INFORMATION TO USERS

While the most advanced technology has been used to photograph and reproduce this manuscript, the quality of the reproduction is heavily dependent upon the quality of the material submitted. For example:

- Manuscript pages may have indistinct print. In such cases, the best available copy has been filmed.
- Manuscripts may not always be complete. In such cases, a note will indicate that it is not possible to obtain missing pages.
- Copyrighted material may have been removed from the manuscript. In such cases, a note will indicate the deletion.

Oversize materials (e.g., maps, drawings, and charts) are photographed by sectioning the original, beginning at the upper left-hand corner and continuing from left to right in equal sections with small overlaps. Each oversize page is also filmed as one exposure and is available, for an additional charge, as a standard 35mm slide or as a 17"x 23" black and white photographic print.

Most photographs reproduce acceptably on positive microfilm or microfiche but lack the clarity on xerographic copies made from the microfilm. For an additional charge, 35mm slides of 6"x 9" black and white photographic prints are available for any photographs or illustrations that cannot be reproduced satisfactorily by xerography.

Ferrall, Charles C., Jr.

TECTONIC STRESS REGIME OF THE CASCADES REGION AND TECTONIC CLASSIFICATION OF LARGE CALDERAS

University of Hawaii PH.D. 1986

PLEASE NOTE:

In all cases this material has been filmed in the best possible way from the available copy. Problems encountered with this document have been identified here with a check mark ✓.

1. Glossy photographs or pages ✓
2. Colored illustrations, paper or print ✓
3. Photographs with dark background ✓
4. Illustrations are poor copy _____
5. Pages with black marks, not original copy _____
6. Print shows through as there is text on both sides of page _____
7. Indistinct, broken or small print on several pages ✓
8. Print exceeds margin requirements _____
9. Tightly bound copy with print lost in spine _____
10. Computer printout pages with indistinct print _____
11. Page(s) _____ lacking when material received, and not available from school or author.
12. Page(s) _____ seem to be missing in numbering only as text follows.
13. Two pages numbered _____. Text follows.
14. Curling and wrinkled pages _____
15. Dissertation contains pages with print at a slant, filmed as received ✓
16. Other _____

_____

_____

TECTONIC STRESS REGIME OF THE CASCADES REGION AND TECTONIC CLASSIFICATION OF LARGE CALDERAS

A DISSERTATION SUBMITTED TO THE GRADUATE DIVISION OF THE
UNIVERSITY OF HAWAII IN PARTIAL FULFILLMENT OF THE
REQUIREMENTS FOR THE DEGREE OF

DOCTOR OF PHILOSOPHY

IN GEOLOGY AND GEOPHYSICS

DECEMBER 1986

By

CHARLES C. FERRALL, JR

Dissertation Comittee:

Michael J. Gaffey, Chairman
George P.L. Walker
John M. Sinton
Thomas B. McCord
James Kellogg
B. Ray Hawke
Everett A. Wingert

ACKNOWLEDGEMENTS

In "The Swordsman and the Cat" (a story from a 17th century book on Japanese swordplay) the most renowned rat-killing cat in the land observes that: "the whole universe is, indeed, not to be sought after outside the mind". To all of the friends, confrers and cohorts that have contributed to the evolution of the mind that produced this monster, you all share in its completion and in my appreciation.

To the folks of PGD I extend my thanks for your support -- both obvious and subtle -- and for being good people to share day-to-day existence with.

To my committee I extend my thanks for your time and energy, and for persevering with me, especially to: Dr. Tom McCord for providing the resources and the breadth of vision to support this project; Dr. B. Ray Hawke for the late night encouragement; and Dr. John Sinton for valuable and entertaining conversations of volcanoes et al.

Dr. Michael Gaffey and Dr. George Walker have been the main forces in support of this effort. Mike's marvelously appropriate advise and encouragement provided exactly the right impetus during the difficult times and contributed immeasurably to the success of the work. George's insight and intuition into things volcanic, his interest in the approach, and his tireless review of early drafts were essential to the evolution of this study. My interaction with these two gentlemen has been a delightful personal experience and the high point of my academic career.

Financial support was provided by NASA, ONR, the Helen Farrar Jones Trust, and GSA. Seasat Radar imagery was provided by the Jet Propulsion Laboratory, Caltech.

It was Dr. Gordon Macdonald who first got me interested in volcanology and planted the seed for this banyan. The inspiration -- the foundation -- of this study lies in the work of H. Williams on caldera processes, Nakaumra on stress trajectories, and Hildreth, and Eichelberger on caldera/tectonic conceptualizations. The project benefited greatly from conversations and field trips with Dr. Lisa Morzel and with Dr. John Gibbons (accompanied by Dr. Wild Turkey). A few of the many others who have contributed and to whom I owe my thanks include: Pam Blake, Cheney Milholland, Dr. Mike Smith, Ab Valencia, Bob Rushforth, Dr. Lionel Wilson, Dr. Brian Taylor, Dr. Charles Rosenfeld (OSU), Dr. Ron Blom (JPL). I also extend my appreciation to the ladies of the libraries, Ms. Pat Price (HIG) and Ms. Mabel Suzuki (Hamilton) who extended great latitude to me in my insatiable need for maps. The final crunch was survived through the support and assistance of Nancy Sadusky -- and Petunia Ferrall.

The most profound inspiration for this work, and life in general, came from my parents who, while enduring their own on-going crisis, encouraged me to persevere. Their courage and selflessness are unsurpassed.

ABSTRACT

This study comprises a tectonic evaluation of the interaction of Basin and Range rifting, that intersects the Cascades Range, with the style of volcanism along the Cascades volcanic axis. Salient results include: a new interpretation of younging trends of rhyolite domes across the northwestern Basin and Range that resolves conflicts in previous tectonic interpretations; a new mechanism for termination of Basin and Range deformation along the Brothers Fault Zone; and the identification of Basin and Range rifts that are propagating into the Cascades at the sites of the large Cascades calderas. A global survey of large-caldera/tectonic association is also presented with a caldera/tectonic classification of calderas greater than 8 km in maximum dimension.

The empirical relationship between the style of volcanism along a magmatic arc and the regional variations in tectonic setting and structure along that arc suggest that the properties of the over-riding plate are more important in volcano-tectonic processes than generally assumed. The present study examines the relationship of tectonic stress orientation and deformation in the over-riding plate to the variation in volcanic style along a magmatic axis. A hypothesis linking these parameters with volcanic style arises from work by Hildreth (1980), Eichelberger and Gooley (1977) and Eichelberger (1977) which studied various volcanic petrologic associations that conform to a model relating relatively compressional tectonics and andesitic stratovolcano-producing volcanism on the one hand; and extensional tectonics and bimodal basalt/rhyolite volcanism characterized by cataclysmic ash flow eruptions

and caldera formation on the other.

The Cascades Range, which demonstrates this relationship, has been chosen for a type-location study. The tectonic setting in the Cascades is such that the subduction-related volcanic arc of the Cascades is becoming progressively convolved at its southern end with the extensional regime of the Basin and Range and the influence of right lateral shear strain related to the transform plate margin (San Andreas) located to the west. The structural, geologic, geophysical, and volcanological environment has been characterized by review and synthesis of the literature, and analysis of remotely sensed images (Landsat, Seasat satellite Radar, airborne Radar, U-2 aerial photography, low altitude oblique aerial photography and pseudo-radar derived from obliquely illuminated relief maps). Volume and area calculations for the entire High Cascades volcanics have been carried out to evaluate distribution of volcanics in relation to various intersecting tectonic elements. Stress trajectory data has been developed from image analysis of vent alignments. A Stress Trajectory Map has been produced which permits tectonic evaluation of stress regimes in the region.

There are two large calderas in the Cascades: Crater Lake and a filled caldera at Mt Lassen (Mt Tehama). There are also two calderas located behind the volcanic front: Medicine Lake and Newberry Calderas. Both Crater Lake and Mt Lassen occur in areas where the Basin and Range faulting has actually reached the axis of the Cascades. Similarly, both Medicine Lake and Newberry calderas occur in areas influenced by this deformation. Medicine Lake caldera is behind the arc in a position

that is arguably within the Basin and Range itself. Newberry occurs at a point where NNW B&R rifting intersects the Cascades arc.

Stress orientations derived from the imagery and volumetric distribution of volcanics indicates that previous interpretations of the significance of NW lineaments -- the Eugene-Denio and Brothers Fault zones -- are difficult to justify. Detailed examination of the Eugene-Denio zone reveals that it is not a discrete zone of enhanced shear. It is discontinuous and fault orientation and fault density within the zone is similar to adjacent areas. The proposed strike-slip deformation of this zone is not in evidence. The Brothers Fault Zone is shown to be most strongly influenced by basin-terminating B&R faults and by extensional deformation. The proposed strike-slip of this zone is also not in evidence.

Study of the style of deformation in the Basin and Range indicates that basins propagated northeastward and stepped westward -- producing the younging previously interpreted to be a NW trend. The orientation of faulting and the ages of rhyolites across the northwestern B&R indicate that a previously unrecognized change in regional maximum horizontal stress orientation took place about 7 mybp. Propagation of B&R rifts into the vicinity of the arc axis beginning about 4 mybp is interpreted to have produced many of the observable variations along the arc. The large calderas (Crater Lake, Newberry, Medicine Lake, Lassen and Bald Mtn. (a possible caldera)) are shown to occur where the B&R rifting has intersected the arc.

From these type examples, a broader study is made of the large calderas of the world (those greater than 8 km in diameter) to examine the tectonic setting of these

volcanoes and thereby test the caldera/tectonic hypothesis on a larger population. This portion of the study is based primarily on the literature and imagery where available. Eighty-two large calderas are identified. These calderas are divided into 13 categories based on the tectonic elements which occur in close proximity to them. Convincing association is found in a statistically significant number of cases between occurrence of calderas and their tectonic environment. 79% of the large calderas occur in an arc environment; 15% in a fundamentally rift environment; and 6% in a hot spot environment. 74% of the total are directly related to extensional tectonics.

Although it is clear that the details of the magma chamber, such as depth, diameter, magma supply rate, viscosity, residence time, etc., are central to the occurrence of major ash flow eruptions, this study implies that for many large-caldera-forming events, the proximity to intersections of active tectonic elements sets the stage for the formation of such magma chambers.

TABLE OF CONTENTS

LIST OF TABLES

LIST OF ILLUSTRATIONS

LIST OF ABBREVIATIONS

AFP	azimuth frequency plot
ARWRL	Abert Rim -- Warner Range Line
B&R	Basin and Range Province
BFZ	Brothers Fault Zone
CIR	Color Infrared
CRB	Columbia River Basalt
EDZ	Eugene-Denio Zone
ERTS	Earth Resources Technology Satellite (early Landsat)
ESRP	Eastern Snake River Plain
HLP	High Lava Plains
MHS	maximum horizontal stress
MPS	maximum principle stress
mybp	million years before present (m.y.b.p.)
my	million years (m.y.)
SRP	Snake River Plain
ybp	years before present (y.b.p.)
WL	Walker Lane

I. INTRODUCTION

In recent years, significant strides have been made in the association of volcanic character with certain tectonic environments. Plate tectonic provinces are a first order discriminant. Among the various elements of the plate tectonic paradigm, magmatic arcs are sources of the majority of subaerial volcanism on the planet. (Primarily for the sake of linguistic variety, the terms volcanic or magmatic arc or axis, and arc environment are used generically and interchangeably herein to refer to the magmatism related to plate subduction.) These features may be thought of as the surface manifestation of a curtain of rising magma produced by the effects of a subducting lithospheric plate (slab) (Marsh, 1981). This magma is thought by some workers to be the result of dehydration of the subducting slab at a depth of about 125 km. The infusion of water into the "fertile" mantle overlying the subducting plate is thought to produce depression of the liquidus and resulting magma production by partial melting of this mantle (Fyfe and McBirney, 1975).

Arc environments can be generally associated with dominant intermediate (andesitic) volcanism whose relatively viscous lava erupts in locally violent, sometimes catastrophic events. Hot spot (plume) volcanism in continental areas (particularly in the early stages of plume conduit development through silicic crust) also tends to have these more violent characteristics. Rift environments, flood basalts, and ocean islands (hot spots in oceanic crust) generally tend to erupt low viscosity mafic magmas in relatively non-violent eruptions. Mafic magmas are also

characteristic of the later stages of continental hot spot and continental rift volcanism.

Intra-province variations in volcanism has also been examined. On the broad scale, study of the distribution of volcanism in the Andes has been correlated with the dip of the subducting plate. Where the dip of the slab (as indicated by seismicity) is shallow -- in Northern Chile -- no volcanism occurs. Where the dip is steep, volcanism is ongoing (Barazangi and Isacks, 1976).

On a much smaller scale, study of the Central American and other magmatic arcs has revealed linear segmentation of these arcs. Volcanic and seismic phenomena within linear segments of the volcanic chain are distinguished from activity at segment offsets (Stoiber and Carr, 1973). These workers characterize segment boundaries in Central America by lower volume, more explosive volcanism, larger spacing between volcanoes, transverse faulting, shallow earthquakes and frequently bimodal basalt/rhyolite volcanism. These varying manifestations of volcanism take place in a setting which, on the broad scale, appears to be one of uniform subduction. Stoiber and Carr (1973) and other workers have proposed that segmentation of the volcanic arc is the result of segmentation in the subducting slab. However, unlike the case for the broad active/inactive volcanic association in the Andes there is no substantial seismic evidence to support this proposal for control of small-scale arc volcanism (Isacks and Barazangi, 1977; Burbach et al, 1984).

What then is the explanation for the along-strike variations in arc volcanic style? The role of crustal stress in the ascent of magma through the overriding plate

is perhaps pertinent to this question.

In the geological literature, extrusive igneous phenomena have commonly been assumed to reflect extensional stresses (eg Shaw, 1980). This arises from the need for a mechanism capable of bringing viscous magma to the near surface environment where it can be erupted. Cracks and fractures generated or opened under the influence of an extensional strain; or rock weakened by the decrease in confining pressure caused by extensional stress, are attractive conduits for the rise of magma. Various mechanisms can produce this extension. These mechanisms range from tectonic stresses related to regional stress fields induced by plate tectonics, to local extension above a rising magma diapir induced by the buoyancy of the magma itself. In both cases the lower density of the molten material, relative to the surrounding rock, is the factor which causes magma to rise (abetted to some degree by excess fluid pressure in the magma produced by volume limitations in the zone of melting).

In the case where the magma is actively forcing its way to the surface by stoping or by diapirism, it induces local extension in the country rock above the magma body (Koide and Bhattacharji, 1975). In this case, the rate of rise is related to the rate at which stress can be built up above the rising mass to the point where the overlying rock fails in tension (or flows -- depending on the regime). In this case larger diapirs move more efficiently because drag associated with the boundaries of the magma body is minimized (Marsh, 1982). The time factor for this mode of magma rise is relatively slow because pods of melt must coalesce before an efficient size is reached to overcome the strength of the overlying rock. This general relationship

applies whether diapirism (or stoping) is taking place in a ductile regime or in a brittle regime. Analyses of this problem have found that for island arc-type magma, a number of diapirs will have to thermally "condition" the crust before subsequent diapirs can actually reach the near surface (Marsh, 1982).

In the case where magma rise takes place in an extensional regime produced by tectonic processes, the magma will behave more passively and follow a path determined less by its own buoyancy and more by the areal forces acting upon it from sources external to the magma body. Since the conduits or zones of weakness that the magma uses in this case precede the arrival of magma, the magma may move in smaller bodies with relatively faster rates of rise. The fact that essentially pristine basalt erupts at some localities, relatively uncontaminated by its passage through the crust, testifies to a process which allows rapid rise of magma. [A more complete discussion of the mechanics of magma ascent are given in Spera (1980) and Shaw (1980).] Clearly, many other factors are involved in the ascent of magma such as: depth of origin and rate of generation of magma; magma composition and rheology; pre-existing regional structure. However the stress relationships discussed above remain among the most critical considerations in the problem of magma ascent.

R.L. Smith (1979) discusses many of these factors in a general consideration of ash-flow magmatism. He considers local conditions in the magma chamber within which these (ash flow) types of eruptions occur -- such as the viscosity window concept (that lavas below a minimum viscosity will not disrupt to form particulate flows; and that lavas above a maximum viscosity (~50% phenocrysts) will not leave the magma

chamber). However, such factors are details of the magma chamber that come to bear once the shallow magma chamber is in place. Smith (1979) observes that these within-chamber processes "probably reveal the overprint of tectonic periodicity that controls both the rate and longevity of primitive magma injection" -- which thermally drives the system.

Eichelberger and Gooley (1977) and Hildreth (1981) have developed a compelling model which relates the influence of stress states to the composition of the resultant magmas. Their model is based on the concept of basalt as the driver of most volcanism. Their evidence for the presence of basalt is summarized by them as follows:

> "Andesitic and rhyolitic volcanism is commonly preceded by the eruption of basalt. Similarly, the earliest phases of granitic plutonic complexes are often gabbro. Thus basaltic magma apparently plays a role in the initiation of a large silicic magma system. Three lines of evidence suggest that basaltic magma also enters silicic chambers and influences their further evolution: (1) Contemporaneous basalt vents flank silicic volcanic centers. (2) Thermal models of silicic magma bodies suggest that their heat must be replenished to maintain them in the upper crust for their observed life-span. (3) Petrologic data indicate that "cognate" mafic clots and xenoliths common in granodiorite and andesite represent basaltic magma quenched within active silicic magma chambers" (Eichelberger & Gooley, 1977).

In their model (Figure 1), the basaltic melt acts as a heat transfer medium by carrying heat from the upper mantle to the crust where it interacts with the crustal rocks in one of three ways: (1) erupting on the surface; (2) assimilating lower crustal rocks and moving toward a more silicic (andesitic) composition; or (3) crystallizing in the crust, thereby providing heat to produce crustal partial melt -- yielding shallow bodies

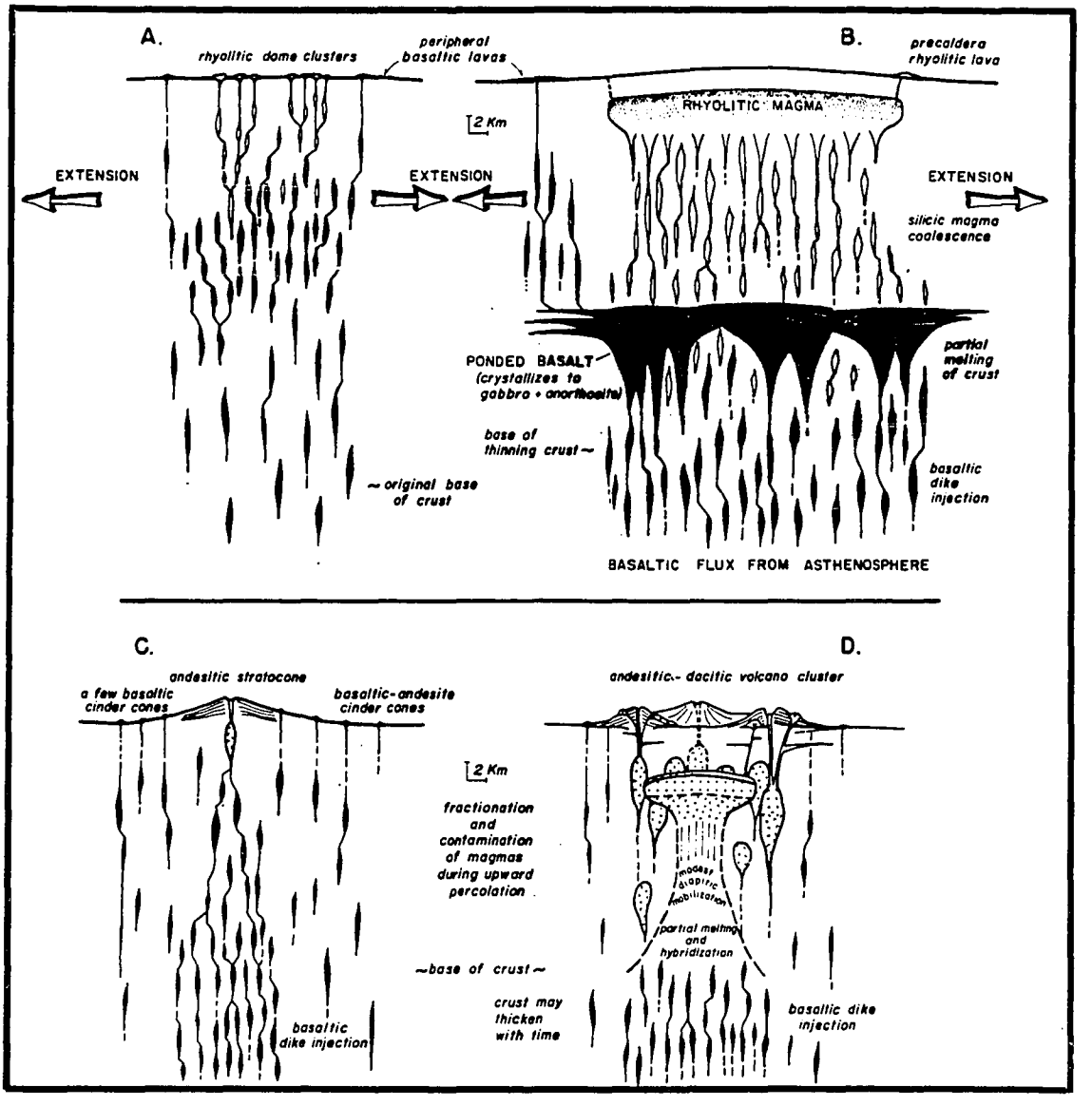

Figure 1. Styles of Lithospheric Magmatism (after Hildreth, 1981). A. Early rise of basalt under extensional regime. B. Advanced stage under extensional regime -- basalt exchanges heat with silicic crust producing a large silicic magma chamber, setting the stage for large caldera collapse by catastrophic venting of the magma chamber. C. Early rise under less extensional regime -- basalt interacts with the crust by fractionation and contamination during magma rise. D. Late stage in less extensional regime -- large andesitic diapir feeds intermediate volcanism.

of siliceous (rhyolitic) magma. The occurrence of numerous examples of rhyolitic centers surrounded by contemporaneous basaltic vents erupting from related structures testifies to simultaneous operation of modes (1) and (3).

The model suggests that compressional environments increase time of residence in the crust and thereby lead to incorporation of crustal rocks producing andesites. Extensional environments permit rapid rise with little loss of heat so that basalts either reach the surface or melt shallower crustal rocks to produce rhyolitic magmas. Exceedingly rapid rise of basaltic melt through silicic crust which is fertile enough to yield large volume rhyolitic partial melts is necessary to produce large rhyolitic chambers. Centers of bimodal rhyolitic/basaltic volcanism then occur in areas of relative extension and their eruption style is either in clusters of domes or as large calderas. Andesitic stratocones are more characteristic of compressional areas.

One test of the validity of the tectonic association which is implicit in this model is to identify along-strike variations in volcanic style and to examine the associated tectonic elements for possible complicity in the process. In plate tectonic terms, the alternatives are that either structure in the subducting plate and/or structure in the overriding plate is responsible for the stress differences that alter magma ascent.

As mentioned above, there is abundant evidence (seismicity and volcano distribution) that broad scale segmentation of the subducting slab is taking place. This is best exemplified in the Andes where volcanism is absent behind arc segments in Peru (15°S - 24°S) and Chile (28°S - 33°S) where shallow, less than 10°, dip of the slab is indicated. Volcanism persists behind areas of steeper-dipping slab (~30°)

(Barazangi and Isacks, 1976; Jordan et al, 1983). These segments are 1550 km and 600 km in length, respectively. On the other hand, Isacks and Barazangi (1977) and more recently Burbach et al (1984), in studying the Central American subduction zone, find no evidence in terms of Benioff Zone seismicity which would indicate variations in slab dip and thus tears in the subducting plate on the appropriate scale (segment length of 100-300 km) that might explain the observed variations in volcanic style discussed by Stoiber and Carr (1973) and ascribed by them to structure in the subducting plate.

This lack of correlation with subducting plate structure is particularly true in arcs on thick continental crust such as the Cascades. Segment boundaries in the Cascades proposed by Hughes, Stoiber and Carr (1980) which link major edifices are lacking supporting data and are, in fact, precluded by actual volcano distribution (see discussion in Chapter 2). These workers invoke NE striking segment boundaries even though the volcanic alignments are at a 45° angle to this trend and transforms in the subducting slab are oriented ESE.

On the other hand, Sykes (1978) cites considerable evidence of structure in the overriding plate apparently influencing tectonic development at the initial continental rifting stage. These structures are profound features in the crust and likely penetrate the entire lithosphere. Hall and Wood (1985) have observed that the northern Andes display some variations (segmentation) in arc volcanism which can be related to structures in the subducting slab (eg. Carnegie Ridge); and some variations in volcanism which do not appear to be related to the slab and are more likely related

to fundamental structure in the overriding plate.

In the Cascades, there is strong indication that such structure is influencing magmatism. However, the examination of such broad-scale features requires a synoptic view of the region to allow integration of the influence and interaction of complex plate tectonic elements. The use of broad-scale satellite imagery provides such a synoptic view of the surface of the earth which facilitates geologic synthesis of large areas that were previously mapped in small segments and perhaps not well integrated with neighboring areas. Satellite synthetic aperture radar (SAR) imagery particularly enhances geologic structure and thus enables tectonic analysis over broad areas -- a capability which was previously not available. The aim of the study described herein has been to utilize this type of imagery (Seasat SAR and Landsat MSS), integrated with other imagery, calculations of the volume distribution of the volcanics, tectonic stress trajectories indicated by well defined vent alignments, and other types of geologic data, to study an area where a number of fundamental tectonic elements are interacting; and to examine the aspects of that interaction -- particularly the volcanic aspects -- which are clarified by the synoptic view. The thrust of this examination is to test the volcano-tectonic model described above: is there an observable correlation between extensional tectonics and the occurrence of large calderas?

Development of the treatment which follows includes a discussion of the plate tectonic setting of the Pacific Northwest and its three principle tectonic elements: Juan de Fuca plate subduction and resultant Cascades volcanic arc; Basin & Range

spreading; San Andreas transform motion. The discussion then centers on the area of interaction of the southern Cascades and northwestern Basin and Range to examine the volcano-tectonic relationships. Evaluation of imagery, maps, etc. allows better characterization of the stress field in the Cascades and the reinterpretation of some problematical structural features. A significant change in the interpretation of the tectonic relationships in the Cascades is proposed. Finally, a review of the large (> 8 km) calderas of the world and their tectonic settings is presented to examine the global significance and implications of this model. If the caldera-tectonic association can be demonstrated in the majority of cases, it may be possible to consider the inverse hypothesis -- that large calderas can be used to find areas of tectonic turmoil!

II. TECTONIC SETTING OF THE CASCADES REGION

The tectonic setting of the Cascades volcanic arc appears, on first look, to be a simple example of an Andean arc -- characterized by volcanism arising from subduction of an oceanic plate beneath a continental plate. The alignment of the volcanoes is linear, with a few exceptions, and spacing is relatively consistent (although it increases from south to north) and the volcanoes generally occur a uniform distance from the coastline. In detail, however, the tectonic setting of the Cascades displays a number of enigmatic characteristics -- most notably the absence of significant Benioff zone seismicity. The significant tectonic elements include the following:

1) oblique subduction of young oceanic crust of the Juan de Fuca plate -- convergence direction: NE-SW;
2) complicated interaction with the Gorda oceanic plate where subduction appears to have ceased;
3) deformation in the Basin and Range province where major crustal extension is dominant to the east of the Cascades;
4) dextral motion between the Pacific and North American plates localized along the San Andreas transform and also distributed to some degree across the western margin of the North American plate as far east as the Basin and Range province;

These elements combine to form a wide variety of geomorphic forms and geophysical characteristics. There have been numerous attempts to synthesize the tectonics of the Western United States (see for example Christiansen and McKee (1978), Stewart (1978), Armstrong (1978), Eaton (1982), Atwater (1970)). However consensus exists only on the broadest issues. The perception of the characteristics of these regions and their significance is constantly evolving as additional data and new perspectives are developed. The present study of synoptic imagery, regional stress trajectories and faulting, and volcanic patterns and distributions has led to new interpretations of some of the tectonics of the southern Cascades. This section presents a discussion of the various tectonic elements and their characteristics, and is intended to provide a background for further discussion in later sections with reference to the imagery.

The oceanic plates will be examined first. Important considerations on the ocean plates include:

1) the oblique subduction of the Juan de Fuca and Gorda plates and the youth of the oceanic crust being subducted;
2) evidence of seismic or aseismic subduction in the absence of unambiguous Benioff zone seismicity;
3) possible coupling of portions of the Gorda plate with the Pacific plate;
4) the significance of structure in, and age of the subducting plate on the development of arc volcanics building on top of the overriding plate;
5) the influence of the Mendocino transform-transform-trench (FFT) triple

junction on Gorda plate subduction/deformation; and on the style of deformation to the east;

Important tectonic considerations on the continental plate includes:

1) the presence of a regional stress oriented with maximum horizontal compression north-south which has produced E-W folding in the northern Cascades;

2) the evolution of the Basin & Range, its tectonic significance, volcanism, seismicity and influence on Cascades magmatism and volcanic style;

3) regional Basin and Range lineaments which are postulated to intersect and offset the Cascades: Brothers Fault zone, Eugene-Denio zone, Mt. McLoughlin zone;

4) the existence and possible influence of the Blue Mountains microplate in Oregon -- an example of so-called allochthanous terrane -- which lies near the arc and may have influenced magmatism/volcanic style;

5) apparent northward termination of the Basin & Range in central Oregon at a proposed northwest-trending right lateral boundary (Brothers Fault Zone) which coincides with the southern margin of the Blue Mountains; and westward younging of silicic volcanism toward Newberry volcano along this boundary;

6) the existence of an ancestor arc to the west of the High Cascades (Western Cascades) and localization of heat flow along the boundary between old and new arcs; and evidence of eastward migration of the volcanic activity

of the arc;

7) the existence of a Cascade graben along which the southern Cascade volcanoes (in Oregon and California) have developed;

8) the dominance of extensional tectonics in the Basin and Range with some strike-slip tectonics along the Walker Lane; and the relative significance of these two modes of deformation in the southern Cascades;

PLATE INTERACTIONS

This study is mainly concerned with the southern Cascades and their interaction with adjacent tectonic elements. The following discussion considers the overall tectonic setting of the region in order to provide a context for the analyses presented in later chapters. Particular note is taken of the dominance of strike-slip deformation at the southern end of the Cascades and the dominance of N-NNW extensional faulting east of the Cascades from Medicine Lake to Newberry and the correspondence between this extensional deformation and caldera location. Work on the details of Basin and Range deformation is examined to provide a context for the discussion in Chapter 3 relating to Basin and Range rifting.

Juan de Fuca and Gorda Oceanic Plates

The Juan de Fuca and the Gorda plates are the remnants of the Farallon plate which has been subducting beneath the western margin of North America throughout most of the Tertiary. This subduction is the ultimate source of Cascades volcanism. The results of modelling of the magnetic anomalies of the Juan de Fuca Plate (Wilson, 1984), indicates that prior to the present configuration, the Juan de Fuca ridge was oriented essentially N-S parallel to the coast of North America. It began to rotate in a clockwise direction about 7.5 m.y.b.p. (Wilson, 1984). This fact may have triggered the change in Basin and Range stress orientation which is an important finding of the present study as discussed in Chapter 3.

The present orientation of the Juan de Fuca and Gorda plates is shown on Figure 2. The Gorda plate is offset relative to the Juan de Fuca plate along the Blanco Fracture Zone. The Blanco once apparently accommodated different rates of spreading between the two plates, however, lack of seismicity on the projection of the Blanco Fracture Zone east of the Gorda Ridge suggests that at least parts of the Gorda plate are now subducting in concert with the Juan de Fuca plate. The Gorda plate is now apparently segmented, with an ill-defined region of differential offset to the south of the Blanco.

Riddihough (1984) identifies a South Gorda plate whose motion is significantly different from the Juan de Fuca since 3-4 m.y.b.p. and which appears to have ceased subduction since that time. The boundary of this plate is shown on Figure 2. Riddihough gives a history of plate motion over the last 6.5 my based on magnetic

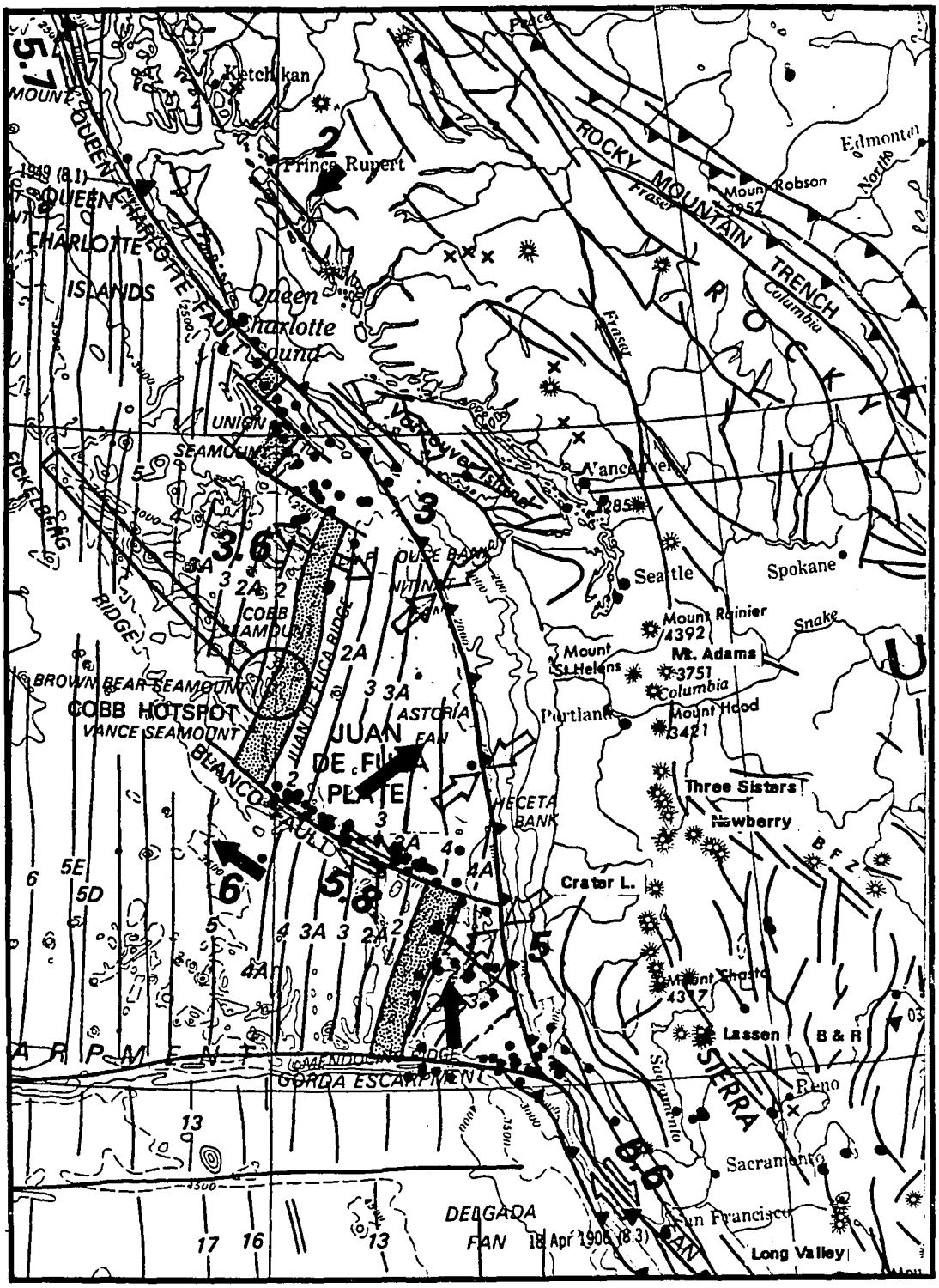

Figure 2. Plate Tectonic setting of the Cascades with relative (open arrows) and absolute (solid arrows) plate motions indicated (modified after AAPG, 1981).

anomaly analysis (Figure 3). Current absolute motion of the Juan de Fuca plate reflects clockwise motion about a pole of rotation nearby to the southeast. This motion interacts with a broadly clockwise absolute rotation of the North American plate (about 22 mm/yr southwest, opposite Mt. Hood) to produce relative convergence with the Juan de Fuca plate (Figure 3) ranging from 46 mm/yr opposite Vancouver Island to 36 mm/yr at Cape Blanco opposite Crater Lake. The South Gorda plate has motion relative to North America that is NW about 40 mm/yr -- roughly parallel to its boundary with the North American plate. Analysis of the magnetic anomaly pattern indicates that this motion has persisted since at least 4 m.y.b.p. (Riddihough, 1984).

Juan de Fuca oblique subduction reflects the final thrashings of slivers of the once formidable Farallon plate as its northern portion approaches complete subduction under North America. The Farallon plate may once have dominated the Pacific plate during the Mesozoic, and maintained right angle convergence with and subduction under North America (Jurdy, 1984). However the Farallon has been progressiviely overrun as the North American plate moved to the southwest. A dextral strike-slip (transform) boundary was established between the North American and Pacific plates north of the Juan de Fuca plate when the Kula plate (and its RRR triple junction with the Farallon and the Pacific plates) was subducted in the late Tertiary. This transform is the Queen Charlotte/Fairweather fault. At present, the Juan de Fuca plate is as flotsam caught in the passage of the North American and Pacific plates past one another. The effect of this relationship is that the Juan de Fuca and North

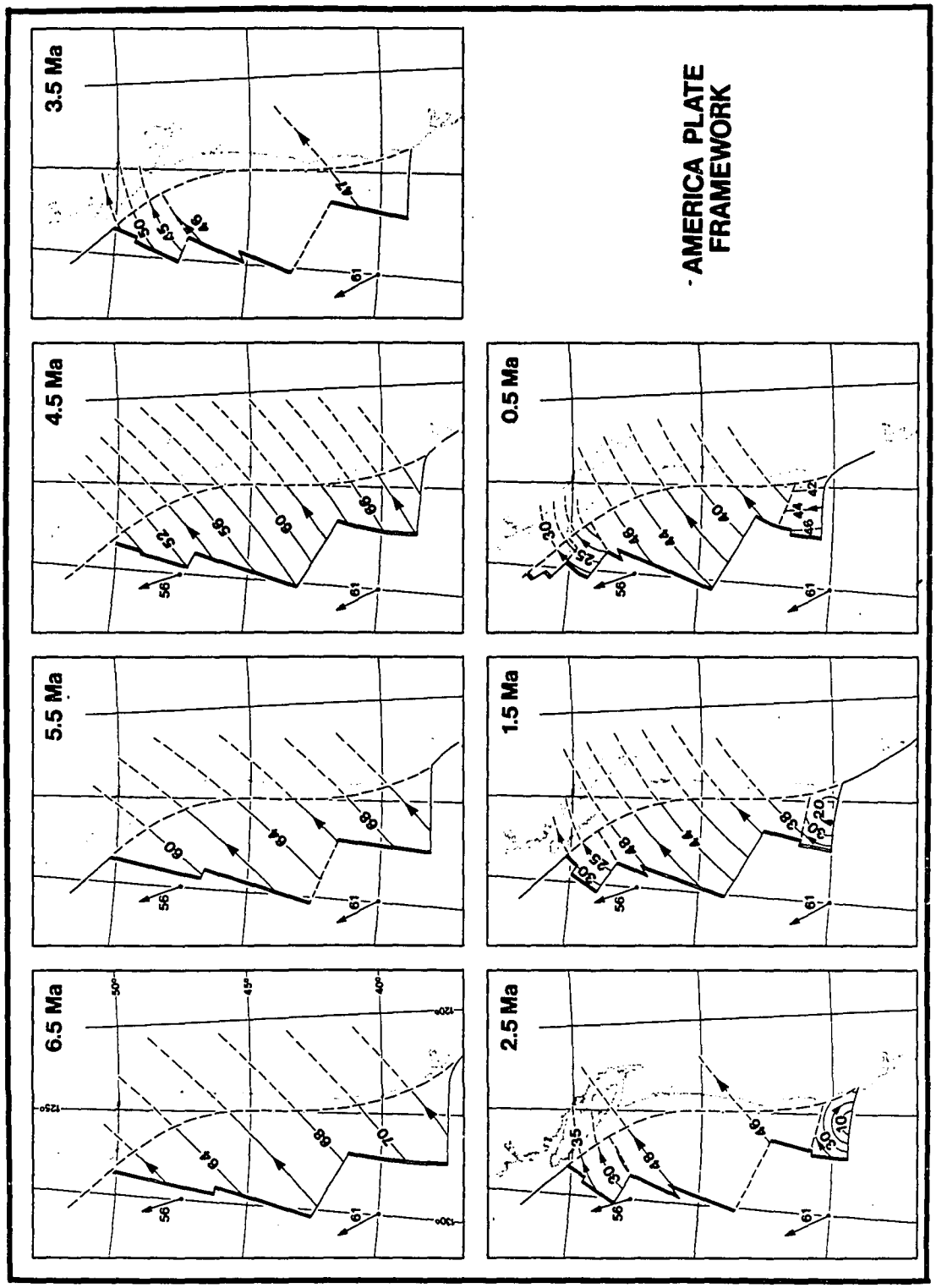

Figure 3. Motion vectors of the Juan de Fuca Plate system since 7 m.y.b.p. relative to the America Plate, errors are at least 20° in azimuth and 10 mm/yr in velocity (Riddihough, 1984).

Gorda ridges are rapidly pivoting -- by propagating new ridges primarily from north to south -- and generating new transforms to adapt to the changing plate motions. Some workers feel that the stress field associated with dextral transforms to the north and south of the Juan de Fuca plate (ie. the Queen Charlotte-Fairweather and the San Andreas) are interacting landward of the subduction zone and that this interaction produces a megashear within the North American plate that plays an important role in the tectonic deformation of the Northwestern US in N. California, N. Nevada, Oregon and Washington (eg. Christiansen and McKee, 1978).

The magnetic anomalies for the Juan de Fuca and Gorda plates are shown on Figure 4. (It is of historical interest that this data set (Raff and Mason, 1961) served as one of the seminal examples of magnetic 'stripes' on the sea floor to be explained in the context of the Plate Tectonic paradigm). The pattern is complex and was initially explained by invoking numerous strike-slip offsets (Silver, 1971) -- a problematical solution in the context of plate tectonic concepts. Recent work by Wilson et al(1984), however, has utilized the propagating rift concept to very convincingly model this magnetic anomaly pattern without requiring strike-slip offsets. Propagating rifting offers a mechanism whereby ridges become reoriented in response to changes in plate motion.

Wilson et al's approach models the magnetic trail made by a propagating ocean ridge as it propagates through older ocean crust. For a single propagating rift the resulting magnetic anomaly pattern looks like the wake of a ship trailing off from the bow (rift tip) (Hey et al, 1980) (see Figure 5). In the model, the propagating rift is

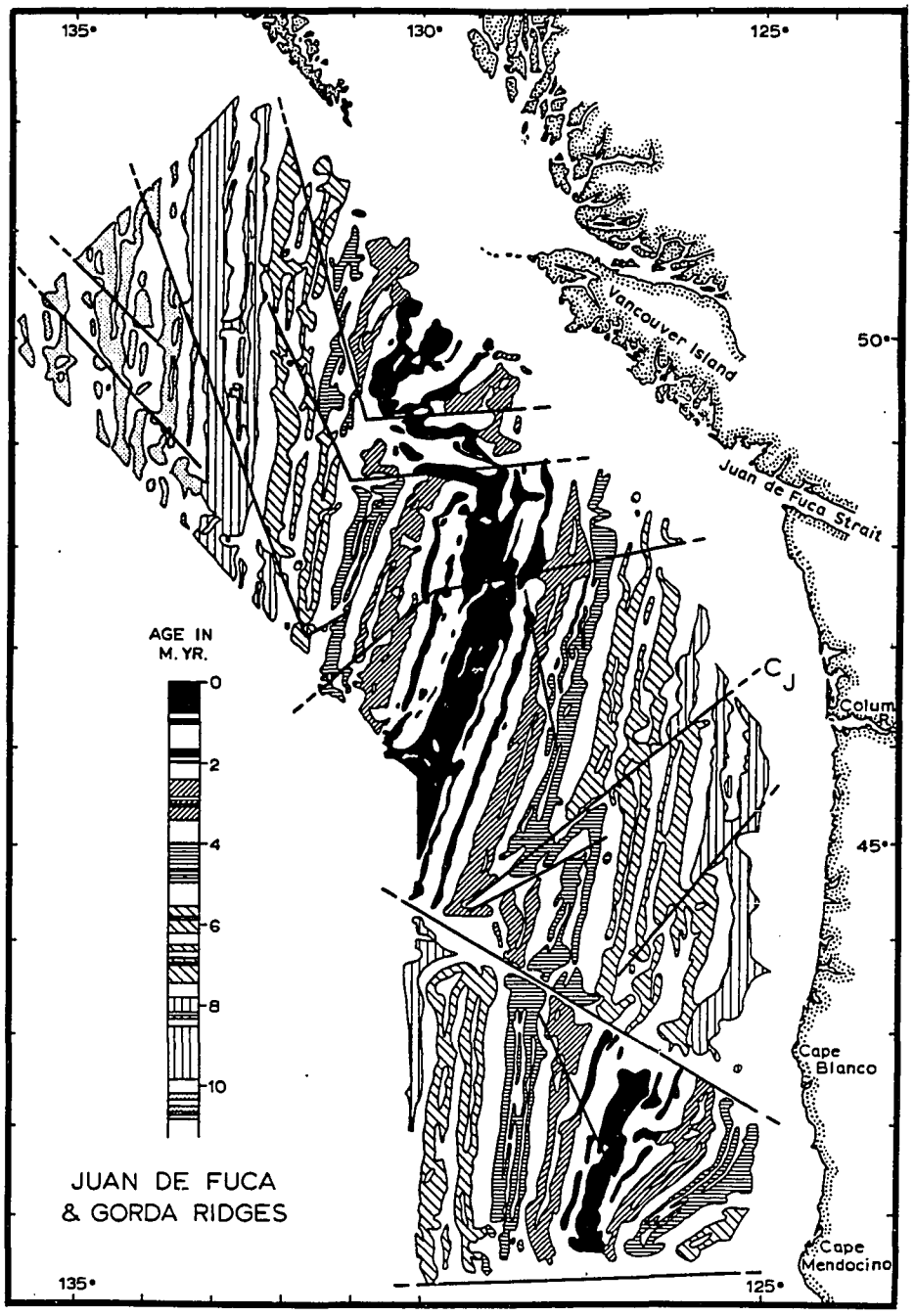

Figure 4. Raff-Mason magnetic anomaly pattern map in the northeast Pacific (Silver, 1971). The current spreading center is shown in black; B-Blanco Fracture Zone; M-Mendocino Fracture Zone; G-Gorda Ridge; J-Juan de Fuca Ridge; dashed lines - possible pseudofaults.

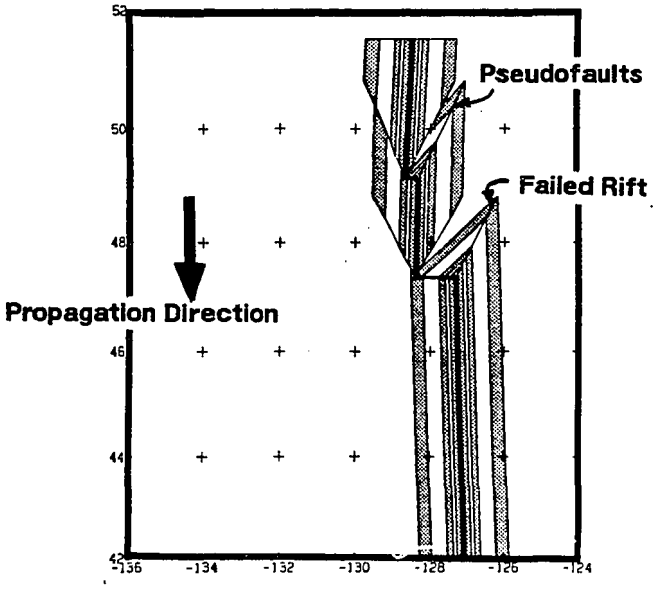

Figure 5. Propagating Rift elements for a ridge propagating from north to south (Wilson et al, 1984).

subparallel to a dying rift of slightly different orientation. As the new rift propagates, it leaves a wake of new crust forming a 'V' pointing along the direction of propagation. These linear anomaly features are termed "pseudofaults" (Hey, 1977). As the old rift dies, it also leaves a linear trace of the intersections of:

a) anomalies that it generated outboard of the new rift; and

b) the ones it generated as it retreated.

This anomaly feature is called the dying rift trace. These two types of features create pairs of subparallel breaks in the anomaly pattern (Figure 5).

Wilson et al. used this propagating rift concept to model the observed Juan de Fuca plate magnetic anomalies. By computer simulation, they propagated a succession of rifts in various geometries in an effort to duplicate the observed anomaly pattern. In their best-fit configuration, the correlation of observed anomalies with the model is compelling. Figure 6 shows the modelled anomalies with respect to the approximate trench location and the major Cascade volcanoes. Figure 6 has been constructed for this dissertation by combining a sequence of figures from Wilson et al. (1985) such that the pattern of magnetic anomalies in the ocean crust is extended beyond the continental margin and into the subduction zone. This represents the first attempt (to the writer's knowledge) to extrapolate anomaly pattern models -- past the subduction zone -- and to examine their possible geometry in the zone of magma generation, and possible relationship to the overlying arc volcanoes.

The validity of the prediction of anomaly geometry under the Cascades is, of course, unknown. But based on the model, the volcanoes appear to arise from crust of

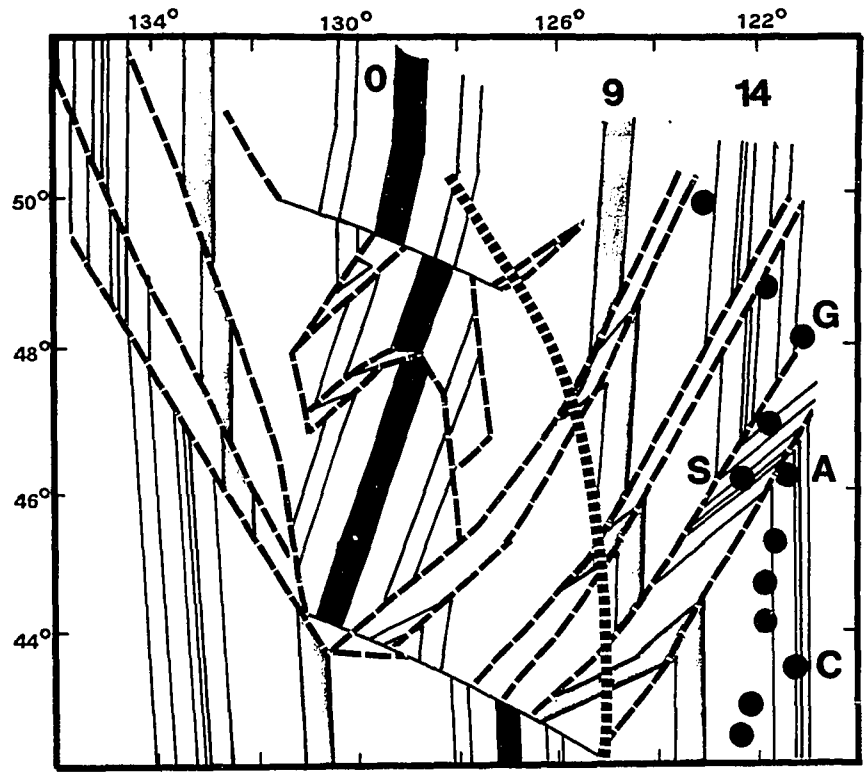

Figure 6. Magnetic Anomaly Model of Juan de Fuca plate resulting from propagating rift geometry (modified after Wilson (1984)). The current spreading center is shown in black (0); anomaly 5 is shaded; solid circles are main volcanoes of the Cascades; narrow dashed lines are pseudofaults and failed rifts; broad dashed line is approximate location of the trench. Numbers are ages of crust in m.y.; C-Crater Lake; A-Mt. Adams; S-Mt. St. Helens; G-Glacier Peak. The volcanoes from Adams northward coincide with the trace of the pseudofault/failed rift zones which are characterized by a high degree of faulting and extensional deformation in the subducting plate.

consistent age. The crust beneath the arc falls in the 11 to 14 m.y.b.p. age interval (anomalies 5A and 5B) for virtually all the major Cascade volcanoes. Only to the north, where the arc-trench gap increases, do volcanoes rise from older crust. (Note: the figure is not corrected for slab dip, which is shallow but ill constrained due to low seismicity. A shallow dip would have no significant effect on the age interpretation.)

The predicted pseudofaults of this model may offer an explanation for the anomalous location of Mt. St. Helens relative to the other volcanoes in the Cascades. Mt. St. Helens lies directly seaward and 52 km west of the Cascade axis which passes through Mt. Adams. St. Helens is in an anomalous position with respect to the otherwise linear N-S alignment of stratovolcanoes in the Cascades although its spacing from adjacent volcanoes (Mt. Adams to the east and Mt. Rainier to the northeast) is typical of stratovolcano spacing found elsewhere in the Cascades. To date, no satisfactory arguments have been put forth to explain St. Helens' spacial relationship to the rest of the Cascades in the context of subducting-margin plate tectonic processes. (The off-axis volcanoes of Newberry and Medicine Lake are in a backarc setting as discussed below and are not relevant in this context).

In the modelled anomalies (Figure 6), St. Helens is overlies a pseudofault/failed rift zone which is an artifact of the propagating rift process. These pseudofault/failed rift zones represent zones where preexisting oceanic crust is transferred from one plate to another. Recent work in the Galapagos area on these features, using Seamarc II side-looking sonar imaging and submersible reconnaissance (John Sinton and Dick Hey, personal communication, 1985), indicates that they are

characterized by considerable local crustal deformation, particularly extensional strain. The anomalous deformation of the pseudofault/failed rift may provide a cause/effect relationship between these zones and the generation of some volcanoes (J. Sinton, pers. comm. 1985). This crustal deformation may localize water and sediment incorporated in the down-going slab and thus provide environments more favorable to localization of partial melting and the subsequent development of a rising magma diapir. The spacing of main vents in the Cascades becomes considerably less consistent north of Mt. St. Helens. However, the locations of the northern Cascades, including: Mt. Adams, Mt. St. Helens, Mt. Rainier, Glacier Peak, Mt. Baker, and Mt. Gariboldi, have in common the fact that they lie close to or on the failed rift/pseudofault zones as modelled by Wilson et al. (1985).

The evaluation of subducting-plate geometry beneath the Cascades is severely impaired by the absence of well defined Benioff zone seismicity. The lack of seismicity is particularly suprising due to the youth of the subducting plate which should be relatively buoyant and therefore resist subduction. Crosson (1972) has argued that the lack of Benioff seismicity implies that within the last 1-2 million years (the resolution of magnetic anomaly data) the Juan de Fuca plate has become attached to the American plate and subduction has effectively ceased. Recent work by Crosson and Yount and others (1980), however, indicates that weak Benioff seismicity may be present under Washington but they note that seismicity does not reflect subduction in any simple way. They observe that seismic moment rates are too low by about a factor of 10 and the stress from fault mechanism solutions is in

the wrong direction compared to other convergence estimates. Heaton and Kanamori (1984) argue that the absence of seismicity data indicates that fault mechanisms are locked and building up for a large stress release. By comparison with other subduction zones where large earthquakes have occurred, they feel that the Northwest is a likely candidate for a large earthquake. Their argument, however, is speculative and based only on broad analogy with other arcs. There is no Cascades data to support their contention. A more straightforward interpretation is that the lack of seismicity implies the absence of stress buildup indicating extensional tectonism. This interpretation is better supported by the character of the arc and adjacent regions as described in the following chapters.

Geodetic measurements in Oregon and Washington, indicating uplift at the coastline relative to areas to the east, have been interpreted to imply aseismic subduction (Ando and Balazs, 1979; Savage et al, 1981; Reilinger and Adams, 1982). The argument is that in the case of seismic subduction, periods between seismic events (preseismic periods) are characterized by coastal subsidence (rather than uplift) which builds up stress that is then released during seismicity (coseismic uplift). The coseismic uplift does not recover completely, leaving a residual uplift (Figure 7) which then subsides with time. In the case of aseismic subduction, it is assumed that stresses built up during subduction may be relaxed by steady-state creep such that the overriding plate is being constantly upthrust over the subducting plate producing uplift at the margin. (It should be noted however, that the resolution of the geodetic data used to distinguish these cases is only marginally better than the uncertainties of the measurements.)

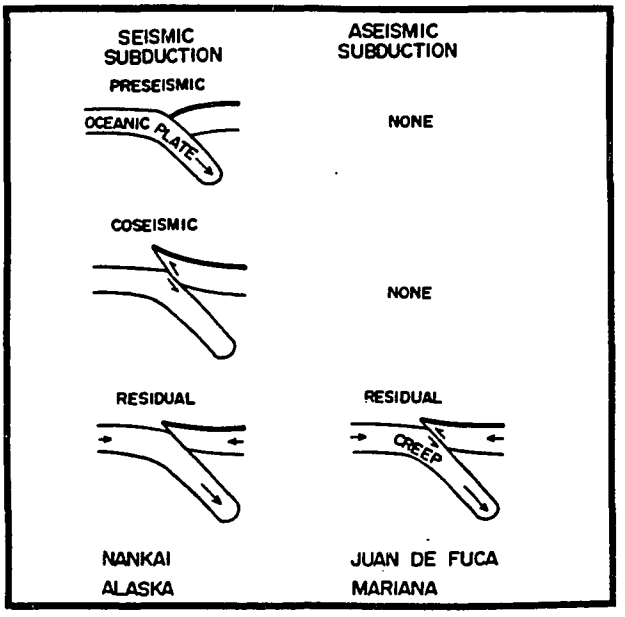

Figure 7. Schematic diagrams of vertical deformation associated with seismic and aseismic subduction (Ando et al, 1979). This scenario has been examined with respect to observed geodetic measurements that suggest aseismic subduction may be taking place beneath the Cascades (see text).

If subduction is taking place, its usual dynamic indicator -- seismicity -- is not obvious here. It is argued that the slow subduction rate and proximity to the ridge (ie. relatively young age of the subducting crust) account for the lack of seismicity (Riddihough and Hyndman, 1976). However, young-age (therefore warm and more buoyant) crust is used by others to infer low angle subduction and resulting compressional (presumably more seismic) linkage to the overriding plate (Uyeda and Kanamori (1979); Heaton and Kanamori (1984)). Such association has also been commonly invoked to explain current Peruvian tectonics and early Cenozoic Laramide tectonics (Cross and Pilger, 1982) which are characterized by a lack of arc volcanism -- clearly not the case in the Cascades.

An alternative explanation which may have merit involves the role of excess pore pressure in the detachment zone of the subducting sediments. High pore pressures have been found at depth in the sediments of the Barbados forearc. It has been proposed that high sediment deposition rates, slow convergence, and high pore fluid pressures may help account for aseismic subduction (Kellogg, 1986). The lack of existing seismic data relating to the Cascades impairs the understanding of the overall tectonics.

The alignment of the major cones in the Cascades Range has been explained from various perspectives. Following the aforementioned approach of Stoiber and Carr (1973) for the Central American volcanoes, Hughes et al. (1980) have applied a similar analysis to the Cascades. They identify arc segments on the basis of "alignments" of major volcanoes and assume that offsets between segments are

indicative of varying slab dip resulting from segmentation of the subducting slab. Consequently, they infer that offsets between segments occur on lines of offset which strike NE -- parallel to the convergence direction. With the exception of pseudofault/failed rift traces discussed above, structure in the subducting plate which is generated at the ridge -- that is, transform faults -- will be oriented perpendicular to the ridge (eg. the Blanco F.Z.), not to the direction of convergence. More importantly, there is no evidence that the offsets in the volcanic arc are taking place parallel to the convergence direction; while there is an abundance of N-S striking structure. The offset in the volcanic arc at Diamond Peak is attributed by Hughes et al. (1980) to slab segmentation on NE-striking structure with the slab northwest of the offset dipping at a shallower angle and thereby generating volcanism farther inland. However, the offset actually trends ESE. Directly east and ESE of Diamond Peak, large recent cones (Odell Butte, Hamner Butte, etc.) occur which are on the volcanic axis that projects down from the north. This precludes the offset taking place on NE-trending structure. Similarly, there is no evidence of transverse faulting or shallow seismicity on their proposed NE segmentation boundaries at Lassen, Three Sisters or Mt. Adams. North of Shasta, the axis of the Cascades arc strikes N-S, and is not perpendicular to the NE convergence direction. On a broad scale, there is little doubt that Juan de Fuca subduction influences arc geometry but the details of the interpretation of Hughes et al. (1980) do not appear supportable.

Weaver and Michaelson (1985) put forth a tectonic model for the Northern Cascades based on seismic focal solutions. Deep earthquakes in the Cascades (> 30 km deep), ascribed to seismic activity in the subducting plate, are limited to areas north of Mt. Rainier. In addition, the focal mechanisms in the area around St. Helens show a NNE regional compressive stress compared to the N-S orientation which dominates areas to the south or east (eg. Mt. Adams) (Weaver and Smith, 1983). This is particularly true along the NNW-striking right lateral St. Helens Fault Zone which passes through the St. Helens stratovolcano. Weaver and Smith suggest that a different stress regime persists from St. Helens northward, which more reflects the plate convergence vector because (they theorize) the subducting slab is in closer contact with the overriding slab. Weaver and Michaelson (1985) propose that the different seismic character in the northern Cascades indicates a shallow dipping slab while that in the Southern Cascades reflects a steeper dip. They speculate that the lack of seismicity in Oregon and further south may be due to the slab actually being broken.

A plausible modification to Weaver and Michaelsons's theory is that the steeper slab dip is due to the slab being relatively less buoyant in the mantle that has been heated by Basin and Range activity. Such thermal activity is supported by higher heat flow and lower Pn velocities in the Southern Cascades versus the Northern Cascades (Blackwell, 1978; R.B. Smith, 1978). However, these models are based on the assumption that subduction is driving seismicity -- or the lack of it. If the dominant tectonic component is the megashear created behind the arc by interaction

of the Queen Charlotte-Fairweather transform with the San Andreas transform, the lack of seismicity in the Southern Cascades could be more related to the dominant extensional deformation caused by the megashear and the geometry of the subducting slab may be less significant. (The details of the Cascades and possible tectonic models are discussed in more detail below.)

In an attempt to approximate slab geometry, one approach is to assume a constant volcanic source depth of 125 km (Hamilton, 1980) and use arc-trench-gap width to calculate slab dip angle. The result of this exercise is a relatively consistent slab true dip of 22° for all of the chain with some shallowing of the angle for the most northerly vents of the Cascades. For the Cascades, this exercise is not straightforward owing to the difficulty in identifying the trench axis. Furthermore, any calculation of this type ignores the fact that, in most arcs, the slab develops a point of flexure landward of the trench so that the slab dips at a shallow angle at the trench and at a steeper angle under the magmatic arc (Taylor and Karner, 1983).

Rodgers (1983) used earthquake hypocenters beneath the Puget Sound area of Washington to estimate slab dip at 12° in the upper part of the subduction zone down to a depth of about 40 km and a 32° dip below 40 km. However, the distribution of hypocenters is diffuse and the geometry is far from well defined. Relative to other subduction zones, this is an average plate geometry, falling at an intermediate point between the very steep and very flat subduction configurations (Jachens and Griscom, 1983).

Although the evidence of Juan de Fuca plate subduction is somewhat ambiguous, the active spreading at the ridge and relative convergence with North America has led most workers to accept the notion that ongoing subduction is taking place. The case for the Gorda Plate, however, is different. Historic seismicity of the Gorda Plate region is shown on Figures 8 and 9 (Riddihough, 1980). This evidence indicates that the Blanco Fracture Zone east of the Gorda Ridge is not a presently active transform. However, young magnetic anomalies terminate at this feature (Figure 4) and there is considerable bathymetric relief across it testifying to tectonic activity in recent geologic history. The magnetic anomalies in the Gorda Plate are distinctive -- with their dominantly northeasterly strike curving to north-south alignment at the ends where the anomalies intersect the Blanco and Mendocino Fracture Zones. The northern portion of the anomaly pattern can be interpreted as that produced by a propagating rift migrating from northeast to southwest and terminating at the prominent offset in the anomalies between latitude 41° and 42° -- initiated at the Blanco Fracture Zone between 4 and 5 m.y.b.p. Riddihough (1980) takes a different view (Figure 9), identifying the Gorda Fracture Zone as a transform between the North and South Gorda plates. This zone is seismically active, although seismic events occur in a somewhat diffuse zone. At the present time, the North Gorda Plate must be moving at the same rate as the Juan de Fuca plate owing to the absence of seismicity between them.

South of this Gorda Fracture Zone the anomaly pattern is problematical. There is a 46° difference in the strike of anomalies between the west side of the Gorda Ridge

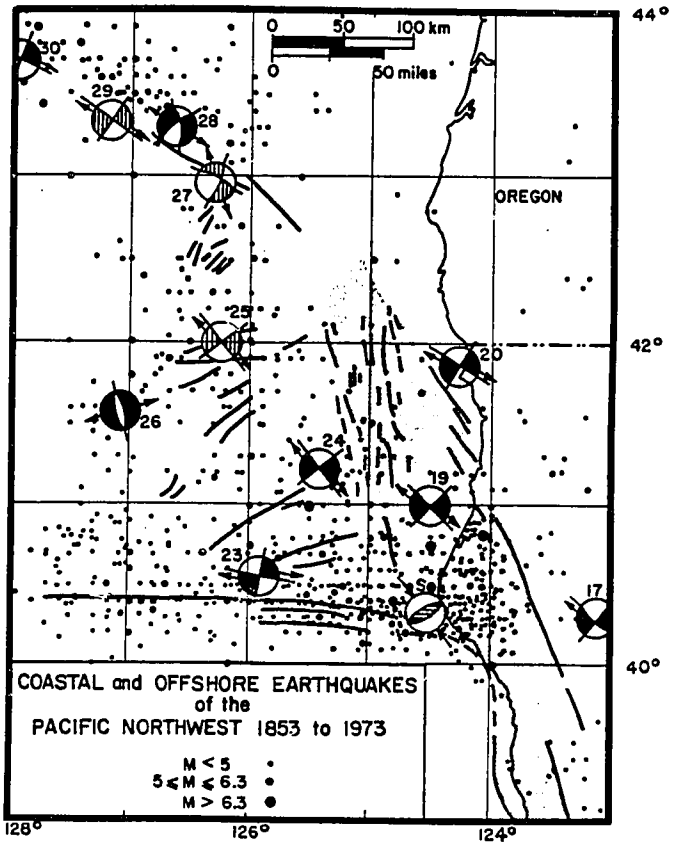

Figure 8. Earthquake epicenters and faults near Cape Mendocino (Herd, 1978). Focal plane solutions are shown indicating right lateral strike-slip within the Gorda Plate which is colinear with the San Andreas Fault.

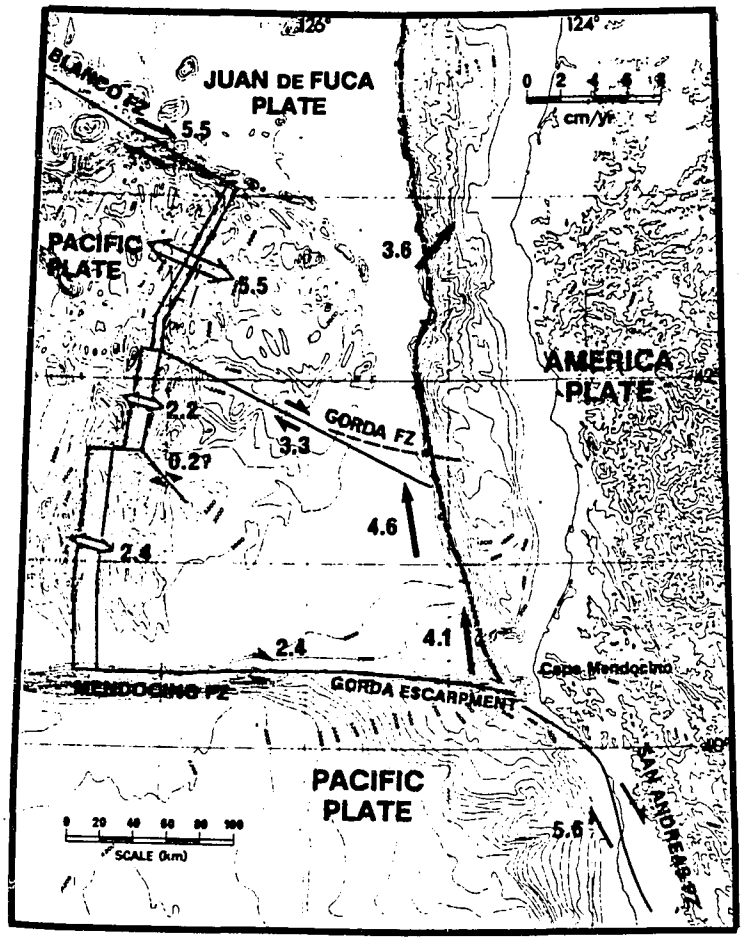

Figure 9. Plate interactions of the Gorda, Juan de Fuca and North America Plates over the last 1 my (Riddihough, 1980) showing the cessation of subduction of the Southern Gorda Plate.

on the Pacific Plate (N85°E) and equivalent anomalies (less than 4 million years old) on the Gorda Plate (N39°E). The absence of significant distortion in the equivalent Pacific plate anomalies to the west make it difficult to explain the pattern to the east of the ridge by the propagating rift model. Similarly, the pivoting subduction model (Menard, 1978) does not pertain -- the fanning of anomalies is in the wrong sense with the apex of the fan centered on the south end of the ridge instead of at the north end of the ridge at the intersection with the trench.

Riddihough (1980) has identified a significant difference between the spreading rate implied by magnetic anomaly spacing and ridge bathymetry north of the Gorda Fracture Zone (about 5.5 cm/yr half rate) versus the spreading rate south of the Gorda Fracture Zone (2.2 to 2.4 cm/yr). Recent work by Wilson (1984) indicates that the South Gorda plate anomalies are best modelled by continuous non-rigid deformation wherein the northeast corner is moving horizontally at close to the motion of the Juan de Fuca plate while the southwest corner is spreading only very slowly if at all. Previously noted anomaly analysis results by Riddihough (1984) indicate that, in the North America/Juan de Fuca reference frame, the South Gorda plate is no longer subducting, and that it has ceased subduction at least 3 m.y.b.p.

Jachens and Griscom (1983) have interpreted residual gravity anomalies in northern California to indicate the southern edge of the subducted Gorda Plate east of the Mendocino triple junction. Their southern edge of the subducted plate shows a change in trend about 120 km inland from the margin. Initially it extends southeast for about 120 km; farther inland, the edge of the plate is oriented more E-W. Plate

theory indicates that this change in strike of the plate edge implies a change in the plate motion 3.6 to 3.9 m.y.b.p. which correlates with a possible change in Gorda plate motion that could have precipitated Gorda deformation.

Fault plane solutions along the trend of the Gorda Fracture Zone indicate right-lateral shear (Figure 8) (assuming NW-striking structure is involved). The geometry of the Mendocino Fracture Zone/San Andreas requires that if the Southern Gorda plate is no longer subducting under North America, the Mendocino Fracture Zone can no longer be a transform fault. If the South Gorda is now part of the Pacific plate, it is possible that the Gorda Fracture Zone may be the locus of some San Andreas transform strain. If so, such strain is being distributed over a wide area because there is no well defined zone of seismicity (Figure 8). Information on land (discussed below), supports this view.

For the present study, the details of Gorda plate motion are not so important, the significant point is the termination of subduction of the Gorda Plate prior to 3 m.y.b.p. This has had a profound effect on the tectonics, broadening Pacific/North American transform strain and further destabilizing the Mendocino Triple Junction long before the Gorda Ridge has actually subducted. The timing of the cessation of Gorda subduction 3-4 m.y.b.p. appears to be paralleled by numerous tectonic and magmatic events in the Pacific Northwest and may mark the initiation of a major reorganization. This fact also has important implications for the southern Cascades since it is the Gorda slab subduction which produces the arc volcanism of Shasta and Lassen. As subduction ceases the influence of the northward moving triple junction and the San

Andreas transform comes to have increasing influence on the volcanic development at the south end of arc.

Figure 10 shows the progress of the Mendocino triple junction along the coast over the last 21 m.y.b.p. This northward progress has been paralleled by cessation of arc volcanism. It appears that the termination of Gorda plate subduction is also a manifestation of the northward migration of the triple junction. However, the magnitude and timing of changes at the arc resulting from changes in subduction are difficult to evaluate with any temporal resolution. There are effects which undoubtedly take place on a number of scales as the plate breaks -- to allow part to subduct and the remainder to fail to subduct -- which vary the plate motions and the magma production geometry; however, these are not understood. Plate motions are probably more quickly effected by the passage of a triple junction than is magma genesis since magma genesis responds after a lag time during which recently subducted crust is still traveling toward the site of melting.

In summary, the evidence from the ocean plates is interpreted as follows:

1) The Gorda plate ceased subduction 3-4 m.y.b.p. This is supported by: magnetic anomaly analysis, implied age of reorientation of the N. Gorda plate propagating rift, change of strike in the southern edge of the subducted Gorda plate, and intraplate seismicity.

2) The Juan de Fuca ridge is reorienting itself to a more NE strike to adjust to the changing tectonic setting. This reorientation began about 7.5 m.y.b.p.

3) Convergence between the Juan de Fuca plate and North America is about 40

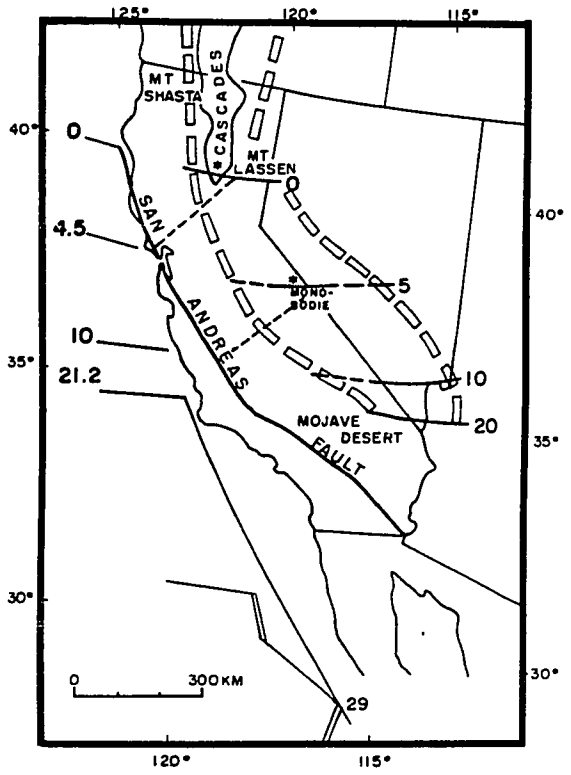

Figure 10. Migration of the Mendocino Triple Junction (age in m.y.) and approximate age of switch off of arc volcanism (Snyder et al, 1976). As the triple junction moves northward, the southern end of the volcanic arc becomes increasingly influenced by dextral deformation as volcanism wanes and eventually ceases.

mm/yr in a northeasterly direction.

4) Magnetic anomaly modelling indicates that the alignments of major edifices in the northern Cascades north of Mt. Hood may be controlled by pseudofault/failed rift structure in the downgoing slab.

5) Benioff zone seismicity beneath the Cascades is diffuse and does not contribute significantly to understanding of the subducting plate geometry.

6) South of Hood there is little evidence for control of magmatism by structure in the subducting plate and there is abundant evidence of the influence of N-S and NNW structure which can be related to tectonic activity in the overriding plate on the landward side of the arc.

Mendicino Triple Junction and The San Andreas Transform

The significance of the San Andreas fault in the plate tectonics of the western US has been widely discussed (Wilson, 1965; Hamilton & Myers, 1966; McKenzie and Morgan, 1969; Atwater, 1970; Dickinson and Snyder, 1976, among many others). Figure 11 shows a broad-scale view of the faulting in Northwestern US and the distribution of probable San Andreas deformation. At the present time, plate tectonics kinematics indicate that right lateral transform motion across the Pacific-North American plate boundary is about 56 mm/yr (Minster and Jordan, 1978). Modern strain measurements by laser ranging suggest that the rate of strike slip may be even larger -- perhaps as high as 80 mm/yr (Savage, 1982). Of this amount, 38 mm/yr is taking place on the San Andreas fault, proper, and the remainder is presumably taking place

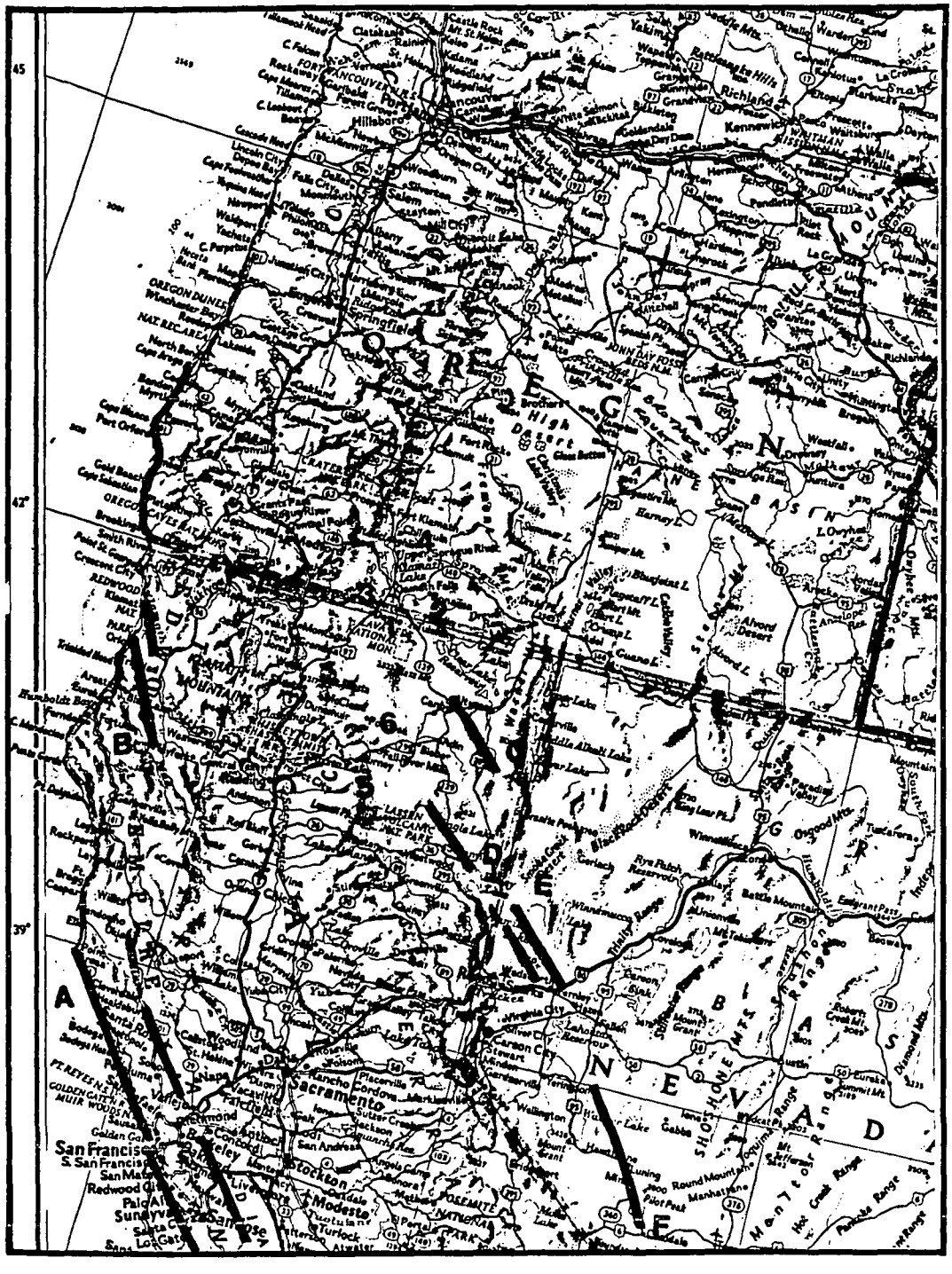

Figure 11. Regional Map of Pacific Northwest (place name reference) showing the right-lateral San Andreas Transform Fault (A) and associated structures: Grogan-Lost Man faults (B); Likely Fault (C); Honey Lake Fault (D); Walker Lane (E to F). Numbers correspond to features demonstrating NNW structural control as discussed in the text (Walker Lane section of Chapter 2).

on a zone of dextral faulting parallel to the San Andreas (Savage, 1982).

In discussing the tectonics of the interaction of the oceanic plates with North America it is important to keep in mind the significance of the Mendocino triple junction and its potential influence on both the regional tectonics of the southern Gorda plate and northern California; and the macro-tectonics of Western North America and the East Pacific. Northward migration of the triple junction converts the margin from a convergent/subduction- dominated system, where an oceanic plate is underthrusting the continental plate, to a strike-slip system with no underthrust plate. This change means that as the triple junction passes a given point, the subducting slab no longer exists in the zone beneath the continental plate. It has been speculated (Dickinson and Snyder, 1979b; Fox et al, 1985) that the 'slab window' generated behind the migrating triple junction would be filled by rising hot aesthenospheric material. In general the ages of volcanics in the Coast Ranges of California appear to correlate with the passage of the triple junction (Dickinson and Snyder, 1979a).

Stability of a triple junction means that three intersecting plate boundaries (the triple junction) remain adjacent after plate motion has taken place. Generally, the motion vectors can only have a restricted relation to one another for stability to exist. In the case of the Mendocino (a transform-transform-trench (FFT) triple junction), for stability to persist, one of the transforms must be parallel (ie colinear) with the trench (McKenzie and Morgan, 1969). Since the San Andreas is not colinear with the Cascadia trench, the triple junction is not stable. There is a tendency of the

transform to jump inland (Ingersol, 1982). This situation is reflected in the morphology of the San Andreas -- a 75-km wide zone in which right lateral motion takes place along several major strike-slip faults. Chronology of deformation in California indicates that this zone is moving generally into the North American plate (Ingersoll, 1982; Herd, 1978) bypassing the Mendocino F.Z. Recent work by Kelsey and Cashman (1983) has identified recent dextral strike-slip faulting of the Grogan-Lost Man faults as far north as the mouth of the Klamath River that they interpret to reflect the most northerly extent (albeit offsets of less than 5 km) of the San Andreas system. These faults are shown on Figure 11.

Such transform instability creates a component of extension in the zone. The extension is reflected in present-day strain measurements (Savage, 1983). The concept of aesthenospheric rise coupled with extensional deformation associated with this eastward jumping of the San Andreas provide both the magma source and structural setting to further support this explanation for the otherwise tectonically anomalous Coast Range volcanics (which are neither arc volcanics nor rise crest nor back arc volcanics).

From a much broader perspective, the passage of the triple junction has been related to the release of 'compressive' stress across the trench and called upon to explain the onset and subsequent northward migration of Basin and Range spreading (Atwater, 1970). Atwater (1970) calls upon the passage of the triple junction to induce distributed right lateral shear which 'opens' the Basin and Range. Ingersoll (1982) presents a slightly different version of this argument whereby the instability

and successive NE jumps of the transform are called upon to rotate lithospheric blocks and thereby open the B&R. Davis (1980), however, deals a significant blow to these ideas by pointing out that northern Basin and Range spreading began 17-14 m.y.b.p. in areas which are still far north of the Mendocino Triple Junction.

The breadth of the San Andreas transform zone is unknown. Figure 18 shows some of the dextral strike-slip faults in the western US. The already described San Andreas system extends as far north as the mouth of the Klamath River. Horizontal deformation beneath the Great (Sacramento) Valley is unknown. However, further east dextral deformation is found at the Honey Lake and Likely Faults and further southeast into Nevada. This zone is the northern end of the Walker Lane Zone of the Basin and Range and many workers have commented on its similarity and possible relationship to the San Andreas (Stewart (1980), Shawe (1965), Wright (1976), Proffett (1977), Albers (1967), Gianella & Callaghan (1934)).

Sbar (1982), in characterizing seismotectonic domains in Western North America has identified an "East Central California" (ECC) domain which extends from the San Andreas domain to and including the western margin of the Basin and Range -- including the Walker Lane (Figure 12). He notes that the orientation of stresses is the same between the ECC and the San Andreas domains and that there is no sharp distinction between the two domains. He distinguished them based on the level and nature of seismicity -- lower strain rate in the ECC and smaller faults. This transitional relationship across northern California appears to have a significant influence on the southernmost Cascades tectonic regime at Lassen. The

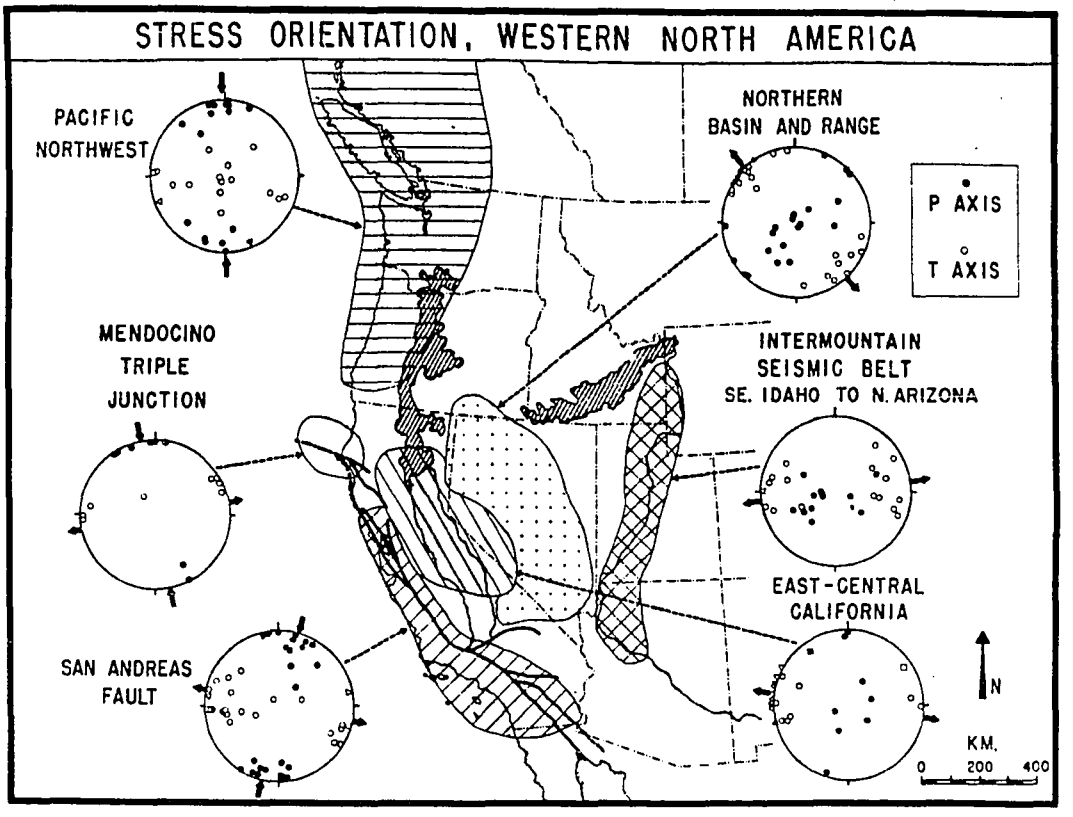

Figure 12. Seismotectonic Domains in Western North America showing stress orientations from focal plane solutions (lower hemisphere projections) and other stress indicators (Sbar, 1982). Note the similarity of stress orientations between the East-Central California domain and the San Andreas domain -- only the magnitude of the maximum horizontal stress is different between these two domains.

characteristics of both the Basin and Range and the Walker Lane will be discussed in the next section.

In summary, the evidence from the Mendocino triple junction and the San Andreas indicates the following.

1) the triple junction is unstable and this tends to broaden the zone across which transform motion is taking place and impose an extensional component to the dominantly strike-slip deformation.
2) Although plate dynamics indicates that transform motion between North America and the Pacific plate is 56 mm/yr, only 38 mm/yr is being taken up on the San Andreas fault with the remainder taking place on distributed subparallel faults, many of which have been identified east of the San Andreas.
3) Tectonic models ascribing the onset of spreading in the Basin and Range to the passage of the now Mendocino triple junction and consequent "relieving of compression" are not tenable in view of the fact that Basin & Range extension started (and continues) in areas that are still North of the triple junction.
4) Occurrence of recent San Andreas deformation to the east (and north) of the main fault system indicates that there is an increasing spacial (if not genetic) coincidence between the San Andreas and the dextral deformation in the western Basin and Range along the Walker Lane.

Basin & Range

The following sections discuss various aspects of the tectonics within the North American plate which influence the Cascades region. Although the Basin & Range is considered to be an extending region analogous to a backarc spreading center, its significance as a tectonic feature is widely debated. In the scheme of global tectonics it is considered to be within the North American plate and is not currently regarded as a plate boundary although perhaps it should be.

For the present study, the examination of the tectonic setting and structural style of the Basin & Range (B&R) is emphasized because B&R deformation is clearly intersecting the Cascades arc. Therefore, an understanding of its characterisitics is essential to the understanding of the interaction between B&R deformation and the Cascades subduction-related volcanoes. Specific considerations include the styles of faulting and the potential for these structures to influence the magma conduit system.

The gradual tectonic transition from the San Andreas to the Walker Lane is an example of the interaction of active tectonic elements that is taking place throughout the western U.S. This interaction also produces significant intraprovince variations in the Basin & Range and the Cascades. Generic B&R deformation in the central portion of the province is multifaceted and different styles pertain, depending on the degree of extension which has taken place. With proximity to the northwestern margin of the province, the extension direction becomes more nearly perpendicular to the Cascades. Similarly, with proximity to the Walker Lane at the west margin of the B&R,

dextral deformation becomes more pronounced. An important point of the present study is that volcanism and deformation in the Cascades within the last 4 m.y.b.p. as well as volcanism and deformation in the Basin and Range indicates increasing interaction and feedback between these provinces.

Clarence Dutton, on viewing the physiographic map of the Basin and Range is reported to have commented that it appeared as "an army of worms crawling northward out of Mexico" (King, 1959). In view of current knowledge of the tectonics of North America, one might add "...and consuming the continent from its core outwards". Dutton was referring to the number, length and subparallelism of the various (over 100) separate ranges (the worms) which are separated by the Quaternary alluvial deposits of the basins (Figure 13). The province is the type example of this remarkable topography of ranges on the order of 10 km wide and up to hundreds of km long separated by basins of similar dimensions. These features are aligned so as to form domains of parallel structures which are separated from those of somewhat different strike by offsets which in some cases demonstrate some form of strike-slip character (Davis, 1980).

The B&R is a region of generally east-west extension which has been tectonically active since about 30 m.y.b.p. and is currently an active tectonic element (Fox et al, 1985). It occurs in a tectonically complex area which has changed geographically, if not genetically, from a back-arc setting when B&R deformation began, to an area which is dominated, in the western part, by distributed dextral strain as well as the extensional strain widely associated with the province.

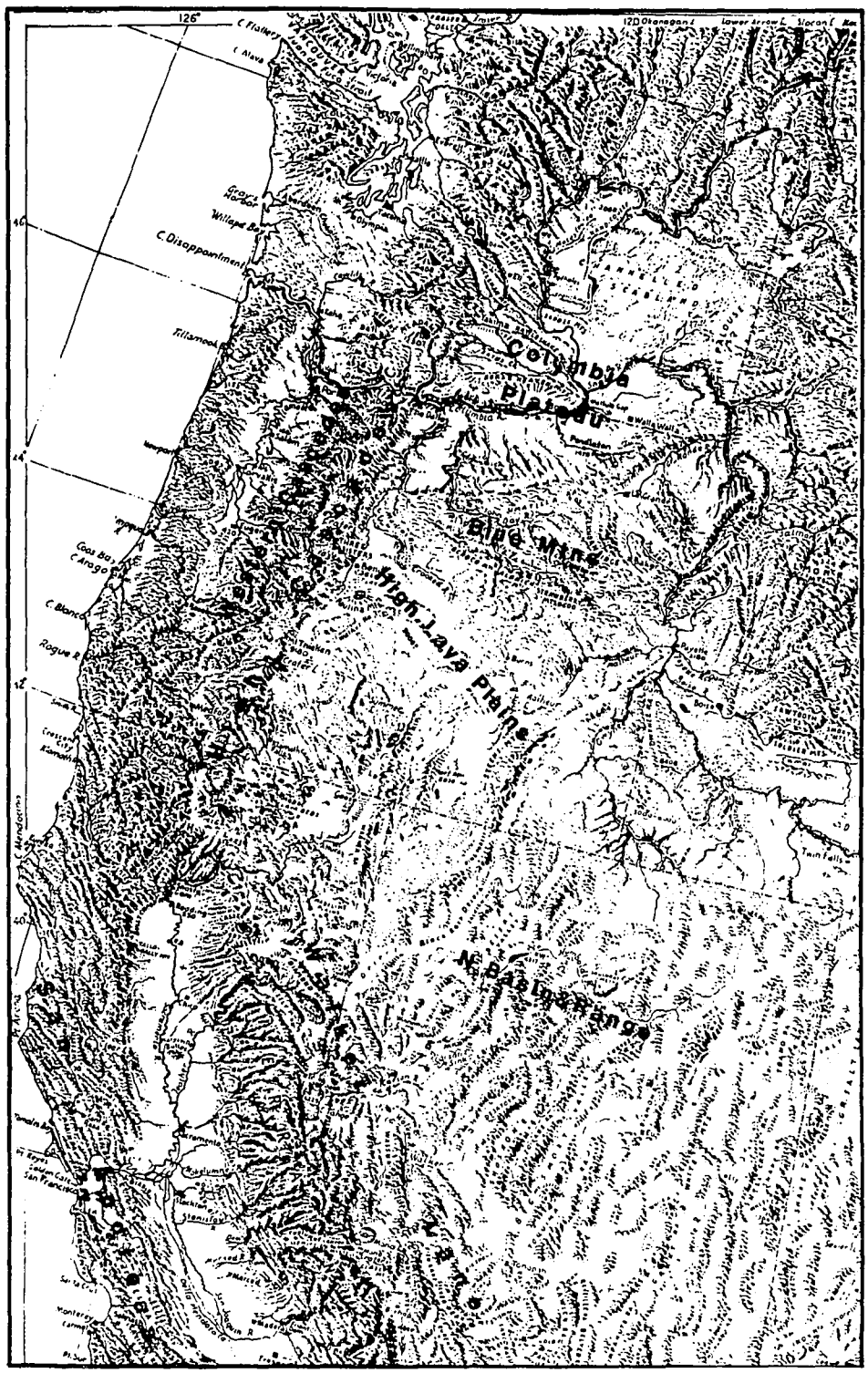

Figure 13. Physiographic Provinces of the Pacific Northwest (modified after Raisz, 1957) showing the subparallel ranges of the Basin and Range in relation to the High Lava Plains and the Cascades.

Geographically, the Basin & Range province encompasses parts of 9 US states and Mexico and it dominates the areas of California and Oregon located immediately east of the Cascades. The physiographic provinces of Western North America are indicated on Figure 13. Tectonically, the province is more active at its margins, particularly the east, west and north margins, than in the interior. This is indicated by higher seismicity along the province boundaries (except the northern boundary) (Christiansen & McKee, 1978) and younger volcanism toward the margins. The eastern margin coincides with the Intermountain Seismic Belt; the western margin coincides with the dextral Walker Lane and the eastern front of the Sierra Nevadas; and the northeast margin roughly coincides with the Snake River Plain volcanic province on the northeast and, on the northwest margin, with the High Lava Plains volcanism and Brothers Fault Zone in central and southeastern Oregon. The Cascades border the northwest boundary.

The Basin & Range province is the subject of much speculation with respect to its detailed deformational style as well as overall tectonic significance. There is general agreement, substantiated by extant strain measurements (Savage, 1983) that it is a region undergoing extension. Spreading rates as high as 2.5 mm/yr across a 40 km base line (equivalent to 36 mm/yr if this rate were province-wide) have been measured on the western edge of the B&R (west of the Walker Lane) by laser ranging (Savage, 1983). Average rates of spreading across the province, based on the seismic moment tensor, are estimated to be 8.4 mm/yr (Eddington et al, 1985). There is debate about the overall percent of extension which has taken place across the

province and good deformational evidence (from fault offsets, intensity of faulting, style of faulting) that the amount of extension varies widely (Proffett, 1977; Stewart, 1978). Essential to the question of deformational style is consideration of the various models of faulting that may be appropriate: steep planar faulting; shallow listric faulting; deep listric faulting; or a combination thereof (these are discussed below).

The direction of B&R extension, if interpreted to be generally perpendicular to the strike of the ranges, has changed during its history from initially NE-SW (which dominates the southern B&R) to NW-SE for more recent ranges in northern Nevada. This change is thought to have taken place prior to about 10 m.y.b.p. (Zoback et al, 1981). Characterizations of the present tectonic stress regimes in the US (Zoback and Zoback, 1980; Sbar, 1982) interpret the regional stress in the northern B&R to be characterized by a NE-SW maximum horizontal stress (Figure 19) and a NW-SE minimum stress (maximum compressive stress is presumably vertical).

The results of the present study indicates that this interpretation may not be appropriate for the extreme northwestern B&R in Oregon and northern California because the orientation of the most recent basins and ranges -- those west of the more or less continuous horst defined by the Warner Ranges and Abert Rim (called herein the Abert Rim-Warner Ranges Line (ARWRL)) -- are typically oriented NNW suggesting a maximum horizontal stress along this bearing for these features. Stress trajectories discussed in Chapter 3 support this interpretation. Such a configuration implies E-W to ENE-WSW direction of extension which is more consistent with

transition to the N-S maximum horizontal stress interpreted for the Cascades Range (Zoback and Zoback, 1980). Basins along the west side of the Basin and Range further south also form along this NNW strike (eg. Owens Valley).

The correspondence between regional stress and strain is, however, complicated by the presence of a pervasive conjugate fault set striking approximately N35°W and N20°E which may have preceded the present stage of faulting (Donath, 1962, discussed later in this chapter; Lawrence, 1976) and upon which strain due to current deformation is being released. Faults of these two trends are evident on fault maps or on the imagery throughout the northwestern B&R at least as far south as Lassen. Some characteristics that can be observed include:

1) in many cases one or the other trend dominates a swarm of faults while an adjacent area is dominated by the conjugate of that trend (this is supported by fault orientation analysis described in the next chapter);
2) the NNW-trending faults are more northwesterly opposite the southernmost Cascades (sub-parallel to the Walker Lane) while striking NNW opposite Crater Lake and Newberry;
3) in a few cases such as Winter Rim (on the west side of Summer Lake), faulting appears to be a combination of offsets on the two conjugate directions to yield a resultant alignment of N-S.

These observations indicate that regardless of whether or not the faults being mobilized are preexisting or primary B&R deformation, basin development is taking place in response to the contemporary stress regime. These factors are discussed in more detail in Chapter 3.

Regional geophysical characteristics of the Basin and Range are summarized as follows:

1) thin crust -- 20 to 35 km compared to 35 to 50 km in the adjacent Rockies and Colorado Plateau (Christiansen and McKee, 1978);

2) absence of seismicity below 20 km (98% of seismicity occurs above 15 km (Eaton, 1982)) -- strong evidence of a shallow detachment surface;

3) upper mantle velocities less than 7.9 km/s compared to 7.9 to 8.1 in the Rockies and Colorado Plateau (R.B. Smith, 1978);

4) high heat flow -- 2 hfu compared to 1.5 continental average (Blackwell, 1978);

5) regional isostatic compensation is indicated but individual ranges are generally not compensated (Eaton, 1978);

6) both volcanism and seismicity are most active at the margins of the province (Eaton, 1982; Christiansen and McKee, 1978; Stewart, 1978).

Eaton (1982) characterizes the Basin & Range as exemplifying predrift rifting of continental lithosphere. He separates the style of deformation into two stages: (1) an early stage which began about 29-30 m.y.b.p. and is characterized by thin-skinned deformation, low-angle normal faults, spatial association of calc-alkaline volcanic activity, listric faulting with shallow detachment surfaces and an extensional regime associated with caldera collapse (ie plutons); followed by (2) a later stage of block faulting, planar and/or large listric faulting, penetrating the crust, with detachment at

the brittle-ductile transition. It is this latter stage which formed the dominant basin and range topography which we see today. This second stage began about 17 m.y.b.p. although the present style of topography is not thought to have become established until about 10 m.y.b.p. (Stewart, 1978). These stages are reflected in angular unconformities, differences in fault trends and associated magmatism. Deformation in the southern part of the province developed earlier and is now less tectonically active than the northern B&R. Stewart (1978) indicates that in SE Oregon (adjacent to the Cascades) the deformation is still in the stage 1 phase. If the formation of the fault pattern in SE Oregon predated the onset of B&R deformation, it may be related to interaction with the Blue Mountains allochthanous block -- a microplate emplaced (accreted) in the Tertiary (Robyn and Hoover, 1982).

Numerous investigators have attempted to evaluate the total amount of strain that has taken place across the B&R. The resultant extension estimates are dependent upon the particular region or transect being evaluated; and on the model of normal faulting which is assumed. Wernicke et al (1982) has summarized much of the evidence for extension across the B&R. The values which have been derived range from 30% to 100%. Types of approaches include the following.

1) Extension estimates based on assumed crustal attenuation from a crustal thickness of 40 to 50 km (typical of Sierran or Colorado Plateau areas) to the present B&R crustal thickness of 20 to 35 km : this approach yields 20%-30% extension (Anderson, 1971; Hamilton, 1978).

2) Extension estimates based on palinspastic restoration of the Mesozoic Sierra

and Idaho bathoiiths which appear to be offset by the northern B&R: this approach yields 50%-100% extension (Hamilton & Myers, 1966).

3) Extension estimates based on the Cenozoic clockwise rotation for the Western Cascades of 27° (+/- 7°), indicated by paleomagnetic data: this approach yields 74% extension for the northern B&R (Magill et al, 1981).

In the southern B&R, larger values are obtained -- eg. 140% for case 3 (tectonic rotation) above (Wernicke et al, 1982). The low intensity of seismic activity and degree of erosional degradation which has taken place in the southern B&R indicate that extension and block faulting is no longer active. Spreading began in the south and has migrated so that active spreading is largely confined to the northern parts of the province and to the areas adjacent to the Sierras west of the Walker Lane.

To better evaluate the mechanisms involved, studies have been carried out to investigate questions pertaining to the detailed style, at depth, of the normal faulting in the B&R -- primarily dealing with the block faulting of stage 2 (above). In one of the most well documented studies, Anderson et al. (1983) examined seismic profiles of a large number of B&R basins to evaluate style of faulting at depth. They identified three general types of faults which have been observed in field mapping and seismic reflection studies. These are:

1) planar, dominantly high angle faults;

2) deeply penetrating listric faults; and

3) listric faulting on shallow detachment surfaces (Figure 14). (Listric faults are curved, concave upward faults which dip steeply near the surface and

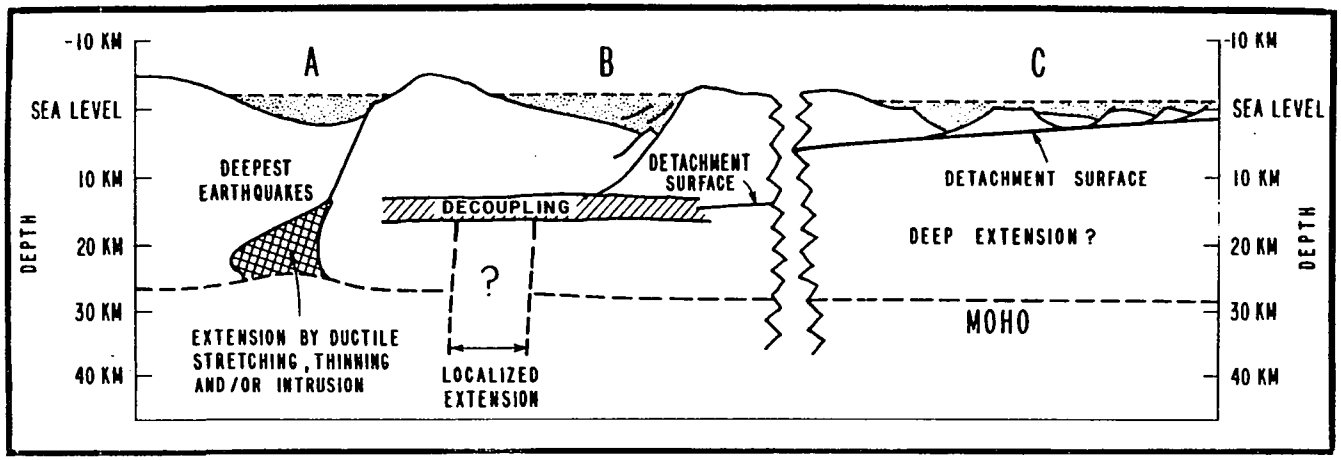

Figure 14. Styles of basin formation in the Basin and Range (Anderson et al, 1983). Mode A: planar dominantly high angle faults; Mode B: deeply penetrating listric faulting soling in a zone of decoupling; Mode C: listric faulting overlying shallow detachment surfaces.

flatten with depth and thereby accommodate greater horizontal extension per unit amount of dip slip (at the surface) than do steep planar faults.)

The conclusions of the study of Anderson et al. were that at least three significantly different styles of basin formation occur:

A) those formed by simple sag adjacent to a major steep planar fault;

B) those formed by tilting related to normal faulting on deeply penetrating listric faults;

C) those which form complex subbasins composed of listric faults and planar faults that sole on shallow detachment surfaces.

They point out that, although their data can only be effectively interpreted to about 5 km depth, significant differences in modes of faulting could be identified. These observations disclose a variety of possible styles and deformation mechanisms. In the past, geologists working in different parts of the B&R have produced conflicting views of THE mechanism of B&R extension. Clearly, either different mechanisms -- or radically different stages of a single mechanism -- are operative in different areas of the province.

Anderson et al. (1983) observe that as basins mature (ie. become older and wider) the structure becomes simpler -- suggesting that extension on widely-spaced, steep, deeply penetrating faults is a late-stage evolution of initially complex shallow closely-spaced listric and rotated planar faults associated with large magnitude, thermally (magmatically?) driven extension. The complexity of early-formed basins suggests intricate patterns of extensional strain domains which, with time, broaden

and simplify (Anderson et al, 1983). In this context it is important to note the "immaturity" of basins in the extreme NW B&R, such as Silver Lake Valley (north of Summer Lake), where basin development is in an early stage. The increasing immaturity of B&R basins with proximity to the Cascades indicates a younger age of onset of deformation in these areas (assuming a steady state extensional process). Anderson et al. (1983) (Figure 14) speculate that the maturing B&R stages could reflect cooling and strengthening of the crust in the mature areas within the last 10 my -- possibly the result of the decreased strain rate. Perhaps the consistent 10-20 km spacing of major normal faults in the mature areas is an optimum dimension of this maturing process. Evolution to this stage may somehow preclude surface-venting magmatism, thus explaining the general absence of ongoing volcanism in the "mature" regions. This may reflect the influence of "depleted" silicic crust which, after yielding early-formed shallow partial melting, is less readily subject to partial melting episodes at shallow levels (Fyfe & Leonardos, 1973).

The concept of mature deformation style agrees with Proffett's (1977) observation that extension was most rapid in the early period of B&R development. In the Yerington area (east of Lake Tahoe), where the magnitude of extension was considerably greater than the province-wide average, deformation was characterized by more complex and subsequently rotated early faulting. Thus the different styles of faulting actually may be rate-limited subdomains within an overall strain continuum (Proffett, 1977).

In the area of the Basin and Range immediately east of the Oregon Cascades, detailed structural studies are not available for most areas. Donath's (1962) study of the northeast corner of Summer Lake is one of the few exceptions. There is significant complexity in this region -- with three prominent directions which may be related to two different tectonic influences. These are: the conjugate set (N35°W an N20°E) noted previously (possibly formed during a period of N-S compression); and to the south, the NW faulting related to Walker Lane shear. This complexity may be a modern analog to the "immature stage" of B&R faulting discussed by Anderson et al (1983) and Proffett (1977).

Anderson et al. (1983) consider that the main variants in the style of faulting are spacing of faults and loci of deep-seated extension. Initial horst and graben and shallow listric faults may give way to deeper listric and eventually planar faulting styles as strain increases and strain rate decreases. In general, planar range-bounding faults are interpreted to directly reflect deep-seated extension (Okaya & Thompson, 1984; Anderson et al, 1983) while shallower listric faulting may be considerably offset from the zone of deep seated extension.

There is evidence that the zone of deep extension may be relatively narrow. Young faulting and large earthquakes occur in the B&R along the 10-30 km-wide N-S Nevada Seismic Zone (NSZ) (Wallace, 1984). The NSZ extends southward from Winnemucca; west of Mt. Tobin; along the east side of the Stillwater Range; and east of Pilot Peak (on the California-Nevada border) where it curves into Owens Valley along the west side of the White Mtns. (see Figures 11, 13 and 15B). The geometry

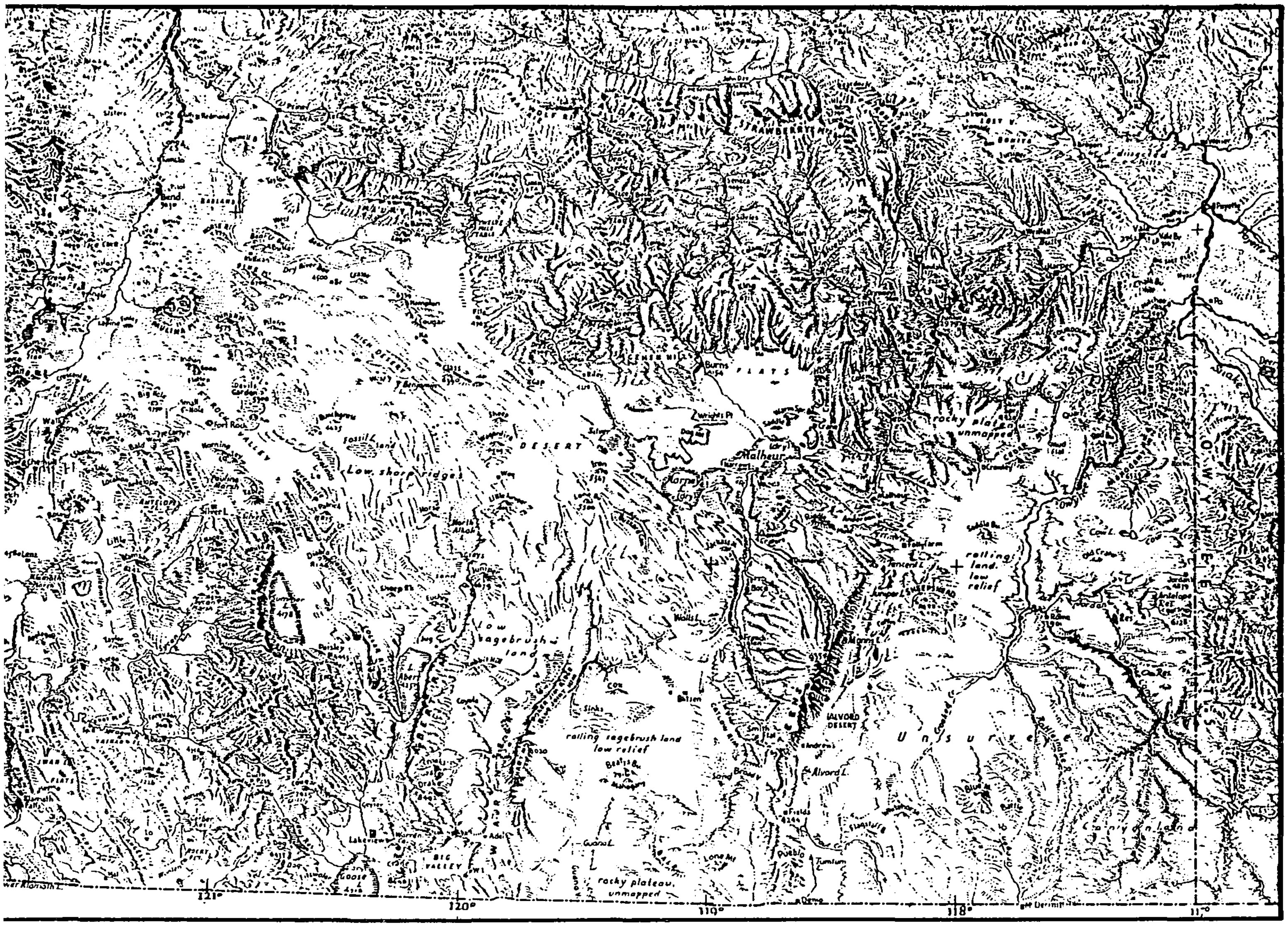
FLATS
Burns
DESERT
Low shore ridges
Malheur L.
rocky plateau unmapped
rolling land low relief
low sagebrush land
rolling sagebrush land low relief
ALVORD DESERT
Alvord L.
Unsurveyed
rocky plateau unmapped
BIG VALLEY
Lakeview
Goose L.
Guano L.
Lone Mt.
Pueblo
Tumtum
Fields
Steens
Cow L.
Owyhee R.
FT. ROCK VALLEY
Fort Rock
Summer L.
L. Abert
Wright Pt.
Harney L.
Sand
Silver L.
121°
120°
119°
118°
117°

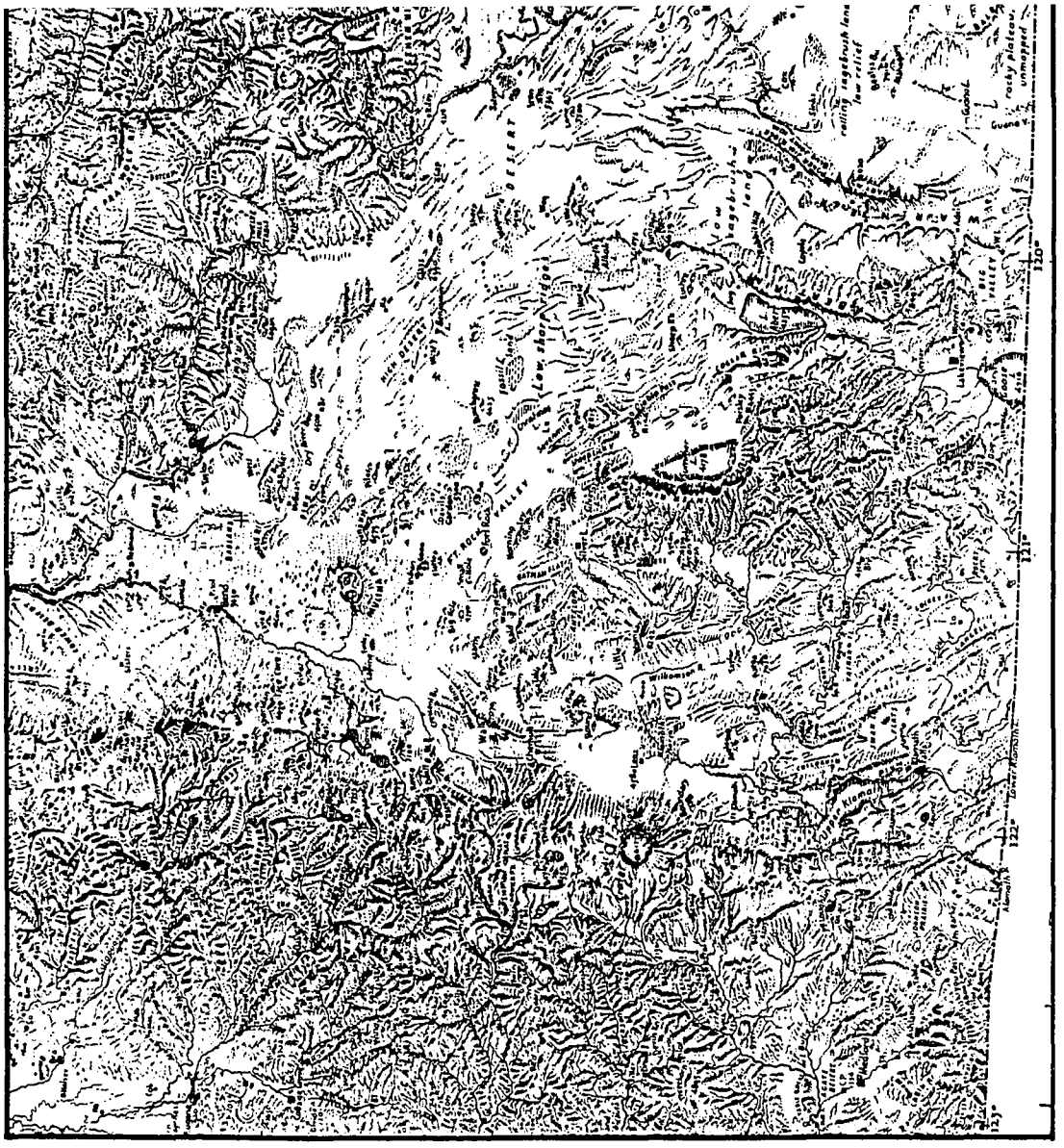

Figure 15. A. Physiographic Map of South Central Oregon (Raisz, 1965).

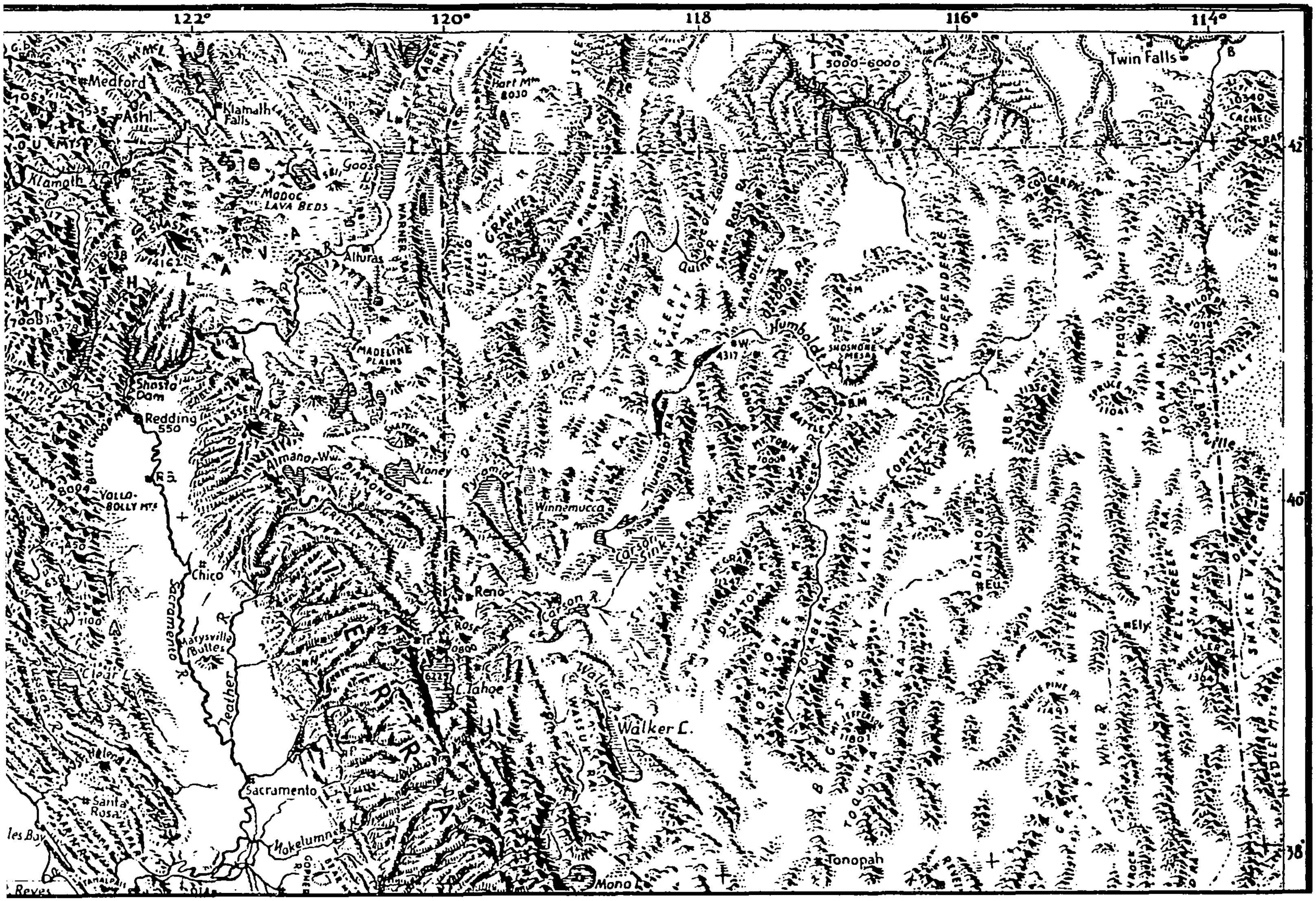

122°
120°
118
116°
114°
42°
40°
38°
Twin Falls
5000-6000
Medford
Klamath Falls
Hart Mtn 8030
Goose
Modoc
LAVA BEDS
Alturas
MADELINE PLAINS
Shasta Dam
Redding 550
Almanor
Honey L.
Pyramid
Winnemucca
Humboldt
Black Rock Desert
DESERT VALLEY
SHOSHONE MESA
MT. TOBIN 10000
RUBY MTS.
TOANA RA.
SALT
DESERT
INDEPENDENCE MTS.
TUSCARORA
Quinn R.
SANTA ROSA RA.
PARADISE
YOLLO-BOLLY MTS.
Chico
Sacramento R.
Marysville Buttes
Feather
Reno
Carson R.
Carson Sink
L. Tahoe
Walker R.
Walker L.
WASSUK RA.
Sacramento
Mokelumne R.
Santa Rosa
Clear L.
Russian R.
Tonopah
Mono L.
Ely
White R.
WHITE PINE MTS.
DIAMOND MTS.
SNAKE RA.
SNAKE VALLEY
SHOSHONE MTS.
TOQUIMA RA.
DESATOIA MTS.
CORTEZ MTS.
Eu

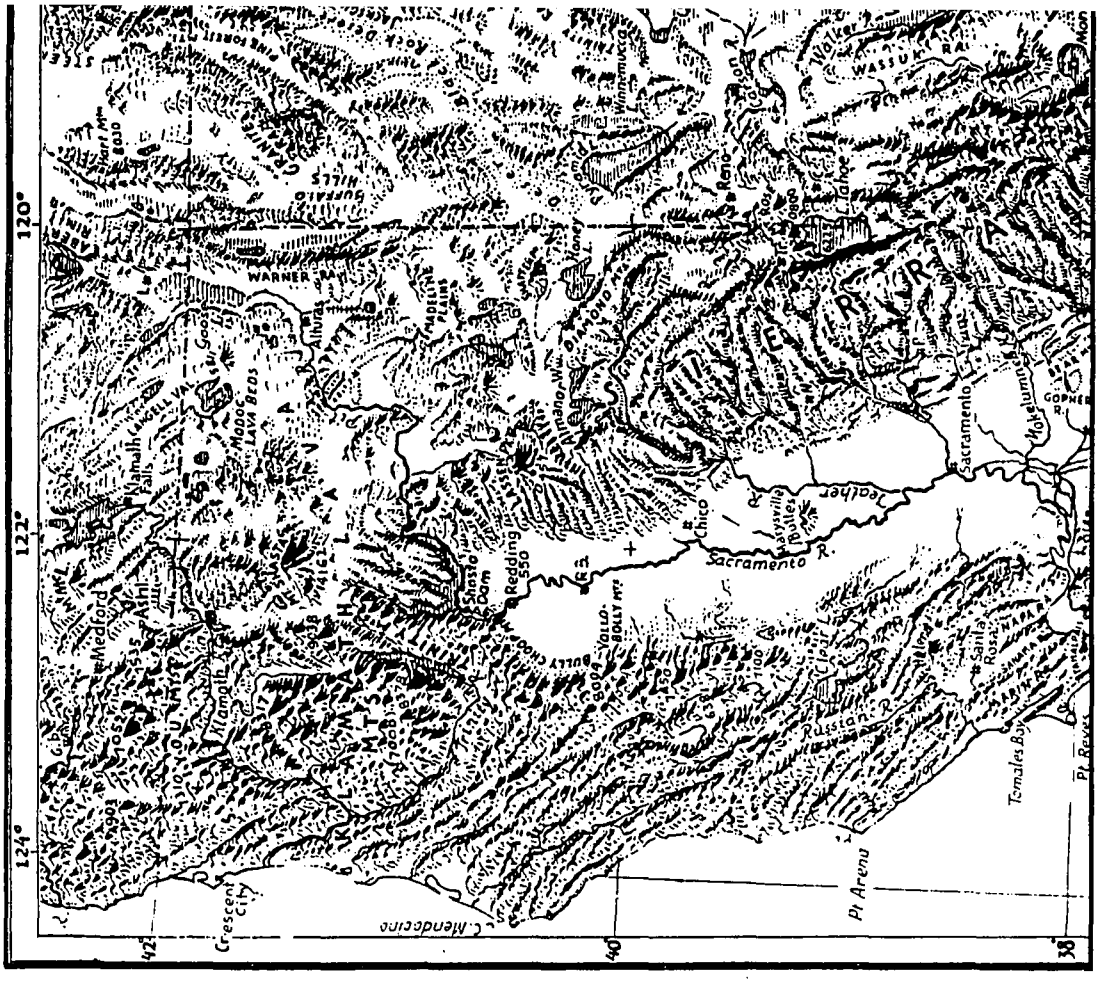

Figure 15. B. Physiographic Map of Northern California and Nevada (Raisz, 1965)

and seismicity of this region within the past 100 years suggests that the high strain rate was confined to a narrow zone. Preexisting faults which cross this zone are active inside the belt but inactive outside of it.

An example of a "typical" Basin & Range faulting event of the "mature" stage within this seismic zone is the Dixie Valley earthquake -- a well studied and often cited case which took place in 1954 on the Dixie Valley portion of the Nevada Seismic Zone east of the Stillwater Range. A magnitude 6.8 earthquake occurred in Fairview Valley to the south (called the Fairview Peak earthquake) followed 4 minutes later by a magnitude 6.8 earthquake in Dixie Valley 50 km to the north. A reevaluation of the teleseismic evidence from this (Dixie Valley) event by Okaya and Thompson (1985) has yielded a source depth of 15 km. This observation coupled with a 2.2 km total vertical displacement on the Stillwater Range fault on the west side of the valley suggest a planar, deeply penetrating fault (the Stillwater) on the west side of the valley and a series of at least three antithetic faults in the eastern half of the valley which terminate on the main fault. Okaya and Thompson interpret seismic reflection profiling to indicate that the antithetic faults are planar. The main fault in turn roots in a detachment or ductile zone at about 15 km.

Microearthquake studies in the Basin and Range indicate that 85% of the seismicity occurs at depths less than 16 km (and 100% < 20 km). Earthquake focal depths also reflect this distribution (Eaton, 1980). The implication is that the lithosphere is perhaps as little as 20 km thick. Okaya and Thompson favor intrusion at depth as a means of filling the excess volume created by continued deformation and

extension on both the main and the antithetic faults. However, no recent volcanism or abnormal heat flow (higher than the already high B&R values) are observed in this area.

This character of B&R basin development, ie. a major steeply-dipping planar fault with either listric or antithetic faults bounding the opposite side of the basin, is a common mode of deformation in the province. The variations on this theme are important constraints on understanding the style of fault development which has produced the basins. The initial phases of this faulting style are not well understood. The relative immaturity of the basin development east of the Cascades and the progressive increase in breadth and depth of basins to the east indicates that the area immediately east of the Cascades is in this initial stage of B&R deformation.

Other styles of deformation characteristic of some B&R areas also occur. One is low-angle normal faulting. Areas of low-angle detachment faulting in the B&R occur on the east side of the province and across central Arizona (Davis, 1980). These tend to occur where the ranges owe their elevation to crustal doming rather than block faulting. Wernicke (1981) holds that low angle (through crust) normal faulting may represent a fundamental structure on which more local listric and planar normal faulting is developed. This mechanism is much like deformation style C (Anderson et al, 1981) shown in Figure 14. Stewart (1980) suggests that originally steep normal faults may be rotated to positions of shallow dip by deformation on subsequent sets of normal faults. Field evidence of low angle normal faulting is most common in the eastern and southern B&R and does not appear to have developed in the

northwestern part of the province (Davis, 1980). Therefore this style is not significant to the present study.

Yet another style of extensional deformation -- discussed briefly above, and most important for this study -- occurs in southern Oregon and has been documented in the Summer Lake area about 100 km east of Crater Lake where Donath (1962) has mapped the structure in this area in great detail. He finds conspicuous evidence for a rhomboid pattern of faults (he considered faults which have a constant-strike length of 0.8 km or more). Evidence indicates that these fault sets -- one striking N35°W, the other N20°E -- were contemporaneous in origin and both cut late-Tertiary basalts. The northwest-striking fault set generally dominates the northeast-striking one. Further west and southwest, the NE-striking faults become considerably less abundant while the NW-striking faults become more prominent (these fault trends are discussed in more detail in Chapter 3). The latest movement on these faults (both sets) is dip slip with minor tilting to accommodate extensional strain (Donath, 1962). This is an area where horst and graben structure is particularly well developed (Stewart, 1978), and the Winter Rim (which bounds Summer Lake on the west) marks the western limit of major block faulting in the northern B&R. As mentioned earlier, Stewart suggests that structure in this part of Oregon may represent an initial stage in the development of B&R structure, before widespread tilting occurs. This point is central to the tectonic model for this area which is discussed in Chapter 3.

The orientation of the ranges in south-central Oregon -- from Abert Rim south to the Warner Ranges in northeastern California is generally N-S but varies from NNW to

NNE. This contrasts with the ranges further east whose average strike is more nearly NE (although also with some variation). West of the Warner Range-Abert Rim line (Plate 1) all basins are oriented along a NNW trend -- including Silver Lake, Summer Lake, Chewaucan Marsh, and Fort Rock Valley). South of the Warner Ranges, within the Walker Lane, the dominant faulting strikes northwesterly.

The significance of the azimuth orientation of ranges, and their adjacent basins, to one another and to the overall deformation scheme is not revealed by strike information alone. The basin-bounding scarps are actually curved in map view with the major basin-bounding fault generally occurring on the convex side of the basin (eg. west side of Summer Lake basin). Moore (1960) first noted the fact that the scarps in the B&R are curved and that the faulted blocks generally tilt toward the convex side of the basin. In the northwestern B&R this relationship is true for Winter Rim/Summer Lake; Warner Ranges/Goose Lake. and Steens Mtn./Alvord Desert (Figure 15A). The bounding fault occurs on the concave basin boundary (east side) at Klamath Lake and in both configurations on the west side of the Warner Range - Abert Rim horst (convex (east side) opposite Abert Lake and south of Goose Lake and concave at Goose Lake). In addition, there is a tendency for the curved-in-plan basins to reverse geometry, that is, if the main bounding fault (on the convex side) is on the west side of the basin (eg. Summer Lake), in the next basin along strike, the main bounding fault will be on the east side with opposite curvature (eg. Coglan Rim vs Winter Rim). Bosworth (1985) and Bosworth et al. (1986) have observed this type of relationship in many of the world's rift valleys; their kinematic model to explain this

is described on Figure 16 and involves along-strike propagation of rifting.

It is not known whether the basins in the Basin and Range form by along-rift propagation but relationships discussed in Chapter 3 suggest that this is a reasonable mechanism. Basins tend to be broader and deeper to the south and east, and to terminate to the north. Summer Lake is at the northwest end of a line of connected basins, while its north end terminates abruptly, although normal faulting continues farther NNW, suggesting that the basin has propagated from south to north. This is also true for Alvord basin, adjacent to Steens Mtn, which gradually narrows and becomes less defined to the north. Similarly, the Klamath Graben appears to have propagated toward the Cascade axis where it narrows and terminates at Crater Lake. The suggestion of sub-parallel structure between the Goose Lake-to-Summer Lake structure and the Klamath Graben (Klamath Falls to Crater Lake) configuration can be seen on the Physiographic Maps (Figure 15A and 15B).

The question of how the basins and ranges actually formed in the first place is an important one which has major implications for Cascades interaction. Unfortunately this question is little understood. Does each basin form when a chunk of continental lithosphere, in effect, calves off the thick lithosphere to the west to form a more-or-less intact range (Model A)? Or do fingers of rift worm their way northward (along the strike of the ranges) in an initially broadly-spaced sinuous pattern which later gets filled in (emptied out?) by later rift fingers (Model B)? Or does the entire region become stressed, necked and finally at once broken into tens or hundreds of boudins (Model C)?

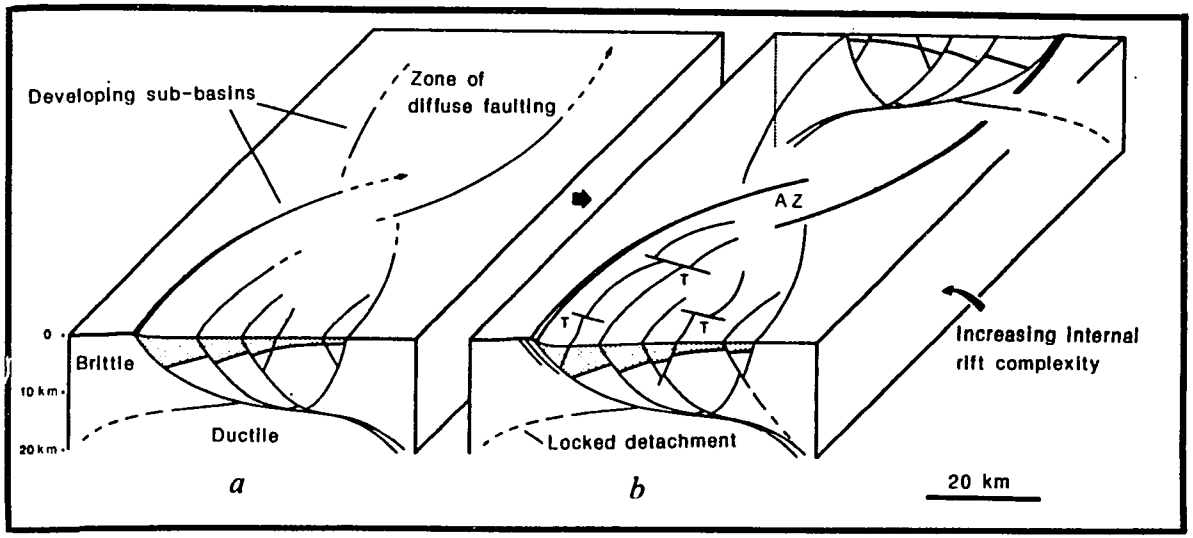

Figure 16. Model of asymmetric rift development and propagation (Bosworth, 1985). Upper crustal extension may initiate as a broad zone of diffuse faulting (a), but quickly evolves to a system of a few main listric (sometimes planar) faults above two oppositely-directed detachments. Judging from the observed asymmetry of most continental rifts, one of these detachments eventually locks. The active detachment propagates along the rift axis (toward the pole of opening) but curves inward to form a large-scale scoop-like structure. Eventually the curving faults depart enough from the overall rift trend to favor a new detachment which links to the old at a complex area referred to as an accommodation zone. If the new detachment takes place on the structure of opposing polarity, a reversal of rift symmetry occurs (b) with the main bounding fault becoming localized on the opposite side of the rift. Detachment systems may overlap or merge at accommodation zones in a variety of configurations.

Evidence pertaining to these models is as follows:

1) the concentration of seismicity and recent volcanism at the margin of the province and the absence of volcanism in the central B&R suggests that processes invoking a progressive outward migrating mechanism are more likely -- favoring models A and B, above;

2) the fact that a feature such as Summer Lake terminates abruptly to the north -- although associated faulting and minor basins extend further NNW -- suggests that a mechanism involving frontal "calving" of an entire range (model A) may not be appropriate;

3) the sinuous configuration of most ranges and the alternating of east-dipping and west-dipping major range-bounding faults, along strike, further argues against "calving" model A;

4) the early stage of B&R deformation, involving distributed complex faulting postulated by previous workers (eg. Eaton, 1982 -- described earlier) best fits models B and C which invoke gradual distributed evolution of structures;

5) the fact that the overall B&R deformation has migrated from south to north suggests that northward propagation of rifts is a viable mechanism. This supports model B and argues against A and C.

Based on these arguments, the concept of basins forming by rifts propagating along strike is the most favorable model. This will be discussed further with respect to the High Lava Plains.

Lawrence (1976) has postulated various NW-striking zones of dextral shear deformation which cross the northwestern B&R and also extend across the Cascades. The most prominent of these is the Brothers Fault Zone (BFZ) which parallels the High Lava Plains. The interpretation of this BFZ as a strike-slip zone has arisen from the perception that the faulting is en echelon and from analogy with the Garlock Fault in the Southern B&R, against which basins terminate (Davis and Burchfiel, 1973). At the Garlock fault, however, strike slip deformation is clearly indicated. A through-going fault with clear evidence of substantial strike-slip supported by significant seismicity provides a clear case for major deep-seated strike-slip termination of basins. On the other hand, the BFZ shows none of these indications. No demonstrable strike slip faulting (all faults in the zone are normal faults); no major through-going structure; and the absence of seismicity leave the BFZ as a poor analog of the Garlock Fault. evident. These and other factors relating to the BFZ are discussed in greater detail in the High Lava Plains section of this chapter and in Chapter 3.

Two other zones, farther south within the B&R, are delineated by Lawrence based on analysis of small scale (1:1 million) black and white ERTS (Landsat) band 5 and band 7 imagery. Lawrence calls these the Eugene-Denio and the Mt. McLoughlin zones. He identifies these zones by higher density of fracturing and he postulates that the fracturing is due to en echelon faulting associated with fundamental dextral strike slip at depth which acts to take up the difference between east-west extended terrain to the south and less extended terrain to the north. He further postulates that the Eugene-Denio zone accounts for the offset in the High Cascades axis at Diamond Peak.

However, analysis of the remote sensing data for the present study indicates that the northwestern B&R is cut by distributed NNW-trending structure -- all of which is capable of releasing shear strain generated by differential extension. When account is taken for the areas obscured by basin-filling sediments, there does not appear to be sufficient evidence of concentrated zones of shear. In addition, workers in the Cascades do not find evidence of shear fracture in the Diamond Peak area (Priest et al, 1983; Barnes, 1978). Finally, stress trajectory data in the Cascades (generated for the present study and discussed in Chapter 3) shows no indication of a stress regime compatible with the proposed dextral strike slip. These questions are discussed further in the High Lava Plains section of this chapter and in Chapter 3.

In summary,

1) Basin and Range deformation comes in various styles but generally with a major fault bounding one side of a basin (range) and step faults or sagging accommodating the other side;
2) faults may be planar or curved with the latter including shallow listric or deeply penetrating listric faulting;
3) a detachment surface is indicated by the fact that 98% of the seismicity occurs above 15 km and 100% above 20 km and this detachment may mark the base of the lithosphere in the B&R;
4) young volcanism is virtually absent in the central B&R and it becomes more prevalent toward the province margins;

5) seismicity is also concentrated at the margins;

6) although many workers consider the regional stress regime for the northern Basin and Range to be NE-SW maximum horizontal stress (based on the orientation of ranges in the northern B&R of Nevada), at the northwestern corner of the province, in Oregon, ranges strike NNW-SSE, indicating a regional maximum stress of NNW-SSE;

7) along strike, basin-bounding ranges are found to have a sinuous pattern and major basin-bounding faults generally occur on the convex (outward curving) sides of the basins; and basins in the northwestern B&R terminate abruptly to the north while associated normal faulting and minor basins continue along strike; both of these characteristics are also found in more localized propagating continental rifts (eg. White Nile rift and Gregory Rift in East Africa) -- suggesting both by analog and observation that the basins form by along-strike propagation;

8) discrete WNW-trending to NW-trending dextral shear zones postulated in the northwestern B&R (eg. Eugene-Denio Zone) are not supported by the fault pattern; such faulting is actually pervasive and relatively uniform in distribution and the identification of these zones as discrete entities does not appear warranted (see Chapter 3 for a detailed discussion).

Walker Lane

The Walker Lane (WL) is a major zone of disruption in the orientation of ranges in the western B&R. It extends southward from the Likely Fault in NE California (just east of Medicine Lake) and parallel to the east margin of the Sierras (Figure 11). It crosses into Nevada about 85 km north of L. Tahoe and extends along the Nevada-California border into the southern part of Nevada.

The WL is obvious on physiographic maps because of the radical change in range orientation from the N to NE trending ranges of the Great Basin to the variable, but generally NW-trend of ranges within the Lane. The WL dominates the western margin of the Northern B&R. However, to the south of Lake Tahoe, the WL is not on the western edge of the B&R. There is a band of "normal" Basin and Range structure west of the Walker Lane within which the ranges strike consistently NNW. This wedge of B&R west of the Walker Lane is apparently actively propagating northwest and westward (Slemmons et al. (1979)) as implied by the recent (2 m.y.b.p.) development of Owens Valley. Active extension west of the WL contrasts with the relatively low level of extension interpreted east of the WL in the southern B&R.

The dimensions of the WL are not completely agreed upon. The width has been interpreted to be 80 km (Albers, 1967) to 200 km (Rowan & Wetlaufer, 1981); and the length has been interpreted to be 480 km (Albers, 1967) to 600 km (Bell & Slemmons, 1979). Near the northwest end of the Nevada portion of the WL, in the Pyramid Lake region, Slemmons et al. (1979) identify at least 5 strands of major strike-slip faulting within the WL zone and estimate 48 km of dextral strike-slip

motion within the last 22 m.y.b.p. there. They base this estimate on fault offsets from historic faults, from offsets of Late Cenozoic rocks, orientation of chevron and en echelon structure, geodetic deformation and focal mechanisms. Working further south -- in the vicinity of Death Valley, Calif. and Las Vegas Valley, Nev., Stewart et al (1968) find evidence for as much as 130-190 km of dextral deformation. Their estimate includes both fault slip and broad scale drag indicated by disruption of facies, offset of thrust faults and offset of thickness trends in rocks ranging from Precambrian to Mesozoic, although the magnitude of these estimates are not universally accepted (eg. Wright, 1976). Stewart et al. (1968) suggest that the magnitude of slip diminishes to the northwest and perhaps indicates that the northwest termination of the WL zone is younger than the southeastern portion.

The timing of WL faulting is not well established. Albers (1967) interprets the abundant evidence of offset in pre-Cretaceous rocks to imply that deformation began in early Jurassic and that much of the offset is pre-Cretaceous. Others (Anderson et al, 1972; Fleck, 1970) interpret a late Cenozoic age for the faulting since Miocene rocks have experienced rotation of similar magnitude to that of Precambrian rocks. Hardyman et al. (1975) and Ekren (1979) note that mid-Tertiary tuffs in the Walker Lake area appear to be offset at least 32 km on NW faults. This represents a minimum offset since late Tertiary.

The seismicity of this zone -- and comparisons with seismicity elsewhere in the province -- indicates ongoing deformation consistent with the fault offsets. Although seismicity is still present in the central part of the Great Basin (Figure 17), the B&R is

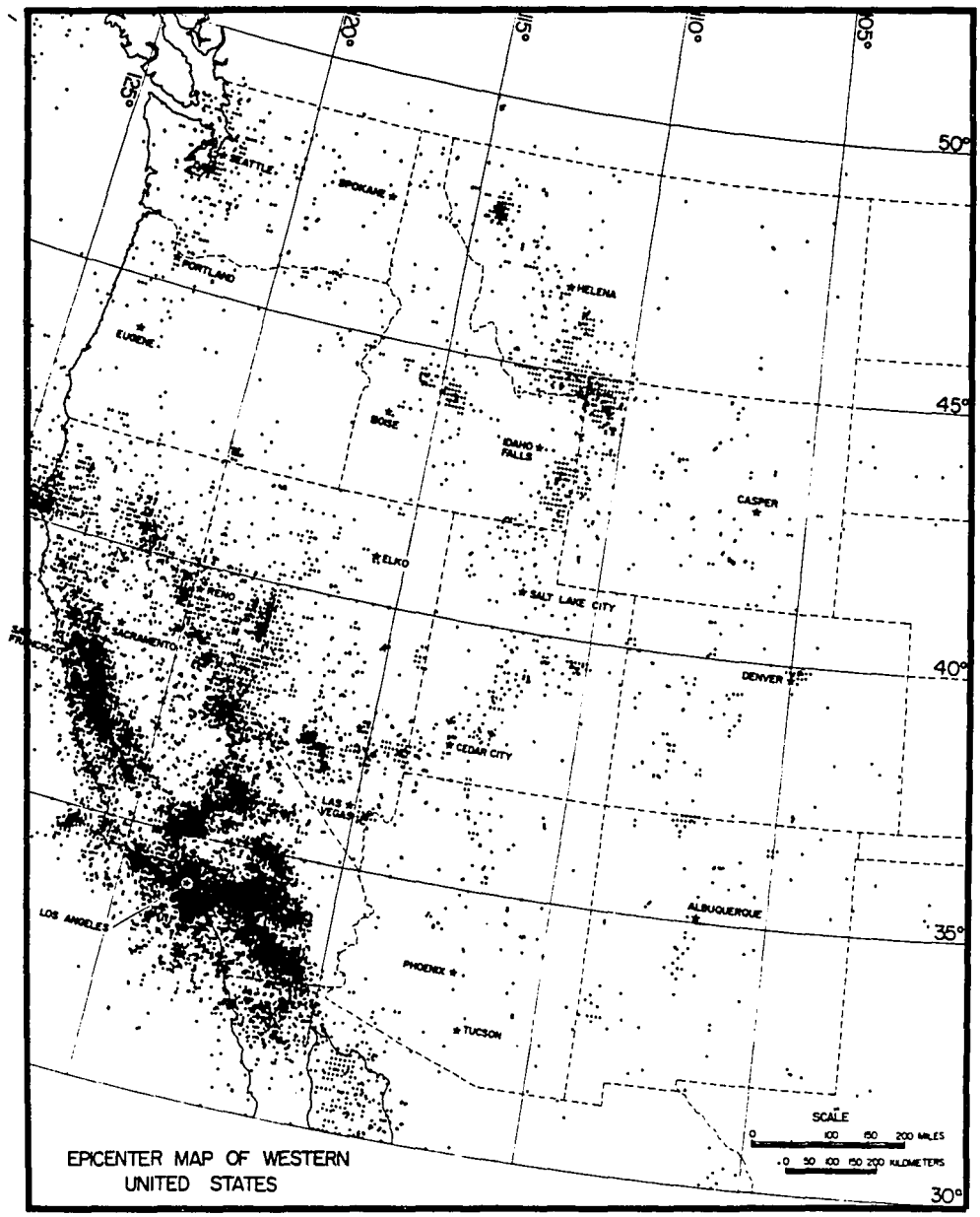

Figure 17. Epicenter map of Western US showing located earthquakes principally from 1950 through 1976. Minimum magnitude plotted for California M=1; elsewhere minimum plotted M=3 (Smith, 1978). Note the lack of seismicity in central and southern Oregon -- the cluster of epicenters NE of the California-Nevada border is located within Warner Lakes basin.

far more active on the margins -- particularly along the WL (Eaton, 1982; Stewart, 1980; Christiansen & McKee, 1978; etc.). Focal plane solutions (Figure 18) indicate varied but dominantly strike-slip solutions along the WL with normal fault solutions elsewhere in the B&R.

Ground break on modern faults also support this interpretation. Ground break on the Fairview Peak earthquake (which accompanied the aforementioned Dixie Valley earthquake in 1954) indicates that the dominant offset was dip-slip at the northern end of the fault system while at the southern end adjacent to the WL offset was dominantly right lateral (Shawe, 1965). This indicates that although the Dixie Valley-Fairview Peak events are rooted in the extensional NNE-trending Nevada Seismic Zone, the deformation at the south end is strongly influenced by the WL.

At its NW end the Walker Lane is marked by a topographic depression which terminates at Honey Lake where the zone breaks up into a series of NW-trending faults (Bonham and Slemmons, 1968). Pease (1969) identifies a number of discrete dextral strike-slip structures in this area, however some of these are not well data-supported. Some of the the better supported of these faults are shown on Figure 11. The Likely and Honey Lake faults are also accompanied by dip slip movement. Faulting between Lake Almanor and Lassen is dominantly dip slip with no strike-slip documented although it was interpreted as a strike-slip feature by Pease (1969).

These faults coexist with an abundance of NNW striking features which occur in Northern California east of Lassen and Shasta and in south central Oregon as far north as the Brothers Fault Zone (Figures 13, 15 and Plate 1). These features

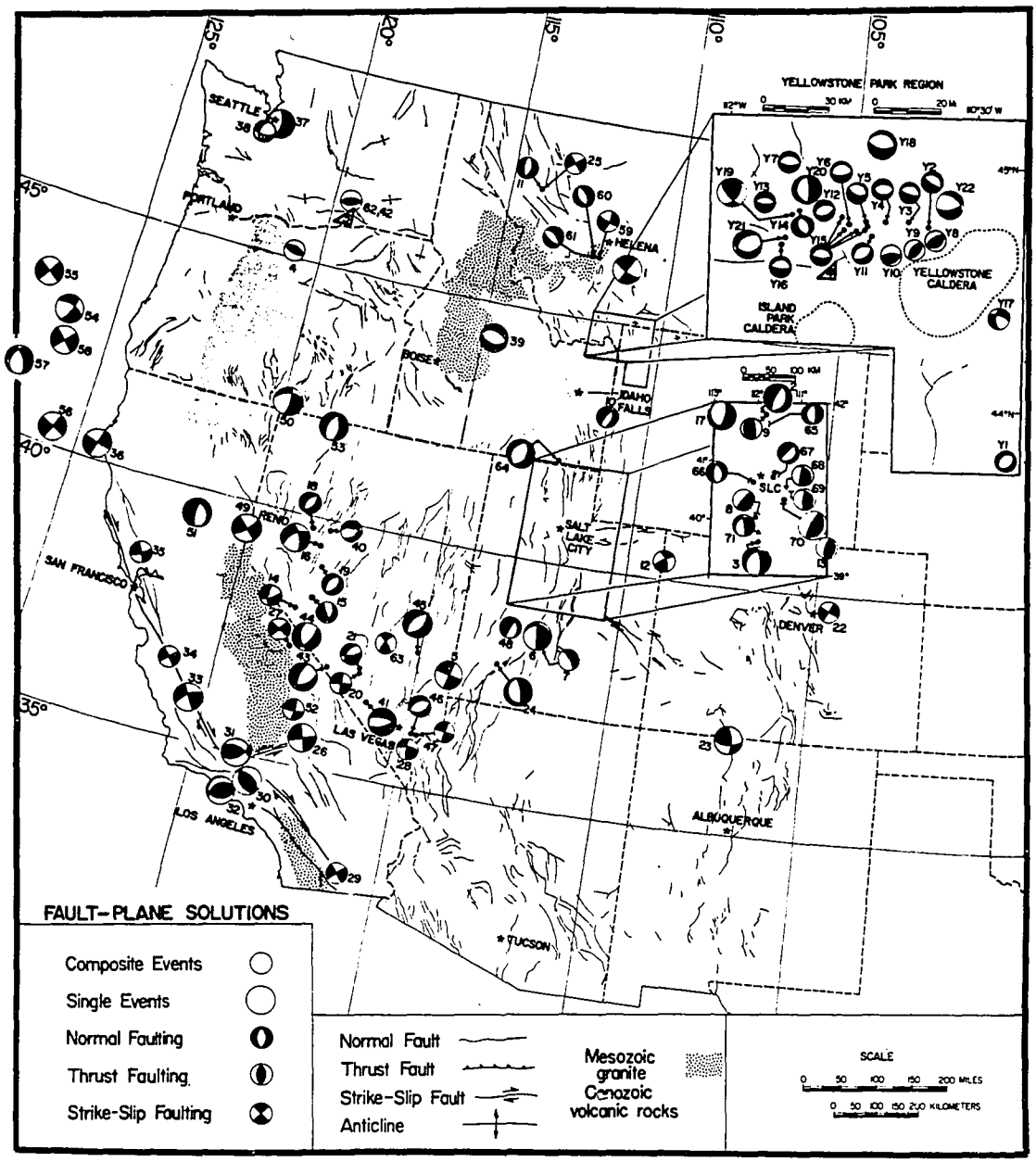

Figure 18. Seismic Focal Plane Solutions of the Western US (dark quadrants = compressional first arrivals) (Smith and Lindh, 1978). There are no focal plane solutions in this compilation for the area of central Oregon.

correspond to the N35°W conjugate of Donath (1962). NNW structural control is demonstrated by such features as Mt. Dome and Mahogany Mtn. in California (25 km NNW of Medicine Lake) (1) (numbers refer to locations shown on Figure 11); and, in Oregon, Bryant Mtn. and Stukel Mtn. (SSE of Klamath Falls) (2); Hamaker Mtn. and Surveyor Mtn (SW of Klamath Falls) (3); and Swan Lake Rim and Hogback Mtn (NE of Klamath Falls) (4). Structures on the west side of Yamsay Mtn., Oregon (east of Crater Lake) and northward from Modoc Point (east side of Klamath Lake) turn to a N-S trend; however, Yamsay Mtn. and areas to the north, east and south, show the NNW structure (eg. the scarp cutting Antelope Mtn north of Yamsay Mtn.). There is also evidence of B&R N-S extensional deformation taking place west of and within the Walker Lane at features such as the Hat Creek Graben (5), north of Lassen, and the Timber Crater Graben (6) north of the Hat Creek. Extensional structures further north -- most notably Klamath Graben (Klamath Lake) and the subsidiary Swan Lake Valley show strong NNW structural control. This NNW structure is thought to be related to B&R extension and it is prevalent throughout the NW B&R.

Summarizing, the Walker Lane is a NW striking dextral boundary on the western margin of the B&R. The end of the WL extends into northern California. Estimates of total displacement on this feature range from 48 to 190 km. Width estimates in Nevada range from 80-200 km and length range from 480 to 600 km. At its northern end it breaks up into a number of NW-trending dextral faults. These areas are also characterized by numerous landform strands controlled by NNW structure.

High Lava Plains

The High Lava Plains (HLP) (Figure 13) is a physiographic province which marks the northward limit of dominant Basin & Range deformation in Oregon. It extends from Newberry Caldera, on the west, to Steens Mountain. Ranges of the B&R extend into and terminate in the southern part of the province east of the Abert Rim-Warner Range Line (ARWRL) (eg. Winter Rim, Abert Rim, Hart Mtn.-Poker Jim Ridge). These ranges strike dominantly NNE, (parallel to the northeast conjugate of the system identified at Summer Lake by Donath (1962)). West of ARWRL the basins trend N to NNW and in the southern HLP, the range-bounding faults appear to curve into the NW-trending swarm of small normal faults which characterize the HLP. The zone of NW faulting within the HLP is called the Brothers Fault Zone (Walker, 1969). The normal fault scarps which make up this zone are generally of small displacement -- a few tens up to a hundred meters. Dip direction varies as shown on the HLP fault map (Figure 19). Thus, in the eastern part of the HLP (east of ARWRL), the B&R ranges strike NNE and terminate against the Brothers Fault Zone (BFZ). West of ARWRL the basins are oriented parallel to the NNW faulting that curves into the BFZ to the north. The difference in trends on either side of ARWRL implies different stress regimes. (This is discussed in Chapter 3.)

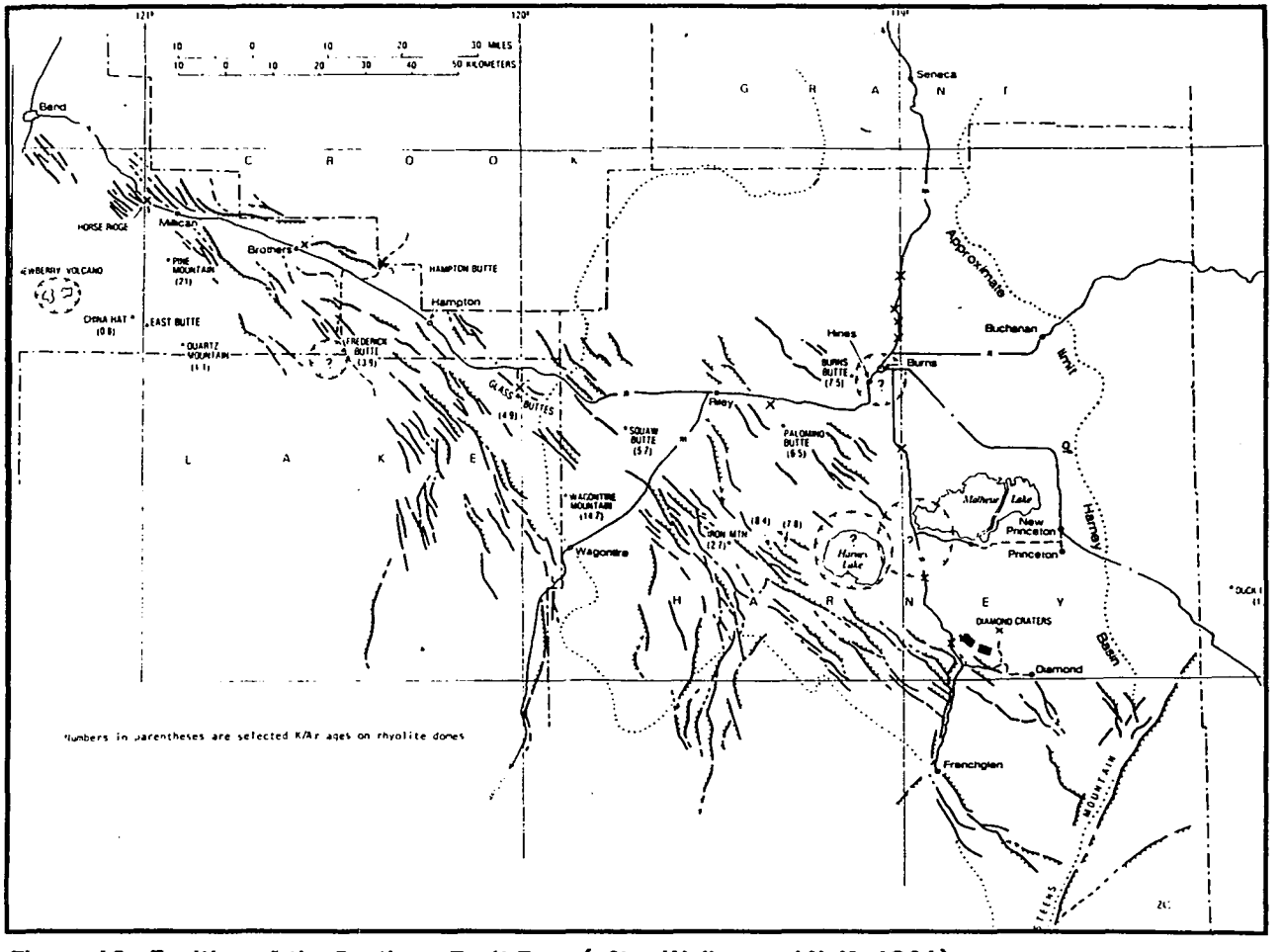

Figure 19. Faulting of the Brothers Fault Zone (after Walker and Nolf, 1981). Note the parallelism of the faults within the main zone of faulting from Frenchglen to Horse Ridge and that the constituent faults are parallel to the overall zone. Stress trajectories at Diamond Craters are shown in broad lines. This fault zone is discussed in detail in Chapter 3.

The High Lava Plains province is dominated by late Cenozoic volcanics -- both basalt flows and rhyolitic domes and ash flows (Figure 20). Basalt is somewhat more voluminous than the rhyolitic rocks. These rocks tend to be youngest along the Brothers Fault Zone and somewhat older to the south of the fault zone (Luedke and Smith, 1982). Basalts less than 5 m.y.b.p. have been identified all along this trend from east of Steens Mtn. to Newberry. Within the rhyolite domes, MacLeod et al. (1975) have identified an age progression across the HLP and northern B&R in rhyolitic domes less than 11 m.y.b.p. This progression has been characterized as a linear younging trend along the Brothers Fault Zone (BFZ) and a more diffuse belt which MacLeod et al. identify across southern Oregon. They have contoured the ages across these two loci, suggesting a general NW younging trend (Figure 20).

These data contain important information about the age progression of deformation across the HLP, however its interpretation is not straightforward. Christiansen and McKee (1978) interpret this data to imply that volcanism propagated across the HLP from SE to NW in concert with this younging of rhyolites. They draw the analogy with the rifting of the Eastern Snake River Plain (ESRP) where it is indicated that rising basaltic magma first initiates crustal melting -- producing silicic volcanics which then become dominated by basaltic volcanism as extension continues and as the lower crust becomes depleted in potential melt components. The result is a younging of the silicic volcanics, in the direction of propagation of rifting, overprinted by contemporaneous basaltic volcanism all along the rift.

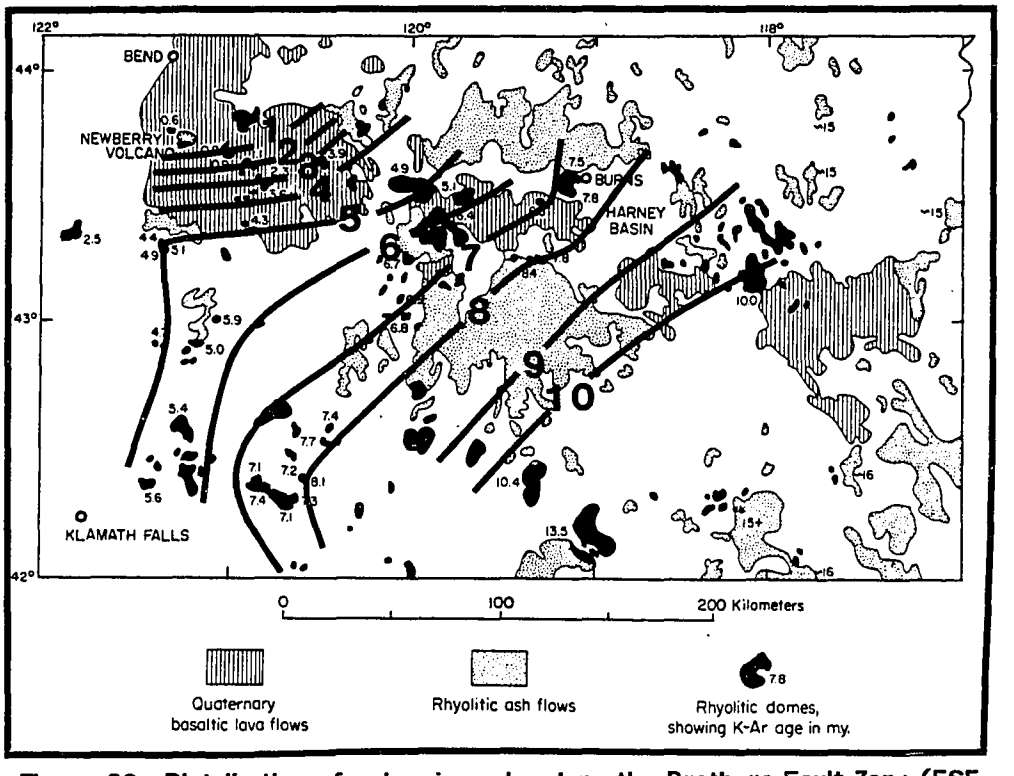

Figure 20. Distribution of volcanic rocks along the Brothers Fault Zone (ESE of Newberry (through Harney Basin)) (Christiansen and McKee, 1978) and age contours of rhyolite domes in m.y. (from MacLeod et al, 1975). Note the extensive rhyolitic ash flows that cover the area of the High Lava Plains south and southwest of Harney Basin. These ashflows are dated around 6 m.y.b.p. (MacLeod et al, 1975).

In the ESRP this propagation direction is NE. It has been postulated that the ESRP represents the track of a stationary hot spot beneath the SE-moving North American Plate. The basalts which initiate crustal melting are interpreted to be related to the hot spot. However, this concept is not compatible with the younging trend that has been interpreted to extend NW through Oregon from the southwestern corner of the ESRP (Christiansen and McKee, 1978; Thompson, 1977). This represents a major conflict in the tectonic interpretation of western North America.

Another problem in the interpretation of these data relates to the identification of the belt of domes in southern Oregon. The interpretation that the domes reflect linear SE to NW younging is challenged in the present study. The line of domes as described by MacLeod et al. (1975) is not a single line but two so-called loci. However, the observation made earlier that pervasive fracture in the B&R is masked by basin sediments also applies to the identification of this locus of rhyolitic domes. Keeping in mind that the younging trend is identified in domes less than 11 my old, Figure 30 shows that the area between the Brothers Fault Zone and the southern locus is covered by ash flow deposits. These are primarily ash flows emanating from the Harney Lake area. MacLeod et al. note that rhyolitic domes are probably concealed beneath these ash flow deposits. If so, the actual distribution of domes is considerably more diffuse than shown and the interpretation of two separate belts must be abandoned. Furthermore, when the pattern of domes in Nevada is included (Plate 1) there is a strong indication in the distribution of domes NE of the Granite Mountains in Nevada that the domes are related to basin structure. This suggests an

alternate view of the younging pattern: that the domes are younging from south to north along the strike of the B&R basins and that the domes in each basin are progressively younger to the west. This view is consistent with the idea that the B&R basins are propagating northward and forming successively westward (this model is discussed further in Chapter 3). Young volcanics also tend to obscure older features.

The HLP is bordered on the north by the Blue Mountains (Plate 1) -- a microplate terrane emplaced prior to mid-Tertiary time. Robyn & Hoover (1982) consider that the Blue Mountians microplate acts as a boundary along which B&R deformation is localized. Since the proposed strike-slip nature of this boundary (Lawrence, 1976) might be expected to be seismically active, Robyn & Hoover postulate that the "microplate" of southern Oregon is "jammed" against the Blue Mtn. microplate. This explanation ignores the fact that all observable deformation along the Brother FZ is normal faulting -- implying deformation of an extensional nature.

Lawrence's (1976) postulated strike-slip origin of the Brothers FZ was discussed above with respect to postulated zones farther south in the HLP and with reference to the Garlock Fault. In contrast to the other zones to the south in the HLP, there can be no doubt that, at the Brothers Fault Zone, there is a zone of enhanced deformation relative to areas to the south. This is quite evident on the fault map (Plate 1). However, interpretation of the significance of the deformation style is not unambiguous. The following points are pertinent.

1) The trend of faults in the Brothers FZ does not parallel the NW conjugate fault set found immediately to the south. Instead, the majority of the

faulting occurs in a zone which is tangent to the Blue Mountains boundary at Horse Ridge.

2) Faulting on the structures to the south curves into the Brothers FZ with a continuous transition; in some cases a single fault curves from one trend to the other. These transitions appear most well developed where major NE basin-bounding faults intersect the BFZ.

3) There is no evidence of actual strike-slip at the surface (Lawrence, 1976; Davis, 1981).

4) Although described by Lawrence (1976) to be "en echelon" and at an angle to the overall trend of the Brothers zone, the faults which make up the BFZ are perhaps more accurately characterized as two overlapping swarms of parallel faults (Figure 20), each striking roughly N48°W and within which the individual faults are parallel to the overall trend of the swarm. One of these swarms extends from Steens Mtn. to Hampton Butte and another from the northern end of Abert Rim (near Wagontire) to Bend. These swarms overlap between Hampton and Wagontire. This geometry suggests that the interpretation of this faulting as being a manifestation of a buried strike-slip fault may not be appropriate. In the next chapter, the theoretical basis of Lawrence's argument will be discussed and possible alternate scenarios evaluated.

The west end of the High Lava Plains adjacent to the Cascades is dominated by Newberry volcano. Newberry has been described by a number of workers, including:

Williams, (1935); Higgins, (1973); MacLeod and Sammel (1982); MacLeod et al. (1981); and Peterson and Groh (1965). Newberry is a shield volcano, roughly 900 m high, with a summit caldera about 8.5 km in diameter. Volumetrically its surface exposures are dominated by basalt with lesser rhyolitic volcanism, particularly in the caldera. It thus qualifies as a bimodal basalt/rhyolite assemblage. Voluminous silicic ash flow deposits have been found on the flanks of the volcano and these were probably related to eruptions which triggered caldera collapse (MacLeod and Sammel, 1982). All volcanics sampled have normal magnetic polarity indicating that the volcano is less than 700,000 years old. The oldest voluminous ash-flow tuff is 510,000 years old and this may reflect the earliest caldera collapse (MacLeod and Sammel, 1982). The caldera is interpreted as the result of several nested collapse features (MacLeod et al, 1982).

Over 400 cinder cones have been identified on the flanks of Newberry and these broadly define: a NNW trend north of the caldera -- parallel to faults to the southeast -- which merges to the north with Green Ridge (a segment of the east side of the Cascade Graben); and a NNE trend parallel to Walker Rim. Newberry therefore occurs at a point of intersection of tectonic elements in this region. In addition, based on the magnetic anomaly maps of the southern Cascades, Blakely et al. (1985) (Figure 21) have observed that there is an apparent magnetic anomaly linking Newberry with the Three Sisters area on the axis of the High Cascades, some 65 km to the NW. This is also indicated to some degree in the gravity data (Blakely et al, 1985) (Figure 22). These data may reflect magmatic communication between these features.

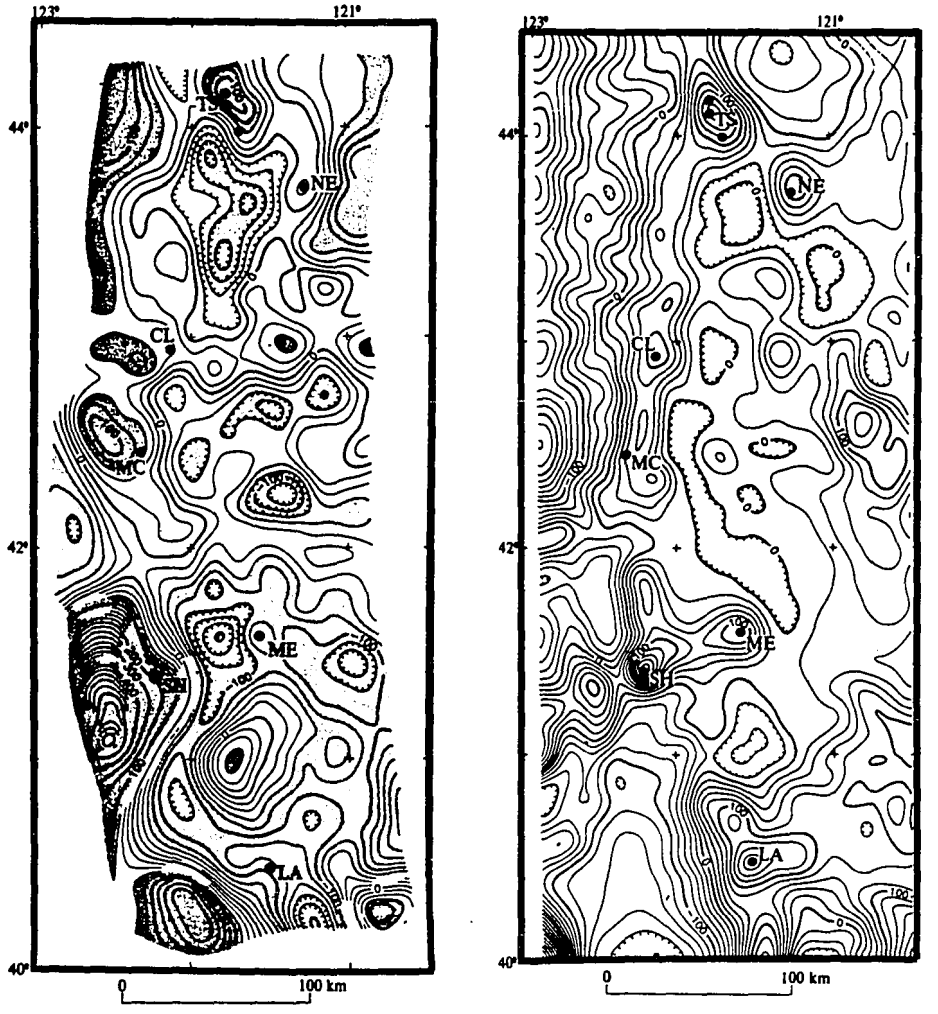

Figure 21. Upward continued aeromagnetic data in the Cascades (A) compared with calculated magnetic anomalies due to an assumed uniformly magnetized upper crust (B). Features in the observed data which do not appear in the calculated anomaly map are due to subsurface anomalies (Blakely et al, 1985). These workers have identified the data in (A) to indicate anomalous magnetic properties between Newberry and Three Sisters.

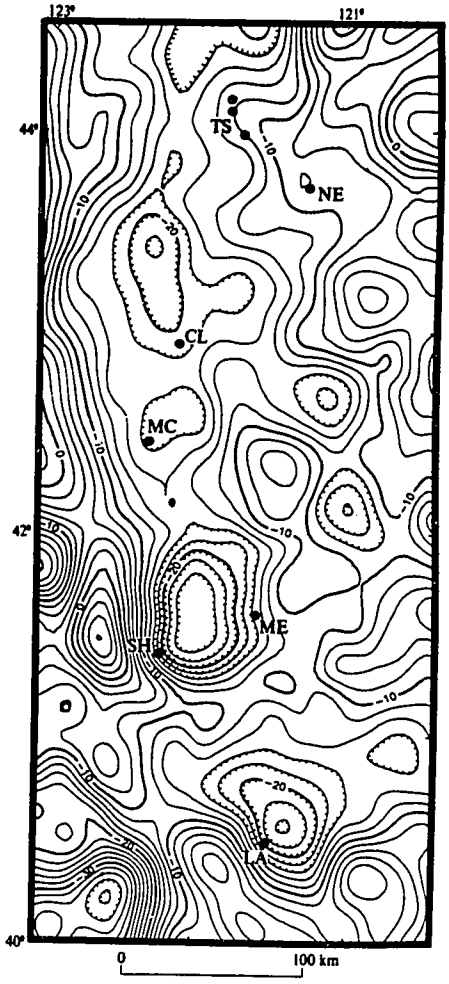

Figure 22. Upward continued gravity data in the Southern Cascades (Blakely et al, 1985).

Recent subsurface drilling has been carried out for geothermal exploration at Newberry. A surprising result is the fact that the shield, at depth, is considerably different from that exposed at the present surface. In particular, andesitic rocks are more abundant (MacLeod and Sammel, 1982) -- suggesting that Newberry may have originated as a more andesitic volcano and evolved toward bimodal (basalt/rhyolite) composition with time.

South of Newberry, there is an area of older volcanics that do not fit conveniently in either the High Lava Plains, the B&R, or the Cascades and may represent the results of former volcano-tectonic settings similar to the present situation at Newberry. These include Bald Mtn -- a proposed ash-flow caldera (Luedke and Smith, 1982) -- and its associated volcanics and Yamsay Mtn. Only reconnaissance mapping has been carried out in this area by Peterson and McIntyre (1970) and some dating by MacLeod et al. (1975). The Bald Mtn complex is dominantly basaltic with a few rhyolitic domes in the summit area. Yamsay Mtn. is dominantly andesitic but rhyolitic domes are located in its summit area and on its east flanks. Extensive basaltic volcanism is not found on Yamsay Mtn. Its rhyolitic domes are dated at 4.7 to 5 m.y.b.p. while those of Bald Mtn. are dated in the 4.4 to 5 m.y.b.p. range.

Both of these centers are cut by NNW-trending faulting. However, the area bounded by Yamsay Mtn. on the south, Walker Rim on the west and the southernmost edge of the flows of Newberry volcano appears to be considerably less effected by extensional deformation. The fault-density is comparable to areas further south and

east but the degree of extensional strain on those faults is less. Basins which occur in this area include: Sycan Marsh, Klamath Marsh, Sprague River Valley. This characteristic will be discussed further with respect to the evolutionary stage of the deformation here in the Chapter 3.

A summary for the High Lava Plains follows.

1) Basin and Range faulting terminates in the southern HLP and extensional deformation which was dominantly NNE-NE curves into NW trending normal faulting on small fault segments with dip slip of variable sense and small magnitude (the Brothers Fault Zone).

2) HLP is a locus of bimodal volcanism which is dominantly basaltic but includes rhyolitic domes and ash flows.

3) The rhyolitic domes which are less than 11 my old become younger monotonically along the BFZ toward Newberry volcano at the west end of the HLP.

4) Rhyolitic domes south of the BFZ locus, form a diffuse E-W pattern. Interpretation of the geometry of this pattern is made difficult by widespread younger ash flows and sediments which obscure older vents.

5) A pattern of rhyolitic volcanism accompanying the northward propagation of B&R basins and the progressive westward stepping of these basins up to the Abert Rim- Warner Ranges line is not inconsistent with the data.

6) The HLP is bordered on the north by the Blue Mtns microplate which appears to act as a boundary to northward propagating deformation.

7) Although the BFZ has been postulated to be a fundamental strike-slip zone, there is no evidence of any strike slip structure. In detail, its faults are not en echelon. Indications exist that it may at present be primarily a locus of extensional deformation.

8) Newberry volcano is a large basaltic shield with a silicic ash flow caldera at its summit. At depth, its dominant composition is andesitic. It shows evidence of 3 well-defined rift zones, two of which parallel the NNW faulting of the northern B&R and one of which parallels Walker Rim.

9) South of Newberry, two broadly similar, but older (about 5 m.y.b.p.) volcanoes occur: Yamsay Mtn. and the Bald Mtn. caldera complex.

The Cascades

Although there has been considerable geologic interest generated in the Cascades in recent years by ongoing geothermal evaluation and volcanologic studies related to volcano hazards, surprisingly few syntheses of the geologic/tectonic evolution of the range have been published compared, for example, to the Basin and Range. This is largely due to the lack of detailed geologic mapping and age dating, although recent work (eg. Priest et al, 1983; Hammond, 1980) is improving this situation. Syntheses that do exist include: Priest et al. (1983) primarily for central Oregon; Hammond (1979); Hammond (1980) primarily southern Washington; McBirney (1978) and White and McBirney (1978).

To the west of the modern magmatic arc, the dissected Western Cascades form a physiographic boundary (the western margin of the Cascades Graben) which is quite distinct in the southern Cascades of north and central Oregon, but less well defined in both the southernmost Cascades (south of Diamond Peak) and in the northern Cascades in Washington. The Western Cascades represent an earlier (Tertiary), larger-volume, and probably more typically Andean volcanic arc which dominated the Pacific Northwest from 40 to about 5 m.y.b.p. (Hammond, 1979). Subduction in the system was initiated when the Pacific-Kula spreading ridge moved north along the continental margin bringing the Farallon Plate (of which the Juan de Fuca is a piece) into contact with the North American plate (Atwater, 1970). Farallon subduction beneath North America, with roughly perpendicular convergence, gave rise to the Western Cascades and has continued into the present.

The Western Cascades are characterized as dominantly silicic lavas and tuffs (Early episode: 40-18 m.y.b.p.) to dominantly intermediate andesitic lavas and dacite tuffs (Late episode: 18-9 m.y.b.p.) (Priest et al, 1983). These episodes were followed by a narrowing of the volcanic axis and a slight eastward shift of the locus of volcanism. This was accompanied by a trend toward more mafic lavas which erupted during the period from about 9-4 m.y.b.p. Because of this mafic trend, Priest et al. (1983) have termed this period the Early High Cascades in central Oregon where it is characterized by the eruption of voluminous high-alumina basalts and later basaltic andesites. They note, however, that in southern Oregon (Smith, 1979) there is no obvious distinction between these rocks and those of the Western Cascades

group. Thus for broader study, the grouping of these "Early High Cascades" rocks into the Western Cascades (eg.Hammond, 1979) may be more useful.

Western Cascades structure is not well established. Few faults have been actually mapped (Wells and Peck, 1961). However, numerous lineaments have been identified (Kienle et al, 1981; Venkatakrishnan, 1980) on U-2, Landsat and SLAR imagery; and structural influence on drainage development is evident. The structure thus implied is dominantly oriented in a northwesterly direction between N50°W and N70°W; and in a northeasterly direction approximately N60°E.

During the later stages of the Western Cascades volcanism, eruptions of the Columbia River flood basalts (CRB) took place on the east side of the arc in southeastern Washington and northeastern Oregon. The main pulse of CRB culminated between 12 and 13 m.y.b.p. although similar, but less voluminous, activity (eg. Simcoe volcanics) has extended to perhaps the end of the Western Cascades volcanism (Washington Public Power Supply, 1981). The CRB erupted from N-S fissures and these basalts have been subject to folding, producing the E-W trending Yakima fold belt deformation which is believed to have initiated prior to the CRB volcanism and been largely completed prior to the eruption of the Simcoe volcanics about 4.5 m.y.b.p. (Davis, 1981).

The tectonic significance of the CRB is not clear. Some workers favor its origin from a mantle plume that was overridden by North America -- the Yellowstone hotspot is the logical candidate (Duncan, 1984). This model has difficulties, however, and this question is not resolved.

The onset of High Cascades (Late High Cascades) volcanism in the Oregon Cascades is marked by extensional faulting, increasing dominance of mafic volcanism and an eastward shift in the arc axis. Cascades volcanism in Washington, and particularly north of Mt. Rainier, has not experienced the same changes, and High Cascades volcanism in Washington is radically different in character from Cascades volcanism to the south. The northern Cascades occur in an area which has experienced more than a kilometer of uplift in the Late Tertiary (Hammond, 1979) and a N-S compressive regime exemplified by the aforementioned E-W trending folds. Volcanism is centralized at relatively small volume andesitic and dacitic stratocones which are superimposed on highly dissected older terrain; and there is little manifestation of the structural influence of this volcanism on the topography -- beyond the cones themselves. Although evidence exists for recent volcanism on all of these volcanic centers the volcanic edifices themselves are heavily glaciated.

By contrast, the onset of the High Cascade episode in Oregon and California (Late High Cascade of Priest et al, 1983) is marked by pronounced down faulting of the High Cascades axis relative to the Western Cascades, forming an abrupt topographic boundary between the Western Cascades and the High Cascades. This deformation is thought to have taken place between 5 and 4 m.y.b.p. (Priest et al, 1983). Lavas erupted during this episode are distinguished by their relative lack of dissection and the influence of existing topography on their emplacement.

Arc-parallel down-faulting is found at numerous points along the axis of the southern Cascades while such faulting is absent north of Mt. Hood. Along the east

side of the Cascades, major normal faults (down to the west) are found at Mt. Hood, Green Ridge, Walker Rim and Klamath Graben (Figure 23). On the west side of the Cascades, normal faulting is found from west of Mt. Jefferson south to Diamond Peak on isolated segments as shown on Figure 23; and along the west side of the Klamath Graben. Such arc-parallel faulting is not present between Diamond Lake and Diamond Peak and also is not found south of Mt. McLoughlin. These areas correspond to the sections of the arc least influenced by Basin and Range deformation.

Volcanism of the (late) High Cascades is characterized by increasingly mafic composition indicative of increased extension (Priest et al, 1983). The down-faulting which accompanied the onset of this volcanism was also accompanied by an eastward shift in the locus of volcanism of the High Cascades north of Diamond Peak. Figure 24 shows the extent of Cascades volcanism less than 5 m.y.b.p. (Luedke and Smith, 1984). This figure depicts volcanic edifices greater than 3.5 km in diameter and the location of volcanic necks. The necks define the axis of late Western Cascades (early High Cascades) volcanism. From Shasta to Diamond Peak the recent volcanism is essentially coincident with the older volcanic axis (also indicated by the overall distribution of older volcanism shown on the maps of Luedke and Smith (1982, 1983, 1984)). The main exception to this is the location of Crater Lake slightly east of the main axis, and a few young cones (eg. Pelican Butte) aligned along the west side of Klamath Graben. North of Diamond Peak the active volcanic axis clearly has a locus displaced eastward relative to the older vents. In general, the areas of active arc volcanism which occur on the older arc are dominated by lower volume, andesitic

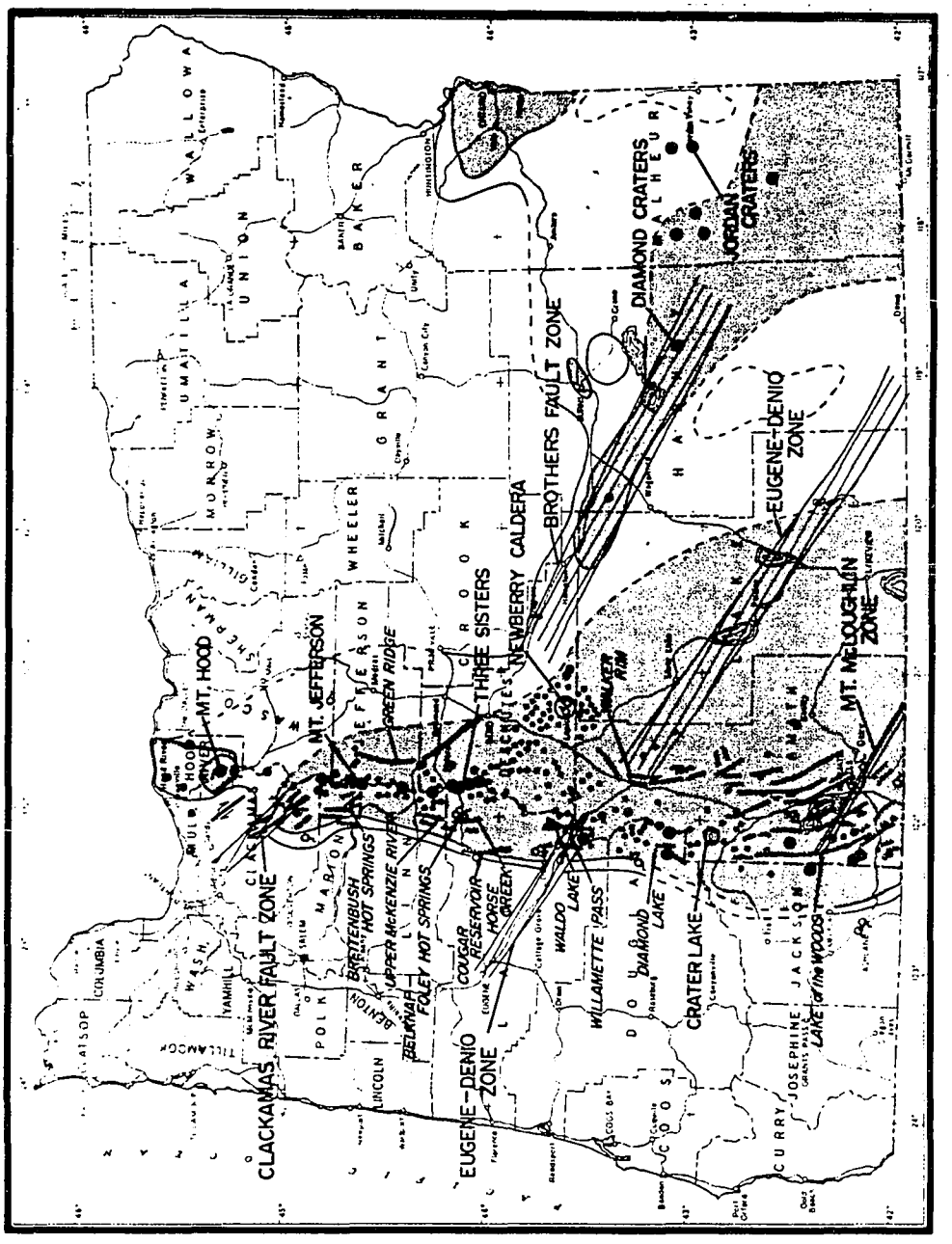

Figure 23. Arc-parallel Faults and Heat Flow in the Cascades (Priest et al, 1983). Major N-S normal faults which mark the boundaries of the active volcanic arc in the Cascades are shown with hachures on the downthrown side. Dark shaded areas incidate areas within which the measured heat flow is over 100 mW/m^2. Filled circles are volcanic centers.

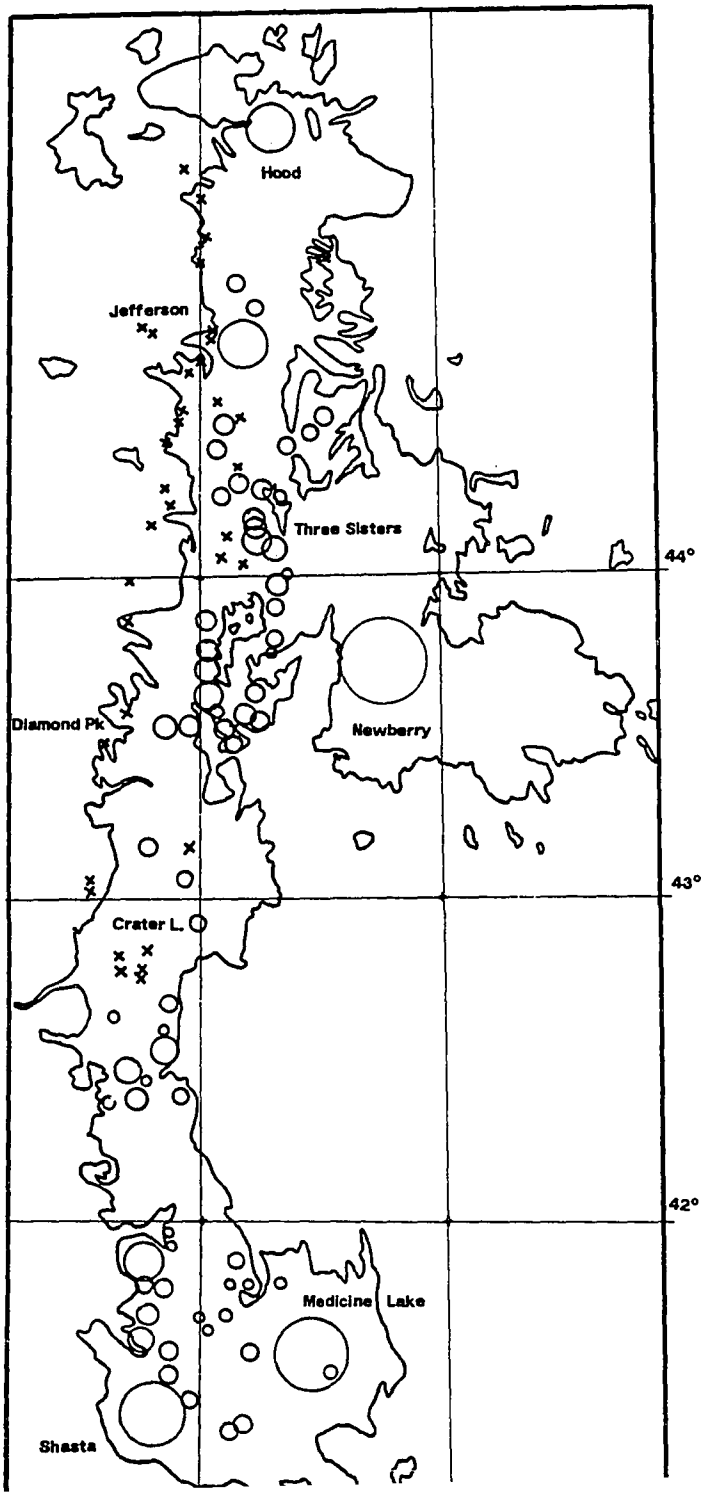
Hood
Jefferson
Three Sisters
44°
Diamond Pk
Newberry
43°
Crater L.
42°
Medicine Lake
Shasta

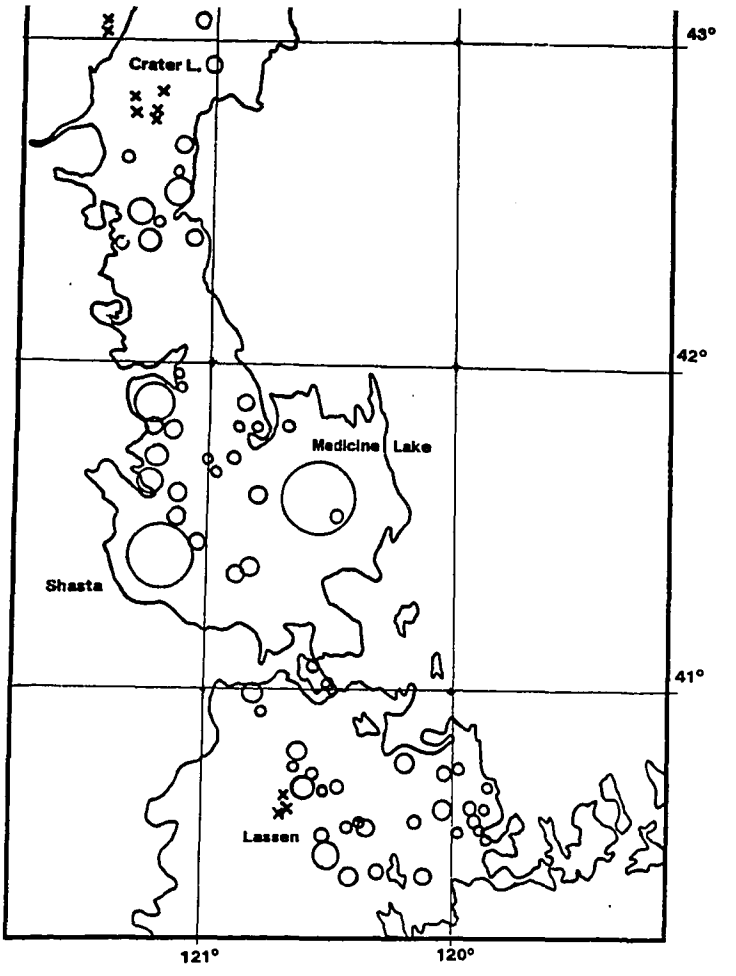

Figure 24. Volcanic distribution and edifice map for the southern Cascades. (Limits of 0-5 m.y.b.p. volcanism from Luedke and Smith (1984).) Circles are relatively undissected edifices (less than 5 m.y.b.p.) and X's are volcanic necks. A eastward shift of Cascades volcanism is evidenced north of Diamond Peak while the arc to the south is essentially coincident with the alignment of the volcanic necks.

volcanism while the areas where volcanism is distributed to the east are dominated by basalts. The eastward displacement and basaltic character also correspond to areas where B&R structure has intersected the arc axis. It is the southern Cascades which display extensional tectonism and caldera formation, that is of main interest to the present study as discussed in Chapter 3.

The geophysical setting of the southern Cascades has been examined by Blakely et al. (1985) (see above with respect to Newberry). Their data is shown on Figures 21 (magnetics) and 22 (gravity). They interpret magnetic lows adjacent to Lassen and between Shasta and Medicine Lake Caldera to reflect upwarp of the Curie temperature -- implying the presence of a shallow magma body. This indicates that there may be some sort of thermal (presumably magmatic) communication between Shasta and Medicine Lake volcanoes. As mentioned above they also interpret magnetic data to imply a connection between Newberry and Three Sisters.

Additional data pertaining to the Cascades is discussed as appropriate in the following sections. Imagery and map analysis is utilized to better define the stress trajectories, examine the Eugene-Denio and Brothers Fault Zones and study the interaction of Basin and Range deformation with the Cascades and the correlation of volume of volcanism and caldera formation with these interactions.

III. IMAGERY AND MAP ANALYSIS

Data Base

The data base utilized for this study of the Cascades/Basin and Range interaction is itemized in detail in Appendix A. This data base includes imagery and maps at a number of different scales. Imagery at scales smaller than 1:500,000 provide a synoptic view of tectonically significant features that is essential to the type of interpretation attempted here. The following imagery was used:

Seasat Synthetic Aperture Radar Image (L band) Mosaic (optically correlated) of the Western US (west of Latitude 119.5°W) 1:500,000;

Landsat (MSS color composite) of the Cascades (west of Latitude 120.5°W) 1:500,000;

U-2 Color IR photography of the Southern Cascades and western Basin and Range (transparencies, most in stereo) 1:500,000 (approximately);

Landsat (Band 7) Mosaic of Oregon, 1:1,000,000;

Return Beam Vidicon Mosaic of Oregon, 1:1,000,000;

Side-looking Airborne Radar (X band) Mosaic of Western Oregon (west of Latitude 122°W) 1:250,000;

Plastic Relief Maps of the Cascades (west of Latitude 120°W) 1:250,000 (vertical exaggeration 2:1) obliquely illuminated from four illumination azimuths;

Low altitude hand held aerial photography of the Cascades (from Mt. Jefferson to Medicine Lake).

These data were combined with geologic maps (from 1:500,000 to 1:62,500), tectonic maps (1:1,000,000), volcanologic maps (1:500,000 and 1:1,000,000), topographic maps (complete coverage at 1:500,000 and 1:250,000; near complete coverage at 1:62,500 and 1:24,000). Additional maps of geophysics (gravity, magnetics, heat flow and seismicity) and other available references were utilized, where appropriate, to synthesize the data available for this area in light of the view offered by means of the imagery.

Low altitude aerial reconnaissance of the Cascades was carried out from Mt. Jefferson to Mt. Shasta including Medicine Lake and Newberry in 1983. Ground reconnaissance was also carried out at this time across the High Lava Plains, and at Crater Lake, Newberry and Medicine Lake.

The Seasat imagery has been the source of much of the first-order inspiration for this study. It has some curious properties which make it simultaneously difficult to work with quantitatively and intriguing for its ability to delineate and enhance geologic structure. Seasat SAR is a high resolution (nominal 20 m per pixel) L-band spaceborne imaging radar that is sensitive to surface roughness on the order of 25 cm in amplitude. Its key characteristic for the present study however is the steep look angle (small incidence angle) of the radar look direction. This produces both undesirable artifacts and enhancement of structural features. An extreme example is the case of large stratovolcanoes such as Mt. Shasta (Figure 25). In this situation, the cylindrical wavefront of the outgoing radar signal encounters the top of the

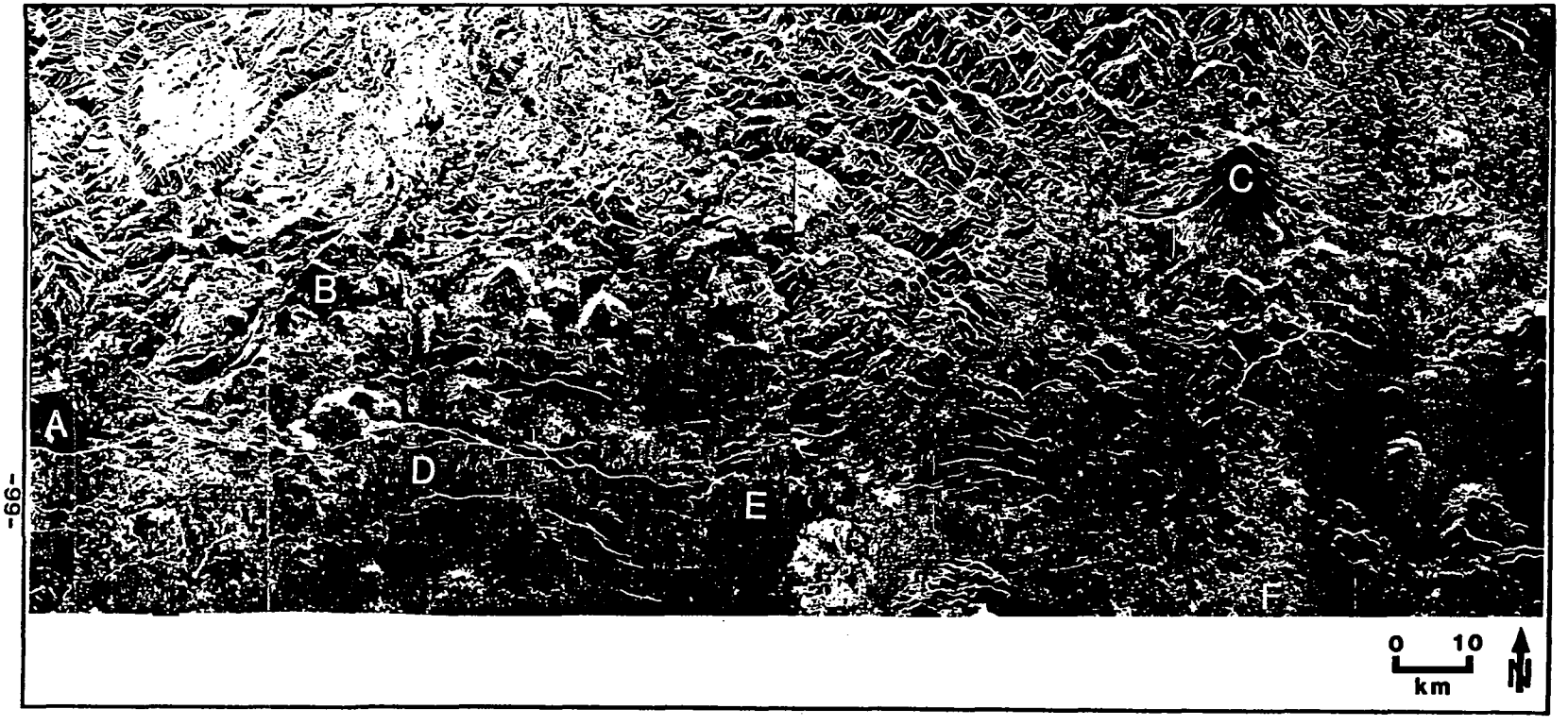

Figure 25. Seasat Radar Image of Mt. Shasta (C), Medicine Lake (F) and Lassen Peak (B), showing examples of extreme layover of high-standing landforms -- Shasta (C) and enhancement of fault scarps (D-E) (also caused by the layover phenomenon). NW-trending structure between Lake Almanor (A) and Lassen is also visible.

volcano at about the same time or slightly sooner than it encounters the base of the volcano. The radar image data is simply a record of the intensity of the radar return as a function of travel time (from source to ground and back to the detector). Therefore, for stratovolcanoes, the return from the top of the volcano frequently occurs before or during the return from the base of the volcano. The result is that the top is mapped superimposed over the volcano flank such that the top appears to have been pulled toward the sensor. This characteristic is called layover. In areas of extreme topographic relief this characteristic completely compromises information content. Valleys can be overlain by adjacent ridges, obscuring any accurate view of the topography (relief can also cause rotation of linear features). Also, scarps whose strike is more than 75° from the flight direction are not well depicted.

On the other hand, in relatively flat-lying regions layover is useful. It has the effect of enhancing fault scarps of various dips because the return-energy is condensed by the layover phenomenon. An example of this is seen on Figure 25 where the fault scarps south of Medicine Lake caldera are clearly depicted. In such flat terrain, the Seasat clearly maps scarps and provides a rendition of fault distribution which supplements maps of recognized faults. Although possessing artifacts, it is a rendition of the actual scene -- not a geologist's conception of the scene. The other main advantage of the Seasat imagery of this study is that it is broad scale (1:500,000) and provides continuous coverage of a wide area. For this study, an area larger than 400 x 500 km can be examined at once. This contrasts with most previous structural geologic and tectonic analyses of the Cascades and

western Basin and Range areas which have traditionally been carried out from the study of small individual structures (eg, Zoback and Anderson, 1981). Utilizing Seasat and other synoptic data of this study, patterns of basins, areal fault distribution and interrelationships of fault elements can be more readily clarified within a regional context.

Although Seasat imagery provides a good synoptic tool, it is not suitable for detailed quantitative analyses of structure because of the artifacts just discussed. Therefore the complementary nature of the other data sets comes into play for such analysis. The strengths of these other data are listed briefly below:

1) Landsat MSS: used in this case at the same scale as Seasat; geometrically correct (excellent baseimage); 80 m resolution; false color provides tonal anomaly information; oblique solar illumination provides some indication of topographic relief;
2) U-2 Color Infrared Imagery: high resolution data (5 m resolution); color tonal anomaly information; utilized in stereo pairs for most of the study area;
3) Plastic Relief Maps: relatively large scale (1:250,000) provides topographic relief information free of other influences; landforms well defined by vertical exaggeration (2:1); can be mosaiced and obliquely illuminated from any angle to enhance various structural orientations;
4) Other data (X-band radar, RBV mosaic, large scale topo) provide additional sources for examining specific areas.

This data set offers the possibility of studying the tectonic setting of the study area on many scales. In particular the broad-scale imagery provides a perspective of the structural interactions of the various tectonic elements present. The goal of this project has been to utilize this synoptic perspective to examine significant aspects of the tectonic setting which can be more clearly stated in the context of the broad scale view supported by finer scale data and previous work.

Problems with Existing interpretations

Chapter 2 discusses the tectonic setting and current tectonic interpretations for the study region. Salient problems with these interpretations that are of particular significance to the Cascades/B&R interaction are reiterated briefly below. These interpretations will be reevaluated in subsequent sections of this chapter.

A) The Eugene-Denio Zone (EDZ), across southern Oregon, is hypothesized as a zone of enhanced, en echelon, NW faulting which reflects WNW-striking right lateral strike-slip faulting (Lawrence, 1976). This interpretation is questionable in view of the following facts.

1) The pattern of faulting is not convincingly en echelon (Lawrence (1976) admits this).

2) Faulting along the extension of the EDZ into the Cascades is found to be inactive since 22 m.y.b.p. in the Lookout Point Reservoir area (Woller and Priest, 1983) and evidence for activity on these structures in

other areas is also lacking (Barnes, 1978 -- Mt. Bailey; Wollelr and Black, 1983 -- Waldo Lake - Swift Creek; Brown et al., 1980 -- west of Willamette Pass).

3) A number of prominent linear features which cross the EDZ east of the Cascades are not offset -- including both Abert Rim and Walker Rim. Normal faults in both of these areas are actually perpendicular to the alleged Eugene-Denio trend -- an orientation which counterindicates ongoing dextral strain across the EDZ.

4) There is no seismicity in the vicinity of the EDZ between the area west of Abert Rim and the Cascades summit.

B) The Brothers Fault Zone (BFZ), which crosses the northern margin of the B&R in Oregon, is hypothesized to be a zone similar to the E-D Zone (Lawrence, 1976), with en echelon normal faults indicating deeper fundamental dextral strike slip. It is interpreted as a strike-slip feature to achieve the transition from extended crust of the B&R to the unextended crust located to the north (Blue Mountains, etc.). This interpretation has been widely referenced and dominates the northern Basin and Range tectonic picture. It is drawn as an analog to the Garlock fault at the southern margin of the B&R where strike slip is clearly indicated (see also Chapter 2). The data on which this interpretation was based is a Landsat (ERTS) black and white mosaic that is similar to the imagery used for the present study -- although lacking the resolution or the other types of imagery used herein. A review of the

information related to the BFZ indicates that several observations are not consistent with the dextral strike slip interpretation.

1) The BFZ is an area of very low seismicity (Figures 17).

2) There are no examples of actual strike-slip deformation -- all the faults of the BFZ and surrounding areas are short normal faults (Walker & Nolf, 1981; Davis, 1981; MacLeod et al, 1982).

3) Examination of the detailed fault pattern in the BFZ (Figure 26) reveals that the fault pattern is not en echelon in any rigorous way. En echelon features are defined as those which are relatively short and oriented in steplike arrangement such that they form a linear zone and the strike of individual features is oblique to the zone as a whole (Bates and Jackson, 1980). The BFZ is perhaps more accurately characterized as swarms of parallel normal faults aligned parallel to the overall strike of the swarm (Figure 26). This pattern is examined more closely below.

4) At the point where the projection of the BFZ intersects the Cascades axis, there is actually a left-lateral offset of the volcanic axis -- between Bachelor Butte and South Sister -- rather than the predicted right-lateral offset.

C) The rhyolite domes (younger than 11 m.y.b.p.) which extend across central Oregon (Figure 20) have been hypothesized to become younger in a linear NW direction along two loci (MacLeod et al., 1975). An examination of the

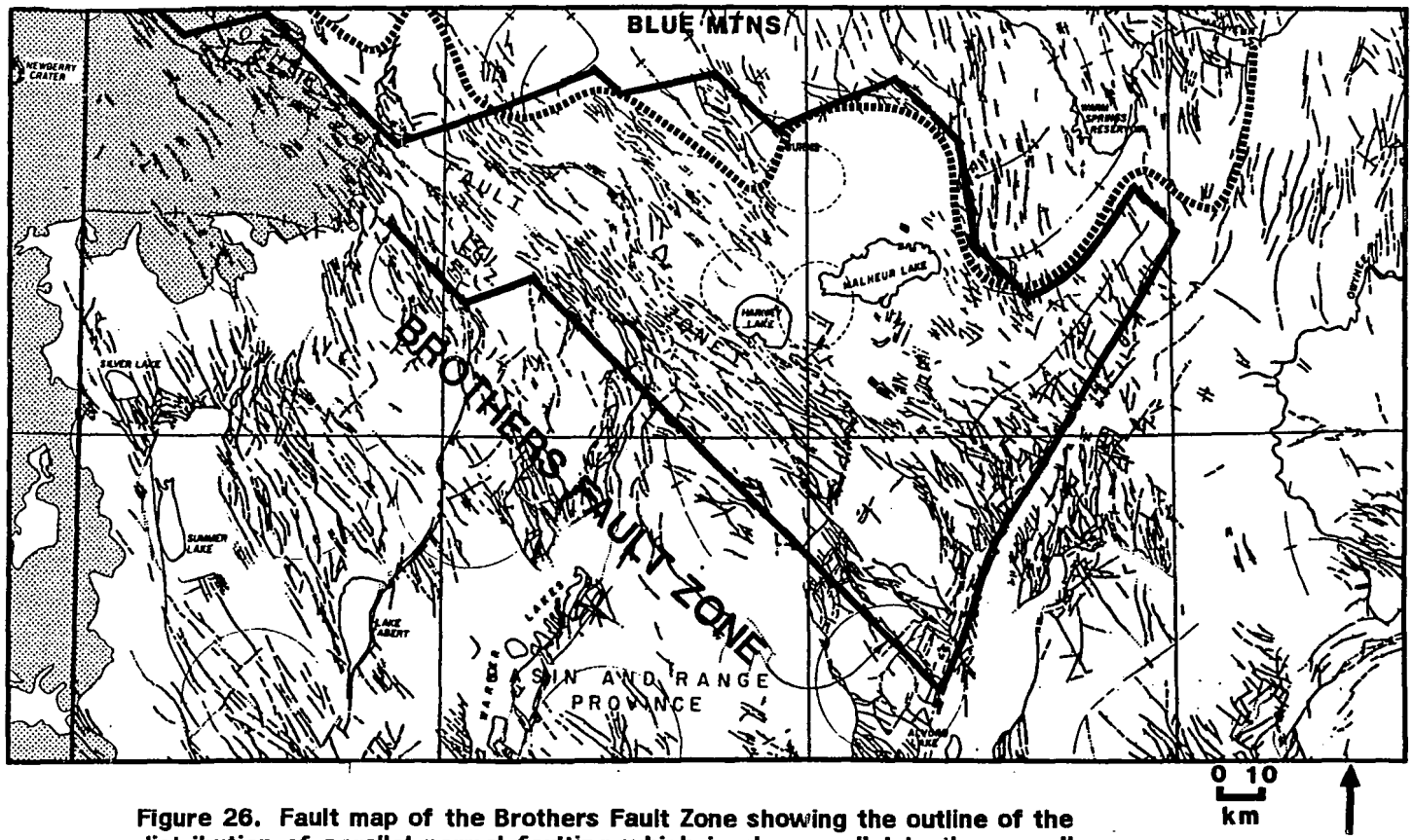

Figure 26. Fault map of the Brothers Fault Zone showing the outline of the distribution of parallel normal faulting which is also parallel to the overall strike of the zone (broad solid line). This faulting is not en enchelon but does appear to coincide with the southern margin of the Blue Mountains (broad dashed line) which is an accreted microplate. Stress trajectories indicated by recent vent alignments at Diamond Craters are shown as short broad lines. The symbols and sources are the same as Plate 1.

distribution of these domes -- particularly when the distribution in northwestern Nevada is also taken into consideration (Plate 1) suggests that reinterpretation of these features is appropriate.

1) The distribution of the rhyolitic domes is not one or two loci, but a relatively diffuse distribution.

2) The volcanism which produces these rhyolites is a more or less continuous extension of older Basin and Range volcanism found to the south and southeast. Such acid volcanism (and caldera formation) is generally considered to be part of the early phase Basin and Range deformational style (Eaton, 1982). However in the NW younging hypothesis for these Oregon domes, the volcanism has not been interpreted in the context of Basin and Range structure.

3) An analogy has been drawn between this NW-younging volcanism and the NE-younging trend of the Snake River Plain/Yellowstone volcanic province (but much smaller in volume) (Christiansen and McKee, 1978; Thompson, 1977). This creates major inconsistencies in the tectonic interpretation of the NW US. Abundant evidence indicates that the SRP is the product of a hot spot, overrun by North America in the mid Tertiary -- producing, in succession, the Columbia River basalts, the Western Snake River Plain volcanics, and the Eastern SRP up to Yellowstone where the hot spot is now thought to be located. The younging trend in a NW direction across Oregon, attributed to a similar

mechanism, has put the entire hot spot model for the SRP in question (Christiansen and McKee, 1978). Workers studying the Columbia River basalt - SRP connection are obliged to ignore the interpretations of the SE Oregon rhyolitic volcanism. Thus both the surrounding tectonic setting and the detailed distribution of these domes indicates that reevaluation of the current interpretation of the domes is appropriate.

D) The maximum horizontal stress in the northern Basin and Range is considered to be oriented NE (Zoback and Anderson, 1981; Zoback and Zoback, 1980). However, in the northwest corner of the Basin and Range, there is evidence that the maximum horizontal stress is oriented NNW.

1) Immediately west of the Abert Rim - Warner Range horst, there is a line of N to NNE trending basins which marks the western boundary of N-NNE oriented basins and ranges (Figure 45). West of this line the dominant strike of the basins is NNW. These NNW tending basins include: Summer Lake, Chewaucan Marsh, Fort Rock Valley, Christmas Valley, Alkali Lake (northeast of L. Abert) and the Klamath graben, plus some smaller basins such as Drews Reservoir and the Devils Garden of the South Fork of the Sprague River.

2) The dominant fault direction outside the limits of the basins is also NNW and the area west of Summer Lake is cut by abundant NNW trending linear landforms.

Data Analysis

Because of these inconsistencies between the generally accepted interpretations and the evidence observable on the imagery and maps, additional analysis has been carried out to further constrain the observations. Six aspects have been examined:

1) Maximum horizontal stress trajectory data has been derived from volcanic vent alignments for the southern Cascades from Lassen to Mt. Jefferson and for the northwestern Basin and Range.
2) The fault density and stress trajectories of the Eugene-Denio Zone have been examined to further evaluate the significance of this zone.
3) The mechanism of Basin and Range deformation in the northwestern part of the province has been reconsidered conceptually in light of the implied evolution of the structures and the concepts of propagating continental rifts.
4) The faulting of the Brothers Fault Zone is reinterpreted in light of closer examination of the fault pattern and stress trajectories.
5) The relationship between Basin and Range structure and the distribution of rhyolite domes has been studied with respect to the implied evolution of the deformation of the region.

6) Volume/area determinations have been carried out and these are used to further examine the relationship between volcanic volume and intersecting B&R structure.

Stress Trajectory Map

An important aspect of evaluating the tectonic setting in any region involves the analysis of the stress regime. Such analysis allows characterization of domains of consistent stress reflecting tectonic processes. In the Cascades and adjacent Basin and Range the low level of seismicity precludes the determination of regional stress by focal plane solutions. An alternative approach is developed herein.

The determination of the stress regime is actually determined by measuring strain. In an otherwise virgin half-space this is an accurate descriptor of the stress field. Strain can take place by elastic or plastic deformation without fracture, for small deviatoric stress, or by mobilization on fracture planes for large stress differences. For example, in unfractured rock undergoing shear by simple compression, the angle between the maximum principle stress and the failure plane will be approximately 45 degrees (eg. Wilcox et al, 1973). Therefore, in previously unfractured rock, the orientation of the maximum principle stress can be determined in an unambiguous way from the geometry of the faults which it produces. If a strike-slip fault is overlain by unfractured overburden, the development of a suite of secondary structures will presage the propagation of the main fault to the surface.

Figure 27 (from Groshong and Rodgers (1978); and Tchalenko (1970)) depicts theoretical and experimental strike-slip fault geometry, including these early-formed second-order structures which can be used to infer stress regime and, therefore, fault sense. It is on the basis of this secondary geometry that the faulting of the BFZ and EDZ has been interpreted to be strike-slip. By contrast, Figure 28 (modified after Withjack, 1982) shows the fault pattern which develops in an experimental clay model on the edge of an uplift in an overall extensional regime -- in this case swarms of short parallel normal faults are characteristic. Therefore, both strike-slip and extension can produce swarms of short faults -- the former producing an en echelon pattern and the latter producing a swarm of faults each parallel to the overall swarm.

In the real world, stress may be mobilized on preexisting faults or joints that occur at angles that do not directly reflect the orientations of the principle stresses. Shear stress may be mobilized on a preexisting plane oriented from 5° to 50° from the maximum stress direction (Sbar, 1982). If the preexisting fractures are oriented greater than 50 degrees from the maximum stress direction, new fractures will form at about 45 ° and the old fractures will not be remobilized. Therefore, for a given slip event, the orientation of the fault plane may be only 5° from the maximum horizontal stress (MHS) and if one assumes the slip to have occurred on a plane 45° from the MHS, the derived MHS will be in error by 40°. Similarly, extensional stress may be released on preexisting fractures that are nct necessarily parallel to the maximum stress.

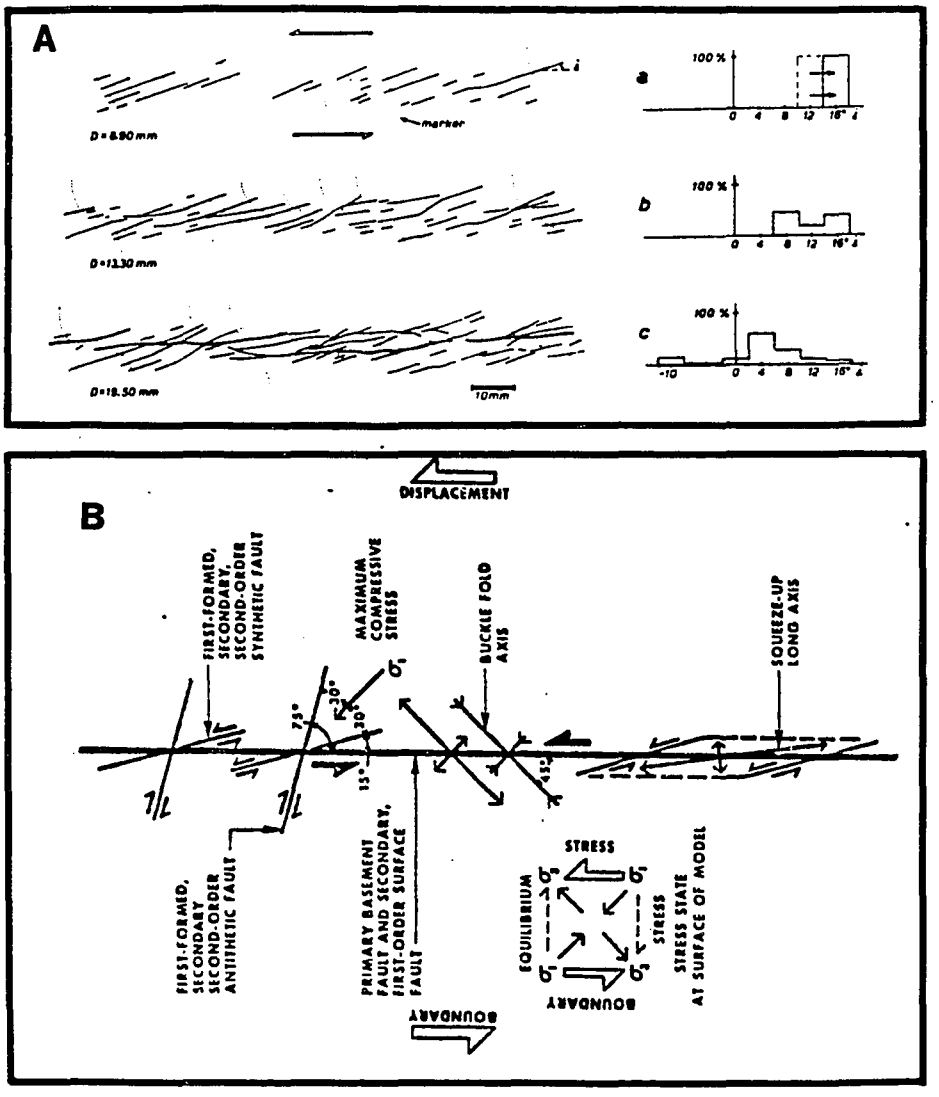

Figure 27. Left lateral Strike-slip Fault Geometry (after Tchalenko, 1970; Groshong and Rodgers, 1978). The upper drawing (A) shows the en echelon structures which develop in the early stages of strike-slip fault scale modelling (Tchalenko, 1970). Before the main fault trace reaches the surface, en echelon structures (top frame) develop. Note that the structures shown are synthetic faults which are short strike-slip faults -- not normal faults. The bottom frame shows the fault pattern after sufficient strain has taken place to propagate the main fault trace to the surface. The lower drawing (B) shows the theoretical structures that can accompany strike-slip faulting where the main fault is covered at depth by unconsolidated (unfaulted) overburden (Groshong and Rodgers, 1978). Tension gashes can also form parallel to the maximum compressive stress but these are less common.

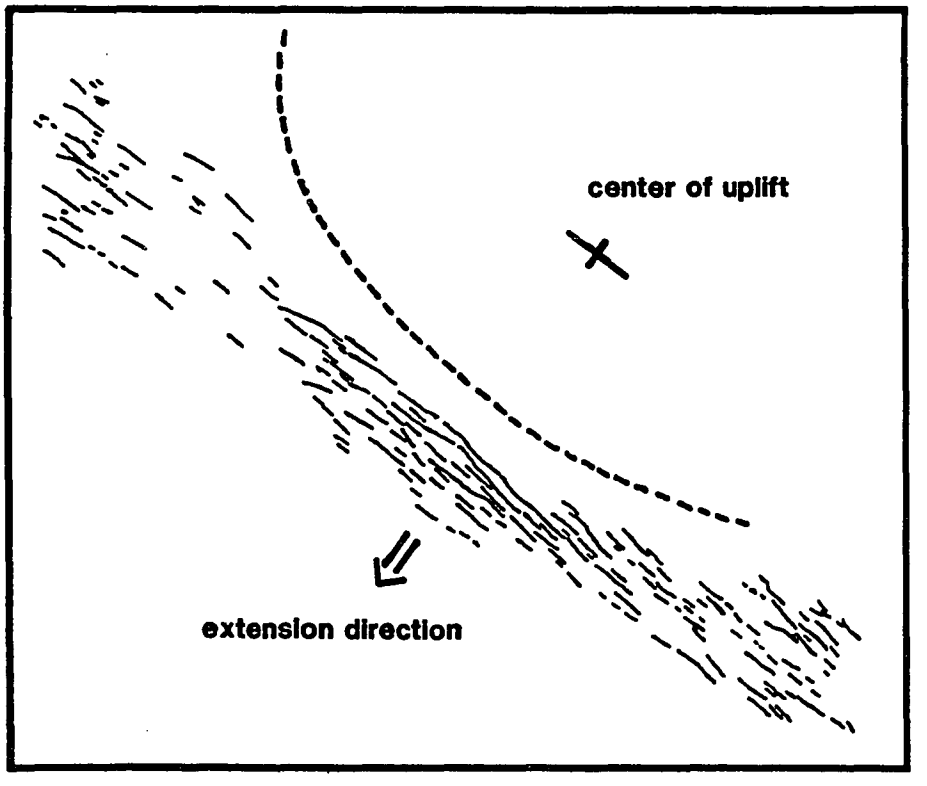

Figure 28. Extensional fault geometry adjacent to an uplift showing tracings of fault patterns produced by elliptical doming and simultaneously applied extension (Withjack and Schneider, 1982). Faults are primarily normal faults. Fault pattern with applied extension rate one and a half times uplift rate. Arrows show applied extension direction. Dashed line is approximate location of the periphery of uplift.

In general, for materials in the brittle regime (ie most crustal rocks), there are three ways of evaluating stress orientation. These are:

1) direct in-situ stress measurements by overcoring or hydrofracting;

2) fault plane solutions for seismic events; and

3) orientations of monogenetic igneous vent alignments and dikes.

Of these methods of stress measurement, overcoring and hydrofracting provide the most controlled and quantitative measure of stress, with overcoring being the more accurate of the two. However, these approaches are costly and such data is not widely available. In addition, measurements made by these methods are a convolution of existing gravitational stresses (overburden or edifice) plus current tectonic stress plus residual tectonic stress from previous tectonic activity (Voight, 1967). They can therefore be influenced by perturbations in the local stress field at and in the vicinity of the borehole. On the other hand, the use of fault plane solutions and vent alignments reflects the stress over a broader area and are less influenced by localized effects -- although less quantitative. In any case, no in-situ stress measurements are available within the Cascades of Oregon or within the NW Basin and Range (Zoback and Zoback, 1980)

Focal plane solutions of earthquake data determine the stress orientation from the distribution and type of the first motion produced at various localities around the earthquake epicenter. The use of fault plane solutions to characterize tectonic stress is widely documented (eg. Cox, 1972). The assumption used to identify the P-axis (compression axis) is that the maximum stress is oriented at 45° to the failure

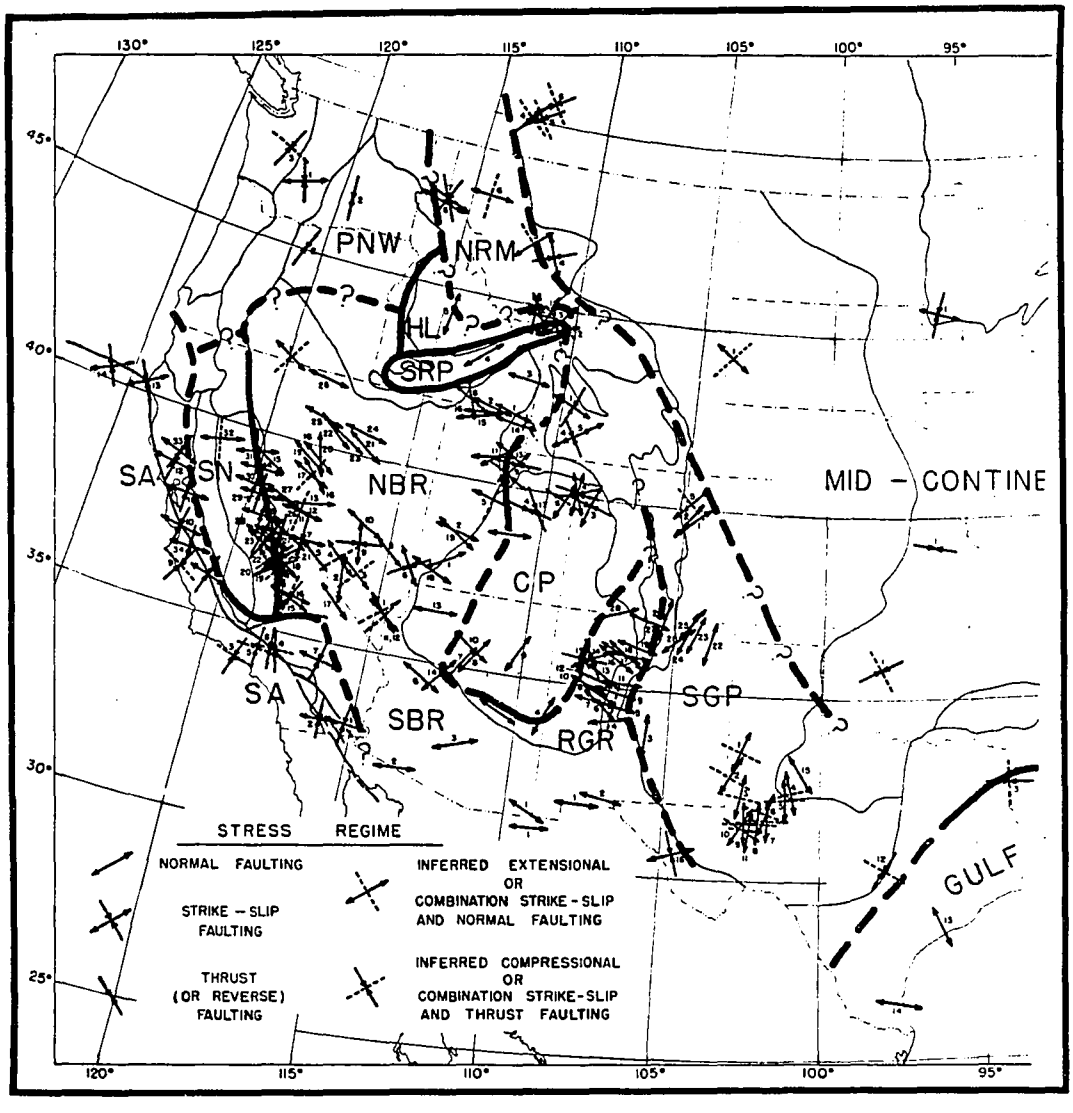

Figure 29. Stress state of conterminous US (west half) (Zoback and Zoback, 1980) showing the stress regimes (broad lines) identified on the basis of stress trajectory information (shown as arrows). Note the absence of any stress trajectory information in the extreme northwestern B&R and only one data point in the Cascades in Southern Washington. SA-San Andreas regime; SN-Sierra Nevada regime; NBR-northern Basin & Range regime; SRP-Snake River Plain regime; HL-Hebgen Lake regime; NRM-Northern Rocky Mountain regime; PNW-Pacific Northwest regime; SBR-Southern Basin & Range regime.

plane. Therefore, for a given earthquake, the calculated P-axis can be off by as much as 40° if preexisting structure is involved (Sbar, 1982), as discussed above.

Characterization of the stress regime in the Cascades is not well constrained. The use of focal plane solutions is limited by the fact that the area is relatively aseismic. Zoback and Zoback (1980) have summarized much of the existing data that pertains to the contemporary stress distribution in the western US. Their data base is shown in Figure 29. They have few in-situ stress measurements in the Pacific Northwest Region, in general, and none in the southern Cascades. In the southern Cascades, they rely heavily on data such as microfaulting in the Sierras (Lockwood and Moore, 1979) which cannot be well constrained in time. The lack of data points in the vicinity of the northwestern B&R and Cascades is particularly noteworthy because these are areas of active contemporary tectonics.

Vent Alignments

For the study of the southern and central Cascades region, emphasis in the present study has been placed on the development of stress trajectory data by the analysis of relatively recent vent alignments in order to better characterize the tectonic stress environment. This is a valuable tool here because of the abundance of such vent alignments and the availability of maps and imagery from which these vents can be evaluated. The value of the use of these vent alignments is enhanced by the lack of seismicity or in-situ measurements for determining stress orientations. The

trajectories used are limited to volcanics less that 5 million years old and the analysis therefore reflects the stress which has dominated the region within the last five million years -- the period during which the High Cascades have developed (Leudke & Smith, 1983; Priest et al., 1983).

The rationale for this effort is as follows. In undeformed rock, intrusions will inject planar dikes perpendicular to the minimum horizontal stress. Alignments of vents which represent the intersection of a given dike with the ground surface will thus trace the orientation of the maximum horizontal stress. Vent alignments which display topographic continuity from one vent to the next in an alignment can be considered to either have been fed by the same dike or to have been channeled during emplacement to parallel the first dike emplaced. In either case, the alignment orientation will reflect the dike orientation and therefore the MHS (within a few degrees of azimuth).

This is an extensional phenomena. In rock possessing preexisting fractures or zones of weakness, intrusions may follow zones of weakness wherever the sum of the tensional strength and the normal stress across the preexisting structure is less than the sum of the minimum horizontal stress plus the tensional strength of intact rock. However, the tensional strength of intact rock is low -- on the order of one-tenth the compressive strength -- and, in general, extensional terrains are characterized by ongoing faulting which is roughly perpendicular to the inferred extension direction.

In the Cascades of Oregon, the dominant preexisting structures -- related to the Western Cascades -- are NE and NW striking faults (Kienle et al., 1981) and Figure .

The general dominance of N-S orientations of vent alignments in the Cascades suggests that these alignments are not following these preexisting trends. In the Cascades of northern California, the vent alignments are dominantly NNW. This trend is parallel to ongoing faulting in the Basin and Range immediately to the east. Because the orientation of these faults does not parallel Western Cascades faulting and does parallel the B&R faulting, the role of preexisting structure is not indicated. Preexisting conjugate faulting (NNE and NNW) in the B&R has been proposed (Donath, 1962). If this faulting preceded Basin and Range deformation (and is therefore preexisting structure) and is being remobilized by extensional deformation, the occurrence of vent alignments still provides information about the stress regime because it indicates which of the two conjugate directions is closer to the MHS. This is very important for determining the contemporaneous tectonic stress regime.

The question of whether the vents are erupting from a dike-like intrusion or from individual pipe-like conduits has been addressed in the literature. With isolated vents, a pipe-like conduit is a possibility, however the presence of multiple aligned vents by itself strongly favors the dike model. This question has been studied in some detail by Fink and Pollard (1983) for silicic domes at Medicine Lake caldera; by Eicheiberger et al. (1985) at the Inyo (rhyolitic) domes north of Long Valley Caldera -- including drilling confirmation; and by Pollard et al. (1983) on Kilauea. They find compelling evidence for the dike-fed model for alignments in these examples which are from a variety of magma environments and compositions. The most convincing evidence for dike intrusion feeding rhyolitic domes is the drilling at Inyo Domes north

of Long Valley where actual drilling and coring of the dike was carried out at two localities along the line of vents -- between vents. The existence of a continuous dike feeding a sequence of domes was confirmed. At Kilauea, typical rift eruptions begin as a curtain of fire (in some cases kilometers in length) which then narrows with time to one or a few isolated vents on the original rift alignment, where the subsequent construction of significant cones takes place. This sequence is best explained by the dike model whereby the original curtain of fire represents the intersection of the upper edge of the dike with the surface.

The use of dike orientations to interpret tectonic stress is most strikingly demonstrated by the pioneer work in the Spanish Peaks area of Colorado by Ode (1957) and later elaboration by Muller and Pollard, 1977. In this effort, mapping of the dikes associated with the intrusion of Spanish Peaks dramatically reflects a stress pattern influenced by the presence of the adjacent Rocky Mountains to the west. Nakamura (1977) and Nakamura et al. (1977) have carried this concept to a more regional scale, utilizing dikes and vent alignments in a number of arc environments to map the minimum horizontal stress; and obtaining stress trajectories that display a regional continuity and describe a stress distribution that can reasonably be interpreted to reflect contemporary tectonic stress.

In the evaluation of vent alignments, stress effects from topography -- particularly volcanic edifices -- must be considered (Fiske and Jackson, 1972). To avoid the influence of edifice effects (gravitational stresses within large volcanic landforms due to the edifice itself) only monogenetic vents (cinder cones and

fissures) are used in the present study. Polygenetic vents (large stratovolcanoes and shields) are likely to reflect a stress distribution which is a convolution of the gravitational stresses within the edifice and the regional stress -- rather than just the regional stress. Therefore, alignments of cones on the slopes of steep-sided polygenetic edifices have been generally avoided as stress trajectory indicators.

One other consideration in evaluating such alignments is the possibility of cases where fortuitous proximity of cones might occur such that parallel, but offset, en echelon dikes are intruded producing an apparent vent alignment at a significant angle to the actual dike orientation. To avoid such situations, alignments are utilized only where the long axis of the cones parallel the overall alignment.

Volcanic vents (less than 5 my old as identified on the 1:1 million mapping of Luedke and Smith (1983)), were examined on topographic maps (1:24,000 and 1:62,500), U-2 imagery (variable scales) and low altitude oblique photography to evaluate the geomorphic continuity between vents. In a number of cases, Luedke and Smith's (L&S) maps omit vents which are evident on the imagery. In the listing in Appendix B, both the actual number of vents observed on the imagery and the number indicated on the L&S map are shown.

Vents are determined to have geomorphic continuity where contours enclose two or more vents, generally at one-quarter to one-third of the cone height. Surrounding topography is taken into consideration and alignments are not used where elongation may be due to topography (eg. eruption on a steep slope). (Although Landsat and Seasat scales alone were found to be too small for satisfactory evaluation of

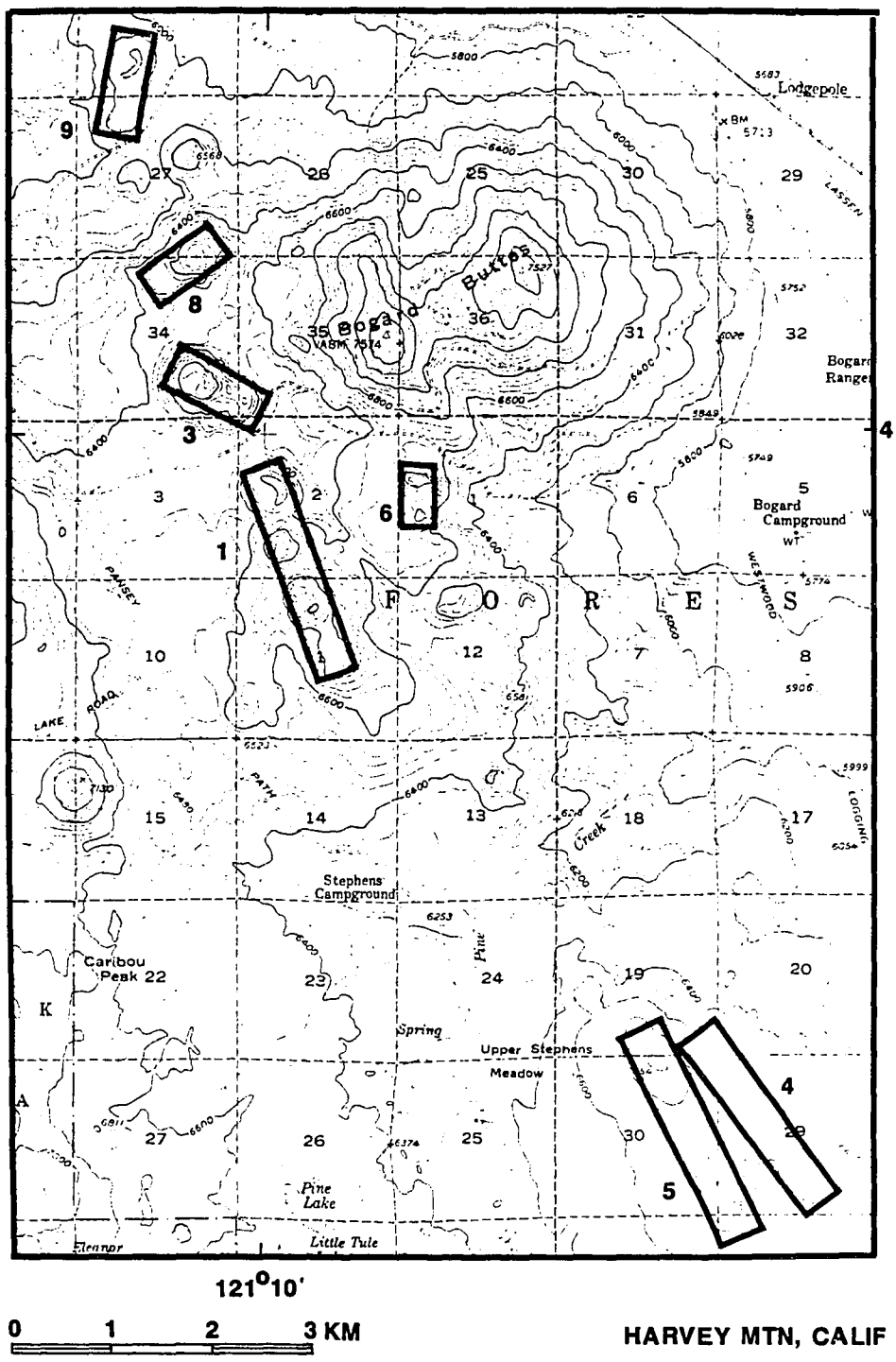

Figure 30. A. Examples of Vent Alignments Used for Stress Trajectory Determinations: Harvey Mtn, Calif., East of Lassen.

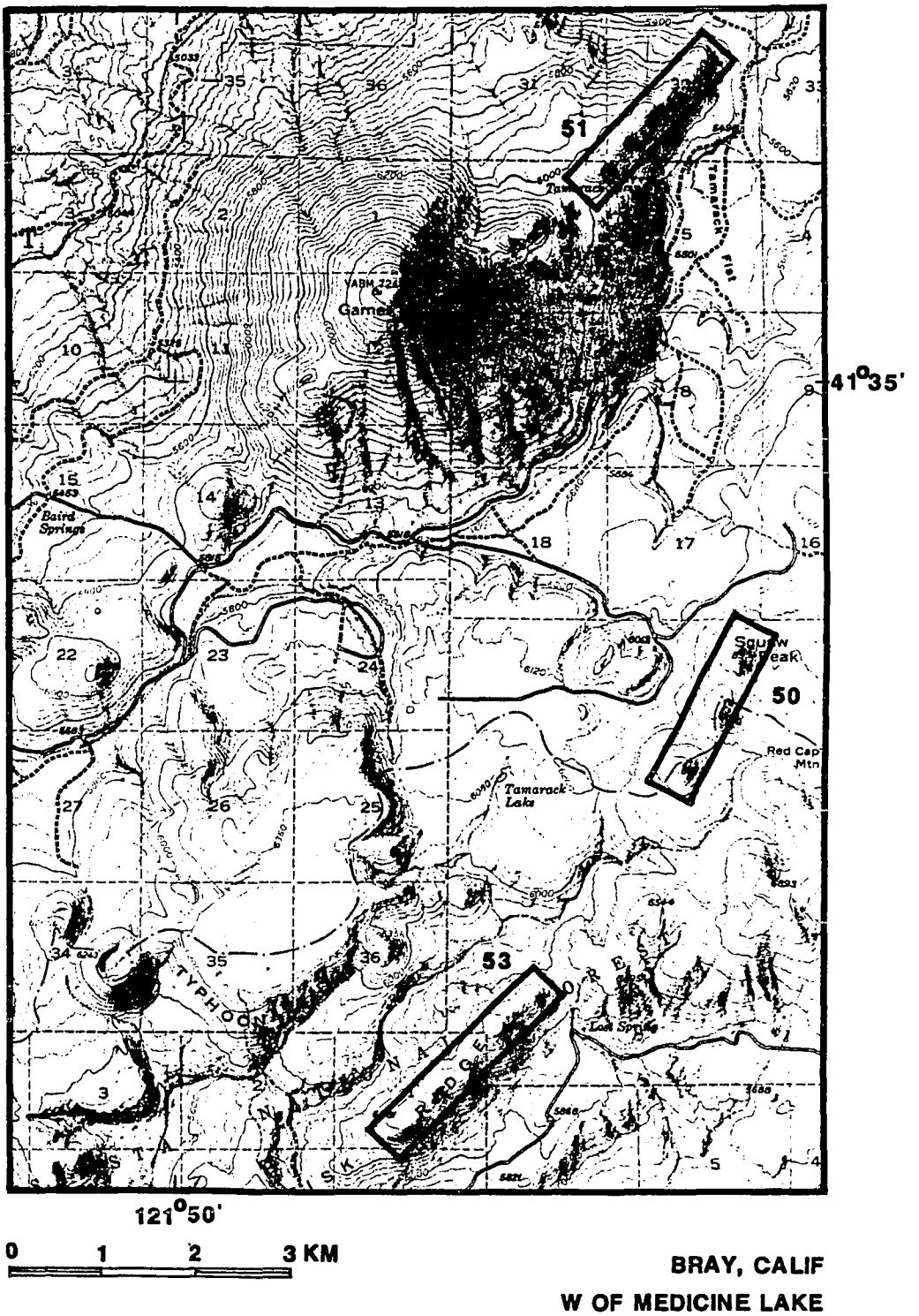

Figure 30. B. Examples of Vent Alignments Used for Stress Trajectory Determinations: Bray, Calif., West of Medicine Lake.

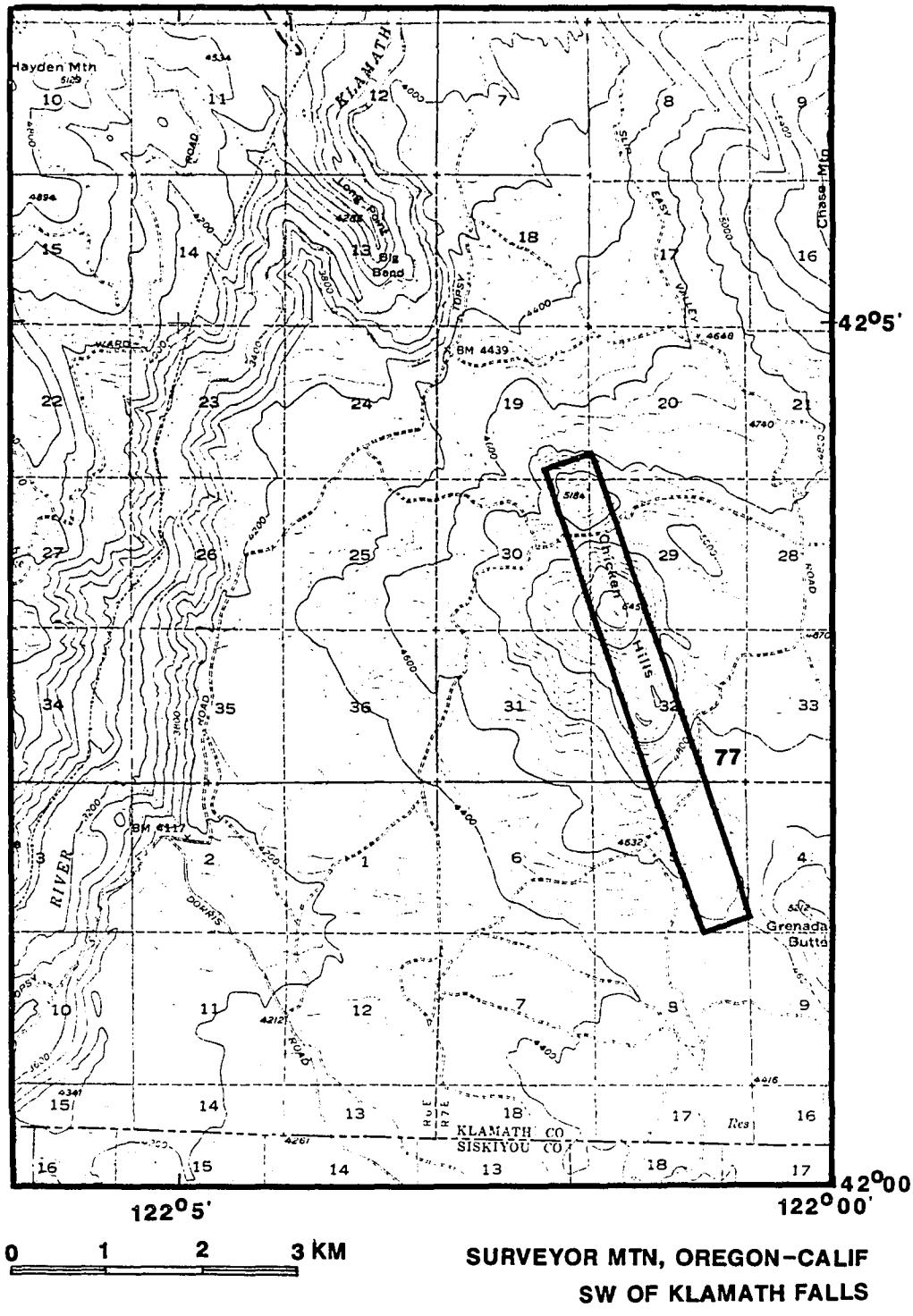

Figure 30. C. Examples of Vent Alignments Used for Stress Trajectory Determinations: Surveyor Mtn., Ore. Calif., Southwest of Klamath Falls, Ore.

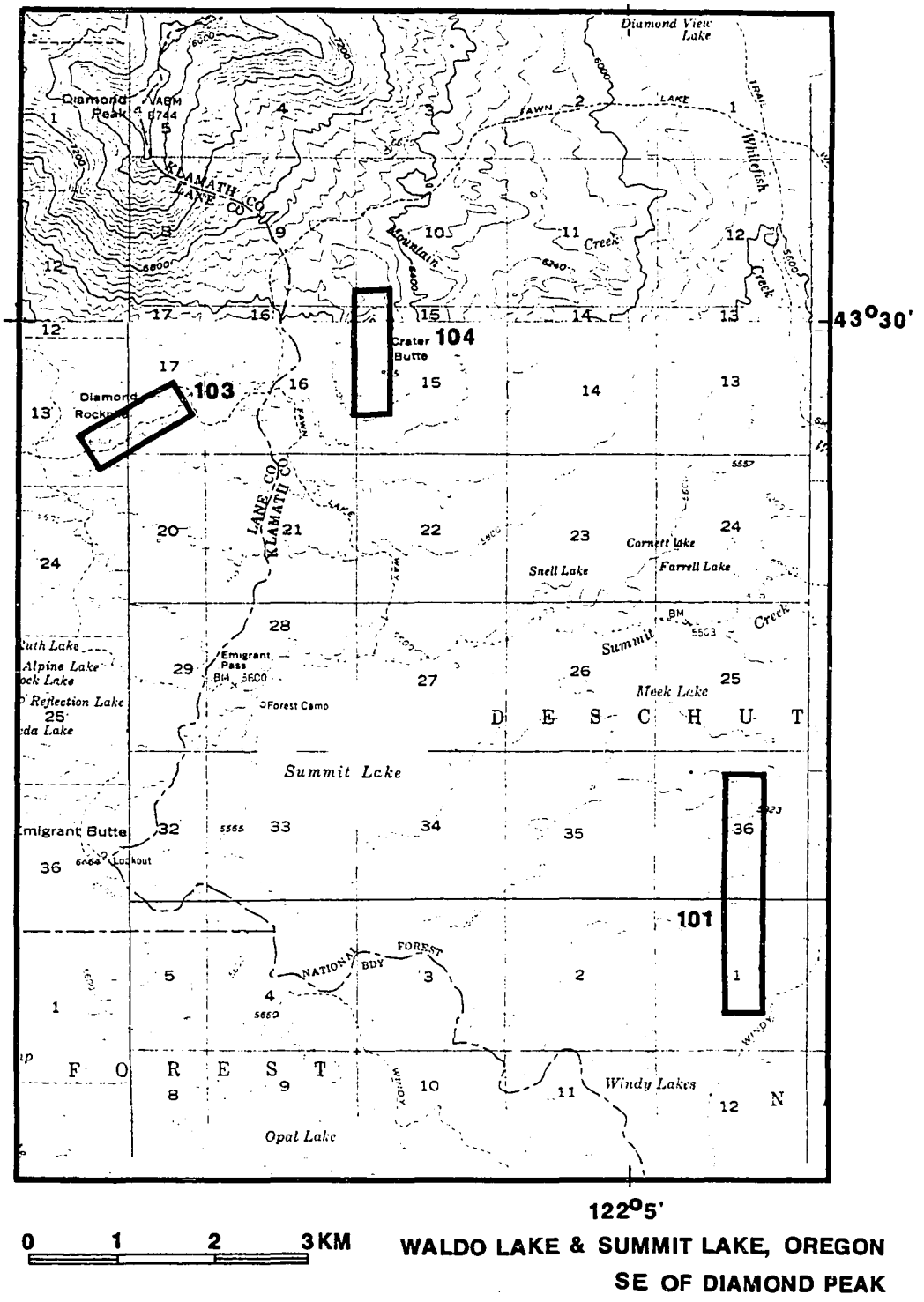

Figure 30. D. Examples of Vent Alignments Used for Stress Trajectory Determinations: Waldo Lake and Summit Lake, Ore., Southeast of Diamond Peak.

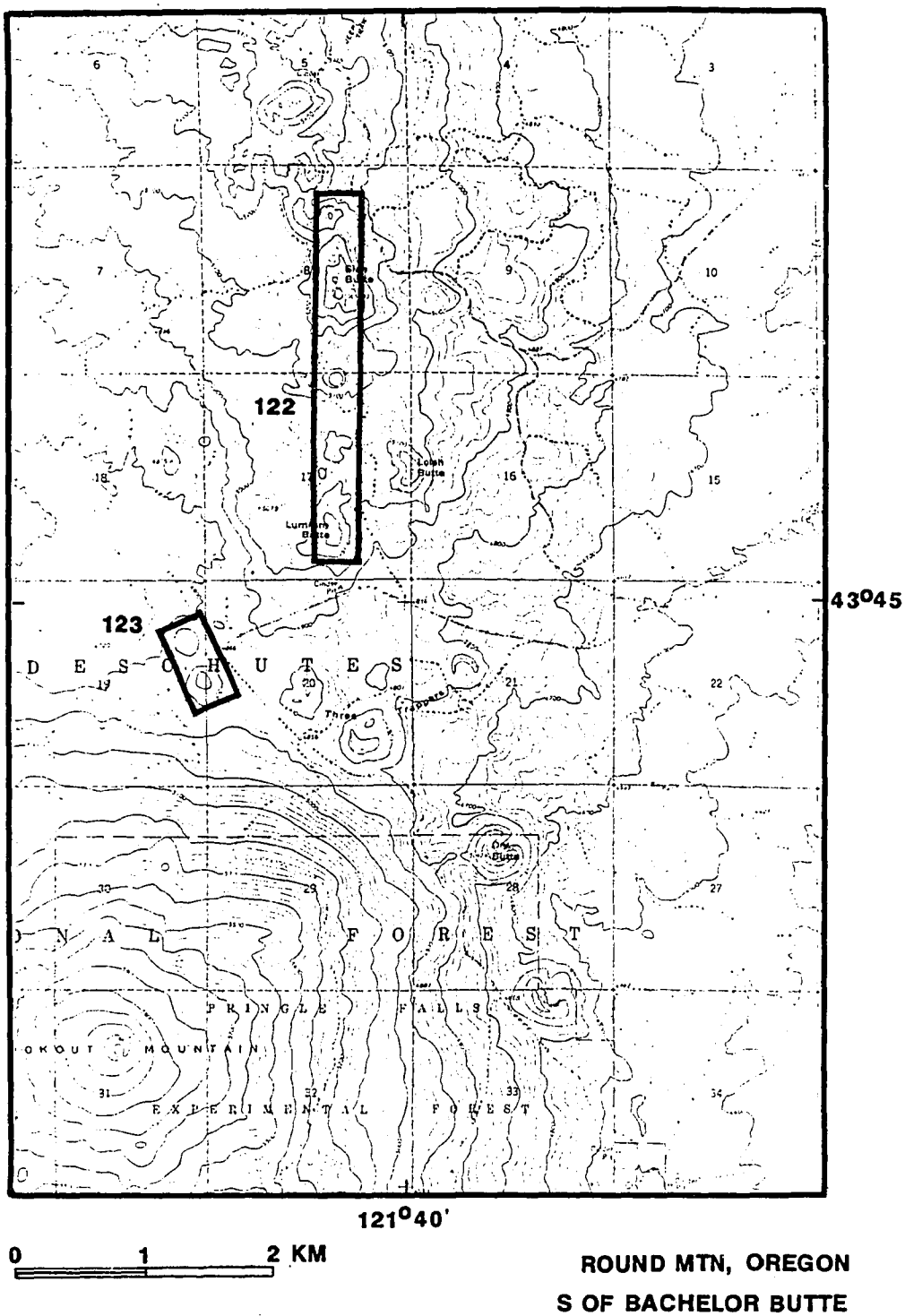

Figure 30. E. Examples of Vent Alignments Used for Stress Trajectory Determinations: Round Mtn., Ore., South of Bachelor Butte.

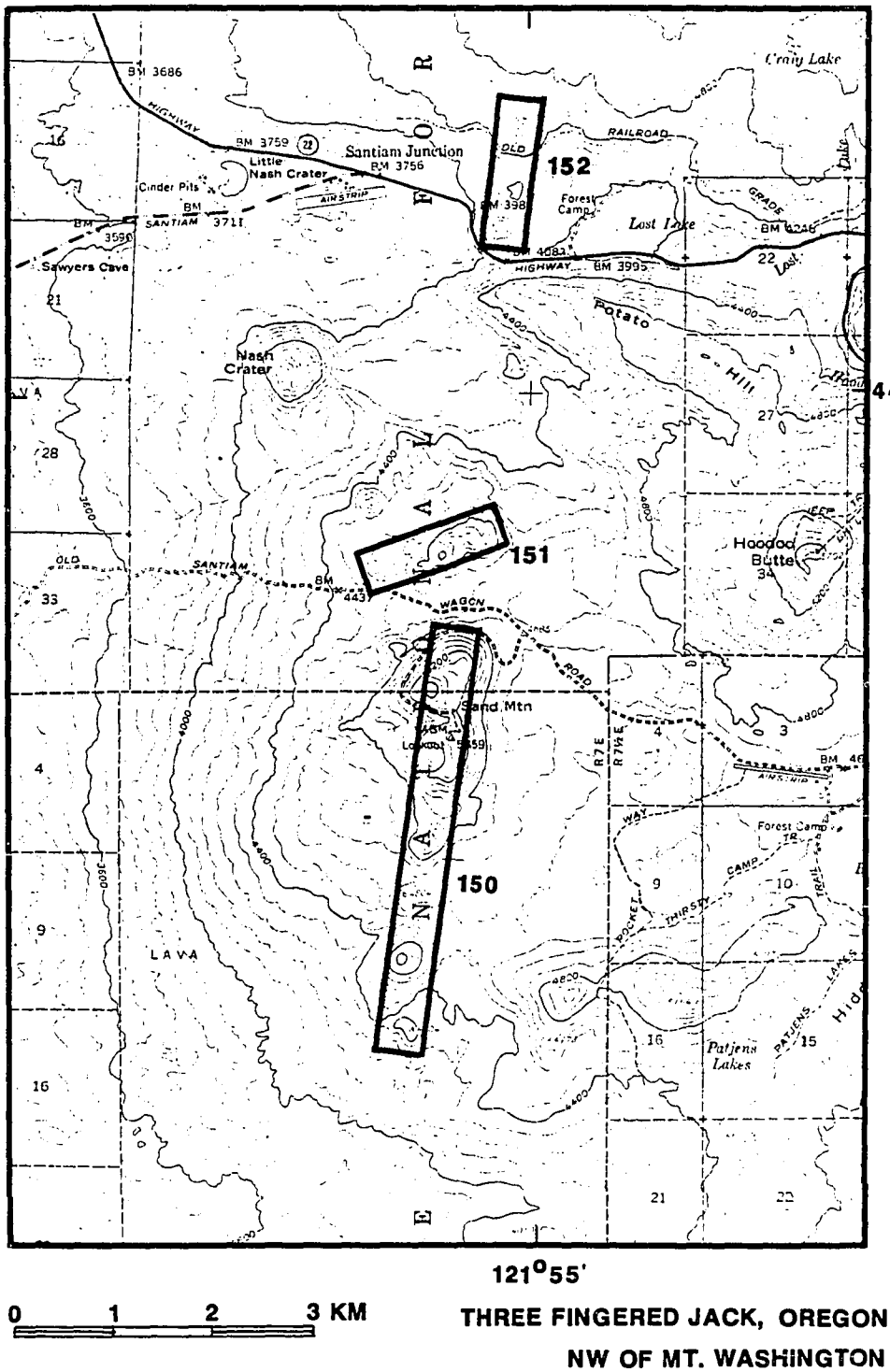

Figure 30. F. Examples of Vent Alignments Used for Stress Trajectory Determinations: Three Fingered Jack, Ore., Northwest of Mt. Washington.

alignments in most cases, a useful data set for this analysis was found to be the combination of Landsat, topographic quads, and the U-2 stereo high altitude CIR. Examples of alignments identified as indicators of maximum horizontal stress trajectories are shown on Figures 30 A through F. Twentyone alignments are shown on these figures out of the total of 175 alignments which were identified during this study (Appendix B).

A detailed geologic map of Newberry Volcano has recently been published (MacLeod et al., 1982) which identifies vent alignments based on field mapping. These alignments could not be rigorously identified by the methods discussed above because in some cases the cones are not geomorphically continuous. Since the continuity of these vent alignments has been verified by field mapping in the Newberry case, these vent alignments (#159 through #178 in Appendix B) have been included on the stress trajectory map (Figure 31). In addition, two vent alignments occur southeast of Newberry in one of the few areas of the US where topographic quadrangle maps are not available at any scale and U-2 imagery is not available. However, these two alignments (#157 and #158, Appendix B) are easily identified on Landsat because each alignment feeds a single recent flow -- the Squaw Mountain and the Bunchgrass Butte flows east of the Devil's Garden. These alignments are also shown on Figure 31. Finally, two vent alignments are found at Diamond Craters, east of Harney Lake, within the BFZ. These are shown on Figure 26.

Where geomorphic continuity was found by the criteria discussed above, alignment location, length and azimuth were recorded. This information is shown on

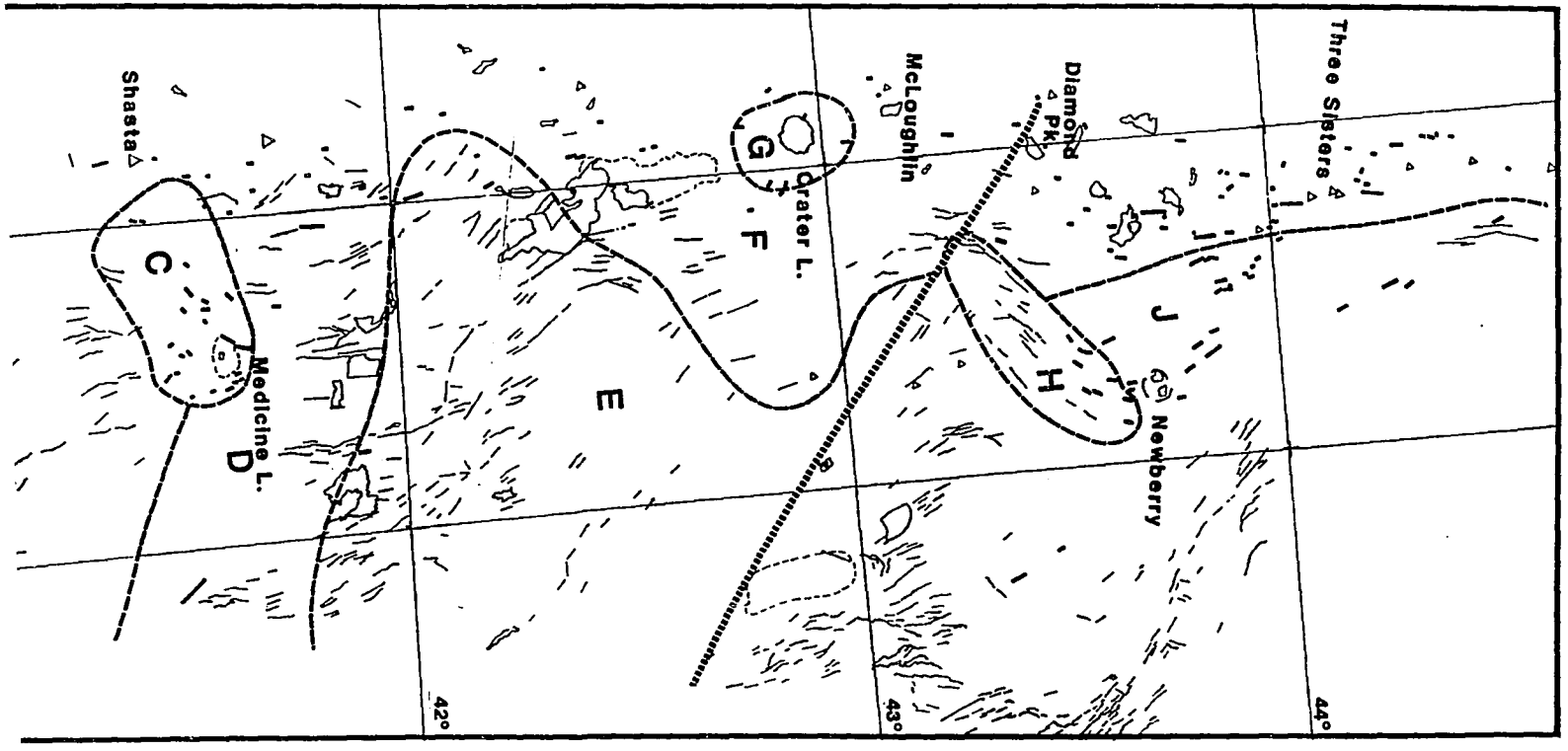

ss Trajectory Map of the Cascades Region showing stress trajectories and dentified on the basis of vent alignments stress trajectory information. Short ıte stress trajectories from vent alignments; fine lines indicate linear landforms with vertical offset indicated; narrow dashed lines indicate stress regime d dashed line is EDZ; triangles indicate major Cascade volcanoes; letters are scussed in text.

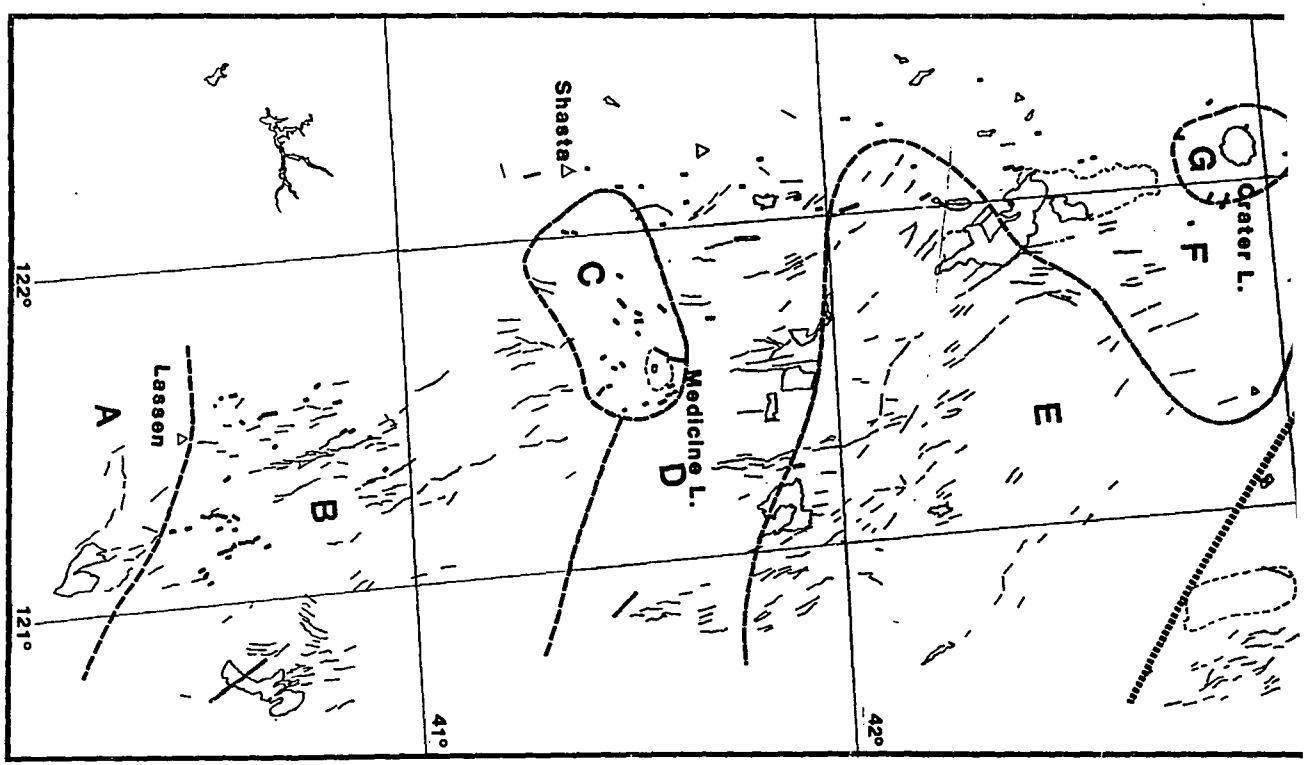

Figure 31. Stress Trajectory Map of the Cascades Region showing stress trajec Stress Regimes identified on the basis of vent alignments stress trajectory informat broad lines indicate stress trajectories from vent alignments; fine lines indicate linear (from Landsat) with vertical offset indicated; narrow dashed lines indicate stre boundaries; broad dashed line is EDZ; triangles indicate major Cascade volcanoes; l stress regimes discussed in text.

the map on Figure 31 and is tabulated in Appendix B. Figures 32 A and B show azimuth frequency plots. In addition, the stress trajectories are shown on Landsat Color composite images in Figuure 33 A and B. The correlation between the stress trajectories and the geomorphic expression of ongoing tectonic deformation associated with Basin and Range elements east of the Cascades is evident.

This data set encompasses all of the obvious indicators of regional stress that can be identified in the vent alignment occurrences. Doubtless some alignments which are valid stress indicators were eliminated because of the restrictions which have been placed on "allowable" alignment identification. However, the continuity of vent alignment orientations within the various regimes identified on Figure 31 argues that the alignments identified do reflect the general regional stress conditions with a degree of accuracy which is at least as good as that derived from other indicators of regional stress -- focal plane solutions and in-situ measurements.

An azimuth frequency plot for this data is shown on Figure 32 A and B. For a given traverse direction (in this case N-S), this plot depicts the number of alignments which fall within a given azimuth range (Wise and McCrory, 1982). Figure 32A gives the azimuth frequency plot (AFP) for all alignments identified; Figure 32B shows the AFP for those alignments of more than three vents. The latter plot therefore represents a higher confidence level (but lower resolution) indication of regional stress. To permit evaluations of these plots as representative of the Cascades axis, the stress trajectories in the vicinity of Newberry (#159 - #178) are not included in these AFP plots (these trajectories are however shown on the map on Figure 31).

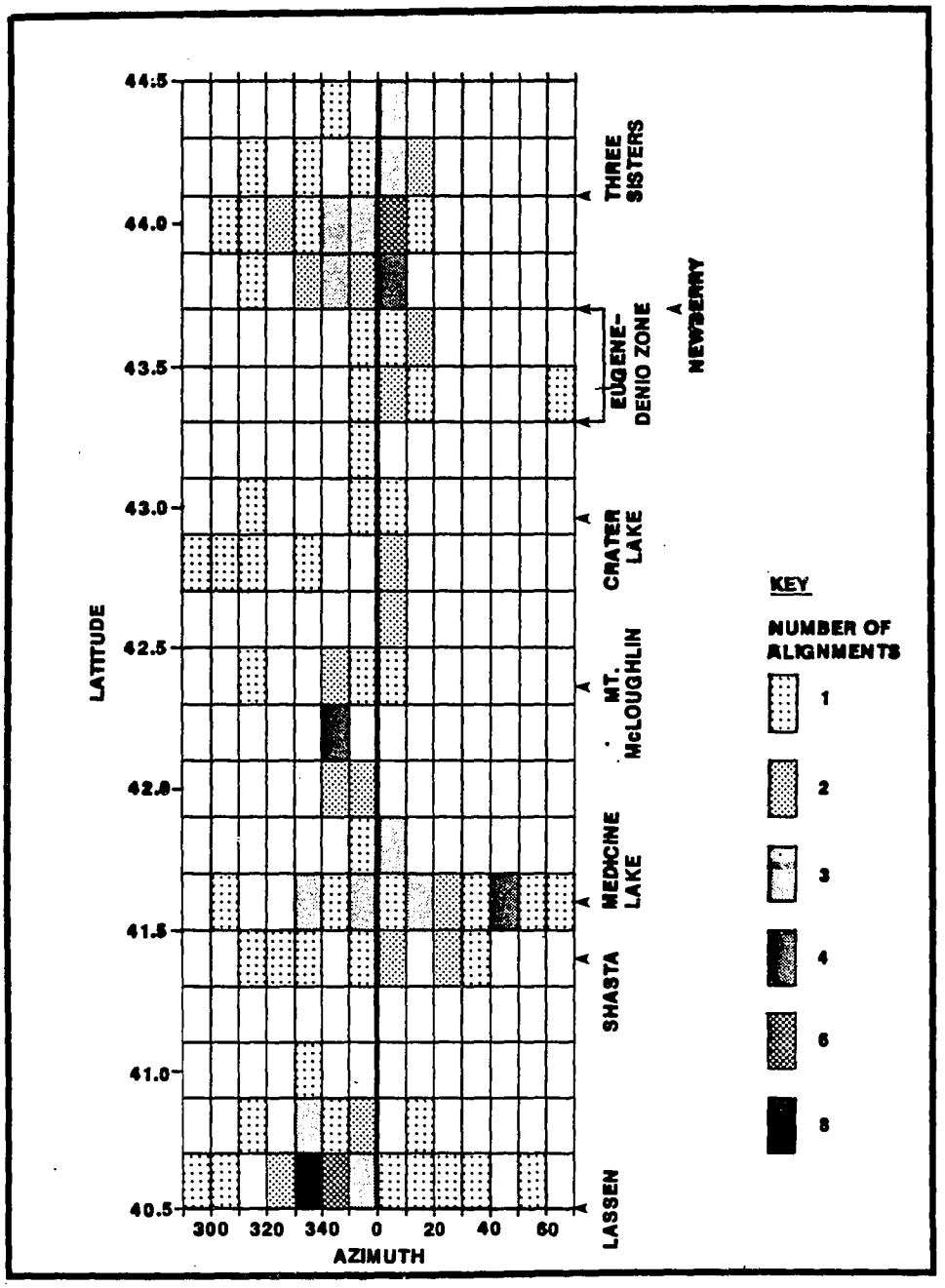

Figure 32. A. Azimuth Frequency Map showing the orientations of Maximum Horizontal Stress trajectories for the High Cascades (exclusive of Newberry) based on the vent alignment trajectories shown on Figure 31 -- all alignments are shown. The plot shows the variation of orientation along a north-south traverse as a function of Latitude. (No alignments occur west of 290° or east of 70°.)

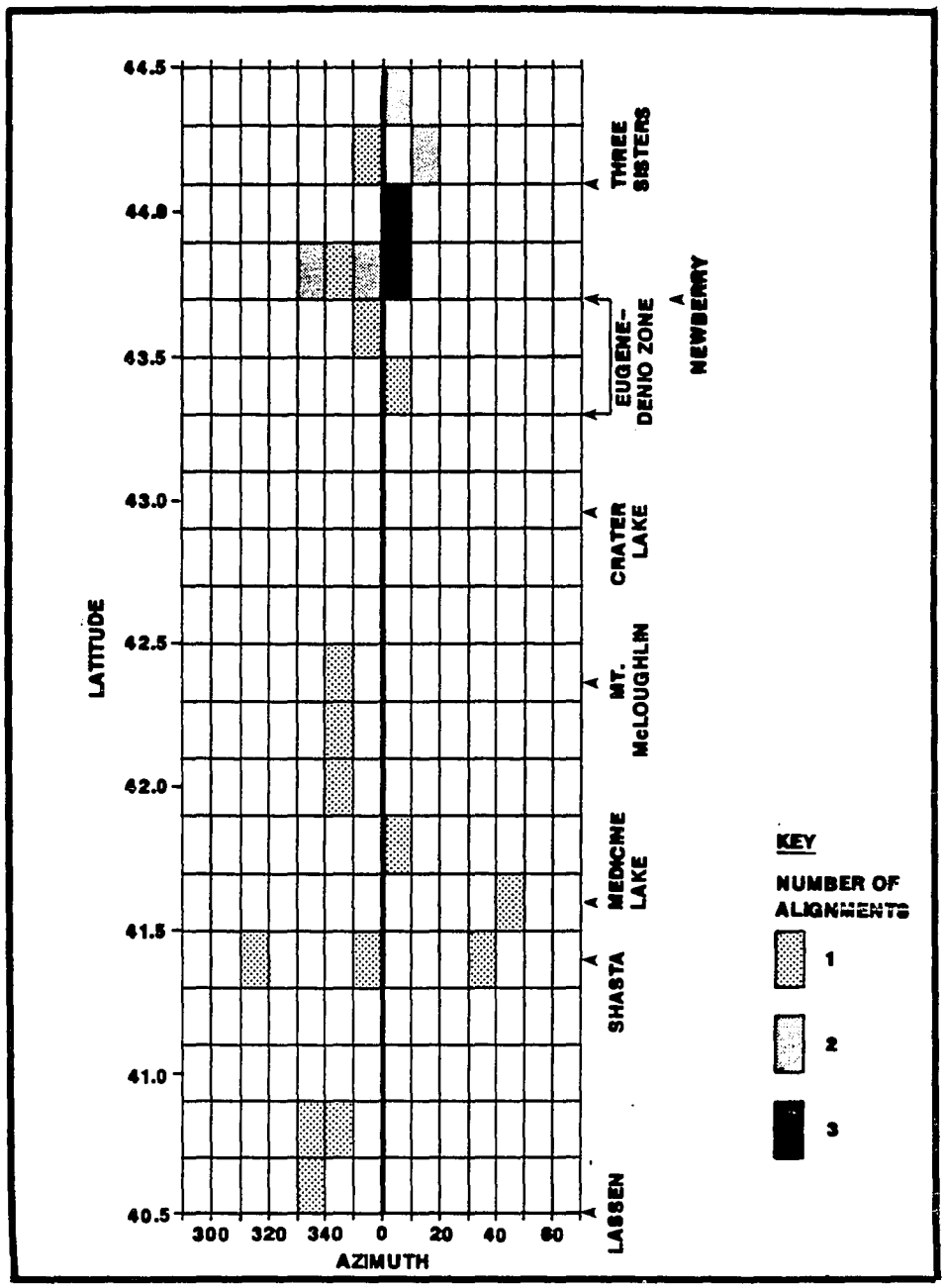

Figure 32. B. Azimuth Frequency Map for the High Cascades (exclusive of Newberry) -- showing only alignments with more than 3 vents. This provides a higher confidence/lower resolution presentation of the data shown in Figure 31 and 32A.

Figure 33. A. Landsat mosaic showing stress trajectories: Lassen to Calif.-Ore. border. Yellow lines are vent alignment stress trajectories; fine lines indicate linear topographic features with vertical offset. A-Lake Almanor; B-Lassen; C-Hat Creek Graben; D-Fall R. Valley; F-Medicine Lake Caldera; G-Shasta; H-Goosenest; dashed line Ore.-Calif. border.

Figure 33. B. Landsat mosaic showing stress trajectories: Calif.-Ore. border to Mt. Jefferson. Line symbols same as Figure 33A; A-Three Sisters; B-Newberry Caldera; C-Blue Mtns.; D-Brothers Fault Zone; E-Bald Mtn. Caldera; F-Diamond Pk.; G-Crater Lake; H-Summer Lake Graben; J-Klamath Graben; K-Mt. McLoughlin; L-Yamsay Mtn.; Sprague R. Valley; Drews Reservoir.

Stress Regimes

From these stress trajectories, nine stress regimes have been identified as indicated by zones A through H and J on Figure 31. Landsat linear features, generally corresponding to mapped fault scarps with a component of vertical motion, are also shown on Figure 31. The stress regime boundaries which are defined on the basis of the stress trajectory orientations are also reflected in the orientations of these linear features. (Stress regime A (for which no vent alignments were identified) is defined solely on the basis of Landsat linear features and mapped faulting.) The Landsat images, with stress trajectories, are shown on Figures 33 A and B. (These may be keyed to associated maps -- particularly Figures 13, 15 and Plate 1.)

The stress regimes are described briefly below and shown on Figure 31). The significance of these zones is integrated with other data in subsequent sections of this chapter.

(A) Lassen - Lake Almanor: Although no stress trajectories were identified in this area, WNW to NW - trending faulting, roughly parallel to the Walker Lane trend characterizes this regime. (The Honey Lake fault, a right-lateral fault thought to be related to the Walker Lane is located 40 km to the east.) Lake Almanor is located in a graben between two NW-trending faults which strike toward Lassen (see Plate 1 and Figure 25). These faults trend in the

direction of Mt. Shasta which is located 120 km to the NW. Some NW faulting extends NW of Lassen (toward Shasta), however this faulting generally cuts older (pre-Quaternary) volcanics.

(B) Between Lassen and Medicine Lake: This regime is dominated by NNW to nearly N-S trajectories that strike from Lassen and vicinity toward Medicine Lake Caldera. The orientation of this regime appears to be influenced by Basin and Range faulting. A number of grabens are controlled by these faults including Hat Creek Graben and Fall River Valley Graben which mark the western limit of Basin and Range development and also are generally coincident with the western limit of Quaternary-Recent volcanism -- suggesting that recent volcanism is more controlled by B&R structure. Stress trajectories at Mt. Shasta also reflect this orientation (although they may be influenced by edifice stresses).

(C) Medicine Lake - Shasta: The area between Medicine Lake caldera and Mt. Shasta is characterized by variable stress trajectories ranging from NW to ENE. These trajectories may reflect the influence of radial maximum stress orientation associated with uplift related to magma chamber development beneath Medicine Lake Caldera (Heiken, 1978). However, an elevated area -- Medicine Lake Highlands -- extends from the foot of Mt. Shasta to Medicine Lake and is about 20 km wide and stands about 330 m above the surrounding landscape. Low gravity and low magnetic signatures corresponding with Medicine Lake Highlands suggest that anomalous thermal

activity (above Curie Point) may be a factor in the stress regime here (Blakely et al., 1985) and that magmatic, or at least thermal, communication may exist between Shasta and Medicine Lake.

(D) Between Medicine Lake and the Oregon border: trajectories in this area are dominantly N-S. On the west, this trajectory orientation parallels the Shasta - Mt. McLoughlin volcanic axis, a long-standing volcanic axis that, farther north, has become inactive as the arc has migrated to the east. In the eastern part of this stress regime zone, N-S faulting parallels faulting of similar orientation located to the east in the Basin and Range.

(E) South Klamath Lake and east of the Cascades: This regime is characterized by NNW-trending stress trajectories south of Klamath Lake which parallel the prominent normal faults that control the southern Klamath Graben. Farther east, NNW to NW Basin and Range faulting parallels this trend. Two vent alignment stress trajectories of this trend are found SE of Newberry (east of Longitude 120°W).

(F) North Klamath Lake and the Cascades Axis to the north: This regime is the dominant orientation for the Cascades axis from Klamath Lake to at least Mt. Adams. N-S stress trajectories are particularly well developed along the east side of the volcanic axis from Hamner Butte (east of Diamond Peak) and northward to Mt. Jefferson. This portion of the Cascades is characterized by a greater abundance of vents, both monogenetic cones and moderate-sized stratocones such as Hamner Butte, Davis Mountain,

Sheridan Mountain and Bachelor Butte. Such a style of volcanism is generally associated with a more extensional regime than the high stratovolcanoes which dominate the Cascades to the north and south. Between Diamond Peak and Three Sisters -- opposite regime H -- the volcanic axis is broader, with a marked increase in vent density (Figure 24). This area is located opposite Newberry Caldera.

(G) Crater Lake: Stress trajectories around Crater Lake are oriented in a roughly radial pattern suggesting control by shallow magma chamber influences (Bacon, 1985).

(H) Walker Rim and the Southwest flank of Newberry Caldera: Stress trajectories in this zone trend NE to NNE and parallel the large normal faults of Walker Rim -- which bounds the Cascades axis on the east. This stress regime appears to reflect interaction between the tectonics of the volcanic axis and accommodation to the more eastward locus of volcanism to the north and to the tectonics of Newberry.

(J) Newberry to Green Ridge: Stress trajectories north of Newberry trend NNW parallel to regime E (which is located SE of the caldera) and with proximity to the volcanic axis these trajectories rotate to a more N-S orientation to parallel regime F (the Cascades axis). This regime therefore appears to reflect stresses that are transitional between Basin and Range and Cascades tectonics.

Fault Character of the Eugene-Denio Zone

The interpretation of the Eugene-Denio Zone (EDZ) is critical to the understanding of Basin and Range/Cascades interaction. The results of the following discussion indicates that the EDZ should not be regarded as an active feature. In its western part, the character of the EDZ has been further elucidated by the stress trajectory data. The EDZ strikes on an azimuth of 305° (its proposed strike, after Lawrence, 1976, is shown on Figure 34). If this is a major right-lateral strike-slip structure, the maximum stress trajectory should be about 45° from the strike of the fault (Figure 27) -- in this case between an azimuth of 340° to 350°. The azimuth frequency plots, Figures 32 A and B, show the location where the EDZ crosses the traverse of the plot. Within this zone, a total of nine stress trajectories are identified which cluster around an azimuth of 5°. However, no trajectories are found with the 340° to 350° azimuth which would indicate fundamental right-lateral faulting along the EDZ.

There is only one landform which crosses the High Cascades that has the WNW strike of the EDZ and upon which the existence of the EDZ across the Cascades is no doubt heavily based. This feature is the drainage valley of the Umpqua River-Miller Creek which cuts the south flank of Miller Mountain -- about 30 km SSE of Diamond Peak. X-band SAR radar imagery of this area is shown on Figure 35 (see also the Landsat image on Figure 33 B). Miller Mountain is part of a high-standing landform which includes Cappy Mtn and Burn Butte to the north. These features are heavily dissected by the major ENE-trending valley of Little Deschutes River and the WNW-

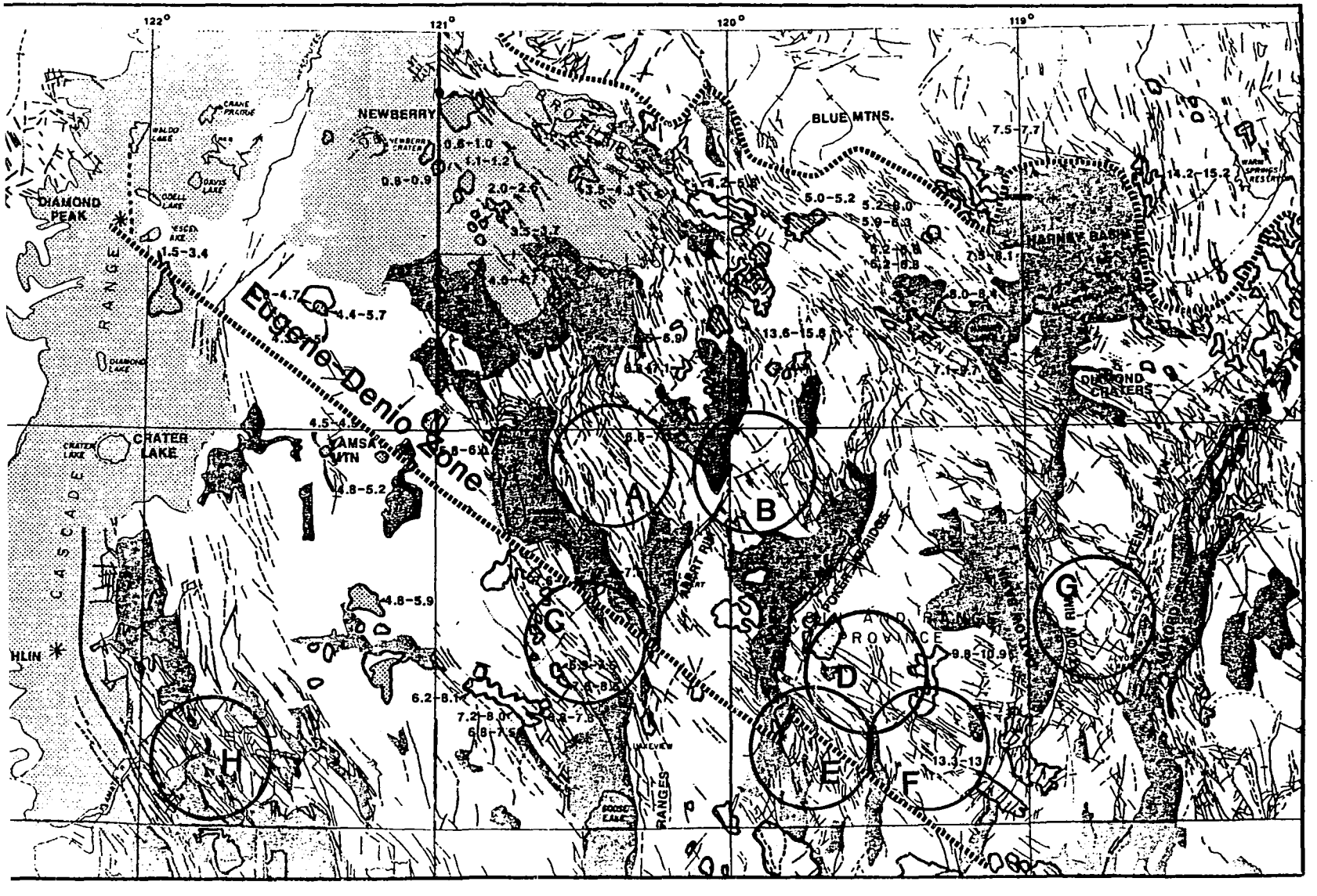
122°
121°
120°
119°
NEWBERRY
BLUE MTNS.
DIAMOND PEAK
CRATER LAKE
HARNEY BASIN
DIAMOND CRATERS
Eugene-Denio Zone
CASCADE RANGE
BASIN AND RANGE PROVINCE
A
B
C
D
E
F
G
H
1
0.8-1.0
1.1-1.2
0.8-0.9
2.0-2.6
1.5-3.4
4.4-5.7
13.6-15.8
4.5-4.8
4.8-5.2
4.8-5.9
6.2-8.1
7.2-8.0
6.8-7.5
9.8-10.9
13.3-13.7
7.5-7.7
14.2-15.2
5.0-5.2
5.2-8.0

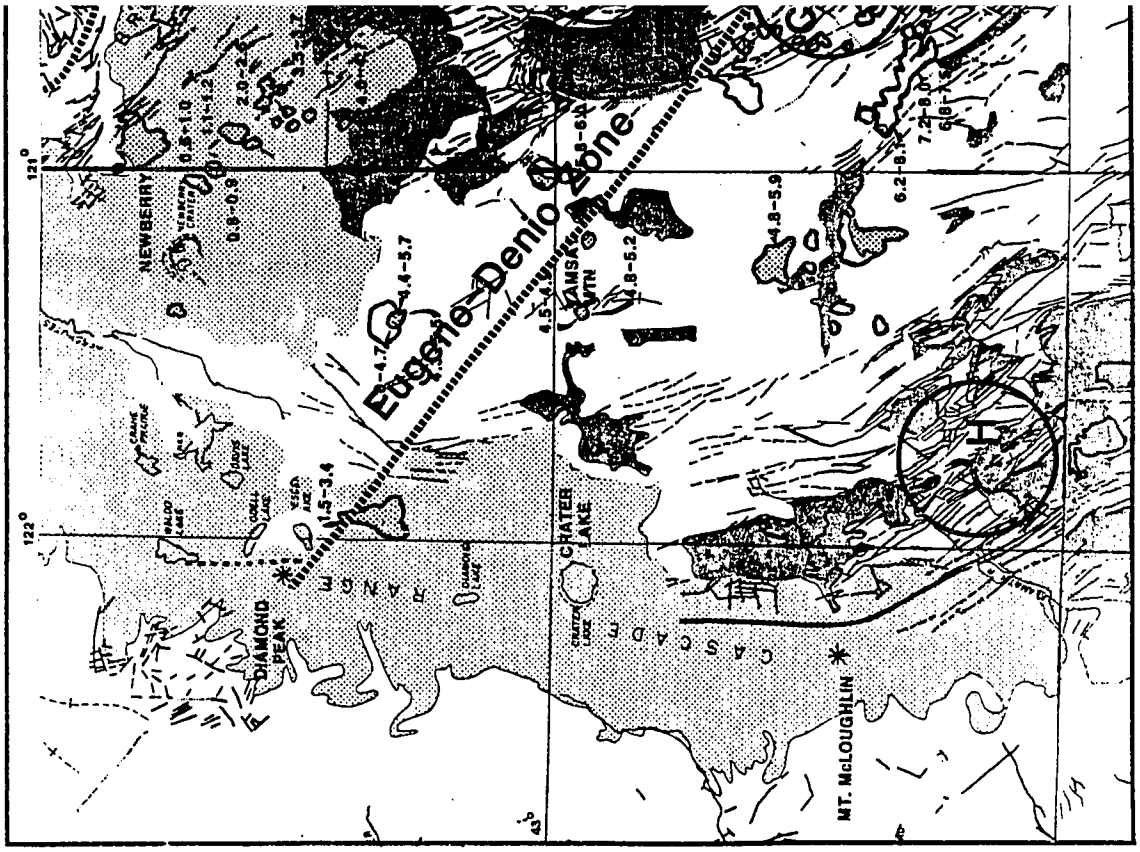

Figure 34. Map of the Eugene-Denio Zone showing faulting and locations of fault-strike analysis subareas (each subarea is 35 km in diameter). Symbols are the same as Plate 1.

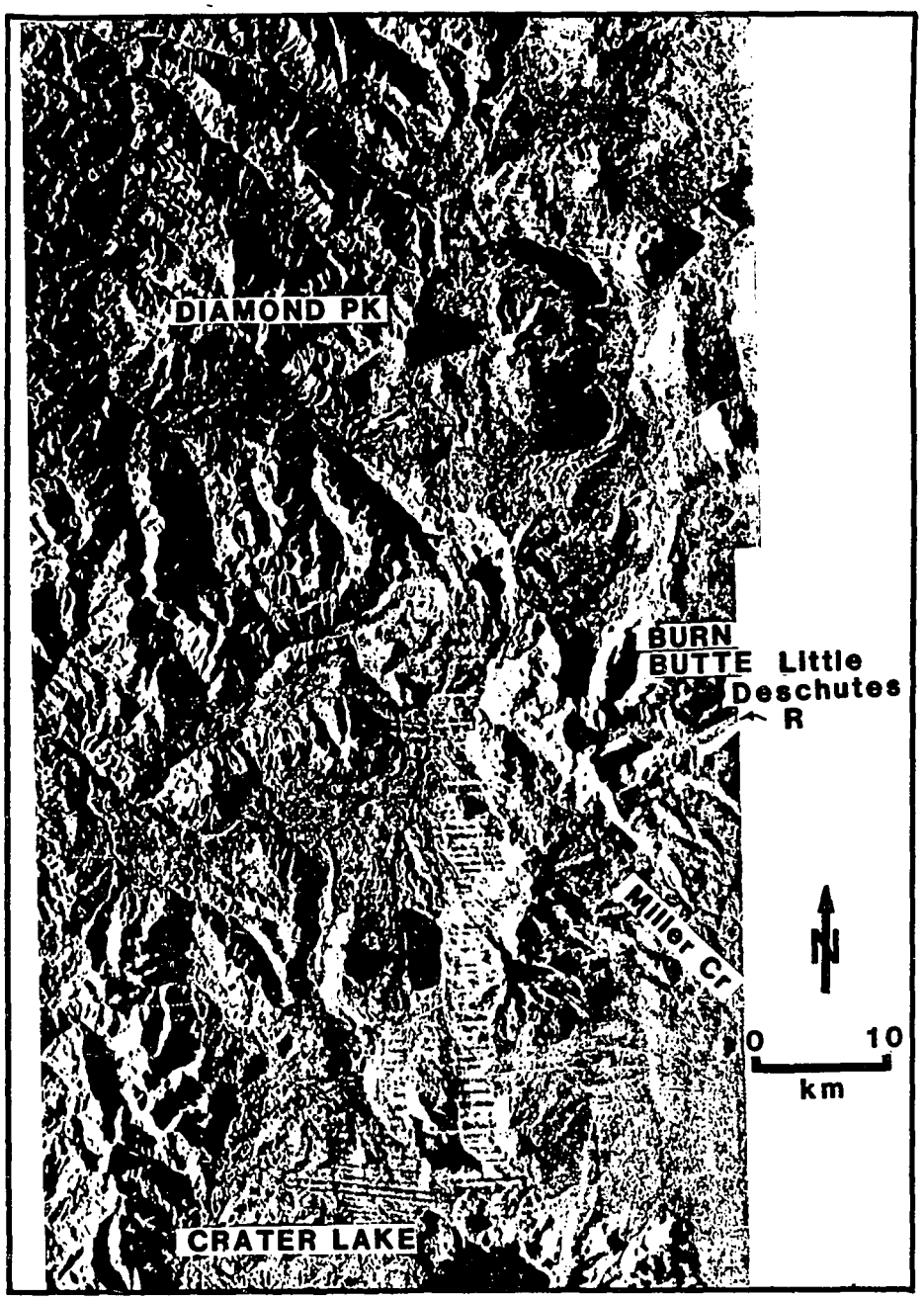

Figure 35. X-band Radar Image of the Burn Butte-Diamond Peak area showing the similarity of the landform of Miller Mountain-Burn Butte to the Western Cascades (western third of the image). Miller Mountain is south of Burn Butte and north of Miller Creek.

trending Umpqua River-Miller Creek Valley. Burn Butte, a rhyolite dome, has erupted on this landform indicating that the landform predates the eruption of Burn Butte which is dated at about 2.45 m.y.b.p. (+/- 0.94). The surrounding High Cascades volcanics are generally less than a million years old in this area (Luedke and Smith, 1982). The WNW trend of Umpqua River-Miller Creek is parallel to one of the directions of stream dissection which is dominant in the Western Cascades (immediately to the west), and Little Deschutes River parallels the other Western Cascades drainage trend. Similarities of this landform to the Western Cascades and the contrast with the surrounding areas of younger volcanism suggests that the Miller Mtn-Cappy Mtn-Burn Butte landform is an outlier of Western Cascades volcanics which reflects the older structure of these mountains and does not reflect any contemporaneous High Cascades-involved deformation. This is supported by the aforementioned lack of post-22 m.y.b.p. movement on WNW faulting farther west (Priest et al., 1983). It is also noteworthy that this Umpqua-Miller feature, even if it was part of the EDZ, strikes south of Diamond Peak and therefore cannot be called upon to account for the offset of the Cascades axis which occurs north of Diamond Peak.

To the east, in the portion of the Basin and Range which is cut by the EDZ, there is little evidence of displacement of landforms indicative of the proposed right slip. Figure 36 shows a Seasat radar image of the Abert Rim area and there is no displacement of Abert Rim evident at the point where the EDZ crosses it. On the other hand, offset is seen on Poker Jim Ridge which may be related to the zone of WNW shearing to the east. The offset, however is left lateral offset -- not the right

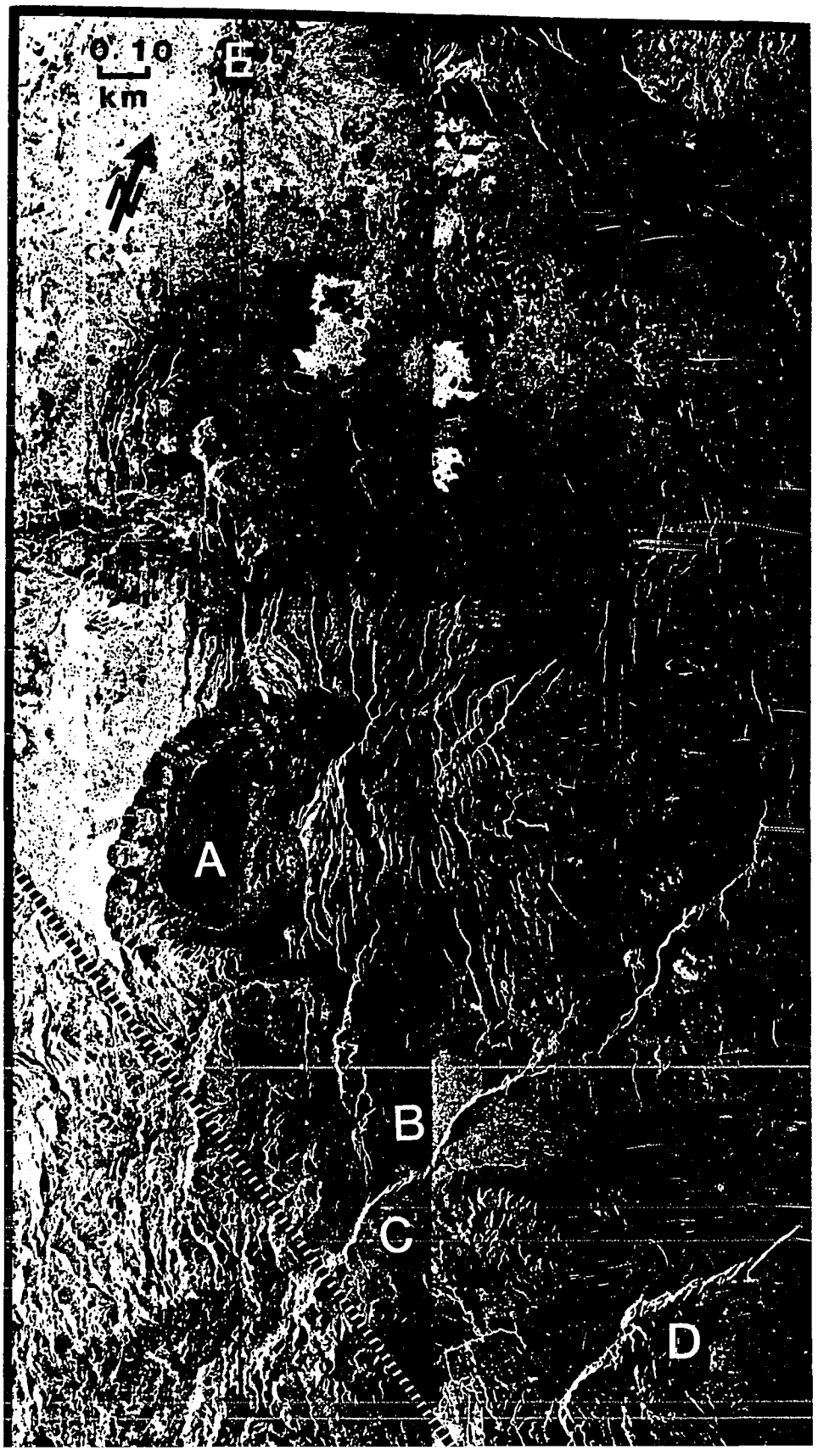
0 10
km
N
A
B
C
D

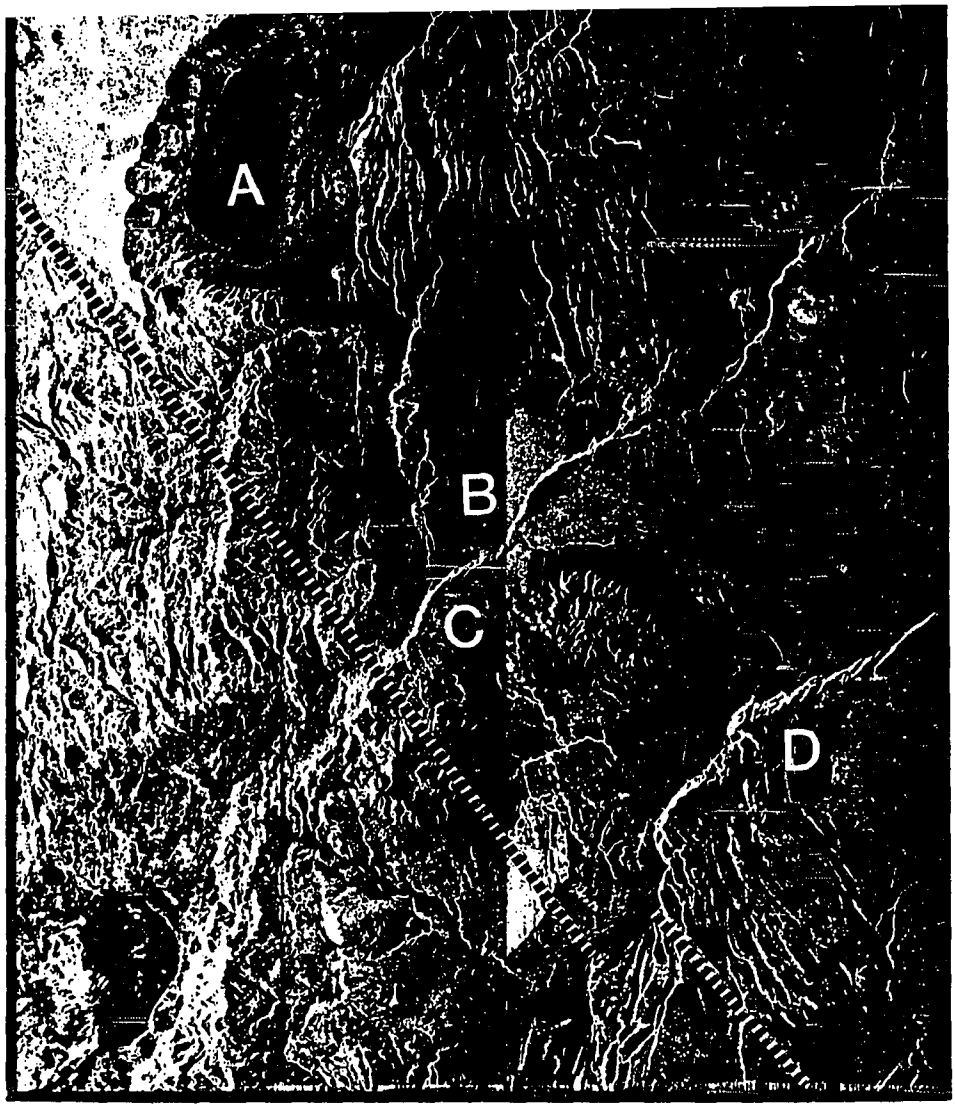

Figure 36. Seasat Radar Image of the Eugene-Denio Zone in the western Basin and Range showing: Summer Lake (A), L. Abert (B), Abert Rim (C), Poker Jim Ridge (D) and Newberry Caldera (E) showing the proposed trace of the Eugene-Denio Zone (dashed line). There is no observable right-lateral offset along the EDZ at Abert Rim and the apparent offset visible at Poker Jim Ridge is left lateral.

lateral displacement proposed for the EDZ. Both Abert Rim and Poker Jim Ridge are major Basin and Range scarps greater than 650m in height. Lack of offset of Abert Rim argues against the existence of a major through-going structure along the EDZ.

Farther east, a fault orientation analysis has been carried out to compare the fault density and orientation of faulting within the EDZ against that found in surrounding areas. At first look, on simple fault maps the EDZ does appear as a zone of higher fault density than surrounding areas. However, numerous basins, filled with recent (unfaulted) sediments, mantle and conceal faulting. These basins are indicated on Figure 34. When the fault map is viewed with the mantled areas excluded, the distinctiveness of the EDZ is decidedly less evident.

This is further examined by the preparation of fault-strike frequency plots which show the number frequency of mapped faults for given azimuth ranges. These plots have been prepared for 8 subareas, each 35 km in diameter, as indicated on Figure 34. Locations of the subareas are chosen to compare areas within the EDZ with those outside it. The results are presented on Figures 37 A,B,C. Such data, conventionally presented as rose diagrams, are presented here as bar plots because of the greater ability of this mode of presentation for discriminating subtle strike variations. Results are presented here in terms of number percent (percent of total number with a given azimuth) and length-weighted percent (percent of total aggregate length with a given azimuth) and data is sorted to bins of 15° of azimuth. In preparation of these data, data was binned to 5°, 10°, 15° and 20° bins. The 15° bin size was found to be the best comprise between resolution and noise.

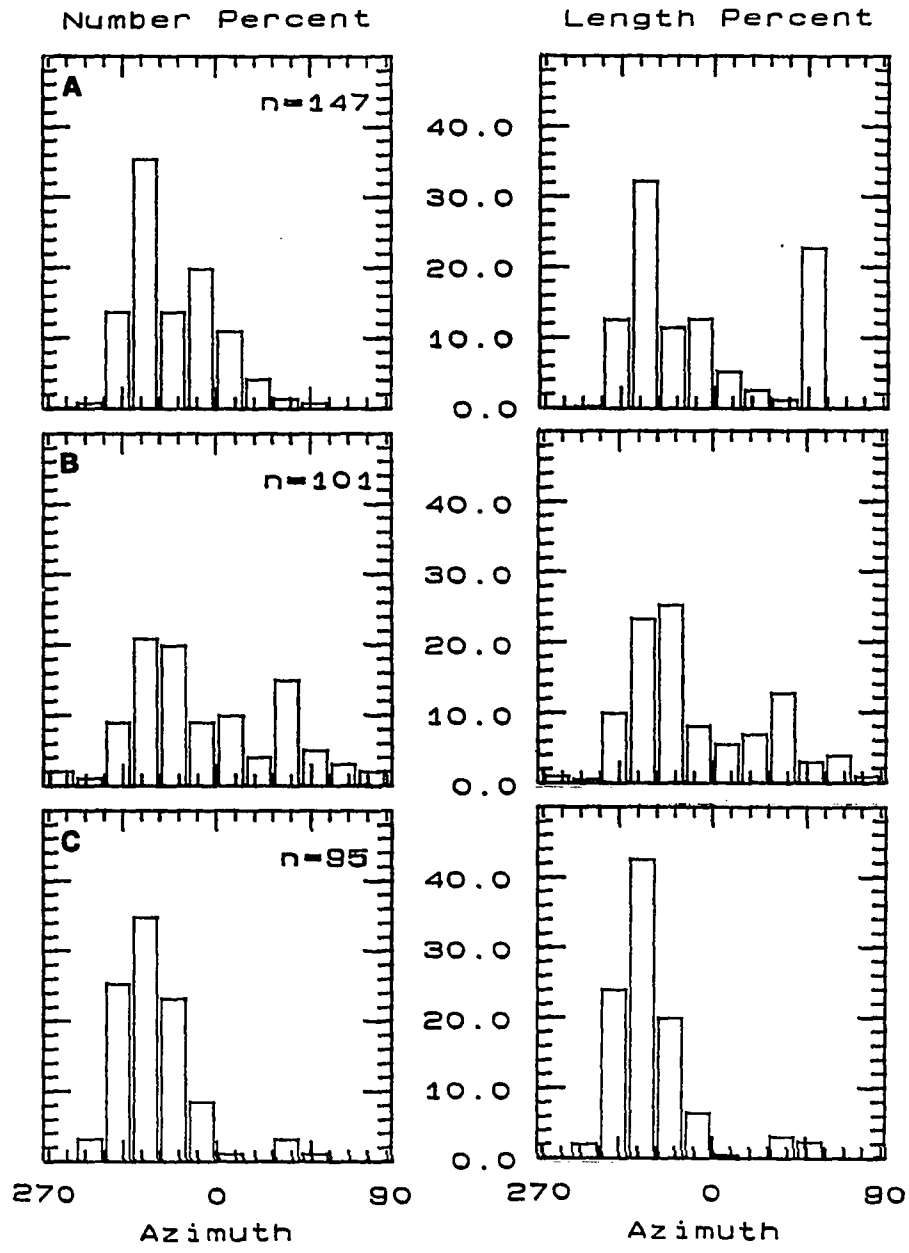

Figure 37. A. Fault strike-frequency plots for the northern Basin and Range for both number percent and length-weighted percent: Subareas A, B, C -- A and B are outside the proposed EDZ while C is within the EDZ. n = number of fault segments used to prepare the plot. See text for additional statistics. Subarea locations shown on Figure 34.

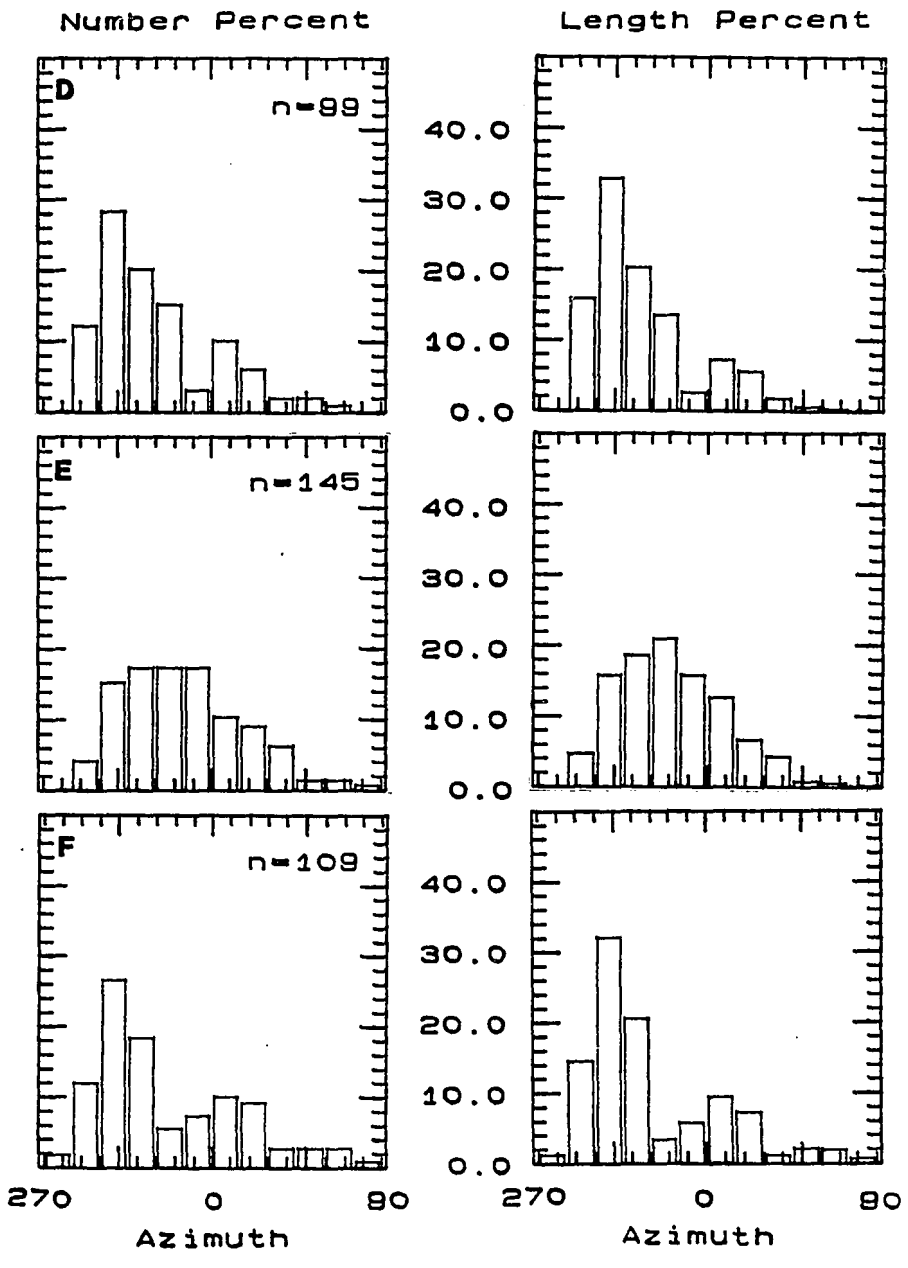

Figure 37. B. Fault strike-frequency plots for the northern Basin and Range for both number percent and length-weighted percent: Subareas D, E, F -- These subareas are within the EDZ. n = number of fault segments used to prepare the plot. See text for additional statistics. Subarea locations shown on Figure 34.

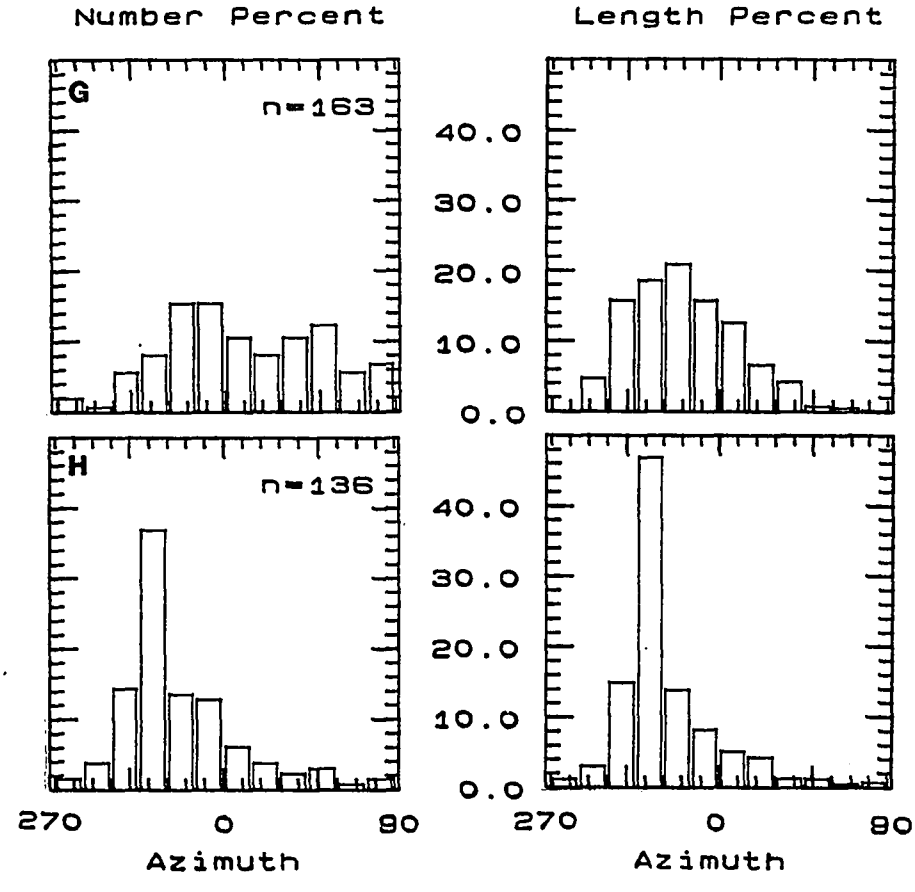

Figure 37. C. Fault strike-frequency plots for the northern Basin and Range for both number percent and length-weighted percent: Subareas G, H -- These subareas are outside the EDZ. n = number of fault segments used to prepare the plot. See text for additional statistics. Subarea locations shown on Figure 34.

The number of straight-line fault segments is shown for each subarea on Figure 37. This is compared with the total number of faults in each subarea and the ratio of straight-line segments to number of faults below.

TABLE 1
Fault Analysis of Subareas Indicated on Figure 34

Subarea	Number of Faults (N)	Number of Straight Segments (n)	Segments/Fault (n/N)
A	103	147	1.43
B	74	101	1.36
C	62	95	1.53
D	60	99	1.65
E	96	145	1.51
F	88	109	1.24
G	103	163	1.58
H	108	136	1.26

Subareas C, D, E and F are within the Eugene-Denio Zone. These areas do not show significant differences in fault density when compared to the areas outside of the zone. Total number of faults for the areas within the EDZ range from 60 to 96 as compared with a range of 74 to 108 outside of the EDZ. The segments/fault parameter -- a measure of the straightness of the constituent faults -- ranges 1.24-1.65 inside the EDZ compared to a range of 1.26-1.58 outside the zone.

Fault orientation does not support the notion of through-going structure. As can be seen on Figure 34, subareas D and F overlap a zone of WNW faulting which is limited to the areas between Catlow Rim (on the east) and Poker Jim Ridge east of Warner Lake. This is reflected in the fact that the highest frequency fault-strike class for subareas D and F, azimuth 300° to 315°, is slightly more westerly than the maximum frequency of surrounding areas, azimuth 315° to 330°. However, this

faulting is absent both to the WNW of Poker Jim Ridge and to the ESE of Catlow Rim -- as well as being less evident immediately to the southwest at Subarea E. The azimuth frequency peak for subareas C and E corresponds to that found outside the EDZ at subareas A, B and H with peak frequency in the 315° to 330° range. Subarea G displays a more diffuse pattern. It is located on Steens Mtn where NNE-NE structure associated with the formation of Alvord basin shows a significant influence on faulting, yielding a second maximum strike frequency at azimuth 45° to 60°, as well as the ubiquitous NNW faulting.

Summarizing the observations relevant to the EDZ:

1) the zone is not continuous in the Basin and Range where its faults are well exposed, and its constituent faults are not en echelon;
2) when the distribution of sediment filled basins, which conceal faulting, is taken into account, there is no significant enhancement of faulting along the EDZ east of the Cascades.
3) the EDZ does not offset prominent linear features which cross it (eg. Abert Rim and Walker Rim);
4) there is no significant seismicity on the zone west of Abert Rim;
5) faults in the Cascades which parallel the EDZ are not active;
6) the vent alignment stress trajectories in the Cascades indicate a stress field inconsistent with the proposed strike-slip of the EDZ;
7) the only landform which actually crosses the Cascades axis and parallels the EDZ is heavily dissected and appears to be an outlier of Western Cascades

volcanism.

The original identification of the EDZ (Lawrence, 1976) was based on the observation of a NW-trending Landsat lineament of anomalous fault density. The lineament appears to be an artifact of the fortuitous distribution of recent sediments which have masked faulting along a NW-trend. No significant anomaly in the distribution of faulting can be demonstrated. It is concluded that the EDZ is not a continuous zone of faulting; is not a manifestation of contemporaneous right-lateral strike-slip faulting; does not offset the Cascades volcanic axis; and is not an active tectonic element. It may be an older feature, or it may not be a significant entity at all.

Basin and Range Propagation

Prior to discussing the relationships in the High Lava Plains to the north, an examination of the mode of deformation likely to be dominating the northwest B&R is useful. (A general consideration of B&R deformation has been presented in Chapter 2.) The stress regimes discussed above imply maximum horizontal stresses oriented between N-S and NW-SE (excepting Stress Regimes C, G, and H (Figure 31) which are local domains). These orientations are consistent with the N to NNW striking basins and dominant faulting which characterize the area between the Abert Rim - Warner Ranges line and the Cascades. On the other hand, east of this line, the basins (and ranges) strike NNE to NE. Based on this NNE to NE orientation of major basins, many workers (Zoback and Anderson, 1981; Zoback and Zoback, 1980; Eaton, 1982) have

interpreted Basin and Range MHS to be NNE to NE.

From this relationship, it is herein interpreted that a significantly different MHS can be identified in the extreme NW Basin and Range that distinguishes the deformation west of the Abert Rim-Warner Ranges Line from that to the east. Namely, east of the ARWRL the basins formed in a stress regime of NNE-NE MHS while west of the ARWRL, basins formed under the influence of NNW-trending MHS. An examination of a possible Basin and Range propagation mechanism for the NE-trending basins is a first step in understanding the process and thereby reconciling these observations. A model of Basin and Range deformation is put forth in the following paragraphs as a hypothesis which is then examined for various specific aspects in the remaining portions of the chapter.

Initially, let us assume that the NE-trending basins did, in fact, develop in a stress regime of NE-trending MHS as interpreted by many workers (Zoback and Thompson, 1978; Zoback and Zoback, 1980; Eaton, 1982). It is well established that Basin and Range extension has migrated from south to north with opening in the northern B&R initiating about 17 m.y.b.p. (as discussed in Chapter 2). The NE-trending basins are thought to have become dominant in the northern B&R between 15 and 6 m.y.b.p. (Zoback et al., 1978). The major basins of the northern B&R extend for hundreds of km along strike (eg. the basin of Black Rock Desert to Alvord Desert -- east of Steens Mtn. is about 260 km long; the continuous Warner Ranges - Abert Rim and its adjacent basins extend for about 240 km). This continuity implies that these individual basins have propagated from southwest to northeast. That is, if

deformation proceeded in general from south to north, and the structures are continuous, then the structures themselves must have evolved from south to north. This concept is further supported by the fact that the basins are broad to the south and become gradually narrower to the north -- eventually terminating at the northern limit of B&R deformation (Plate 1). Models of such individual propagating rifts in a continental setting have been discussed by Bosworth (1985) and Courtillot (1982).

It is also well established that Basin and Range volcanism (both basalt and rhyolite) is generally younger at its western margin and progressively older to the east (McKee et al., 1983; Eaton 1982; Christiansen and McKee, 1978) -- although the basalt ages are more scattered -- with some small-volume eruptions occurring in the older portions of the province. Also, seismicity is most active at the margins of the province (as discussed in Chapter 2). These factors suggest that deformation has proceeded as a combination of NE propagating basins (rifts) which have stepped progressively westward as deformation proceeds. Province-wide extension may be the result of some broad tectonic stress field such as a mega-couple between the San Andreas and the Queen Charlotte-Fairweather transforms (Christiansen and Mckee, 1978); or caused by broad lithospheric thinning due to anomalous mantle activity. In either case, westward stepping of basins could reflect the progressive buildup of stress in unfractured unattenuated lithosphere at the margins of the province. This is evidenced by the thinner crust of the Basin and Range and the rapid crustal thickening and higher Pn values at the province margins. As fracture occurs in a section of lithosphere parallel to a basin, that section loses its capacity to sustain

stress so that the stress concentrates in unfractured lithosphere farther west, until that too fails and a new basin starts to evolve and propagate northward.

The assumption that is essential to this concept of outward stepping rifting is that the stress which causes rifting must be externally applied over a broad region. The cartoon on Figure 38 shows an idealized situation for a right-lateral force couple with potential lines of extensional fracture shown. If the upper right portion (BCD) were somewhat weaker than the rest of the block (eg. weakened by crustal heating due to B&R activity further east) the first extensional fracture would be in the upper right portion of the block. This rift would facilitate additional heating (migration of magma and other heated fluids) causing the next section (ABDE) of the block to become weakened. Stress would continue to build in the unrifted portion of the block (ABDFG) and stress would be concentrated in the weakened but unrifted edge ABDE. Eventually fracture would take place in this portion of the block, in the vicinity of line AE -- as a propagating rift. Once this fracture (rift) was completed, the same cycle would be repeated in block AEFG. This concept explains the younging-outward relationships of the B&R and the fact that no anomalously broad basins occur. Once a rift forms, it can no longer support stress and the stress which caused it becomes concentrated in the unfractured lithosphere which is still being stressed.

In cases where the northward propagating basins (rifts) encounter older, thicker, colder and therefore stronger lithosphere (eg. the Blue Mountains microplate), a consequence of this model would be that the extensional deformation would either: (a) change strike to propagate around the obstacle; (b) terminate against the edge of

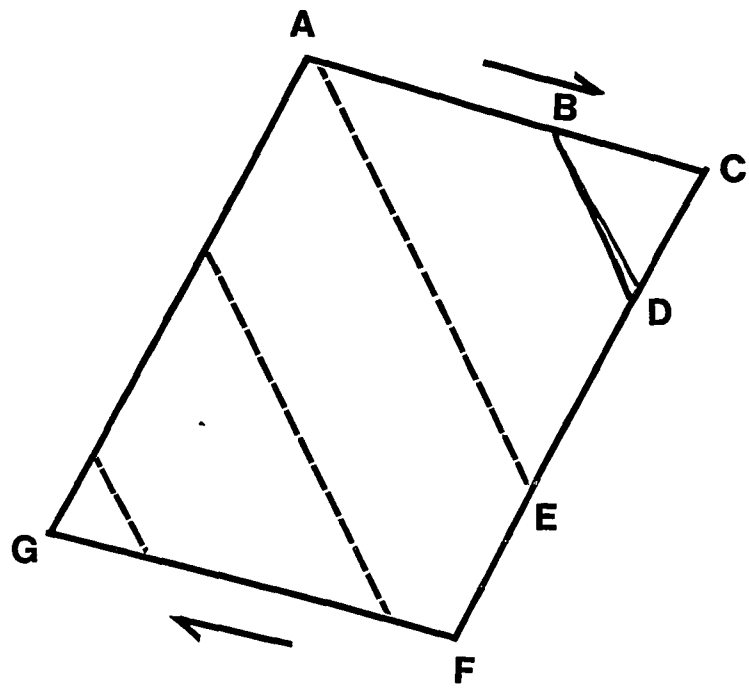

Figure 38. Idealized case of a block subjected to an external force couple. If the upper right (BCD) has been thermally weakened, tensional fracture (rifting) will mobilize here first. Once rifting occurs on BD, stress will become concentrated in the unfractured block ABDFG until rifting takes place along AE, etc. This rifting, once started, apparently propagates along strike. This model of stepping-out of rifting explains the westward younging of volcanism and the concentration of seismicity along the margins of the B&R.

the thicker lithosphere which represents a material boundary; or (c) propagate into the thicker lithosphere perhaps at a reduced rate. Examples are discussed below.

In the case where the basins terminate against the thicker block, deformation is expected where the dip slip B&R faults terminate against short strike-slip faults, as shown schematically in Figure 39. These strike-slip faults, which mark the ends of the basins, should be manifest at the surface as short, parallel normal faults because the downdropping of the fault block would leave a vertical scarp, as depicted on Figure 39. Their length is limited to the width of the basin which they terminate. The fact that the basin-terminating faults do not align is evidence that this termination is a result of termination of individual basins as they are propagating northward, not the result of control on some fundamental right-lateral fault. It is also important to note that there is no reason to expect that these basin-terminating faults would be en echelon, however, the geometry does predict that they would be parallel. These faults, which reflect short strike-slip faults at depth, are therefore secondary to the extensional deformation. This is very different from the secondary structures (en echelon normal, synthetic and antithetic faulting) which result from primary strike-slip at depth beneath unconsolidated overburden (Figure 27).

This model of northeast propagating basins, stepping northwestward and terminating in short strike-slip faults is well supported by the style of deformation in the Basin and Range and a number of basin-terminating structures are identified in the following section. This model of B&R deformation has important implications for the regional tectonic interpretation, as discussed below.

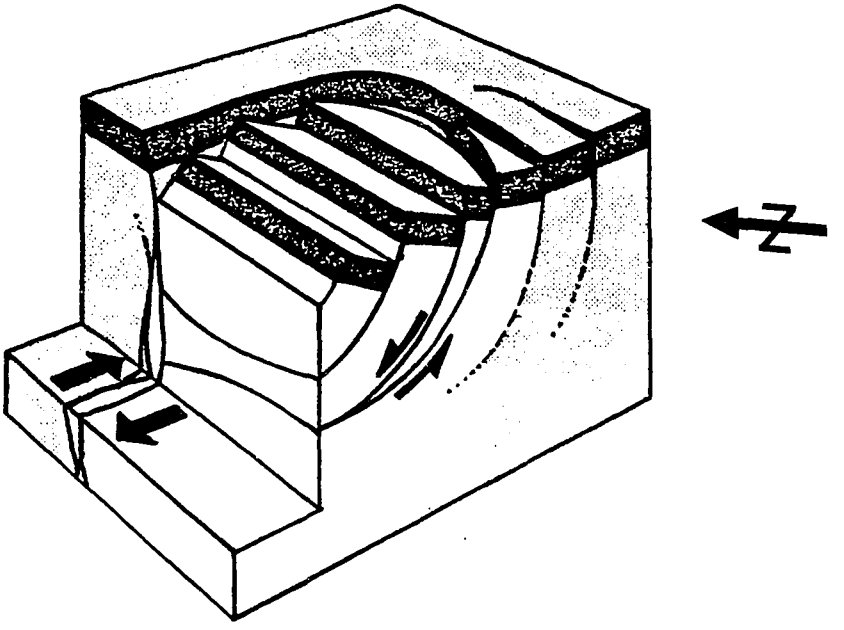

Figure 39. Block diagram showing termination of basin normal faults as short strike-slip faults which are manifest at the surface as short normal faults roughly perpendicular to the strike of the basins (Pecora Symposium, 1975). Structures along the southern edge of the Brothers Fault Zone show this relationship (the north arrow indicates the orientation of these features along the BFZ).

Brothers Fault Zone

The BFZ has been proposed as a right-lateral transform fault termination of the northern Basin and Range (Lawrence, 1976). This is a frequently referenced interpretation which is analogous to the termination of part of the southern Basin and Range against the strike-slip (left lateral) Garlock Fault (Davis and Burchfiel, 1974). However, the Garlock is well established as a major strike-slip fault with the appropriate seismicity and well documented lateral offset (Figure 40). The BFZ lacks both of these characteristics, although there can be no doubt that the BFZ is a significant fracture zone, with higher fault density, distinct from Basin and Range terrain to the south. However, most maps used to examine the BFZ do not show the full distribution and density of short normal faults which comprise and characterize the zone (eg. Figure 24). By comparison, Figure 26 shows the complete BFZ with its constituent faults. The faults of the BFZ are distinctive because of their NW strike versus the dominant NNW strike of the B&R faulting to the south. Indeed, in some cases single NNW faults strike into the BFZ and in doing so curve to the NW strike.

The broad straight lines on Figure 26 outline the area of NW-striking faults. This area is much broader than the zone generally defined as the Brothers Fault Zone. As with the Eugene-Denio Zone, discussed above, part of the reason for the way the BFZ is defined is due to masking of large areas to the north (eg. Harney Basin) by recent

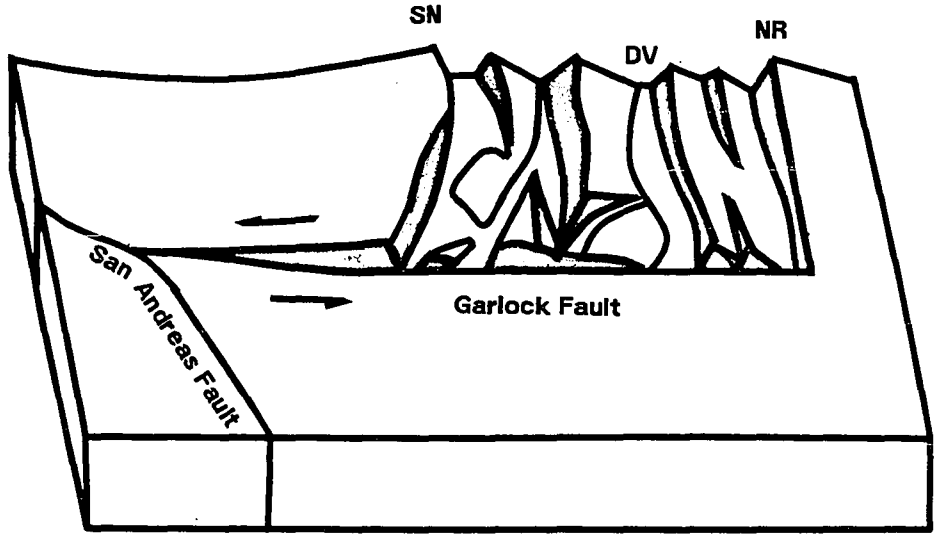

Figure 40. Block Diagram of the Garlock Fault and the abrupt termination of fault blocks of the southern Basin and Range against this well defined left lateral strike-slip fault: SN-Sierra Nevada; DV-Death Valley; NR-Nopah Range (after Davis and Burchfiel, 1973).

sediments. The actual extent of NW-trending faults coincides closely with the southern margin of the Blue Mountains -- an allocthanous terrain (microplate) of presumably older, colder and stronger lithosphere.

As discussed earlier, within the BFZ, the constituent faults form a swarm of parallel faults which are parallel to the zone as a whole. The overall swarm steps to the SW at about Longitude 120°W. Swarms of short parallel normal faults, which are parallel to the overall zone in which they occur, are characteristic of extensional terrain. Figure 28 is an example of such structure developed in a clay model by distributed extension adjacent to an uplift. The structural style bears more than a vague similarity to the BFZ. The possibility that extension is dominant in the BFZ is also indicated by the fact that the vent alignment stress trajectories at Diamond Craters (#179 and #180, Appendix B), located within the BFZ east of Harney Lake (and shown on Figures 19 and 26) are oriented parallel to the BFZ rather than at a 45° to the zone as should be the case if a strike-slip stress regime were dominant. Diamond Craters is young basaltic volcanism -- possibly less than 20,000 years old (Walker and Nolf, 1981). An extensional regime within the BFZ (broadly similar to that depicted in the clay model results shown in Figure 28) is therefore more consistent with the mode of deformation, with the stress trajectory indicators with the presence of ongoing volcanism and, perhaps most significantly, with the observed low seismicity.

At the southern limits of the BFZ, evidence is found for the basin-terminating structure discussed in the preceding section and depicted schematically on Figure

39. Figure 41 shows the faults which are in the appropriate position and have appropriate displacement to represent such basin-terminating faults. These basin-terminating structures are well depicted on the Seasat mosaic of this area (Figure 42). The identification of these features by means of the Seasat imagery is a good example of the special qualities of this imagery. Seasat shows the strike of the faults clearly as well as the dip (facing direction). Bright (white) features have a west-facing component while the verification of the presence of these basin-terminating structures is somewhat ambiguous on the fault maps and Landsat data. The bright signature and clear definition of these features identifies them as the major structures in an area of ubiquitous small-displacement faulting.

Therefore, the NNE-NE trending basins of the northern B&R terminate along the Brothers Fault Zone. Basin bounding normal faults (NNE-NE) gradually diminish in the magnitude of dip slip to the north; and turn into short normal faults of variable dip which generally strike WNW at angles of 60 to 90 degrees from the trend of the basin-bounding (NNE-NE) faults. This geometry indicates basins which are propagating NNE-NE and terminating against a material boundary. In this case, the material boundary appears to be the Blue Mountains exotic terrane -- a former microplate.

The significance of the role of the Blue Mountains microplate is further evidenced by the geometry of the eastern end of the Brothers Fault Zone. The BFZ terminates abruptly at Steens Mountain (Figure 26). East of Steens Mountain, the basin of Alvord Desert - Turnbull Lake continues northeast, around the east side of the Blue

Figure 41. Brothers Fault Zone with Basin-terminating Faults shown as broad lines. These faults are also shown on Plate 1. The strikes and dips of these faults are equivalent to the schematic case shown on Figure 39. Note that these basins do not terminate at a through-going structure and are therefore not analogous to the Garlock fault case (Figure 40). Symbols are the same as Plate 1.

A
E
F
G
B

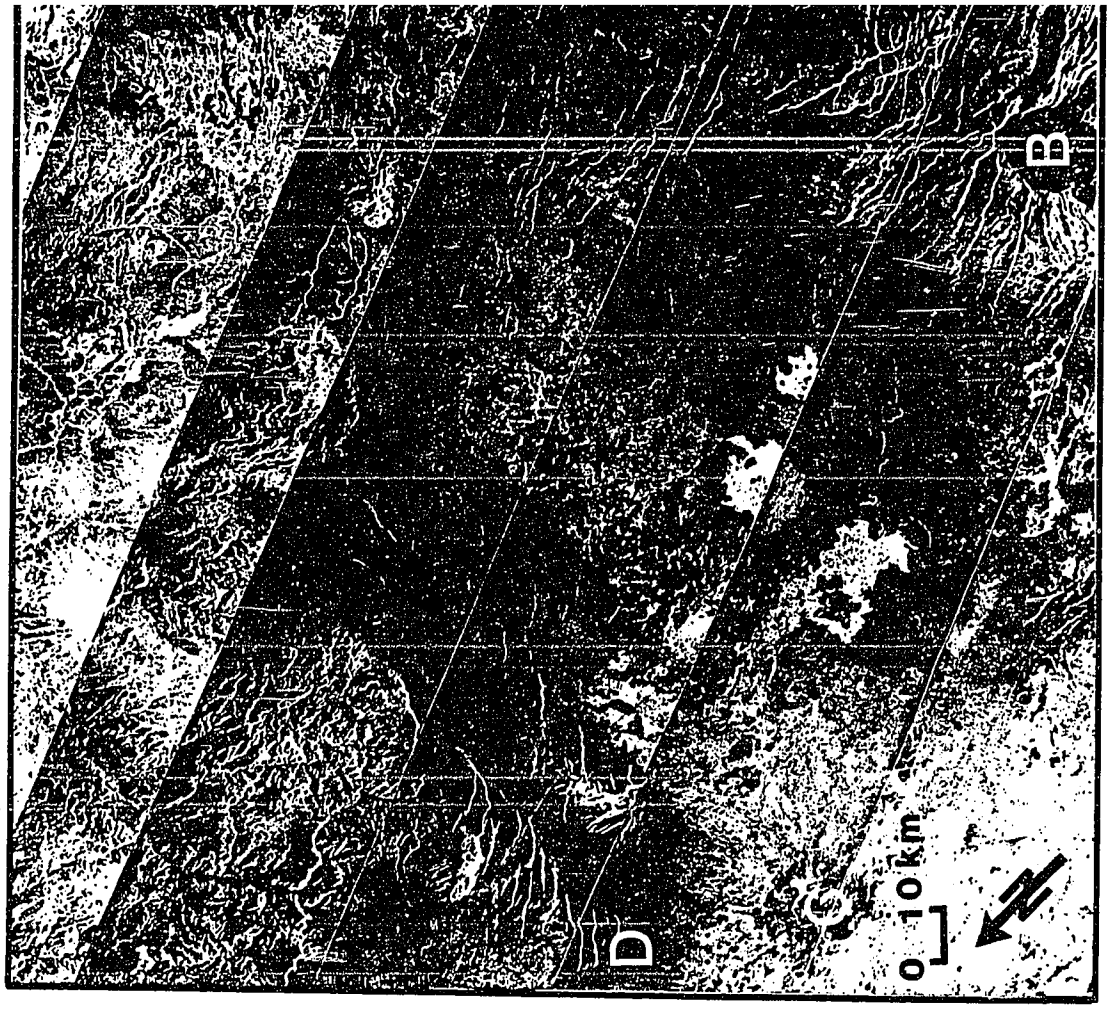

Figure 42. Seasat Imagery Mosaic of the Brothers Fault Zone (D to E) depicting Basin-terminating structure. The structures shown on Figure 41 are depicted well by the radar imagery which looks ENE and therefore displays faults as bright (white) lines if they strike between NNW and NE and have scarps that have a NW-facing component. Localities identified include: Silver Lake (B), Abert Rim (G), and Poker Jim Ridge (F).

Mountains and normal faulting is mapped continuing northward along the extension of this basin which passes west of the town of Harper and gradually rotates to N-S and then NNW along Bully and Clover Creeks eventually passing NNW between the Elkhorn and Strawberry Mountains (the latter part of the Blue Mtns block) (see Figure 15A and 43). Thus the basin adjacent to Steens Mountain appears to be an example of a B&R structure which propagated around the Blue Mountains block rather than terminating against it. The NNE-trending basins west of Steens Mtn intersect the southern margin of the Blue Mountains at essentially right angles and cannot propagate around the Blue Mountains as long as they are under the influence of a NNE-NE MHS.

Subsequent to the termination of these basins -- or possibly a cause of this termination, the evidence indicates that a NNW MHS came to dominate the BFZ. The evidence includes the NNW trend of the basins and normal faulting in the northwesternmost B&R, the distribution and style of the dominant BFZ faulting, the lack of seismicity, the vent alignment stress trajectories, and the advent of abundant volcanism along the BFZ, including ashflow caldera formation beginning about 6 m.y.b.p.

A critical question which cannot be answered explicitly by this evidence deals with the extent of the NNW MHS regime -- both geographically and temporally. The two most obvious possibilities are as follows.

Hypothesis 1) The NNW MHS is geographically controlled by the transition from a NNE-NE MHS regime to the east in the B&R to a N-S regime in the Cascades.

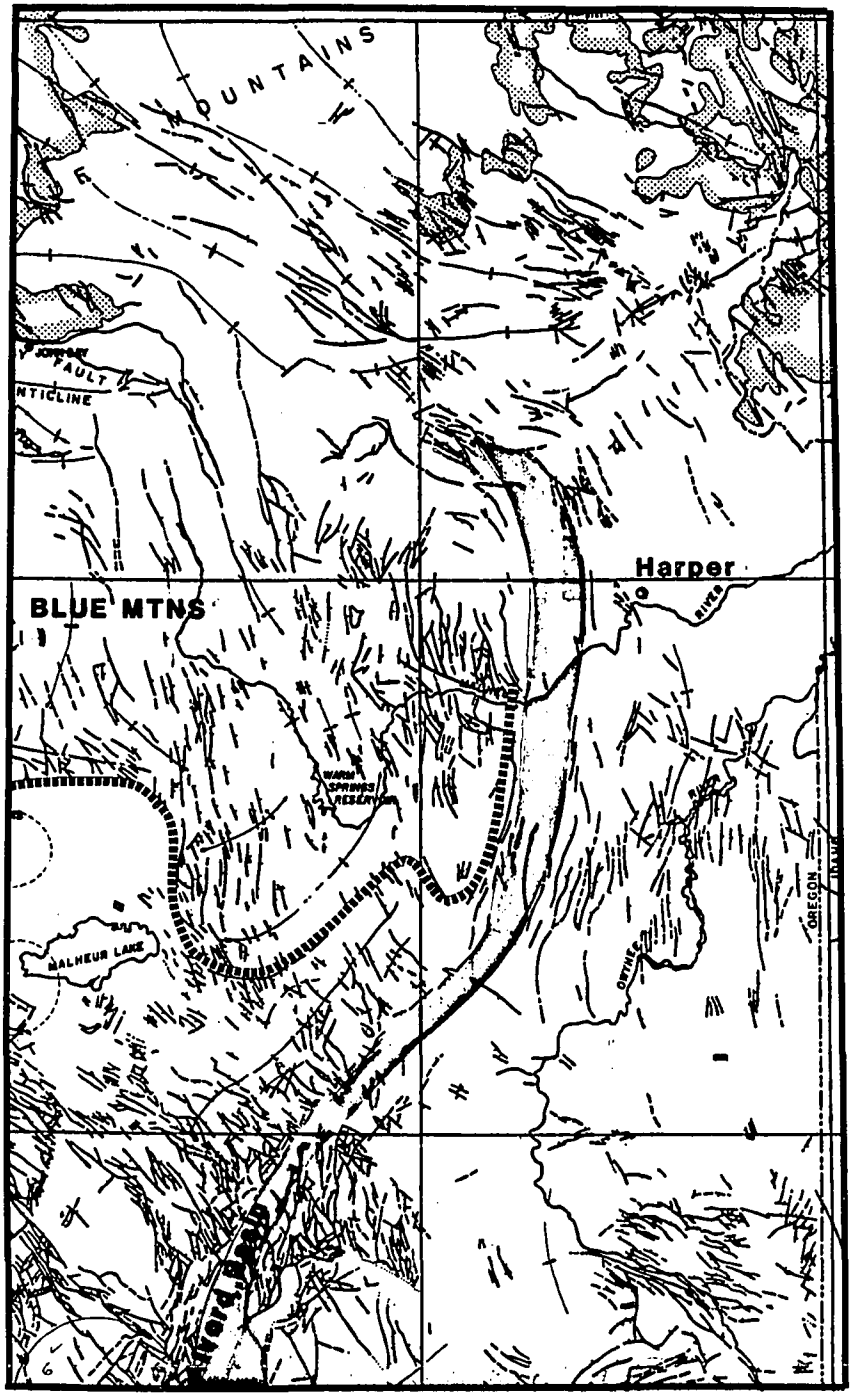

Figure 43. Fault Map of the northern extension of the Alvord Desert-Turnbull Lake Basin. The shaded area is the generalized strike of the northern end of the Alvord Basin, where it has propagated around the east end of the Blue Mountians microplate. Symbols are the same as Plate 1.

That is, the NNW regime represents a transition from one regime to another. Arguments against this notion is the abrupt nature of the change in geometry across the ARWRL and the NNW MHS trajectory indicated far to the east within the BFZ at Diamond Craters.

Hypothesis 2) The NNW MHS represents a stress regime that has, with time, come to dominate the entire northern B&R in Oregon. The observed curving of normal faults east and north of the Blue Mountains tends to suggest that a NNW regime also persists northeast of this terrane, supporting broad temporal change rather than the local transitional regime of hypothesis 1.

In the following section the ages of rhyolite domes are examined as a possible indicator of age-progressive rifting. However, these data cannot really resolve the question of the significance of the NNW regime. The NNE-NE regime, which is responsible for the major landforms of the NNE-trending basins, only became dominant at most 15 m.y.b.p. (Zoback and Thompson, 1978) and probably closer to 10 m.y.b.p. (Zoback et al., 1981). This implies that it is a relatively recent tectonic development. As discussed below, the rhyolites indicate that NNW rifting initiated west of the ARWRL about 6-7 m.y.b.p. coincident with the onset of ashflow volcanism. Such rapid "global" regime changes (as required in case 2 above) is problematical. Unfortunately, a great deal more data is needed to resolve these questions. At this point, case 2 -- even with its implied rapid stress change -- appears to be the most palatable owing to the NNW stress trajectory at Diamond Craters, far east of the Cascades, and the high heat flow characteristic of this area (Figures 19, 23 and 26).

Structural Control of 0-11 my Rhyolite Domes

The distribution of rhyolite domes across the northern Basin and Range is shown in detail on Plate 1. In northern Nevada, at Granite Range and extending NNE toward Steens Mtn. there is obvious coincidence between the distribution of rhyolite vent rocks and the NNE-trending B&R structure. In SE Oregon, the occurrence of broad alluvial basins such as Catlow and Harney Basins and the abundance of ash flow deposits and Quaternary basalt lava flows (Figure 30) obscures this structural relationship somewhat. However, immediately to the east of the ARWRL, a line of 5 domes is mapped which roughly parallels the ARWRL. Given the masking effects of subsequent sedimentary and volcanic deposits, it is possible that similar NNE control of dome emplacement persists in the subsurface along basins farther east.

The discussion which follows with respect to the ages of these rhyolite domes is based on the hypothesis that as rifts (basins) propagate along strike, basaltic magma finds easier access to the shallow crust where crustal melting takes place generating silicic lavas. This is also consistent with the idea that the crust would already be heated due to B&R activity to the east so that when fracture developed, partial melting may result. An analog of this case has been encountered in the case of propagating oceanic rifts where lavas as silicic as rhyolites (thought to be differentiates in this case) are found at the propagating rift tip (Sinton et al, 1983).

Although the timing between the onset of lithospheric fracture and the generation of silicic melt is not known, the younging trends can yield rates of rift propagation rather than absolute ages the onset of rifting. The only known evidence

that this process may be operative is as follows.

1) The B&R is known to be a region of anomalously high heat flow and volcanism -- particularly in the early stages of rifting.

2) The ages of the rhyolite domes, when interpreted in the context of the structures observed, do show the appropriate age progression.

These are not particularly strong arguments, but the resultant interpretation is no less supportable than that which has been proposed previously (MacLeod et al., 1975; Christiansen and McKee, 1978; Thompson, 1977) which invoke some hot spot-like feature produced by an enigmatic "sublithospheric transform". The interpretation discussed herein is preferable in that it takes account of the B&R structural environment in which these rhyolites have been emplaced.

MacLeod et al. (1975) have assumed that the few rhyolite domes which occur in this area that are greater than 11 m.y.b.p. are not related to the processes that produced the younger domes. This interpretation is reasonable in that the two examples of older domes -- a 14.7 my age on the east edge of Harney Basin and a 14.7 my age at the north end of the ARWRL both occur in the BFZ within which the next oldest dome is 9.8 m.y.b.p. This is a 5 m.y.b.p. hiatus -- a significant period in this region of rapid recent tectonic evolution.

South of the Brothers Fault Zone and east of the ARWRL (assuming NNE structural control), there is not much information available by which to constrain any ageing pattern. South of the BFZ, there is only one rhyolite dome (less than 11 m.y.b.p.) which has been dated -- Beattys Butte south of Catlow Basin (Plate 1).

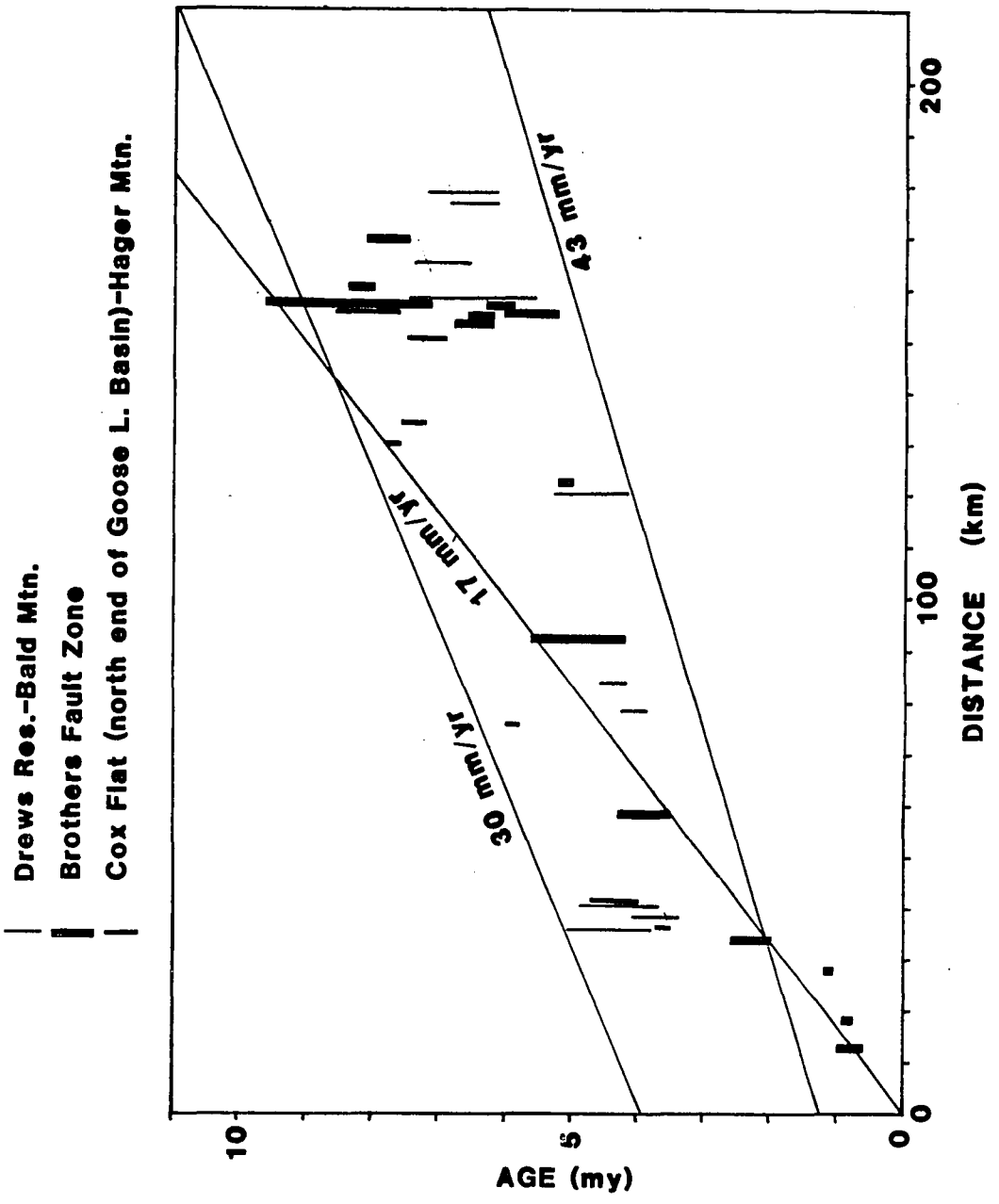

Figure 44. Age-distance plot for rhyolite dome trends east of the Cascades. The structures corresponding to these trends are shown on Figure 45. The Drews Res-Bald Mtn. trend corresponds to Structure B and the Cox Flat-Hager Mtn. trend corresponds to Structure A. The Brothers Fault Zone domes show a uniform younging trend of about 43 mm/yr from 7-14 m.y.b.p., and about 17 mm/yr since that time. Prior to 7 m.y.b.p., there is no uniform age progression. The Cox Flat-Hager Mtn. trend (Structure A) shows a 30 mm/yr propagation (younging) rate. The Drews Res-Bald Mtn. rate (Structure B) is about 43 mm/yr.

Within the BFZ to the NE, one date (east of Diamond Craters at the north end of Alvord Basin) is similar to Beatty's Butte (average 9.8 m.y.b.p. vs average 10.3 m.y.b.p. at Beatty's Butte). Because these domes occur in successive basins, these dates are (tentatively) interpreted to imply that Catlow Basin propagation lagged behind Alvord Basin by roughly 100 km. North of Beatty's Butte, within the BFZ just east of Harney Lake, there is a dome which is dated at about 8 m.y.b.p. It appears to be older than the NW-trending 43 mm/yr younging trend which parallels the BFZ farther west because it plots well above the age-distance plot for the western BFZ (see discussion below and Figure 44). This dome is therefore assumed to be related to NE basin formation. It may be related to Warner Lakes Basin, but is located north of the basin-terminating faults. There is a possibility that this dome is related to the basin-terminating faults of Catlow Basin (Figure 41). If so, a NE rift-propagation velocity of about 45 mm/yr is indicated between Beatty's Butte and this dome. If the 8 my dome is related to younger (than Catlow) basin structure, then this 45 mm/yr represents a minimum rate of NE-basin rhyolite propagation for Catlow Basin.

The age data along the NNW-trending structures west of ARWRL is much better resolved. This structure has evolved since a change in the MHS orientation from NNE to NNW as indicated by the stress trajectory data and basin orientation discussed above. West of the ARWRL and along the BFZ from west of Harney Lake to Newberry, well defined younging trends are found. These trends are shown on an age vs distance plot on Figure 44. The data for the Brothers Fault Zone from about 7 m.y.b.p. - 3.5 m.y.b.p. fall on a velocity of about 43 mm/yr. As mentioned in the preceding

paragraph, the dates greater than 7 my west of Harney L. fall well above this 43 mm/yr trend and are interpreted to be related to NNE propagating structure. For this reason, it is proposed that NNW structure development was in progress by about 7 m.y.b.p. and that domes older than 7 m.y.b.p. are probably related to NE-trending basin development. Seven m.y.b.p. may therefore be the date of an overall change in MHS or the date at which B&R deformation reached far enough west to be influenced by a different MHS regime. For dates less than 3.5 my the rate of propagation diminishes to about 17 mm/yr (Figure 44).

Additional support for the 7 m.y.b.p. date for the change in stress regime is the fact that the BFZ became a locus of rhyolitic ashflow volcanism shortly after this time. The Harney Ash (which may have erupted from one of a number of proposed (but not well established) caldera structures (Figure 19) is dated at 6.2 m.y.b.p. (MacLeod et al., 1975).

West of the ARWRL, two structures occur which appear to control dome emplacement. These structures are shown on Figure 45 and their geomorphic form can be identified on Figure 46 (Structure A: QLN; Structure B: QSP). These structures are identified by the younging trend of the rhyolites viewed in the context of the adjacent faulting. The boundaries of these structures are drawn to conform to the mapped fault trends. The Cox-Flat-to-Hager-Mtn domes (Structure A, Figure 45) are structurally associated with faulting of the series of grabens which extend from the south end of L. Abert through Chewaucan Marsh, Summer Lake, Silver Lake and Fort Rock Valley. Rhyolites probably exist within these basins but are covered by

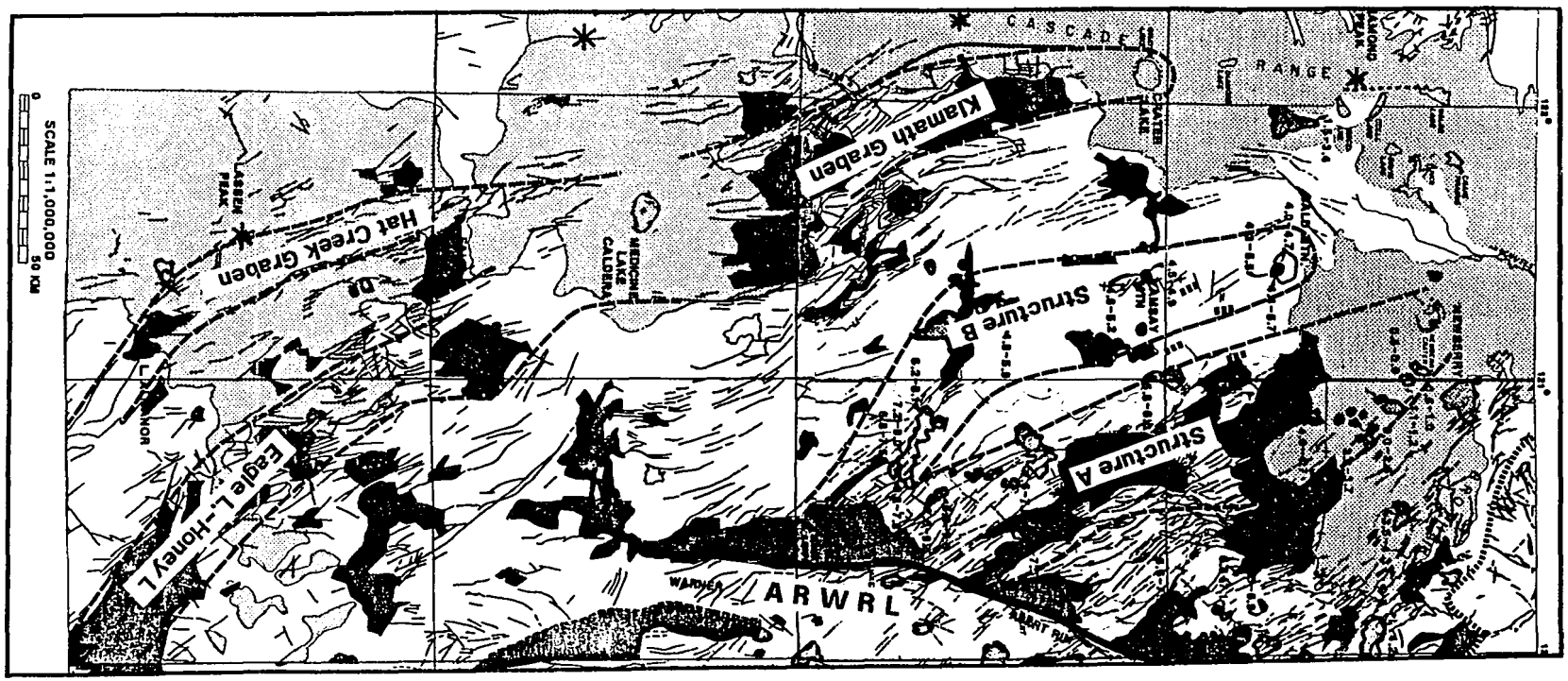

Figure 45. Area between ARWRL and the Cascades showing two propagating structures (A & B) that are correlated with caldera formation. These structures are defined by fault orientation, landform development, rhyolite dome ageing trends, and older vent alignments (shown in short broad dashed lines). These structures propagate toward Newberry and Bald Mtn. calderas -- and rhyolite ages indicate that rifting arrives at the calderas at roughly the date of the inception of caldera formation. Similar structures shown to the west are the Klamath Graben (intersecting the arc at Crater Lake) and the Hat Creek Graben and Eagle L.-Honey L. Graben which interact with the arc at Lassen and Medicine Lake Calderas.


H
E
N
D
P
A
L
S
R
K
Q
M
B

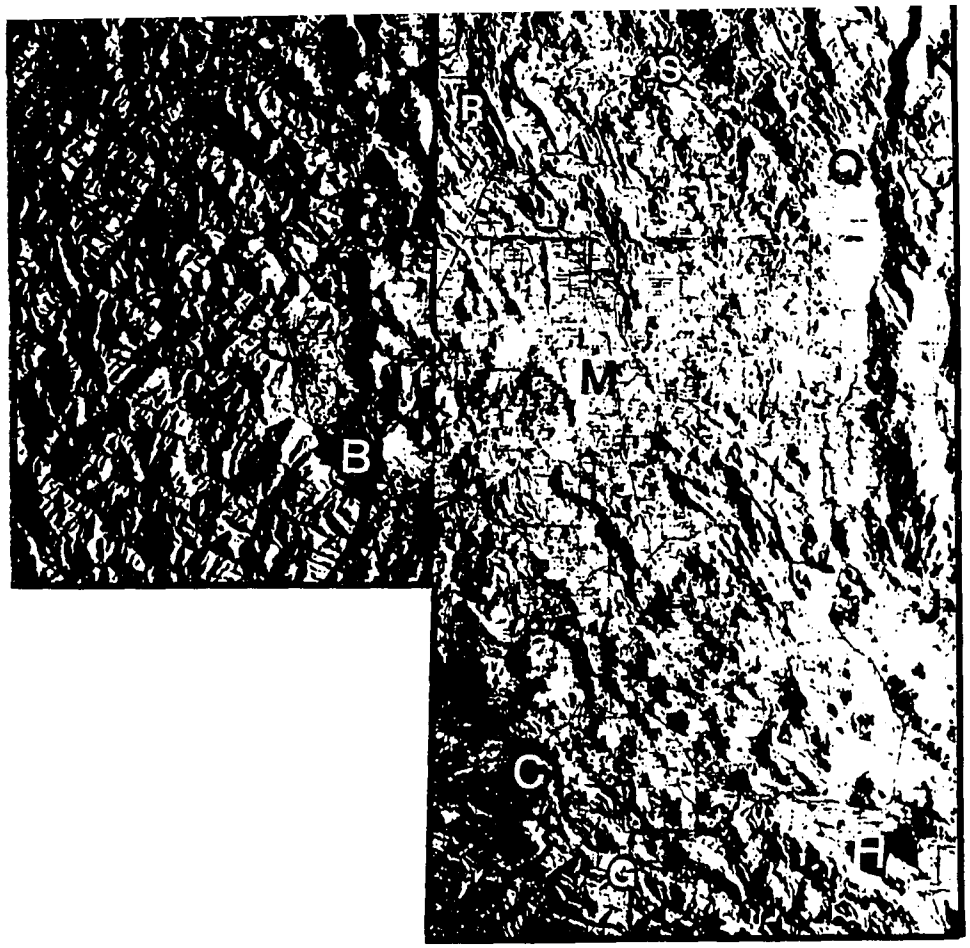

Figure 46. Oblique Illuminated Relief Map Mosaic showing geomorphological expression of rhyolite dome structural trends. Illumination direction is from the east. Letters identify the following features: A-Crater Lake; B-Shasta; C-Lassen; D-Diamond Peak; E-Three Sisters; F-Jefferson; G-L. Almanor; H-Honey Lake; L-Summer L.; N-Newberry; P-Bald Mtn.; R-Klamath Graben; S-Devil's Garden (Sprague R.); Structure A (Figure 44) = QLN; Structure B = QSP.

sedimentary fill. From Hager Mtn to Newberry the west boundary of this structure is not constrained by dome ages but is separated from Structure B (Plate 2) by down-to-the-west normal faulting (eg. at Antelope Mtn). The rate of propagation along this trend from Cox Flat to Hager Mtn is about 30 mm/yr. The area of this structure is depicted on the Seasat image, Figure 36.

The Drews-Reservoir-to-Bald Mtn. trend (which parallels the Klamath Graben) strikes NE to the Sycan River and then strikes northward through Yamsay Mtn. parallel to faulting to the west. This trend terminates at the approximately 4 my old Bald Mtn complex which is considered by some workers (eg. Luedke and Smith, 1982) to be a caldera. Bald Mtn possesses a bimodal basalt/rhyolite assemblage and has a geomorphic expression suggesting a maximum dimension of about 7 km. The age-distance relationship for this Drews-Bald Mtn trend indicates a propagation of about 43 mm/yr.

The identification of these structure-age progression domains is supported by faulting trends and geomorphic expression -- best depicted on the obliquely illuminated relief map mosaic, Figure 46. The Brothers Fault Zone trend is supported by the abundant faulting of extensional character, absence of NE structure north of the basin terminations (discussed above), stress trajectories at Diamond Craters and near Newberry. The Cox Flat - Hager Mtn trend is supported by (older) apparent vent alignments (Luedke and Smith, 1982) SSE and W of Hager Mtn, and abundant faulting and basin structure (Summer L. et al.), and recent stress trajectories SE of Newberry. The Drews Reservoir - Bald Mtn trend is geomorphically the least well defined.

However, it is paralleled by major drainage features (Drews Reservoir, Sycan River, Williamson River, Jack Creek), and (older) apparent vent alignments both north and south of Yamsay Mtn. (Luedke and Smith, 1982). The older vent alignments are shown on Figure 45 and are identified as geomorphically continuous on the basis of topographic maps. (Imagery of these areas was not available to this study.)

It is the contention of this study that these structures represent B&R propagating basins which appear to be becoming progressively more involved in Cascades volcanism with time. The Klamath Graben is a similar structure although it lacks the age dating information. Clearly, the Klamath Graben is a well defined graben and probably represents the most active of these three features. The Drews-Bald Mtn. structure is the least evolved and may have ceased to be active as indicated by the fact that the faulting of Walker Rim and the stress trajectories of the SW flank of Newberry cuts across this structure. However, the Drews-Bald Mtn structure has the most consistent trend of rhyolite domes. Such domes may exist within Klamath Graben and the Summer Lake-Fort Rock valley structures, but are covered by sediments. Two extensional features -- the Honey Lake-Eagle Lake trend and the Hat Creek trend, converge on Medicine Lake caldera. These features are continuous with the Klamath Graben although because of the cover of recent Medicine Lake volcanism the structural connection is not clearly visible. These structures differ from those to the north in that they branch off NW-trending faults related to the Walker Lane rather than those related to N-NE Basin & Range structure (Figure 45).

Volume Distribution of Cascades Volcanism

Volume/area determinations for the Cascades volcanism in the 0-5 m.y.b.p. time interval has been determined to examine variations in volcanism along the volcanic arc which may relate to tectonic perturbations. These determinations are described and data plots are presented in Appendix C. Basalts of Simcoe, Deschutes Basin and Newberry are excluded from the determinations in order to eliminate offarc influences and older (pre-late High Cascades) volcanism (see the discussion in Appendix C).

The most relevant aspects to the present study are shown on Figures A-4 and A-5 and summarized below.

1) Two peaks in overall volume of volcanics occur (Figure A-5): one south of latitude 42°N in the vicinity of Shasta and Lassen; and one in the vicinity of Three Sisters (latitude 44°N). These peaks occur at locations where B&R structure most obviously dominates recent deformation along the arc axis.

2) These peaks correspond to an increased proportion of basalt in the volcanic volume (Figure A-4). (Note that the large spike in percent basaltic component at 45.5°N is less significant because it is a point of low total volume.)

3) There is a significant drop in the relative volume of volcanism between Mt. McLoughlin and Diamond Peak (latitude 42° to 44°N) (Figure A-5).

There is a relatively strong coincidence between low overall volume of volcanism and those areas where the arc has remained on the older locus of Cascades volcanism (defined by the location of volcanic necks (Figure 24)). Areas where the arc has stepped east (north of Diamond Peak) or is heavily influenced by Basin and

Range deformation (Shasta-Lassen) are also areas of higher total volume of volcanism and higher proportion of basaltic volcanism.

Summary Observations

To summarize the study described herein, a model is proposed which emphasizes the role of the interaction of Basin and Range and Cascades structure. The major elements of this model are the NNW MHS east of the Cascades in the northwestern B&R, and the propagation of B&R deformation by the propagation of rifts parallel to the MHS. This model reconciles many heretofore unresolved relationships within this region.

1. Prior to about 7 m.y.b.p. rifting of the northern Basin and Range within a regime of NE to NNE MHS was causing basins to propagate NNE and step westward.
2. Basins terminated in small strike-slip faults, along the south margin of the Blue Mountains microplate, at the southern BFZ.
3. An exception was the Alvord Desert basin which propagated around the east end of the Blue Mtns.
4. Major strike slip structure is not involved in the northern termination of B&R structure, nor in the Eugene-Denio Zone.
5. After about 7 m.y.b.p., the B&R deformation became dominated by NNE MHS. B&R basins forming after this time -- those west of the Abert Rim - Warner Lakes Line -- propagated along this NNW trend.

6. With this change, distributed extension, characterized by swarms of extensional fissures, came to dominate the BFZ as extension was localized along the southern margin of the Blue Mountains block. The general aseismicity of the area is a reflection of the dominant extensional regime which continues to dominate.

7. Small volume rhyolite magmas appear to have been produced as rifting propagated along the strike of the basins. This volcanism shows a general younging trend which may be a reflection of the rate of propagation of the basins.

8. With proximity to the axis of the Cascades, the rift propagation has rotated to a north-south trajectory parallel to the axis of volcanism. Volcanic interaction has taken place between the arc-driven volcanoes and the rift-associated volcanoes -- producing back arc edifices paired with major arc volcanoes: Newberry (opposite Three Sisters); Medicine Lake (opposite Shasta); Yamsay Mountain (opposite Crater Lake). Calderas have developed at three points where the rifting has come within about 50 km of the volcanic axis: Medicine Lake, Newberry and Bald Mtn.

9. At Crater Lake the intersection of the Basin and Range structure with the volcanic axis has generated caldera-producing volcanism.

10. The arc has stepped east, north of Diamond Peak, to follow extensional structure that has been imposed on the eastern side of the axis by the propagation of rifts into the vicinity of the axis.

11. The coincidence of the age of Bald Mtn. (~4.5 my) with the proposed age of this eastward shift of volcanism at Hamner Butte, NW of Bald Mtn, suggests that these features may be related.

12. The structural shift of the Cascades from a western locus -- essentially coincident with the long-standing axis along the McLoughlin - Diamond Peak alignment, to a more easterly locus appears to now be primarily influenced by the rifting which has reached Newberry and created magmatic communication with the axis. This has produced slowing of the rift progression as volcanism has become more steady state in character.

13. The stress transition at Walker Rim (Regime H) has been produced to accommodate the transition from the western to the eastern volcanic locus. Walker Rim is relatively recent (probably postdating the Bald Mtn volcanism) as indicated by its relatively shallow character (it is not reflected in the gravity data (Couch, 1981)).

14. An analogous situation is seen to the north of Newberry (Regime J) where there is a transition from the NNW B&R structure to the N-S Cascades stress regime at Green Ridge.

15. The volume calculations for the Cascades reflect these relationships with the high volume areas coinciding with the points where the B&R deformation is associated with an eastward shift of the locus of volcanism (Shasta-Medicine Lake and Three Sisters).

Tectonic Interpretation

Three of the conclusions of this disertation have major tectonic implications including:

A) Basin & Range formation in eastern Oregon takes place by NE-propagating rifts which step progressively westward with time;

B) a change from NE MHS to NNW MHS takes place about 6-7 m.y.b.p.; and

C) there is a progressive incursion of NNW to N-S propagating B&R structure on the Cascades arc.

A general model of a megashear caused by the interaction of the Queen Charlotte-Fairweather Fault, north of the Juan de Fuca plate, and the San Andreas has been described by Christiansen and McKee to explain deformation in the Basin & Range in general. (A version of this model was actually put forward first, on kinematic grounds, by Wise (1963) in the pre-plate tectonic era.) Christiansen and McKee (C&M) invoke their model to explain the NE-trending MHS in the Basin & Range and most post-17 m.y.b.p. deformation. Although the present study looks beyond the details of their interpretation, the general concept of the C&M/Wise model provides a possible broad mechanism for imposing an external stress regime which could produce the style of deformation consistent with the findings of the present study. The fact remains, however, that the basic overall cause of Basin & Range tectonism is not understood.

The basic tectonic elements are shown on Figure 2 and a cartoon is presented on Figure 47 showing the elements arising from the present study. The analyses of this

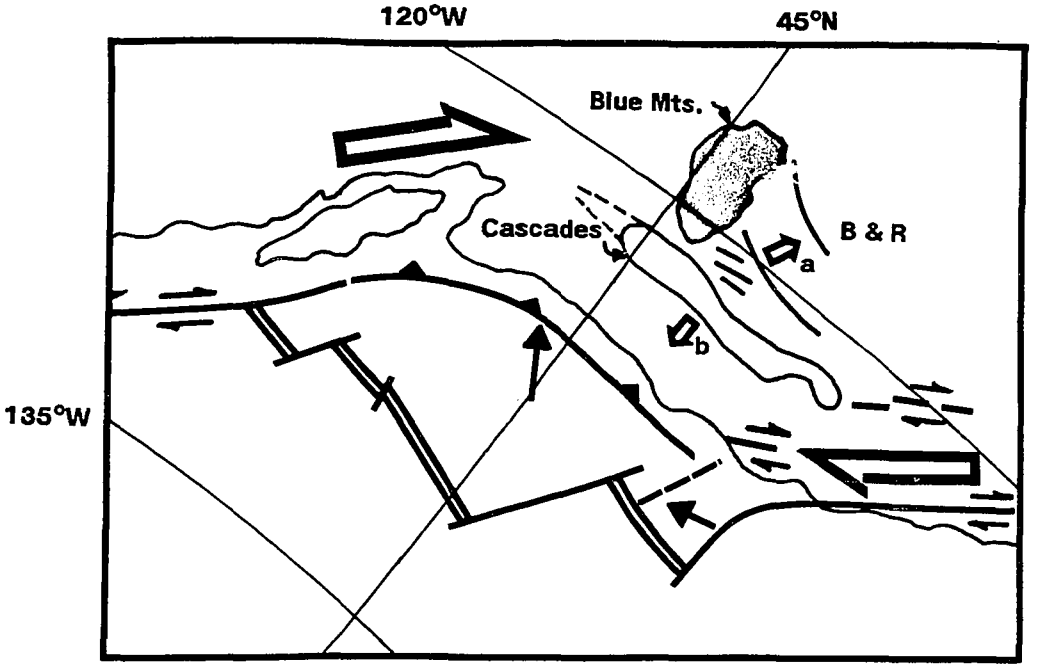

Figure 47. Oblique Mercator projection of the Pacific Northwest showing tectonic features from this study. (Projection is about the pole of relative rotation between the Pacific and North American plates (Atwater, 1970).) The basic tectonic factors are shown including: the direction of minimum horizontal stress prior to 6 m.y.b.p. associated with NE-trending basins (small open arrow a.) and since 6 m.y.b.p. associated with NNW-trending basins and the N-S volcanic arc (small open arrow b.); San Andreas-related strike slip (small half arrows); the San Andreas/Queen Charlotte-Fairweather couple (large half arrows); the Blue Mountains microplate (shaded); and relative plate motion vectors (solid arrows).

study strongly imply that an overall external stress field is being imposed on the area of the study, causing basins to step westward into unfractured lithosphere as deformation progresses (see the discussion of this concept earlier in this chapter). The consequences of this outward stepping of rifting are explored in a scenario depicted on Figure 48. The stages of rift development are shown for the period from 10 m.y.b.p. to 6 m.y.b.p. A rift propagation rate of 45 mm/yr is used for the propagation of each NE-trending basin along strike. An overall spreading rate of 10 mm/yr across the region is used -- a low value for general Basin & Range estimates (Chapter 2) but consistent with the cumulative opening implied by the width of basins in eastern Oregon. Most of the E-W B&R opening has taken place on the NE-basins and the apparent absence of major NE basin formation since 6 m.y.b.p. indicates that most of the opening was completed by 6 m.y.b.p. Paleomagnetic measurements of post-Miocene rotation of the Western Cascades of Oregon indicates 27° of rotation in the last 20 m.y. about a pole of rotation near Mt. St. Helens (Magill and Cox, 1981). The scenario of Figure 48 produces a rotation, about the same pole, of 10°-11° -- consistent with the paleomagnetic data.

In this context, it is noteworthy that rotation of the Western Cascades about a nearby pole of rotation is consistent with the concept of progressive propagation of basins toward the BFZ causing gradual rotation with the passage of each rift. On the other hand, the concept of through-going strike-slip termination of the B&R at the BFZ would produce translation of the Western Cascades which would be manifest as relative minor rotation about a distant pole. Thus the paleomagnetic evidence further

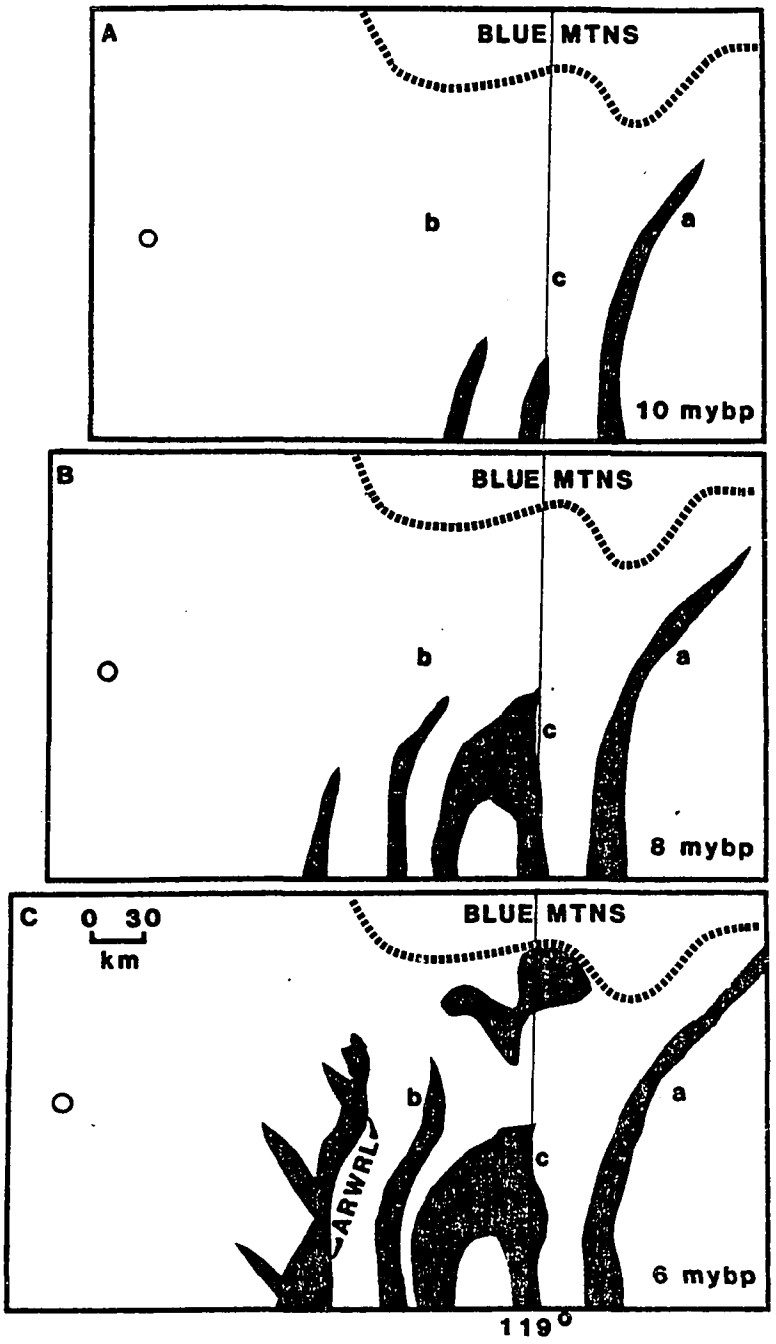

Figure 48. Cartoon of the implied evolution of NE propagating rifts (basins) of the Basin & Range from 10-6 m.y.b.p. As deformation proceeds, rifts step westward. This scenario uses a rift propagation rate of 45 mm/yr and an overall E-W spreading rate of 10 mm/yr. The circle is a reference point (Crater L.); basins are shaded areas: a-Alvord Basin; b-Warner Lakes Basin; c-Catlow Basin. The Blue Mtns. is a stable block not influenced by B&R spreading.

supports the conclusions of the present study discussed earlier in this chapter.

The N-NE MHS implied by the N-NE-trending basins in the northern B&R east of the ARWRL is interpreted to reflect backarc spreading behind the basically E-W convergence of the JDF plate with North America which predated 7.5 m.y.b.p. (Wilson, 1984). At this time the Mendocino triple junction was south of San Francisco (Figure 10) and the bounding dextral faults of the megashear were therefore considerably further apart -- possibly minimizing the influence of this interaction on the intervening crust. Furthermore, the lithosphere between the ARWRL and the Cascades was essentially undisturbed by B&R deformation (since rifting had not reached this point yet) so that there was a broad belt of strong lithosphere between the backarc activity and the arc. As a result of these two factors, little evidence of interaction between the two transforms is observed in the style of deformation.

At about 6-7 m.y.b.p. this situation changed. The development of NNW structure suggests that the eastward stepping N-NE basins had sufficiently narrowed the zone of unfractured lithosphere between the B&R and the Cascades such that interaction of the two provinces started to evolve. As it did so, the southern boundary of the Blue Mtns microplate became a locus of extension. Stress was released on what were probably preexisting NNW-trending faults. With time, this initial extension has evolved into basins (Summer Lake, Silver Lake, Klamath Graben) which, with proximity to the arc, rotate to a more N-S trend. The arc itself is dominated by N-S MHS stress trajectory. Large calderas (Crater Lake, Medicine Lake, Newberry and Lassen) occur at the points where these rifts intersect or come close to the arc axis (a smaller

caldera -- Bald Mtn -- also corresponds to this geometry). In the vicinity of Walker Rim, the arrival, at the volcanic axis, of the propagating rifts associated with this NNW propagating extension, Structure B, at about 4 m.y.b.p. coincides with the initiation of the late High Cascades volcanism (Priest et al., 1983) which was accompanied by an eastward shift in the locus of volcanism north of Diamond Peak, and the development of more mafic affinity. Subsequent rifting reaching the volcanic axis, eg. Structure A (Figure 45) has enhanced this more basaltic volcanism as demonstrated by the volcanic volume data discussed earlier (Figure A-5).

These ideas suggest that the present setting of the Cascades has evolved into one where backarc rifting has become colinear with the magmatic arc. This situation is analogous to the Taupo Volcanic Zone (Table 2-MM) where 'backarc' rifting is apparently propagating along the arc producing the transition from the large bimodal (basalt/rhyolite) calderas of the Taupo Zone to the large andesitic stratovolcanoes of the Tongarirro Volcanic Center. This transition is similar to the transition from the southern Cascades to the northern Cascades. The propagation of more mafic, extensional volcanism northward along the arc is shown schematically on Figure 48. The development of extensional features such as Green Ridge and the Hood River Fault within the last 4 m.y.b.p. supports the concept of northward propagation of extensional character.

At the south end of the Cascades, the Mendocino triple junction is moving northward, resulting in increasing interaction between the arc and the two transforms. At about 3.5 m.y.b.p. the South Gorda plate ceased subduction -- presumably

reflecting the northward motion of the triple junction. This has produced dextral strike-slip structure at the south end of the Cascades axis. The most northerly evidence of San Andreas deformation, at the mouth of the Klamath River is only about 120 km west of Mt. Shasta; and the Walker Lane trends into the southern end of the Cascades.

The conspiracy of Basin & Range extension and the northward propagation of the Mendocino triple junction appears to have set the stage for a period of extensional rejuvenation of Cascades volcanism -- immediately prior to the cessation of subduction-driven magmatism. Such complex tectonic interactions are presumably no uncommon. The next chapter undertakes a study of the large calderas elsewhere in the world to examine the correlation of such calderas with areas of tectonic complexity such as those just described in the Cascades.

III. TECTONIC ASSOCIATION OF LARGE CALDERAS

The preceding sections have discussed the tectonic setting of the southern Cascade Range and made some observations about the relationship between large caldera-forming volcanoes and tectonic setting. The premise is that, given the availability of high temperature mantle which is capable of producing melt, volcanism displaying a bimodal, generally basalt/rhyolite assemblage, is particularly likely to develop in areas where intersecting tectonic elements occur. The intersecting elements presumably cause enhanced deformation which more readily allows migration of magma. The large calderas in and adjacent to the Cascades are consistent with this model (as discussed in detail above).

1) Crater Lake occurs at the intersection of the Klamath Graben with the Cascades magmatic arc. The Klamath Graben is a Basin and Range graben which has propagated into the arc within the last 4 m.y.b.p. At its SE end the Klamath Graben strikes NNW; with proximity to the Cascades arc, it curves to a N-S strike. The Klamath Graben trajectory changes strike under the influence of the arc and the arc is influenced by the intersecting graben -- producing Crater Lake Caldera. This is a situation where arc volcanism is influenced by an intersecting (graben) rift.

2) Medicine Lake caldera is located behind the magmatic arc at a point where

contrasting trends of Basin and Range structure occur. The Fall River Valley and Big Valley grabens -- on either side of the Big Valley Mountains -- strikes NNW toward Medicine Lake. North of Medicine Lake, faulting -- as well as tectonic stress trajectories -- strike N-S. In addition there is geophysical evidence for interaction of Medicine Lake caldera magmatism with the adjacent magmatic arc at Mt. Shasta. Thus Medicine Lake Caldera has formed where extensional tectonism has interacted with arc volcanism. Again, this is a situation of arc volcanism influenced by intersecting rifting (graben).

3) Lassen Peak, the site of the former caldera Mt. Tehama (now filled), occurs at the intersection of the magmatic arc with a locus of contrasting directions of Basin and Range faulting similar to Crater Lake and Medicine Lake. Lassen also appears to be influenced to some degree by the northern end of the right lateral Walker Lane. SE of Lassen the Lake Almanor graben strikes NW (parallel to the Walker Lane) toward Lassen; whereas north of Lassen, Hat Creek Graben strikes along a NNW trend which parallels the trend of the volcanic arc between Lassen and Shasta. Thus Lassen appears to have developed at a point of intersecting rift (graben) structure.

4) Newberry caldera is located at the intersection of the shallow graben of Fort Rock Valley which is an extension of the NW trending Silver Lake Valley - Summer Lake Graben. In addition, like Medicine Lake, there is geophysical evidence of

magmatic interaction with the Three Sisters volcanic complex which is on the magmatic arc. Quaternary tectonic stress trajectories indicate that Newberry is located at a point where the NNW trending Basin and Range extension is curving to parallel the Cascades N-S trend. This is also supported by the fact that the axis of Cascades volcanism has stepped east within the last 4 my and extensional structures parallel to the arc have developed. Newberry, also, appears to have developed at a point where extensional tectonism has intersected the arc.

There are very few locations within the Cascades, where B&R structure intersects the arc, that have not been the site of large caldera formation. These relationships indicate that the location of the large calderas in the Cascades is not arbitrary but rather controlled by intersecting tectonic structure. Analysis of tectonic stress trajectory indicated by geomorphically contiguous vent alignments which coincide with the age of collapse events that formed these calderas indicates that Basin and Range deformation was influencing the stress regime in each case at the time of collapse (Ferrall, 1983). The orientation of Basin and Range structure at an angle to the arc trend implies that its deformation is not directly related to current plate tectonic processes of the North American plate margin. It is thought that the B&R originated as a backarc spreading feature but has subsequently become influenced by the transform plate margins to the north and south of the Cascades and resultant rotational strains. It is known that the direction of extension has changed

at least once (Zoback and Anderson, 1981) and probably twice (see Chapter 3) since opening of the northern Basin and Range began 17 m.y.b.p. Also, subduction of the Gorda Plate had ceased prior to about 3 m.y.b.p. Thus, in the Cascades, the structure of the volcanic arc and backarc do not appear to be directly related to the contemporaneous configuration of the subducting plate and are responding to processes that appear to be in the overriding plate.

This type of interaction may not be an unusual phenomenon. It is a premise of the following discussion that the locations of large calderas may be indicative of the intersection of structure in the overriding plate with the arc. This overriding plate structure may be due to deformation induced by contemporaneous subduction-induced stresses or to structure inherited from preexisting tectonic activity. To test this caldera/tectonic association, a broad study of the large calderas elsewhere in the world has been carried out. Utilizing the available literature and maps, the regional setting of these calderas has been examined to identify the tectonic elements which are present. Where available, imagery is also utilized. Calderas are characterized according to: location; size; a brief description of the volcanic geology; and a description of the tectonic setting.

This study is aimed at an examination of the association of broad regional tectonic features with caldera location for a statistically significant number of large calderas. Local structural relationships within one or two caldera diameters of the vent, although discussed, are not the main emphasis. The goal of this section is to examine and categorize the tectonic character of large caldera locations.

Rationale and Approach

The initial step in such an examination is the determination of the minimum caldera size which characterizes a tectonically significant feature -- that is, a feature which is developed in the sub-volcanic crust rather than one that is a manifestation of processes taking place in the volcanic edifice which sits on the crust. Abundant examples exist of small calderas which form at the summits of large volcanoes (eg. Kilauea, Mauna Loa and Mt. St. Helens). Where sufficient data exists to identify the location of the magma chambers, these small calderas are shown to result from activity of small chambers within the edifice of the volcano.

Two well documented examples are Mt. St. Helens and Kilauea. The May 18, 1980 eruption of Mt. St. Helens produced a 1 km caldera (amphitheatre). Seismicity immediately preceding the eruption was localized in a small volume less than 2.5 km (el 675 m) below the pre-eruption summit (el 3175 m) (Endo et al, 1981) -- indicating that the roof of a shallow magma chamber was at this level -- above the base of the edifice. The active caldera at the summit of Kilauea is approximately 3 km in diameter and the top of the magma chamber here has been shown to be located at the 1 to 3 km levels. This level is between the el +200 m and el -1200 m -- well above the base of the edifice of the volcano which is located at about el -2000 m.

This is in contrast with crustal silicic magma chambers. For example, the depth of the top of the crustal magma chamber at Long Valley caldera (maximum caldera dimension: 32 km) is thought to be about 4.5 km -- although the chamber was probably deeper at the time of the cataclysmic eruption which formed the caldera

(Sanders, 1984). Because there is essentially no volcanic edifice below the caldera at Long Valley, this magma chamber is located well down into the underlying crust where it is influenced most strongly by regional crustal stresses. Similarly, recent seismicity at the Phlegrean Fields caldera (maximum caldera dimension: 12 km) indicates that the top of the magma chamber is at least 3-4 km below the base of the volcano (Barberi et al, 1984). At Rabaul (maximum caldera dimension: 14.7 km), during the seismic crisis of 1983-84, 95% of the earthquakes were shallower than 3 km depth indicating that the roof of the magma chamber is below this depth and therefore well below the volcano edifice (McKee et al, 1984).

These large calderas clearly arise from crustal chambers. It therefore appears that the choice of a sample of large calderas lacking major edifices -- such as the oceanic island volcanic edifices which extend kilometers below sea level -- may be expected to filter out calderas which are the result of activity of shallow within-edifice magma chambers and thereby avoid confusing the effect of tectonic stresses with the effect of edifice stresses,

In his evaluation of caldera structural styles, Walker (1984) presents a histogram of diameters of Quaternary calderas. He found a bimodal relationship in which a strong mode was found for calderas less than 20 km in diameter and a weak mode for those with diameters 22-27 km (Figure 49a). However, within the 1-20 km class of calderas, there is a strong minimum at 4-5 km diameter which separates diameters smaller than 4 km from calderas with larger diameters. In Walker's histogram of Tertiary Basin and Range calderas (Figure 49d), the minimum caldera diameter is 8

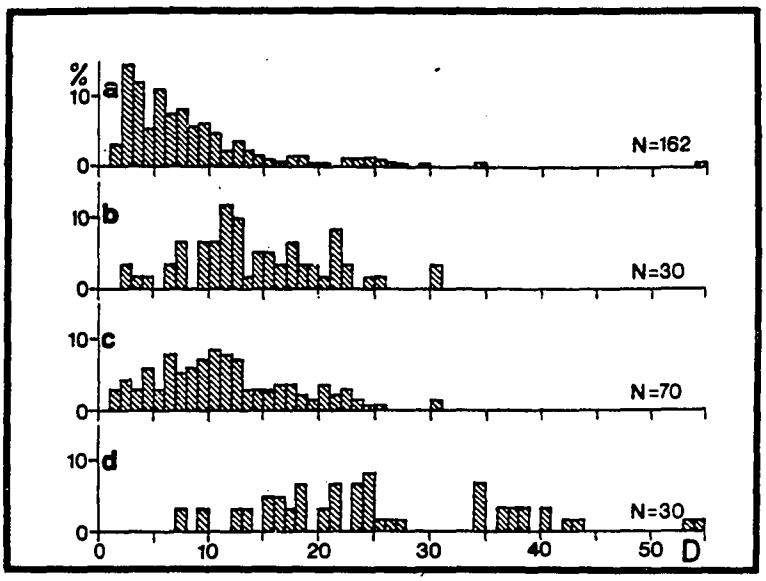

Figure 49. Histogram of caldera sizes (Walker, 1984) showing Quaternary calderas (a), cauldrons that have a subsided block of volcanic rocks (b), cauldrons irrespective of the character of the subsided block (c), and Tertiary calderas of the Basin and Range province. Note the low occurrence of quaternary calderas (a) in the 4 to 5 km range and the absence of Basin and Range calderas (d) less than 7 km in diameter.

km. Basin and Range calderas are thought to be the result of the activity of crustal magma chambers which may or may not be preceded by the formation of significant volcanic edifices (Lipman, 1984). It is possible that the smaller calderas, less than 5 km in diameter, form a class which is the result of activity in shallow (perhaps transient) edifice magma chambers while the larger ones (greater than 8 km) are characteristic of deeper crustal chambers. Intermediate sized calderas 5-8 km in diameter may represent transitional cases.

The smallest of the Cascades calderas which have been shown in the preceding chapters to be related to intersecting tectonic influences is Newberry, which is 8.1 km in diameter. Therefore, based on Walker's histogram of the Basin & Range calderas and the Cascades cases which are demonstrably influenced by crustal tectonic structure, a minimum caldera diameter of 8 km has been chosen for this general study of large calderas tectonic association. In addition, the sample has been limited to Quaternary calderas for two reasons:

1) Plate tectonic relationships are best understood for currently active processes where ongoing seismicity can be utilized. As a result, plate margins and motions as well as more localized intra-plate tectonic activity are best resolved for contemporaneous tectonics. Since calderas are relatively localized features, such resolution is essential;

2) Recognition of calderas older than the Quaternary is frequently difficult. Both erosion and volcanic processes tend to obscure them within a few hundred thousand years (eg. Los Humeros, Mexico). Since the aim of the present study is to

examine the caldera-tectonic issue in light of the current global population of calderas, the age limitation to the Quaternary increases the chance of obtaining an unbiased population.

Accordingly, a listing of the world's large calderas greater than 8 km has been compiled and is presented on Table 2. Caldera dimensions are also shown. (Calderas of the Andes have been excluded from the compilation because of the incompleteness of the data set -- see the Andes sheet in Table 3.) A total of eighty two such calderas are identified. Such a compilation has not been carried out previously. Basic sources used for compiling this list include: Pike & Clow (1981), Spera & Crisp (1981), Macdonald (1972), Simkin et al (1981), and IAVCEI (1951-1976). However, it was necessary to review considerable supplementary sources to produce a complete inventory. Supplementary sources are listed for each caldera. Caldera dimensions have been taken in most instances from direct measurements on maps and imagery and some are considerably more reliable than many published compilations.

These calderas have each been investigated in order to characterize them in terms of the volcanic character, local structure, regional structure, tectonic elements present and tectonic association. This information is presented in a tabulated form on Table 3A through 3XX at the end of this section. In some cases, this information is not easily acquired or is simply not available. Remote areas such as the Aleutians, Kamchatka, the Philippines, Indonesia, New Britain and the Afar are not well studied in general -- although specific calderas in these provinces may be well studied. Language is also a problem. The bulk of information on Kamchatka and the Kuriles is in

Table 2

CALDERAS OF THE WORLD WITH MAXIMUM DIMENSION > 8 km	
Caldera	Dimensions (km)
CASCADES (arc)	
Crater Lake, Oregon	10 x 9
Medicine Lake, California	9 x 7
Newberry Caldera, Oregon	8 diam
BASIN & RANGE (rift/backarc)	
Long Valley, California	32 x 17
SNAKE RIVER PLAIN (hot spot/rift)	
Island Park, Idaho	25 diam
Yellowstone, Wyoming	75 x 45
RIO GRANDE RIFT (rift)	
Jemez (Valles) Caldera, New Mexico	23 diam
MEXICO (arc)	
Sierra la Primavera, Mexico (west)	11 diam
Los Humeros, Mexico (east)	21 x 15
CENTRAL AMERICA (arc)	
L. Atitlan, Guatemala	24 x 21
Amatitlan, Guatemala	16 x 14
L. Coatepeque, El Salvador	11 x 6.5
L. Ilopango, El Salvador	11 x 8
Masaya, Nicaragua	10.8 x 6.6
ANDES (arc)	not catalogued
SOUTH SHETLAND ISLANDS (arc)	
Deception Island, Antarctica	11.3 x 9.7
ALEUTIAN ISLANDS & ALASKA (arc)	
Veniaminoff, Alaska Peninsula	8.2 diam
Aniakchak, Alaska Peninsula	10 x 9.2
Okmok, Umnak I., Aleutian Is.	11 x 10
Fischer, Unimak I., Aleutian Is.	16.5 x 11

Table 2 (Continued)

CALDERAS OF THE WORLD WITH MAXIMUM DIMENSION > 8 km	
Caldera	Dimensions (km)
KAMCHATKA (arc)	
Krashennikov (central)	10 x 9
Uzon (central)	18 x 9
Bolshoy Semyachik (central)	12 x 10
Maly Semyachik (central)	10 x 8.4
Ksudach (south)	10.3 x 6.6
Gorley Khrebet (south)	14 x 9
Opala (south central)	18.7 x 13
Kurile Lake Caldera (south)	9.7 x 7
Pauzhetskaya (south)	29 x 21
KURILE ISLANDS (arc)	
Nemo, Onekotan I., (north)	10.7 x 9
Lion's Jaw [Lvinaya Past], Iturup I. (south)	10 x 8
JAPAN (arc)	
Kutcharo, Hokkaido (east)	23 x 20
Akan, Hokkaido (east)	22 x 14.7
Toya, Hokkaido (west)	12 diam
Shikotsu, Hokkaido (west)	15 x 14
Towada, Honshu (north)	13 square
Hakone, Honshu (central)	13.5 x 10
Aso, Kyushu (central)	24 x 17
Aira, Kagoshima Bay, Kyushu	23 square
Atta, Kagoshima Bay, Kyushu (south)	16 x 12
Kikai, south of Kyushu	22 x 13
PHILIPINES (arc)	
L. Taal, Luzon (south)	26 x 25
Laguna de Bay, Luzon	25 x 12
INDONESIA (arc)	
Tondano Depression, Suluwesi (north)	15.5 x 6
Toba, Sumatra (north)	100 x 31
Manindjau, Sumatra (central)	21.5 x 10
Ranau, Sumatra (south)	16.6 x 13.5
Gedonsurlan, Sumatra (south)	20 x 16.5
Krakatau, Sunda Straights	8 x 4
Danau, Java (west)	15 x 13.5
Tengger [Bromo?], Java (east)	11 x 8
Idjen, Java (west)	17 x 14
Bratan, Bali	10.5 x 6.3
Batur, Bali	12.5 x 9.3
Segera, Lompok	8.1 x 3.6

Table 2 (Continued)

CALDERAS OF THE WORLD WITH MAXIMUM DIMENSION > 8 km	
Caldera	Dimensions (km)
NEW BRITAIN (arc)	
Long Island, Papua N.G. (west of New Britian)	14.9 x 10.9
Dakataua [Benda or Talasea], New Britain (central)	13 x 10
Hargy [Gallosuelo], New Britain (central)	13 x 10.8
Rabaul, New Britain (east)	14.7 x 9
NEW HEBRIDES (arc)	
Ambrym I.	13 x 12
NEW ZEALAND (arc)	
Taupo, North Island	30 x 26
Rotorua, North Island	17 diam
Haroharo caldera [Okataina], North Island	28 x 16
ITALY (arc/backarc)	
Latera caldera [Vulsini]	11 diam
Lago di Bolsena [Vulsini]	13 x 11
Sacrofano caldera [Sabatini]	10 x 6
Lago di Bracciano [Sabatini]	10 diam
Alban Hills [Artemisio]	10 diam
Phlegrean Fields	12 x 11
AEGEAN (arc)	
Santorin [Thera]	10.8 x 7
CENTRAL AFRICA (hot spot)	
Tibesti, northeast Chad, Africa:	
Emi Koussi	12.9 x 11.3
Tarso Voon	18 x 11
Tarso Toon	11 x 9
Tarso Yega	17 x 11
Yirrique	14 x 13
EAST AFRICAN RIFT (rift)	
Nabro [Bidu Pile], Afar, Ethiopia	8 x 7.5(?)
Asavyo, Afar, Ethiopia	8.2 diam
O'A, Ethiopia, (south)	16 x 13
Corbetti, Ethiopia (south)	12.5 x 10
Menengai, Kenya (south)	12 diam
Suswa, Kenya (south)	12 x 8
Ngorongoro, Tanzania	20 x 17

Table 2 (Continued)

CALDERAS OF THE WORLD WITH MAXIMUM DIMENSION > 8 km	
Caldera	Dimensions (km)
ICELAND (rift/hot spot)	
Askja (central)	9.5 x 8.7

Russian, Japan in Japanese, Italy in Italian and Central America in Spanish. These sources have been used sparingly -- where willing translators were available. In general, however, only the literature written or abstracted in English has been utilized.

Volcanic character is described in terms of the presence of ashflows and their association with caldera collapse; the presence of a bimodal assemblage; and the petrologic affinity of the volcanic suite. Where this information is omitted, it is not available. For example, if ashflows are present but association with caldera collapse is not known, it is stated that ashflows are present. If the area has been studied and ashflows are demonstrably not associated with a given caldera collapse, (eg. Askja), this is discussed explicitly. Similarly, if no note is made of the volcanic assemblage, it is not known.

Local structure generally refers to geologic structure within a few tens of km of the caldera which might point to more regional influences. Caldera rim alignments, vent alignments and local faulting fall in this category. Regional structure is discussed in terms of faulting, seismicity, gravity anomalies, etc. which relate the tectonics to the caldera location. Tectonic elements are the plate tectonic features (arcs, rifts and transform faults) which are operative in the vicinity of a given caldera. In this context, the term rift has been given special usage. It is used in a generic sense to imply significant tectonic extension and faulting. In many cases the genetic significance of rifting in terms of an oceanic spreading axis or backarc spreading axis is not clear -- although tectonic rifting is clearly taking place. Both the Basin and Range and the East African Rift are features which do not fall easily into the ridge-

trench-transform triumvirate of the plate tectonic paradigm. A possible explanation of this difficulty may relate to the inheritance of one tectonic environment by another (eg. B&R: backarc inherited by transform couple, see preceding chapters). In any case, in the present treatment, both of these provinces are discussed as generic rifts.

Finally, each caldera is categorized in terms of the tectonic elements which appear most directly related to its occurrence. Particular attention is given to intersecting structures that may act to localize the caldera. The tectonic-association categories which have been identified are:

AIR Arc / Intersecting Rift
AAR Arc / Arc-parallel Rift
AAR/S Arc / Arc-parallel Rift with strike-slip indicated
ATE Arc / Transform / Secondary extension
AOI Arc / Offset or Inflection in volcanic axis
ACZ Arc / Collision Zone
APF Arc / Preexisting Fault
AA Arc / Arc
ROI Rift / Rift Offset or Inflection
RL Rift / Lineament
RRR Rift / Rift / Rift
RHS Rift / Hot Spot
HS Hot Spot

These categories have been identified with the goal of providing a tectonic context for the study of large calderas and to examine the variety of tectonic settings where they occur. The result indicates that in some cases, tectonic processes may be operating in a complex manner producing a variety of deformational styles in environments that appear at first look to be straight-forward types. An example is the case of collision zones where platelets are being accreted from a subducting

plate to an overriding plate. Simple compression is indicated at such a location however localized extension is indicated by the presence of calderas such as Hakone and Ambrym. These concepts and the individual categories are discussed below.

Of these categories, AIR, AAR, AAR/S, ATE are related -- all involving arc-rift interaction. 49% of all the calderas fall in these four classes. AOI is a classification for calderas located at points where variations in arc axis alignment can be observed but for which the tectonics of the overriding plate in the vicinity of the caldera is not well known. Many of the members of this category are islands. ACZ, APF and AA represent special cases and each of them has no more than two members.

The rift categories are less populated with a total of 12 members. RL, RRR and RHS are special cases each with no more than 2 members. The ROI category calderas represent 75% of the rift calderas. These are dominated by East African Rift calderas and are generally well constrained. The HS category is established for the five large Tibesti calderas.

The details of each caldera are presented on Table 3A through 3XX with numerous figures for illustration. This information is the basis of the caldera-tectonic categories. A discussion of the classification results and other implications of this information is presented at the end of the Table.

Table 3

The caldera summary sheets of Table 3 follow this listing -- grouped as indicated above on Table 3A through 3XX.

Table 3A

Caldera Name		Location		
Long Valley Caldera (LVC)		west central California		
Elongation	Volcanic Character	Local Structure	Regional Structure	Tectonic Elements
E-W 32 x 17 km	Abundant high silica rhyolite ash-flows accompany caldera formation; bimodal basalt/rhyolite assemblage; resurgent doming	Elongation parallels E-W B&R extension; seismic activity on the Hilton Creek Fault, a B&R fault bounding the west side of Owens Valley, is interpreted to be related to magma movement beneath the caldera (E)	Eastern bouding fault of the Sierras; Pancake (PL) and Warm Springs (WSL) Landsat lineaments trending ENE; Nevada Seismic Zone trending NNE	Western edge of Basin & Range spreading
Additional Information				
The caldera was formed 0.7 mybp associated with the eruption of the Bishop Tuff. LVC is localized at the western margin of the B&R at the north end of Owens Valley (OV) -- an active B&R basin formed in the last 2 my (D) which appears to be propagating northward into the Sierras through Long Valley. Seismic activity on Hilton Creek Fault (outside the caldera) is associated with magma movement (E). The Nevada Seismic Zone (NSZ) enters Owens Valley from the NNE opposite LVC. The NSZ is a generally NNE trending zone of historic seismicity (A) which extends across Nevada. LVC occurs at a major change in the trend of the NSZ at the north end of OV where the NSZ bends to the SE to parallel OV. LVC also occurs on the strike of two ENE-trending Landsat Lineaments: PL and WSL. These features strike across central Nevada and are marked by termination of N-trending ranges, aligned streams, tonal boundaries (B), and mapped faults (C). The tectonic significance of these lineaments and the NSZ is not established.				
References				
(A) Wallace, 1984; (B) Rowan and Wetlaufer, 1981; (C) Sabins, 1978; (D) Slemmons et al, 1979; (E) Savage and Clarke, 1979; (F) Hildreth, 1981 FIGURE 50 and 51				
Category: RIFT (Owens Valley/Basin & Range) / LINEAMENT (PL and WSL) / FAULT (Sierran Fault)				

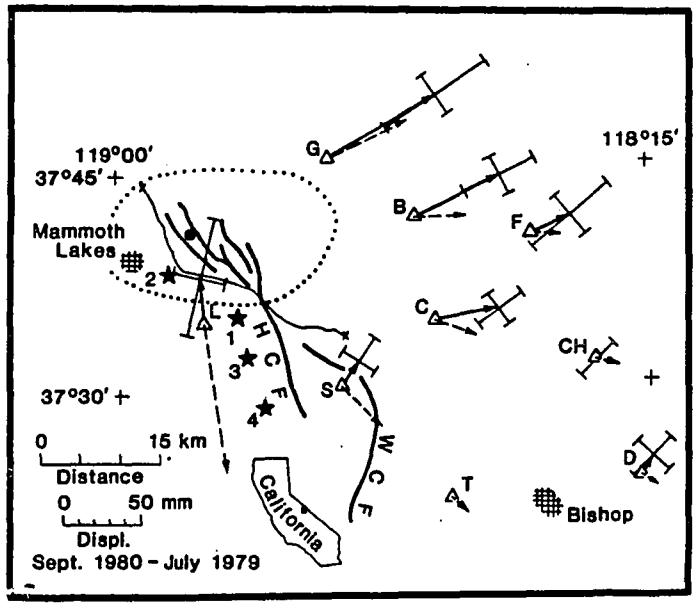

Figure 50. Long Valley Structure Map (Savage and Clark, 1982) showing recent earthquakes (stars) paralleling a mapped Basin and Range fault (HCF). This seismicity has been related to magma movement beneath long valley caldera.

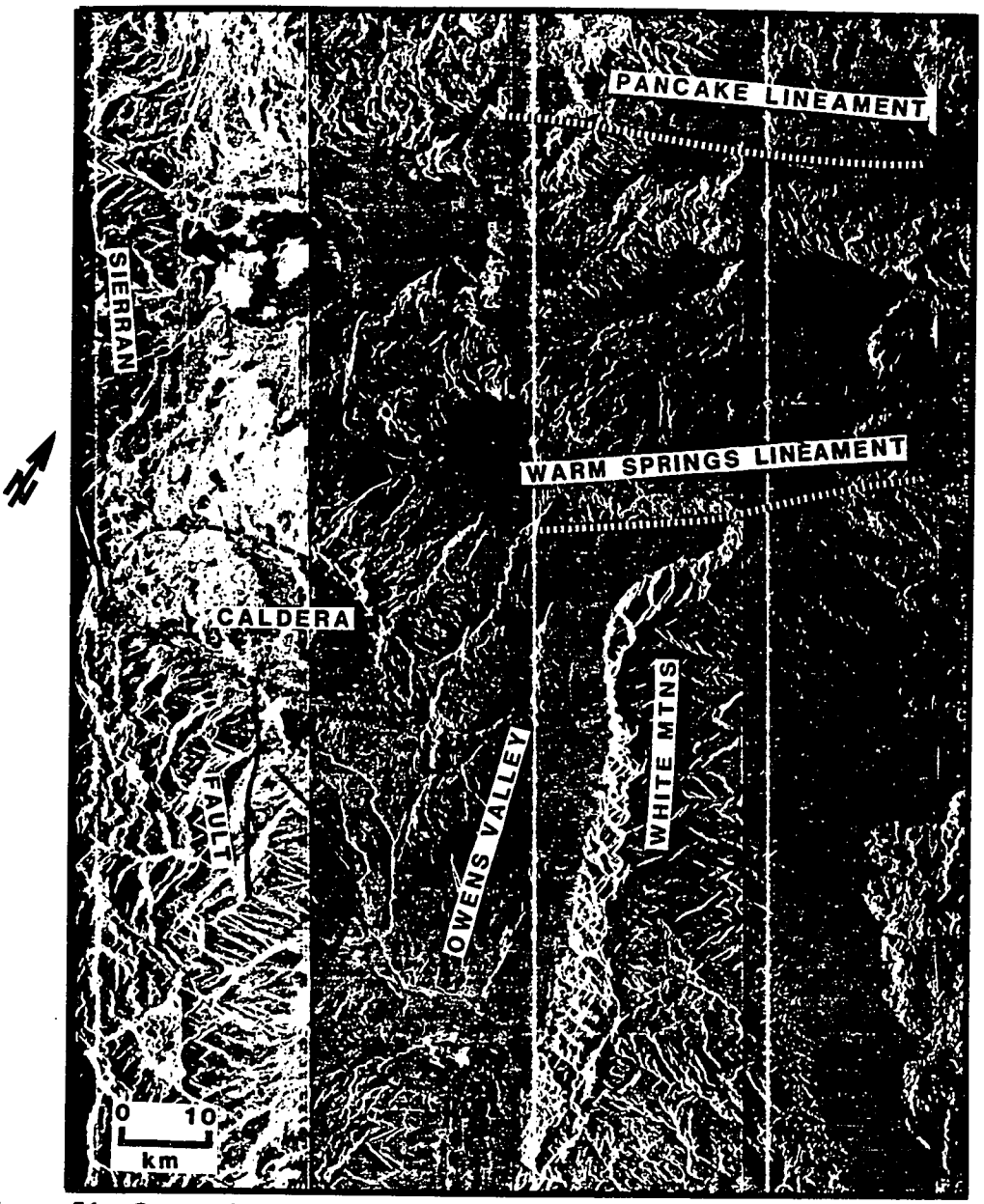

Figure 51. Seasat image of Long Valley Caldera showing structural features associated with the caldera including: the Sierran Fault, Pancake and Warm Springs lineaments. Nevada Seismic Zone enters the north end of Owens Valley from the NNE and bends to strike parallel to the valley.

Table 3B

Caldera Name		Location		
Island Park Yellowstone		Snake River Plain (SRP) 20 km SW of Yellowstone, Eastern Idaho Northwestern Wyoming		
Elongation	Volcanic Character	Local Structure	Regional Structure	Tectonic Elements
Island Park: Circular 25 km	basalt/rhyolite assemblage; abundant high silica (H) rhyolitic ashflows associated with caldera formation; multiple caldera-forming episodes (A)	NW wall of caldera strikes NE parallel to SRP axis (F)	SRP follows regional structure of Precambrian basement (D,E); N-S faults verge from the south -- related to faulting on the east margin of Basin and Range; E-W to NW-SE faults verge from the west and northwest related to Rocky Mountains deformation (A)	Yellowstone Hot Spot; Eastern margin of the Basin and Range
Yellowstone: NE 75 x 45 km		elongation parallels long axis of the Snake River Plain (SRP); elongation of two late stage resurgent domes is NW -- parallel to SRP extension (B)		
Additional Information				
	Although the exact margins of the Yellowstone caldera are not as well defined as many calderas, the dimensions indicated by extensive mapping of the most recent and largest caldera-forming stage place it as the second largest caldera in the world -- second to Toba's 100 km length. However, it lacks the striking tectonic influence of Toba and appears to be related to a combination of distributed preexisting faulting, Basin and Range deformation, and hot spot activity.			
	Silicic volcanism has a monotonic younging trend to the NE with the youngest silicic volcanism occurring at Yellowstone. This is interpreted to be the track of a deep thermal plume -- the Yellowstone Hot Spot. Silicic volcanism is followed by volumetrically much smaller basaltic volcanism. Island Park (IP) has evolved to the basaltic stage while Yellowstone is still dominated by silicic volcanism.			
	The Precambrian structural trend, which the SRP parallels, is marked by magnetic anomalies which extend both NE and SW of the limits of SRP volcanism (E). Specific tectonically active regional features include: the Teton Basin -- a NW-trending Basin and Range feature which strikes toward and merges into IP from the south; the NW-trending Teton Fault Zone and Jackson Hole basin which project into Yellowstone from the south; and the E-W Centennial Fault Zone and the NW-SE trending Hebgen Lake Fault Zone which verge from the W and NW and intersect beneath the Yellowstone Caldera. Considerable seismicity is released on these features in the vicinity of Yellowstone and to the south on the eastern margin of the Basin and Range.			
References				

25 km	dant high silica (H) rhyolitic ashflows associated with caldera formation; multiple caldera-forming episodes (A)	NW wall of caldera strikes NE parallel to SRP axis (F)	N-S faults verge from the south -- related to faulting on the east margin of Basin and Range; E-W to NW-SE faults verge from the west and northwest related to Rocky Mountains deformation (A)	Yellowstone Hot Spot; Eastern margin of the Basin and Range
Yellowstone: NE 75 x 45 km		elongation parallels long axis of the Snake River Plain (SRP); elongation of two late stage resurgent domes is NW -- parallel to SRP extension (B)		

Additional Information

Although the exact margins of the Yellowstone caldera are not as well defined as many calderas, the dimensions indicated by extensive mapping of the most recent and largest caldera-forming stage place it as the second largest caldera in the world -- second to Toba's 100 km length. However, it lacks the striking tectonic influence of Toba and appears to be related to a combination of distributed preexisting faulting, Basin and Range deformation, and hot spot activity.

Silicic volcanism has a monotonic younging trend to the NE with the youngest silicic volcanism occurring at Yellowstone. This is interpreted to be the track of a deep thermal plume -- the Yellowstone Hot Spot. Silicic volcanism is followed by volumetrically much smaller basaltic volcanism. Island Park (IP) has evolved to the basaltic stage while Yellowstone is still dominated by silicic volcanism.

The Precambrian structural trend, which the SRP parallels, is marked by magnetic anomalies which extend both NE and SW of the limits of SRP volcanism (E). Specific tectonically active regional features include: the Teton Basin -- a NW-trending Basin and Range feature which strikes toward and merges into IP from the south; the NW-trending Teton Fault Zone and Jackson Hole basin which project into Yellowstone from the south; and the E-W Centennial Fault Zone and the NW-SE trending Hebgen Lake Fault Zone which verge from the W and NW and intersect beneath the Yellowstone Caldera. Considerable seismicity is released on these features in the vicinity of Yellowstone and to the south on the eastern margin of the Basin and Range.

References

(A) Christiansen, 1984; (B) Christiansen, 1982; (C) Smith and Christiansen, 1980; (D) Eaton et al, 1980; (E) Mabey et al, 1978; (F) Landsat Image: Short et al, 1976, Pl 98; (G) Smith, 1978; (H) Hildreth, 1981

FIGURE 52

Category: RIFT (Basin and Range) / HOT SPOT (Yellowstone) / PREEXISTING FAULTS (Centennial; Hebgen Lake)

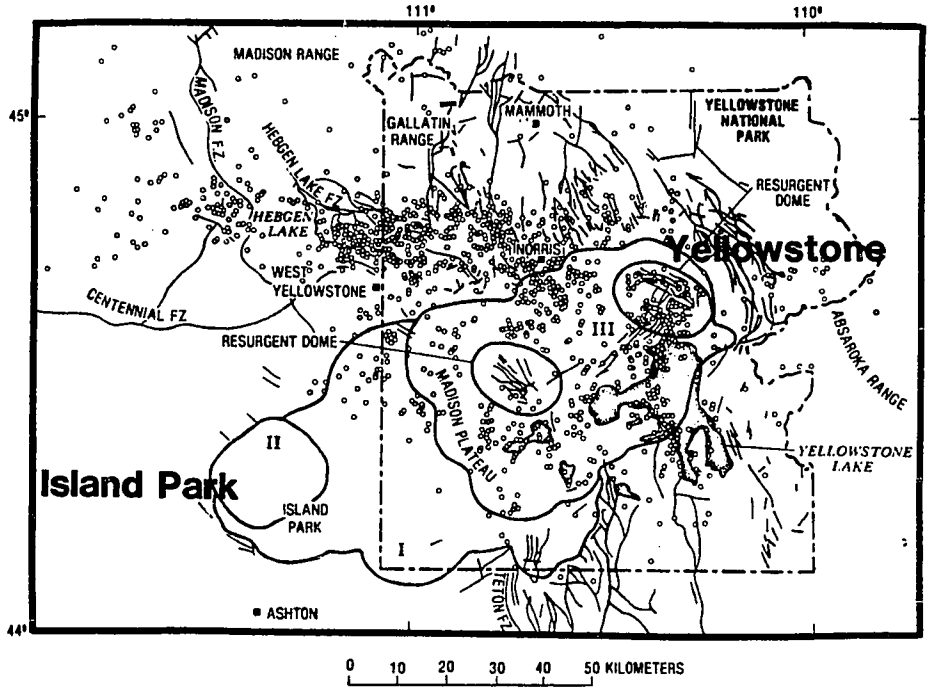

Figure 52. Yellowstone caldera-forming phases (Christiansen, 1982) showing calderas of the Yellowstone-Island Park complex. Note the Centennial and Hebgen Lake Zones which intersect in the vicinity of the most recent caldera stage. These faults are likely related to Rocky Mountain deformation which predates Snake River Plain volcanism. Faults related to the eastern margin of the Basin and Range include the N-S Teton Fault Zone and related faults to the east.

Table 3C

Caldera Name		Location		
Valles--Toledo caldera		Jemez Mountains, northern New Mexico		
Elongation	**Volcanic Character**	**Local Structure**	**Regional Structure**	**Tectonic Elements**
Circular 23 km diameter	Abundant zoned rhyolite-intermediate (F) ashflows (Bandolier Tuff) accompany caldera formation; bimodal basalt/rhyolite assemblage; multiple caldera with resurgent activity (A)	The southeast wall of the caldera has a linear aspect trending NE parallel to the Jemez Lineament (JL) (B,A); Some structure within the caldera parallels the JL (B)	Located astride the Rio Grande Rift (RGR) at its intersection with the Jemez Volcanic Lineament; the RGR is a northward propagating N-S rift which marks the easternmost edge of Basin and Range deformation; the JL is a 700 km-long alignment of dominantly basaltic volcanism striking NE-SW across New Mexico and Arizona	Eastern margin of Basin and Range; Jemez Lineament
Additional Information				
Valles is the only example of a large caldera along the Rio Grande Rift and it occurs where the Jemez lineament crosses the rift. It is considered to be a classic example of tectonic control of caldera development (C). Valles is located on the northern RGR. At this point the RGR is a single rift propagating northward. Volcanism on the JL is not time-transgressive and there is little surface expression of tectonic structure (C). There is some evidence of Tertiary strike-slip along the JL but evidence of the sense of motion is ambigous (E). The tectonic significance of the JL is not understood. It lies parallel to regional Precambrian structure and is regarded as a manifestation of a fundamental zone of weakness (C). There is a similar, less well developed volcanic lineament in central N.M. -- the Morenci (D) -- which parallels the JL. The JL is seismically active to the southwest of the caldera but there is no historic seismicity associated with the caldera itself, which formed about 1 mybp (B). Volcanism along both the RGR and the JL is primarily basaltic. In terms of intensity of volcanism, the JL is at least as profound a feature as the RGR and it may be related to deeper, perhaps mantle processes (C).				
References				
(A) Smith and Bailey, 1968; (B) Self et al, 1985; (C) Smith and Luedke, 1984; (D) Baldridge and Kron, 1980; (E) Aldrich, 1985; (F) Hildreth, 1981				
FIGURE 53				
Category: RIO GRANDE RIFT (Basin & Range) / LINEAMENT (Jemez Lineament)				

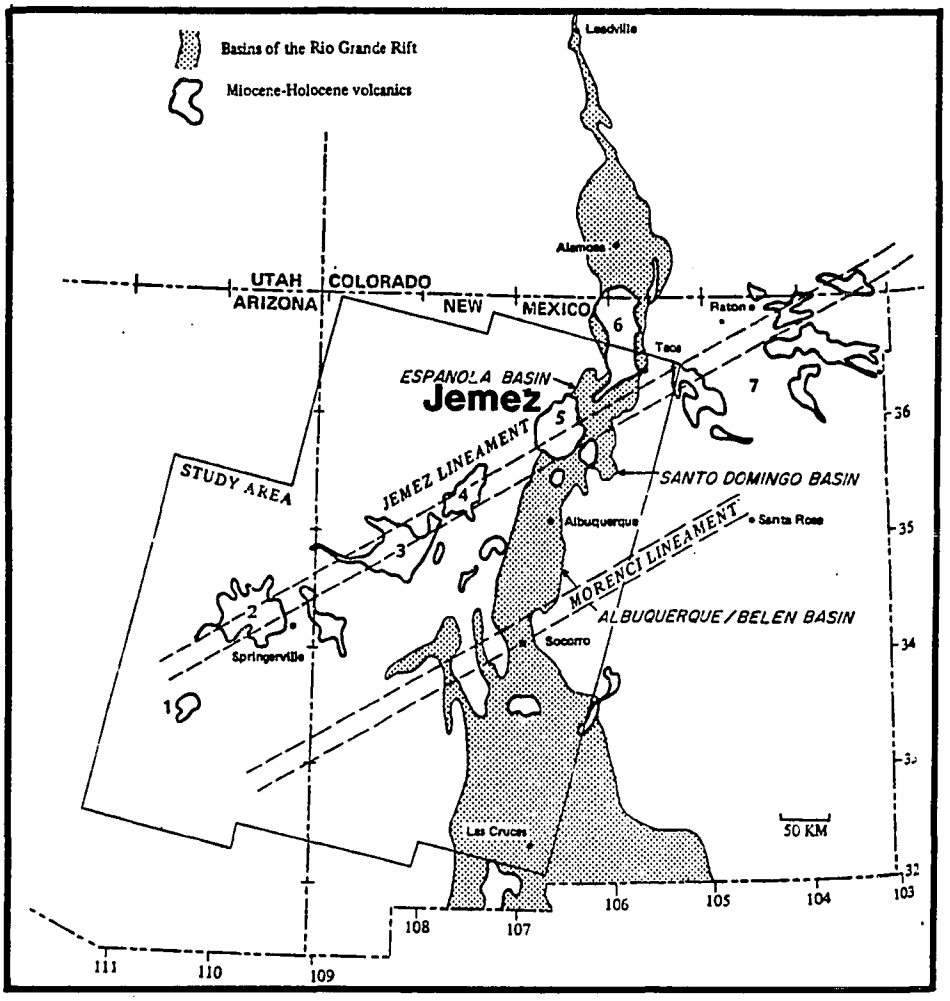

Figure 53. Jemez Caldera and Jemez Lineament (Baldridge et al., 1980). Valles and Toledo calderas are located within the Jemez Mountains (5). Volcanism along the Jemez Lineament is contemporaneous, not time transgressive and follows the trend of Precambrian structure.

Table 3D

Caldera Name	Location			
Sierra La Primavera	Western Mexico			
Elongation	**Volcanic Character**	**Local Structure**	**Regional Structure**	**Tectonic Elements**
Circular 11 km (A)	dominant high-silica rhyolite (peralkaline) composition; abundant ashflows accompany caldera collapse (A)	a WNW alignment of 10 cinder cones strikes toward Sierra La Primavera (SLP) from the SE (A)	Located at the west end of the Trans-Mexican Volcanic Belt (TMVB) adjacent to its intersection with the N-S extensional Colima (Tepic) Graben. NW of SLP the character of the TMVB changes, becoming more extensional, and influence of Rivera Plate subduction is indicated (B). Arc strike changes from a diffuse E-W orientation on the East TMVB to a relatively well-defined NW trend west of SLP	Trans-Mexican Volcanic Belt (Arc); extensional tectonics of the NW Segment of the TMVB

Additional Information

SLP is a peralkaline center in close proximity (within 20 km) of contemporaneous (less than 0.1 mybp) calc-alkalic andesitic volcanic centers. The region surrounding the caldera is characterized by extensional faulting along three trends: the graben of Lake Chapala, which strikes E-W and parallels the main TMVB to the east; Zacoalco Graben, which strikes NW and merges with the Northwestern Segment of the TMVB; and the Colima Graben, which strikes N-S and contains the active Volcan Colima, 60 km south (in front of) the main volcanic belt (B). SLP is on the main volcanic axis on the strike of the Colima Graben, and at the point of inflection in the arc. SLP is 20 km north of the intersection of these three grabens. NW of SLP, the intimate association of alkaline and calc-alkaline volcanics is more common (B). It has been interpreted (B) that the evolving extensional volcanism of this area is a precursor to a spreading ridge jump from the East Pacific Rise, along the west side of the Rivera Plate, to the Colima-Chapala-Zacoalco rift intersection. (This would result in the Colima Graben becoming a spreading ridge and the Zacoalco graben becoming a dextral transform (B).

References

(A) Mahood, 1981; (B) Luhr et al, 1985

FIGURES 54, 55, 56

Category: ARC (Trans-Mexican Volcanic Belt) / INTERSECTING RIFT (Colima Graben) / INFLECTION IN ARC

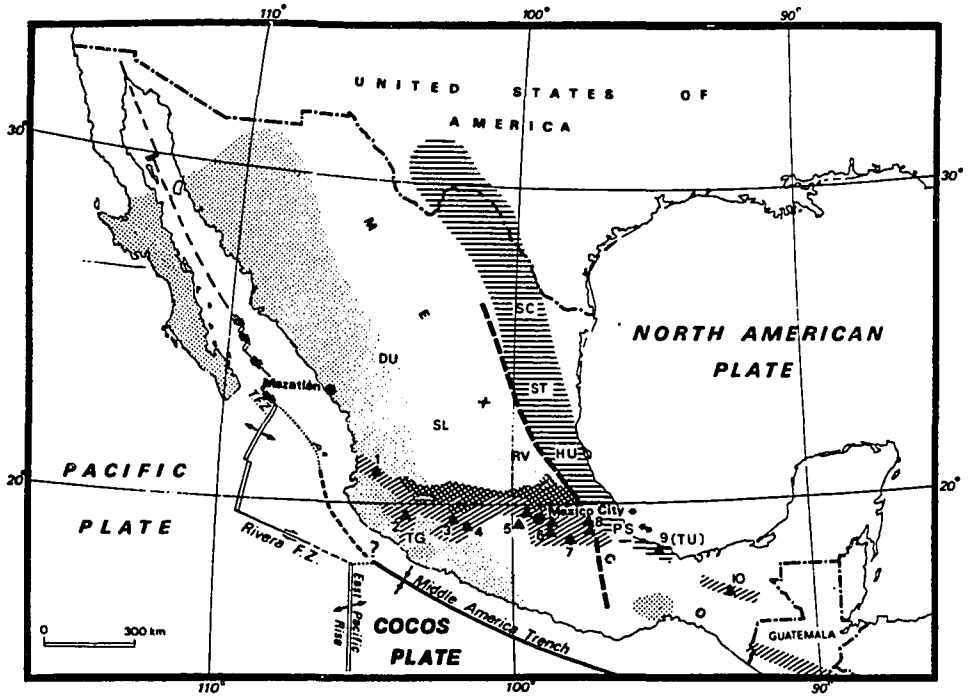

Figure 54. Tectonics of volcanic belts in Mexico showing the plate boundaries in relation to the volcanic belts. The Trans-Mexican Volcanic Belt (TMVB) (or Neovolcanic Zone) is the WNW-ESE trending belt which is the result of subduction of the Cocos Plate into the Middle America Trench. The lack of parallelism of the TMVB with the trench is not well understood. At the west end of the TMVB the subduction of the Rivera Platelet (NW of the Cocos Plate) influences the volcanism (see text). The NNW-trending zone along the east coast of Mexico is an alkaline province thought to be related to the tensional margin of the Gulf of Mexico and to continental rifting to the north (Robin, 1982).

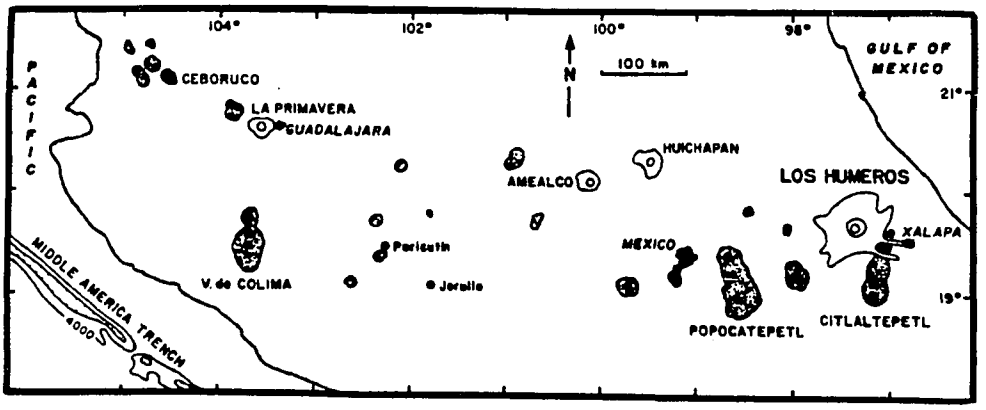

Figure 55. Distribution of Volcanism along the Trans-Mexican Volcanic Belt showing the locations of Los Humeros and (Sierra) la Primavera are shown. The apparent NNE alignment of vents north of Citlaltepetl is not supported by the actual morphology of the vents, while the alignment NNW from Popocatepetl is strongly indicated by continuity of recent volcanic deposits along this trend.

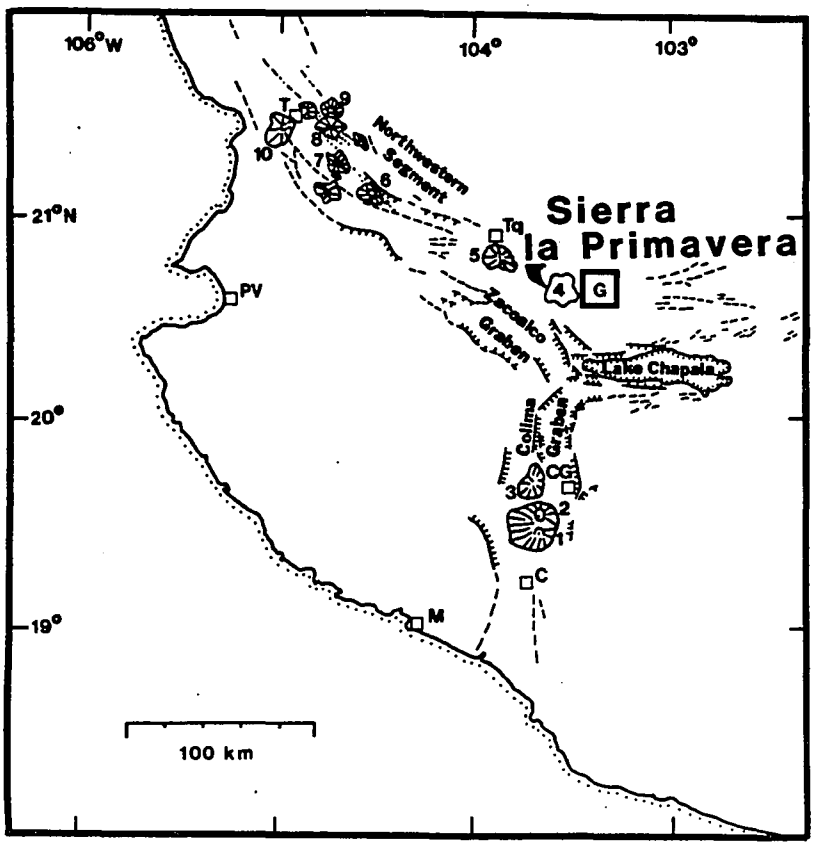

Figure 56. Tectonic Map of Western TMVB and Sierra la Primavera (Luhr et al, 1985). Sierra La Primavera (4) is located adjacent to the triple rift intersection of the Lake Chapala Graben, Zacoalco Graben and the Colima Graben. Numerous extensional faults occur in the region. SLP also occurs at the point where the Trans-Mexican Volcanic Belt changes from a W-WNW trend (east of SLP) to a NW trend west of SLP. This structural situation is attributed to an incipient eastward jump of the East Pacific Rise to the Colima Graben (Luhr et al, 1985).

Table 3E

Caldera Name		Location		
Los Humeros		Eastern Mexico		
Elongation	**Volcanic Character**	**Local Structure**	**Regional Structure**	**Tectonic Elements**
E-W 21 x 15 km (A)	high silica rhyolitic and zoned ash-flows associated with caldera collapse; andesite-rhyolite-basalt assemblage (A)	NNW trending normal faults occur within the caldera (C)	the Altiplano Border Fault strikes NNW-SSE parallel to the coast. Los Humeros occurs at the intersection of this fault with the arc	Trans-Mexican Volcanic Belt (Arc); Altiplano Border Fault
Additional Information				
	Los Humeros is located at the east end of the Trans-Mexican Volcanic Belt (TMVB) 50-80 km behind the volcanic front. It occurs where the TMVB is cut by the N to NNW rifting of eastern Mexico along the border of the Altiplano. This rifting has produced a NNW zone of alkaline volcanism within the last 8 mybp, which as been associated by some workers with tensional faulting of the Gulf of Mexico margin (B,D).			
	The Los Humeros caldera has only recently been identified due to the fact that its ring scarps are largely obscured by subsequent volcanism. It was formed as a result of high silica rhyolite to rhyodacite ashflow eruptions 0.46 mybp (Xaltipan Tuff). The most recent caldera-forming eruption here is dated at about 0.1 mybp (A) (Faby Tuff). It therefore provides one example of the time required to obscure a large caldera to the point where recognition becomes difficult. This factor is important in evaluating the distribution of recognized large calderas relative to their causative factors.			
References				
	(A) Ferriz and Mahood, 1984; (B) Robin, 1982; (C) NASA Apollo Photography, Frame A39-25-3686; (D) Robin and Tournon, 1978			
FIGURES 54, 55				
Category: ARC (Trans-Mexican Volcanic Belt) / FAULT-RIFT (Altiplano Border Fault)				

Table 3F

Caldera Name	Location			
Atitlan Amatitlan	southwestern Guatemala, Central America 50 km ESE of Atitlan, Guatemala, Central America			
Elongation	**Volcanic Character**	**Local Structure**	**Regional Structure**	**Tectonic Elements**
Atitlan: E-W 24 x 21 km (A)	abundant silicic ashflows associated with collapse of both calderas (B,C); calc-alkaline andesite/basalt/rhyolite assemblage (C); N-S alignment of cones within both calderas (A,B)	Caldera is within a N-S trending negative gravity anomaly (D); N-S structure exists tangential to sides of caldera (E)	located on the convex side of a bend in the left-lateral Polochic-Motagua transform (PMT); N-S extensional faulting caused by accomodation to change in strike of PMT transform	Middle America Arc; Polochic-Motagua Transform Fault between Caribbean and North American Plates
Amatitlan: N-S 16 x 14 km (B)	collapse resulted from ashflow volcanism within the last 0.3 my	within the N-S Guatemala Graben (D); faulting within the caldera is dominantly N-S; also NW-SE faulting occurs across the caldera where the arc-parallel Jalpatagua Fault crosses the caldera (SE-NW) (B)		
Additional Information				
Both of these calderas appear to occur in extensional settings developed as secondary structures related to the major change in strike of the PMT. At Amatitlan the NW-SE trending Jalpatagua fault crosses the caldera and terminates on the west side of the caldera (B). The Jalpatagua is a right-lateral arc-parallel distensional strike-slip fault which is related to relative motion of the Caribbean plate parallel to and away from the trench (D). Extensional movement on the Jalpatagua Fault is more pronounced further SE in El Salvador.				
References				
(A) IAVCEI, 1958; (B) Wunderman and Rose, 1984; (C) Rose et al, 1980; (D) Burkart and Self, 1985; (E) Seasat SAR Imagery, 1978				
FIGURE 57, 58				
Category: ARC (Middle America) / INTERSECTING RIFT (secondary graben structures related to change in PMT strike)				

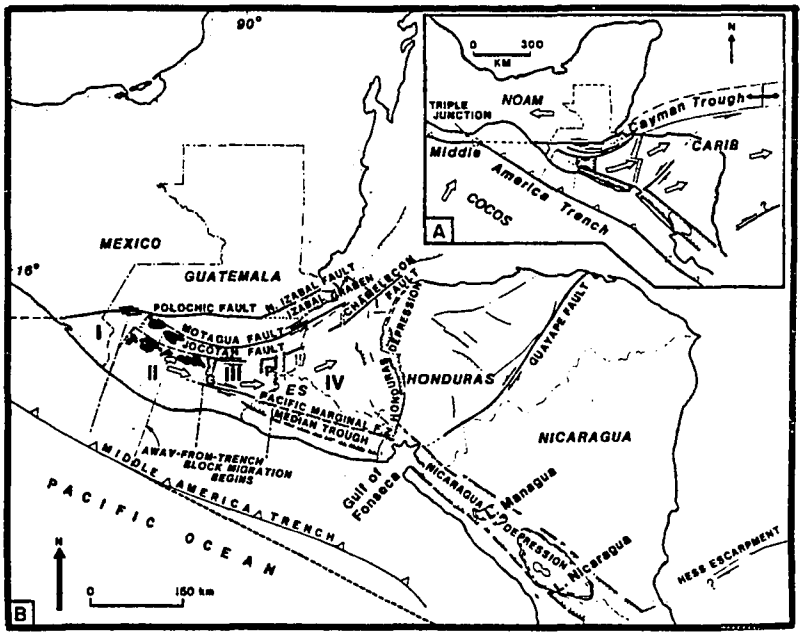

Figure 57. Central America Tectonic Map (Burkart and Self, 1985) showing the plate tectonic elements of the Central American region. Evidence indicates that the Caribbean Plate motion is to the east away from the Middle American Trench (open arrows). This results in the right lateral motion on the Jalpatagua Fault in Guatemala which, to the SE, becomes the Pacific Marginal Fault zone and the Median Trough of El Salvador.

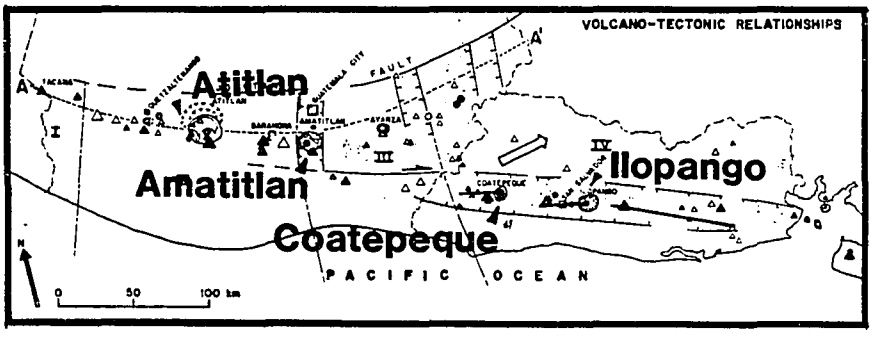

Figure 58. Central American Calderas (modified after Burkart and Self, 1985) showing large calderas of Guatemala and El Salvador in relation to secondary tectonic features associated with the left-lateral Jocotan Transform Fault. Lines drawn through Coatepeque and Ilopango indicate the alignment of volcanic vents and the en echelon development of segments within the Median Trough of El Salvador.

Table 3G

Caldera Name	Location
Coatepeque [Santa Ana] Ilopango [Islas Quemadas]	western El Salvador, Central America 45 km ESE of Coatepeque, El Salvador, Central America

Elongation	Volcanic Character	Local Structure	Regional Structure	Tectonic Elements
Coatepeque: ENE 11 x 6.5 km (B)	abundant silicic ashflows associated with caldera collapse (A,B); calc-alkaline andesite/basalt/dacite assemblage (B);	Linear segments of the N and S caldera walls indicate control on E-W structure; NNW trending fissures west of the caldera mark a right-stepping offset in the volcanic axis of 20 km to the NE (B,E)	These calderas occur in the Median Trough of El Salvador -- a distensional right-lateral zone which parallels the arc (A)	Middle America Arc; Median Trough of El Salvador
Ilopango E-W 11 x 8 km (B)	at Ilopango major ashflow eruptions occurred about 2000 ybp and may date the last major caldera collapse (D)	elongation of the caldera and linear wall segments indicate E-W structure (B); Ilopango occurs at a 15° inflection in the volcanic axis		

Additional Information

Both of these calderas are lake-filled depressions with normal faulting along caldera rims. They occur in the Median Trough of El Salvador (A). The Median Trough is the result of relative motion of the Caribbean and Pacific Plates (Figure 57). A combination of extension and right-lateral strike slip is indicated. This motion is manifest as an arc-parallel trough with right-stepping offsets of the volcanic axis within the trough. To the NW of Coatepeque, the strike-slip components are more pronounced while to the SE, in the Nicaragua Depression, extension is more dominant. Ilopango marks an apparent change from en echelon to arc-parallel alignment of the volcanic axis. SE of Ilopango, the volcanic axis more closely parallels the ESE trend of the Median Trough -- possibly reflecting the increasing dominance of extension. Seismic focal plane solutions (G) support this interpretation. Parallels have been drawn between the tecotnic setting of the Median Trough and Nicaraguan Depression, and similar settings in the Semangka Graben and Toba Depression of Sumatra (F).

References

(A) Burkart and Self, 1985; (B) IAVCEI, 1958; (C) Stolber and Carr, 1974; (D) Sheets, 1979; (E) Seasat SAR Mosaic Imagery, 1978; (F) McBirney and Williams, 1964; (G) Burbach et al, 1984; (H) Carr et al, 1982

FIGURE 57, 58

Category: ARC (Middle America) / ARC-PARALLEL RIFT (Median Trough) / OFFSET or INFLECTION IN VOLCANIC AXIS

Table 3H

Caldera Name		Location		
Masaya		southwest Nicaragua, Central America		
Elongation	**Volcanic Character**	**Local Structure**	**Regional Structure**	**Tectonic Elements**
WNW rectangular 10.8 x 6.6 km (A)	Basaltic ignimbrite eruption accompanied caldera collapse; dominantly basaltic (tholeiitic) assemblage (C)	elongation of the caldera is parallel to the Nicaraguan Depression; NE and SW caldera walls are aligned WNW parallel to the Depression; at the NW end of the caldera there is an 8 km-long NE-trending alignment of cinder cones which parallels regional faulting (E)	historical activity has taken place on NE-trending faults in the vicinity of Masaya (D); the extensional Nicaraguan Depression is oriented WNW-ESE; this region is dominated by mafic (oceanic) crust	Middle America Arc; Nicaraguan Depression
Additional Information				
Masaya, scene of historic volcanism, is most notable for its unusual basaltic ashflows and general basaltic character. Although the caldera was previously thought to be the result of lateral draining of the magma chamber (B), basaltic ashflows correlated with caldera collapse have recently been identified (C). (This contrasts with Apoya caldera, located 5 km to the SE, that is a 6 km caldera which has been the site of silicic, not basaltic, ashflows.) Masaya lies within the Nicaraguan Depression and is strongly controlled by its WNW-trending structure. Its rectangular shape oriented parallel to the rift axis is similar to that of Toba in Sumatra (G). Active NE-trending faulting adjacent to the caldera includes the 1972 Managua earthquake -- a left-lateral event (D). Vent alignments parallel this direction. The sense of motion of this event has been interpreted to indicate that true transform motion is taking place on an offset in the Nicaraguan Depression spreading (F, figure 59).				
References				
(A) IAVCEI, 1958; (B) Williams and McBirney, 1979; (C) S. Williams, 1982; (D) Niccum et al, 1974; (E) Ui, 1972; (F) Dewey and Algermissen, 1974; (G) McBirney and Williams, 1964				
FIGURE 57, 59				
Category: ARC (Middle America) / ARC-PARALLEL RIFT (Nicaraguan Depression)				

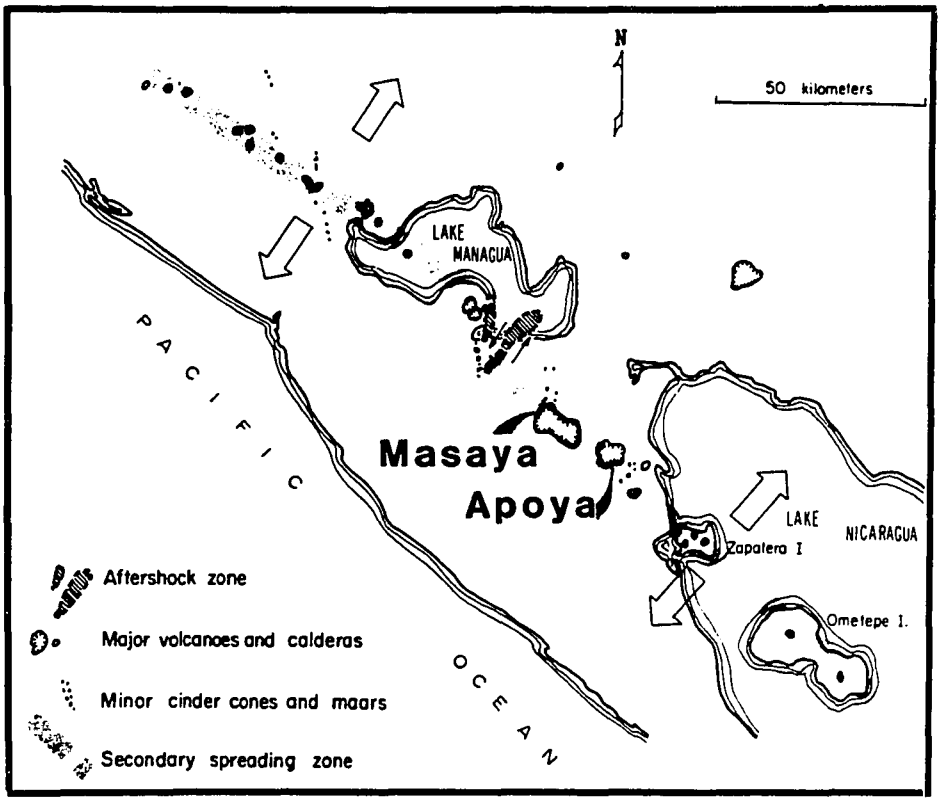

Figure 59. Tectonics of the Masaya Region (Dewey and Algermissen, 1974) showing secondary extension (broad arrows) indicated across the Nicaraguan Depression and left-lateral offset on strike-slip faults at the SE end of Lake Nicaragua that suggests these faults are acting as true transform faults. Masaya caldera is characterized by unusual basaltic ashflows while silicic ashflows are found at the smaller Apoya Caldera.

Table 3I

Caldera Name	Location
The Andes	South America

The Andes is an area of extensive long term subduction and consequent arc volcanism. Volcanics over 20 my old are located adjacent to vents active within the last few thousand years. In this setting, numerous silicic ignimbrite sheets have been identified via field reconnaissance or image interpretation. However, the general inaccessibility and hostile conditions have left these volcanics understudied. In particular, the inventory of calderas in the Andes is not adequate for making significant statements at this time about the distribution and tectonic associations of the large Quaternary calderas here.

A representative review of available literature reveals that only six well-defined calderas that have been identified in the Andes Arc which runs the length of South America. These six calderas include: Calabozos (D), Mt. Hudson (C) and Wheelwright (I) in Chile; Cerro Galan (B,F) and Payun Matru in Argentina and Pampas Galeras in Peru (B). All of these calderas are associated with voluminous ignimbrite eruptions. However, Calabozos and Mt. Hudson are the only ones in this list which are Quaternary (the age of Payun Matru is unspecified). By contrast, Baker (B) has identified on the order of 20 Quaternary ignimbrite sheets in just the area between Latitude 15° and 28° (ie. parts of southern Peru, western Bolivia, northern Chile and western Argentina). This may reflect either a lack of recognition of the calderas or a real lack of caldera collapse accompanying relatively large ignimbrite eruptions. If the latter is the case, it would provide an important limiting case for the caldera/ignimbrite association, but the resolution of the data will not be adequate to support or refute such a statement for many years.

A number of workers have attempted to evaluate possible effects of segmentation of the subducting Nazca Plate on the Andes structure (eg H and G). These efforts suggest that although the Andes can be divided into broad segments which possess differing structural and volcanological characteristics, these segments do not always correlate with segmentation in the Nazca plate (H), ie. a segment of constant Benioff zone geometry. Pre-existing crustal geometry also appears to be involved (H). In general, seismicity indicates that the Andes magmatic arc is under east-west compressive horizontal stress -- in contrast to many other arcs.

An important example of the evolution of possible caldera-tectonic association is found in the work of Gonzalez-Ferran et al (I) which examines the record of volcanic activity in the area of Ojos Del Salado -- on the north edge of the shallow-dipping slab (and magmatic gap) of central Chile opposite the Easter 'Hot Line' (seamounts). A number of calderas -- including the large (20 km) Wheelwright Caldera -- occur in this area. These calderas fall in a 23 to 6 my old group of volcanics which are characterized by N-S alignment of vents and fissures indicating E-W extension. However, post 6 my old volcanism in the area is developed on a different trend and fissures associated with these younger volcanics strike N65°E -- suggesting increased E-W compression in the Plio-Pleistocene. (Also there is Paleozoic structure in the area paralleling the N65°E trend.) Large calderas do not occur in this second, younger group of volcanics. This

A representative review of available literature reveals that only six well-defined calderas that have been identified in the Andes Arc which runs the length of South America. These six calderas include: Calabozos (D), Mt. Hudson (C) and Wheelwright (I) in Chile; Cerro Galan (B,F) and Payun Matru in Argentina and Pampas Galeras in Peru (B). All of these calderas are associated with voluminous ignimbrite eruptions. However, Calabozos and Mt. Hudson are the only ones in this list which are Quaternary (the age of Payun Matru is unspecified). By contrast, Baker (B) has identified on the order of 20 Quaternary ignimbrite sheets in just the area between Latitude 15° and 28° (ie. parts of southern Peru, western Bolivia, northern Chile and western Argentina). This may reflect either a lack of recognition of the calderas or a real lack of caldera collapse accompanying relatively large ignimbrite eruptions. If the latter is the case, it would provide an important limiting case for the caldera/ignimbrite association, but the resolution of the data will not be adequate to support or refute such a statement for many years.

A number of workers have attempted to evaluate possible effects of segmentation of the subducting Nazca Plate on the Andes structure (eg H and G). These efforts suggest that although the Andes can be divided into broad segments which possess differing structural and volcanological characteristics, these segments do not always correlate with segmentation in the Nazca plate (H), ie. a segment of constant Benioff zone geometry. Pre-existing crustal geometry also appears to be involved (H). In general, seismicity indicates that the Andes magmatic arc is under east-west compressive horizontal stress -- in contrast to many other arcs.

An important example of the evolution of possible caldera-tectonic association is found in the work of Gonzalez-Ferran et al (I) which examines the record of volcanic activity in the area of Ojos Del Salado -- on the north edge of the shallow-dipping slab (and magmatic gap) of central Chile opposite the Easter 'Hot Line' (seamounts). A number of calderas -- including the large (20 km) Wheelwright Caldera -- occur in this area. These calderas fall in a 23 to 6 my old group of volcanics which are characterized by N-S alignment of vents and fissures indicating E-W extension. However, post 6 my old volcanism in the area is developed on a different trend and fissures associated with these younger volcanics strike N65°E -- suggesting increased E-W compression in the Plio-Pleistocene. (Also there is Paleozoic structure in the area paralleling the N65°E trend.) Large calderas do not occur in this second, younger group of volcanics. This association suggests the correspondence between extensional stress and caldera development.

References

(A) Thorpe et al, 1982; (B) Baker, 1981; (C) Fuenzalida and Espinosa, 1974; (D) Hildreth et al, 1984; (E) Baker and Francis, 1978; (F) Francis, 1983; (G) Hall and Wood, 1985; (H) Jordan et al, 1983; (I) Gonzalez-Ferran et al, 1985

Table 3J

Caldera Name		Location		
Deception Island		South Shetland Islands, Antarctica		
Elongation	**Volcanic Character**	**Local Structure**	**Regional Structure**	**Tectonic Elements**
NW 11.3 x 9.7 km (A)	Abundant ashflows accompany caldera collapse; bimodal alkaline basalt/rhyolite assemblage (A)	elongation parallels a NW fault system which cuts across the Bransfield backarc trough and also parallels the SW Drake transform fault; this trend is manifest by numerous alignments of bathymmetric features (A)	located astride the NE-trending fault which bounds the NW side of the Bransfield Trough (BT); and at the intersection of this fault with the NW-trending transform fault on the SW side of the Drake plate (B)	South Shetland Arc; Bransfield Trough (BT); SW Drake Transform
Additional Information				
The South Shetland Islands are a volcanic arc which results from the subduction of the Drake Plate (from the NW) beneath the Antarctic Peninsula (C). The fault-bounded Bransfield Trough occurs between the S. Shetland Is. and the Peninsula and is the result of backarc spreading (B). Deception Island caldera occurs on the back side of the arc -- about 20 km behind the volcanic front -- on the strike of the bounding normal fault on the NW side of the Brandsfield Trough. It is in an intermediate location between the arc and the backarc -- broadly similar to Medicine Lake caldera. Also it occurs at the SW end of the Trough where the bathymmetric expression of the Trough narrows and terminates NE of Deception Is. Spreading on the Drake Passage Ridge slowed or stopped 4 mybp (B) and spreading in the BT initiated about 2 mybp. The crust of the South Shetlands is continental while that of the BT is oceanic (B). The BT is considered to be in the initial stages of backarc rifting (B). Therefore, it is speculative but not unlikely that BT spreading is propagating SW through continental crust beneath Deception Island -- similar to the situation in Kamchatka where the Central Kamchatka Depression appears to be propagating south through Opala Caldera.				
References				
(A) Baker et al, 1975; (B) Tarney et al, 1982; (C) Barker et al, 1984 FIGURE 60, 61				
Category: ARC (South Shetland) / ARC-PARALLEL RIFT (Bransfield Trough) / TRANSFORM (SW Drake Transform)				

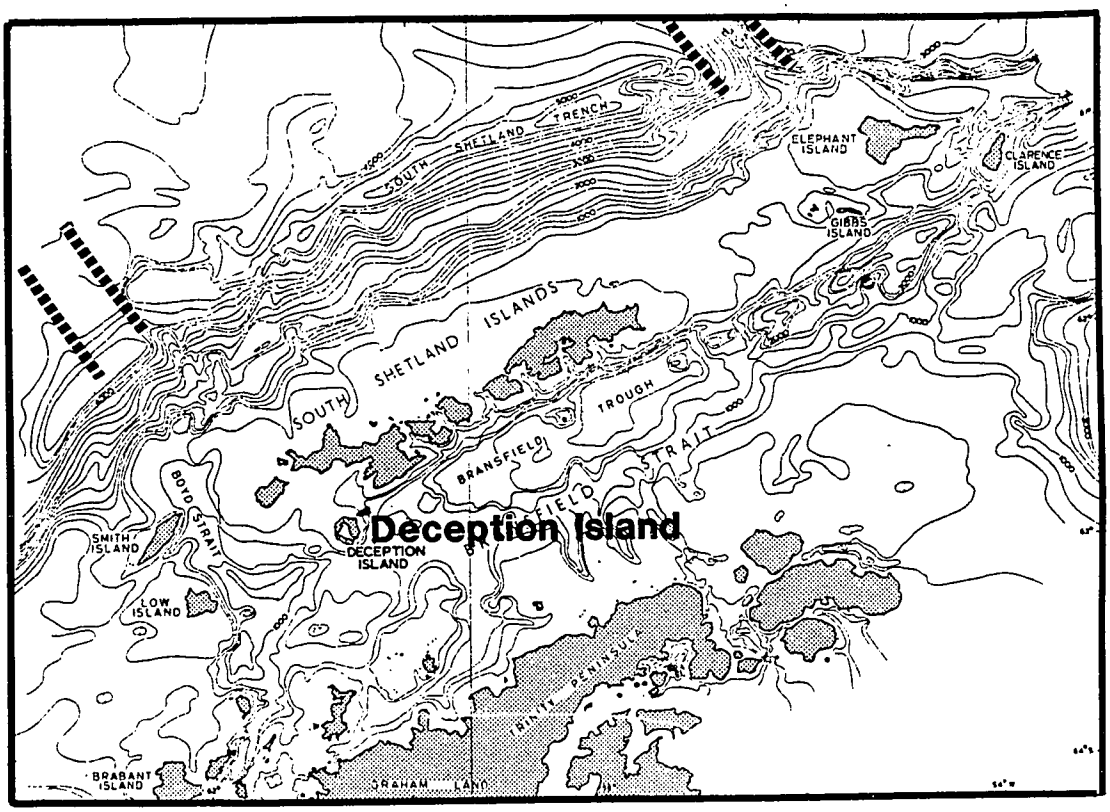

Figure 60. Bathymetric Map of the South Shetland Islands (Baker et al, 1975) reveals the main tectonic elements adjacent to Deception Island: Bransfield Trough -- an active backarc basin which shallows to the SE; and NW-trending transform faults on the NE and SW ends of the Arc (broad dashed lines).

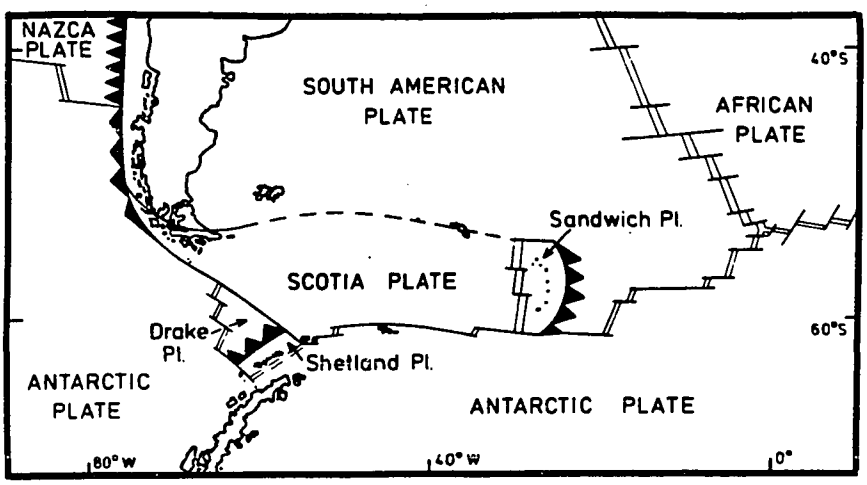

Figure 61. Tectonic Map of the South Shetland -- Scotia Plate Region (Tarney et al, 1982) showing subduction of the Drake Plate beneath the Antarctic Peninsula which produces the South Shetland Arc -- although Drake Ridge spreading is thought to have ceased within the last 2 m.y.b.p. Spreading in the Bransfield Trough between the South Shetlands and the Antarctic Plate isolates the South Shetlands on the Shetland Platelet.

Table 3K

Caldera Name		Location		
Veniaminof Aniakchak		Alaska Peninsula, Alaska Alaska Peninsula 100 km NE of Veniaminof, Alaska		
Elongation	Volcanic Character	Local Structure	Regional Structure	Tectonic Elements
Veniaminof: circular 8.2 km	abundant ashflows occur on both volcanoes (~3500 ybp); rhyolite/basalt/dacite assemblage (C)	a strong alignment of cinder cones trending NW crosses the entire peninsula at Veniaminof (one cone occurs within the caldera and the largest concentration of cones is on the north flank of the volcano)	located at the NE end of an arc segment striking NE; regional structure (faults and folds) parallel this trend (A)	Aleutian Arc
Aniakchak: NE 10 x 9.2 km (A)	zoned intermediate ashflows (D)	a major linear scarp cuts the east and west flanks of the volcano parallel to ENE regional faulting (A,B)	located at the SW end of an ENE-trending arc segment which is paralleled by regional folds and faults as well as local structure	
Additional Information				
From west of Veniaminof, the volcanic arc strikes NE. At Veniaminof the arc takes a left step (north) of about 30 km to Aniakchak. Black Peak volcano occurs midway between Aniakchak and Veniaminof, but the ENE alignment of vents and faults -- en echelon to the segments west of Veniaminof and east of Aniakchak -- indicates that Black Peak is isolated between segments rather than there being a Veniaminof-Black Peak-Aniakchak volcanic segment. From Aniakchak, an arc segment strikes to the ENE parallel to volcanic vents and faulting in the vicinity.				
References				
(A) Burk, 1965; (B) Shuttle photography of Aniakchak: STS-41G-17-33-043; (C) Miller and Smith, 1977; (D) Hildreth, 1981				
FIGURE 62				
Category: ARC (Aleutian) / OFFSET IN VOLCANIC AXIS / FAULTING (regional)				

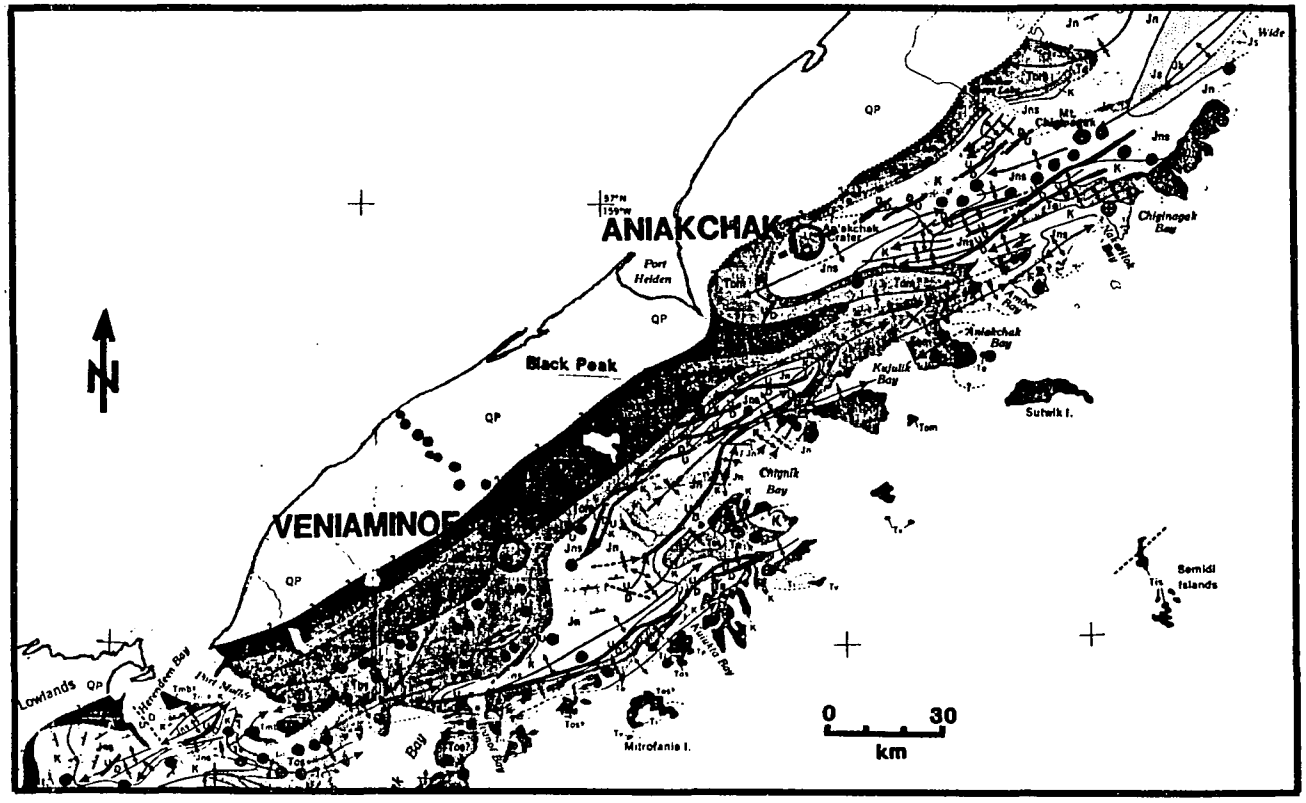

Figure 62. Tectonic Map of Alaskan Peninsula (modified after Burk, 1965) Veniaminof and Aniakchak are shown in relation to surrounding structure and volcanic vents. Broad dashed lines indicate volcanic arc segments (as implied by vent distribution), medium lines are normal faults, and fine lines are fold axes.

Table 3L

Caldera Name		Location		
Okmok Fisher Caldera		Umnak I., eastern Aleutian Is. Unimak I., 250 km ENE of Okmok, 370 km SW of Veniaminof		
Elongation	**Volcanic Character**	**Local Structure**	**Regional Structure**	**Tectonic Elements**
Okmok: NE 11 x 10 km (E)	rhyolitic and zoned intermediate (G) ashflows accompany caldera collapse (A,C); bimodal basalt/rhyolite assemblage (A)	elongation parallel to Vsevidof-Okmok arc segment	located at a major break and inflection in the volcanic axis; occurs in the transition zone from continental to oceanic crust	Aleutian Arc
Fisher Caldera: NE 16.5 x 11 km (E)	abundant primarily dacitic ashflows (F); bimodal assemblage implied (H)	faulting beyond NE and SW ends of the caldera trends NE (D) parallel to the elongation of the caldera; this trend is also along the line of the Akutan-Westahl segment.	located at an inflection in the volcanic arc between the Akutan-Westahl and Shishaldin-Isanotski trends	
Additional Information				
	Okmok exists at the NE end of the Vsevidof-Okmok (VO) segment. To the east there is an 82 km gap (to Makushin) in the volcanic arc. The Makushin-Akutan segment (E of Makushin) strikes 20° more easterly than the VO segment. The inflection and gap in volcanism indicates that a structural anomaly exists here. This is supported by the presence of the recently erupted Bogoslof Island which is located 34 km behind the VO segment, opposite a point on the arc 32 km ENE of Okmok. Such behind-arc volcanism is rare in the Aleutians (C).			
	Fisher Caldera occurs at a 20° inflection in the strike of the arc from an ENE striking Makushin-Akutan-Westahl segment to a more easterly Shishaldin-Isanoski-Frosty trend. Its size and strong elongation belies the relatively small inflection in the arc. The tectonic association of this caldera is not well established. The local bathymmetry (E) to the south of Fisher suggests possible NNW-striking intersecting structure.			
	It is noteworthy that west of Okmok -- where oceanic crust occurs -- there are no clear examples of calderas greater than 8 km in diameter. Tanaga is a possible exception, however only a small portion of its caldera is exposed (less than 70°) preventing significant interpolation of its caldera walls.			
References				
	(A) Byers, 1959; (B) Marsh, 1979; (C) Marsh, 1982; (D) Seasat image of Fisher Caldera, Ford, 1980; (E) USGS, 1951, 1:250,000 Topographic (Shaded Relief) Maps, Unimak and Umnak Quads, Alaska; (F) Miller and Smith, 1977; (G) Hildreth, 1981; (H) Pike and Clow, 1981			
FIGURE 64, 65				
Category: ARC (Aleutian) / OFFSET OR INFLECTION IN VOLCANIC AXIS				

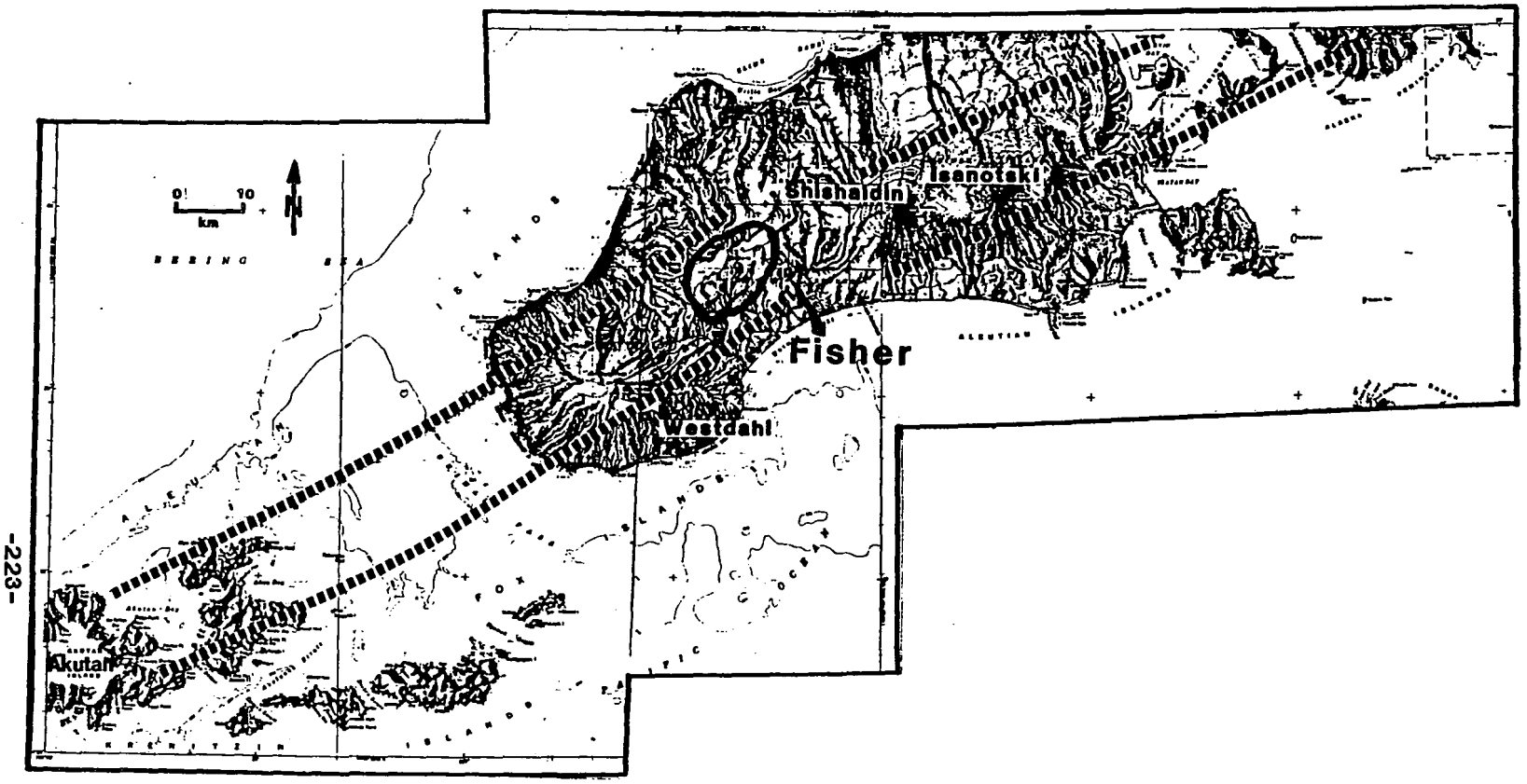

Figure 63. Relief Map of Fisher Caldera, Unimak I. and Akutan I. (basemap USGS 1:250,000 Unimak and False Pass Topographic Quads) Fisher Caldera occurs at a 20° inflection in the volcanic arc between the Makushin-Akutan-Westdahl volcanic segment (Makushin not shown to the SW) and the Shishaldin-Isanotski-Frosty segment (Frosty not shown to the NE). Segments are shown as broad dashed lines. This inflection is well defined on Unimak I, however, extrapolation of the segment alignment beyond Unimak is speculative.

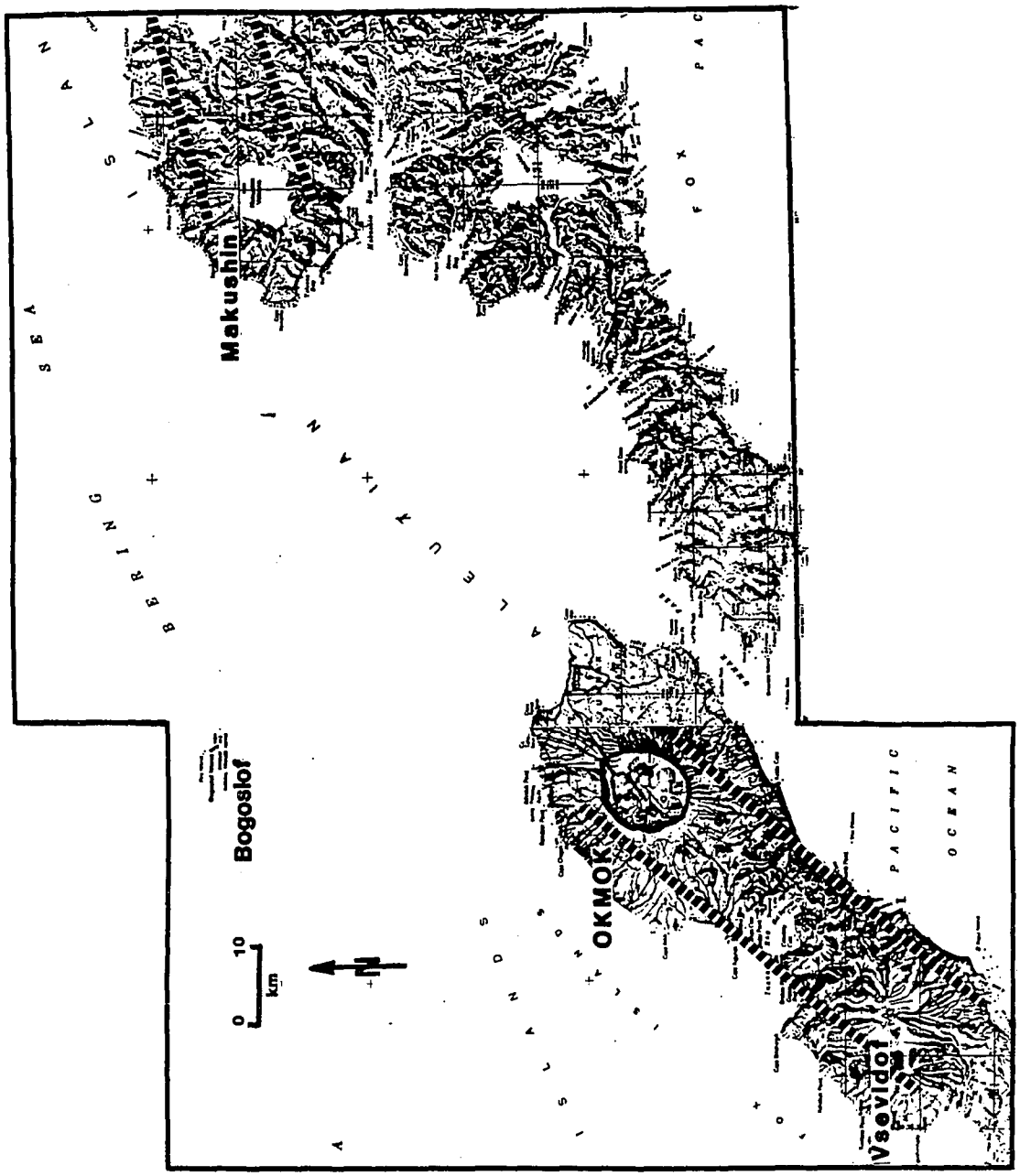

Figure 64. Map of Okmok Caldera, Umnak I. and Unalaska I. (basemap USGS 1:250,000 Umnak and Unalaska Topographic Quads) Okmok occurs at the NE end of a segment of the volcanic arc. NE of Okmok there is a gap in volcanism on the volcanic front and behind-arc activity at Bogoslof. East of this gap the arc strikes ENE. Segments are shown as broad dashed lines.

Table 3M

Caldera Name	Location
Maly Semyachik Bolshoy Semyachik Uzon Krashenninikov	east central Kamchatka 16 km north of Maly Semyachik 8 km north of Bolshoy Semyachik 3 km north of Uzon

Elongation	Volcanic Character	Local Structure	Regional Structure	Tectonic Elements
Maly Semyachik: WNW 10 x 8.4 km (A) Bolshoy Semyachik: NE 12 x 10 km (A) Uzon: WNW 18 x 9 km (A) Krashenninikov: WNW 10 x 9 km	extensive areas of acid pyroclastic rocks, pumice and ignimbrites occur associated with these calderas (B); at Uzon and Krasheninnikov a bimodal assemblage is implied (J)	Maly Semyachik is within the larger Zhupanovsky depression which includes the smaller Karymsky and Academy of Sciences calderas. In general, the calderas display NE-trending faulting parallel to the East Kamchatka Graben (EKG) and WNW elongation parallel to the EKG extension direction (B). Krasheninnikov has a well defined NNE alignment of vents on its N flank (outside the caldera) (A,G).	These calderas lie in the NE-trending, single-sided EKG. This structure is paralleled by the Central Kamchatka Depression to the west (B). The EKG and its extensional character is well defined by a distinct decrease in Benioff Zone Seismicity opposite the Karymsky-Krasheninnikov calderas segment (I)	Kurile Arc; Central Kamchatka Depression

Additional Information

With the exception of Bolshoy Semyachik (which is aligned NE), all of these calderas are located at right-step offsets of about 12 km in the volcanic arc and are elongate parallel to the extension direction of the East Kamchatka Graben (EKG) within which they occur. Maly Semyachik occurs at the southwest end of the Maly-Bolshoy-Uzon segment; Uzon spans both the NE end of this segment and the SW end of the Uzon-Krasheninnikov segment; and Krasheninnikov is at the NE end of this Uzon-Krasheninnikov segment. These calderas lie in the EKG -- a single-sided graben whose fault (west side) boundary is located west of, and parallel to the volcanic arc (B). There is little evidence of any fault bounding the EKG on the seaward side of the arc. Farther west, the Central Kamchatka Depression (CKD) parallels the EKG yielding a block faulted topography behind the arc (E). Both the EKG and the CKD are actively extending, with evidence indicating southward propagation of the CKD (B). In addition, some left lateral strike-slip has been suggested along the CKD (H). North of Krasheninnikov, volcanic volume diminishes, effectively ceasing along this arc alignment at the Kronotsky Peninsula opposite the point where the Meiji Guyot -- an oceanic plateu on the Pacific Plate -- is entering the subduction zone. The total length of the volcanic arc occupied by large calderas along the 84 km portion of the arc from Maly Semyachik to Krasheninnikov is 34.4 km -- an area of exceptionally high density of large calderas.

References

(A) Melekestsev, 1974; (B) Erlich, 1979; (C) IAVCEI, 1959; (D) Erlich et al, 1973; (E) Shuttle photograph of Gorley Khrebet: STS-9-31-1097; (F) Erlich et al, 1979; (G) Volcanic Map of Kamchatka, 1960; (H) Savostin, 1983; (I) Fedotov and Tokarev, 1974; (J) Pike and Clow, 1981

FIGURE 65, 66

Category: ARC (Kurile) / ARC-PARALLEL RIFT (EKG) / OFFSET IN VOLCANIC AXIS

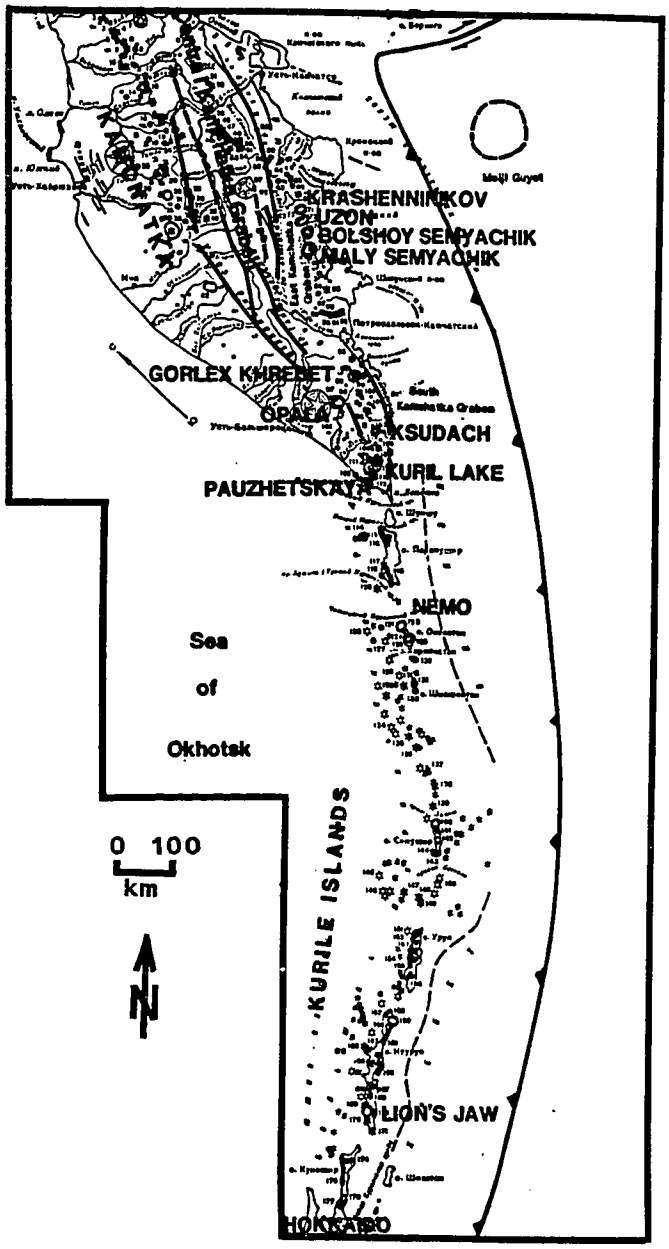

Figure 65. Calderas and Tectonic Elements of Kamchatka and the Kurile Arc (modified after Melekestsev, 1974). The faults shown on Kamchatka reflect Maps by Melekestsev (1974) and by Erlich (1979). The Central Kamchatka Graben (Depression) -- CKD -- is a well defined extensional feature in which the onset of faulting becomes younger further south -- suggesting propagation in that direction. The East Kamchatka Graben, a one sided graben, localizes four large calderas that represent one of the post prolific caldera-alleys in the world. The South Kamchatka Graben is a less defined feature within which the large calderas of southern Kamchatka occur. Opala occurs at the southern extension of the CKD. Nemo and Lion's Jaw, in the Kuriles, occur at points where the arc is cut by cross-structure.

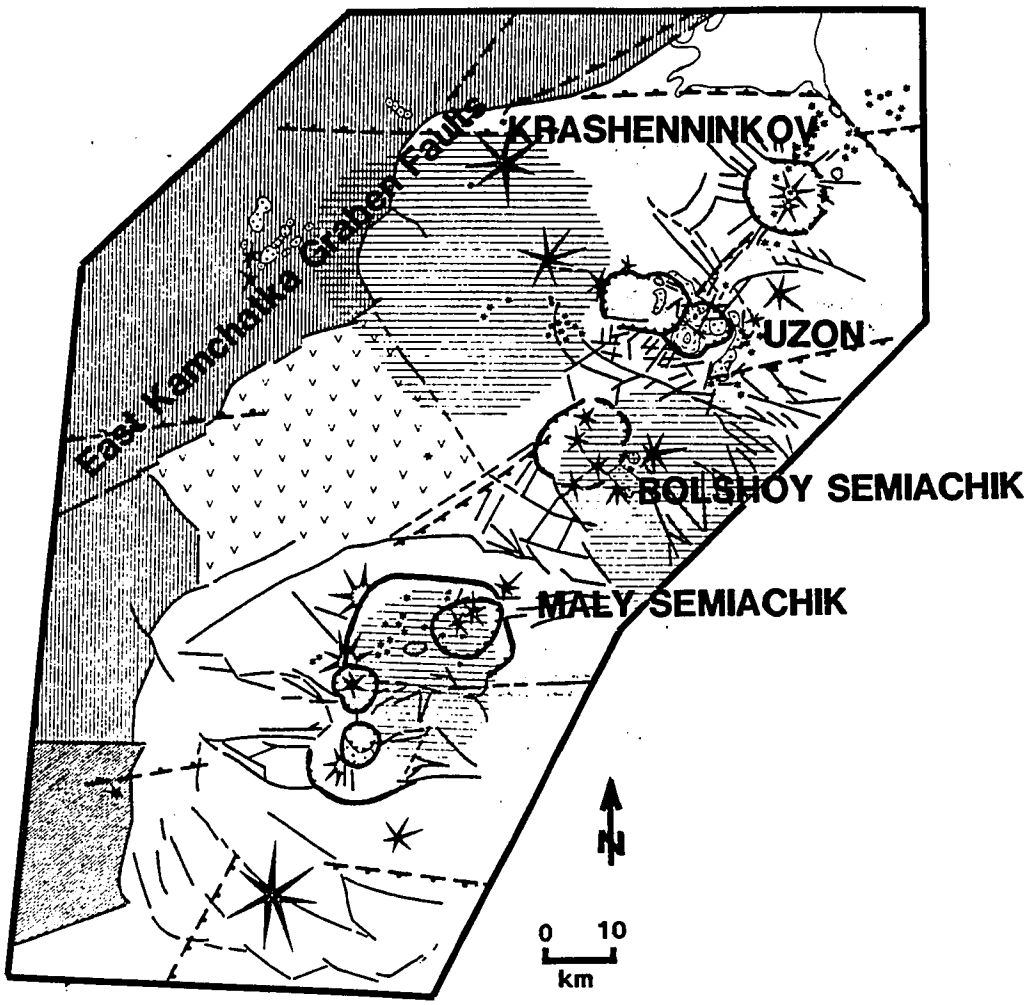

Figure 66. Calderas of the Karymsky-Krasheninnikov region (modified after Meleketsev, 1974) showing caldera outlines and East Kamchatka Graben faults.

Table 3N

Caldera Name		Location		
Opala		south central Kamchatka		
Elongation	**Volcanic Character**	**Local Structure**	**Regional Structure**	**Tectonic Elements**
N-S 18.7 x 13 km (D)	Abundant ashflows -- probably related to caldera formation (A)	linear segments of caldera walls align NNE; elongation parallels Central Kamchatka Depression (CKD) located north of the caldera; alignment of monogenetic vents to the NE of the caldera are aligned NNE to NE; negative gravity anomaly	located east of Gorley Khrebet , about 40 km east of the volcanic front, opposite the north end of the South Kamchatka Graben (SKG) (C) and at the southern end of the CKD which widens to the north; strike-slip faults extend transverse to the volcanic axis NW of Gorley (C)	Kurile Arc; south end of the CKD; opposite north end of the SKG
Additional Information				
	Opala is located near the northern boundary of the South Kamchatka block (C). The South Kamchatka Graben, which parallels the coast and acts as the locus of the S. Kamchatka volcanic front, terminates to the east of Opala, suggesting that Opala lies near some fundamental NW-trending transverse structure. In addition, Opala is at the southern extremity of the CKD which becomes younger to the south and appears to be propagating to the south. Its location behind the arc and on the strike of a major active graben (CKD) is similar to Newberry and Medicine Lake calderas in the Cascades (Newberry is located 50 km behind the volcanic front). Thus it is associated with backarc block faulting and associated caldera volcanism analogous to Basin and Range activity.			
References				
	(A) Erlich et al, 1973; ; (B) IAVCEI, 1959; (C) Erlich, 1979; (D) Melekestsev, 1974			
FIGURE 65, 67				
Category: ARC (Kurile) / ARC-PARALLEL RIFT (Central Kamchatka Depression)				

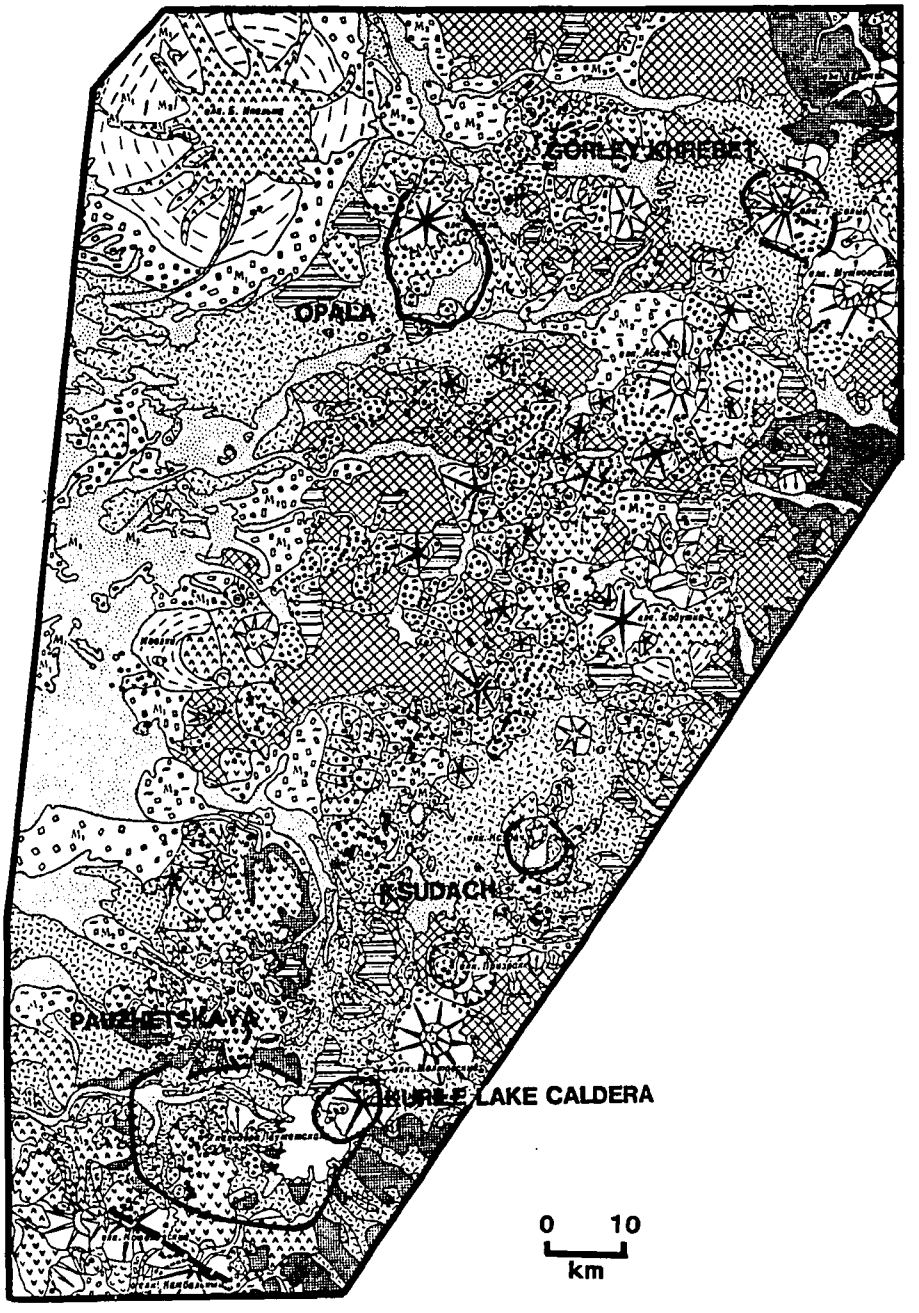

Figure 67. Calderas of Southern Kamchatka (modified after Meleketsev, 1974). The details of caldera margins and relationship to other volcanism are shown. Large stlylized asterisks are shield volcanoes (black: active; white: inactive), small asterisks are cinder cones. The broad dashed line south of Pauzhetskaya denotes the Kambalny-Koshelevsky vent alignment discussed in the text.

Table 30

Caldera Name	Location
Pauzhetskaya	south central Kamchatka
Kuril Lake Caldera	on NE corner of Pauzhetskaya
Ksudach	36 km NE of Kurile Lake, southeast Kamchatka
Gorley Khrebet	84 km NE of Ksudach, southeast Kamchatka

Elongation	Volcanic Character	Local Structure	Regional Structure	Tectonic Elements
Pauzhetskaya: WNW 29 x 21 km (A)	abundant silicic ashflows found in the vicinity of these calderas (C)	elongation, and southwest caldera wall, parallels WNW-trending strike-slip faulting along which the Kambalny-Koshelevsky Volcanic (KKV) ridge (to south of the caldera) is aligned (A,B)	Pauzhetskaya marks the south boundary of the South Kamchatka block along which WNW transverse strike-slip faulting is found (B); a right-step offset in the volcanic arc occurs along the KKV between the Kurile trend to the south and the SKG to the north	Kurile Arc; offset in volcanic axis; South Kamchatka Graben
Kurile Lake Caldera: ENE 9.7 x 7 km (A)		elongation parallels South Kamchatka Graben (SKG) and also aligns with the (NE-striking) SE wall of Pauzhetskaya (A)	Kurile Lake and Ksudach calderas occur within the arc-parallel SKG at offsets in the arc	
Ksudach: WNW 10.3 x 6.6 km (A)	abundant ashflows in the caldera vicinity (F); double caldera; bimodal assemblage implied (G)	located on a line of NE fractures which cross the caldera (C); the locus of active volcanoes steps left (west) 14 km to the north of Ksudach		
Gorley Khrebet: NW 14 x 9 km	abundant pyroclastic ashflows (D)	WNW striking fissures cross the caldera (C,D); elongation parallels SKG extension	Gorley is at the NE termination of the SKG (B) and at the northern edge of a zone of prolific arc volcanism -- there is only one volcano found in 90 km NE of Gorley (A,B)	

Additional Information

Pauzhetskaya occurs at the south edge of the South Kamchatka block where the Kurile volcanic trend steps east; this step is paralleled by WNW aligned volcanoes. North of Pauzhetskaya, arc volcanism is centered in the NE-trending South Kamchatka Graben. At Ksudach, the locus of volcanism steps slightly west but remains in the SKG. Abundant monogenetic cone alignments trend NE (parallel to the SKG) between Ksudach and Gorley. Gorley Khrebet marks the northeast end of the SKG. NE of Gorley a 90 km gap in arc volcanism occurs. Opala caldera (see separate sheet) is located landward of Gorley at the southern end of the Central Kamchatka Depression. All of these calderas are negative gravity anomaly types except Ksudach.

References

(A) Melekestsev, 1974; (B) Erlich, 1979; (C) IAVCEI, 1959; (D) Erlich et al, 1973; (E) Shuttle photograph of Gorley Khrebet: STS-9-31-1097; (F) Erlich et al, 1979; (G) Pike and Clow, 1981

FIGURE 65, 67

Category: ARC (Kurile) / ARC-PARALLEL RIFT (SKG) / OFFSET IN VOLCANIC AXIS

Table 3P

Caldera Name	Location
Nemo Lion's Jaw [Lvinaya Past]	northern Onekotan I., northern Kurile Is. southern Iturup I., southern Kurile Is.

Elongation	Volcanic Character	Local Structure	Regional Structure	Tectonic Elements
Nemo: NE 10.7 x 9 km (B)	abundant ignimbrite related to caldera collapse; andesite/basalt/dacite assemblage; double caldera, partly overlapping (C)	elongation parallels the forearc trough axis	located at the north end of Onekotan Island which also includes a caldera at its southern end; these calderas align on the strike of a trough -- the Central Kuril Graben (CKG) -- located between the frontal arc and the volcanic arc (G, D); also opposite the off-axis (behind arc) volcano of Makarushi I. which is 29 km to the NW	Kurile Arc
Lion's Jaw: NNE 10 x 8 km (B)	abundant dacitic ashflows accompany caldera collapse (C)	elongation parallels the alignment of the arc segment and is perpendicular to the intersecting trough	at the north end of an arc segment; north of Lion's Jaw the volcanic arc steps right (east) 15 km; also a trough in the acoustic basement on the Sea of Okhotsk side of the arc (E) strikes into the caldera from the NW	

Additional Information

Both of these calderas occur at locations where arc-intersecting structure is indicated. Kimura (G) proposes that the Kurile Arc is composed of the Kurile Forearc Plate (KFAP) produced by the oblique subduction of the Pacific Plate at the Kurile Trench (see also Kutcharo/Akan sheet). He interprets the trough which cuts the arc at the Bussol Straits as the northeast margin of the KFAP. He cites a trough which parallels the arc and separates the frontal arc from the volcanic arc between the KFAP and the North American Plate (Sea of Okhotsk). Northeast of the Bussol Straits, another trough (CKG) strikes NNW and intersects the arc at Onekotan Island (D,G). Nemo and Tao-Rusyr calderas occur on Onekotan and are aligned on the strike of this CKG.

Lion's Jaw caldera occurs on the SW Kurile Arc at a point where a trough in the acoustic basement (E) intersects the arc from the NNE (backarc) side. This trough is more localized than that related to Onekotan I. However, it is the most significant arc-vergent backarc feature found along the Kurile Islands chain.

Other calderas occur in the Kuriles which fall slightly below the 8 km size limitation of this study. These include: Tao-Rusyr (7.9 km), noted above; and Brouton Caldera (7.9 km), on the north end of Simushir I. Medvezhi Caldera, on the north end of Iturup I., is heavily eroded and its dimensions are a ill-defined. In assessing the tectonic association of the Kurile calderas it must be noted that data resolution in this part of the world is limited and the significance of the cross structures is not clear.

References

(A) IAVCEI, 1958; (B) Army Map Service, 1944, 1:250,000 Topographic Maps, Kunashiri, Etorofu, Onnekotan Quads, Kuriles (Northern Japan); (C) Gorshkov, 1970; (D) Gnibidenko et al, 1983; (E) Gnibidenko and Svarichevsky, 1984; (F) Savostin et al, 1983; (G) Kimura, 1986

FIGURE 65, 68

Category: ARC (Kurile) / INTERSECTING STRUCTURE / OFFSET IN VOLCANIC ARC

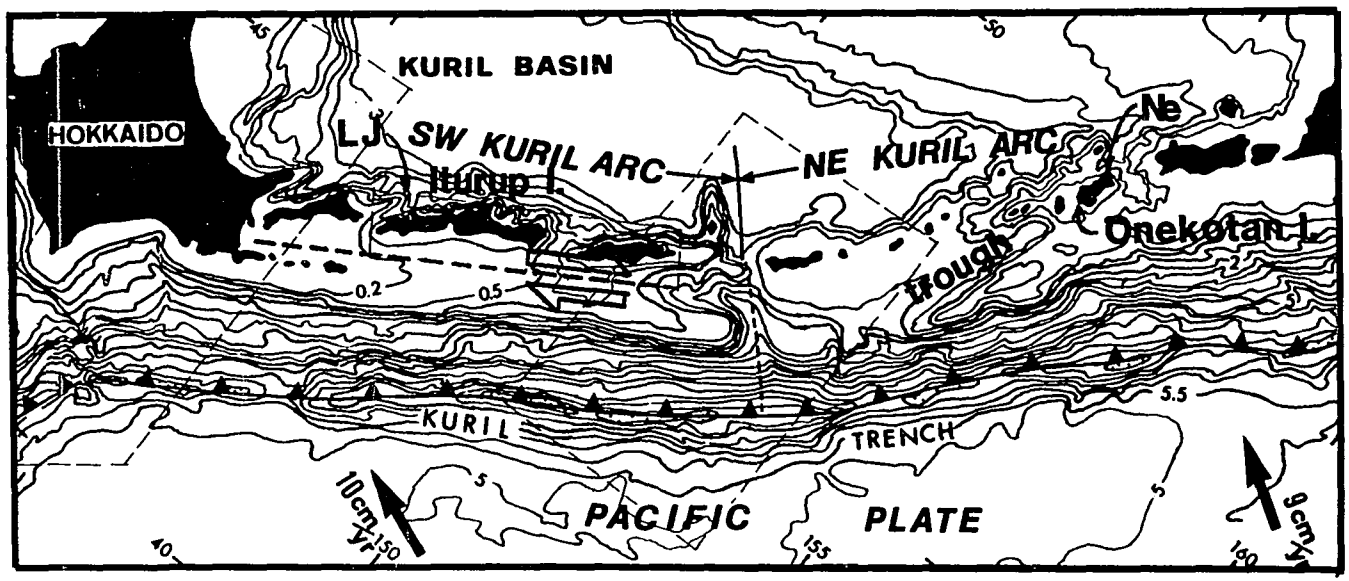

Figure 68. Bathymetric Map of the Kurile Arc (modified after Kimura, 1986) showing bathymetry and tectonic details of the Kurile Arc, including the transform fault between the Kurile Forearc Plate (KFAP) and the Kuril Basin. The trough which strikes toward Onekotan I. is also shown (see text): Ne = Nemo Caldera; LJ = Lion's Jaw Caldera.

Table 3Q

Caldera Name		Location		
Kutcharo Akan		eastern Hokkaido, Japan 8 km southwest of Kutcharo		
Elongation	Volcanic Character	Local Structure	Regional Structure	Tectonic Elements
Kutcharo: E-W 23 x 20 km (C)	caldera collapse about 30,000 ybp accompanied by abundant zoned intermediate ash-flows (B); basalt/andesite/dacite assemblage (C)	nearly circular caldera with slight elongation E-W; caldera is associated with a NW-trending graben which cuts the Shiretoko-Akan Volcanic chain (SAVC) (F)	these calderas occur on the SAVC which is an en echelon NNE ridge across the dextral ENE Kurile Forearc Transform	Kurile Arc; Kurile Forearc Plate Transform
Akan: NE 22 x 14.7 km (C)	abundant silicic ashflows associated with caldera collapse; basalt/andesite/silicic pumice assemblage (C)	caldera walls aligned NE parallel to the trend of the SAVC (B)		

Additional Information

The tectonic setting of eastern Hokkaido has not been completely resolved, however, current thinking (D,E) points to the existence of a Kurile Forearc Plate (KFAP) between the volcanic arc and the trench. This KFAP allegedly results from the fact that the Pacific Plate motion is oblique to the trench inducing a dextral strike-slip component which is translated to the KFAP (D,F). The NW margin of the KFAP forms a strike-slip boundary along the volcanic arc and a collisional boundary to the SW between the KFAP and the Eurasian Plate along the Hidaka Shear Zone (HDZ) in central Hokkaido. Seismicity indicates ENE-trending P-axes which contrast sharply with those on the west side of the HSZ (see also Shikotsu caldera). The SAVC is paralleled by en echelon right stepping structures: the Tokachi-Asahi volcanic chain and the Kamishiyubetsu Tectonic Line (E) -- both to the west; and to the east by the en echelon volcanic islands of the southern Kuriles. It has been proposed that this en echelon structure is a secondary structure related to the dextral KFAP transform motion (D,E). This interpretation implies that these en echelon structures are analogous to buckle folds and that the maximum horizontal stress (MHS) is oriented roughly NW-SE. This interpretation is supported by the alignment of the NW-trending graben at Kutcharo and by the seismic focal plane solutions for this part of Hokkaido. However, it also implies that the alignment of Kutcharo and Akan is not parallel to the MHS but for each caldera is controlled by NW-striking extensional structure. The elongation of Akan NE, parallel to the extension of such NW-trending structures is consistent with this interpretation, however, no reference to NW-striking extensional structures specifically at Akan where found.

References

(A) IAVCEI, 1962; (B) Katsui et al, 1975; (C) Army Map Service, 1944, 1:250,000 Topographic Maps, Shari Quad, Japan; (D) Kimura et al, 1983; (E) Seno, 1985; (F) Olde, 1968; (G) Hildreth, 1981; (H) Kimura, 1986

FIGURE 68, 69, 70, 71, 73

Category: ARC (Kurile) / TRANSFORM (KFAP transform) / SECONDARY EXTENSION

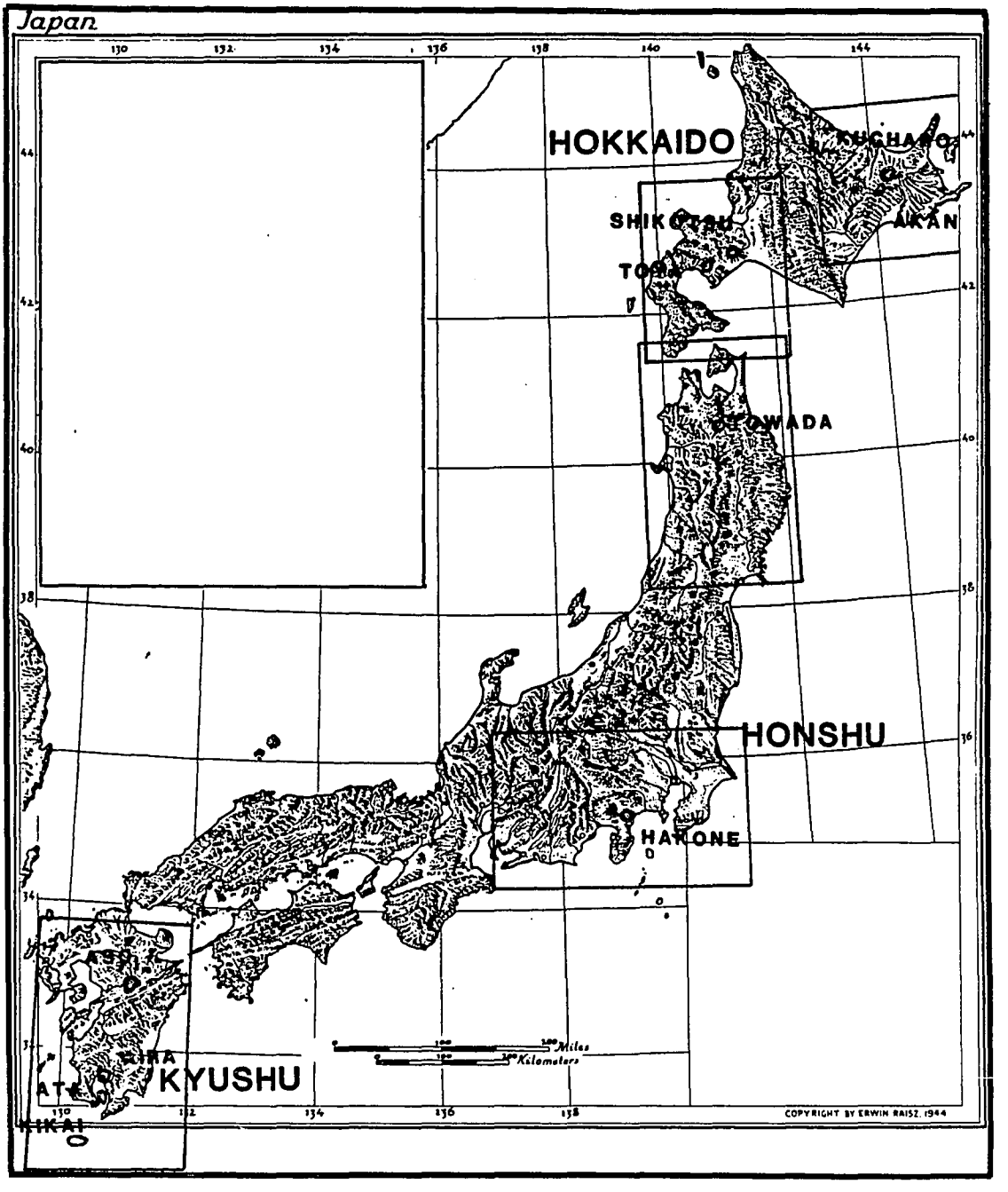

Figure 69. Index Map showing the outlines of Japan Large Caldera Maps (after Raisz, 1944) -- Figures 70, 72, 74, 76 and 78.

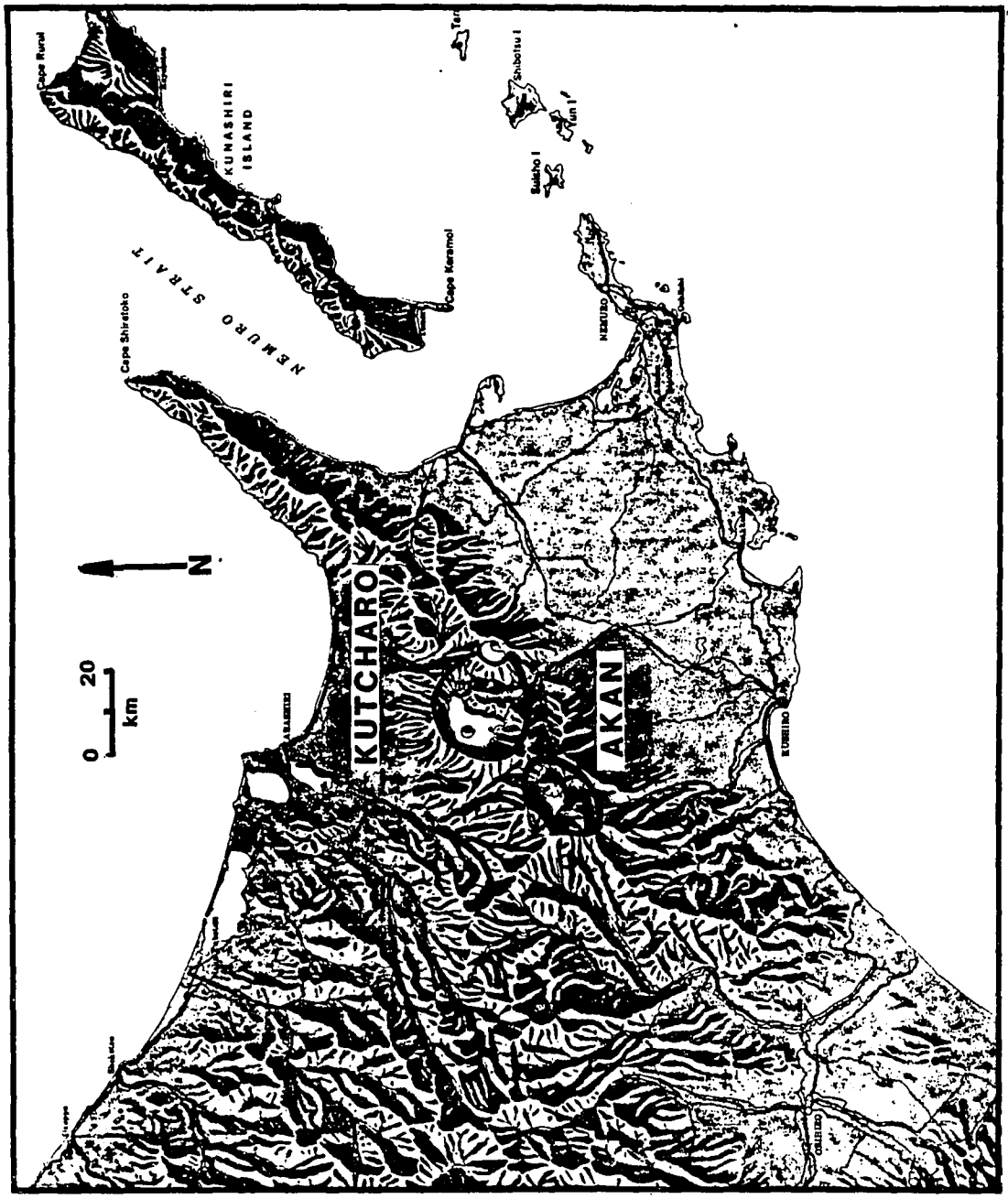

Figure 70. Shaded Relief Map of Kucharo and Akan Calderas showing the location of the calderas on the axis of a compressional ridge (Kunashir Is. is another such ridge). The location of Kutcharo is controlled by a NW-SE striking graben. The ridge in this case appears to be a buckle ridge associated with right lateral transform motion between the Kuril Forearc Plate and the North American Plate.

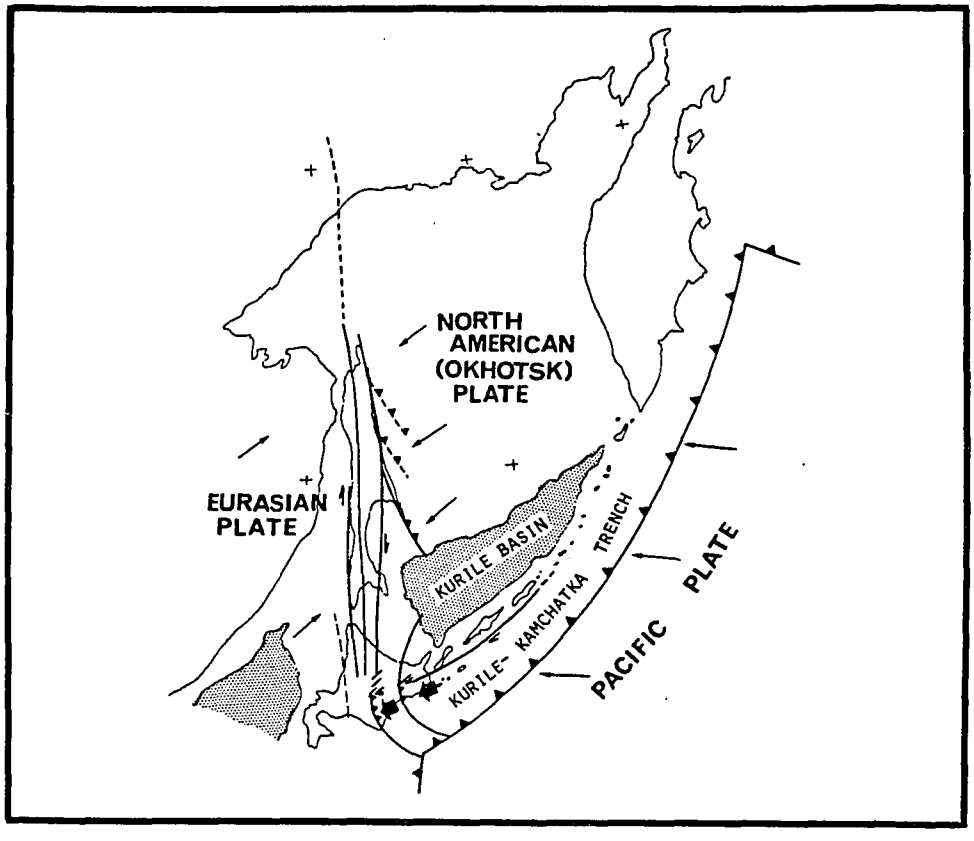

Figure 71. Tectonic Setting of the Kurile Arc and eastern Hokkaido (Kimura, 1983) showing the motion of the Kurile Forearc Plate and its southwest subduction beneath central Hokkaido (see also Figure 68).

Table 3R

Caldera Name	Location			
Shikotsu [Tarumai] Toya [Usu]	southwestern Hokkaido, Japan 25 km west of Shikotsu			
Elongation	**Volcanic Character**	**Local Structure**	**Regional Structure**	**Tectonic Elements**
Shikotsu: NNW 15 x 14 km (C)	abundant silicic ashflows associated with caldera collapse (B); andesite/dacite assemblage (B); ashflows associated with Shikotsu are zoned intermediate (I)	linear wall segment on NE indicates NW to NNW structure (C); NNW alignment of post-caldera vents (B)	Shikotsu is located on the western margin of the Ishikari Graben -- an active N to NNW trending extensional feature. This graben is bound on the east by the N-S Ishikari-Teshio deformation belt (D). Both Shikotsu and Toya are located on the edge of Uchiura Bay -- which appears to be related to the NNW-trending arm of the trench which issues from the intersection of the NE-trending Kurile Trench and the Japan Trench (Figure 73). This area is generally subsiding (E).	Japan Arc; Kurile Arc; Ishikari Graben
Toya circular 12 km (C)		linear wall segment on the SE indicates NNW structural control		

Additional Information

These two relatively circular calderas are located at the intersection of the Japan Arc and the Kurile Arc. In addition, the Ishikari-Teshio tectonic belt -- to which both right-lateral strike-slip and collision has been ascribed -- bounds this area on the west (D). Seismic data indicates NNW to N trending P-axes (maximum horizontal stress (MHS)) consistent with the orientation of Ishikari Graben and the alignment of vents at both calderas (ie. parallel to MHS) (B). Figure 73 shows the free-air gravity anomaly map of northern Japan. The trenches are well defined by the negative gravity anomaly. The arm which extends NNW from the intersection of the two trenches trends toward Ishikari Graben and Uchiura Bay. Seismicity here displays diverse stress orientations (F) and the tectonics of this area is not well constrained. The presence of the Ishkari Graben -- an actively subsiding area (E) -- indicates that western Hokkaido is an area of N to NNW MHS. It has been noted (G) that petrologic evidence indicates that the profile of the slab under Toya/Shikotsu is dipping in two directions (NE and SW) away from a high point which corresponds to the change from the Japan Trench to the Kurile Trench. This bend (analogous to the axis of a plunging anticline) may account for the extensional setting of Ishikari Graben. The profile is somewhat similar to that at Long Island caldera although the horizontal geometry is quite different.

References

(A) Williams, 1941; (B) IAVCEI, 1962; (C) Army Map Service, 1944, 1:250,000 Topographic Maps, Tomakomai and Muroran Quads, Japan; (D) Kimura et al, 1983; (E) Seno, 1985; (F) Hayes and Taylor, 1978; (G) Blot et al, 1975; (H) Olde, 1968; (I) Hildreth, 1981

FIGURE 69, 71, 72, 73

Category: ARC (Japan) / ARC (Kurile) / INTERSECTING RIFT (Ishikari Graben)

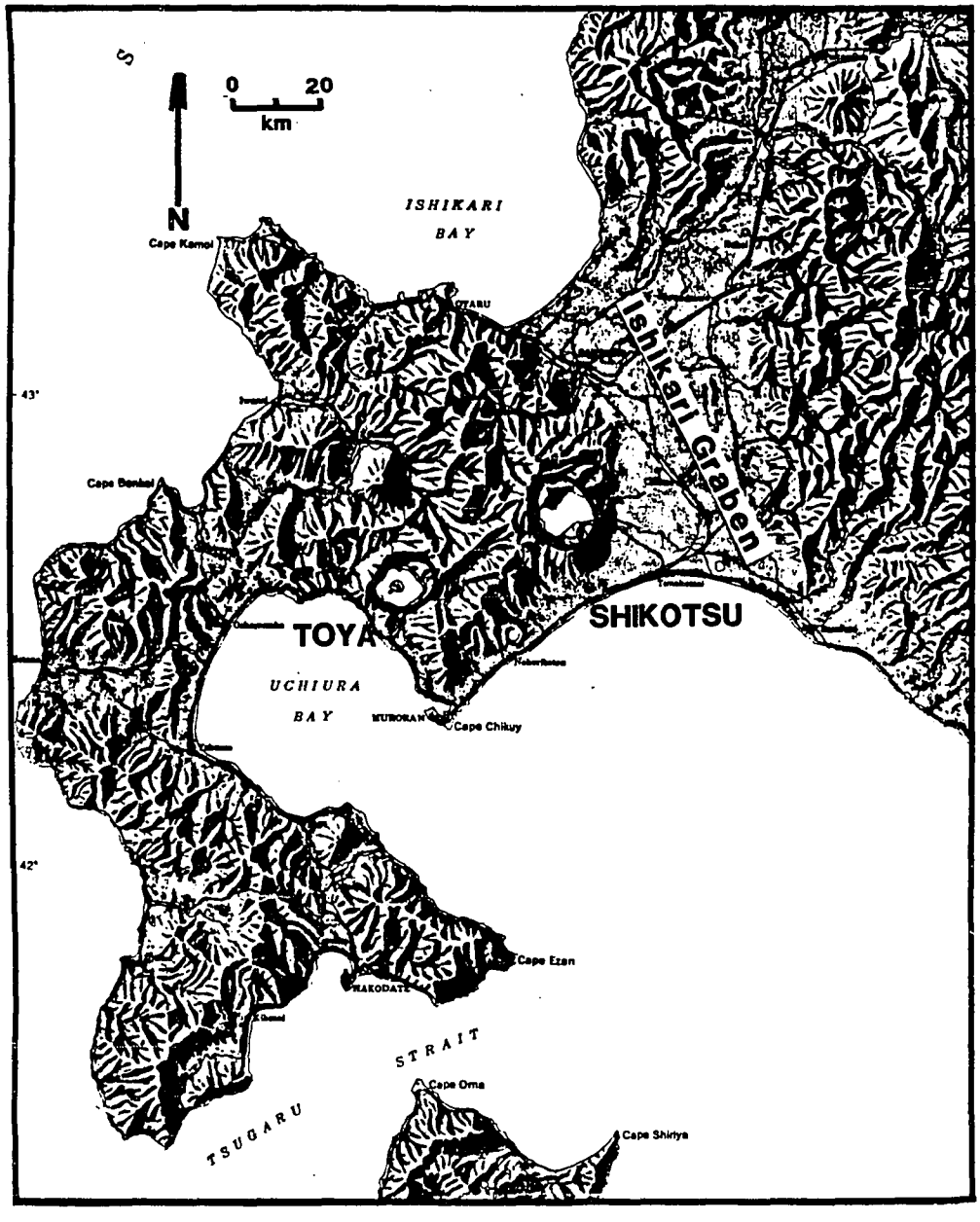

Figure 72. Shaded Relief Map of Toya and Shikotsu Calderas and vicinity.

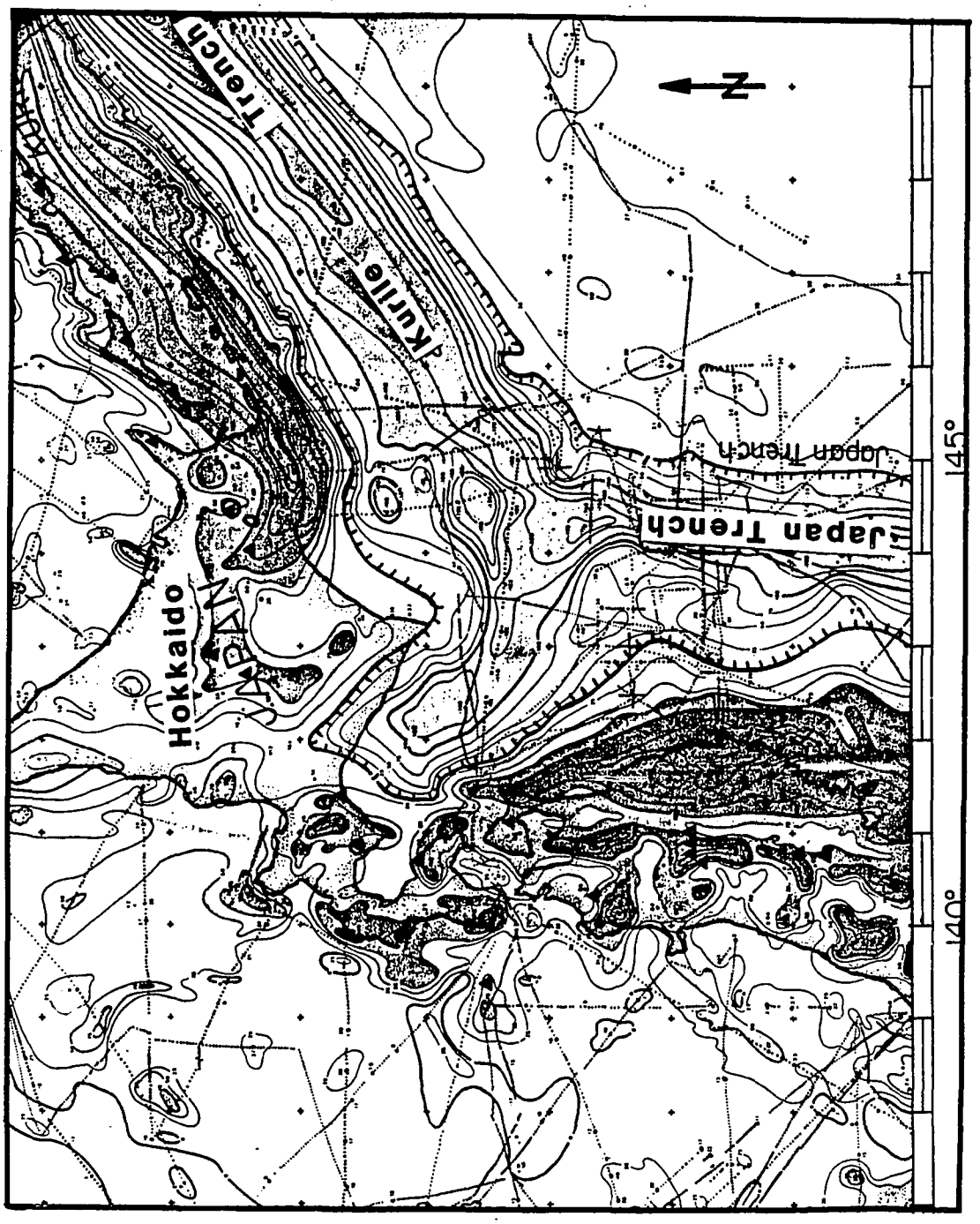

Figure 73. Free Air Gravity Anomaly Map of the Japan and Kurile Trench intersection (Watts es et al, 1978) showing the intersection of these trenches is shown in relation to Hokkaido and the large calderas. The trench-arm which extends NNW from the trench intersection aligns with the extensional Ishikari Graben (Figure 72). With the Kurile Benioff Zone dipping NE and the Japan Benioff Zone dippng west, the Pacific Plate beneath this arm must form an anticlinal bend beneath Toya and Shikotsu.

Table 3S

Caldera Name		Location		
Towada		northern Honshu, 225 km S of Toya, Japan		
Elongation	Volcanic Character	Local Structure	Regional Structure	Tectonic Elements
13 km square aligned NNW	Abundant silicic ashflows accompany caldera formation; bimodal basalt/dacite/andesite assemblage; double nested caldera (A); positive gravity anomaly	NE and SW walls of caldera are aligned NNW indicating control by NNW structures of Pliocene age. Topographic grain NE of caldera indicates possible NNE structure.	regional faulting broadly N-S (from NNW to NNE) (E); maximum horizontal stress E-W due to Japan Trench Subduction (on east) and incipient Japan Sea subduction on west (E,F)	Japan Arc; Japan Sea Subduction

Additional Information

Up to 7 mybp this area was dominated by E-W extension which produced N-S trending block faulting and N-S dike orientations (C,B). Subsequent tectonics have apparently produced E-W compression. Seismicity indicates E-W to NE-SW P-axes (E) and young (maximum horizontal) stress trajectories (dike orientations) are E-W (C). These observations conflict somewhat with evidence of caldera development. Both Towada caldera and Tazawa (a 7.5 km caldera 80 km to the south) lie in grabens bounded by NNE and NNW trending faults. At the Head of the broad NNE-striking Omonogawa River valley, Tazawa occurs in a structural setting similar to that of Crater Lake at the head of the Klamath Graben (H). Although these grabens may be residual from the earlier period of E-W extension, the structure in the vicinity of Towada caldera (alignment of caldera walls and surrounding landforms, dominance of block faulting style) appears to be controlled by normal faulting on these NNW to NNE faults (G,H,I). One P-axis identified (E) nearby on the south end of Tazawa indicates NE maximum horizontal stress. This orientation is in better agreement with the aparent caldera control on NNE structure. Additional information is necessary to resolve the differences between regional and local stress indicators here.

One additional large caldera is referenced sparingly in the literature. This caldera, Onikoube, occurs about 180 km south of Towada in a similar tectonic setting of older block faulting currently under a compressive regime. The diameter of this feature is on the order of 15 km and it is associated with Pleistocene pyroclastic flows (I). Little documentation is available for this caldera and one writer claims that it is not a caldera at all but a preexisting basin (J). Therefore, it is noted here but not tabulated in the summary lists.

References

(A) Williams, 1941; (B) Sugi et al, 1983; (C) Nakamura and Uyeda, 1980; (D) Yokoyama (1966); (E) Wesnousky et al, 1982; (F) Tamaki and Honza, 1985; (G) Newton Magazine, July, 1981; (H) Army Map Service, 1944, 1:250000 Topographic Maps, Aomori and Hachinohe Quads, Japan; (I) Mukaiyama et al, 1983 and 1984; (J) Olde, 1968

FIGURE 69, 74, 75

Category: ARC (Japan) / FAULT (preexisting faulting)

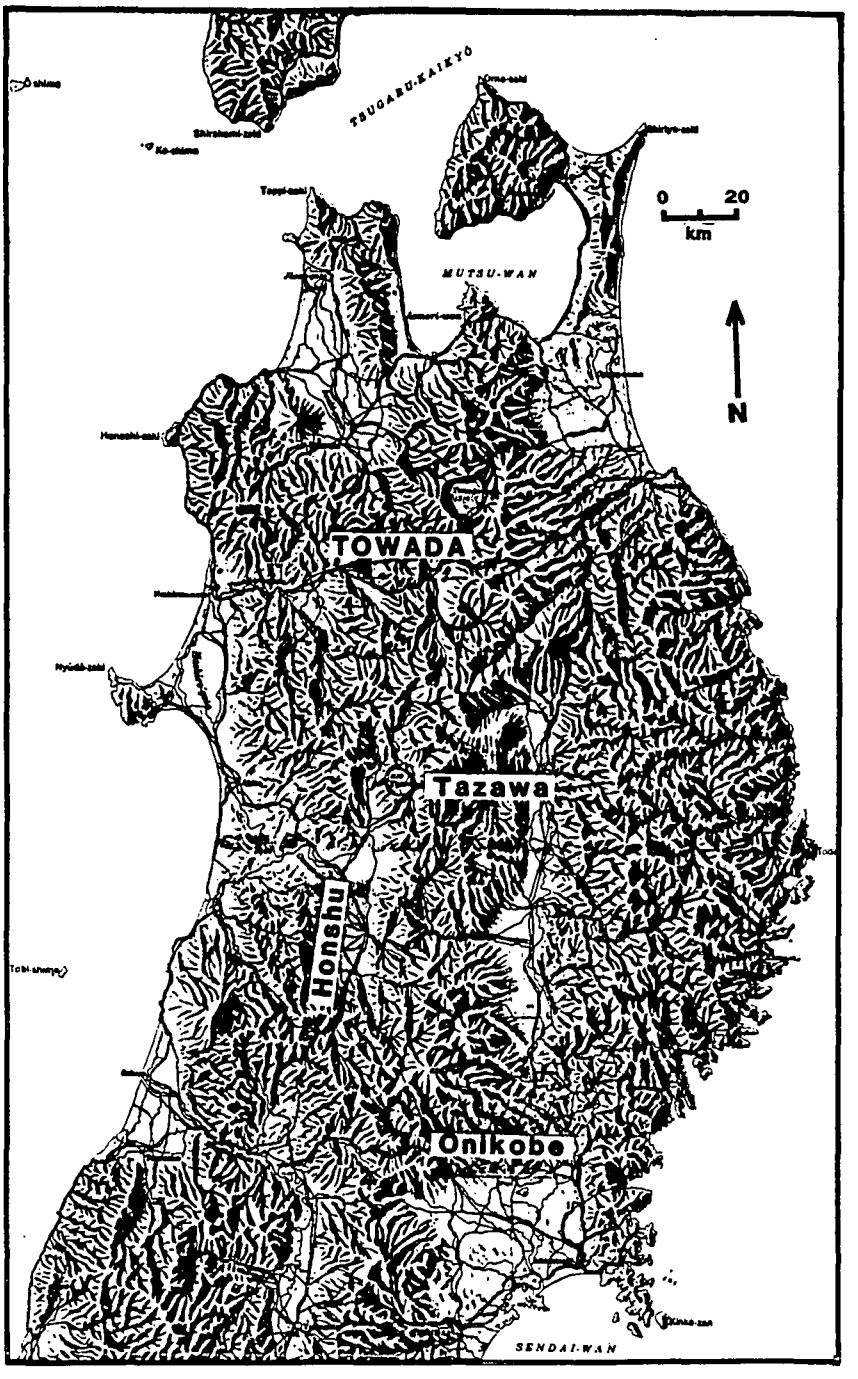

Figure 74. Shaded Relief Map of Northern Honshu showing Towada caldera showing the NE to NW striking block faulting (attributed to extensional tectonism > 7 m.y.b.p.) which dominates caldera development.

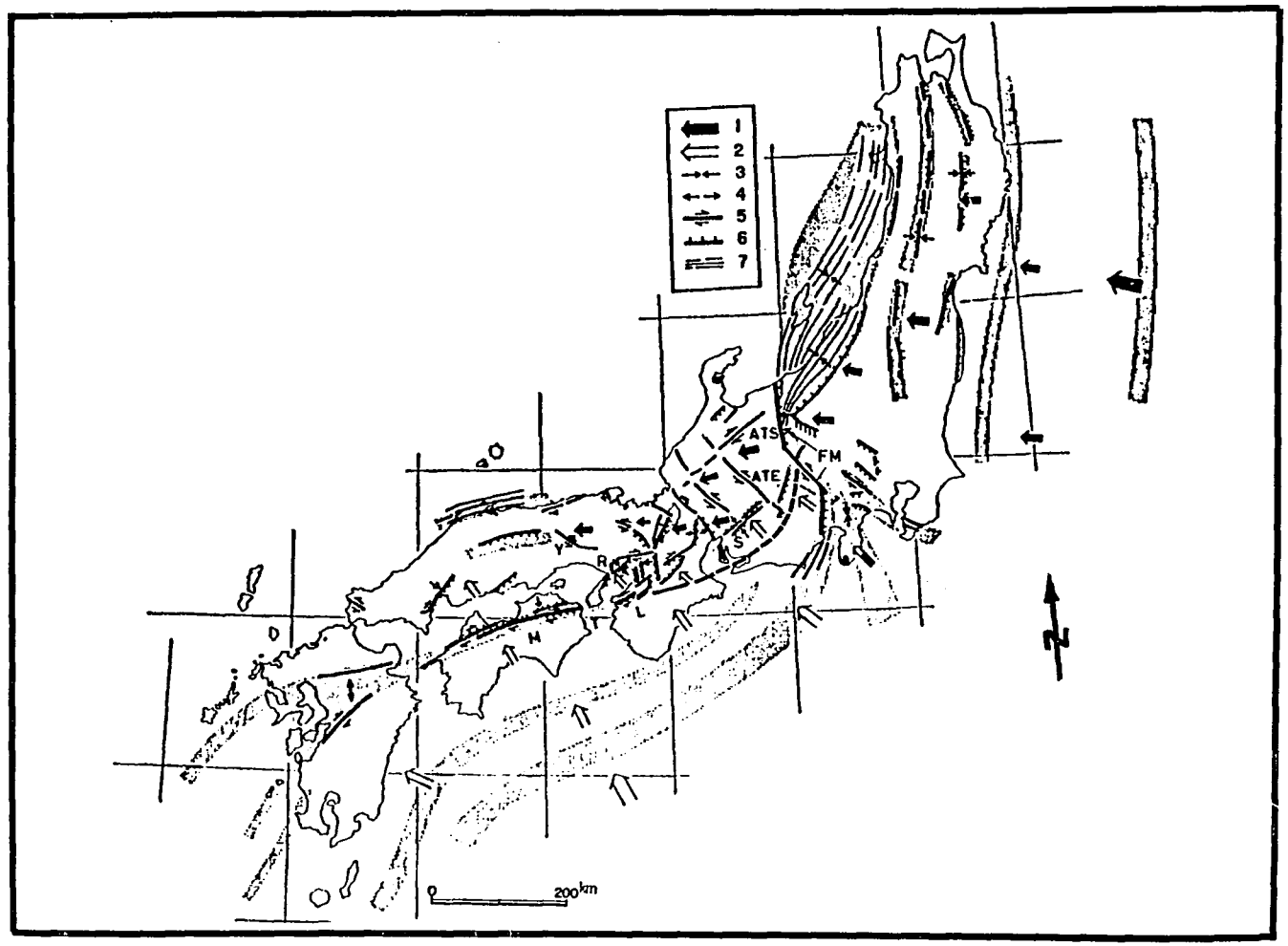

Figure 75. Tectonics of Honshu and Kyushu, Japan (Seno, 1985) showing Quaternary tectonic movements. The setting of northern Honshu and Towada caldera is presently considered to be undergoing compression across previously extensional normal faults.

Table 3T

Caldera Name		Location		
Hakone		central Honshu, Japan		
Elongation	**Volcanic Character**	**Local Structure**	**Regional Structure**	**Tectonic Elements**
NW 13.5 x 10 km	Abundant dacitic ashflows accompany caldera formation; bimodal basalt/dacite/andesite assemblage; double nested caldera formed in preexisting shield (A); caldera formation took place roughly contemporaneous with Izu-Honshu collision (A)	post-caldera vents aligned NW-SE (A); N to NNW-striking dextral fault intersects the south wall of the caldera -- the Kita-Izu fault system (G); within-caldera faults also parallel this NNW-N trend (D)	Sagami Trough (to the east) is a right-lateral transform zone; Suruga Trough (to the west) is a subduction boundary; these mark convergent plate boundaries and bound the Izu Peninsula -- allocthanous terrain of the Philippine Sea Plate (PHS) plate which has collided with Honshu. Hakone occurs adjacent to the collision zone and also at the north end of the Izu-Bonin volcanic arc.	Sagami Trough; Suruga Trough; PHS/Honshu (EUR Plate) collision; Izu-Bonin arc and backarc spreading
Additional Information				
Hakone caldera occurs at a complex tectonic intersection. The Izu Peninsula -- composed of Miocene submarine rocks formed on the PHS (B) -- has collided with Honshu (on the Eurasian (EUR) plate) starting about 1 mybp (B). Plate margins occur on either side of the Peninsula: the Sagami, largely dextral (D), and the Suruga, a subduction zone which becomes the Nankai Trough further south. Verging NNW, from the south, is the Izu-Bonin volcanic arc which is paralleled by backarc spreading. Hakone, the heat for which is produced by the subduction of the Pacific plate beneath the PHS (yielding the Izu-Bonin arc), is located on the edge of the indenting block (Izu) where localized extension can occur (see also Ambrym caldera). The Fossa Magna, a possible NNW-trending convergent zone, intersects the Suruga Trough on the west side of the Izu collision zone.				
References				
(A) IAVCEI, 1962; (B) Nakamura et al, 1984; (C) Thatcher and Savage, 1982; (D) Huchon, 1986; (E) Shuttle Image STS 2-9-390; (F) Minato, 1977; (G) Yoshikawa et al, 1981				
FIGURE 69, 75, 76, 77				
Category: ARC (Nankai) / ARC (Izu-Bonin) / COLLISION (PHS-EUR) / TRANSFORM (Sagami)				

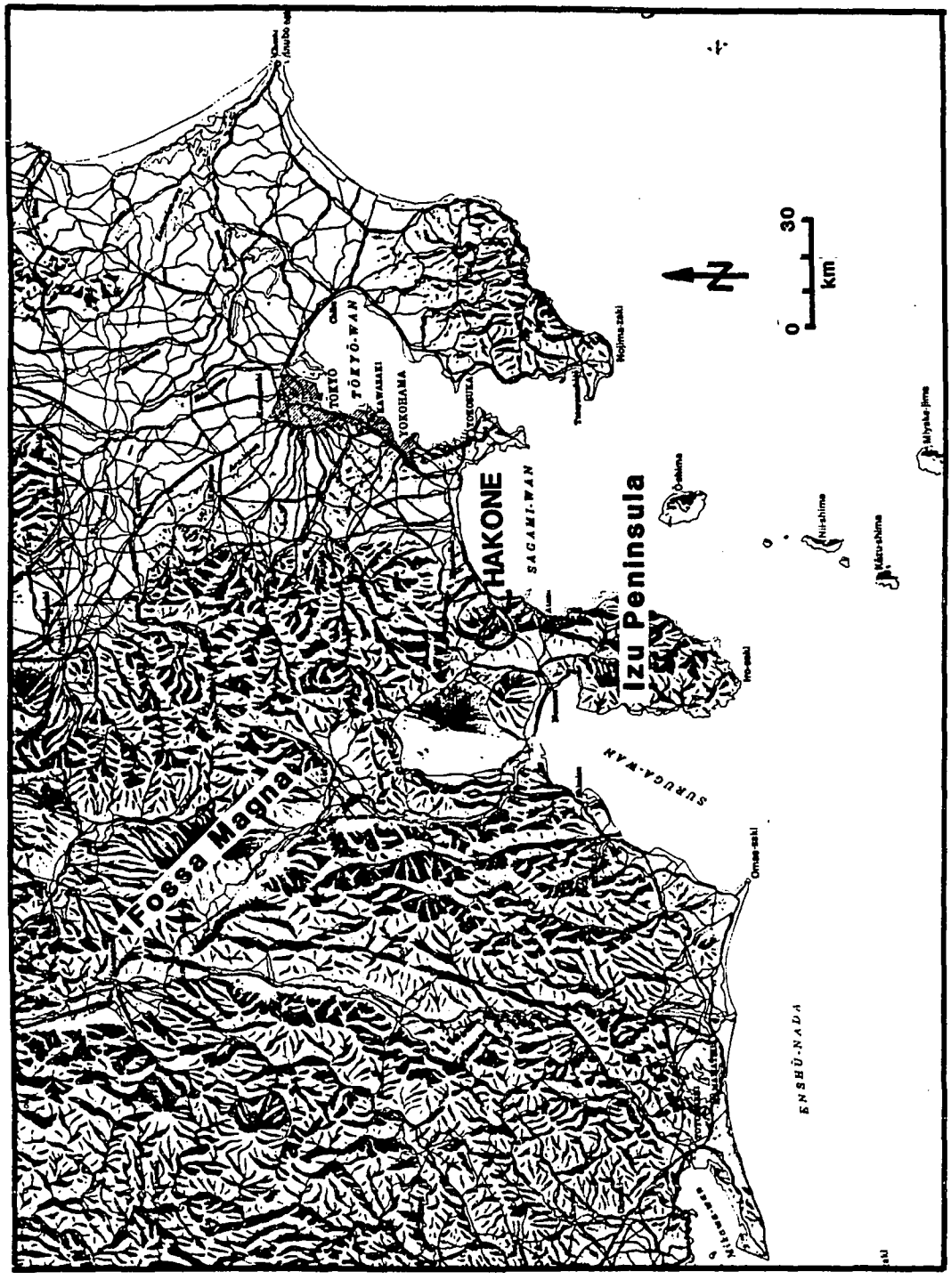

Figure 76. Shaded Relief Map of Hakone Caldera and vicinity.

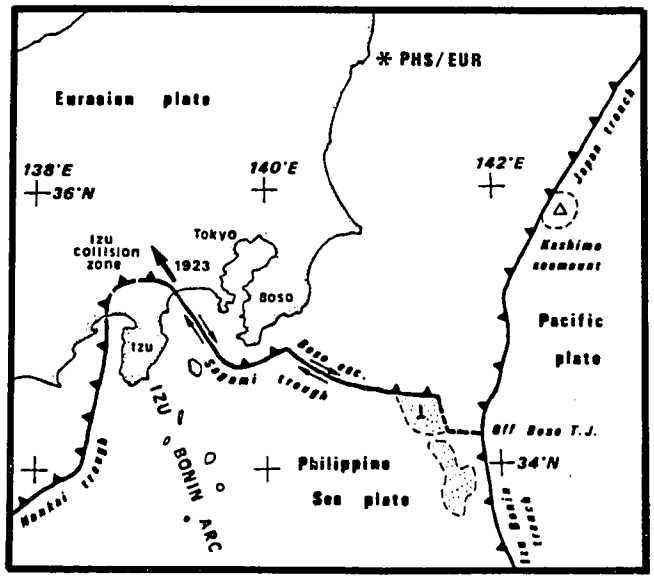

Figure 77. Tectonics of the Izu Peninsula Region around Hakone Caldera (Huchon, 1986). Hakone is located adjacent to a collisional regime where the Izu Peninsula -- formerly on the Pacific Plate -- has collided with, and become accreted to Honshu. Hakone is located at the edge of the collision point.

Table 3U

Caldera Name		Location		
Aso		central Kyushu, Japan		
Elongation	**Volcanic Character**	**Local Structure**	**Regional Structure**	**Tectonic Elements**
N-S 24 x 17 km	Abundant zoned intermediate (F) ashflows accompany caldera collapse; probable multiple collapse (D)	Linear walls on NW and E sides indicate NNE structural control; alignment of vents within the caldera (and scarps west of the caldera) along an E to ENE trend; recent cone alignment NNW-SSE within the caldera	WSW trending right-lateral MTL trends through the caldera; Beppu Shimabara Graben -- an extension of the Okinawa Trough (OT) -- trends ENE and intersects Aso	Ryuku Arc; Okinawa Trough (OT); Median Tectonic Line (MTL)
Additional Information				
	The MTL is a long-standing tectonic feature of central and southern Japan to which Quaternary right-lateral motion has been ascribed (E). It trends toward Aso from the ENE. The Beppu Shimabara Graben trends toward Aso from the WSW. It has been ascribed to extension related to spreading in the Okinawa Trough (D). These two features (MTL and OT) are parallel and intersect in the vicinity of Aso. They presumably interact with one another to produce enhanced localized extension. Additional NNE and NNW structure (similar to that found at Kagoshima Bay to the south) may reflect mobilization of preexisting structure. The OT represents the intersection of the backarc tectonics with the magmatic arc. It intersects the arc at a small angle and is transitional between an arc-parallel rift and an intersecting rift.			
	It is noteworthy that Yokoyama (C) has interpreted gravity and limited drilling data (2 holes 150m and 600m deep) to imply that Aso caldera is a superficial structure narrowing at shallow depth to a small fraction of the caldera diameter at the surface. He also applies this reasoning to many other of Japan's large calderas as well as Long Valley caldera. Unfortunately, the basis of his interpretations are problematical. He assumes basement/caldera fill density contrast of 0.3 and basement density of 2.4. However, potential caldera fill material ranges in density from basalt (density 2.8) to andesite (density 2.6) to rhyolite (density 2.4) (E); while granite -- the country rock ("basement") -- is typically 2.6. (The probable dominant caldera fill -- andesite -- differs little from granite in density.) The borings which he cites are not deep enough, nor in sufficient number to distinguish between "basement" and magma-chamber roof rock. The available models cannot be distinguished using the data he cites.			
References				
	(A) Williams, 1941; (B) IAVCEI, 1962; (C) Yokoyama, 1983; (D) Letouzey and Kimura, 1985; (E) Carmichael, 1984; (F) Hildreth, 1981 FIGURE 69, 75, 78, 79			
Category: ARC (Ryuku) / INTERSECTING to ARC-PARALLEL RIFT (OT) [with possible strike-slip (MTL)]				

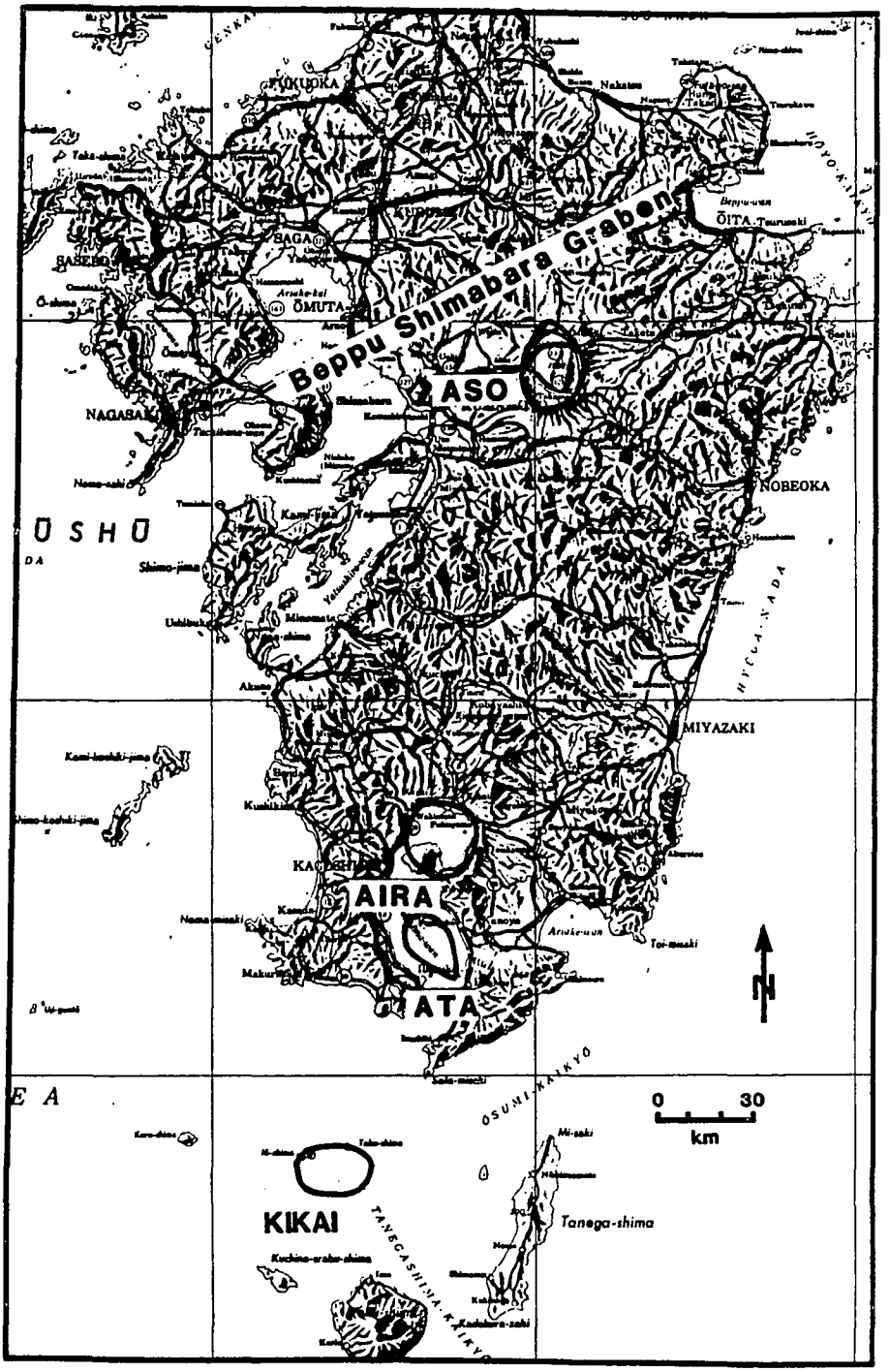

Figure 78. Shaded Relief Map of Kyushu and Aso, Aira, Ata and Kikai Calderas showing the relationship of Aso with the Beppu Shimabara Graben.

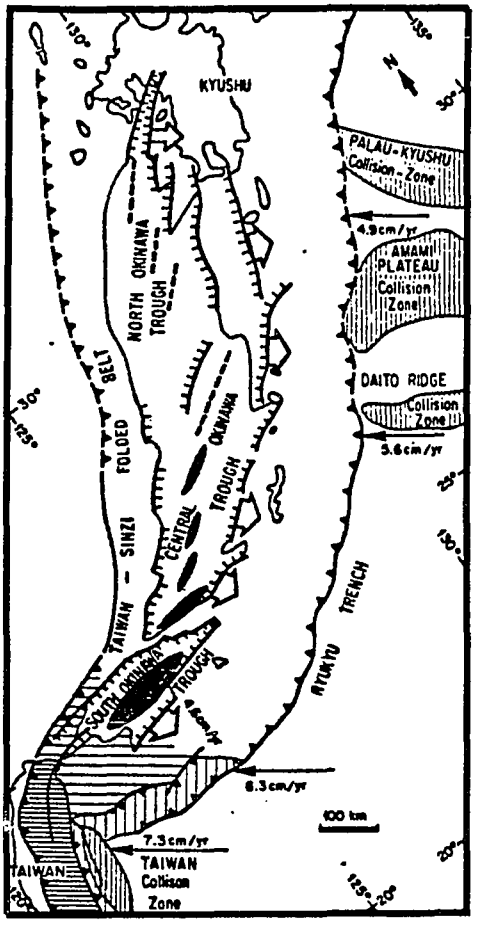

Figure 79. Tectonics of Kyushu and the Okinawa Trough (Letouzey and Kimura, 1985). The active backarc extension of the Okinawa Trought becomes distributed to the north and intersects Kyushu both at Kagoshima Bay (location of Aira, Ata and Kikai calderas) and at the Beppu-Shimabara Graben where Aso caldera is located (see Figure 78).

Table 3V

Caldera Name	Location
Aira Atta Kikai	northern Kagoshima Bay, southern Kyushu, 120 km SSW of Aso, Japan central Kagoshima Bay, 17 km S of Aira, Japan offshore south of Kyushu, 60 km S of Atta, Japan

Elongation	Volcanic Character	Local Structure	Regional Structure	Tectonic Elements
Aira 23 km (square) (A)	abundant silicic ashflows associated with caldera collapse (A); at Aira, post-caldera volcanism is andesitic (A)	east and west caldera walls aligned NNE; normal faults within caldera parallel this trend	Kagoshima Bay is S-shaped, developed on active NNE aand NNW trending normal faults. The right-lateral Median Tectonic Line passes 100 km north of the Bay; South of the Bay the NNW extensional faults of the Okinawa trough verge from the south.	Ryukyu Arc; Okinawa Trough
Atta: NNE 16 x 12 km	Atta ashflows are zoned intermediate (E)	elongate parallel to the trend of the bay; shape implies multiple collapse		
Kikai: E-W 22 x 13 km (D)		elongation of caldera parallel to extension direction; southern caldera wall is breached by a NE-trending graben which parallels the orientation of the southern end of Kagoshima Bay (to the north) (E)		

Additional Information

Kagoshima Bay is a rift which is an extension of normal faulting associated with the Okinawa Trough (a backarc spreading center verging from the south) (C). Kagoshima Bay also occurs opposite an inflection in the Ryuku Arc where the arc changes strike from NNW-SSE, south of Kagoshima to NNE-SSW to the north. The NNW-trending faults within the Bay are an extension of Okinawa Trough faulting (C). The NNE-trending faults may be related to the older (but still active) NE-trending Median Tectonic Line. Kagoshima Bay is characterized by negative gravity anomaly along its length (A). Atta is completely submarine, while two islands (Iwo-zima and Take-sima) occur on the rim of the otherwise submarine Kikai caldera. The calderas become geomorphically younger looking to the north with Aso (north of the Bay) the youngest in appearance (B) (the formation of Aira caldera has been dated at 22,000 yr ago (A)). The large calderas in and adjacent to Kagoshima Bay occur in an area of intense caldera development -- 32 km of aggregate caldera width within 105 km of arc -- rivaled (in terms of number and breadth of calderas) only by the calderas of central Kamchatka, New Zealand, and Italy.

References

(A) Aramaki, 1984; (B) Williams, 1941; (C) Letouzey and Kimura, 1985; (D) IAVCEI, 1962; (E) Hildreth, 1981

FIGURE 69, 78, 79

Category: ARC (Ryukyu) / INTERSECTING to ARC-PARALLEL RIFT (Okinawa Trough) / INFLECTION IN THE ARC

Table 3W

Caldera Name	Location
Taal Laguna de Bay	southern Luzon I., Philippine Is. 10 km NE of Taal, Philippine Is.

Elongation	Volcanic Character	Local Structure	Regional Structure	Tectonic Elements
Taal: N-S 26 x 25 km (A)	abundant andesitic ashflows associated with caldera collapse (A); dominant andesitic assemblage with minor dacite (A);	the 700 m high SE wall of the caldera coincides with the Palawan-Macolod Lineament (PML) and the Marikina Fault crosses Taal from N to SW	both calderas are located in a NNE-trending zone of normal faults (with N to NE strikes) which are bound on the west by the Marikina Fault and on the east by the PML; located 20 to 50 km behind the volcanic front	Bataan Lineament (Arc associated with the Manilla Trench); PML/Marikina graben
Laguna de Bay: NNE 25 x 12 km (A)	mildly alkaline dominantly andesitic assemblage; abundant andesitic ignimbrites are found adjacent to the caldera (A)	east side of the caldera coincides with the NE to NNE PML and the WNW trending Manilla Fault crosses the caldera (A); numerous en echelon normal faults parallel and define the east and west walls of the caldera (A); south of Laguna de Bay (LdB) well defined vent alignments coincide with the PML (A)		

Additional Information

The northern Philippines occur in an area of complex tectonics with east-dipping subduction of the SE Asian Plate taking place at the Manilla Trench west of Luzon; and west-dipping subduction of the Philippine Sea Plate taking place in the East Luzon Trough to the NE. Also the major sinistral strike-slip Philippine fault passes 20 km east of LdB. The Bataan Lineament (Arc) is the volcanic arc associated with the Manilla Trench subduction (a waning subduction zone (D)). The PML is a major NNE-trending zone of extensional deformation which has been traced for at least 100 km (A). The PML is closely related to caldera development at both Taal and LdB, although its tectonic significance is not well understood. On the basis of available information, it appears to be an extensional rift-like feature intersecting the volcanic arc.

References

(A) Wolfe and Self, 1985; (B) Wolfe, 1981; (C) Landsat Imagery, Short et al, 1976, PI 369; (D) Karig, 1973

FIGURE 80, 81

Category: ARC (Bataan Lineament) / INTERSECTING RIFT (PML/Marikina extensional zone)

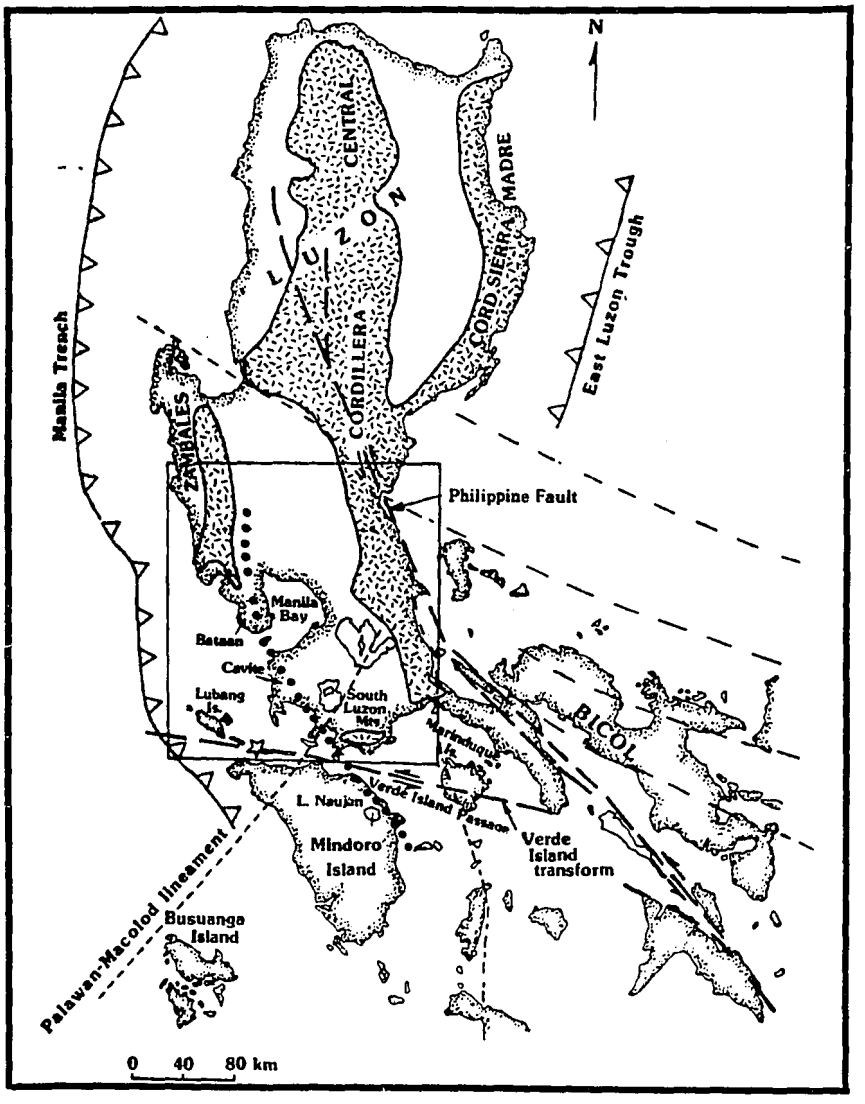

Figure 80. Tectonic Map of the northern Philippines (Wolfe and Self, 1982) The dotted line marks the calc-alkalic volcanic front. Taal is located about 20 km behind the front while Laguna de Bay is about 50 km behind the volcanic front. The Palawan-Mocolod Lineament (PML) marks the east side of an extensional zone which intersects the arc.

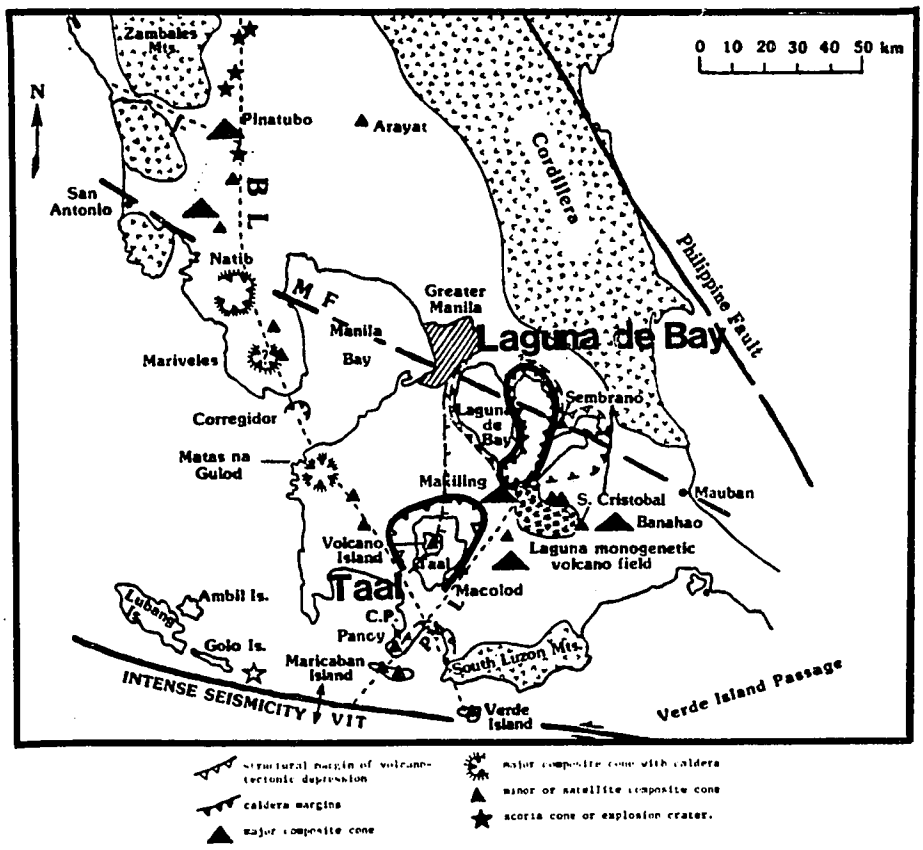

Figure 81. Volcanoes and Structure of the Taal and Laguna de Bay Region (Wolfe and Self, 1982). Both calderas are located on the (PML). This zone is bounded on the west by the Marikina Fault. These faults influence the development of the caldera walls of both Taal and Laguna de Bay.

Table 3X

Caldera Name		Location		
Tondano Depression		North Arm, Sulawesi, Indonesia		
Elongation	Volcanic Character	Local Structure	Regional Structure	Tectonic Elements
NNE 15.5 x 6 km rectangular	character of volcanic deposits unknown; rhyolites, basalts (tholeiitic and calcalkalic) and andesites occur in the Tondano vicinity (C) but their relationship to Tondano is undefined	NNE-trending vent alignment parallels elongation; linear segments of E and W walls of caldera imply control on NNE structure	occurs 10 km south of the intersection of two volcanic arcs; located west of the complex Molucca Sea Plate double subduction	North Sulawesi Arc and East Sangihe Arc

Additional Information

Tondano Caldera is identified in the compilation of Pike and Clow (D) but little information on the caldera is available. Tondano is rectangular in shape, suggesting significant tectonic influence on caldera wall orientation, however no graben extending beyond the caldera is evident on the topographic maps (B). There is little information on the volcanic deposits or structure of Tondano. Topography of the outer flanks of Tondano suggest the presence of ashflow deposits. Its tectonic setting is unusual in that it is located at the intersection of two volcanic arcs representing the subduction of two different microplates. These arcs represent the volcanism derived from the E. Sangihe subduction zone, where the Molucca Sea Plate is subducting from the east -- producing a short arc trending NNE; and the North Sulawesi subduction zone, where the plate to the north of the North Sulawesi Trench is subducting from the north -- producing an ENE-trending arc. It is noteworthy that Tondano is located opposite the extremely complex Molucca Sea subduction where the 150 km-wide Molucca Sea Plate is being subducted both eastward, beneath Halmahera, and westward beneath Tondano. It has been noted that the east end of the North Sulawesi Trench has migrated eastward with time (A). This implies a retreat of the subducted Molucca Sea Plate beneath Tondano. The complexities of these tectonic interactions may produce localized extension.

References

(A) Hamilton, 1979; (B) Army Map Service, 1:200,000 Topographic Maps, Amderang and Menado Quads., 1943; (C) Pike and Clow, 1981

FIGURE 82, 83

Category: ARC (North Sulawesi) / ARC (East Sangihe)

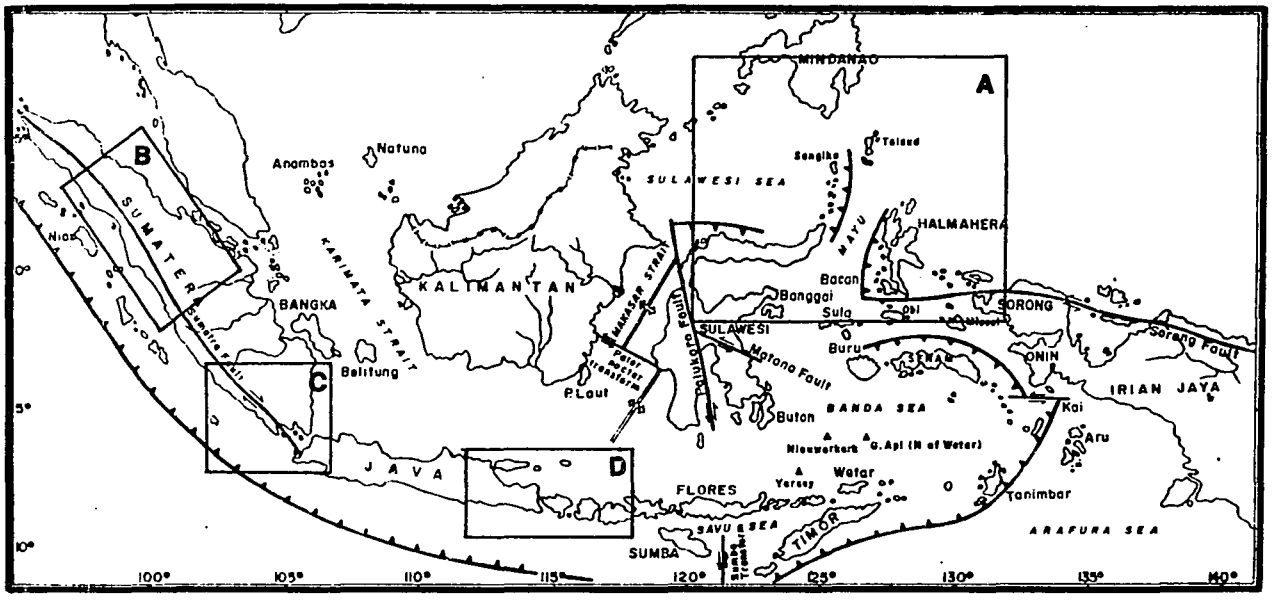

Figure 82. Tectonics of the Indonesian Region (modified after Katili and Hatono, 1983). This map indexes the caldera maps of the four regions which contain large calderas in Indonesia (A- Toba and Manindjau; B- Ranau, Gedonsurian, Krakatau and Danau; C- Tengger, Idjen, Batur, Bratan, Segera; D- Tondano. General tectonic relationships are indicated. Note the dextral strike-slip character of the (Great) Sumatra Fault (GSF) which parallels the arc on Sumatra. This is a transform fault related to the NW-SE spreading in the Andaman Sea (NW of Sumatra) and also reflects the oblique NNW-ESE convergence at the trench.

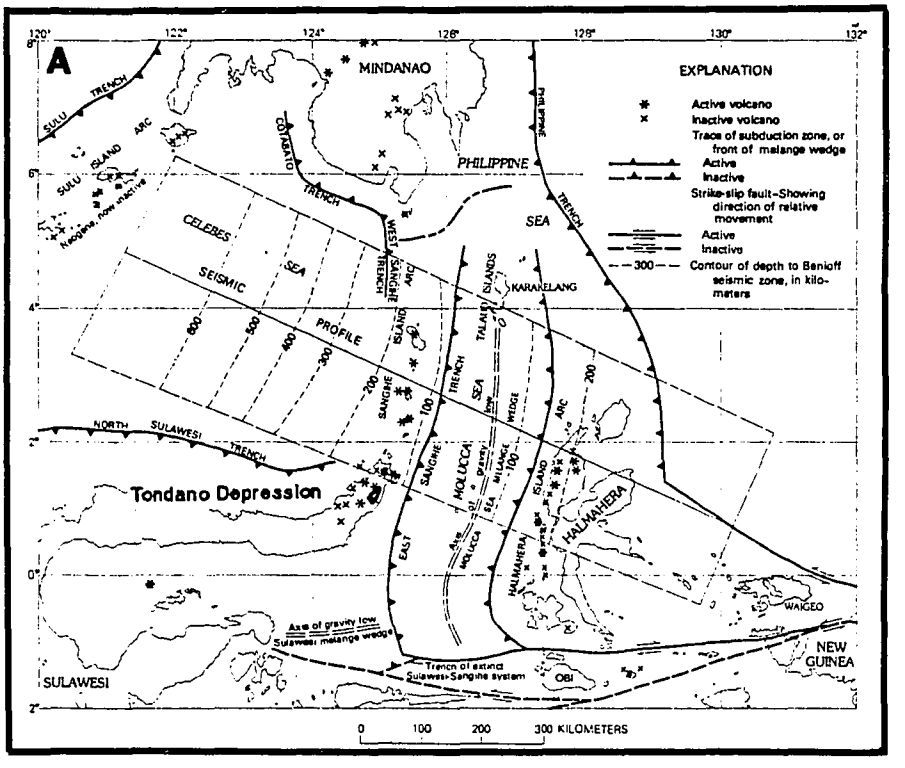

Figure 83. Tectonics and caldera location of Tondano Depression (Hamilton, 1979). Tondano is the only caldera within the isolated volcanic arc of the north arm of Sulawesi. Its linear walls and rectangular shape indicate tectonic control. It is located at the intersection of two volcanic arcs: one related to the south dipping subduction in North Sulawesi Trench and one related to the east dipping subduction in th East Sangihe Trench. It is also adjacent to the doubly subducting Molucca Sea Plate (note that along subduction zones the barbs occur on the over-riding plate except in the Molucca Sea where the barbs occur on the subducting Molucca Sea Plate).

Table 3Y

Caldera Name		Location		
Toba Caldera		northern Sumatra, Indonesia		
Elongation	Volcanic Character	Local Structure	Regional Structure	Tectonic Elements
NE 100 x 31 km (B) rectangular	abundant rhyolitic ashflows associated with the caldera collapse; primarily rhyolitic/dacitic assemblage; evidence of associated mafic volcanism is absent (H); resurgent doming has occurred	NE and SW caldera walls are linear and parallel to the elongation direction of the caldera; parallelogram shape of the caldera indicates strong tectonic control	Long axis parallels the Great Sumatra Fault (GSF). The main trace of the GSF makes a 15° bend at Toba from a NW strike (north of the caldera) to a NNW strike (to the south)	Sunda Arc; Great Sumatra Fault (inflection)

Additional Information

The tectonics of Sumatra is dominated by the superposition of a major transform fault -- the Great Sumatra Fault -- on the volcanic arc associated with the Sunda Arc. The arc is the result of the N-S subduction of the Indo-Australian Plate beneath Sumatra. The GSF transform is a right-lateral fault resulting from spreading in the Andaman Sea NW of Sumatra. This relationship has been ascribed to the oblique subduction taking place along this Sunda Arc (I). In addition to strike-slip motion, the GSF has a significant component of extension which produces a discontinous en echelon rift morphology along its length within which volcanism occurs.

Toba is the largest caldera in the world. It is occupied by Lake Toba and Samosir Island, a resurgent dome (F). Its present morphology is probably the result of more than one collapse event and the strong structural control implied by the caldera shape implies an intimate linkage between volcanic and tectonic processes. The existence of Lake Singkarak, south of Manindjau, which is not attributed to caldera collapse (E), demonstrates that tectonic processes on the GSF alone are capable of producing caldera-like depressions. On the other hand, the presence of the large (20 x 46 km) updomed block of Samosir Island within Toba caldera testifies to the deformation role that volcanic processes have produced here. The location of Toba along the GSF appears to be dictated by the tectonic setting on two scales. Extensional tectonics at Toba is enhanced on the north side of the GSF as a result of the bend which the fault takes -- striking SE north of the caldera vs SSE south of the caldera. Also, the area adjacent to Toba on the NE (east of the GSF) is characterized by a higher density of mapped faults (dominantly NE and ENE). The inflections in the trace of the GSF (inflections which are probably the result of undefined cross structures) interact with the overall right-lateral sense of this transform to produce an extensional tectonic environment favorable to volcanism.

References

(A) Williams, 1941; (B) van Bemmelen, 1949; (C) Geologic Map of Pematangsiantar Quad, Sumatra, 1982 (1:250,000), Geol. Res. and Dev. Center, Bandung, Indonesia; (D) Army Map Service, Topographic Maps (1:250,000); (E) van Bemmelen, 1929; (F) Smith and Bailey, 1968; (G) Landsat Image E-1437-03081-7; (H) Walker, pers. comm., 1986; (G) Hamilton (1979)

FIGURE 82, 84

Category: ARC (Sunda) / ARC-PARALLEL RIFT (inflection in GSF) / TRANSFORM (GSF)

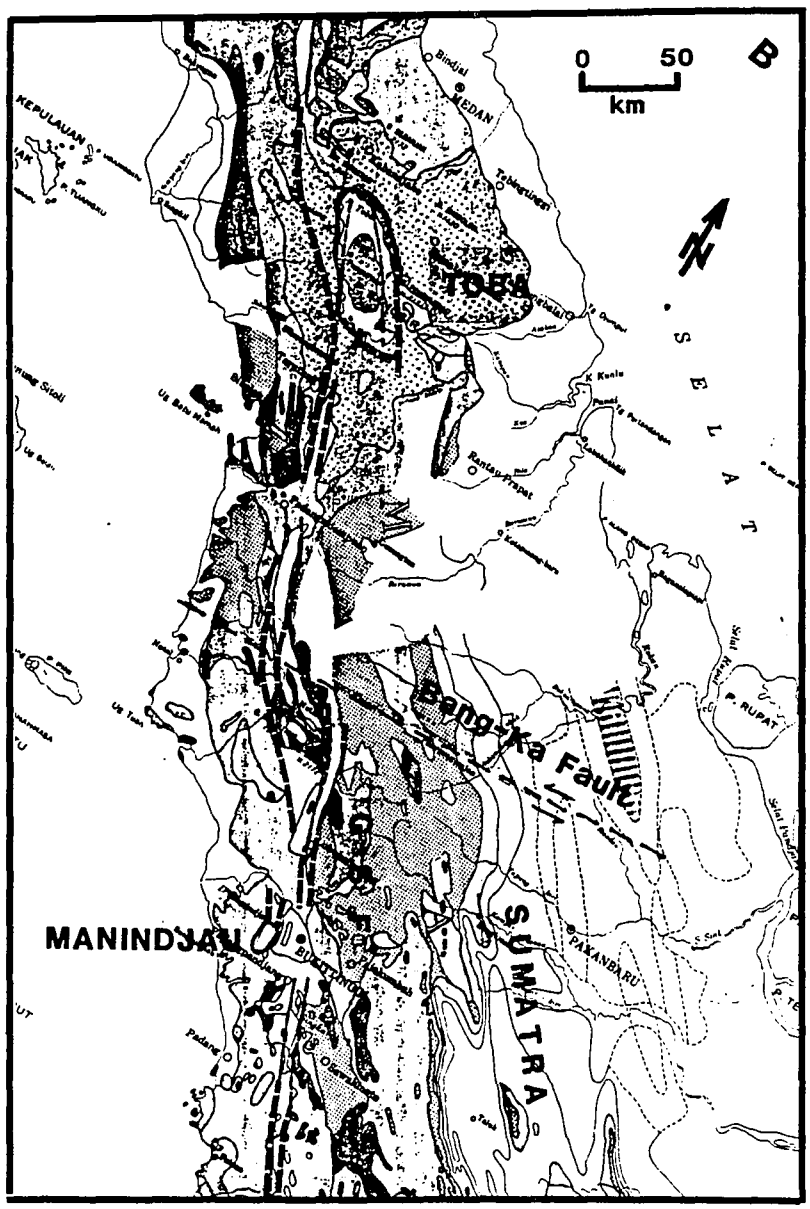

Figure 84. Caldera Map of Northern Sumatra (basemap Geologic Map of Indonesia, 1965). Calderas and mapped faults of northern Sumatra are shown. Bold dashed lines indicate faults mapped from other sources (see text). The dextral Great Sumatra Fault (GSF) is manifest as an arc-parallel graben structure of generally SE strike. It is paralleled by graben structures reflecting a component of extension across this feature. Calderas occur within or adjacent to these graben structures. Perturbations in the trend of this fault zone are in many cases marked by large calderas, eg. Toba and Manindjau in this figure. Oblique (N-S) convergence dominates this arc.

Table 3Z

Caldera Name		Location		
Manindjau		central Sumatra, 325 km SSE of Toba, Indonesia		
Elongation	**Volcanic Character**	**Local Structure**	**Regional Structure**	**Tectonic Elements**
N-S to NNE 21.5 x 10 km (B)	abundant acid tuffs associated with the caldera (B); bimodal assemblage implied (E)	broadly rectangular caldera shape; long axis of caldera oriented N-S, curving to NNW at the north end of the caldera -- parallel to the GSF trend. East wall of the caldera is excavated into basement.	Located west of the GSF at a point where the geomorphic form of the axial graben of the GSF is not well developed.	Sunda Arc; Great Sumatra Fault (GSF) (offset)

Additional Information

The regional tectonics of Sumatra is described on the Toba Sheet. Manindjau is a well-formed lake-filled caldera which has linear wall segments on its E and W sides -- parallel to its elongation direction -- indicating structural control along N to NNW trends. At its south end the long axis of the caldera is oriented N-S, an orientation parallel to the maximum horizontal stress direction associated with the right-lateral strike-slip of the GSF (mapped faults with similar strike are found about 25 km SE of Manindjau (B)). Van Bemmelen (A) notes that the location of Manindjau west of the axial graben suggests that cross faulting, intersecting the GSF, is present. However, good geologic mapping of Sumatra is generally not available (D) and such cross faulting is not indicated on available maps. It is noteworthy that about 100 km north of Manindjau, a major WNW-strikng sinistral strike-slip fault -- the Bang-Ka Fault Zone is identified (C) crossing the GSF -- producing the large left-step which occurs in the vicinity of Gunung Malintang. Similar, as yet unidentified cross faulting may be present at Manindjau.

References

(A) van Bemmelen, 1949; (B) Geologic Map of Padang Quad, 1972 (1:250,000), Geol. Res. and Dev. Center, Bandung, Indonesia; (C) Holcombe, (1977); (D) Hamilton, 1979; (E) Pike and Clow, 1981

FIGURE 82, 84

Category: ARC (Sunda) / ARC-PARALLEL RIFT / TRANSFORM (GSF)

Table 3AA

Caldera Name		Location		
Ranau		southern Sumatra, 210 km NW of Krakatau, Indonesia		
Elongation	**Volcanic Character**	**Local Structure**	**Regional Structure**	**Tectonic Elements**
NNE 16.6 x 13.5 km	abundant acid tuffs accompanying caldera collapse	NW and SW caldera walls are linear indicating strong NW structural control parallel to the Semangka Graben and SW control perpendicular to the Graben. The caldera elongation parallels the extension direction of the main graben.	The GSF (graben) strikes SE intersecting Ranau on its NE side. the GSF steps to the right, about 5 km, at Ranau and continues SE of the caldera	Sunda Arc; Great Sumatra Fault -- Semangka Graben
Additional Information				
The regional tectonics of Sumatra is described on the Toba Sheet. Ranau is located within the axial rift of the GSF at a slight offset in the Semangka Graben. Van Bemmelen (A) also indicates a fault scarp trending N from the NE wall of the caldera. The caldera width in the long dimension is typically reported as the width of Lake Ranau which occupies the caldera. However, low topography to the NE of the lake indicates that caldera width may be as much as 23 km. Ranau's rectangular shape, parallel to the Semangka Rift, indicates tectonic influences.				
References				
(A) van Bemmelen, 1949; (B) Westerveld, 1954; (C) Williams, 1941				
FIGURE 82, 85				
Category: ARC (Sunda) / ARC-PARALLEL RIFT / TRANSFORM (GSF)				

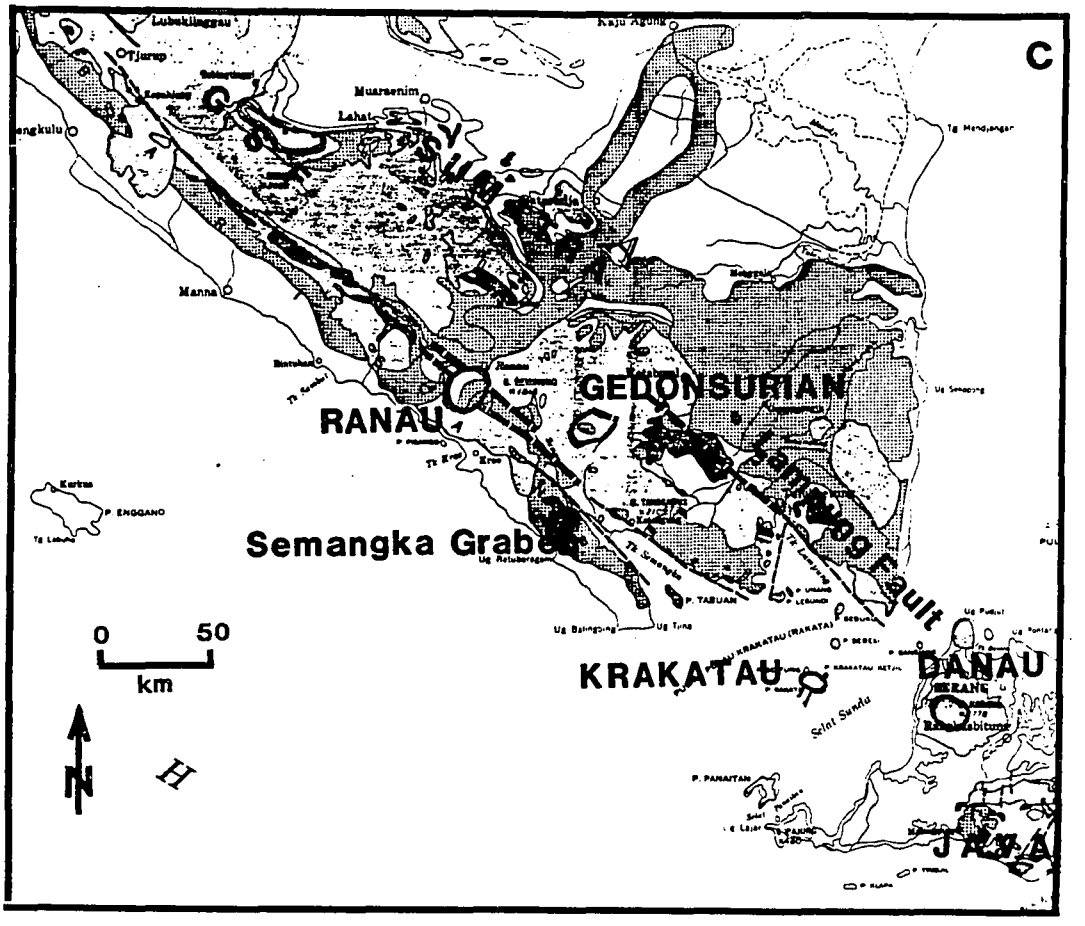

Figure 85. Caldera Map of southern Sumatra and western Java (basemap Geologic Map of Indonesia, 1965). The southeast end of Sumatra coincides with the SE termination of the GSF. Bold dashed lines indicate faults mapped from other sources (see text). At this point the GSF broadens and includes the Semangka Graben on the SW and the Lampung Fault on the NE. Ranau caldera, Gedonsurian and Danau appear to be associated with this broader distribution of the strain associated with the fault termination. Ranau is also associated with minor offset of the Semangka Graben.

Table 3BB

Caldera Name		Location		
Gedonsurlan		south central Sumatra, 160 km NNW of Krakatau, Indonesia		
Elongation	Volcanic Character	Local Structure	Regional Structure	Tectonic Elements
E-W 20 x 16.5 km	silicic ashflows accompany caldera collapse (A); mafic volcanism not noted	NW-striking fault scarps define linear caldera walls and a fault (the Rigis) within the caldera (A); the SE wall of the caldera is also linear	located between the Semangka Graben and the northern termination of the Lampong fault	Sunda Arc; Great Sumatra Fault -- Semangka/Lampong faults
Additional Information				
The tectonics of Sumatra is described on the Toba Sheet. Volcanism of Gedonsurlan caldera is not well characterized. Gedonsurlan is a broad parallelogram-shaped depression characterized by abundant silicic ashflows. At the south end of Sumatra, the GSFZ broadens and becomes a series of parallel faults. Major elements of this part of the zone are the Semangka Graben and the Lampung Fault (east of the Semangka). The Lampung extends NW from the south tip of Sumatra along the east side of Lampung Bay and inland as far as Gedonsurlan (B). Gedonsurlan is located between the northern termination of the Lampung Fault and the Semangka Graben and may reflect interactive strain fields of these faults within the overall fault zone.				
References				
(A) van Bemmelen, 1949; (B) Westerveld, 1954				
FIGURE 82, 85				
Category: ARC (Sunda) / ARC-PARALLEL RIFT (Semangka Graben) / TRANSFORM (GSF)				

Table 3CC

Caldera Name		Location		
Krakatau		Sunda Strait, Indonesia (between Sumatra and Java)		
Elongation	**Volcanic Character**	**Local Structure**	**Regional Structure**	**Tectonic Elements**
E-W 8 x 4 km	zoned intermediate ashflows accompany historic caldera collapse (D); bimodal basalt/rhyolite/andesite assemblage	NE and NW-trending faulting is indicated in linear structure of NE (submarine) and NW walls of the caldera (C)	lies on the strike of the Semangka Graben; on a NE fissure alignment of 3 volcanoes 15-20 km NE of Krakatau (A)	Sunda Arc; Great Sumatra Fault (south termination)
Additional Information				
	The tectonics of Sumatra is described on the Toba sheet. Krakatau occurs near the southern termination of the Great Sumatra transform. To the east, the Indo-Australian Plate subduction is more perpendicular to the trench. The termination of the transform is characterized by a broadening of the fault zone and accompanying subsidence on both NE and NW trending faults. The E-W elongation of the caldera appears to reflect the interacting of these structures rather than a direct control on the Semangka Graben faults.			
	Krakatau is the primary historic example of a large-cladera-forming event. It is characterized as the classic caldera collapse preceded by voluminous silicic eruptions. Local NE and NW-trending structure of the caldera walls parallels the major tectonic trends which intersect at the caldera: the Semangka Graben (manifestation of the strike-slip/extensional Great Sumatra Fault); and the NE-striking fissure along which volcanic vents in the Sunda Strait are aligned (A).			
References				
	(A) Simkin and Fiske, 1983; (B) van Bemmelen, 1949; (C) Williams, 1941; (D) Hildreth, 1981			
FIGURE 82, 85				
Category: ARC (Sunda) / ARC-PARALLEL RIFT (Semangka Graben) / TRANSFORM TERMINATION (GSF)				

Table 3DD

Caldera Name		Location		
Danau		west end, 60 km east of Krakatau, Java, Indonesia		
Elongation	**Volcanic Character**	**Local Structure**	**Regional Structure**	**Tectonic Elements**
E-W 15 x 13.5 km	large volume silicic "Bantam" tuffs accompanied caldera collapse (A); bimodal assemblage (A)	a NW-SE fault cuts the north flank of Danau (A)	located at the south end of the NW-trending Lampong Fault	Sunda Arc; Great Sumatra Fault (south termination)
Additional Information				
The tectonics of Sumatra and the termination of the GSF are described on the Toba and Krakatau sheets. A fault from the NW passes NE of the caldera (A) and appears to be an extension of the Lampung Fault (see also Gedonsurian) from SE Sumatra. The Great Sumatra Fault (GSF) Zone terminates here and further east convergence is more perpindicular to the arc. East of Danau localized arc-parallel left-lateral fault movements have been discussed (B,C). Volcanism and structure of Danau caldera is not well characterized. The E-W elongation of the caldera, similar to Krakatau, does not parallel the Lampung Fault and appears to be related to localized strain associated with termination of the GSF.				
References				
(A) van Bemmelen, 1949; (B) Katili, 1970; (C) Fitch, 1972				
FIGURE 82, 86				
Category: ARC (Sunda) / ARC-PARALLEL RIFT (Lampung Fault) / TRANSFORM TERMINATION (GSF)				

Table 3EE

Caldera Name		Location		
Tengger [Sandsea] Idjen		East Java, 320 km E of Idjen, Indonesia East end, Java, Indonesia		
Elongation	Volcanic Character	Local Structure	Regional Structure	Tectonic Elements
Tengger: NE 11 x 8 km	poorly defined, bimodal assemblage implied (C)	two fissure alignments E-W and NNE (A)	occurs at the west end of an E-W trending arc segment	Sunda Arc
Idjen: E-W 17 x 14 km	poorly defined, bimodal assemblage implied (C)	ENE-trending vent alignment tangent to the south side of the caldera (B)	at a 20° rotation in arc alignment trend and 10 km right step	Sunda Arc

Additional Information

Eastern Java is characterized by the perpendicular convergence of the Indo-Australian Plate with the Banda Trench. The details of contemporaneous tectonics are not well studied however. The crust of the overriding plate beneath Java is dominantly ensimatic versus Sumatra where the overriding crust is dominantly ensialic (F). It may also be noteworthy that on E. Java, large calderas only occur where the island is narrow -- opposite the Madura Straits which bound the north side of the island. By analogy with other caldera provinces, the implication is that the Madura Straits might be an arc-parallel extensional feature. However the Madura Straits are considered to be the result of Tertiary compression-induced folding (E). The volcano tectonics of this region cannot be considered to be well understood.

Tengger is located at the north end of a 20 km left step in the arc alignment. (The alignment of arc segments is defined by actual distribution of stratocones and other vents.) A local NNE fissure alignment parallels the alignment of the arc offset and there is a NNE trending vent alignment along this offset. Thus Tengger is located at the west end of an arc alignment which extends ESE to Idjen. The arc segment to the west of Tengger trends WNW for over 350 km and its SE end, opposite Tengger, is marked by the large stratocone, Mahameru. Two scarps and adjacent valleys cut the NE and NW flanks of Tengger. These have been ascribed to large scale slumping (toward the north) of the north flank of the volcano (G).

Idjen is located at a point where the nearly E-W arc segment from Tengger to Idjen rotates 20° to an ESE strike from Idjen to near Bratan on Bali. Unlike other locations on Java, there is no significant offset in the arc at Idjen, although volcanic volume at Idjen is large and volcanism appears to be more active along the ESE trend than the E-W trend.

References

(A) IAVCEI, 1951-1962; (B) van Bemmelen, 1949; (C) Pike and Clow, 1981; (D) ONC; (E) Hamilton, 1979; (F) Hutchison, 1982; (G) Williams, 1941

FIGURE 82, 85

Category: ARC (Sunda) / OFFSET AND INFLECTION IN ARC

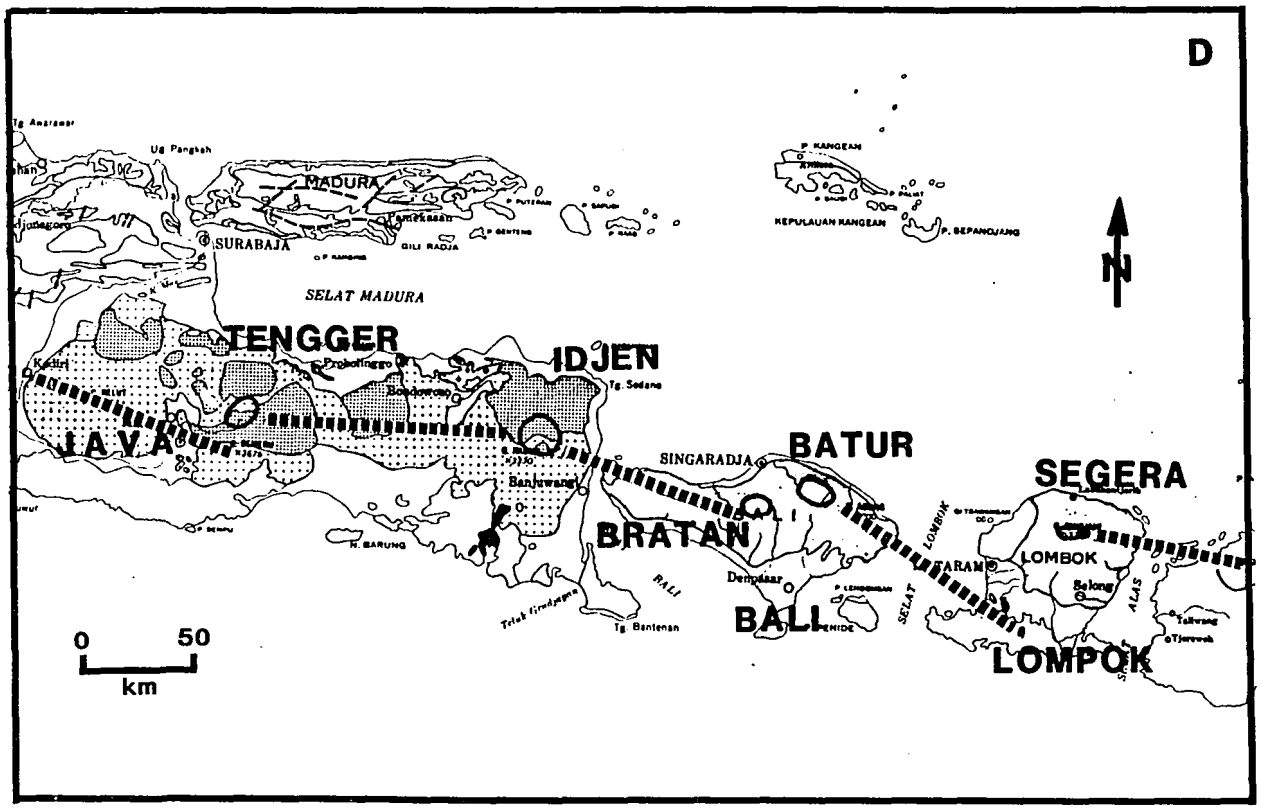

Figure 86. Caldera Map of eastern Java, Bali and Lompok (basemap Geologic Map of Indonesia, 1965). The calderas of Tengger, Idjen, Bratan, Batur and Segera occur at points of inflection and/or offset in the volcanic axis which is otherwise characterized by stratocones. Arc segments determined by alignment of vents are indicated by broad dashed lines. Plate convergence here is essentially perpendicular to the trench. Considerable mapping remains before this area can be well characterized.

Table 3FF

Caldera Name		Location		
Bratan Batur		central Bali, 94 km ESE of Idjen, Indonesia eastern Bali, 18 km ENE of Bratan, Indonesia		
Elongation	Volcanic Character	Local Structure	Regional Structure	Tectonic Elements
Bratan: E-W 10.5 x 6.3 km	poorly defined, bimodal assemblage indicated (F)	elongation parallels WNW arc segment west of the caldera	located at a 25 km left offset of the WNW-trending arc segment	Sunda Arc
Batur: NW-SE 12.5 x 9.3 km	poorly defined, silicic ashflows are present, bimodal acid/basalt (A); nested double caldera	at the NW end of SE-trending alignment of vents (A) (parallel to elongation of caldera); a NE-trending line of fissures also crosses the caldera (A)	located the same arc offset (left step) as Bratan at the NW end of a SE trending arc segment; the arc trend also changes strike	Sunda Arc
Additional Information				
	Bratan is poorly documented. It is located at a 25 km left step in the WNW-trending arc. East of Bratan, the arc steps north to Batur and rotates to a NW-SE trend. West of Bratan the arc segment strikes WNW toward Idjen. Bratan actually occurs within the zone of offset at an intermediate point between the ends of the two arc segments.			
	Batur is composed of two nested calderas (A,D). Although acid ashflows are noted (A), their relatively low volumes are problemmatical (B) with respect to caldera collapse mechanisms. This caldera is a high-gravity anomaly type (E).			
References				
	(A) van Bemmelen, 1949; (B) Williams, 1941; (C) Purbo-Hadiwidjojo, 1971; (D IAVCEI, 1951-62; (E) Yokoyama and Suparto, 1970; (F) Pike and Clow, 1981			
FIGURE 82, 85				
Category: ARC (Sunda) / ARC OFFSET AND INFLECTION				

Table 3GG

Caldera Name		Location		
Segera [Rindjani]		Lompok, 105 km ESE of Batur, Indonesia		
Elongation	Volcanic Character	Local Structure	Regional Structure	Tectonic Elements
E-W 8.1 x 3.6 km	poorly defined, bimodal assemblage implied (D)	the north wall of the caldera is aligned WNW-ESE -- parallel to the arc segment trend	located at the west end of a WNW-trending arc segment at a 63 km left step in the arc	Sunda Arc
Additional Information				
Segera Caldera has an irregular, angular shape indicating E-W structural control. The morphology of the caldera suggests that it is the result of superposition of two smaller calderas along a WNW line (A,C). Segera occurs on the west end of an arc segment which is offset from the "Batur" segment and is parallel to the "Idjen-Bratan" segment.				
References				
(A) Landsat Image, Sheffield, p 92, 1981; (B) IAVCEI, 1951-62; (C) van Bemmelen, 1949; (D) Pike and Clow, 1981				
FIGURE 82, 85				
Category: ARC (Sunda) / ARC OFFSET				

Table 3HH

Caldera Name		Location		
Long Island caldera		east of New Britain, 315 km E of Dakataua, Papua New Guinea		
Elongation	Volcanic Character	Local Structure	Regional Structure	Tectonic Elements
NW 14.9 x 10.9 km (A)	abundant ashflows of intermediate composition and basalt lavas (A,C)	elongation parallels direction of en echelon orientation of adjacent volcanoes (B)	The NW-SE series of island volcanoes between New Guinea and New Britain form a left-stepping en echelon arrangement; tectonically these volcanoes are located over the double-dipping Solomon Sea Plate which is now completely subducted in this area	Double subduction zone: Solomon Sea Plate (SSP) subducting to the northeast beneath the South Bismarch Plate; and the SSP subducting to the SW beneath the Indo-Australian Plate (New Guinea) (D)
Additional Information				
The western arc of the New Britain (NB) subduction zone bordering the south side of the Bismarck Sea extends NW from the west end of NB. Long Island caldera (LIC) is located near the southern end of this volcanic line where the island volcanoes occur in a left-stepping pattern as exemplified by NNW elongation of the islands, bathymmetric trend between the islands, and elongation of the LIC. NNW en echelon segments include Karkar-Bagabag, Hankow Reef-Crown I.-Long I., Tolokiwa-Umboi. There is an essentially vertical seismic zone beneath this area which apparently results from the final stages of the subduction of the SSP in the Vitiaz Strait. The SSP is subducting both NE beneath the Bismarck Plate and SW beneath the Indo-Australian Plate. The volcanoes therefore mark the locus of incipient collision of two parallel arcs. The en echelon character of the volcanics suggests that a component of left lateral strike-slip may occur along the volcanic axis; and such deformation is supported by shallow seismic focal plane solutions (E).				
References				
(A) Ball and Johnson, 1976; (B) Johnson, 1976; (C) Pain et al, 1981; (D) B. Taylor, personal communication, 1986; (E) Hamilton, 1979				
FIGURE 87				
Category: ARC / ARC (collision of parallel subduction zones) / OFFSET IN VOLCANIC ARC (en echelon volcanic alignment)				

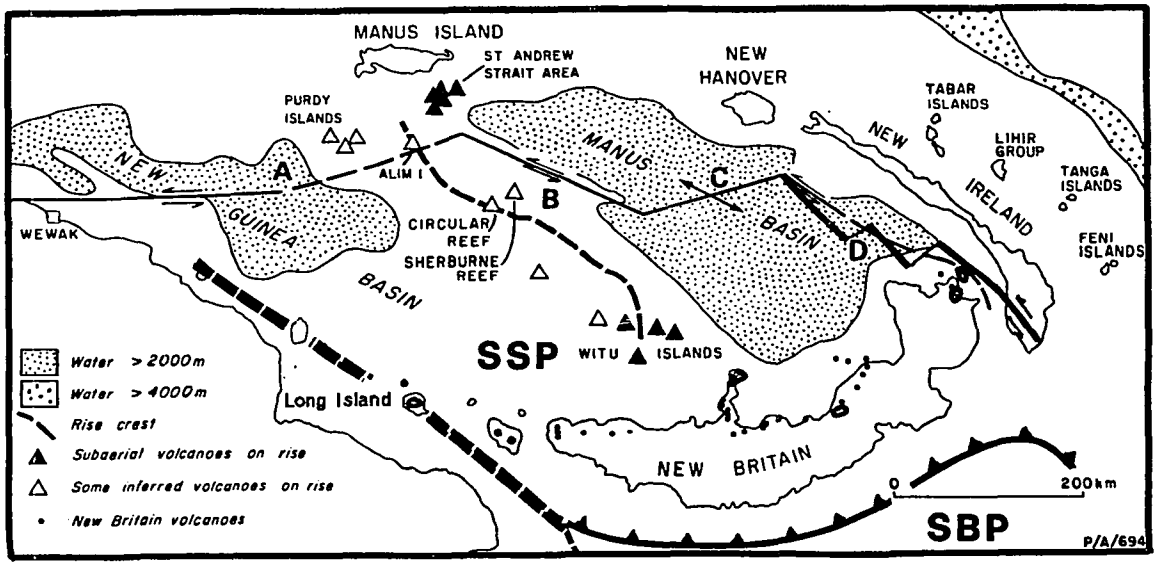

Figure 87. Tectonic Map of New Britain Arc (modified after Johnson et al, 1979) showing caldera locations relative to the principle tectonic elements. A subduction zone is located south of New Britain (NB) (Solomon Sea Plate subducting beneath NB) which curves to the south at its east end. The broad dashed line at the west end of the trench denotes the alignment of the zone where the Solomon Sea Plate (SSP) is subducting both NE beneath the South Bismarck Plate (SBP) (on which New Britain is located) and SW beneath New Guinea. A left lateral transform bounds the arc on its east end. Note the angular relationship which the alignment of Rabaul and the proposed submarine caldera to the north forms with respect to the transform. This situation is analagous to that found at Kutcharo and Akan calderas on Hokkaido.

Table 311

Caldera Name		Location		
Dakataua [Benda] [Sandsea]		Willaumez Peninsula, central New Britain		
Elongation	Volcanic Character	Local Structure	Regional Structure	Tectonic Elements
E-W 13 x 10 km (A)	basalt/dacite/andesite calc-alkalic assemblage; rhyolite found adjacent to but not within the caldera; possibly a nested double caldera (A); the association of silicic ashflows with caldera collapse is not clearly established (A)	Dakataua is located on the seaward (N) end of the Willaumez Peninsula (WP) -- a N-trending peninsula characterized by NE-SW en echelon alignments of vents -- many of which have erupted rhyolitic lavas	Dakataua occurs 50 km behind the main volcanic arc and on the west end of active arc volcanism; east of Dakataua, there is a gap in recent arc volcanism of over 150 km extending to Langila on the east end of New Britain (NB); the volcanoes of the Witu Islands (in the Bismark Sea 70 km WNW of Dakataua) may be related to the caldera-tectonic setting (C)	New Britain Arc; Willaumez-Manus Rise

Additional Information

The NB arc of the east half of the island of NB is a relatively normal island arc resulting from northward subduction of the Solomon Plate beneath NB. However, the large gap in arc volcanism between Dakataua and Langila is difficult to explain in light of the fact that ongoing subduction (evidenced by seismicity (E)) is also taking place in this gap (the volcanoes Schrader and Andewa, in western NB are heavily dissected and considered older than the active arc (D)). Dakataua is located on the east side of this gap well behind the arc and its composition is more alkalic than the volcanoes on the arc front (D). Examination of the tectonic setting behind the arc indicates that tectonic elements possibly related to the arc are present -- although not well understood. One hundred km behind the volcanic gap of western NB (70 km WNW of Dakataua) is an arc-parallel line of recent volcanics -- the Witu Islands -- which include basaltic through rhyolitic compositions. Johnson (C) finds these rocks to be most similar to backarc basin lavas (however, no backarc trough is associated with them). The alignment of these islands projects toward the north end of the Willaumez Peninsula at right angles to the peninsula. Northwest of the Witu Islands is a NW-striking bathymetric high called the Willaumez-Manus Rise. This feature has been proposed as an extinct spreading axis, a remnant arc or a hot spot trace, although Johnson (D) supports a 'tectonic' origin related to uplift at the edge of the active backarc spreading in the Manus Basin which is located behind the active volcanic arc of eastern NB. Available data does not permit clarification of the tectonic setting of Dakataua although work currently underway in this area may provide some clarification. The location of a large caldera at Dakataua indicates probable localization of tectonism and represents a case where the existence of a large caldera may be used as a significant indicator for tectonic interpretation of a complex tectonic setting. If the Wittu Islands do represent manfestation of backarc spreading, the setting of Dakataua may be dictated by the propagation of the backarc toward the arc -- analogous to Deception Island.

References

(A) Lowder and Carmichael, 1970; (B) IAVCEI, 1957; (C) Johnson et al, 1979; (D) Johnson, 1976; (E) Johnson, 1982

FIGURE 87, 88

Category: ARC (New Britain) / OFFSET AND TERMINATION OF VOLCANIC ARC (unclear tectonic association)

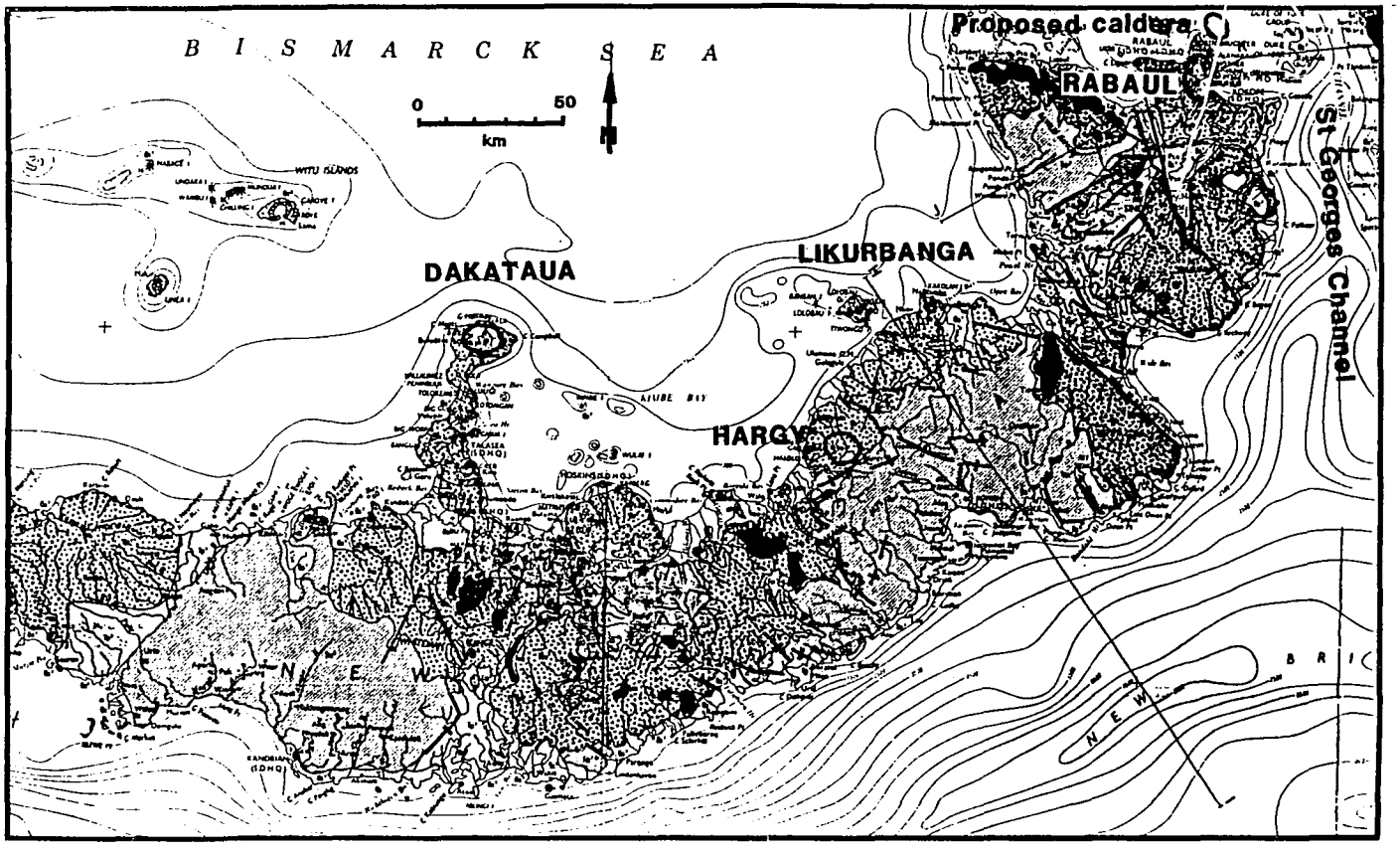

Figure 88. Calderas of Eastern New Britain (basemap Bureau of Mineral Resources, Geologic Map of New Guinea, 1972) showing calderas in relation to mapped faulting. Likurbanga (a 7 km caldera) is located on the west edge of the graben which cuts the island at its narrowest point (E of Likurbanga). There are no large calderas located within the graben. Quaternary volcanism covers the Willaumez Peninsula (Dakataua); is less voluminous between the Willaumez Pen. and Hargy; and is continuous from Hargy to Likurbanga. Rabaul (and a recently proposed caldera to the north) occur on the east end of the island.

Table 3JJ

Caldera Name		Location		
Hargy [Galloseulo]		central New Britain, 130 km SW of Rabaul		
Elongation	Volcanic Character	Local Structure	Regional Structure	Tectonic Elements
WNW 13 x 10.8 km (B)	an inner caldera rim suggests nested calderas; volcanic character not determined; bimodal assemblage implied (C)	little is known about caldera structure; caldera elongation parallels mapped normal faults east of the caldera (B)	Hargy is located at a 50° inflection point in the volcanic arc alignment; to the NE voluminous recent volcanism is found on a continous NE-trending line of volcanoes including: Bamus, Uluwan and further north, Lolobau ; to the west, volcanism is aligned E-W and is less voluminous and discontinous	New Britain Arc
Additional Information				
A number of E-trending normal faults intersect the arc at Hargy. In addition, parallel drainage across the island follows the trend of these faults. The tectonic significance of the major inflection in the axis here is not known.				
References				
(A) IAVCEI, 1957; (B) Geologic Map of Papua New Guinea, 1972; (C) Pike and Clow, 1981				
FIGURE 87, 88				
Category: ARC (New Britain) / INFLECTION IN VOLCANIC AXIS				

Table 3KK

Caldera Name		Location		
Rabaul		east end of New Britain		
Elongation	**Volcanic Character**	**Local Structure**	**Regional Structure**	**Tectonic Elements**
N-S 14.7 x 9 km (A)	basalt/andesite/dacite assemblage; abundant silicic ash-flows accompany caldera collapse 3500 ybp; multiple nested calderas are indicated (A); latest large ash-flow 1400 ybp (C)	elongation is parallel to mapped normal faulting 30 km S and SW of the caldera	located adjacent to NW faulting related to left lateral transform motion (D); the strike of the main transform is proposed to pass down St. Georges Channel, east of Rabaul; Rabaul is at the east end of a 100 km gap in arc volcanism	New Britain Arc; transform fault
Additional Information				
	Rabaul is among the most active large calderas in the world with seismic activity defining caldera ring faulting beneath the caldera (H). A proposed NW-striking transform fault between the Manus Basin spreading and New Ireland passes east of Rabaul in St. Georges Channel and is exposed on the south end of New Ireland as the Weitin fault. This transform is a left-lateral fault which steps left from NW of the Gazelle Peninsula (where Rabaul is located) to the St. Georges channel -- indicating a distensional aspect to the transform motion. Extensional deformation (normal faulting) on NNW-striking faults is indicated, west and south of the caldera, extending across the eastern end of New Britain. This includes the Baining Fault (E) which bounds the west side of the graben of Kavavas River Valley, south of Rabaul. A N-S trending, down to the west, normal fault bounds the east side of this graben and strikes toward Rabaul, dissappearing beneath alluvium 20 km south of the caldera.			
	Rabaul occurs at the west end of a 100 km gap in Quaternary arc volcanism which extends from Likurbanga caldera (NE of Uluwan) to Rabaul. This gap is bounded on the west by the Wide Bay fault and on the east by the Baining fault; and it includes a 25 km-wide graben (striking NW) immediately northeast of the Wide Bay Fault. The 7 km-long (NW) Likurbanga caldera occurs on the Wide Bay Fault at the west edge of this graben. However, the graben itself is devoid of Quaternary arc volcanics. The absence of arc volcanics at a point on the arc where such transverse extensional structure occurs is difficult to explain. Open Bay at the NW end of this structure may be a good place to look for submarine caldera activity.			
	Rabaul marks the east edge of the subaerial New Britain volcanic arc. Recent marine surveys (F) have disclosed the existence of a probable large submarine caldera less than 10 km NNE of Rabaul. The elongation of this caldera is NW to NNW. The close proximity of these calderas and the orientation of their overall trend to the adjacent transform is similar to that of Kuctharo and Akan calderas on Hokkaido. The New Britain trench bends nearly 90° to the south of Rabaul -- accounting for the termination of the New Britain Arc. By their orientation relative to the overall left-lateral transform stress field, these calderas align along the buckle fold trend predicted by strike-slip fault geometry (G). Rabaul caldera appears to be localized by the arc-intersecting normal faulting vergent from the south.			
References				
	(A) Heming, 1974; (B) IAVCEI, 1957; (C) Walker et al, 1981; (D) Johnson, 1979; (E) Davies, 1973; (F) B. Taylor and J. Sinton, pers. comm. 1986; (G) Wilcox et al, 1973; (H) McKee et al, 1984			
FIGURE 87, 88				
Category: ARC (New Britain) / TRANSFORM / SECONDARY EXTENSION (Baining Fault)				

Table 3LL

Caldera Name		Location		
Ambrym		Ambrym I., central Vanuatu (New Hebrides)		
Elongation	**Volcanic Character**	**Local Structure**	**Regional Structure**	**Tectonic Elements**
N-S 13 x 12 km (A)	Dominantly basaltic lavas and ash of alkaline affinity (no silicic pyroclastics found to date) (A)	WNW-trending fissure zone dominates both flanks of the volcano indicating WNW-ESE compression; linear segments of north and south walls of the caldera parallel the fissure zones; elongation of the caldera broadly reflects the direction of extension indicated by fissure orientations	D'Entrecasteaux Zone subducts beneath the arc North of Ambrym	New Hebrides Arc; D'Entrecasteaux Zone

Additional Information

The N-S striking central New Hebrides Arc presents a relatively unique arc environment. Here, the Indo-Australian Plate is subducting eastward beneath the Pacific Plate. The uniqueness of the configuration lies in the fact that the E-W trending D'Entrecasteaux Zone -- an aseismic ridge -- is riding on the subducting plate and colliding with the overriding plate as it enters the trench. This D'Entrecasteaux Zone (D'EZ) -- either an old (Miocene) arc or a Fracture zone -- is a bathymetric ridge up to 100 km wide and standing over one km above the surrounding sea floor. In addition, it is subducting at a point on the arc where the older, rigid Santos-Malekula block (SMB) sits on the edge of the overriding plate. The D'EZ is apparently colliding with the SMB. This is reflected in the absence of both the trench and the backarc trough (which persist to the north and south) and geologic evidence (dike orientations, etc.) and shallow seismicity suggesting horizontal stress trajectories and slip lines radiating away from the collision zone similar to that produced by a die indenting a semi-infinite rigid-plastic medium (C). In this setting, Ambrym occurs south of the south edge of the D'EZ (the indenter) in a zone which (by the indenting model) would be dominated by either strike-slip or secondary tension resulting from the indenting process (C). This interpretation is supported by the fact that Ambrym occurs at the north end of a continous N-S zone of Pleistocene-Recent volcanics which become discontinous north of Ambrym (opposite the collision zone where enhanced compression prevails). The arc volcanics adjacent to the collision zone (Ambrym, Aoba and Gaua) are of alkaline afinity while those of the rest of the arc are calcalkalic.

References

(A) McCall et al, 1970; (B) IAVCEI, 1957; (C) Collot et al, 1985

FIGURE 89, 90

Category: ARC (Hebrides) / COLLISION (with D'EZ yielding secondary tension)

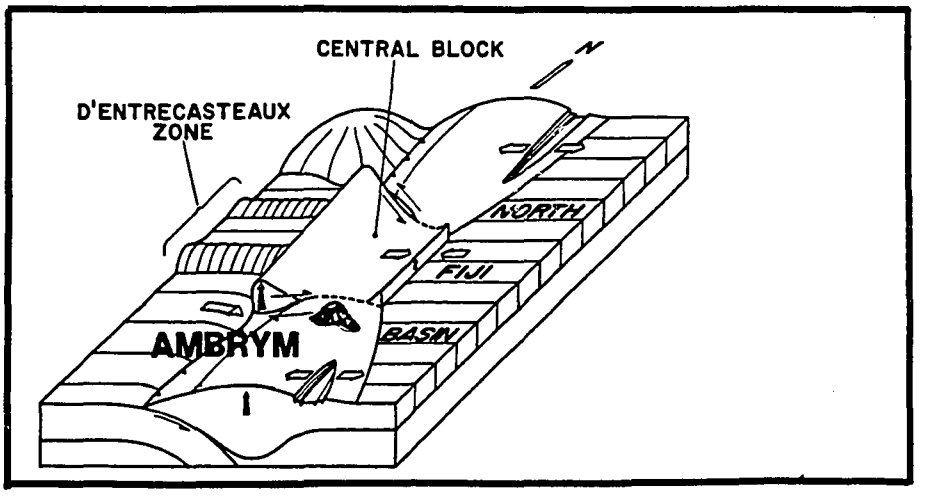

Figure 89. Block diagram of the subduction of the D'Entrecasteaux Zone into the New Hebrides Trench (modified after Collot et al, 1985). Ambrym caldera is shown in relation to adjacent structural elements. The subduction of the D'Entrecasteaux Zone is proposed to generate indention stresses in the overriding plate. Ambrym is located outside of the compressional zone, on strike of backarc spreading rifts in a region of possible secondary extension related to the indention.

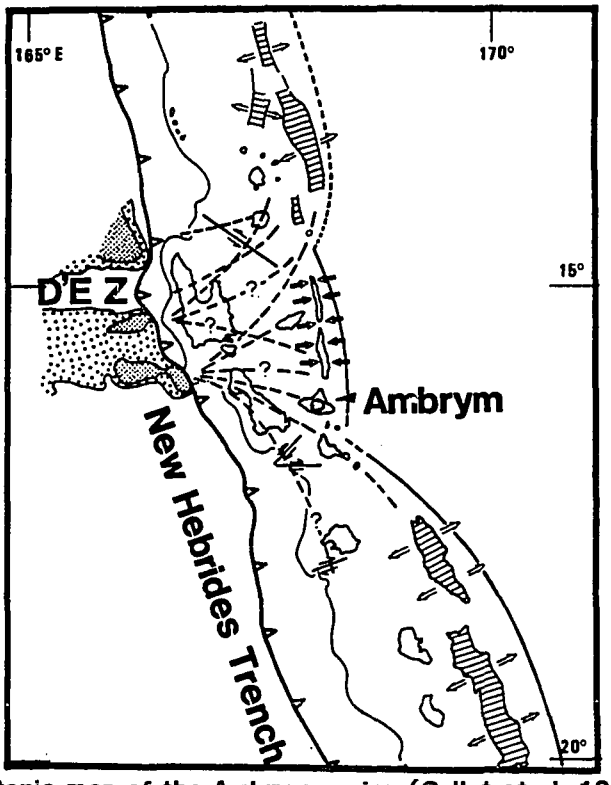

Figure 90. Tectonic map of the Ambrym region (Collot et al, 1985) showing tectonic elements including the location of Ambrym on the edge of the proposed indention zone caused by the subduction/collision of the overriding Pacific Plate with the D'Entrecasteaux Zone (D'E Z) -- which has 1-2 km relief relative to surrounding ocean floor.

Table 3MM

Caldera Name	Location
Taupo	south Taupo Volcanic Zone, North Island, New Zealand
Rotorua	north Taupo Volcanic Zone, 65 km N of Taupo
Haroharo	north Taupo Volcanic Zone, 6 km E of Rotorua

Elongation	Volcanic Character	Local Structure	Regional Structure	Tectonic Elements
Taupo: NW 30 x 26 km Rotorua: circular 17 km Haroharo: N-S 28 x 16 (A)	bimodal calcalkalic basalt/rhyolite assemblage; multiple collapse (except Rotorua) (A); abundant rhyolitic ashflows accompany caldera collapse (A)	NNW-trending normal faults (fissure swarms) dominate the Taupo Volcanic Zone (TVZ) N of Taupo and turn to a NE-trend near Haroharo (B,D)	located on the volcanic front on strike with andesitic stratocones to the SW; aligned with the backarc spreading rift of the Havre Trough; and located at the intersection of the SE-trending Hauraki Graben (D) with the arc	Hikurangi Trough (Arc); Havre Trough; Hauraki Graben

Additional Information

The TVZ is a zone of rhyolitic (and minor basaltic) volcanism. The arc, a result of oblique subduction of the Pacific plate into the Hikurangi Trough, is colinear with the Kermadec Trench to the north. It became active within the last 6 my (C) prior to which subduction took place along the NW-striking NE coast of the North Island (C). The change from SW convergence to E-W convergence has imposed a tensional regime with extension perpendicular to the TVZ which may be a southern extension of the backarc spreading in the Havre Trough. South of the TVZ is the Tongariro Volcanic Center -- a line of andesitic stratocones colinear with the TVZ. (Most of these stratocones have erupted from NW-trending vent alignments (C).) The arc undergoes this abrupt change from the tension-dominated TVZ to the andesitic stratocones over a distance of 20 km. Further SW the plate boundary becomes a dextral transform -- the Hope-Alpine Fault (C). The Hauraki Graben is an active extensional feature, located NNW of the TVZ, which strikes toward Taupo (C). It is the site of young volcanism which decreases in age toward Taupo. Pre-Quaternary "basement faults" trending NW (D) are also present across the TVZ (D). A component of dextral strike-slip on the TVZ has been proposed based on remote sensing data (D).

The TVZ is the site of intense caldera development -- perhaps six calderas -- of which Taupo, Haraharo and Rotorua are the largest. The aggregate NNE width of these calderas is 73 km over 125 km of arc. The fissure swarms which extend between these calderas are similar to those in the East Africa Rift or in Iceland's Eastern Volcanic Zone. At the south end of the TVZ, one NE-SW normal fault (the Waihi Fault) continues to the southwest into the Tongariro Volcanics, whereas to the northeast of Taupo numerous fissures occur. Also earliest volcanism in the TVZ was andesitic (A). These facts suggest that the tensional regime is propagating to the southwest along the TVZ. The fissures NE of Taupo trend NNE to the vicinity of Maroa caldera where they rotate to a NE strike. The mapped normal faults along the TVZ step left (to the NW) about 5 km at Taupo caldera, 5 km at Maroa caldera, and 15 km at Rotorua/Haraharo caldera. NE of Rotorua/Haraharo, the fissure zone becomes less well developed and appears to step back to the right (SE) 30 km.

TVZ caldera-forming events have erupted in an extremely explosive manner producing exceptionally wide dispersal of volcanic products. The pronounced rift aspect of TVZ structure is unusual for an arc environment and the influence of extensional tectonism on the arc is indicated.

References

(A) Wilson et al, 1984; (B) Rogan, 1982; (C) Cole and Lewis, 1981; (D) Cochrane and Tianfeng, 1983; (E) Walker, 1981

FIGURE 91, 92

Category: ARC (Hikurangi Trough) / ARC-PARALLEL RIFT (TVZ-Havre Trough) / INTERSECTING RIFT (Hauraki Graben)

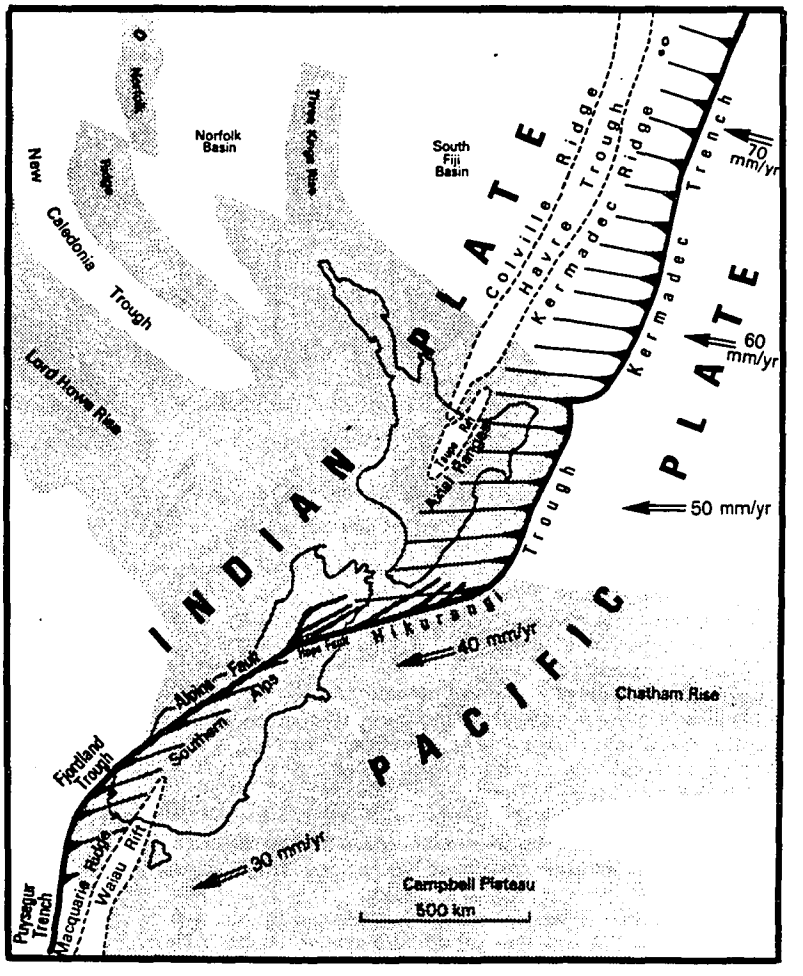

Figure 91. Tectonic Map of New Zealand (Cole and Lewis, 1981). The Taupo Volcanic Zone is located on the volcanic arc associated with oblique subduction at the Hikurangi Trough. The extensional character of the Taupo Zone appears to be related to the backarc spreading basin of the Havre Trough which intersects and becomes colinear with the arc at Taupo.

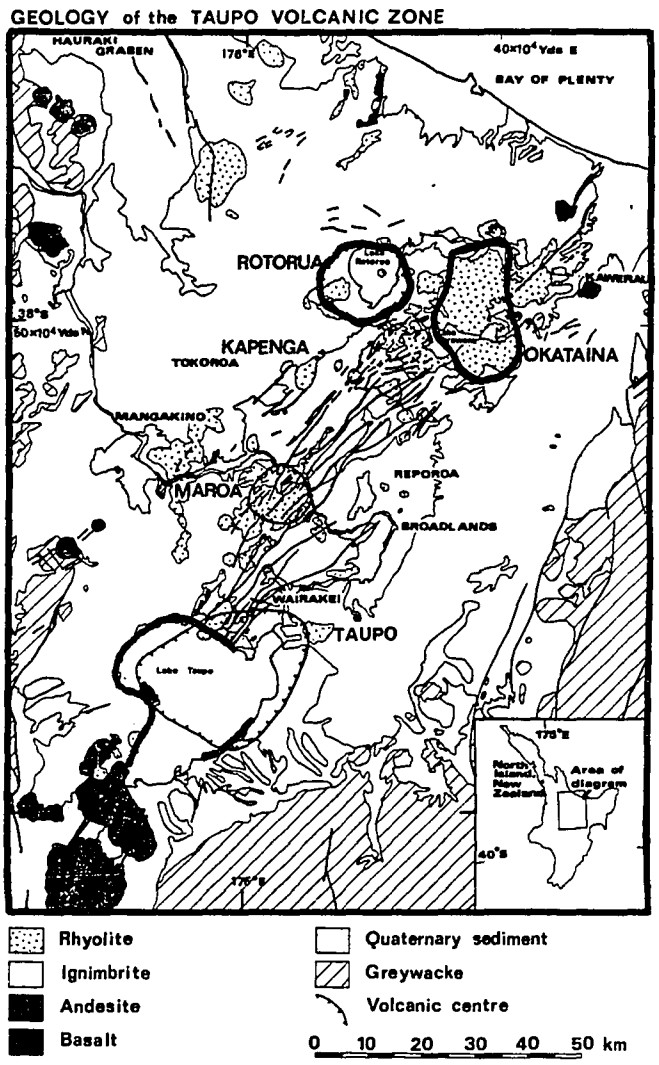

Figure 92. Structure of the Taupo Volcanic Zone (modified after Rogan, 1982). This figure is modified to reflect the caldera boundaries indicated by Wilson et al (1984). Andesitic (Tongarirro) stratocones are located 20 km SW of Taupo. Fissure swarms trend NNW to NW northeast of Taupo. The Hauraki Graben strikes from the NNW toward Taupo.

Table 3NN

Caldera Name		Location		
Latera Bolsena L.		Vulsini Volcanic Complex, Roman (Latian) Volcanic Province, Italy Vulsini Volcanic Complex, 2 km east of Latera		
Elongation	Volcanic Character	Local Structure	Regional Structure	Tectonic Elements
Latera: circular 11 km Bolsena: N-S 13 x 11 km (I)	abundant ashflows associated with caldera collapse (I,G); alkaline bimodal leucitite trachybasalt phonolite assemblage (G)	these calderas are located within the S to SSE trending Radicofani-Tiber Graben (G) which verge from the north; the east caldera wall of Bolsena strikes N-S, parallel to the intersecting graben	within block faulted terrane of NNW, N-S and NE striking extensional tectonism	Arc (preexisting Appennine Arc); Rifting of Tyrrhennian Sea Margin

Additional Information

The tectonic environment of Italy is complex and considerable rotation of tectonic elements is indicated. The Apennine Mtns. are presently oriented NW-SE and run the length of the Italy. The Appennines were formed, when they were oriented E-W along the southern coast of France (A), by microplate collision as the Adriatic (Apulian) Plate (now east of the Italian Peninsula) was moving northward and underthrusting the European continent (A). Subsequent to collision, spreading in the Ligurean and Tyrrhennian Seas (to the west of Italy) has rotated the Apennines to their present NW-SE orientation. Lack of Benioff zone seismicity indicates that subduction has ceased beneath the Roman Volcanic Province although subduction does continue along this arc farther south. West-dipping subduction may have been active opposite the Roman Province as late as Mid-Pliocene (C). Roman Province magmatism has therefore been described as remnant from the subduction driven system (D). In this context it can be noted that a subduction system dipping 45° and consuming 3 cm of plate per year would continue to supply subducted plate to the zone of magma generation (say 125 km depth) for almost 6 my after the trailing edge of the plate entered the trench. Late in the evolution of this system (Late Miocene (E)) E-W back-arc spreading in the Tyrrhenian Sea became dominant. With time, general sinking of the Tyrrhenian sea has spread outward and widespread normal faulting has come to characterize the magmatic axis. This has been accompanied by eastward migration of the volcanic belt (F). These facts and the alkaline character of some of the volcanics has been interpreted by some workers (C) to imply that the Roman volcanism is the result of backarc spreading and Tyrrhennian Sea opening. The extensional character of the province tends to support the latter view although the superposition of extensional tectonism on a former arc environment is an equally plausible mechanism. The distribution of extensional faulting in the vicinity of the four large caldera complexes: Vulsini, Vico, Sabatini and Albani may be generally characterized as an arc-parallel NW trend and a NE trend. The NE trend is paralleled by and in some cases appears to be a landward continuation of similar trending faults in the Tyrrhenian Sea floor to the west (E). Much of the extensional structure is manifest along the volcanic front as single-sided grabens similar to the setting of the Karymsky-Krasheninnikov calderas of Kamchatka.

Latera and Bolsena calderas occur in close proximity to one another (2 km apart). Their petrologic assemblage is an undersaturated equivalent of the basalt/rhyolite association. To date the ashflows associated with Bolsena collapse do not account for the caldera volume (G). Post-

moving northward and underthrusting the European continent (A). Subsequent to collision, spreading in the Ligurean and Tyrrhennian Seas (to the west of Italy) has rotated the Apennines to their present NW-SE orientation. Lack of Benioff zone seismicity indicates that subduction has ceased beneath the Roman Volcanic Province although subduction does continue along this arc farther south. West-dipping subduction may have been active opposite the Roman Province as late as Mid-Pliocene (C). Roman Province magmatism has therefore been described as remnant from the subduction driven system (D). In this context it can be noted that a subduction system dipping 45° and consuming 3 cm of plate per year would continue to supply subducted plate to the zone of magma generation (say 125 km depth) for almost 6 my after the trailing edge of the plate entered the trench. Late in the evolution of this system (Late Miocene (E)) E-W back-arc spreading in the Tyrrhennian Sea became dominant. With time, general sinking of the Tyrrhenian sea has spread outward and widespread normal faulting has come to characterize the magmatic axis. This has been accompanied by eastward migration of the volcanic belt (F). These facts and the alkaline character of some of the volcanics has been interpreted by some workers (C) to imply that the Roman volcanism is the result of backarc spreading and Tyrrhennian Sea opening. The extensional character of the province tends to support the latter view although the superposition of extensional tectonism on a former arc environment is an equally plausible mechanism. The distribution of extensional faulting in the vicinity of the four large caldera complexes: Vulsini, Vico, Sabatini and Albani may be generally characterized as an arc-parallel NW trend and a NE trend. The NE trend is paralleled by and in some cases appears to be a landward continuation of similar trending faults in the Tyrrhenian Sea floor to the west (E). Much of the extensional structure is manifest along the volcanic front as single-sided grabens similar to the setting of the Karymsky-Krasheninnikov calderas of Kamchatka.

Latera and Bolsena calderas occur in close proximity to one another (2 km apart). Their petrologic assemblage is an undersaturated equivalent of the basalt/rhyolite association. To date the ashflows associated with Bolsena collapse do not account for the caldera volume (G). Post-Bolsena ercsion may account for this discrepancy (I). This complex has developed within the Radicofani-Tiber graben which formed about 1 mybp (G). Bolsena caldera formed 0.4 mybp and Latera developed about 0.1 mybp (G). These calderas have evolved in an extensional terrain with NNW to NE normal faulting -- generally related to Tyrrhenninan Sea opening.

References

(A) Rehault et al, 1984; (B) Boccaletti et al, 1984; (C) Reutter et al, 1978; (D) Peccerillo, 1985; (E) Wise et al, 1985; (F) Puxeddu, 1984; (G) Varecamp, 1980; (H) Landsat Image, Short et al, 1976, Pl 244; (I) Sparks, 1975; (J) Barberi et al, 1984

FIGURE 93, 94

Category: ARC (preexisting Appennine Arc) / ARC-PARALLEL RIFT (Tyrrhennian Sea Margin extensional deformation)

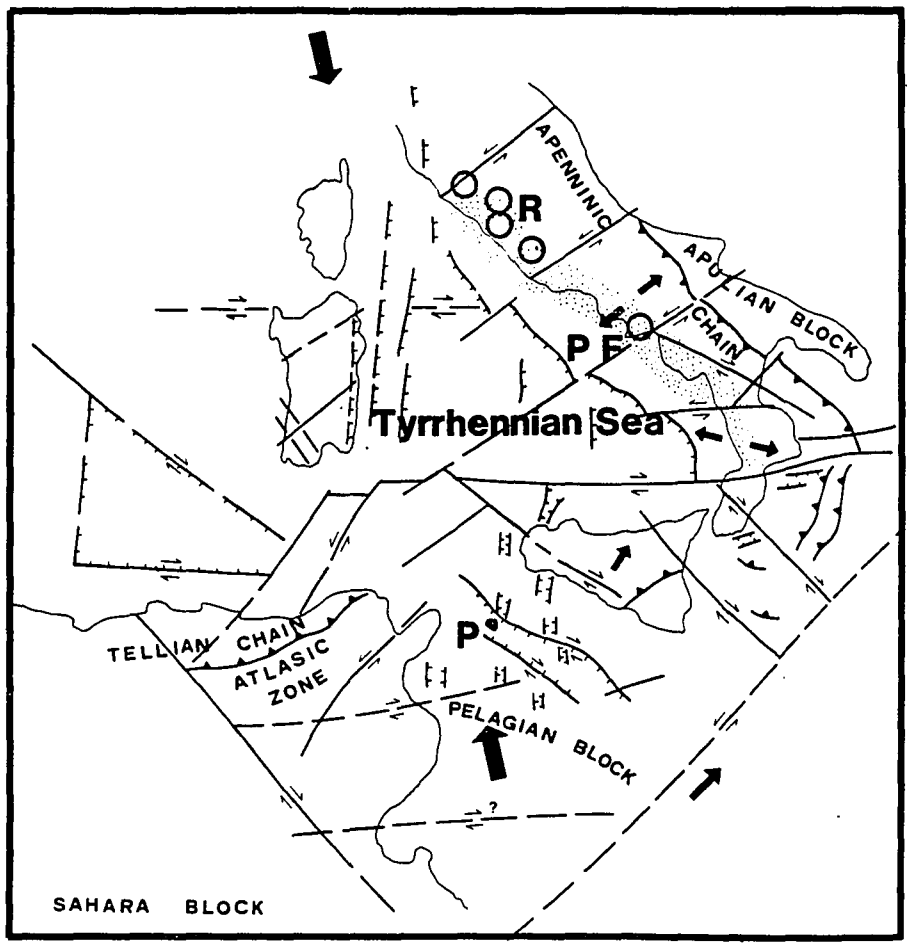

Figure 93. Tectonic Map of southern Italy and the Tyrrhennian Sea (modified after Boccaletti et al, 1984). The tectonic elements related to the Roman Volcanic Province (R) include the spreading in the Tyrrhennian Sea and the preexisting subduction of the Adriatic Plate (Apulian Block) beneath the Italian Peninsula. Along the east coast of the southern part of Italy, opposite the Phlegrean Fields (PF), the Apulian Block is still actively subducting. The location of Pantellaria caldera (P) -- somewhat less than 8 km in diameter -- is also shown.

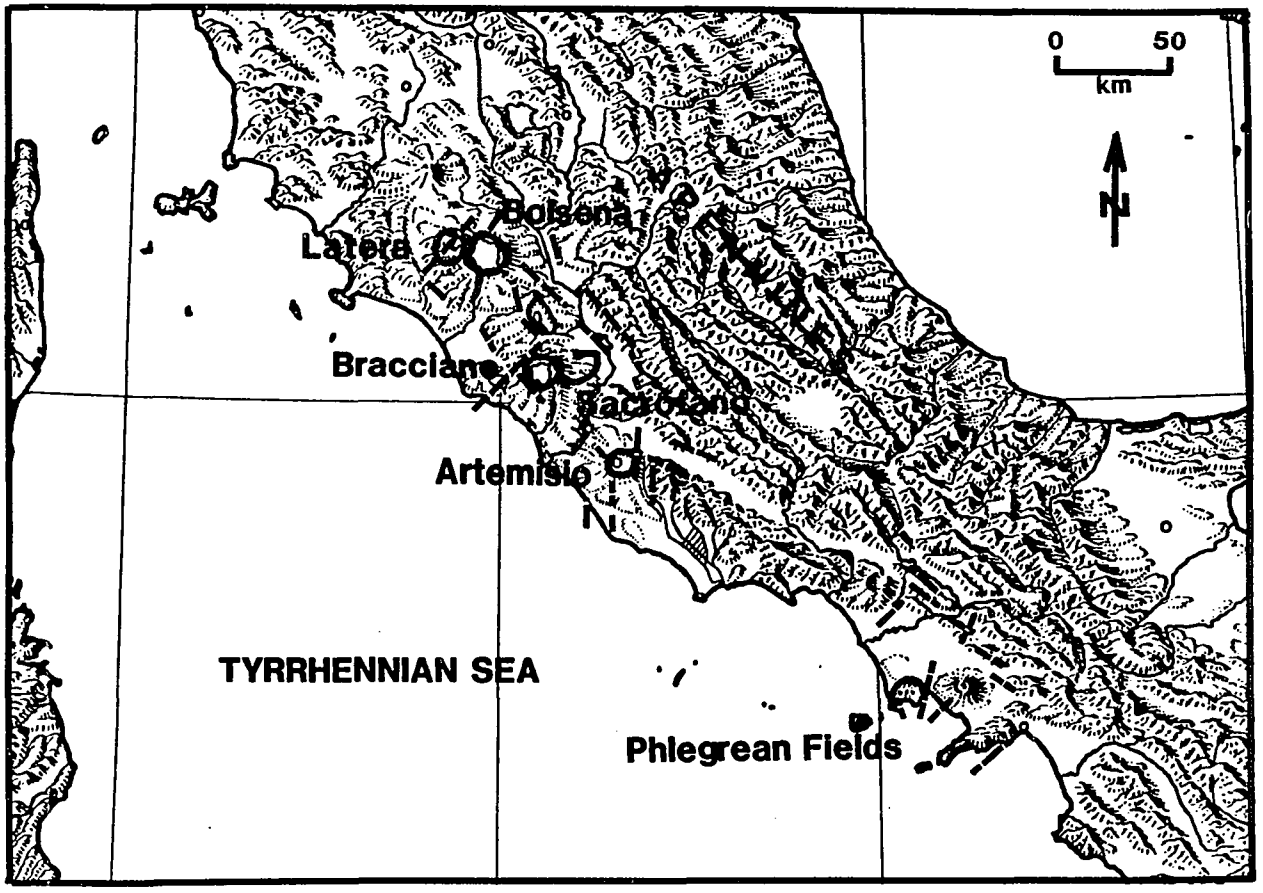

Figure 94. Structure and Caldera Map of western Italy (basemap Raisz, 1944). The large calderas of the Roman Volcanic Province and the Campanian Volcanics (Phlegrean Fields) are shown with adjacent landforms and faulting (bold dashed lines). (Faults are shown only for the areas adjacent to the calderas; generalized after De Rita and Funiciello, 1982.) Extensional block faulting associated with Tyrrhenninan Sea opening along NW to NE trends and single sided down-to-the-west structures dominate.

Table 300

Caldera Name		Location		
Sacrofano Bracciano L.		Sabatini Volcanic Complex, Roman (Latian) Volcanic Province, Italy Sabatini Volcanic Complex, 4 km west of Sacrofano		
Elongation	Volcanic Character	Local Structure	Regional Structure	Tectonic Elements
Sacrofano: NE 10 x 6 km	double caldera; abundant ashflows accompany caldera collapse (A); alkaline leucitite phonolite assemblage.	these calderas are located on the west edge of the NNW-trending Tiber Graben; Sacrofano is elongate parallel to the graben extension direction	within block faulted terrane of NW and NE striking extensional tectonism	Arc (preexisting Appennine Arc); Rifting of Tyrrhennian Sea Margin
Bracciano: circular 10 km (A)	latest of the three calderas of this complex; no ashflows directly attributed to collapse of this feature			
Additional Information				
	The regional tectonic environment of these calderas is described on the Latera/Bolsena sheet. These calderas occur in an area where the graben is one sided and there is no obvious seaward graben bounding fault. Vico caldera, a caldera slightly less than 8 km, is located between Sacrofano/Bracciano to the south and Latera/Bolsena to the north within the same Tiber Graben within which these other calderas are localized.			
	Sacrofano cladera is the scene of multiple caldera forming events with the smaller Baccano caldera nested on its W side. It is located on the edge of the Tiber Graben and reflects an extension direction perpendicular to the graben axis.			
	Bracciano is a circular lake-filled depression. However, no large volume ashflow or air fall deposits have been identified to date that can be correlated with the collapse of this caldera (A). Volcanism has been associated with fractures which bound the Lake (A). Some workers (A) prefer to refer to Bracciano as a volcano-tectonic depression. It is included herein because it classifies as a caldera for the purposes of this study -- ie a fault bounded collapse structure related to volcanic activity (the term volcano-tectonic depression is an abused and misused term in general). It is not unlikely that collapse-related deposits associated with Bracciano may be identified in the future. An alternative is that collapse is the result of a succession of smaller-volume eruptions (C).			
References				
	(A) De Rita and Funiciello, 1982; (B) De Rita et al, 1982; (C) Walker, 1984			
FIGURE 93, 94				
Category: ARC (preexisting Appennine Arc) / ARC-PARALLEL RIFT (Tyrrhennian Sea Margin extensional deformation)				

Table 3PP

Caldera Name		Location		
Artemisio		Alban Hills Complex, Roman (Latian) Volcanic Province, Italy		
Elongation	**Volcanic Character**	**Local Structure**	**Regional Structure**	**Tectonic Elements**
circular 10 km	abundant ashflows associated with caldera collapse (B); alkaline bimodal leucitite phonolite assemblage (A)	located at the southern end of the Roman Volcanic Province, aligned with the complexes to the north and bounded to the east by the same extensional structures; occurs at the NW end of the Latina Valley graben	within block faulted terrane of NW, N-S and NE striking extensional tectonism	Arc (preexisting Appennine Arc); Rifting of Tyrrhennian Sea Margin
Additional Information				
	Artemisio caldera occurs within the Alban Hills Volcanic Complex at the south end of the Roman Volcanic Province. This caldera (also referred to as Tuscolano-Artemisio) formed within the last 0.7 my. It occurs in the block faulted terrane of the west coast of Italy in the tectonic setting described on the Latera/Bolsena sheet. Artemisio is located at the NW end of the northwest-trending graben of Latina Valley where this graben cuts the N-S faults of the Appennine front. These N-S to NW trending normal faults form a one-sided graben with no scarp evident on the seaward side.			
References				
	(A) Short et al, 1976, Pl 244; (B) De Rita and Funiciello, 1982			
FIGURE 93, 94				
Category: ARC (preexisting Appennine Arc) / ARC-PARALLEL RIFT (Tyrrhennian Sea Margin extensional deformation)				

Table 3QQ

Caldera Name		Location		
Phlegrean Fields		Campanian Volcanic Region, Gulf of Naples, Italy		
Elongation	Volcanic Character	Local Structure	Regional Structure	Tectonic Elements
NE: 12 x 11 km	abundant trachytic ashflows associated with caldera collapse (A); alkaline bimodal leucitite trachyte phonolite assemblage (A)	located within the graben of the Campanian Plain (A); caldera morphology dissected by subsequent phreatomagmatic activity; elongation parallel to graben extension direction; recent vents and seismicity align along NW and NE striking structures (B)	within block faulted terrane of NW, NNW and NE striking extensional tectonism	Arc (active Appennine Arc); Rifting of Tyrrhennian Sea Margin
Additional Information				
The regional tectonic environment of this caldera is described on the Latera/Bolsena sheet. The Phlegrean Fields is the site of frequent seismicity and rapid uplift and is at this writing among the most active large calderas in the world (C). The existing caldera, which was formed by the eruption of the Campanian ignimbrite about 36,000 years ago (B), has been subsequently dissected by phreatomagmatic explosions. This caldera is located within the single-sided Campanian graben which has no seaward bounding scarp. This graben is also the location of Somma Vesuvius -- a 5 km caldera located 14 km east of the Phlegrean Fields. In contrast to the Roman Volcanic Province to the north which is located opposite a no longer actively subducting trench, the Phlegrean Fields is on the arc front opposite the active ongoing Appennine Trench of southern Italy.				
References				
(A) Principe et al, 1982; (B) Barberi, 1978; (C) Barberi et al, 1984				
FIGURE 93, 94				
Category: ARC (active Appennine Arc) / ARC-PARALLEL RIFT (Tyrrhennian Sea Margin extensional deformation)				

Table 3RR

Caldera Name		Location		
Santorini [Thira]		Thira I., Cyclades, Greece, central Aegean Sea		
Elongation	Volcanic Character	Local Structure	Regional Structure	Tectonic Elements
NNW 10.8 x 7 km	abundant rhyodacitic ashflows accompany caldera collapse (A,B,C); staged caldera collapse (A); bimodal basalt-andesite-dacite-rhyolite calc-alkalic assemblage (D)	the caldera occupies a 3-4 km wide graben which trends NE -- toward Colombo Bank (a large submarine volcano to the NE -- last active in 1650); a normal fault on the south end of Thira parallels this graben	the caldera is located on the NW-trending volcanic front of Hellenic Arc at a point where it is cut by the NE-trending graben (called here the Christiana-Colombo graben); this graben extends from 60 km NE of Thira to 18 km SW of the island (A,F); arc-parallel extensional structures are also indicated (E,F)	Hellenic Arc; extensional Christiana-Colombo graben
Additional Information				
The caldera of Santorini is the result of a number of caldera-forming events which took place about 1400 BC. Caldera collapse occurred in stages from an initial caldera about 7 x 6 km to the final 10.8 x 7 km feature. The caldera occurs in a NE-trending graben which intersects the volcanic arc and has bathymetric expression from the Christiana Is., 28 km to the SW, to Amorgos I. about 60 km NE of Thira (A,E,F). Focal plane solutions support the interpretation of this graben as an actively extending structure (E). Arc-parallel graben structures are also indicated in the bathymetric data (E,F). These structures are located trenchward of the arc as well as along the volcanic axis (F). This eruption essentially destroyed the Minoan culture, opening the way for subsequent Greek and Roman dominance. This represents the best example of the socio-geologic impact of eruptions that accompany large caldera formation.				
References				
(A) Heiken and McCoy, 1984; (B) Williams, 1941; (C) Bond and Sparks, 1976; (D) Keller, 1982; (E) McKenzie, 1978; (F) Jacobshagen et al, 1978				
FIGURES 95, 96				
Category: ARC (Hellenic) / INTERSECTING RIFT (Christiana-Colombo graben) / ARC-PARALLEL RIFT (submarine graben structures)				

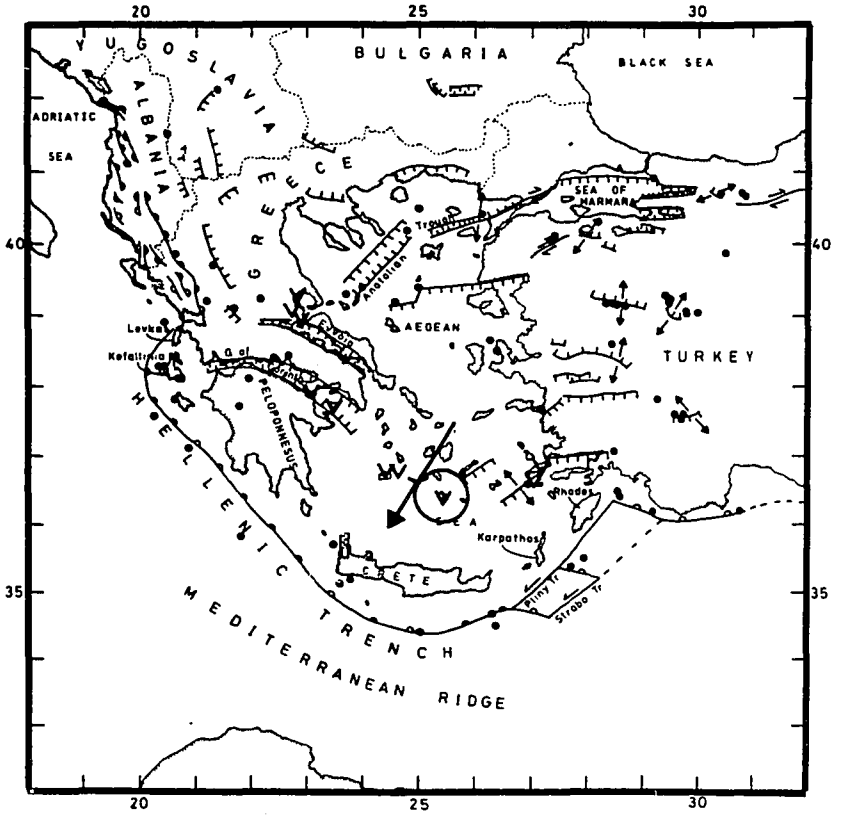

Figure 95. Tectonic Map of the Aegean (McKenzie, 1978). The Hellenic Volcanic Arc (marked by V's) is the result of north and northeast dipping subduction into the Hellenic Trench. The circle denotes Santorin. Stress trajectories indicated by extensional structures in the backarc region indicate extension parallel to the volcanic axis (Nakamura and Uyeda, 1980).

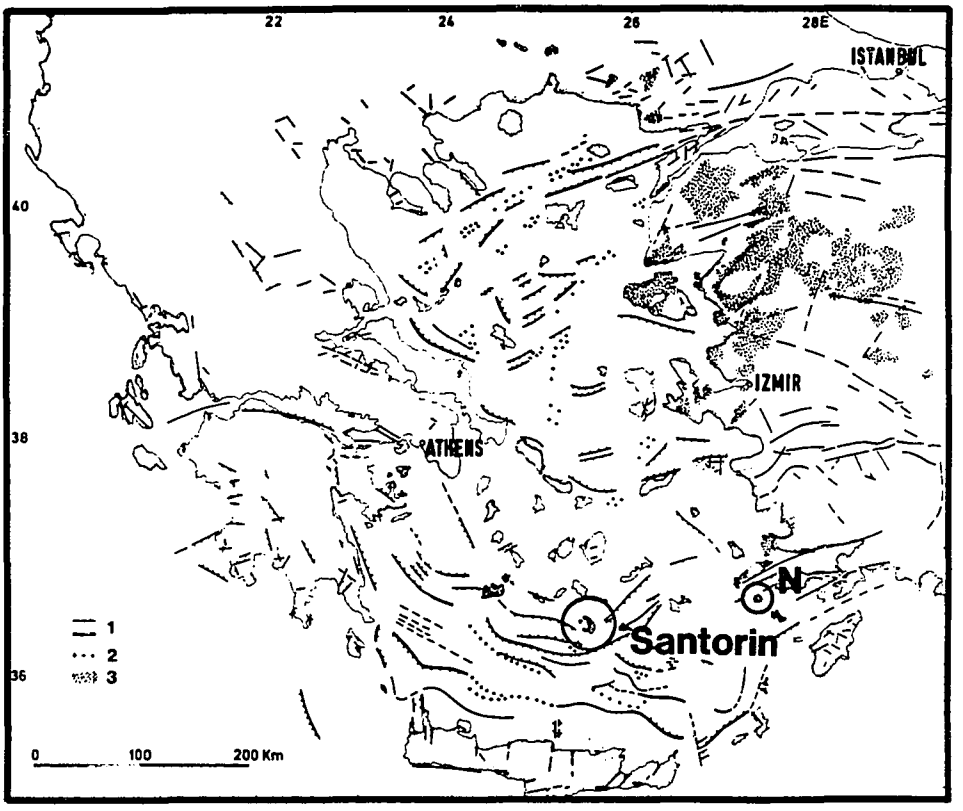

Figure 96. Fault Map of the Aegean (Jacobshagen et al, 1978) showing the intersection of NE-SW trending graben structures, from behind the arc, with the volcanic axis at Santorini (circle). Arc-parallel extensional structure trenchward of the arc striking WNW indicates extension, in the forearc region, that parallels the direction of plate convergence. This is contrary to the common situation of compression in the forearc paralleling convergence (Nakamura and Uyeda, 1980). The location of Nisyros caldera (N) -- somewhat less than 8 km across -- is also shown.

Table 3SS

Caldera Name	Location
Emi Koussi	east Tibesti, Chad, north central Africa
Tarso Yega	central Tibesti, 180 km NE of Emi Koussi
Tarso Toon	south central Tibesti, 50 km NNE of Tarso Yega
Tarso Voon	central Tibesti, 20 km NNW of Tarso Yega
Yirrique	west Tibesti, 85 km WNW of Tarso Voon

Elongation	Volcanic Character	Local Structure	Regional Structure	Tectonic Elements
Emi Koussi: WNW 12.9 x 11.3 km (B) Tarso Yega: NNW ~17 x 11 km (A) Tarso Toon: NW 11 x 9 (A) Tarso Voon: NW 18 x 11 (A) Yirrique: NNW 14 x 13 (A)	abundant ashflows adjacent to calderas (A); bimodal alkaline basalt-rhyolite assemblage (A; alkaline affinity (F)	NW trending vent alignments and caldera elongation	NW-striking flextures; NE-trending Precambrian structure	Tibesti Hot Spot

Additional Information

Tibesti is located in an intraplate setting far from any tectonic plate boundary. The province is 420 km long (NW) and 225 km at its widest point. The large calderas are limited to the central 120 km of its width (NE). The province has been active since Mid-Eocene time and includes the development of at least five large Quaternary calderas . Volcanism is dominantly basaltic with significant volumes of rhyolite (37% by volume (A)). Tibesti overlies Precambrian basement with structural grain striking NNE to NE. This faulting is displayed on Landsat imagery (C,B). Uplift and tilting accompanying volcanism has produced flexures which strike NW. The volcanism has taken place along a NW-striking zone -- although some alignment of major centers may occur along the NNE faults (eg Tarso Toon to Tarso Yega). Flexure and volcanism has migrated to the SW during the Quaternary (A). The flexures have been related to the rise of magma and act to localize eruptions. The NE-trending faults have not been injected by volcanics and are generally passive. Volcanism has apparently taken place in a tectonic stress field characterized by NW-SE maximum horizontal stress (Mil3). The NW alignment of monogenetic vents NW of Emi Koussi, (visible on the NASA Apollo orbiter photography (D)), supports this view; as does the absence of the emplacement of volcanics into the NE-trending preexisting faults.

The Tibesti province appears to be the result of a hot spot located beneath a stationary African plate that has remained stationary for the last 25 my (E). This idea is consistent with the petrology of the volcanics which falls in the alkalic suite at the beginning of province volcanism and in the recent (low volume), presumably waning, stage; while during the middle, most active stage, tholeiitic volcanics were dominant (A). The Hawaiian Hot Spot also shows this pattern.

18 x 11 (A) Yirrique: NNW 14 x 13 (A)	affinity (F)			

Additional Information

Tibesti is located in an intraplate setting far from any tectonic plate boundary. The province is 420 km long (NW) and 225 km at its widest point. The large calderas are limited to the central 120 km of its width (NE). The province has been active since Mid-Eocene time and includes the development of at least five large Quaternary calderas . Volcanism is dominantly basaltic with significant volumes of rhyolite (37% by volume (A)). Tibesti overlies Precambrian basement with structural grain striking NNE to NE. This faulting is displayed on Landsat imagery (C,B). Uplift and tilting accompanying volcanism has produced flexures which strike NW. The volcanism has taken place along a NW-striking zone -- although some alignment of major centers may occur along the NNE faults (eg Tarso Toon to Tarso Yega). Flexure and volcanism has migrated to the SW during the Quaternary (A). The flexures have been related to the rise of magma and act to localize eruptions. The NE-trending faults have not been injected by volcanics and are generally passive. Volcanism has apparently taken place in a tectonic stress field characterized by NW-SE maximum horizontal stress (MHS). The NW alignment of monogenetic vents NW of Emi Koussi, (visible on the NASA Apollo orbiter photography (D)), supports this view; as does the absence of the emplacement of volcanics into the NE-trending preexisting faults.

The Tibesti province appears to be the result of a hot spot located beneath a stationary African plate that has remained stationary for the last 25 my (E). This idea is consistent with the petrology of the volcanics which falls in the alkalic suite at the beginning of province volcanism and in the recent (low volume), presumably waning, stage; while during the middle, most active stage, tholeiitic volcanics were dominant (A). The Hawaiian Hot Spot also shows this pattern. There is no evidence that the location of the Tibesti volcanics is associated with the structure in the overriding plate beyond being influenced by the regional NW-SE MHS. The magma produced by a thermal plume resulting from heat buildup under a stationary plate, was presumably produced in sufficient volume to stope its way to the surface over a broad 420 km area and produce uplift, extensional faulting, volcanism and caldera formation.

References

(A) Vincent, 1970; (B) Main, 1977; (C) Short et al, 1976, Pl 334; (D) Nicks, 1980, p 81; (E) Burke and Wilson, 1972; (F) Pike and Clow, 1981

FIGURE 97

Category: HOT SPOT (Tibesti)

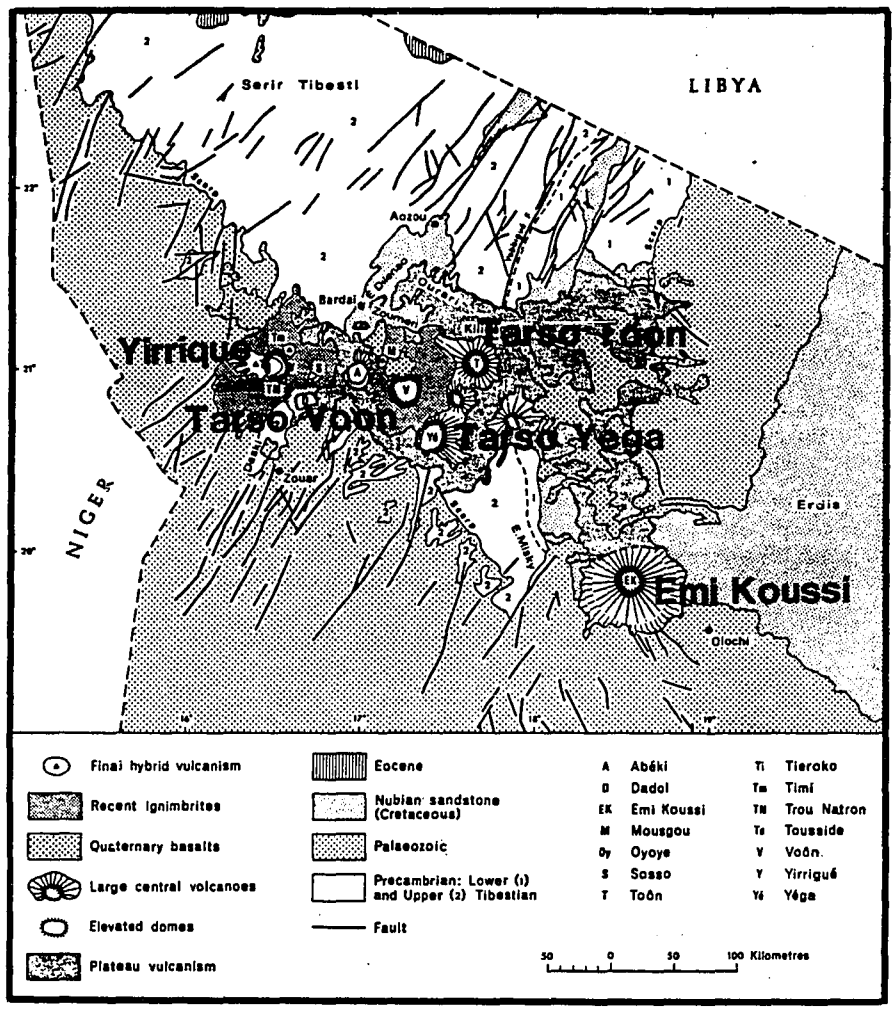

Figure 97. Structure and Volcanic Map of the Tibesti Region (Vincent, 1970) showing the five large calderas that occur in this region of intraplate hot spot volcanism. The African plate has been stationary for the last 25 m.y. and volcanism has dominated the Tibesiti area since the Miocene. Early alkaline volcanism was replaced by a voluminous tholeiitic phase followed by a return to low volume alkalic volcanics of the Recent -- similar to the cycle of the Hawaiian Hot Spot.

Table 3TT

Caldera Name		Location		
Nabro [Bidu Pile] Asavyo		Dubbi line, north central Afar, Ethiopia, Africa Dubbi line, 15 km SW of Nabro		
Elongation	Volcanic Character	Local Structure	Regional Structure	Tectonic Elements
Nabro: NNE 8 x 7.5(?) km (A) Asavyo: circular 8.2 km (G)	abundant silicic ashflows adjacent to calderas (A,C); alkaline bimodal basalt/rhyolite with adjacent contemporaneous tholeiitic basalts (A,C)	calderas occur on the Dubbi volcanic line of silicic vents at points where the line is cut by NW-SE trending extensional faults (A); elongation is parallel to extension on these NW structures	the Dubbi volcanic line -- a 130 km long of silicic volcanism and calderas -- cuts across the Danakil Horst and associated NW structure localizing vents at these intersections; volcanoes of the Dubbi line become younger to the NE; NW structures parallel the Red Sea Rift at a right step (SW) from the Red Sea Rift to Afar	Red Sea Rift offset; extension of East Africa Rift
Additional Information				
	The Afar region of Ethiopia is a unique locality where three spreading ridges -- the Red Sea Rift (RSR), the Gulf of Aden, and the East African Rift -- intersect in a subaerial environment. This has been regarded by most workers as a RRR triple junction (D) but recent work (E) indicates that a second generation of Red Sea rifting is propagating toward -- but has not yet reached -- the East African Rift at the Afar; while rifting in the Afar is concentrated in the central part of the region on NW-trending spreading ridges (B) which parallel the RSR.			
	The Navbro and Asavyo calderas occur along the NE-trending Dubbi line of bimodal silicic/basaltic volcanoes which has been interpreted as a transform zone between the RSR and Afar spreading (B). Younging to the NE, this line may reflect a rift propagating NE toward the RSR termination with volcanism localized at points where NW extensional faults cross the "transform". The tectonic significance of these features is not well constrained. It is not clear whether these volcanoes should be taken as diffuse deformation within a soon-to-be-rifted zone or as individual mini-propagating rifts (F).			
References				
	(A) Mohr and Wood, 1976; (B) Barberi and Varet, 1977; (C) Mohr, 1983; (D) McKenzie and Morgan, 1969; (E) Courtillot and Vink, 1983; (F) Courtillot, 1982; (G) NASA Large Format Camera Neg. 1329			
FIGURE 98, 99				
Category: RIFT (Afar) / RIFT OFFSET (transform to RSR)				

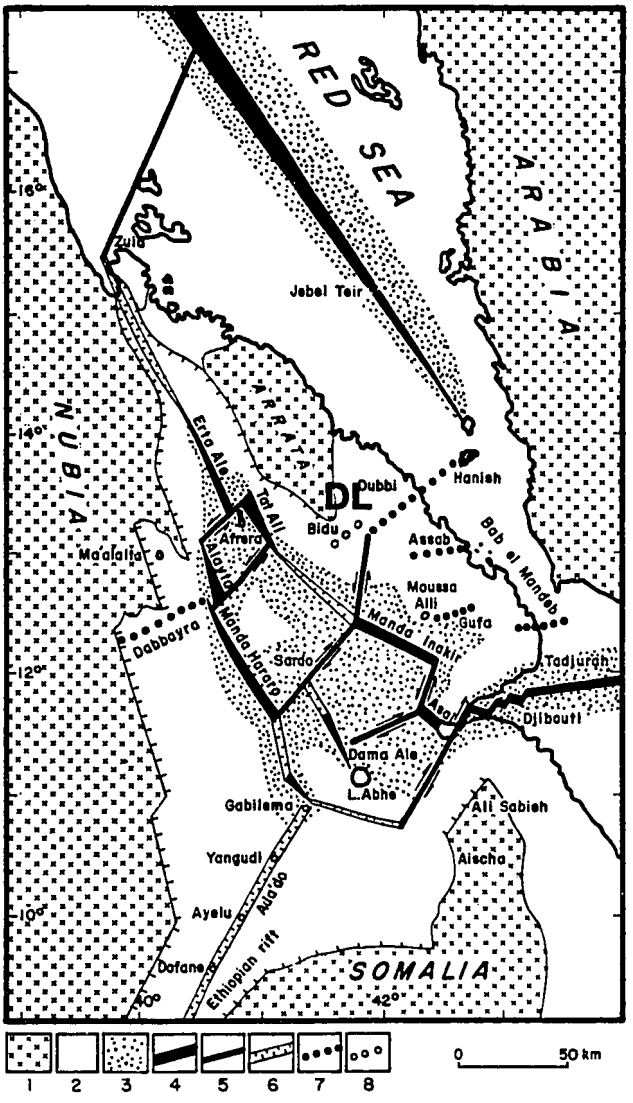

Figure 98. Tectonic Map of Afar (Barberi and Varet, 1977) showing the termination of the Red Sea Rift in relation to the Dubbi Line (DL) and its orientation in a transform position between the Red Sea Rift and the spreading in the Afar region. The silicic volcanism of the Dubbi calderas appears to become younger to the NE.

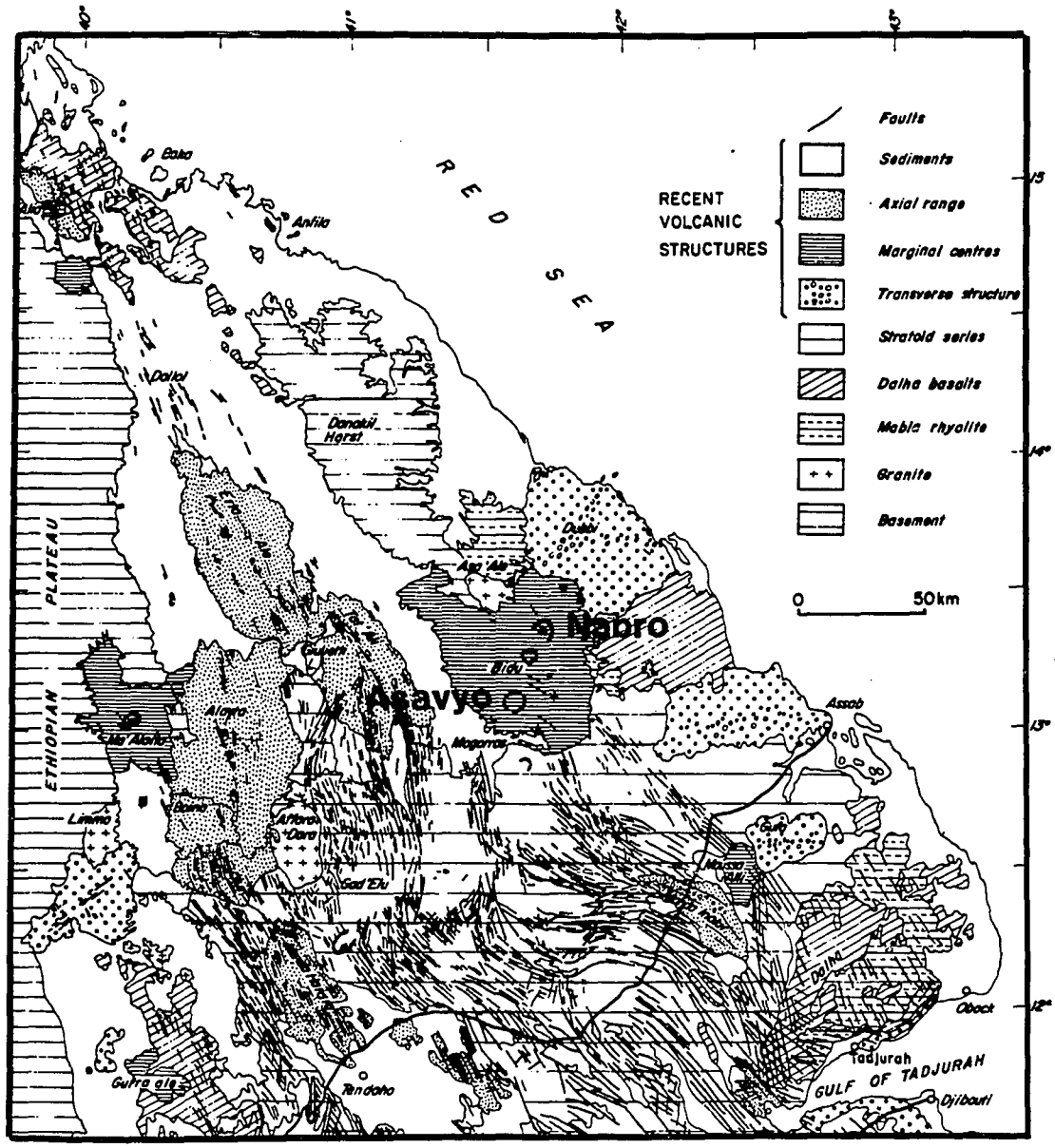

Figure 99. Structure and Volcanic Map of Afar (Barberi and Varet, 1977) showing the Dubbi Line calderas relative to surrounding structure. Although not shown, NW trending faulting cuts Danakil Horst and extends across the Dubbi Line; calderas occur at these intersections (Mohr and Wood, 1976).

Table 3UU

Caldera Name		Location		
O'a [Lake Shalla] Corbetti		Main Ethiopian Rift, East African Rift, central Ethiopia 17 km SW of O'A		
Elongation	**Volcanic Character**	**Local Structure**	**Regional Structure**	**Tectonic Elements**
O'a: WNW 16 x 13 km (A) Corbetti: WNW 12.5 x 10 km (A)	abundant silicic ashflows accompany caldera collapse (A); alkaline bimodal basalt-rhyolite with adjacent contemporaneous tholeiites (A,B)	elongation of calderas parallels extension direction of the Rift; numerous NNE fissures south of O'a, NE trending fissures NE of O'a; linear NW wall of Corbetti strikes NE; dominant fissures in the vicinity of Corbetti strike NNE	these calderas occur in a zone of inflection in the main Rift from NE (NE of O'a) to NNE (S of O'a)	East African Rift (EAR)

Additional Information

The large calderas of the EAR occur in an extensional environment where alkaline volcanism and normal faulting are ubiquitous. The development of rifting is similar to that described for the propagation of individual rifts of the Basin and Range. Typically the rifts develop as half grabens with one side formed by a major normal fault and the other side formed by a combination of downwarping and step faulting (H). The rift forms in segments which are slightly curved basins and the main fault generally occurs on the convex (outward) side of the basin (G). Curvature alternates along the strike of the rift with inflection points occurring at the end of each segment, producing a subtle zigzag pattern in the rift trend. The large calderas of the rift appear to occur at these inflection points in the rift. Within the EAR, linear fissure swarms occur in the floor of the rift valley -- the Wonji Fault Belt (WFB). These have developed after the initial rift event and vary from swarms parallel to the sides of the rift -- typical of the main Rift; to swarms trending at a small angle to the rift -- as in the northern rift/Afar region. King (F) considers that these inflection points relate to the control of rifting by crustal characteristics and Precambrian structure. In a regional sense the rift follows, and bifurcates around the margins of the Tanganyika Shield -- an area of thicker continental crust (F).

Both O'A and Corbetti calderas occur within the axial rift zone at an inflection point in its alignment. The geology and structural setting of these calderas is discussed in references A,B,C,D. Mohr (C) characterizes the WFB as en echelon faulting and notes that these calderas occur at right-step offsets in the WFB. Exposures in the central rift are covered by lacustrine sediments, however, so that fault maps give a deceptive picture. Wherever continous exposures of the WFB are found, the Wonji occurs as parallel fissure swarms (I) -- not en echelon (stepping) fissures. The presence of parallel fissures on both sides of the sediment ponds suggests that the WFB occurs as a parallel swarm here also -- not en echelon.

O'a caldera occurs in the central rift valley at a 20° inflection in the dominant strike of the WFB fissures from a NE trend, NE of O'a, to a NNE trend south of the caldera. This inflection is evident on fault maps (D) and on Landsat (E). The change in trend of the WFB reflects an inflection in the main rift walls which occurs to the south, adjacent to Corbetti caldera. Corbetti is located on the east side of the rift close to the rift boundary scarp. At this point the main rift scarp changes trend by about 20°. The interaction of the two WFB trends is seen at Corbetti where the NW wall of the caldera parallels the NE fissure set although the swarm most pro-

and the main fault generally occurs on the convex (outward) side of the basin (G). Curvature alternates along the strike of the rift with inflection points occurring at the end of each segment, producing a subtle zigzag pattern in the rift trend. The large calderas of the rift appear to occur at these inflection points in the rift. Within the EAR, linear fissure swarms occur in the floor of the rift valley -- the Wonji Fault Belt (WFB). These have developed after the initial rift event and vary from swarms parallel to the sides of the rift -- typical of the main Rift; to swarms trending at a small angle to the rift -- as in the northern rift/Afar region. King (F) considers that these inflection points relate to the control of rifting by crustal characteristics and Precambrian structure. In a regional sense the rift follows, and bifurcates around the margins of the Tanganyika Shield -- an area of thicker continental crust (F).

Both O'A and Corbetti calderas occur within the axial rift zone at an inflection point in its alignment. The geology and structural setting of these calderas is discussed in references A,B,C,D. Mohr (C) characterizes the WFB as en echelon faulting and notes that these calderas occur at right-step offsets in the WFB. Exposures in the central rift are covered by lacustrine sediments, however, so that fault maps give a deceptive picture. Wherever continous exposures of the WFB are found, the Wonji occurs as parallel fissure swarms (I) -- not en echelon (stepping) fissures. The presence of parallel fissures on both sides of the sediment ponds suggests that the WFB occurs as a parallel swarm here also -- not en echelon.

O'a caldera occurs in the central rift valley at a 20° inflection in the dominant strike of the WFB fissures from a NE trend, NE of O'a, to a NNE trend south of the caldera. This inflection is evident on fault maps (D) and on Landsat (E). The change in trend of the WFB reflects an inflection in the main rift walls which occurs to the south, adjacent to Corbetti caldera. Corbetti is located on the east side of the rift close to the rift boundary scarp. At this point the main rift scarp changes trend by about 20°. The interaction of the two WFB trends is seen at Corbetti where the NW wall of the caldera parallels the NE fissure set although the swarm most prevalent around Corbetti is the NNE WFB set. The prevalence of lakes and depressions and ash-flow deposits in the vicinity of O'a/Corbetti may reflect the influence of the broad extension and resulting shallow-chamber magmatism which dominates this rift inflection area.

References

(A) Di Paola, 1972; (B) Mohr et al, 1980; (C) Mohr, 1983; (D) Di Paola, 1973; (E) Short et al, 1976, Pl 365; (F) King, 1970; (G) Bosworth, 1985; (H) Williams et al, 1984; (I) Mohr, 1973

FIGURE 100

Category: RIFT (Ethiopian Rift) / RIFT INFLECTION (Wonji Fault Belt)

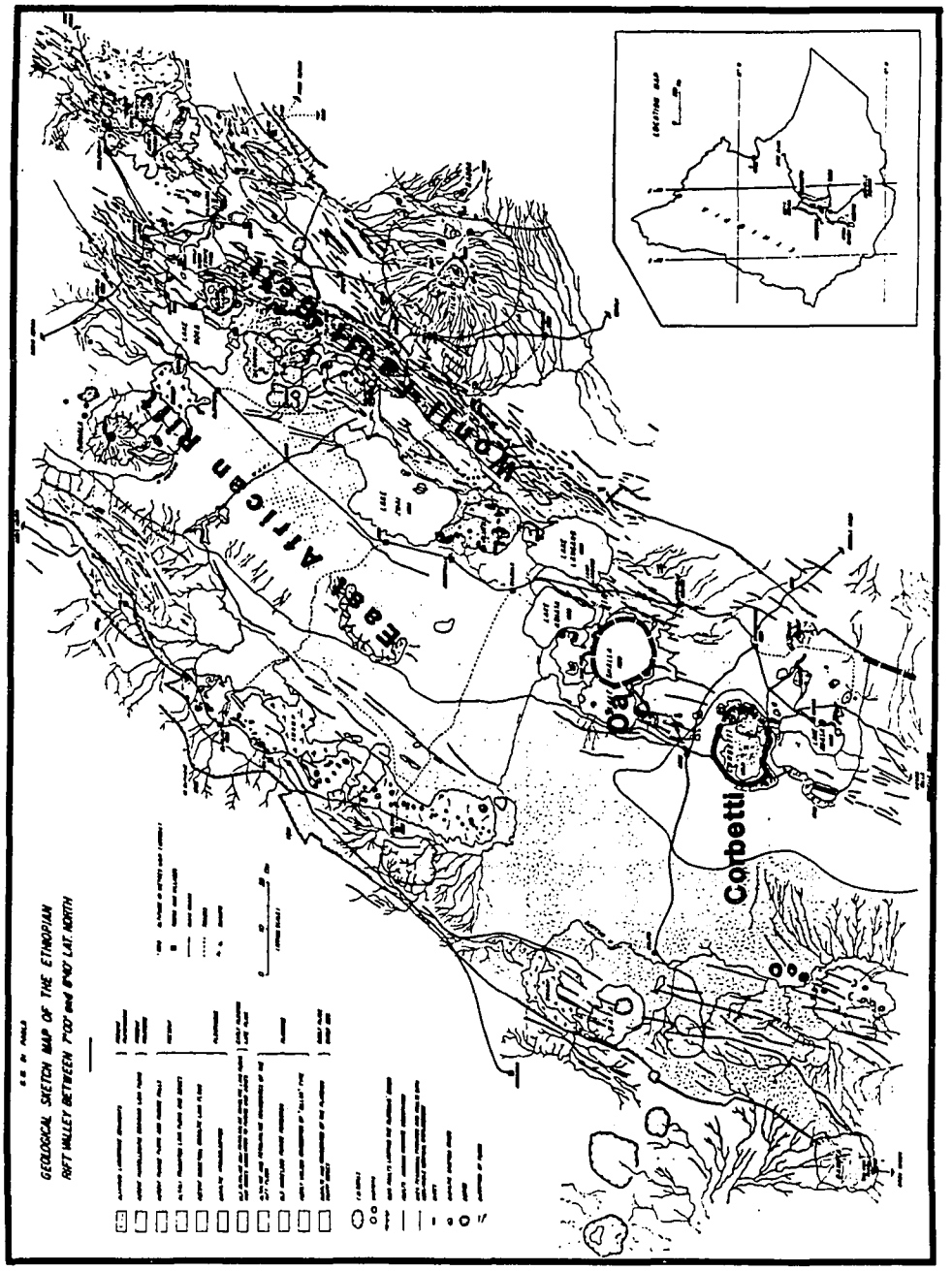

Figure 100. East African Rift -- Ethiopia (modified after Di Paola, 1973). The Wonji Fault Belt is the swarm of fissures which cut the floor of the East African Rift in Ethiopia (faults of the system can also be seen on the west side of the rift). Corbetti and O'a occur at a 20° inflection of both the Wonji (at O'a) and the main rift wall (at Corbetti). The bold dashed line southeast of Corbetti shows the trend of the rift south of Corbetti. Extensive lacustrine sediments and ash deposits occur west and north of the caldera and obscure fault trends in the central area of the rift.

Table 3W

Caldera Name		Location		
Menengai Suswa		Gregory Rift, East African Rift, south central Kenya 100 km SSE of Menengai, Kenya		
Elongation	**Volcanic Character**	**Local Structure**	**Regional Structure**	**Tectonic Elements**
Menengai: circular 12 km (A) Suswa: ENE 12 x 8 km (A)	abundant silicic ashflows accompany caldera collapse (D); dominant peralkaline silicic assmeblage (D) abundant ashflows accompany caldera collapse (A); peralkaline trachyte-phonolite assemblage (A)	NNW fissures S of Menengai and N-S trending fissures N of Menengai; the N-S set offsets the NNW set. At Suswa elongation parallels extension of the Rift; NNW fissures strike toward the caldea from the north while N-S to NNE fissures intersect the caldera from the south	these calderas occur in a zone of inflection of about 30° in the main Rift which strikes broadly N-S to the North of Menengai, NNW between Menengai and Suswa, and N-S to NNE south of Suswa; a NE striking Landsat lineament crosses the rift at Suswa bisecting the caldera	East African Rift (EAR)
Additional Information				
	The tectonic setting of the EAR and its structural development is discussed on the O'a/Corbetti sheet. Fissure swarms formed after the initial rifting are ubiquitous on the floor of the rift valley and are analagous to the Wonji Fault Belt discussed on the O'a/Corbetti sheet (E).			
	Menengai occours at an inflection point in the rift system where it diverges from a NE trend, south of Menengai, to a N-S trend, north of the caldera. Viewed on Landsat imagery (F) a NE-trending fissure swarm terminates at the caldera and a few of the faults curve to a nearly E-W strike within 10 km of the caldera and verge colinear with the northern wall of the caldera. The N-S fissures pass through the caldera and control the caldera wall orientation. Where the NW and N-S fault sets interact (east of the caldera) the N-S set is consistently offset by the curving NW trend, implying a younger relative age for this faulting.			
	Suswa is known for its "circumferential graben" inside of the caldera-bounding fault which probably results from resurgent activity (A). Tectonically, Suswa is located at a point of inflection where the rift trend deviates from N-S (south of Suswa) to NNW (north of the caldera). Landsat imagery of the area (G) depicts the trends of normal faults on the floor of the rift valley parallel to these directions of rifting. Immediately north of the caldera, the fissures are obscured by ash deposits. South of the caldera, both sets of faults are well developed, and can be seen to offset each other -- indicating contemporaneity. Either preexisting structure is being remobilized or the sets have been generated to the north and south of the inflection point and propagated toward one another so that crack propagation drive the two trends into one another. Also, a 180 km long Landsat lineament occurs at Suswa and strikes NE across the caldera. It is characterized by lineation in vegetation, channelization of a lava flow from the east side of the caldera, and offset of fault scarps on both E and W margins of the rift. The structural significance of this lineament is not yet evaluated.			
References				
	(A) Williams et al, 1984; (B) Baker and Mitchell, 1976; (C) Mohr and Wood, 1976; (D) Leat et al, 1984; (E) Johnson, 1969; (F) Sheffield, 1981; (G) Short et al, 1976, PI 359; (H) USGS Landsat Mosaic of Kenya, Map 8586R, 1:1,000,000			
FIGURE 101				
Category: RIFT (Ethiopian Rift) / RIFT INFLECTION				

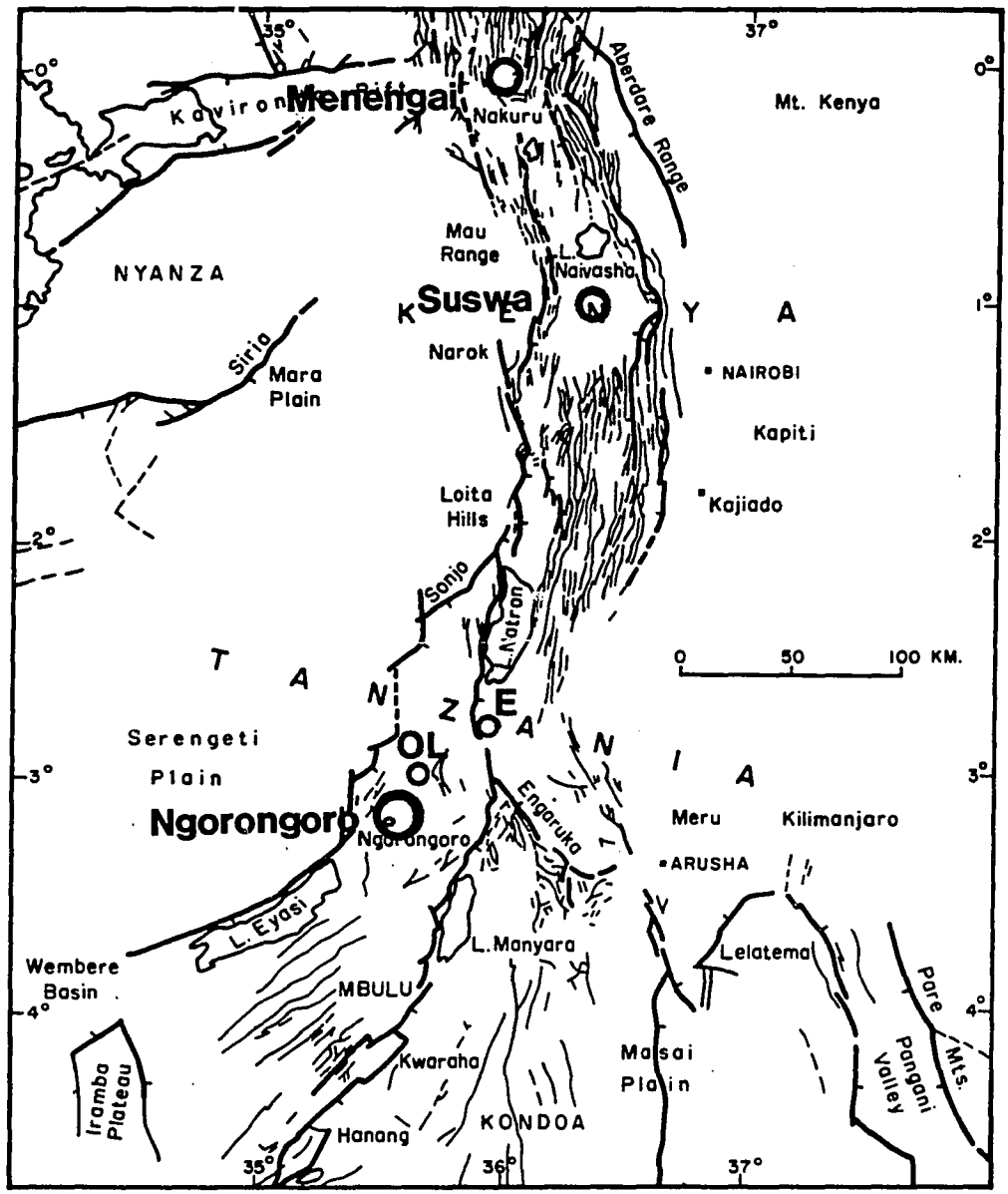

Figure 101. East African Rift -- Kenya and Tanzania (Baker et al, 1972) showing the location of large calderas in southern Kenya and Tanzania in relation to faulting. Menengai and Suswa both occur at points where the trend of the fissure swarm within the rift valley undergoes a 30° change. Ngorongoro occurs where the rift bifurcates and becomes more distributed to the south. Elanaibori (E) and Olmoti (OL), both of which are somewhat less than 8 km across, are also shown.

Table 3WW

Caldera Name		Location		
Ngorongoro		Gregory Rift, East African Rift, north central Tanzania		
Elongation	**Volcanic Character**	**Local Structure**	**Regional Structure**	**Tectonic Elements**
E-W: 20 x 17 km (B)	abundant silicic ashflows adjacent to caldera (D); alkaline bimodal basalt-trachyte-phonolite assemblage (A,D); multiple caldera	the NW wall of the caldera is linear and aligns with the Lake Eyasi branch of the rift (B); elongation parallels extension of main EAR extension to the north	this caldera occurs on strike with the Lake Eyasi Rift at the intersecIton of NW and NNW trending faults from the Lake Manyara Rift branch which merges into the Main EAR to the north	Triple junction within the East African Rift (EAR)

Additional Information

Ngorongoro is a large primarily circular caldera slightly elongate E-W. Its west side has been obscured by a satellite caldera of about 6 km diameter giving a total width of the geomorphic caldera of 26 km. It is located near two other calderas which are about 7.5 km diameter. These are Olmoti, 10 km to the NE, and Elanaibori (Embagai), 26 km to the NE. All of these calderas are located at a point on the rift where narrow well-defined rifting to the north gives way to more distributed rifting and bifurcation of the locus of major extension to the south. Landsat imagery of this area (B) depicts three directions of structure -- a NNW trend from the southeast (Lake Manyara); a N-S trend from the north (main EAR); and a NE trend from the southwest (Lake Eyasi). Ngorongoro is most directly influenced by the NE trend which is related to the rift arm occupied by Lake Eyasi. This structure appears to control the NW and SE walls of Ngorongoro caldera. The NNW-trending faulting extends from an area of broad rifting to the east of Lake Manyara. Landsat lineaments extending northwest from the north end of Lake Manyara project to the NE and SW walls of the caldera but direct association with caldera geometry is not visible. The N-S structure on the west side of the main EAR curves into the NE (Eyasi) structure between Ela Naibori and Ngorongoro while the N-S structure which forms the east wall of the rift continues south to the east side of Lake Manyara. The large diameter of Ngorongoro and the anomalous number of calderas in this area (relative to elsewhere on the EAR) indicate that enhanced rifting at a point where structural transition from localized extension to distributed extension is taking place. This is similar to that described for Askja.

References

(A) Searle, 1970; (B)Sheffield, 1981, p. 110; (C) USGS Landsat Mosaic of Kenya, Map 8586R, 1:1,000,000; (D) Pike and Clow, 1981

FIGURE 101, 102

Category: RIFT (East African Rift) / RIFT (L. Eyasi trend) / RIFT (L. Manyara trend)

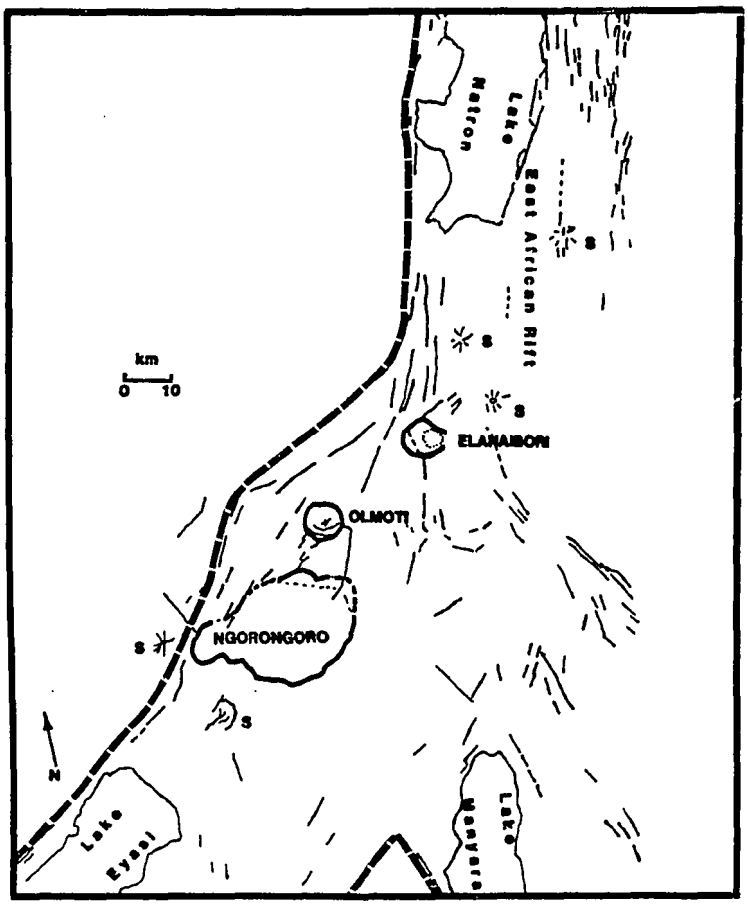

Figure 102. Fault Map (from Landsat) of Ngorongoro and vicinity showing the detailed relationship of Ngorongoro and adjacent calderas to the change in rift style. In the north rifting is localized to a central rift while to the south rifting becomes more distributed and takes place on two trends: NNW and ENE.

Table 3XX

Caldera Name		Location		
Askja		central Iceland		
Elongation	Volcanic Character	Local Structure	Regional Structure	Tectonic Elements
NW 9.5 x 8.7 km	no voluminous ash-flows associated with caldera formation are found; bimodal basalt/rhyolite assemblage	elongation parallels direction of extension; normal faulting adjacent to the caldera trends NE (C)	occurs in the Eastern Volcanic Zone (EVZ) of Iceland just north of the point where the broad active spreading of south Iceland narrows and becomes localized to the EVZ (D); ubiquitous N to NE normal fault scarps parallel the rift (extension is E-W)	Mid Atlantic Ridge (EVZ); offset and widening of spreading axis; Iceland Hot Spot
Additional Information				
	Askja caldera was formed in a subglacial environment. It is dominated by basaltic volcanism with volumetrically small silicic lavas. No pyroclastic deposits have been associated with caldera collapse. Historic accounts of the 1875 formation of Oskjuvatn Caldera -- a 4 x 5 km caldera nested within Askja -- indicates caldera collapse was preceded by a basalt eruption on the volcano flank (50 to 70 km north) which apparently precipitated collapse. This eruption accounted for 60% of the eventual caldera volume, while a silicic ashflow eruption at the caldera accounted for 40% of the caldera volume -- 5 weeks after caldera collapse had begun (G). It is thought that evacuation of the magma chamber, by lateral draining, caused the caldera collapse (G). Given the lack of significant pyroclastics associated with the main Askja collapse, the collapse of Oskjuvatn may provide the best analog for Askja. However, the pyroclastics may have been removed by glacial action. Another factor is that Iceland overlies basaltic crust. It is difficult to produce large volumes of silicic magma from basaltic crust. This may be a limiting factor in the evolution of larger silicic chambers in mafic crust.			
	Iceland represents a subaerial exposure of the Mid Atlantic Ridge (MAR) convolved with Hot Spot volcanism. Two modes of spreading (rifting) are found. One is spreading isolated to the EVZ (north half of the island) the strike of which is NNE at its south end in the vicinity of Askja, and N-S at its north end; with the changes in direction made by successive inflections along left-stepping spreading segments. A second mode is where the spreading is distributed across the southern half of the island with zones of most active spreading on the southern EVZ and on the Langjokull Zone which dominates the west side of southern Iceland. Both of these zones trend consistently NE -- at an angle to the northern EVZ. The Langjokull zone is the more long-lived zone with spreading on the EVZ thought to have initiated in the Plio-Pleistocene.			
	There is a broad E-W zone of en echelon spreading which connects the north end of the Langjokull with the EVZ. A number of calderas (less than 8 km) and possible, but subglacial calderas are found in this zone of tectonic accomodation. (Subglacial calderas likely greater than 8 km in size include Bardarbunga and Grimsvotn.) Their tectonic association is similar to that of Askja. Grimsvotn has experienced eruptive activity within the caldera (evidenced by historic jokulhlaups) and is thought to have fed basaltic fissure eruptions on its flanks. However, lack of structural information (due to ice cover) prevents structural categorization of Grimsvotn. Other calderas of Iceland are not discussed here because they are [illegible]			

nested within Askja -- indicates caldera collapse was preceded by a basalt eruption on the volcano flank (50 to 70 km north) which apparently precipitated collapse. This eruption accounted for 60% of the eventual caldera volume, while a silicic ashflow eruption at the caldera accounted for 40% of the caldera volume -- 5 weeks after caldera collapse had begun (G). It is thought that evacuation of the magma chamber, by lateral draining, caused the caldera collapse (G). Given the lack of significant pyroclastics associated with the main Askja collapse, the collapse of Oskjuvatn may provide the best analog for Askja. However, the pyroclastics may have been removed by glacial action. Another factor is that Iceland overlies basaltic crust. It is difficult to produce large volumes of silicic magma from basaltic crust. This may be a limiting factor in the evolution of larger silicic chambers in mafic crust.

Iceland represents a subaerial exposure of the Mid Atlantic Ridge (MAR) convolved with Hot Spot volcanism. Two modes of spreading (rifting) are found. One is spreading isolated to the EVZ (north half of the island) the strike of which is NNE at its south end in the vicinity of Askja, and N-S at its north end; with the changes in direction made by successive inflections along left-stepping spreading segments. A second mode is where the spreading is distributed across the southern half of the island with zones of most active spreading on the southern EVZ and on the Langjokull Zone which dominates the west side of southern Iceland. Both of these zones trend consistently NE -- at an angle to the northern EVZ. The Langjokull zone is the more long-lived zone with spreading on the EVZ thought to have initiated in the Plio-Pleistocene.

There is a broad E-W zone of en echelon spreading which connects the north end of the Langjokull with the EVZ. A number of calderas (less than 8 km) and possible, but subglacial calderas are found in this zone of tectonic accomodation. (Subglacial calderas likely greater than 8 km in size include Bardarbunga and Grimsvotn.) Their tectonic association is similar to that of Askja. Grimsvotn has experienced eruptive activity within the caldera (evidenced by historic jokulhlaups) and is thought to have fed basaltic fissure eruptions on its flanks. However, lack of structural information (due to ice cover) prevents structural categorization of Grimsvotn. Other calderas of Iceland are not discussed here because they are less than 8 km (Torfajokull, Tungnafellsjokull, Kverfjokull) or there is question about their identity as calderas (Krafla (E)).

References

(A) Volcano News, 1980; (B) Thorarinsson et al, 1973; (C) Seasat image of Askja, 1978; (D) Saemundsson, 1979; (E) Walker, pers. comm., 1986; (F) Sparks et al, 1982; (G) Sigurdsson and Sparks, 1978

FIGURE 103

Category: RIFT (MAR) / RIFT OFFSET & INFLECTION (south vs north Iceland)

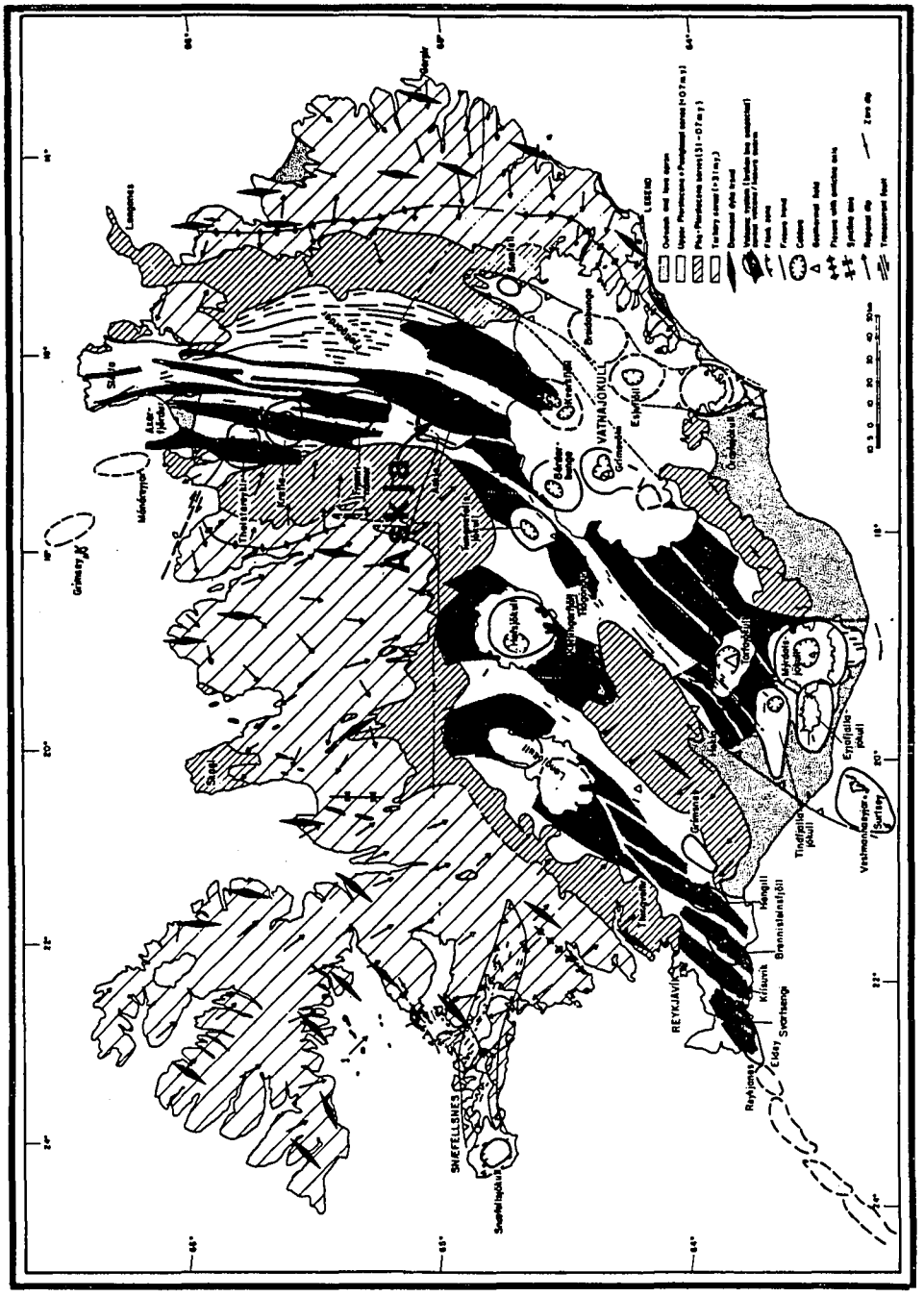

Figure 103. Tectonic Map of Iceland (Saemundsson, 1980) Many possible calderas occur in the Eastern Volcanic Zone (EVZ) of Iceland and in the E-W zone which marks the termination of the broad spreading of southern Iceland. Candidate large calderas Bardarbunga and Grimsvotn are subglacial and therefore difficult to document. Krafla is not well defined as a caldera. Askja -- the only well defined large caldera in Iceland -- occurs at the point where the broad southern spreading becomes localized to the EVZ.

Discussion

The remaining sections are a distillation of the information contained in Table 3. Reference to Table 3 and its attendant figures is implicit in this discussion.

It is clear that the recognition of plate boundaries and other fundamental tectonic features is in an evolutionary stage and that some of the assignments given here may be superseded in the future. This is particularly true because of the fact that most of these calderas occur in areas of complex plate tectonics involving small plates and complicated geometry which is not well resolved. The tectonic associations discussed are for the most part based on data and interpretations currently extant in the literature. However, it is anticipated that further study of these calderas in a tectonic context may contribute both to the understanding of large calderas and to the further understanding of tectonic processes.

Significance of the Caldera Landform

The discussion of the significance of caldera-tectonic associations is not a simple one. Logically, the demonstration that identifiable caldera localities correspond to identifiable tectonic intersections DOES imply that calderas may be limited to such localities but does not imply that large calderas will form at all such tectonic intersections (assuming the presence of an available magma source). Additional study of the tectonics of these localities is necessary to quantitatively compare types of intersections and characterize those most prone to the development of a large shallow crustal magma chamber. Furthermore, the processes which cause such a

magma chamber to erupt catastrophically must be better understood in order to complete the tectonics/magma chamber/large caldera connection. This is a broad question which cannot be answered unequivocally and, like many important questions in geology, might never be completely resolved. The following points are pertinent, however:

1) Calderas appear to evolve, in most cases, from areas of preexisting volcanism (Lipman, 1984) and therefore the absence of a caldera in a "promising" volcanic locality (obvious intersection of tectonic elements) does not necessarily imply that one will not develop in the future.

2) If thermal pre-conditioning of the crust (Smith, 1979; Hildreth, 1981) (by early rise of basaltic magma) is necessary to set the stage for large scale partial melting and the resulting development of a large shallow silicic chamber, there may be considerable time lag between the development of a favorable tectonic environment and the ultimate caldera-forming eruption. At Crater Lake it is thought that radial vent alignments considered to be evidence of a shallow silicic magma chamber, developed about 63,000 years before the cataclysmic caldera-forming eruption took place 6850 ybp (Bacon, 1985).

3) Large calderas are not particularly durable in the geologic record. They become rapidly obscured by subsequent volcanism and/or erosion. For example, at Los Humeros in Mexico the presence of a 21 km caldera which first formed about 460,000 ybp with a subsequent collapse 100,000 ybp has eluded recognition until the last few years.

Thus the time between the establishment of a magma chamber and caldera formation may be on the order of 0.1 my and the time it takes to obscure the caldera may be on the order of 0.1 my. The time lag between the development of a favorable tectonic regime and the actual development of a shallow silicic chamber is not constrained but the implication is that a caldera may not be in evidence a significant portion of the time during which the tectonic setting is favorable for caldera formation. In any case it is most likely that the tectonic association is more specifically one related to the development of large crustal magma chambers than it is to the specific formation of large calderas. Large calderas are, however, a good way to identify locations of large crustal magma chambers.

Some useful observations can be made, based on the compilations of Table 3A through 3XX, pertinent to the currently favored caldera model of Eichelberger and Gooley (1977), Smith (1979), etc., and to the caldera-tectonic association.

Ashflows

Of the 82 large calderas identified, 98% occur in close proximity to large ashflows. Only one -- Askja -- is demonstrably lacking such ashflows in the caldera vicinity. At another -- Ambrym -- such ashflows have not yet been identified but are not sufficiently studied to eliminate their existence. For 45 (55%) of the calderas studied, ashflows have been specifically correlated with the caldera collapse events. 34 of the remaining 37 are not sufficiently studied and one (Ilopango) is very likely associated with a recent large-volume ashflow. At only two which have been

extensively studied, Bolsena and Bracciano, have the correlations of large ashflows with the caldera collapse not been made. These may be examples of incremental down sag due to smaller-volume eruptions (Walker, 1984). However, the possibility remains that ashflows accompanied the formation of these calderas but have not been identified as such. The example of Masaya is pertinent. Masaya was extensively studied previous to 1980 (eg. Williams and McBirney, 1979) and no significant ashflows were identified. However, recent work (S. Williams, 1982) has identified large volume ashflows which have been correlated with collapse of the caldera.

Bimodal Assemblages

The nature of the volcanic assemblage is known for 72 calderas (88%). Of these, 67 (93% of those for which data is known) display a bimodal assemblage. (The term bimodal is used in the sense of Hildreth (1981) and can include assemblages ranging from zoned intermediate to basalt/rhyolite (and undersaturated equivalents).) Three calderas do not have the mafic member of the bimodal assemblage: Toba, Gedonsurian (which is not particularly well studied) and Menengai; and two calderas are missing the silicic member: Masaya and Ambrym -- both of which are basaltic. The absence of the mafic member is not conclusive because basaltic volcanism may have reached the surface prior to the establishment of the silicic chamber and then been covered by subsequent silicic volcanism and blocked from further eruption by the density contrast of the two magma types.

The absence of silicic volcanism at Masaya and Ambrym may be problemmatical to the current caldera model (discussed in Chapter 1) and additional study of these calderas is appropriate to further resolve this difficulty. Of possible significance at Masaya is the presence of silicic ashflow volcanism accompanying caldera collapse of Apoya Caldera -- located about 5 km SE of Masaya. Ambrym is not sufficiently studied at this time.

Summarizing: given the resolution of the data, there is close to 100% correspondence between the large calderas identified in this study, and the presence of large-volume ashflow volcanism and a bimodal volcanic assemblage. This strongly supports the premises on which this study is based.

Caldera/Tectonic Classification

Simkin et al (1981) have identified 1343 "recent" volcanoes in the world (1213 excluding the Andes). Given the number of volcanoes which are considered extinct but are actually dormant, the number of capable volcanoes is probably over 2000 (not including the submarine spreading ridges). Of this number, only 82 large Quaternary calderas have been documented. When grouped in the tectonic categories described above, these calderas fall in 13 classes. The calderas are listed according to Caldera/Tectonic categories on Table 4. The most populous of these classes are those in which extensional tectonism -- rifting -- is explicitly involved. Of the 82 calderas, 74% of them are directly associated with rifting. This includes rift-involved arc volcanism and fundamental, primarily continental, plate-rifting volcanism.

Table 4
Caldera/Tectonic Classification

Tectonic Environment: ARC / INTERSECTING RIFT		
Arc	**Location**	**Caldera names**
Cascades	US	Crater Lake Medicine Lake * Newberry Caldera
Trans Mexican Volcanic Belt	western Mexico eastern Mexico	Sierra La Primavera * Los Humeros *
Central America	Guatemala	Atitlan Amatitlan
Kurile	Hokkaido, Japan Onekotan I., Kuriles Iturup I., Kuriles	Shikotsu Toya Nemo Lion's Jaw (Lvinaya Past)
Manilla	southern Luzon, Philippines	Lake Taal Laguna de Bay *
Aegean	Aegean Sea	Santorin

Tectonic Environment: ARC / ARC-PARALLEL RIFT		
Arc	**Location**	**Caldera names**
South Shetland	west of Antarctica Peninsula	Deception Island *
Kamchatka	east central Kamchatka south central Kamchatka southeastern Kamchatka	Krasheninnikov Uzon Bolshoy Semyachik Maly Semyachik Opala * Gorley Khrebet Ksudach Kurile Lake Pauzhetskaya *
Ryuku	Kyushu, Japan	Aira * Ata Kikai
Italy	west central Italy	Latera Lago di Bolsena Sacrofano-Baccano Lago di Bracciano Artemisio Phlegrean Fields

Table 4 (Continued)
Caldera/Tectonic Classification

Tectonic Environment: ARC / ARC-PARALLEL RIFT (strike-slip indicated)		
Arc	Location	Caldera names
Central America	El Salvador	Coatepeque Ilopango
	Nicaragua	Masaya
Ryuku	Kyushu, Japan	Aso
Sunda	central Sumatra, Indonesia	Toba Manindjau
	southern Sumatra, Indonesia	Ranau Gedonsurian
	Sunda Straits, Indonesia	Krakatau
	western Java, Indonesia	Danau
New Zealand	North Island, New Zealand	Taupo Rotorua Haraharo

Tectonic Environment: ARC / TRANSFORM FAULT / SECONDARY EXTENSION		
Arc	Location	Caldera names
Kurile	Hokkaido, Japan	Kutcharo Akan
New Britain	eastern New Britain	Rabaul

Tectonic Environment: ARC / OFFSET OR INFLECTION IN VOLCANIC AXIS		
Arc	Location	Caldera names
Aleutian	Alaskan Peninsula	Aniakchak Veniaminof
	Umnak I., Aleutians	Okmok
	Unimak I., Aleutians	Fisher
Banda	eastern Java, Indonesia	Tengger Idjen
	Bali	Bratan Batur
	Lompok	Segera
New Britain	central New Britain	Dakataua * Hargy

Table 4 (Continued)
Caldera/Tectonic Classification

Tectonic Environment: ARC / COLLISION ZONE (conjugate)		
Arc	Location	Caldera names
Japan	central Honshu	Hakone
New Hebrides	Ambrym I.	Ambrym

Tectonic Environment: ARC / PREEXISTING FAULT		
Arc	Location	Caldera names
Japan	northern Honshu	Towada

Tectonic Environment: ARC / ARC		
Arc	Location	Caldera names
North Suluwesi and Sangihe	North Arm, Suluwesi	Tondano Depression
New Britain and New Guinea (Solomon)	east of New Britain	Long Island

Tectonic Environment: RIFT / LINEAMENT		
Rift	Location	Caldera names
Rio Grande	northern New Mexico	Jemez (Valles) Caldera
Basin and Range	east central California	Long Valley Caldera

Tectonic Environment: RIFT / RIFT OFFSET OR INFLECTION		
Rift	Location	Caldera names
East Africa	Dubbi Line,Afar, Ethiopia	Nabro
		Asavyo
	southern Ethiopia	O'A
		Corbetti
	central Kenya	Menengai
		Suswa
Mid Atlantic Ridge	central Iceland	Askja

Tectonic Environment: RIFT / RIFT / RIFT		
Rift	Location	Caldera name
East Africa	northern Tanzania	Ngorongoro

Table 4 (Continued)
Caldera/Tectonic Classification

Tectonic Environment: RIFT / HOT SPOT		
Rift	**Location**	**Caldera names**
Snake River Plain	eastern Idaho western Wyoming	Island Park Caldera Yellowstone

Tectonic Environment: HOT SPOT		
Hot Spot	**Location**	**Caldera names**
Tibesti	northern Chad, Sahara	Emi Koussi Tarso Voon Tarso Toon Tarso Yega Yirrique

Arc Volcanism

As already discussed, of the arc-volcanism categories, AIR, AAR, AAR/S and ATE are related to rifting. Of the 65 arc calderas in this compilation, 75% (49) fall in these four classes.

Arc / Intersecting Rift

AIR is best exemplified by the situation described for the three Cascades calderas with extensional structure verging from the backarc area and intersecting at a significant angle to the volcanic arc and localizing large calderas. Other calderas where extensional tectonism verges from the backarc include: Los Humeros, Atitlan, Amatitlan, Lake Taal, Laguna de Bay, Santorini and Lion's Jaw. The types of intersecting structure for each caldera are detailed on Table 3. Los Humeros, Atitlan and Amatitlan are located where structure in the overriding plate intersects the arc: Los Humeros -- the intersecting Altiplano border Fault verging from northern Mexico; Atitlan and Amatitlan -- secondary structure related to the Polochic-Motagua Transform Fault. Santorini is related to arc-perpendicular grabens of the Aegean Sea which are of unknown tectonic origin but which, by their orientation perpendicular to the arc, do not appear to be related to arc-parallel backarc spreading. The reasoning is similar for the Palawan-Macolod Lineament which influences both Lake Taal and Laguna de Bay. This extensional feature is perpendicular to the arc and of unknown tectonic origin. Lion's Jaw caldera is intersected by a small trough verging at an angle to the arc from the backarc -- its tectonic significance is not known.

Other examples are found where the extensional structure intersects the arc from the forearc. These include: Sierra la Primavera, Shikotsu, Toya and Nemo. Sierra la Primavera is located where an arc-perpendicular graben intersects the arc. This graben is interpreted to be a possible site of imminent ridge jump of the East Pacific Rise (Luhr et al, 1985). The geometry of the trench, arc orientation, and plate convergence directions do not follow the classic pattern -- the arc does not parallel the trench -- and many interpretations can be made. However, the proximity of the ocean ridge to the trench, the abrupt change in arc strike at Sierra La Primavera, and the change in arc characteristics on either side of this intersection indicates that the subducting slab and surrounding contemporary plate tectonics are influencing volcanism and enhancing extension. This may also be true of Shikotsu and Toya which appear to coincide with the intersection of structure resulting from the interaction of the Kurile and Japan subduction zones. The location of Nemo caldera apparently coincides with contemporary (though not well understood) structure related to Kurile Forearc Plate Tectonics.

Those calderas influenced by structure intersecting from behind the arc outnumber those with structure verging from the forearc 9 to 5. The total population of this class (14) represents 17% of the total number of large calderas. Four of these calderas occur in a setting behind the main volcanic axis: Medicine Lake, Sierra La Primavera, Los Humeros and Laguna de Bay. As discussed for the Cascades, the fact that the intersecting structure is not parallel with the arc suggests that it is not related directly to backarc spreading influenced only by the subducting slab; but

is instead related to structure in the overriding plate. This situation is indicated for 10 of these calderas while the remaining four may be more directly influenced by contemporary tectonics of the subducting slab.

Arc / Arc-Parallel Rift

AAR represents the case where extensional structure is parallel to, or nearly parallel to, the volcanic arc. While this suggests similarities to backarc spreading structure, only two of these calderas occur in locations which can be unambiguously characterized as behind-the-arc: Opala and Deception Island. Deception Island does appear to be a case where backarc spreading, subparallel to the arc, comes very close to the volcanic axis of the arc. At Opala the situation is similar, with the Central Kamchatka Depression (CKD) propagating into the Opala area. However, the CKD is not a simple manifestation of backarc spreading due to contemporary Pacific Plate subduction. The CKD obviously predates the current subduction geometry because it is widest and oldest in the north -- behind an area north of the West Aleutians Transform, where subduction is no longer taking place. It therefore appears to be an inherited structure.

Other AAR calderas which occur somewhat behind the volcanic arc axis include: Pauzhetskaya and Aira. Pauzhetskaya occurs at an offset in the axis of volcanism where the Kamchatka volcanic axis steps west to the north end of the Kuriles. Although the seismicity does not reflect major changes in subduction geometry here, this offset could be related to variations in the subducting plate. Aira occurs in the

graben of Kagoshima Bay, which has been shown to be opening along preexisting structure (Aramaki, 1984). In addition, arc geometry is changing here due to the change in strike between the Nankai Trough and the Ryuku Arc. With the exception of Deception Island, none of these examples of arc-parallel structure (Deception Is., Opala, Pauzhetskaya and Aira) can be attributed to the geometry of the subducted slab in an unambiguous way.

Other calderas of this AAR class include the remaining Kamchatka calderas -- all of which occur in grabens that are colinear with the volcanic axis. The Southern Kamchatka Graben is a two-sided graben within which Kurile Lake, Ksudach and Gorley Khrebet calderas are localized. The East Kamchatka Graben is a single-sided down-to-the-east graben which localizes Maly Semyachik, Bolshoy Semyachik, Uzon and Krasheninnikov calderas -- a most impressive array of calderas. Although the CKD appears to predate the present plate geometry, the arc is segmented with some calderas occurring at segment boundaries (Pauzhetskaya, Gorley Khrebet, Maly Semyachik and Krasheninnikov). Also arc volcanism is absent opposite the subduction of Meiji Guyot. Other calderas, however, do not appear to be related to segment boundaries: Bolshoy Semyachik, Uzon and Ksudach.

Ata and Kikai calderas of Kyushu also occur in Kagoshima Bay. Although these calderas occur more or less on the volcanic axis, the opening of Kagoshima Bay has been related to the backarc spreading within the Okinawa Trough to the south. However, the geometry becomes complicated where the northern end of the Trough intersects Kyushu and preexisting structure influences deformation.

The Italian calderas (Latera, Bolsena, Sacrofano, Bracciano, Artemisio and the Phlegrean Fields) occur in a block faulted region of intersecting Apennine and anti-Apennine structure which has been overprinted by extension (presumably related to backarc spreading of the Tyrrhenian Sea). Like the Kyushu volcanics, interaction between backarc extension and overriding plate structure is indicated.

A total of 19 calderas fall in the AAR class -- 23% of the total calderas. Only one, Deception Island, is clearly related to contemporary backarc spreading. In addition, 4 of the Kamchatka calderas may relate to segmentation of the arc that could be caused by subducting plate geometry. For the sites of the remaining 14 calderas, overriding plate structure is implicated in the structural evolution of the arc and the localization of these calderas.

Arc / Arc-Parallel Rift With Strike-Slip Indicated

The AAR/S category includes those members of the AAR class for which arc-parallel strike-slip is indicated. This distinction is made because the calderas of this class tend to demonstrate more obvious tectonic control of caldera walls and large size -- including the largest caldera in the world, Toba. There are no behind-arc examples in this class. All of these calderas occur on the main volcanic axis. The role of strike-slip strongly implicates the significance of overriding plate tectonics in localizing the calderas. Coatepeque, Ilopango, Masaya and Aso all occur at offsets in the arc axis and at localities where extension and moderate strike-slip occurs due to transform plate motions. Transform faulting is a process which involves overriding

plates (ie. those that are not subducting). Therefore, the role of transform faulting at these calderas (Burkart and Self, 1985) indicates that they are localized on structures that to some degree are related to tectonics in the overriding plate.

The calderas of Sumatra and western Java occur in a classic tectonic environment where interaction of subduction-driven arc volcanism, major strike-slip transform motion and extension is taking place. The volcanic arc coincides with the locus of right-lateral distensional strike slip producing a series of en echelon extensional valleys within which arc volcanism occurs. Transform motion along this zone is on the order of 40 mm/yr. Toba, Manindjau and Ranau occur within these graben segments and are clearly controlled by the arc-parallel transform-related structure. The transform fault (Great Sumatra Fault -- GSF) ends at the southern end of Sumatra. At the southern termination of the fault, the extensional zone broadens and becomes more distributed on several normal faults -- the Semangka and Lampong Faults. Gedonsurian, Krakatau and Danau occur in this setting. East of this termination, no large calderas are found until the east end of Java (see AOI). The dominance of major transform motion at Sumatra indicates that structure in the overriding plate has a major influence on the caldera-tectonics.

At Taupo, Rotorua and Haroharo, the strike-slip is less pronounced and the dominant tectonism is extensional. As with Sumatra, the strike-slip may be related to oblique convergence between the subducting plate and the overriding plate. In these cases, however, backarc spreading appears to be a significant factor in the development of these calderas -- as they occur on strike of the Havre Trough to the

north. In the Taupo Zone, extension is colinear with the volcanic axis -- not behind the arc.

The AAR/S category includes 13 members -- 16% of the calderas. Of these, 10 reflect overriding plate structure while 3 appear more directly related to contemporary plate geometry.

Arc / Transform Fault / Secondary Extension

The ATE category includes only 3 studied examples: Kutcharo, Akan and Rabaul. The proposed submarine caldera north of Rabaul may constitute a fourth. ATE calderas occur in a setting where their localization appears to be related to structures secondary to the strike-slip transform fault geometry. In both cases, the calderas are aligned en echelon to the transform, perpendicular to the maximum principle stress (MPS). This is the orientation of secondary backarc folds (Figure 27). Extensional faulting intersects these calderas in an orientation roughly parallel to MPS. These calderas therefore appear related to the overriding-plate structure developed in response to contemporary transform plate motion.

Summarizing for rift-involved arc calderas, a total of 49 calderas fall in AIR, AAR, AAR/S and ATE classifications. This represents 60% of the total of all large calderas. Of these, indications are that 37 are dominantly influenced by structure in the overriding plate -- 76% of the total of rift-involved arc calderas.

Arc / Offset and Inflection in Volcanic Axis

Calderas of this category occur at horizontal variations in the volcanic axis -- offsets or inflections in the overall volcanic axis alignment -- with no observable influence from active tectonics in the overriding plate. However, the regions surrounding these calderas are extremely remote or covered by water. The large calderas of the Aleutians and the Alaskan Peninsula occur where long-standing subduction has taken place, and they may be passively influenced by preexisting arc-parallel folds and faults. The correlation of caldera locations with arc offsets or inflections and the lack of other evidence suggests that variations in the subducting slab (Marsh, 1982) may be influencing the location of these calderas, however these cases are ill-constrained.

The Banda Arc calderas (Tengger, Idjen, Bratan, Batur and Segera) are similar. They occur at volcanic axis alignment offsets and inflections and no other variations are evident. This situation also pertains at Hargy caldera on New Britain, although some mapped faulting crosses the island trenchward of Hargy. The significance of this faulting is unknown. Dakataua caldera is also included in the AOI category -- primarily due to lack of structural information in the surrounding submarine areas. It is located in a behind-arc setting at the edge of a broad gap in arc volcanism. There are a total of 11 calderas in this category -- 17% of the total -- all of which may be dominated by subducting plate influence.

Arc / Collision Zone

ACZ calderas occur at two localities: Hakone -- landward of the collision of the Izu Peninsula (the northern end of the Izu-Bonin Arc) with Honshu; and Ambrym -- behind the collision of the D'Entrecasteaux Zone with the Pacific Plate. The detailed structural interaction at both of these calderas remains to be determined. Workers have discussed this type of situation utilizing the indenting die model (Collot et al, 1985). Enhanced faulting (dominantly conjugate sets) is predicted outside of the zone of indention compression (Tapponier and Molnar, 1976). In relation to the direction of collision and the geometry of the collision front, both of these calderas appear to occur in areas where such enhanced faulting may be taking place. Subduction is no longer taking place in these cases, suggesting that faulting in the overriding plate is creating sites favorable for development of a shallow crustal magma chamber. Localized extension may be occurring in zones of high fault density.

Arc / Preexisting Fault

The APF category includes only one caldera -- Towada. Here is a caldera that occurs in an area that was dominated by extensional block faulting on both NNE and NNW-trending faults up to 7 m.y.b.p. but has subsequently evolved into a compressional province. Maximum compression is now considered to be perpendicular to the former normal faults such that thrusting on these faults is suggested by focal plate solutions. Caldera location may be related to magma pathways established in zones of enhanced preexisting faulting or to thinned lithosphere inherited from the

preceding extensional regime. On the other hand, the presence of Towada, and two smaller calderas (~7 km), Tazawa and Onikobe, and the obvious structural control of the calderas on the block faults suggests that extension may still be taking place. This is an excellent case where the interpretation of the tectonics in a region (compression in this case) should be carefully reevaluated in light of the caldera/tectonic implications.

Arc / Arc

There are two AA calderas -- ones which occur in settings where two arcs intersect. Tondano and Long Island are classified in this category (Toya and Shikotsu might also fit here). Tondano occurs where two arcs intersect at an acute angle -- the North Suluwesi Arc, site of southward subduction; and the East Sangihe Arc, site of WNW subduction. The E. Sangihe Arc appears to be retreating to the east, perhaps resulting in enhanced extension normal to the arc. Tondano is oriented parallel to this arc and is a narrow but long rectangular depression indicative of strong fault control of caldera collapse.

Long Island caldera is in a very different setting where two parallel arcs appear to be coming together as the plate between them (Solomon Sea Plate) is consumed in both directions. Control of volcano tectonism by subduction-related processes is indicated for both of these cases.

Rift Volcanism

Nine large calderas occur in continental rift settings, two in a transitional continental/oceanic rift setting (Afar), and one (Askja) in an oceanic rift setting. These represent 15% of the total of large calderas. Whereas the heat source for arc volcanism is subduction related, the heat source for rifting is less obvious. Mantle upwelling -- a vague concept -- is indicated. Elevated temperatures in the crust and upper mantle clearly occur but the cause and effect relationship is not well established.

Rift / Lineament

The RL category is the least constrained of the rift categories because it involves lineaments whose basic tectonic significance is not understood. Two calderas fall in the RL category: Jemez (Valles) Caldera and Long Valley Caldera. The Valles caldera occurs at the intersection of the Rio Grande Rift with the Jemez Lineament. This lineament is well defined by volcanism and is thought to represent a zone of preexisting weakness in the continental crust. Long Valley caldera is more problematical. It occurs at the intersection of the margin of the Basin and Range (where tectonic activity is most prevalent) with a number of elements including 2 E-W Landsat lineaments, the Nevada Seismic Zone, and the northward propagating Owens Valley (graben). These observations provide abundant possibilities for structural interaction, but do not provide clear evidence of the nature of such interaction; the conclusion that Long Vallley Caldera is related to B&R marginal volcanism is unavoidable.

Rift / Offset or Inflection

The ROI category includes calderas localized by either changes in rift alignment or offsets in the axis of rifting. Unlike the AOI category, calderas in this category are quite well constrained in most cases. There are 7 members of this class -- representing 9% of the total of large calderas and 58% of the non-arc rift examples.

Nabro and Asavyo are the least constrained of these cases. They fall on a line of silicic calderas which trend from the southern termination of the Red Sea rifting toward the spreading locus of the Afar. This is characterized here as a major rift offset. Some workers consider it to be the site of incipient propagating rifting (Courtillot and Vink, 1983). Such deformation in a basaltic crust of elevated temperature may produce partial melting yielding silicic volcanism.

East African Rift calderas occur at changes in strike of the rift axis. These include: O'a, Corbetti, Menengai and Suswa. These changes in strike appear to result from the adjustments of the emplacement of fissure swarms to the rift geometry of rift basins of alternating curvature.

Askja occurs at a point where the centrally restricted rifting of the northern Eastern Volcanic Zone of Iceland (EVZ) gives way to more distributed rifting across most of the width of southern Iceland. Other calderas in Iceland occur at this transition.

Rift / Rift / Rift

The RRR category is a special case of the ROI category. The sole example is Ngorongoro caldera. This caldera occurs at the intersection of three rift trends. In addition, it is located at a point where, like Askja, rifting to the north is relatively confined to a single rift valley while to the south of the caldera rifting is more distributed with numerous basins and ranges in evidence.

Rift / Hot Spot and Hot Spot

The RHS and HS categories are the calderas where hot spot volcanism is directly implicated in the caldera/large crustal magma chamber development. (Iceland -- also thought to be a Hot Spot -- is considered elsewhere and, as noted above, the examples of large ocean island calderas are not studied here on the grounds that edifice effects may strongly influence their caldera development.) There is one example of an RHS environment -- the Snake River Plain (SRP) -- which has produced two large Quaternary calderas: Yellowstone and Island Park. Although these caldera locations may be influenced to some degree by intersecting preexisting structure, the two dominant tectonic influences are the Yellowstone Hot Spot and the eastern margin of the B&R. It is known that voluminous silicic volcanism has characterized the SRP as the Hot Spot traversed from southwest Idaho toward Yellowstone. Some workers (Thompson, 1977; Christiansen and McKee, 1978) have postulated that SRP volcanism has coincided with the eastward movement of the B&R deformational front. Observationally, the calderas now occur at the intersection of B&R faulting with the Hot Spot trajectory.

The only example, on earth, of large calderas associated solely with hot spot volcanism -- the HS category -- is the Tibesti province of Africa. 5 calderas occur here which have not been influenced by preexisting structure (Vincent, 1970) and whose main observable structural relationship to crustal rocks is that they are generally distributed along a NW-trending flexure thought to be contemporaneous with magma rise (Vincent, 1970). Three of them align NE parallel to the maximum compressive stress. These calderas and associated volcanism is thought to overlie a hot spot beneath a stationary African Plate. Such a hot spot may arise due to a buildup of heat within mantle that is not being cooled by the injection of subducting slabs (Anderson, 1984). This heat would presumably produce uplift and extensional stresses that could facilitate magma rise. Another example of this type of tectonism may be the Tharsis region of Mars -- although the Tharsis calderas are probably related to edifice magma chambers.

Caldera Dimensions

The sizes and shapes of the large calderas have been compiled and examined, in the light of the caldera-tectonic categories just described, to determine if size or shape has tectonic significance.

Caldera Size

A histogram of the maximum dimension of the 82 calderas is shown on Figure 104. The clustering of the data at the 8 km minimum caldera size indicates that the hypothesized size gap, between large calderas associated with crustal tectonics and those related to edifice magma chambers does not occur above 8 km. Indeed, a number of calderas less than 8 km have been encountered during this study for which an arc/intersecting rift environment is clearly indicated, eg. Pantellaria (Strait of Sicily), Nisyros (Aegean), Vico (Italy), Tazawa (Honshu) and Tao Rusyr (Kuriles). In the non-arc rift environment, examples of sub 8 km calderas occurring at structural intersections include: Gadamsa (Ethiopia) and Elanaibori (Tanzania).

The broad spread of the limbs of the histogram caused by the anomalous size of Yellowstone and Toba suggest that the processes causing these calderas are not linear. Also, these features are the result of the formation of multiple nested calderas. Such large examples presumably reflect the existence of particularly favorable conditions -- presumably made possible by favorable tectonic conditions.

A histogram of size for each caldera/tectonic category is presented on Figure 105 A and B. In these subsets, the following observations can be made:

1) the AOI and ROI calderas tend to be smallest -- averaging 11.9 and 11.2 km, respectively;

2) the AAR/S category is more dominated by large calderas than the other classes -- averaging 24.1 km;

3) both of the RHS calderas of the Snake River Plain are anomalously large --

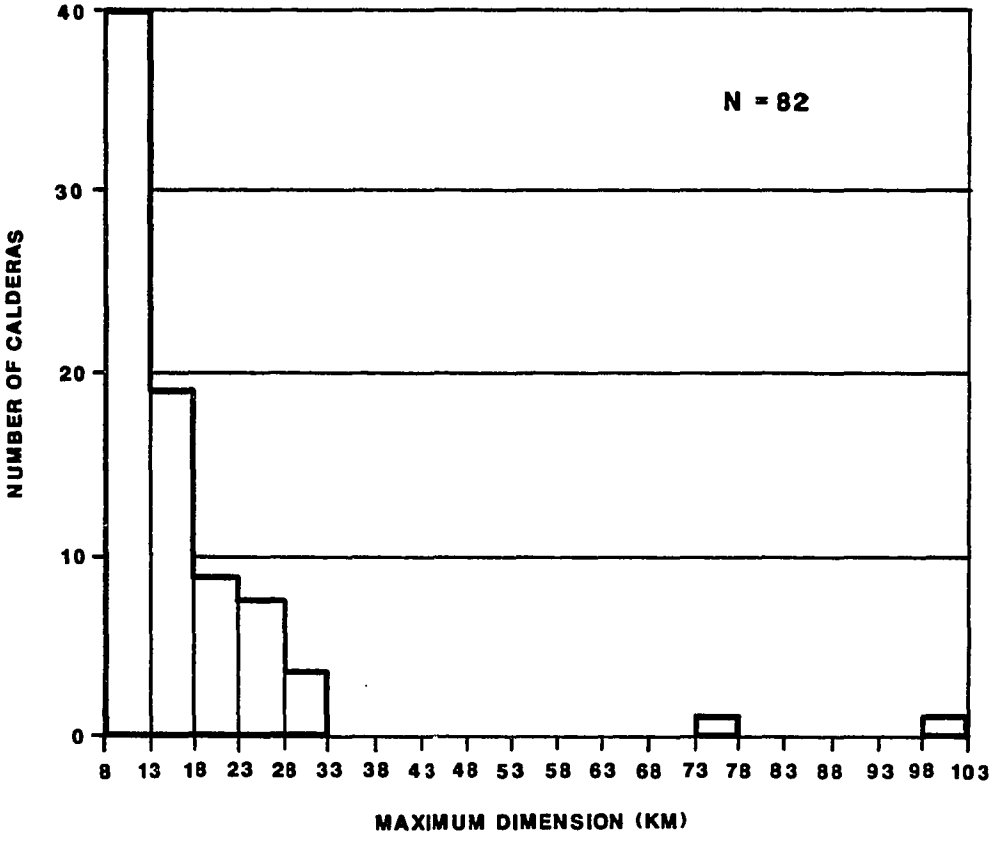

HISTOGRAM OF MAXIMUM CALDERA DIMENSION

Figure 104. Histogram of Maximum Caldera Dimension showing the number of calderas (greater than 8 km in maximum dimension) for each size range. The total population is 82 calderas.

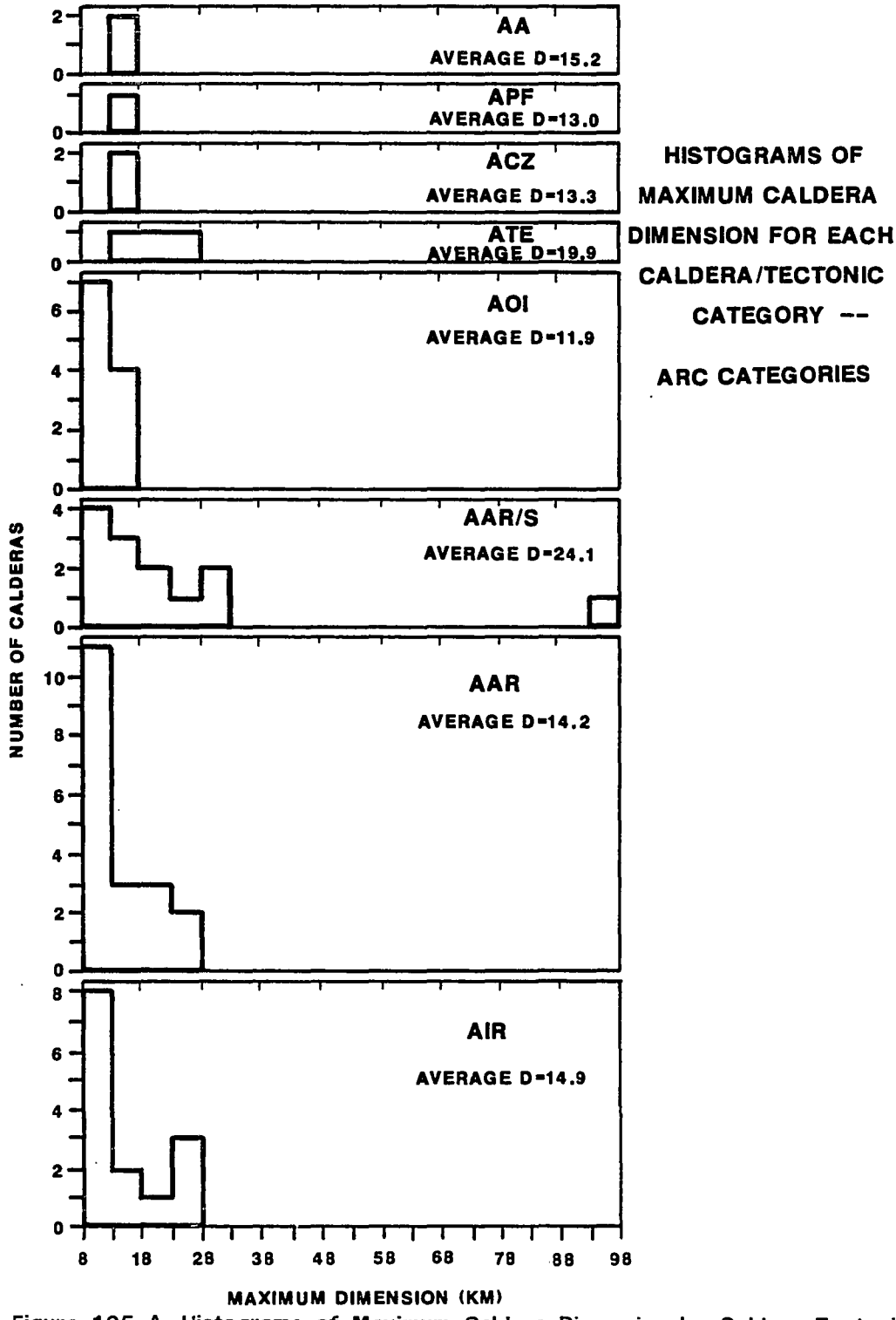

Figure 105 A. Histograms of Maximum Caldera Dimension by Caldera-Tectonic Category showing the size histogram for each separate caldera-tectonic category discussed in the text -- Arc Categories.

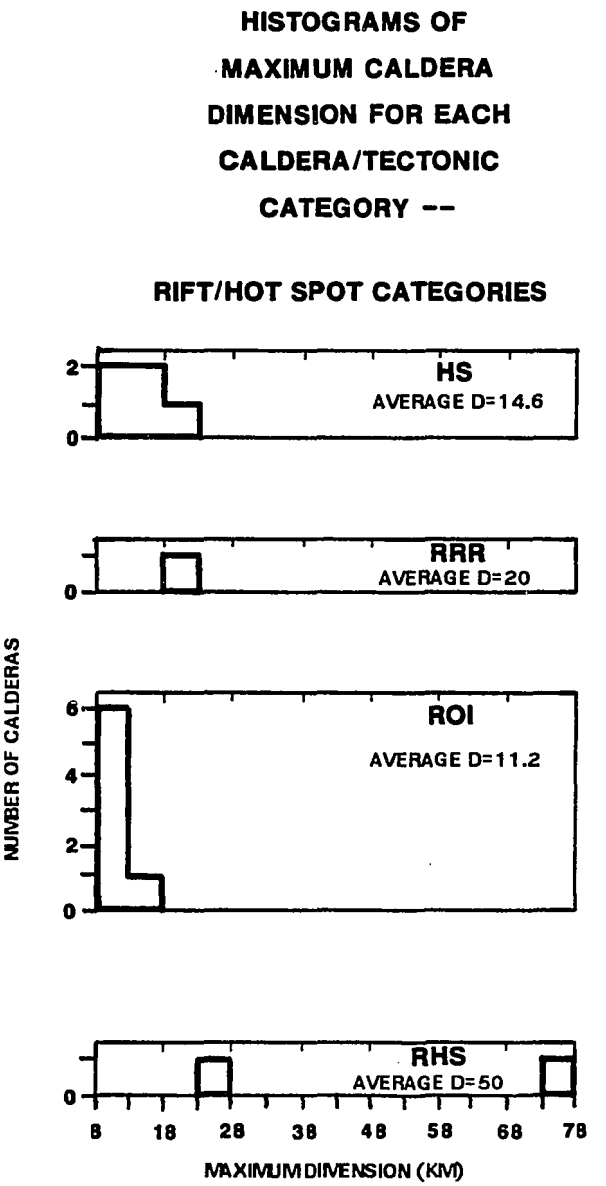

Figure 105 B. Histograms of Maximum Caldera Dimension by Caldera-Tectonic Category showing the size histogram for each separate caldera-tectonic category discussed in the text -- Rift/Hot Spot Categories.

averageing 50 km, the largest class average.

Caldera Shape

The caldera shapes have been evaluated by means of a width/length ratio, defined herein as: minimum dimension / maximum dimension; and called the aspect ratio (AR). This is a measure of caldera elongation. A histogram of aspect ratio for all 82 calderas is shown on Fig 106. A list of aspect ratio, elongation orientation relative to structure, and the crustal type for each caldera is shown on Table 5. The largest number of calderas are equidimensional with 33% greater than 0.9 AR. However, a broad range of elongation is seen. Histograms of AR are shown for each caldera/tectonic category (Figure 107). AAR/S calderas are the most dominated by elongate calderas. ROI calderas are commonly equidimensional -- not typically elongate parallel to the extension direction. This implies that the intersecting structures of ROI settings produce multiple directions of faulting such that no dominant trend controls caldera shape.

The association of elongation with extension direction is examined by means of Table 6. Calderas with an AR greater than 0.9 are essentially equidimensional within the accuracies of map measurements and caldera boundary identification. For those with an AR less than 0.9, Table 6 presents the comparison of elongation orientation relative to the orientation of the associated tectonic elements -- particularly extension direction.

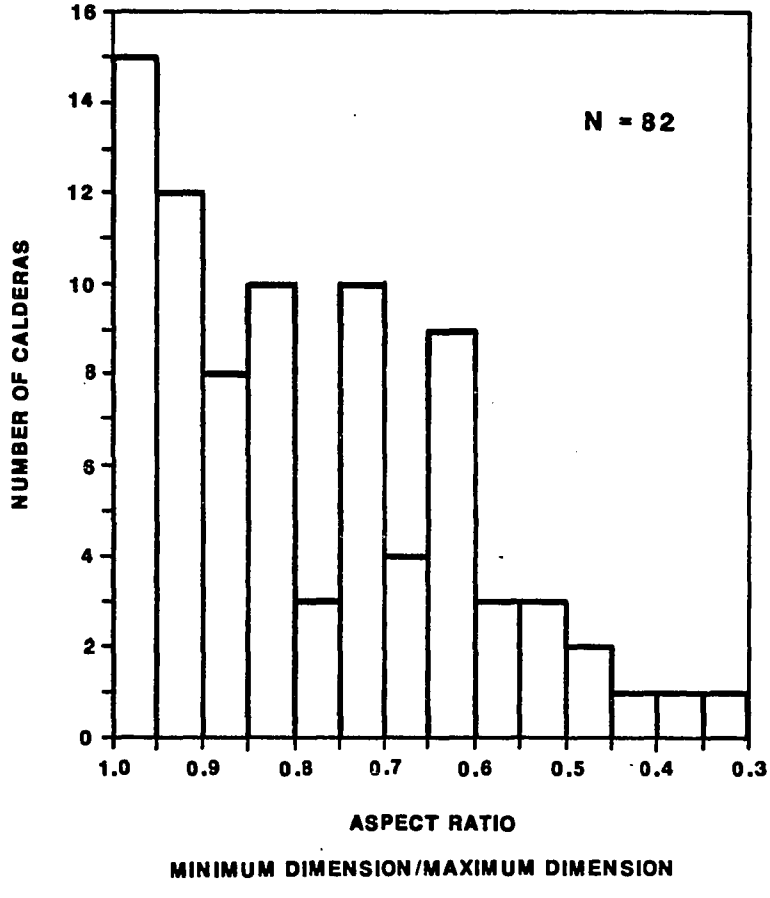

HISTOGRAM OF MINIMUM / MAXIMUM CALDERA DIMENSION

Figure 106. Histogram of the Ratio of Minimum to Maximum Caldera Dimension (Aspect Ratio) showing the number of calderas (greater than 8 km in maximum dimension) occurring within each range of aspect ratio category. The total population is 82.

Table 5
Caldera Aspect Ratio, Elongation, Crustal Type

CALDERAS OF THE WORLD WITH MAXIMUM DIMENSION > 8 km			
Caldera	Aspect Ratio AR	Elongation Orientation (for AR < 0.9)	Crustal Type
CASCADES (arc)			
Crater Lake	0.90		EC
Medicine Lake	0.78	X: B&R faulting	EC
Newberry	1.00		EC
BASIN & RANGE (rift/backarc)			
Long Valley	0.53	X: B&R faulting	EC
SNAKE RIVER PLAIN (hot spot/rift)			
Island Park	1.00		EC
Yellowstone	0.60	RA/X: B&R faulting/Snake River Plain rifting	EC
RIO GRANDE RIFT (rift)			
Jemez	1.00		EC
MEXICO (arc)			
Sierra la Primavera	1.00		EC/NC ?
Los Humeros	0.71	X/AP: Altiplano Fault/TMVB	EC/NC ?
CENTRAL AMERICA (arc)			
Atitlan	0.88	X: Secondary Graben	EC
Amatitlan	0.88	X: Secondary Graben	EC
Coatepeque	0.59	X: Median Trough	EC
Ilopango	0.73	X: Median Trough	EC
Masaya	0.61	RA: Nicaraguan Depression	EM

Table 5 (Continued)
Caldera Aspect Ratio, Elongation, Crustal Type

CALDERAS OF THE WORLD WITH MAXIMUM DIMENSION > 8 km			
Caldera	Aspect Ratio AR	Elongation Orientation (for AR < 0.9)	Crustal Type
ANDES (arc)	not catalogued		
SOUTH SHETLAND ISLANDS (arc)			
Deception Is.	0.86	X: Bransfield Trough	EC
ALEUTIAN ISLANDS & ALASKA (arc)			
Veniaminoff	1.00		CN
Aniakchak	0.92		CN
Okmok	0.91		CN/MN
Fischer	0.67	AA: volcanic axis	CN/MN
KAMCHATKA (arc)			
Krashennikov	0.90		EC
Uzon	0.50	X: East Kamchatka Graben	EC
Bolshoy Semyachik	0.83	AP: East Kamchatka Graben	EC
Maly Semyachik	0.84	X: East Kamchatka Graben	EC
Ksudach	0.64	X: South Kamchatka Graben	EC
Gorley Khrebet	0.64	X: South Kamchatka Graben	EC
Opala	0.70	RA: Central Kamchatka Depression	EC
Kurile L. Caldera	0.72	RA: South Kamchatka Graben	EC
Pauzhetskaya	0.72	X: South Kamchatka Graben	EC

Table 5 (Continued)
Caldera Aspect Ratio, Elongation, Crustal Type

CALDERAS OF THE WORLD WITH MAXIMUM DIMENSION > 8 km			
Caldera	Aspect Ratio AR	Elongation Orientation (for AR < 0.9)	Crustal Type
KURILE ISLANDS (arc)			
Nemo	0.84	RA: Central Kurile Graben	EC
Lion's Jaw	0.80	X/AA: Intersecting trough / volcanic axis	EC/NC ?
JAPAN (arc)			
Kutcharo	0.87	RA: Intersecting graben	EC
Akan	0.67	X: Intersecting graben ?	EC
Toya	0.93		
Shikotsu	1.00		
Towada	1.00		EC
Hakone	0.74	X: minimum stress adjacent to collision zone	NC
Aso	0.71	X: Beppu Shimabara Graben	EC
Aira	1.00		EC
Atta	0.75	RA: Kagoshima Graben	EC
Kikai	0.59	X: Okinawa Trough	EC
PHILIPINES (arc)			
L. Taal	0.96		EC
Laguna de Bay	0.48	RA: Palawan Macolod Lineament	EC

Table 5 (Continued)
Caldera Aspect Ratio, Elongation, Crustal Type

CALDERAS OF THE WORLD WITH MAXIMUM DIMENSION > 8 km			
Caldera	Aspect Ratio AR	Elongation Orientation (for AR < 0.9)	Crustal Type
INDONESIA (arc)			
Tondano	0.39	AA: E. Sanghe Arc	EC/NC ?
Toba	0.31	RA: Great Sumatra Fault	EC
Manindjau	0.47	RA: Great Sumatra Fault	EC
Ranau	0.81	X: Great Sumatra Fault	EC
Gedonsurian	0.83	X: Great Sumatra Fault/Lampong Fault	EC
Krakatau	0.50	X/RA: Intersecting trough/Great Sumatra Fault	EC
Danau	0.90		EC
Tengger	0.73	O: offset in volcanic axis	M/C ?
Idjen	0.82	AA: volcanic axis	M/C ?
Bratan	0.60	AA: volcanic axis	M/C ?
Batur	0.74	AA: volcanic axis	M/C ?
Segera	0.44	AA: volcanic axis	M/C ?
NEW BRITAIN (arc)			
Long Island	0.73	AA: volcanic axis	M
Dakataua	0.77	AA: New Britain Arc	EC/NC ?
Hargy	0.83	O: offset in volcanic axis	EC/NC ?
Rabaul	0.61	RA: Baining Fault	EC
NEW HEBRIDES (arc)			
Ambrym I.	0.92		M

Table 5 (Continued)
Caldera Aspect Ratio, Elongation, Crustal Type

CALDERAS OF THE WORLD WITH MAXIMUM DIMENSION > 8 km			
Caldera	Aspect Ratio AR	Elongation Orientation (for AR < 0.9)	Crustal Type
NEW ZEALAND (arc)			
Taupo	0.87	X: Taupo Volcanic Zone	EC
Rotorua	1.00		EC
Haroharo	0.57	RA: Taupo Volcanic Zone	EC
ITALY (arc/backarc)			
Latera	1.00		EC
Bolsena	0.85	RA: Radicofani-Tiber Graben	EC
Sacrofano	0.60	X: Tiber Graben	EC
Bracciano	1.00		EC
Alban Hills	1.00		EC
Phlegrean Fields	0.91		EC
AEGEAN (arc)			
Santorin	0.65	RA: Christiana-Colombo Graben	EC
CENTRAL AFRICA (hot spot)			
Tibesti			
Emi Koussi	0.88	X: NW flexure	NC
Tarso Voon	0.61	X: NW flexure	NC
Tarso Toon	0.82	X: NW flexure	NC
Tarso Yega	0.64	X: NW flexure	NC
Yirrique	0.92		NC

Table 5 (Continued)
Caldera Aspect Ratio, Elongation, Crustal Type

CALDERAS OF THE WORLD WITH MAXIMUM DIMENSION > 8 km			
Caldera	Aspect Ratio AR	Elongation Orientation (for AR < 0.9)	Crustal Type
EAST AFRICAN RIFT (rift)			
Nabro	0.94		ME
Asavyo	1.00		ME
O'A	0.91		EC
Corbetti	0.81	X: East African Rift	EC
Menengai	1.00		EC
Suswa	0.67	X: East African Rift	EC
Ngorongoro	0.85	X: East African Rift	EC
ICELAND (rift/hot spot)			
Askja	0.92		EM

Codes:	
Orientation	Crustal Type
X: parallel to extension direction	EC: extended continental crust
RA: parallel to axis of extensional structure	NC: unextended continental crust
AA: parallel to arc	EC/NC: continental crust - degree of extension unknown
O: parallel to the structure indicated	M/C: transitional mafic/continental crust
	M: mafic crust - degree of extension
	EM: extended mafic crust

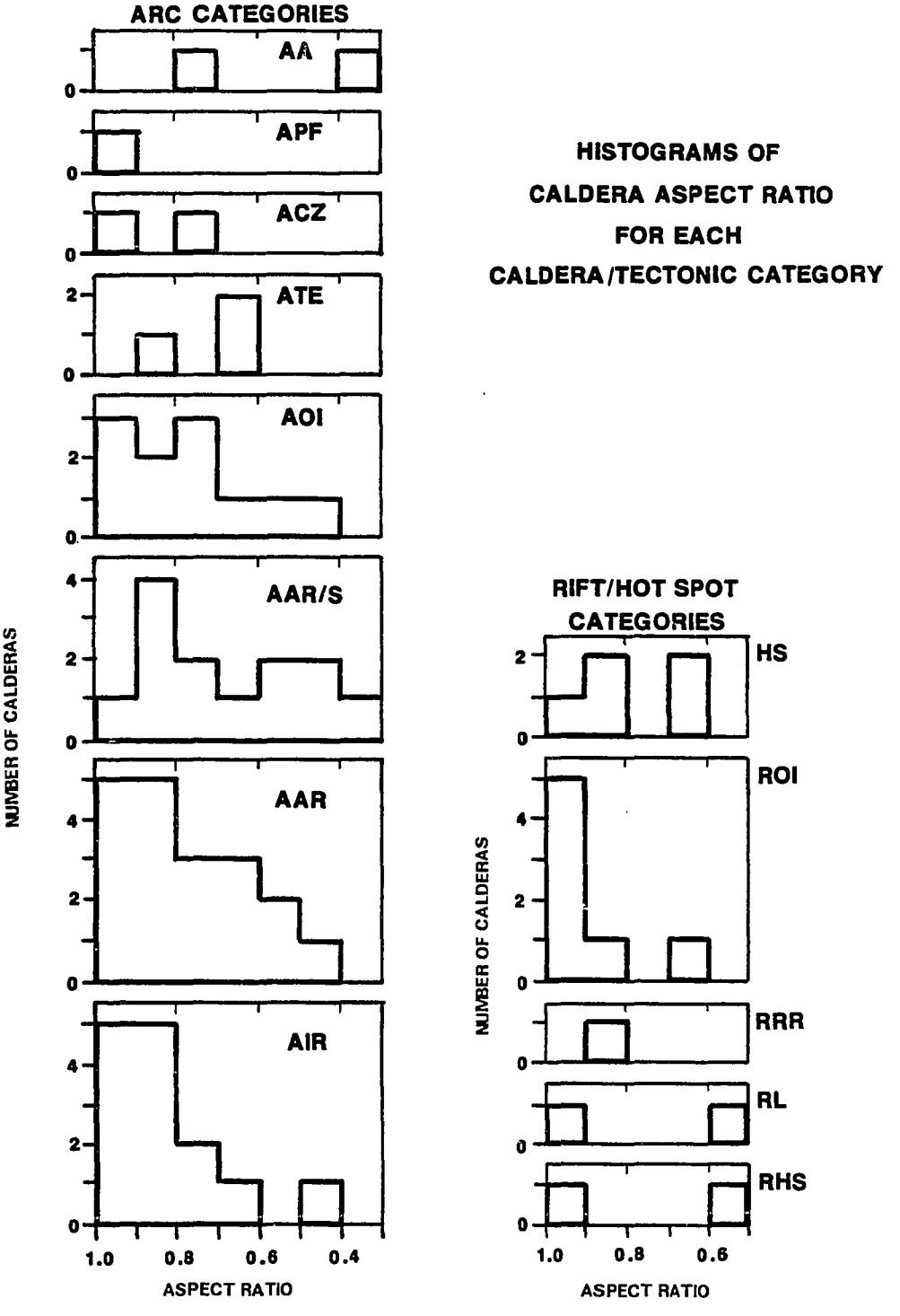

Figure 107. Histograms of Caldera Aspect Ratio by Caldera-Tectonic Category showing the aspect ratio histogram for each separate caldera-tectonic category.

Table 6
Caldera Elongation

ELONGATION OF LARGE CALDERAS RELATIVE TO TECTONIC SETTING -- figures denote numbers of calderas				
Caldera Category	X	RA	AP	O
AIR	4 (1 AP)	4 (2 AP)	1	0
AAR	8	5 (3 AP)	0	0
AAR/S	5	7 (6 AP)	0	0
ATE	1	2	0	0
AOI	0	0	6	2 (arc offset)
ACZ	1	0	0	0
APF	0	0	0	0
AA	0	0	2	0
Subtotal for arc calderas	18	18 (11 AP)	9	3
ROI	2	0	0	0
RL	1	0	0	0
RRR	1	0	0	0
RHS	0	0	0	1 (Yellowstone anomalous)
HS	4	0	0	0
Total	26	17	8	4

Orientation
X: parallel to extension direction
RA: parallel to axis of extensional structure
AP: parallel to arc
O: parallel to the indicated structure

For non-arc rift environments all 4 elongate calderas (of a rift total of 12) are parallel to the rift extension direction. Yellowstone is anomalous in that the overall elongation is parallel to the rift axis; while the two smaller, late stage calderas are elongate parallel to the extension direction. For HS calderas four of the total of five have AR less than 0.9 and are elongate parallel to the minimum horizontal stress (minimum horizontal stress). However, in the arc-involved cases, this expected relationship does not hold. Of the 47 elongate arc calderas (72% of all arc calderas), 18 are elongate parallel to the extension direction (or minimum horizontal stress); however, another 18 are parallel to the rift axis (ie. perpendicular to extension) and of these, 11 are parallel to the arc axis as well. Also 9 other calderas are parallel to the arc rather than to a rift element (one caldera, Los Humeros, is listed twice -- parallel to extension and to the arc). Two calderas are elongate parallel to arc offsets in no obvious relationship to the inferred tectonic elements.

These results indicate that for the arc calderas, in many cases arc-parallel structure (perhaps simply the geometry of the rising magma curtain) overwhelms the tendency to form elongate calderas which parallel the minimum horizontal stress. Clearly, in the arc environment the elongation of a caldera is not unequivocally related to the extension direction. The relationship between size and elongation has also been investigated; however, these factors do not correlate beyond a generai tendency for the larger calderas to be less equidimensional than the smaller ones.

Summary of Large Caldera Tectonic Charcteristics

The following points can be made from this categorization of large calderas:

1) 82 calderas greater than 8 km in maximum dimension have been identified;
2) 74% are related to rifting (localized extension may occur at the others);
3) 79% of the large calderas are related to arc volcanism and three quarters of these are related to arc / rift-involved localities;
4) for the arc calderas, indications are that 62% (40) of the caldera locations are primarily influenced by structure in the overriding plate while 38% (25) appear more directly influenced by the subducting plate geometry.
5) 7 of the 65 large arc calderas occur in behind-arc positions and 6 of these are related to rifting (the tectonic setting of Dakataua is not constrained);
6) all of the 12 calderas which occur in non-arc rift environments appear to be localized at intersections with other structural/tectonic elements;
7) the hot spot calderas of Tibesti are a special case, on a stationary plate, which do not occur at any significant structural or tectonic intersection;
8) there is a broad range of caldera sizes, 8-100 km, of which the AAR/S calderas are dominated by large calderas and the AOI and ROI calderas are dominated by the smaller-size population; however, sizes are widely scattered among the categories;
9) non-arc rift calderas are generally equidimensional but the few elongate members of this class are oriented with the maximum dimension parallel to the rift extension direction;
10) elongate arc calderas do not consistently align parallel to extension: 38% are elongate parallel to the extension direction; 38% parallel the rift axis; 43% parallel the arc axis (including 11 of those that parallel the rift axis); and 2 parallel rift offsets.

Crustal Type and Lithospheric Thickness

The role of crustal type in the formation of large calderas has not been directly addressed although observations about some provinces have been made (eg. Walker, 1984). Crustal information for the calderas of this study is given on Table 5. Distinctions are made between calderas occurring on mafic crust, continental crust (non-extended), extended continental crust and transitional cases. The breakdown of large caldera crustal type is presented in Table 7 below.

Table 7.
Large Caldera Crustal Environment
(Numbers of Calderas in each Environment)

continental crust	69
not extended (excluding hot spot)	3
not extended (hot spot)	5
extended continental crust	55
degree of extension unknown	6
transitional continental to mafic crust	7
degree of extension unknown	7
mafic crust	6
extended mafic crust	4
degree of extension unknown	2

Eighty-four percent of the large calderas occur on continental crust, and 7% occur on mafic crust. It is important to note, however, that the data base of this study is confined to calderas which occur subaerially. The proposed submarine caldera north of Rabaul is an example of a large caldera which has been obscured until early this year because of its submarine location. An additional submarine

caldera, Sumisu Jima, about 9.5 km in maximum dimension, occurs in the northern part of the Izu arc, at latitude 31°N. Little information is available on this caldera and the tectonic association is not obvious. It does occur opposite a point where the backarc spreading trough, which is absent to the north, becomes a well defined bathymetric feature. These examples indicate that additional large calderas may exist in the oceans where mafic crust is most common.

The type of crust has obvious petrologic significance to the caldera model and this has been discussed at length in earlier sections. However, consideration should be given to the idea that the lithospheric thickness is more significant than the crustal type. Lithospheric thickness is, however, very difficult to determine and, in most cases, data which does exist is integrated over great distances with low resolution. In the Basin and Range, however, the possibility of a radically thinned lithosphere is indicated by the fact that no earthquakes occur below a depth of 20 km. The fact that the large calderas of this study have been shown to have affinity for extensional areas may indicate an affinity for areas of thinned lithosphere. If we exclude hot spot related calderas on the grounds that they are "autotectonic", only 3 calderas (4%) -- Hakone, Aniakchak and Veniaminof -- occur in areas where some component of crustal extension, either primary or secondary, is not taking place.

On the other hand the thinnest lithosphere occurs at the mid-ocean ridges. In this environment large calderas are generally not known. Given the necessity for a shallow crustal magma chamber to form and remain sealed long enough for the development of a large volume of silicic melt and the associated volatiles required for

cataclysmic eruption, it is reasonable to suppose that a certain minimum lithospheric thickness is also necessary -- thereby explaining the absence of large young calderas in areas of extremely thinned crust. The association of the Cascades calderas with the recently-rifted margins of the B&R, where it intersects the arc, further indicates that the proper combination of lithospheric strength and lithospheric thinness may be optimized at such locations.

FINAL COMMENTS

In recent years, great insights have been achieved in the volcanological study of the great ignimbrite eruptions in the geological record. This has enabled the development of some conceptualizations of the broad-scale processes operating that cause these catastrophic events. By studying the tectonic regime associated with the large calderas, the preceding discussion has examined the tectonic significance of some of these conceptualizations. The presence of rifting, on variable scales, is indicated for most of the large calderas. Rifting may provide easier access to the surface for magma. On the other hand, rifting may be a reflection of thinned lithosphere and thinned lithosphere may be the necessary condition for producing the conditions that culminate -- at a moment in time -- with a 10 km wide void, 2 km thick, 5 km below the surface of the earth.

This study can only be considered a reconnaissance. However it points this writer toward one major conclusion: the presence of these large calderas constitutes important tectonic information ... in many ways more profound than the currently

favored tools of Plate Tectonic study. Our challenge is to figure out how to use the tool.

APPENDIX A

List of Imagery and Maps

LANDSAT COLOR COMPOSITES			
ID NUMBER		DATE AND LOCATION	
E-2	630-18002	10/13/76	Crater Lake
E-2	310-18000	10/13/76	Horse Ridge
E-2	630-18005	10/13/76	Shasta
E-2	630-18011	10/13/76	Lassen
E-1	041-18271	09/01/72	Crater Lake Western Cascades
E-1	077-18265	10/08/72	Three Sisters
E-2	596-18120	09/09/76	St. Helens
E-1	419-18253	09/15/73	Adams/Hood

SEASAT OPTICALLY CORRELATED RADAR IMAGES (1978)	
REV	NW SWATHS
308	Cape Blanco, Ore. - Anacapa Is., Calif.
595	Cascade Head, Ore. - San Diego, Calif.
107	Cape Meares, Ore. - Ensenada, Mex.
394	Cape Flattery, Wash. - Mexicali, Mex.
1269	Vancouver Is., Canada - Vancouver, Wash.
193	Vancouver Is. Canada - Yuma, Ariz.
1140	Vancouver Is., Canada - Yuma, Ariz.
480	Vancouver, Canada - Gila Bend, Ariz.
236	Vancouver, Canada - Seattle, Wash.
1197	Montpelier, Idaho - Chaco Canyon, N.M.
	NE SWATHS
1449	Bodega Bay, Calif. - Spokane, Wash.
761	Cape Meares, Ore. - Kamloops, B.C., Canada
230	Grays Harbor, Wash. - Gott Peak, B.C., Canada
474	Grays Harbor, Wash. - Gott Peak, B.C. Canada

SEASAT DIGITALLY CORRELATED RADAR IMAGES (1978)	
REV	LOCATION
1441	Newberry, Ore.
681	Newberry, Ore.
1406	Shasta - Medicine Lake, Calif.
107	Shasta - Medicine Lake, Calif.
351	Lassen Peak, Calif.
681	Mt. St. Helens, Wash.

U-2 HIGH ALTITUDE COLOR INFRARED PHOTOGRAPHY (188 FRAMES TOTAL)	
FLIGHT LINE NO.	75-125 (7/31/75)
AREA COVERED:	Shasta, Calif - Diamond Peak, Ore. - Silver Lake, Ore. - Lakeview, Ore.
FRAMES:	5770-5775, 5781-5782, 5791-5793, 5795-5805, 5807-5808, 5812, 5818-5839, 5841-5862, 5864
FLIGHT LINE NO.	78-107B (8/2/78)
AREA COVERED:	Maiden Peak, Ore. - Rhododendron Ridge, Ore. - Sourdough Ridge, Ore. - Riley, Ore.
FRAMES:	2331, 2333-2341, 2343-2345, 2347-2361, 2363-2370, 2373-2378, 2380, 2382, 2384-2385, 2387, 2389-2394, 2396-2403, 2405, 2407-2408, 2418, 2420, 2422, 2424-2428, 2430-2434, 2441
FLIGHT LINE NO.	79-083 (6/27/79)
AREA COVERED:	Dorris, Calif - Klamath Falls, Ore. - Lassen Peak, Calif.
FRAMES:	5149-5155, 5157-5163, 5168, 5170,5172-5180, 5268

LANDSAT BAND 7 Black and White Mosaic of Oregon (ERSAL, Oregon State University, 1973)
RETURN BEAM VIDICON Mosaic Of Oregon (ERSAL, Oregon State University, 1982)
SYNTHETIC APERTURE RADAR (X-BAND) Mosaic of Western Oregon and Washington (Washington Public Power Supply, Inc., 1981)
SIDE-LOOKING AIRBORNE RADAR (X-BAND) Image of Newberry Caldera (C. Rosenfeld, Oregon State University)
RELIEF MAP Mosaic of the Cascades (U.S.G.S., 1:250,000, Plastic)
OBLIQUELY ILLUMINATED RELIEF Mosaic of the Southern Cascades: Illumination Directions: east, northeast, west and south
GEOLOGICAL, GEOPHYSICAL and VOLCANOLOGICAL MAPS as referenced in the text
ALL AVAILABLE TOPOGRAPHICAL MAPS for the areas discussed in the text (see U.S.G.S. Index for quadrangle names)

APPENDIX B

Vent Alignment Data

Quadrangle Name	No.	Vent Alignment	Latitude N	Longitude W	Length (km)	Azimuth (°)
Harvey Mtn Calif.	1	4 Unnamed Cones - 1.9 km SW of Bogard Buttes	40.58	121.17	2.12	338
	2	2 Round Valley Butte	40.53	121.08	0.62	343
	3	2 Unnamed Cone - 1.7 km West of Bogard B.	40.59	121.18	0.60	297
	4	3 Unnamed Cones next to Larger Elongate Cone (Line 5) 3 km West of Round Valley Butte	40.53	121.12	1.80	332
	5	2 Large (el 7054') Elongate Cone Adjacent to Line 4	40.53	121.12	2.20	344
	6	2 Unnamed Cones 1 km South of Bogard Buttes	40.59	121.15	0.50	350
	7	2 large cones N of Black Butte	40.56	121.23	1.7	338
	8	2 Unnamed Cones Due West 1 km from Bogard Butte	40.60	121.16	0.62	50
	9	2 Unnamed Cones 3 km NW of Bogard & due East of Grays Flat	40.62	121.8	0.80	11
	10	2 Unnamed Cones 5 km SW of Cal Mtn	40.63	121.18	0.6	25
	11	2-3 Unnamed Cones (el 6375') 2 km SW of Cal Mtn	40.64	121.19	0.80	328
	12	3 Vents on Cal Mtn	40.67	121.16	1.1	341
Prospect	13	2 Elongate Cones on Edge of Lava Flow South of Butte Creek Ranch	40.6	121.25	0.6	332
Harvey Mtn	14	2 Cones 2 km NNE from Twin Buttes	40.60	121.23	0.6	331
Lassen	15	2 Cones 1.5 km NW from Twin Buttes	40.59	121.25	0.55	352
	16	2 Cones on Scarp at Sunrise PK	40.57	121.28	1.9	341
	17	2 Cones on Scarp at Sunrise PK	40.55	121.28	1.2	332
	18	2-3 Cones at Ash Butte	40.53	121.28	0.9	351
	19	3 Cones at Red Cender Cone	40.50	121.26	0.9	335
	20	3 Cones at Black Cinder Cone	40.46	121.23	1.6	348
	21	2-3 Cones on Summit of West Prospect Pk	40.60	121.38	0.9	1
	22	2 Cones, Red Lake Mtn	40.59	121.60	1.1	300
	23	2 Unnamed Cones NW of Red Lake Mtn	40.60	121.61	.8	330
Manzanita L.	24	3 Cones SW of Grayback Ridge	40.61	121.63	1.6	345
	25	3 Cones, Bear Wallow Bte	40.63	121.54	0.6	35
Prospect	26	2 Cones Sugar Loaf Pk	40.70	121.46	0.9	338
Burney	27	2 Cones Twin Buttes SE of Burney Mtn	40.78	121.58	1.1	350
Manzanita L.	28	2 Cones, Tumble Buttes SE	40.67	121.55	0.7	325
	29	5 Cones, Hall Bte et al unnamed, East of Freydonyer	40.70	121.55	3.8	347
Burney	30	3 Cones on Burney Mtn	40.80	121.61	1.9	314

Quadrangle Name	No.	Vent Alignment	Latitude N	Longitude W	Length (km)	Azimuth (°)
	31	3-4 Cones on NE Flank of Burney Mtn	40.83	121.58	3.1	350
	32	4 Cones on Cinder Butte (Hat Creek Flow)	40.87	121.50	2.0	333
	33	2 Cones on Cinder Butte	40.88	121.50	1.6	339
	34	2 Cones on Hat Creek Flow North of Cinder Butte	40.91	121.41	1.0	16
Jellico	35	2-3 Cones	40.96	121.28	0.5	334
Hambone	36	2 Cones NW of Deep Crater (SW Edge of Burnt Lava Flow)	41.47	121.56	0.4	334
	37	4+ Cones along SW Side of Burnt Lava Flow	41.46	121.56	2.0	312
	38	3 Cones, Snag Hill	41.46	121.63	2.0	322
	39	2-3 Cones, unnamed, South of Six Shooter Butte	41.50	121.61	1.2	30
Medicine L.	40	2 Cones, Six Shooter Bte	41.51	121.61	1.0	46
	41	3 Cones (Silicic) NNW of Glass Mtn	41.61	121.53	0.8	351
	42	Fissure Vent (Silicic) NE Flank MT Hoffman	41.62	121.55	0.7	322
	43	3-4 Cones (Silicic), Pumice Mine NNW of Glass Mtn	41.60	121.52	0.9	333
	44	3-4 Silicic Vents Glass Mtn	41.59	121.50	2.5	335
Timber Mtn	45	2 Cones on S Flank of Black Mtn	41.51	121.48	0.3	341
	46	2 Vents (Basaltic) between Lyons PK & Black Mtn	41.56	121.49	0.8	337
Medicine L.	47	3 Cones, Three Sisters	41.72	121.74	1.9	N-S
	48	3-4 Cones, Red Cap Mtn	41.55	121.75	1.7	10
	49	1 Cone and Explosion PTS Paint Pot Crater	41.55	121.71	0.4	48
Bray	50	3 Cones, Squaw Peak +2	41.55	121.77	1.4	23
	51	5 Cones (Silicic), Garner Mtn	41.60	121.77	1.4	41
Medicine L.	52	Explosion Pits. Doe Peak	41.50	121.75	0.8	51
Bray	53	3-4 Cones, Fisk Ridge	41.51	121.80	2.0	47
	54	2 Cones, Stevens Butte	41.51	121.88	0.6	45
Medicine L	55	Ground Cracks Connecting Vents (Fink & Pollard,1983)	41.58	121.63	4.1	27
	56	Ground Cracks (Fink & Pollard,1983)	41.63	121.61	4.4	16
Shasta	57	4 Cones N of Swamp Cr. Ridge	41.41	122.0	2.0	37
	58	2 Cones, Swamp Cr. Ridge	41.40	122.01	1.9	3
	59	2 Cones, Sugar Pine Butte	41.38	122.01	2.0	26
	60	4 Domes, S. Flank Shasta, Gray Butte to McKenzie Butte	41.33	122.20	3.8	354
	61	2 Cones, N Flank of Shasta East of Coquette Falls	41.45	127.20	0.7	N-S
Whaleback	62	3 Cones, Whaleback	41.53	122.13	0.9	6
	63	2 Cones between Whaleback and Deer Mtn	41.58	122.12	0.6	19
	64	2 Cones just N of Deer Mtn on N side of Grass L.	41.68	122.15	1.3	354
	65	2 Cones E of Whaleback	41.53	122.11	0.4	69
	66	2 Cones, W side of Haight Mtn	41.56	122.05	0.6	309
	67	3 Cones SW of Orr Mtn	41.61	122.03	0.6	350

Quadrangle Name	No.	Vent Alignment	Latitude	Longitude	Length (km)	Azimuth (°)
	68	2 Cones between Little Deer Mtn and Horsethief Butte	41.68	122.08	0.6	14
Dorris	69	6+ Cones, not rigorously attached, but unambiguously aligned parallel to a fault which extends from south of the alignment	41.83	121.96	8.1	N-S
Macdoel	70	2 Cones E of Ball Mtn	41.81	122.10	0.8	N-S
	71	2 Cones NE of Willow Cr. Mtn	41.85	122.20	1.2	355
	72	2 Cones N of Meiss Lake	41.93	122.07	1.4	342
	73	2 Cones SW of Pleasant Valley just below Oregon border	41.96	122.10	0.8	351
	74	3 Cones on N side of Parker Mtn	42.13	122.27	2.1	347
Hyatt Resevoir	75	3 Cones on summit of Grizzly Mtn (possibly > 5 m.y. old)	42.05	122.28	1.9	358
Surveyor Mtn	76	3 Cones on E flank of Buck & Surveyor Mtns	42.20	122.11	1.3	345
	77	5 Cones of Chicken Hills	42.03	122.05	5.3	342
	78	4 Cones west of the S end of Aspen Lake	42.33	122.05	2.8	344
Modoc Pt	79	3 Cones at Ball PT (Klamath L.)	42.42	122.00	2.5	315
Mt. McLoughlin	80	2 Cones W of Brown Mtn Robinson Bte	42.36	122.38	1.3	359
Lake o the Woods	81	one of 2 en echelon alignments of 3 Cones each, N flank of Mt Harriman (NE of L. of the Woods)	42.40	122.10	4.5	345
	82	en echelon mate to 81	42.43	122.10	4.0	345
	85	2 Cones SW of Pelican Bte (near Lost Cr)	42.48	122.20	1.3	N-S
Pelican Bte	86	2 Cones NE of Pelican Bte (E of Cherry PK)	42.58	122.08	1.1	N-S
	87	2 Cones, N of #86	42.61	122.11	1.5	N-S
Crater L.	88	3 Cones N of Goosenest	42.80	121.15	1.4	7
	89	3 Domes E of Mt Scott (N of Scott Cr)	42.91	121.95	2.3	290
	90	2 Domes SE of Mt Scott (S of Scott CR)	42.90	121.96	1.9	307
	91	2 Vents at end of #89	43.00	122.00	1.2	39
	92	2 vents SW of Crater L. at Castle PT	42.88	122.25	1.8	337
	93	2-3 Domes at Sharp Pk (Bacon, 1983)	42.88	122.25	1.8	337
	94	Devil's Backbone (Dike) W Wall of Crater	42.95	122.16	0.4	316
Diamond L.	95	2 Cones at Timber Crater N of Crater L	43.05	122.07	2.2	356
Lenz	97	2 Cones ENE of Boundary Bte (SE of Crater L)	42.81	121.86	1.4	N-S
Garwood Bte	98	Garwood Bte, 3-4 vents (mapped as one on Luedke and Smith Map)	43.15	122.28	1.2	355
Summit L.	100	3 Cones at Red Cinder Bte	43.30	122.07	2.7	356
	101	(3-5) Small cones E of Summit L.	43.45	121.07	2.5	N-S

Quadrangle Name	No.	Vent Alignment	Latitude	Longitude	Length (km)	Azimuth (°)
Crescent	102	Crescent Butte & 4 other cones (possibly > 5 my old, not shown on azimuth frequency plots)	43.74	121.65	4.6	7
Summit L.	103	2 Cones, Diamond Rockpile (S of Diamond PK)	43.48	122.15	1.2	62
	104	2 Cones at summit of Crater Bte (elongation and alignment)	43.50	122.12	0.9	N-S
Odell L.	105	2 Cones, Royce Mtn (elongation and alignment)	43.52	121.90	1.4	N-S
Hamner Bte	106	2 Cones, Saddle Bte N flank of Hamner Bte	43.58	121.78	1.8	N-S
	107	3 Cones on summit of Ringo Bte	43.55	121.75	2.6	N-S
Davis Mtn	109	2 Cones at NW foot of Davis Mtn	43.63	121.82	0.8	5
Wickiup Dam	110	4 Cones at NE foot of Davis Mtn	43.63	121.72	2.3	356
	111	3 Cones, Gilchrist Butte, parallel to elongation and faulting	43.63	121.65	0.8	12
	112	3 Cones, Hamner Butte, Wright Butte and one other	43.67	121.63	3.8	12
Irish Mtn	113	4 Cones S of Irish Mtn	43.82	121.97	3.0	5
Elk L.	114	4-5 Cones W of Elk Lake	43.95	121.87	2.5	3
	115	2 Cones W of Senoj L. continuation of #114	43.92	121.87	0.9	12
	116	Lucky Butte S of #114 & #115	43.88	121.87	0.7	315
	117	3 Cones, Williamson Mtn, parallel to elongation	43.93	121.82	1.6	312
	118	2 Cones S of Lucky L.	43.90	121.80	1.4	344
Davis Mtn/ Crane Prarie Reservoir	119	4 Maars N & S Twin lakes, an unnamed, Shukash Butte and Wuks Butte	43.75	121.77	6.9	N-S
Round Mtn	120	2 vents of Palanush Bte	43.77	121.75	0.6	310
	121	2 Cones, Round Mtn + one other	43.77	121.70	1.9	N-S
Round Mtn + Bachelor Bte	122	11 Cones from Lumrum Bte to S side of Sheridan Mtn (sum of 2 en echelon segments)	43.87	121.68	5.0	353
	123	2 Cones on N side of Lookout Mtn	43.83	121.68	0.7	340
	124	4-5 Cones on N flank of Sheridan Mtn	43.90	121.70	2.1	4
Pistol Bte	125	4-5 Maars of Wake Bte	43.83	121.62	4.8	333
Pistol Bte + Wanoga Bte	126	7 Cones incl: Lolo Bte, Klak Bte 2 sections: Lolo +2; Klak-Northward	43.87	121.62	 1.3 2.1	 343 9
Wanoga Bte	127	6 Cones SE of Wanoga Bte	43.88	121.53	4.0	350
Wanoga Bte + Ann's Bte + Pistol Bte	128	4 Cones SE of Wanoga Bte	43.87	121.50	2.4	335
Wanoga Bte	129	3 Cones N of #128 plus 2 cones en echelon and to the west	43.90	121.52	0.6	344
	130	2 Cones SE of Katalo Bte	43.95	121.53	1.6	353
	131	3 Cones (Dogleg) E of Katalo Bte. N. Leg. S. Leg.	43.95	121.55	 1.1 0.8	 327 354

Quadrangle Name	No.	Vent Alignment	Latitude	Longitude	Length (km)	Azimuth (°)
	132	2 Cones E of Kapka Bte	43.96	121.57	1.1	326
	133	2 Cones (L & S map one) N of Kapka Bte	43.98	121.60	1.1	326
Ann's Bte	134	5-6 Cones E of Sun River	43.87	121.38	3.0	347
Broken Top	135	3 Cones SW of Todd L. (S of Broken Top)	44.00	121.70	1.6	N-S
	136	2 Cones at N foot of Tumalo Mtn	44.01	121.65	1.6	331
	137	2 Cones at N base of Bachelor Bte	44.00	121.68	0.9	N-S
Three Sisters	138	2 Cones Telapus Bte & Fatsuk Bte	44.01	121.75	2.2	355
	139	Silicic Domes on S. flank of S. Sister, 2 en Echelon segments	44.03	121.75	6.0	N-S
	140	2 Cones on Burnt Top between Top L & Nash L.	44.03	121.87	1.3	305
	141	3 Small Cones SE of Koosah Mtn	44.01	121.80	0.5	N-S
Tumalo Dam	142	3 Cones adjacent to Tumalo Dam	44.15	121.42	3.1	333
Three Sisters	143	2 Cones of Two Butte, W. of N Sister & NW of Linton L.	44.20	121.92	1.3	N-S
	144	2 Cones, Condon Bte and small cone to SE	44.22	121.83	1.5	315
	145	2-4 Cones of Four-In-One NE of N Sister	44.20	121.80	0.9	15
	146	2 Cones on "The Island" N of N Sister	44.23	121.78	1.2	8
Three Sisters + Three Finger Jack	147	6-8 Cones N of N Sister (N of Yopah L.)	44.25	121.76	5.0	18
	148	3-4 Cones, W side of the Belknap Flows	44.30	121.90	4.1	N-S
Three Finger Jack	149	2 Cones at Twin Craters NE Flank of Scott Mtn	44.25	121.89	0.6	N-S
	150	6 Cones across Sand Mtn	44.36	121.93	4.0	5
	151	3 Small Cones next to Lost L.	44.43	121.90	1.4	7
	152	2 Cones transverse to #150	44.37	121.93	1.3	71
Henkle Bte	153	3 Cones S of Henkle Bte	44.32	121.47	5.3	342
	154	6 Small Cones W of Fryer Bte	44.25	121.48	4.8	356
Mt. Jefferson	155	2 Cones, S. Cinder Pk and 1 lava vent N of Rockpile Mtn	44.57	121.82	1.6	14
Whitewater River	156	3-4 Cones W of Metolius R., W of Wizard Falls	44.52	121.65	3.7	346
Crescent 2° Sheet	157	4 Cones of Bunchgrass Buttes (same lava flow)	43.33	121.67	38	326
Hogback Butte	158	6 Cones of Squaw Butte	43.45	121.75	2.5	337
Geolgic Map of Newberrry (MacLeod et al, 1982)	159	3 vents, Moffit Bte + 2 unnamed	43.52	121.45	1.8	38
	160	A) Ipsoot Bte and 3 unnamed cones at south end of this alignment, 3.5 km N. of Spring Bte B) Ipsoot Bte and 2 unnamed cones which merge with 160A	43.55	121.37	1.2 1.5	24 60

Quadrangle Name	No.	Vent Alignment	Latitude	Longitude	Length (km)	Azimuth (°)
		C) 3 unnamed cones. Segments #160 A & B merge and curve into #160C			2.1	355
	161	6 Cones, SW flank of Newberry 10 km NNW of Spring Bte	43.62	121.38	3.4	338
	162	5 small cones, 1.8 km NE of Spring Bte (SW of Green Bte)	43.53	121.30	2.5	35
	163	2 en echelon segments summed (7 cones) 4.3 km W of Willow Bte	43.55	121.22	2.8	23
	164	3 en echelon segments summed (13 cones) S. of #163	43.54	121.22	5.6	33
	165	6 Cones, 7 km S of Newberry Caldera	43.62	121.25	2.5	10
	166	5 Cones, Topso Bte, Kweo Bte + 3 others, 4 km S of Newberry Caldera	43.65	121.20	3.8	17
	167	5 Cones, 2.2 km S of Newberry Caldera	43.65	121.23	2.2	N-S
	168	4 Cones, 1.5 km S of Newberry Caldera	43.65	121.25	3.1	347
	169	3 Cones, + fissure: Cinder Cone + 2 unnamed cones 8 km SW of China Hat	43.65	121.12	2.8	4
	170	3 Cones, Lowullo Bte + 2 unnamed, 3.8 km NE of East Lake	43.77	121.18	1.6	335
	171	Fissure of the Lava Cascade Flow 6 km N of Newberrry Caldera	43.80	121.27	2.0	339
	172	6 Cones adjacent to Mokst Bte flow, 11 km N of Newberry	43.85	121.32	4.7	321
	173	3 Cones, Sugarpine Bte + 2 unnamed	43.82	121.38	3.4	325
	174	10cones, 3 km NNW of #173	43.87	121.39	3.6	349
	175	1 Cone, Fuzztail Bte, + fissure	43.87	121.20	1.8	N-S
	176	1 Cone + 3 fissure segments, 3.8 km E of Bessie Bte	43.95	122.22	3.1	348
	177	3 Cones + fissure segment, 1 km N of #176	43.98	121.22	2.4	335
	178	Fissure cutting N. rim of Newberry Caldera from E. Lake	43.75	121.25	3.5	229
Diamond Swamp	179	1 Cone + 4 pit craters, Diamond Craters East of Malheur and Harney Lakes, central Oregon	43.08	118.77	1.2	293
	180	Vent-filled fault-bounded depression (16-20 vents) with strong elongation	43.10	118.78	1.2	306

APPENDIX C

Volume/Area calculation

Volume and area calculations have been completed for the Cascades volcanics (< 5 m.y.b.p.) in order to compare the volcanic distribution along the Cascades axis with the occurrence of intersecting tectonic elements. The details of the calculations and plots of the results are presented in this appendix. A discussion of the significance of these data is included in Chapter 3. Volume calculations were carried out at a scale of 1:500,000 utilizing the existing topographic maps of the states of Washington, Oregon and California, and the maps of the occurrences of recent volcanics published by Leudke and Smith (1983, 1984). Luedke and Smith have divided the occurrence of volcanic rocks in the western US to time intervals of 0-5; 5-10; and 10-16 m.y.b.p.. Volume for the 0-5 m.y. volcanics were calculated. Existing outcrops are extrapolated across erosional features to approximate their original extent. Areas of outcrop were divided into subareas within which the topography could be approximated by geometric volumes (cones, pyramids, etc.). Base areas were determined utilizing a Tamaya Planix 3 digital linear-type planimeter (resolution: 0.1 square cm; accuracy: 0.2%).

The determination of base elevation is the most subjective aspect of this exercise (assuming that the mapping of units is accurate). To estimate base area, the mapped extent of units was overlain on the topographic maps and the minimum elevation of outcrop was used for the local base elevation. Two offsetting considerations are involved in this approximation. First, this approximation will in

some cases overestimate the volume of volcanics in cases where a lava flow which has flowed over sloping older ground such that the bottom of the flow is not a horizontal base. On the other hand, in areas of extensive young volcanics where the bottom of the volcanics is not exposed and where the volcanics likely accumulated in graben-like depressions, the accumulations of volcanic deposits may be underestimated. Recent drilling on Mt. Hood and at Newberry has demonstrated thicknesses of High Cascades volcanics far greater than anticipated based on volcano morphology. In order to examine the volcanism along the Cascades axis (as opposed to backarc volcanism), the volcanics associated with Newberry Volcano have not been included in the calculation. Although Medicine Lake is also a backarc volcano, it has been included on the grounds that it is more intimately associated (geographically) with contemporaneous Cascades volcanism in California. There is no disctinct geographic separation between Medicine Lake and Shasta, while there is between Newberry and the Cascades axis. Additional adjustments arise from the fact that the (late) High Cascades volcanism started about 4 m.y.b.p. while the maps show volcanism greater than 5 m.y.b.p. Thus there is a need to do some filtering in order to represent the (late) High Cascades episode for which the tectonics are being considered. For the present calculations, the following adjustments have been made: the exclusion of the Simcoe basalts (east of Mt. Adams) -- thought to have been erupted prior to the (late) High Cascades (Washington Public Power Supply, Inc., 1981); and the exclusion of basalts of the Deschutes basin (NNW of Newberry) which are thought to precede (late) High Cascades volcanism (Taylor, 1973). These

areas are indicated on Figure A-1 east of the dashed line. Also, in areas on the west side of the Cascades where High Cascades volcanism manties Western Cascades landforms (eg. Diamond Peak) the base elevation used for calculation was raised to reflect these pre-existing landforms.

The methods of volume calculation utilized herein are approximate owing the the assumptions made about volcanic thickness controlled by a horizontal base elevation. However, the method is applied consistently throughout and provides a reasonable and systematic estimate of volume which is appropriate for general interpretations and relative comparisons of along axis distribution of volcanism. For detailed analyses of individual volcanic centers, more specific calculations combined with field checking would be appropriate.

The total area of volcanics is determined to be 44997 km^2 and the average area per 0.5° latitude is 2363 km^2 which translates to 42 km^2 per km. A maximum value for area of volcanics is 5212 km^2 per 0.5° latitude (95 km^2/km), found between 40.5° and 41°N; and a minimum value of 0 is found between 47.5° - 48°N. Total volume of volcanics for the Cascades is determined to be 13094 km^3 and the average volume per 0.5° latitude is 689 km^3 which amounts to 1.7 km^3 per km. A maximum volume of 1483 km^3 is found between 44° and 44.5°N (Three Sisters) which is 27 km^3 per km and a volume of 1376 km^3 is found between 41.5° and 42°N (Shasta) which is about 25 km^3 per km.

The following figures complete this appendix:

Figure A-1. Map of volcanic rocks less than 5 m.y.b.p. (Smith & Luedke, 1985).

Areas excluded from Volume/Area calculations are those located east of the broad dashed line.

Figure A-2. Volume of volcanics in the Cascades for 0.5 degree latitude increments: total volume; and separate curves for andesite, basalt, dacite and rhyolite.

Figure A-3. Area of volcanics in the Cascades for 0.5 degree latitude increments: total area, and separate curves for andesite, basalt, dacite and rhyolite.

Figure A-4. Percent andesite, basalt, dacite and rhyolite for each 0.5 latitude degree bin.

Figure A-5. Percent of total Cascades volcanic volume occurring at each 0.5° latitude bin. A smoothed curve of this data is shown as a dashed line (see text).

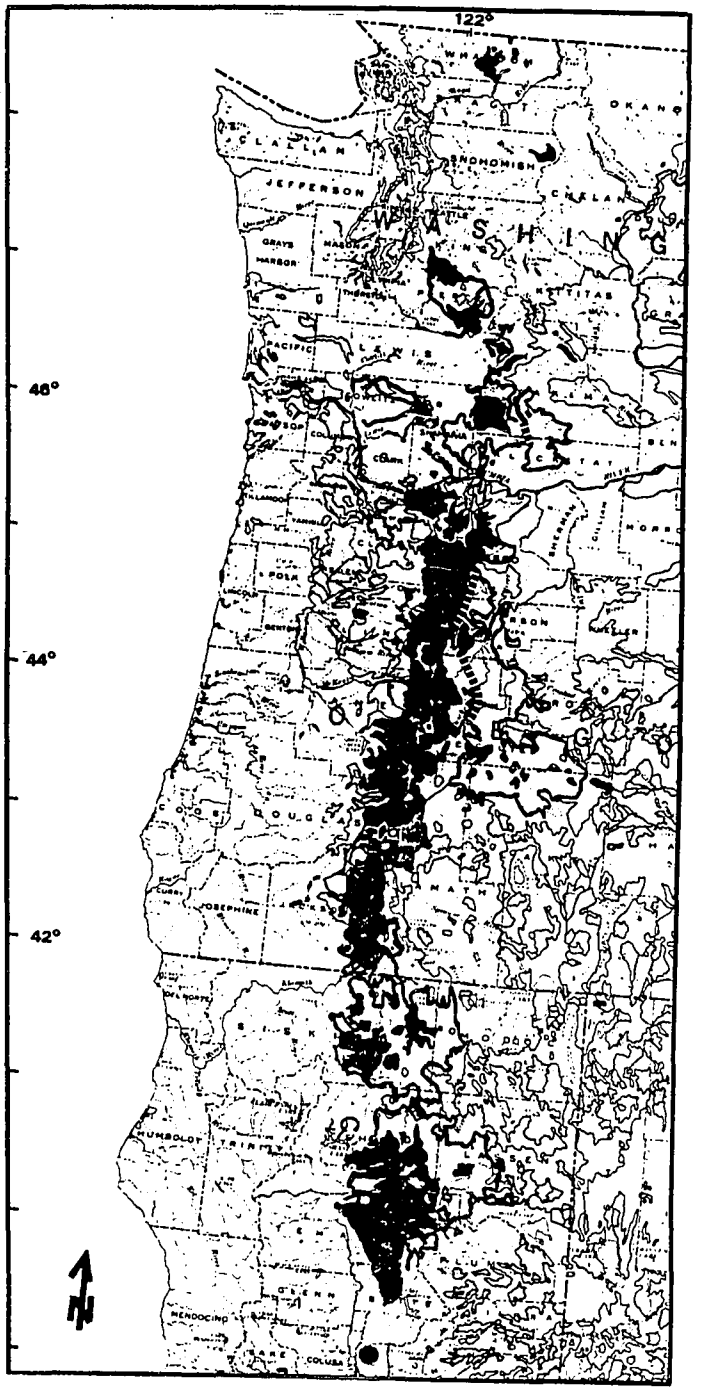

Figure A-1. Map of volcanic rocks less than 5 m.y.b.p. (Smith & Luedke, 1985). Areas excluded from Volume/Area calculations are those located east of the broad dashed line.

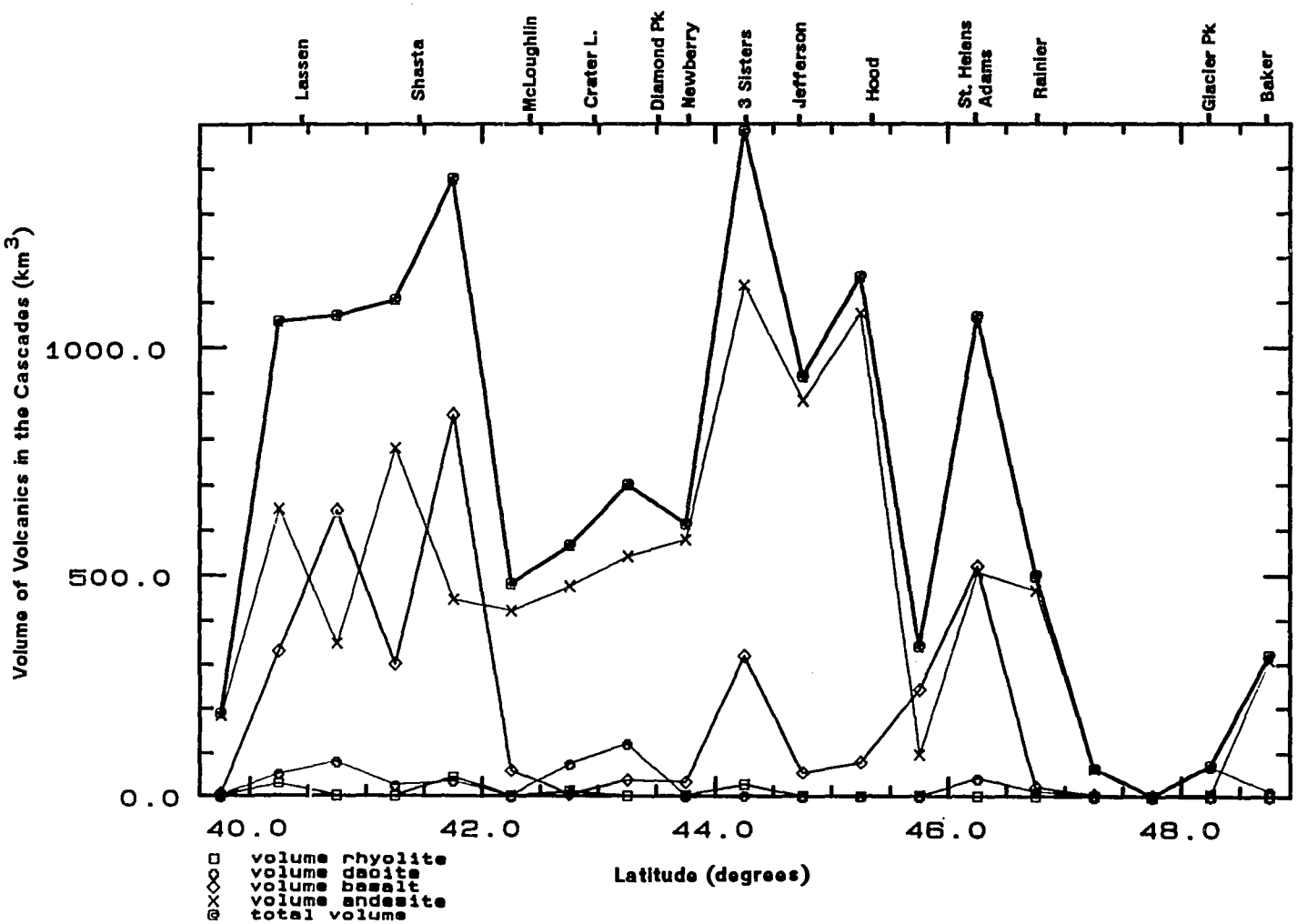

Figure A-2. Volume of volcanics in the Cascades for 0.5 degree latitude increments: total volume; and separate curves for andesite, basalt, dacite and rhyolite.

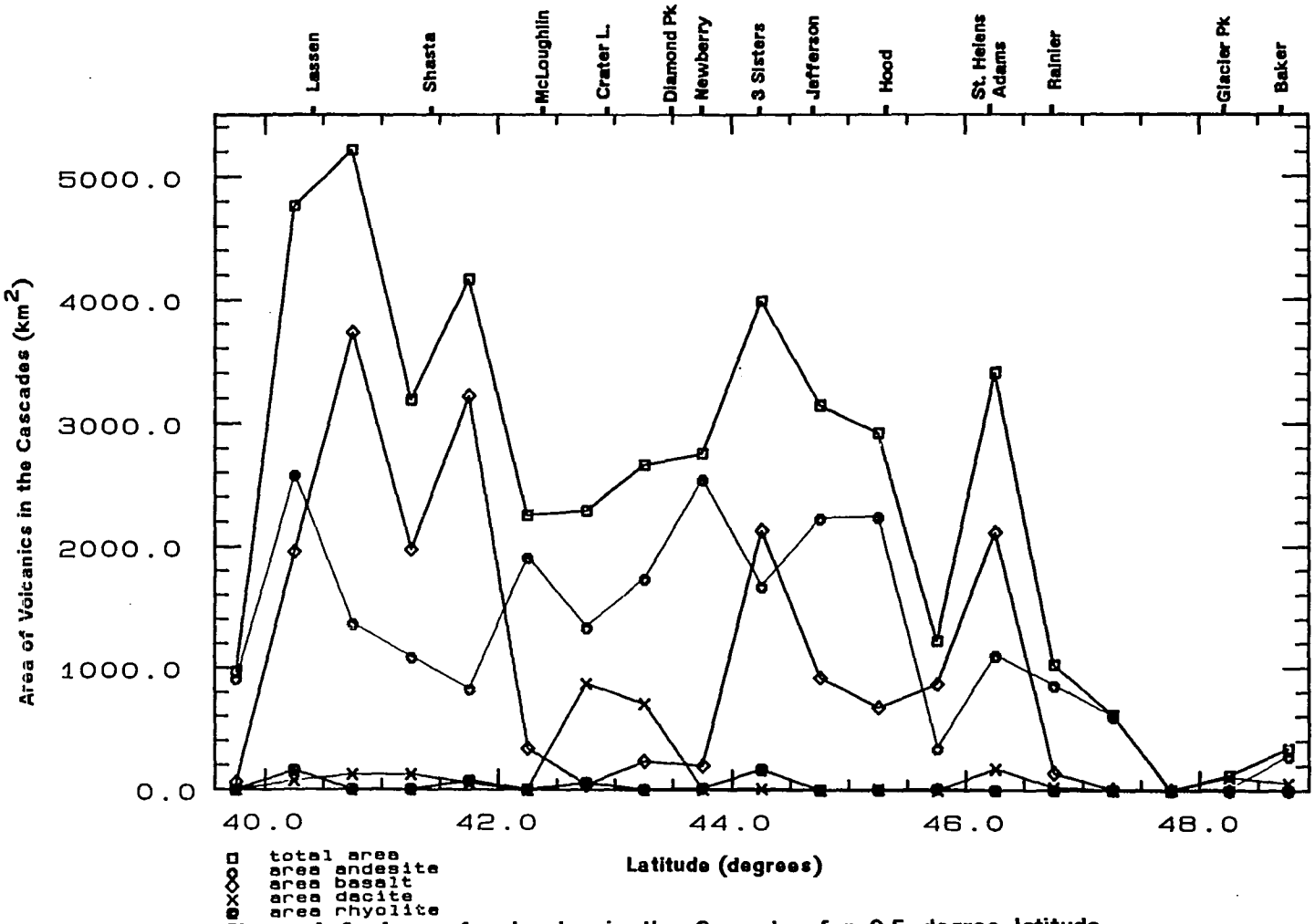

Figure A-3. Area of volcanics in the Cascades for 0.5 degree latitude increments: total area, and separate curves for andesite, basalt, dacite and rhyolite.

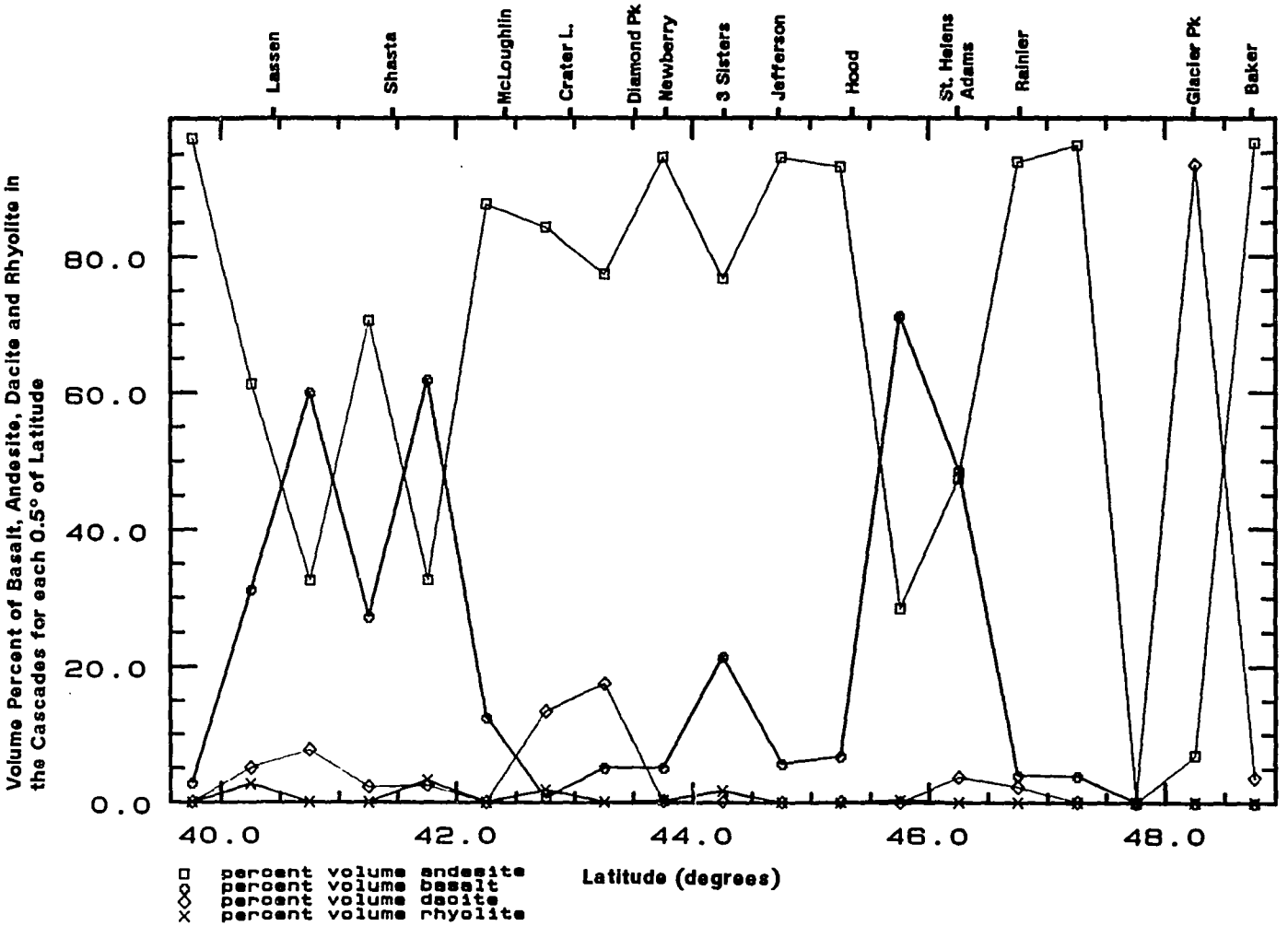

Figure A-4. Percent andesite, basalt, dacite and rhyolite for each 0.5 latitude degree bin.

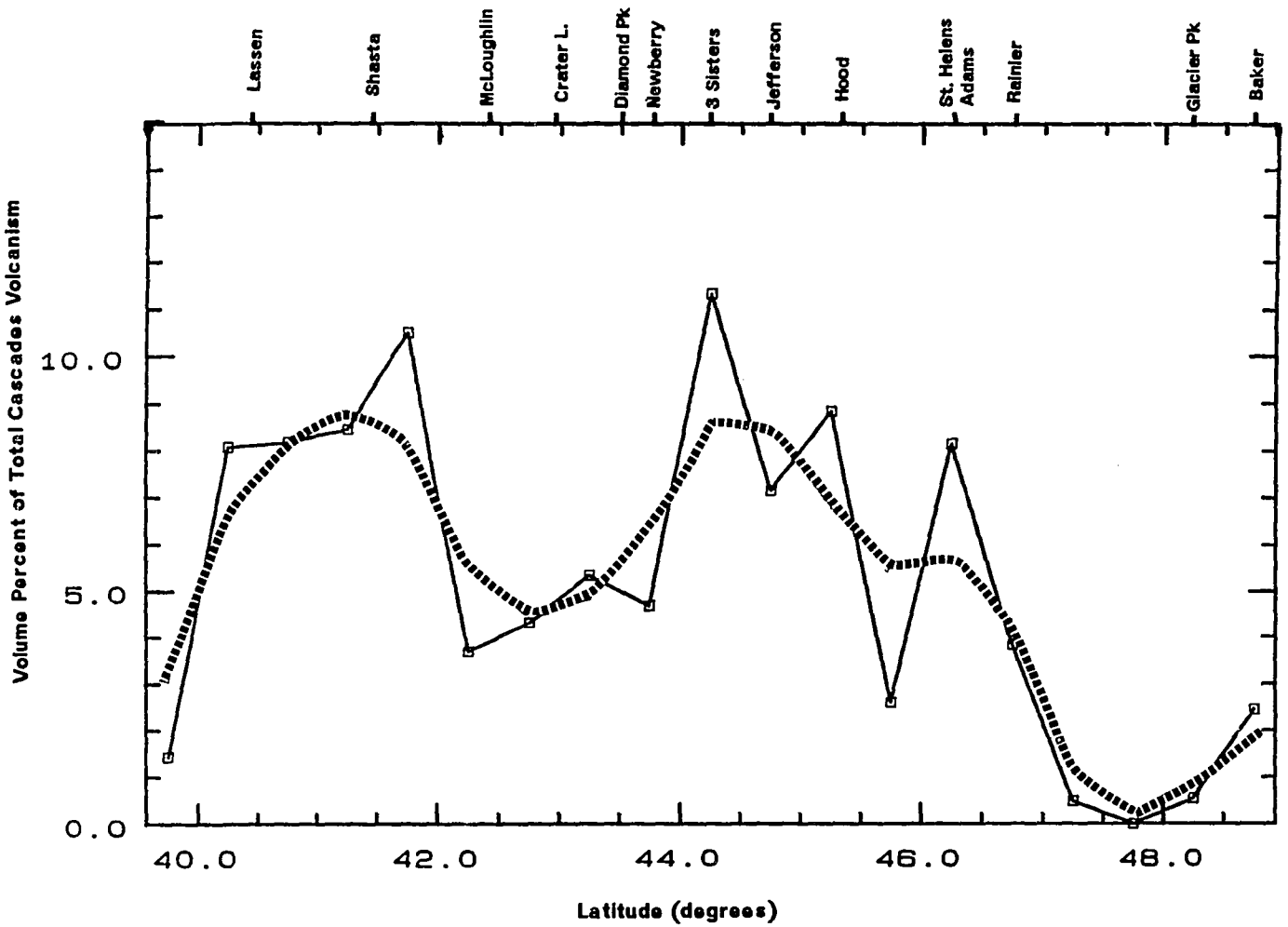

Figure A-5. Percent of total Cascades volcanic volume occurring at each 0.5 latitude degree bin. A smoothed curve of this data is shown as a dashed line (see text).

REFERENCES

American Association of Petroleum Geologists, 1981, Plate Tectonic Map of the Pacific (NE Quadrant), 1981

Albers, J.P., 1967, Belt of Sigmoidal Bending and Right-lateral Faulting in the Western Great Basin, GSA Bull 78, 143-156.

Aldrich, M.J., Jr. and C.E. Chapin, 1985, Stress History and Tectonic Development of the Rio Grande Rift, New Mexico, JGR in press, (abstract in EOS 66 711).

Aldrich, M.J., Jr., 1985, Tectonics of the Jemez Lineament in the Jemez Mountains and Rio Grande Rift (Abstract), EOS 66, 33, 600.

Anderson, C.A., 1941, Volcanoes of the Medicine Lake Highland, California, University of California Publications in Geological Sciences, 25, 347-422.

Anderson, D.A., 1984, The Earth as a Planet: Paradigms and Paradoxes, Science 223, 347-355.

Anderson, E.M., 1951, The Dynamics of Faulting, Oliver & Boyd, Ltd: Edinburgh, 240 p.

Anderson, R.E., M.L. Zoback and G.A. Thompson, 1983, Implications of Selected Subsurface Data on the Structural Form and Evolution of Some Basins in the Northern Basin and Range Province, Nevada and Utah, GSA Bull 94, 1055-1072.

Anderson, R.E., 1971, Thin-skinned distension in Teritary rocks of southeastern Nevada, GSA Bull. 82, 3533-3536.

Anderson, R.E., C.R. Longwell, R.L. Armstrong and R.F. Marvin, 1972, Singificance of K-Ar ages of Tertiary rocks from the Lake Mead Region, Nevada-Arizona, GSA Bull. 83, 273-287.

Ando, M. and Balazs, E.I., 1979, Geodetic evidence for aseismic subduction of the Juan de Fuca plate, JGR 84, 3023-3028.

Aramaki, S., 1984, Formation of Aira Caldera, Southern Kyushu, ~22,000 Years Ago, JGR 89, 8485-8501.

Armstrong, R.L., 1978, Cenozoic Igneous history of the U.S. Cordillera from Lat 42 degrees to 49 degrees N, in Smith, R.B. and G.P. Eaton, eds., Cenozoic Tectonics and regional geophysics of the Western Cordillera: GSA Memoir 152.

Atwater, T., 1970, Implications of plate tectonics for the Cenozoic plate tectonic evolution of western North America, Geol. Soc. Am. Bull. 81, 3513-3536.

Aydin, A. and A. Nur, 1982, Evolution of Pull-Apart Basins and their Scale Independence, Tectonics 1, 91-105.

Bacon, C.R., 1980, Quaternary Volcanism in the Cascades (Abstract), EOS 61, 1050.

Bacon, C.R., 1983, Eruptive History of Mount Mazama and Crater Lake Caldera, Cascade Range, USA, JVGR 18, 57-115.

Bacon, C.R., 1985, Implications of Silicic Vent Patterns for the Presence of Large Crustal Magma Chambers, JGR 90, 11243-11252.

Bailey, R.A., G.B. Dalrymple and M.A. Lanphere, 1976, Volcanism, Structure and Geochronology of Long Valley Caldera, Mono County, Calif., JGR 81, 725-744.

Baker, B.H. and J.G. Mitchell, 1976, Volcanic Stratigraphy and Geochronology of the Kedong-Olorgesailie Area and the Evolution of the South Kenya Rift Valley, Jour. Geol. Soc. London 132, 467-484.

Baker, B.H., P.A. Mohr, and L.A.J. Williams, 1972, Geology of the Eastern Rift System of Africa, GSA Special Paper 136, 67p.

Baker, M.C.W., 1981, The Nature and Distribution of Upper Cenozoic Ignimbrite Centres in the Central Andes, JVGR 11, 293-315.

Baker, M.C.W. and P.W. Francis, 1978, Upper Cenozoic Volcanism in the Central Andes -- Ages and Volumes, EPSL 41, 175-187.

Baker, P.E., I. McReath, M.R. Harvey, M.J. Roobol, and T.G. Davies, 1975, The Geology of the South Shetland Islands. V. Volcanic Evolution of Deception Island, British Antarctic Survey Scientific Reports: No. 78, 1-81.

Baldridge, W.S. and A. Kron, 1980, The Role of Lineaments and Preexisting structure on the Late Cenozoic Rio Grande Rift (Abstract), in Rio Grande Rift workshop on Crustal Modelling and Applications of Remote Sensing, Lunar Planetary Inst. Tech Report 81-07.

Barazangi, M. and B. Isacks, 1976, Spatial Distribution of Earthquakes and Subduction on the Nazca Plate Beneath South America, Geology 4, 686-692.

Barberi, F., G. Corrado, F. Innocenti, and G. Luongo, 1984, Phlegraean Fields 1982-1984: Brief Chronicle of a Volcano Emergency in a Densely Populated Area, Bull. Volc. 47-2. 175-185.

Barberi, F., F. Innocenti, P. Landi, U. Rossi, M. Saitta, R. Santacroce, I.M. Villa, 1984, The Evolution of Latera Caldera (Central Italy) in the Light of Subsurface Data, Bull. Volc. 47-1, 125-141.

Barberi, F., F. Innocenti, L. Lirer, R. Munno, T. Pescatore, and R. Santacroce, 1978, The Campanian Ignimbrite: a major Prehistoric Eruption in the Neopolitan Area (Italy), Bull. Volc. 41-1, 10-31.

Barberi, F. and J. Varet, 1977, Volcanism of Afar: Small-scale plate tectonics implications, GSA Bull. 88, 1251-1266.

Barberi, F., G. Ferrara, R. Santacroce and J. Varet, 1975, Structural Evolution of the Afar triple junction, in A. Pilger and A. Rosler, eds, 1975, Afar Depression of Ethiopia, Schweizerbart, Stuttgart, 19-37.

Barker, P.F., P.L. Barber and E.C. King, 1984, An Early Miocene Ridge Crest-Trench Collision on the South Scotia Ridge near 36 W, Tectonophys. 102, 315-332.

Barnes, C.G., 1978, The Geology of the Mount Bailey area, Oregon: Eugene, Oreg., University of Oregon M.S.Thesis, 123 p.

Bates, R.L. and J.A. Jackson, 1980, Glossary of Geology, American Geological Institute: Falls Church, Va., 749p.

Beget, J.E., 1982, Recent Volcanic Activity at Glacier Peak, Science 215, 1389-1390.

van Bemmelen, R.W., 1949, The Geology of Indonesia, Volume 1A: General Geology of Indonesia and Adjacent Archipelagoes, Government Printing Office: The Hague, Netherlands.

van Bemmelen, R.W., 1929, The Origin of Lake Toba, Proc. 4th Pacific Sci. Cong., v. 2A, Batavia, Indonesia, 115-124.

Billings, M.P., 1960, Diastrophism and Mountain Building, GSA Bull. 71, 363-397.

Blackwell, D.D., R.G. Bowen, D.A. Hull, J. Ricco, and J.L. Steele, 1982, Heat Flow, Arc Volcanism, and Subduction in Northern Oregon, JGR 87, 8735-8754.

Blakely, R.J., R.C. Jachens, R.W. Simpson and R.W. Couch, 1985, Tectonic setting of the southern Cascade Range as interpreted from its magnetic and gravity fields, GSA Bull 96, 43-48.

Bonham, H.F. and D.B. Slemmons, 1968, Faulting Associated with the Northern Part of the Walker Lane, GSA Spec. Pap. 101, p 290.

Bosworth, W., 1985, Geometry of Propagating Continental Rifts, Nature 316, 625-627.

Bosworth, W., J. Lambiase, and R. Keisler, 1986, A New Look at Gregory's Rift: The Structural Style of Continental Rifting, EOS 67, 577-583.

Brown, D.E., G.D. McLean, N.M. Woller and G.L. Black, 1980, Preliminary geology and geothermal resource potential of the Willamette Pass area, Oregon: Oregon Dept of Geol and Min Ind Open File Report O-80-3, Portland, Ore, 65 p.

Brun, J-P and Choukroune, P., 1983, Normal Faulting, Block Tilting and Decollement in a Stretched Crust, Tectonics 2, 345-356.

Burchfiel, B.C., G.S. Hamill and D.E. Wilhelms, 1983, Structural Geology of the Montgomery Mountains and the Northern Half of the Nopah and Resting Spring Ranges, Nevada and California, GSA Bull 94, 1359-1376.

Burbach, G.V., C. Frohlich, W.D. Pennington and T. Matumoto, 1984, Seismicity and Tectonics of the Subducted Cocos Plate, JGR 89, 7719-7735.

Bureau Mineral Resources, Geology and Geophysics, Canberra A.C.T., 1972, Geologic Map of Papua New Guinea, 1:1 million scale.

Burk, C.A., 1965, Geologic Map of the Alaska Peninsula, GSA Memoir 99.

Burkart, B. and S. Self, 1985, Extension and Rotation of crustal blocks in northern Central America and effect on the volcanic arc, Geology 13, 22-26.

Burke, K. and J.T. Wilson, 1972, Is the African Plate Stationary?, Nature 239, 287-289.

Byerlee, J., 1978, Friction of Rocks, Pageoph 116, 615-626.

Byers, F.M.Jr., 1959, Geology of Umnak and Bogoslof Islands, Aleutian Is., Alaska, USGS Bull. 1028-L, 267-369.

Carmichael, R.S., 1984, CRC Handbook of Phyysical Properties of Rocks, Volume III, CRC Press, Inc: Boca Raton, Florida.

Carr, M.J., 1976, Underthrusting and Quaternary Faulting in Northern Central America, GSA Bull 87, 825-829.

Carr, M.J., W.I. Rose, and R.E. Stoiber, 1982, Central America, in Thorpe, R.S., 1982, Andesites, John Wiley & Sons, 149-166.

Carlson, R.W., 1984, Tectonic Influence on Magma Composition of Cenozoic Basalts from the Columbia Plateau and Northwestern Great Basin, USA, in Explosive Volcanism, National Research Council Geophysics Study Committee, National Academy Press, Washington, DC.

Carlson, R.L., 1981, Late Cenozoic rotations of the Juan de Fuca Ridge and the Gorda Rise: a case study, Tectonophysics 77, 171-188.

Case, J.E. and T.L. Holcombe, 1980, Geologic-Tectonic Map of the Caribbean Region, USGS Map I-1100.

Christiansen, R.L., 1984, Yellowstone Magmatic Evolution: Its bearing on Understanding Large-Volume Explosive Volcanism, in Explosive Volcanism, National Research Council Geophysics Study Committee, National Academy Press, Washington, DC., 84-95.

Christiansen, R.L., 1982, Late Cenozoic Volcanism of the Island Park Area, Eastern Idaho, in Bonnichsen, B. and R.M. Breckenridge, eds, Cenozoic Geology of Idaho: Idaho Bur Mines & Geology Bull 26, 345-368.

Christiansen, R.L., 1979, Cooling Units and Composite Sheets in Relation to Caldera Structure, in Chapin, C.E. and W.E. Elston, eds., Ash-Flow Tuffs, GSA Special Paper 180, 29-42.

Christiansen, R.L., 1976, Volcanic Evolution of Mt. Shasta, Calif., GSA Abstracts with Programs 8, 3, 360-361.

Christiansen, R.L., P.W. Lipman, P.P. Orkild, F.M. Byers, 1965, Structure of the Timber Mountain Caldera, South Nevada, and Its Relation to Basin-Range Structure, USGS Prof. Pap. 525-B, B43-B48.

Christiansen, R.L. and P.W. Lipman, 1972, Cenozoic Volcanism and Plate Tectonic evolution of the Western U.S. II: Late Cenozoic, Phil. Trans. Roy. Soc. London A 271, 249-284.

Christiansen, R.L. and E.H. McKee, 1978, Late Cenozoic volcanic and tectonic evolution of the Great Basin and Columbia Intermontane Regions, in Smith, R.B. and G.P. Eaton, eds., Cenozoic Tectonics and regional geophysics of the Western Cordillera: GSA Memoir 152.

Cochrane, G.R. and W. Tianfeng, 1983, Interpretation of Structural Characteristics of the Taupo Volcanic Zone, New Zealand, from Landsat imagery, Int. J. Remote Sensing 4, 111-128.

Cole, J.W. and K.B. Lewis, 1981, Evolution of the Taupo--Hikurangi Subduction System, Tectonophys. 72, 1-21.

Collot, J.Y., J. Daniel and R.V. Burne, 1985, Recent Tectonics Associated With The Subduction/Collision of the D'Entrecasteaux Zone in the Central New Hebrides, Tectonophys. 112, 325-356.

Couch, R.W., G.S. Pitts, M. Gemperle, D.E. Braman and C.A. Veen, 1982, Gravity Anomalies in the Cascade Range in Oregon: Structural and Thermal Implications, State of Oregon Department of Geology and Mineral Industries Open File Report O-82-9, Portland, Oregon.

Courtillot, V. and G.E. Vink, 1983, How Continents Break Up, Sci. Am. 249, July, 43-49.

Courtillot, V., 1982, Propagating Rifts and Continental Breakup, Tectonics 1, 239-250.

Cox, A., 1973, Plate Tectonics and Geomagnetic Reversals, W H Freeman and Company: San Francisco, 285-287.

Cross, T.A. and Pilger, R.H.Jr., 1982, Controls of subduction geometry, location of magmatic arcs, and tectonics of arc and back-arc regions, Geol. Soc. Am. Bull. 93, 545-562.

Crosson, R., 1972, Small earthquakes structure and tectonics of the Puget Sound region, Bull. Seis. Soc. Am. 62, 1133-1171.

Crosson, R.S., 1983, Review of Seismicity in the Puget Sound Region From 1970 through 1978, in Yount, J.C. and R.S. Crosson, USGS Open File Report 83-19.

Davies, H.L., 1973, Gazelle Peninsula, New Britain, Sht SB/56-2, International Index, 1:250,000 Geol. Series, Aust. Govt. Pub. Svc., Canberra.

Davis, G.A., 1981, Late Cenozoic tectonics of the Pacific Northwest with Special Reference to the Columbia Plateau, Washington Public Power Supply System, Final Safety Analysis Report, Nuclear Project 2, Appendix 2.5N, 44p.

Davis, G.A., 1980, Problems of Intraplate Extensional Tectonics, Western U.S., in Burchfiel, B.C., E.T. Silver, J.E. Oliver, eds, Continental Tectonics, Washington, D.C., National Academy of Sciences.

Davis, G.A. and B.C. Burchfiel, 1973, Garlock Fault: An Intracontinental Transform Structure, Southern California, GSA Bull 84, 1407-1422.

De Rita, D., and R. Funiciello, 1982, Guidebook for the Field Excursion to the Sabatini and Sacrofano-Baccano Volcanic Areas, Consiglio Naz. De. Ricerche (It.) and NSF (US), Workshop on Explosive Volcanism.

De Rita, D., R. Funiciello, U. Rossi and A. Sposato, Structure and Evolution of the Sacrofano-Baccano Caldera (Sabatini Volcanic Complex, Rome), in preparation.

De Rita, D., and R. Funiciello, 1982, Guidebook for the Field Excursion to the Alban Hills, Consiglio Naz. De. Ricerche (It.) and NSF (US), Workshop on Explosive Volcanism.

De Rita, D., and R. Funiciello, 1982, Guidebook for the Field Excursion to Alban Hills, Consiglio Naz. De. Ricerche (It.) and NSF (US), Workshop on Explosive Volcanism.

Dewey, J.W. and J.T. Algermissen, Seismicity of the Middle America Arc-Trench System near Managua, Nicaragua, Seis. Soc. Am. Bull. 64, 1033-1048.

Dickinson, W.R., and Snyder, W.S., 1979a, Geometry of triple junctions related to San Andreas transform, JGR 84, 561-572.

Dickinson, W.R. and Snyder, W.S., 1979b, Geometry of Subducted Slabs related to San Andreas Transform, Jour. Geol. 87, 609-627.

Diment, W.H. and T.C. Urban, 1981, Average Elevation Map of the Conterminous United States (Gilluly Averaging Method), US Geol. Surv. Map GP-933.

Di Paola, G.M., 1973, The Ethiopian Rift Valley (Between 7 00' and 8 40' lat. North), Bull. Volcanol. 36, 517-560.

Di Paola, G.M., 1972, Geology of the Corbetti Caldera Area (Main Ethiopian Rift Valley), Bull. Volcanol. 35, 497-506.

Dokka, R.K., 1983, Displacements on Late Cenozoic Strike-slip Faults of the Central Mojave Desert, California, Geology 11, 305-308.

Donath, F.A., 1962, Analysis of Basin-Range Structure, South-Central Oregon, GSA Bull 73, 1-16.

Donnelly-Nolan, J.M., E.V. Ciancanelli, J.C. Eichelberger, J.H. Fink and G. Heiken, Roadlog for Fieldtrip to Medicine Lake Highlands, in Johnston, D.A. and J. Donnelly-Nolan, eds., USGS Circular 838, 1981.

Drake, E.T., 1982, Tectonic Evolution of the Oregon Continental Margin, Oregon Geology 44, 15-21.

Duncan, R.A., 1984, A Captured Island Chain in the Coast range of Oregon and Washington, JGR (in press).

Eaton, G.P., 1979, A Plate Tectonic Model for Late Cenozoic Crustal Spreading in the Western U.S., in Reicker, R.E., ed, Rio Grande Rift Tectonics and Magmatism, AGU, Washington, D.C.

Eaton, G.P., 1980, Geophysical and Geological Characteristics of the Crust of the Basin and Range Province, in Burchfiel, B.C., E.T. Silver, J.E. Oliver, eds, Continental Tectonics, Washington, D.C., National Academy of Sciences.

Eaton, G.P., 1982, The Basin & Range Province: Origin and Tectonic Significance, Ann. Rev. Earth and Planet. Sci. 10, 409-440.

Eaton, G.P., R.L. Christiansen, H.M. Iyer, A.M. Pitt, D.R. Mabey, H.R. Blank Jr., and M.E. Gettings, 1975, Magma Beneath Yellowstone National Park: Science 188, 787-796.

Eaton, G.P., R.R. Wahl, H.J. Prostka, D.R. Mabey, M.D. Kleinkopf, 1978, Regional Gravity and Tectonic Patterns: Their Relation to Late Cenozoic Epierogeny and Lateral Spreading in the Western Cordillera, in Smith, R.B. and G.P. Eaton, eds., Cenozoic Tectonics and regional geophysics of the Western Cordillera: GSA Memoir 152, 51-92.

Eddington, P.K., R.B. Smith and C. Renggli, 1985, Kinematics of the Great Basin Intraplate Extension, EOS 66, 1056.

Eichelberger, J.C. and R. Gooley, 1977, Evolution of Silicic Magma Chambers and their Relationship to Basaltic Volcanism, in AGU Monograph 20: The Earth's Crust.

Eichelberger, J.C., P.C. Lysne, C.D. Miller and L.W. Younker, Research Drilling at Inyo Domes, California: 1984 Results, EOS 66, 186-187.

Ekren, E.B., F.M. Byers, Jr., R.F. Hardyman, R.F. Marvin and M.L. Silberman, 1979, Stratigraphy, Geochronology and Preliminary Petrology of Tertiary Volcanic Rocks in the Gabbs Valley and Gillis Ranges, Mineral County, Nevada, USGS Bull. 1464.

Endo, E.T., S.D. Malone, L.L. Noson and C.S. Weaver, 1981, The 1980 Eruptions of Mount St. Helens, Washington: Locations, Magnitudes and Statistics of the March 20 - May 18 Earthquake Sequence, in Lipman, P.W. and D.R. Mullineaux, USGS Professional Paper 1250, 93-108.

Erdlac, R.J.Jr, and T.H. Anderson, 1982, The Chixoy-Polochic Fault and Its Associated Fractures in Western Guatemala, GSA Bull. 93, 57-67.

Erlich, E.N., 1979, Recent Structure of Kamchatka and Position of Quaternary Calderas, Bull. Volc. 42, 13-43.

Erlich, E.N., I.V. Melekestsev and O.A. Braitseva, 1979, Evolution of Recent Volcanism, Bull. Volc. 42, 93-112.

Erlich, E.N., I.V. Melekestsev, A.A. Tarakanovsky, and M.I. Zubin, 1973, Quaternary Calderas of Kamchatka, Bull. Volc. 36, 222-237.

Fedotov, S.A. and P.I. Tokarev, 1974, Earthquakes, Characteristics of the Upper Mantle under Kamchatka, and Their Connection with Volcanism (according to data collected up to 1971), Bull. Volc. 37-1, 245-257.

Ferrall, C.C., 1983, Interpretation of Tectonic Stress Regime vs Volcanic Style in the Cascade Range (abstract), EOS 64, n. 45, p. 886.

Ferriz, H. and G.A. Mahood, 1984, Eruption Rates and Compositional Trends at Los Humeros Volcanic Center, Puebla, Mexico, JGR 89, 8511-8524.

Finch, R.H., 1930, Activity of a California Volcano in 1786, The Volcano Letter, 308, 3.

Fink, J.H., 1983, Structure and emplacement of a rhyolitic obsidian flow: Little Glass Mountain, Medicine Lake Highland, northern California, GSA Bull 94, 362-380.

Fink, J.H. and D.D. Pollard, 1983, Structural evidence for dikes beneath silicic domes, Medicine Lake Highland Volcano, California, Geology 11, 458-461.

Finn, C. and D.L. Williams, 1982, Gravity Evidence for a shallow intrusion under Medicine Lake volcano, California, Geology 10, 503-507.

Fiske, R.S. and E.D. Jackson, 1972, Orientation and Growth of Hawaiian Volcanic Rifts: The effect of Regional Structure and Gravitational stress, Roy. Soc. (London) Proc. A, 329, 299-326.

Fitch, T.J., 1972, Plate Convergence, Transcurrent Faults, and Internal Deformation Adjacent to Southeast Asia and the Western Pacific, JGR 77, 4432-4460.

Fletcher, R.C. and B. Hallet, 1983, Unstable Extension of the Lithosphere: A Mechanical Model for Basin-and-Range Structure, JGR 88, 7457-7466.

Fleck, R.J., 1970, Age and Possible Origin of the Las Vegas Valley Shear Zone, Clark and Nye Counties, Nevada, GSA Abs. with Prog. 2, 333.

Ford, J.P., R.G. Blom, M.L. Bryan, M.I. Daily, T.H. Dixon, C. Elachi, and E.C. Xenos, 1980, Seasat Views North America, the Caribbean, and Western Europe with Imaging Radar, JPL Pub. 80-67: Pasadena, Calif.

Fox, K.F.Jr., R.J. Fleck, G.H. Curtis and C.E. Meyer, 1985, Implications of the northwestwardly younger age of volcanic rocks of west-central California, GSA Bull 96, 647-654.

Friedman, I., 1977, Hydration Dating of Volcanism at Newberry Crater, Oregon, USGS Jour. of Res. 5, 337-342.

Fuenzalida, R.P. and W.N. Espinosa, 1974, Hallargo de una Caldera Volcanica en la Provincia de Aisen, Revista Geologica de Chile, 64-66.

Fyfe, W.S. and O.H. Leonardos, 1973, Ancient Metamorphic Migmatite Belts of the Brazilian African Coasts, Nature 244, 501-502.

Fyfe, W.S. and A.R. McBirney, 1975, Subduction and the Structure of Andesitic Volcanic Belts, AJS 275-A, 285-297.

Gay, T.E.Jr and Q.A. Aune, 1958, Alturas Sheet, Geologic Map of California, Olaf P. Jenkins Edition, California Division of Mines.

Geologic Map of Indonesia, 1965, 1:2,000,000, prepared by Indonesia Directorate of Geology, published by USGS.

Gianella, V.P. and Callaghan, E., 1934, Cedar Mountain, Nevada, Earthquake of December 20, 1932, Seism. Soc. Am. Bull. 24, 345-377.

Gilbert, C.M. and M.W. Reynolds, 1973, Character and Chronology of Basin Development, Western Margin of the Basin and Range Province, GSA Bull 84, 2489-2510.

Gnibidenko, H., T.G. Bykova, O.V. Veselov, V.M. Vorobiev and A.S. Svarichevsky, The Tectonics of the Kuril-Kamchatka Deep-Sea Trench, in T.W.C. Hilde and S. Uyeda, Geodynamics of the Western Pacific-Indonesian Region, Geodynamics Series V. 11, AGU: Washington, D.C., 249-283.

Gnibedenko, H. and A.S. Svarichevsky, 1984, Tectonics of the South Okhotsk Deep-Sea Basin, Tectonophys. 102, 225-244. Gonzalez-Ferran, O., P.E. Baker and D.C. Rex, 1985, Tectonic-Volcanic Discontinuity at Latitude 27 South Andean Range, Associated with Nazca Plate Subduction, Tectonophys. 112, 423-441.

Gorshkov, G.S., 1970, Volcanism and the Upper Mantle, Plenum Press: New York, 385p.

Grose, T.L.T. and E.H. McKee, 1982, Late Cenozoic Westward Volcanic Progression East of Lassen Peak, Northeastern California (Abstract), EOS 63, 1149.

Groshong, R.H.Jr. and D.A. Rodgers, 1978, Left-Lateral Strike-Slip Model, in Wickham, J. and R. Denison, Structural Style of the Arbuckle Region, GSA South Central Section, Field Trip #3.

Hall, M.L. and C.A. Wood, 1985, Volcano-tectonic segmentation of the northern Andes, Geology 13, 203-207.

Hamblin, W.K., 1984, Direction of Absolute Movement Along the Boundary Faults of the Basin and Range -- Colorado Plateau Margin, Geology 12, 116-119.

Hamilton, W., 1980, Complexities of Modern and Ancient Subduction systems, in Continental Tectonics, National Academy for the Advancement of Science.

Hamilton, W., 1979, Tectonics of the Indonesian Region, USGS Prof. Paper 1078, US Govt. Print. Ofc.: Washington, D.C., 345p.

Hamilton, W., 1978, Mesozoic Tectonics of the Western United States, in Howell, D.G. and K.A. McDougall, eds., Mesozoic paleogeography of the western United States, Soc. Econ. Paleont. & Min., Pacific Section, Pacific Coast Paleograph. Sympos. 2, 33-70.

Hamilton, W. and W.B. Myers, 1966, Cenozoic Tectonics of the Western United States, Rev. Geophys. 4, 509-549.

Hammond, P.E., 1979, A tectonic model for Evolution of the Cascade Range, in Armentrout, J.M., M.R. Cole and H. Terbest, Jr., eds. Pacific Coast Paleogeography Symposium 3, Soc. Econ. Paleontol. and Mineralologists, Los Angeles, Calif. 219-237.

Hammond, P.E., S.A. Pedersen, K.D. Hopkins, D. Aiken, D.S. Harle, Z.F. Danes, D.L. Konicek, C.R. Stricklin, 1975, Geology and Gravimetry of the Quaternary Basaltic Volcanic Field, Southern Cascade Range, Washington, Proc. 2nd U.N. Sympos. on Develop. of Geotherm. Res. 1, 397-405.

Hardyman, R.F., E.B. Ekren and F.M. Byers, Jr., 1975, Cenozoic Strike-Slip, Normal, and Detachment Faults in Northern Part of Walker Lane, West-central Nevada, GSA Abs. with Prog. 7, 1100.

Hart, W.K., 1982, Isotopic Characteristics of Basalts from the N.W. Great Basin, U.S.A. (Abstract), EOS 62, 457.

Hart, W.K., J.L. Aronson and S.A. Mertzman, 1984, Areal Distribution and Age of Low-K High-Alumina Olivine Tholeiite Magmatism in the Northwestern Great Basin, GSA Bull 95, 186-195.

Hart, W.K. and S.A. Mertzman, 1983, Late Cenozoic Volcanic Stratigraphy of the Jordan Valley area, Southeastern Oregon, Oregon Geol 45, 15-19.

Hayes, D.E. and B. Taylor, 1978, Tectonics, in D.E. Hayes, A Geophysical Atlas of the East and Southeast Asian Seas, GSA Map MC-25: Boulder, Colo.

Heaton, T.H. and H. Kanamori, 1984, Seismic Potential Associated with Subduction in the Northwestern US, Bull Seism Soc Am 74, 933-941.

Heiken, G., 1978, Plinian-type Eruptions in the Medicine Lake Highland, Calfornia, and the Nature of the Underlying Magma, Jour. Volc. Geotherm. Res. 4, 375-402.

Herd, D., 1978, Intracontinental plate boundary east of Cape Mendocino, Calif., Geol 6, 721-725.

Hey, R.N., Dunnebier, F.K., and Wilson, W.J., 1980, Propagating Rifts on midocean ridges, JGR 85, 3647-3658.

Higgins, M.W., 1973, Petrology of Newberry Volcano, Central Oregon, GSA Bull 84, 455-488.

Hildreth, W., 1981, Gradients in Silicic Magma Chambers: Implications for Lithospheric Magmatism, JGR 86, 10153-10192.

Hildreth, W., A.L. Grunder and R.E. Drake, 1984, The Loma Seca tuff and the Calabozos caldera: A major ash-flow and caldera complex in the southern Andes of Central Chile, GSA Bull. 95, 45-54.

Hill, D.P., 1982, Contemporary Block Tectonics: California and Nevada, JGR 87, 5433-5450.

Holcombe, C.J., 1977, How rigid are the lithospheric plates? Fault and Shear Rotations in Southeast Asia, J. Geol. Soc. London 134, 325-342.

Huchon, P., 1986, Comment on "Kinematics of the Philippine Sea Plate" by B. Ranken, R.K. Cardwell, and D.E. Karig, Tectonics 5, 165-168.

Hughes, J.M., R.E. Stoiber and M.J. Carr, 1980, Segmentation of the Cascade Volcanic Chain, Geology 8, 15-17.

Humphrey, J.R. and I.G. Wong, 1983, Recent Seismicity near Capitol Reef National Park, Utah, and its Tectonic Implications, Geology 11, 447-451.

Hutchison, C.S., 1982, Indonesia, in R.S. Thorpe, Andesites, John Wiley and Sons: New York, 207-224.

Ingersoll, R.V., 1982, Triple-junction instability as cause for late Cenozoic extension and fragmentation of the western United States, Geol 10, 621-624.

International Assoc. Volcanology and Chemistry Earth's Interior (IAVCEI), 1951-1976, Catalog of the Active Volcanoes of the World, v. 1-23.

Isacks, B.L. and M. Barazangi, 1977, Geometry of Benioff Zones: Lateral Segmentation and Downward Bending of the Subducted Lithosphere, in Talwani, M. and W. Pitman, eds, Island Arcs, Deep Sea Trenches and Back-arc Basins, Maurice Ewing Series 1, AGU Washington, DC, 99-114.

Isacks, B., J. Oliver and L.R. Sykes, 1968, Seismology and the New Global Tectonics, JGR 73, 5855-5899.

Jachens, R.C. and Griscom, A., 1983 Three-dimensional geometry of the Gorda Plate beneath Northern California, JGR 88, 9375-9392.

Jacobshagen, V., St. Durr, F. Kockel, K. Kopp and G. Kowalczyk, 1978, Structure and Geodynamic Evolution of the Aegean Region, in Cloos, H., D. Roeder, and K. Schmidt, eds., Alps, Apennines, Hellenides: Interunion Commission on Geodynamics, Science Report no. 38, Schweizerbartsche Verlag, 299-311.

Johnson, R.W., 1982, Papua New Guinea, in R.S. Thorpe, ed., Andesites, John Wiley and Sons: New York, 225-244.

Johnson, R.W., 1976, Late Cainozoic Volcanism and Plate Tectonics at the Southern Margin of the Bismarck Sea, Papua New Guinea, in R.W. Johnson, ed., Volcanism in Australasia, Elsevier Sci. Pub. Co.: New York, 101-116.

Johnson, R.W., J.C. Mutter and R.J. Argulus, 1979, Origin of the Willaumez-Manus Rise, Papua New Guinea, EPSL 44, 247-260.

Johnson, R.W., 1969, Volcanic Geology of Mount Suswa, Kenya, Phil. Trans. R. Soc. London A 265, 283-412.

Jones, D.A., A. Cox, P. Coney and M. Beck, 1982, The Growth of Western North America, Sci. Am. 247, n. 5.

Jordan, T.E., B.L. Isacks, R.W. Allmendinger, J.A. Brewer, V.A. Ramos, C.J. Ando, 1983, Andean Tectonics related to geometry of subducted Nazca plate, GSA Bull 94, 341-361.

Jurdy, D.M., 1984, The Subduction of the Farallon Plate Beneath North America as Derived from Relative Plate Motions, Tectonics 3, 107-114.

Karig, D.E., 1973, Plate convergence between the Philippines and Ryukyu Islands, Mar. Geol. 14, 153-168.

Katili, J.A., 1970, Large transcurrent faults in southeast Asia with spherical reference to Indonesia, Geol. Rundsch. 59, 581-600.

Katili, J.A. and H.M.S. Hatono, 1983, Complications of Cenozoic Tectonic Development in Eastern Indonesia, in T.W.C. Hilde and S. Uyeda, eds., Geodynamics of the Western Pacific -- Indonesian Region, Geodynamics Ser. 11, AGU: Washington, D.C., 387-400.

Katsui, Y., A. Shigeyuki, and I. Kunimaru, 1975, Formation and Magmatic Evolution of Mashu Volcano, East Hokkaido, Japan, Jour. Fac. Hokkaido Univ. Ser IV, 16, 533-552.

Kellogg, J.N., 1986, Aseismic Accretion of the South Caribbean and North Panama deformed belts: Analogs for the Barbados Forarc, Abs. 11th Caribbean Geological Conference, Barbados, 1986, p. 52.

Kelsey, H.M. and S.M. Cashman, 1983, Wrench Faulting in Northern California and its Tectonic Implications, Tectonics 2, 565-576.

Kienle, C.F., C.A. Nelson and R.D. Lawrence, 1981, Faults and Lineaments of the Southern Cascades, Oregon, Special Paper 13, Oregon Dept of Geol and Min Ind, Portland, Ore.

Kilbourne, R.T. and C.L. Anderson, 1981, Volcanic History and "Active" Volcanism in California, Calif Geol, August 1981.

Kimura, G., 1986, Oblique Subduction and Collision: Forearc tectonics of the Kuril arc, Geology 14, 404-407.

Kimura, G., S. Miyashita, and S. Miyasaka, 1983, Collision Tectonics in Hokkaido and Sakhalin, in M. Hashimoto and S. Uyeda, eds., Accretion Tectonics in the Circum-Pacific Regions, Terra Scientific Pub. Co.: Tokyo, 123-134.

King, B.C., 1970, Vulcanicity and Rift Tectonics in East Africa, in T.N. Clifford and I.G. Gass, eds, African Magmatism and Tectonics: Oliver and Boyd, Edinburgh, 263-282.

King, P.B., 1959, The Evolution of North America, Princeton Univ. Press, Princeton, New Jersey, 190 pp.

Koide, H. and S. Battacharji, 1975, Formation of Fractures Around Magmatic Intrusions and Their Role in Ore Localization, Econ Geol 70, 781-799.

Kohler, W.M., J.H. Healy, and S. Wegener, 1982, Upper Crustal Structure of the Mt. Hood, Oregon Region as Revealed by Time-Term Analysis, JGR 87, 339-355.

Kronberg, P., M. Schonfeld, R. Gunther, and P.Tsombos, 1975, ERTS 1 -- data on the geology and tectonics of the Afar/Ethiopia and adjacent regions, in A. Pilger and A. Rosler, eds, 1975, Afar Depression of Ethiopia, Schweizerbart, Stuttgart, 19-37.

La Torre, P., R. Nannini, F. Sollevanti, 1981, Geothermal Exploration in Central Italy: Geophysical Surveys in Cimini Range Area, 43rd Meeting, Eur. Assn. Ex. Geophysicists (proceedings).

Lawrence, R.D., 1976, Strike-slip faulting terminates the Basin and Range province in Oregon, GSA Bull 87, 846-850.

Leat, P.T., R. Macdonald and R.L. Smith, 1984, Geochemical Evolution of the Menengai Caldera Volcano, Kenya, JGR 89, 8571-8592.

Leaver, D.S., W.D. Mooney and W.M. Kohler, 1984, A Seismic Refraction Study of the Oregon Cascades, JGR 89, 3121-3134.

Letouzey, J. and M. Kimura, 1985, Okinawa Trough genesis: Structure and Evolution of a Backarc Basin Developed in a Continent, Marine and Petroleum Geology 2, 111-130.

Lipman, P.W., 1984, The Roots of Ash Flow Calderas in Western North America: Windows Into the Tops of Granitic Batholiths, JGR 89, 8801-8841.

Lipman, P., 1980, Cenozoic Volcanism in the Western U.S.: Implications for Continental Tectonics, in Studies in Geophysics: Continental Tectonics, National Academy of Sciences, Washington, D.C.

Lockwood, J.P. and J.G. Moore, 1979, Regional Deformation of the Sierra Nevada, California on Conjugate Microfault Sets, JGR 84, 6041-6049.

Lowder, G.G. and I.S.E. Carmichael, 1970, The Volcanoes and Caldera of Talasea, New Britain: Geology and Petrology, GSA Bull. 81, 17-38.

Luedke, R.G. and R.L. Smith, 1981, Map Showing Distribution, Composition and Age of Late Cenozoic Volcanic Centers in California and Nevada, USGS Map I-1091-C, 1:1 million.

Luedke, R.G. and R.L. Smith, 1982, Map Showing Distribution, Composition and Age of Late Cenozoic Volcanic Centers in Oregon and Washington, USGS Map I-1091-D, 1:1 million.

Luedke, R.G. and R.L. Smith, 1983, Map Showing Distribution, Composition and Age of Late Cenozoic Volcanoes and Volcanic Rocks of the Cascade Range and Vicinity, Northwestern United States, USGS Map I-1507, 1:500,000.

Lustig, L.K., 1969, Trend-Surface Analysis of the Basin and Range Province, and Some Geomorphic Implications, USGS Prof. Paper 500-D, D1-D79.

Luhr, J.F., S.A. Nelson, J.F. Allan, I.S.E. Carmichael, 1985, Active rifting in southwestern Mexico: Manifestations of an incipient eastward spreading-ridge jump, Geology 13, 54-57.

Lydon, P.A., T.E. Gay, Jr. and C.W. Jennings, 1960, Westwood Sheet, Geologic Map of California, Olaf P. Jenkins Edition, California Division of Mines.

Mabey, D.R., I. Zeitz, G.P. Eaton, and M.D. Kleinkopf, 1978, Regional magnetic patterns in part of the Cordillera in the Western United States, in Smith, R.B. and G.P. Eaton, eds, GSA Memoir 152.

McBirney, A.R. and H. Williams, 1964, The Origin of the Nicaraguan Depression, Bull. Volc. 27, 63.

McCall, G.J.H., R.W. Le Maitre, A. Malahoff, G.P. Robinson, P.J. Stephenson, 1970, The Geology and Geophysics of the Ambrym Caldera, New Hebrides, Bull. Volc. 34, 681-696.

Macdonald, G.A., 1972, Volcanoes, Prentice-Hall, Inc., Englewood Cliffs, N.J., 510p.

Macdonald, G.A., 1966, Geology of the Cascade Range and Modoc Plateau, in E.H. Bailey, ed., Geology of Northern California, California Division of Mines and Geology Bull 190, 65-96.

Magill, J., and A. Cox, 1981, Post-Oligocene Tectonic Rotation of the Oregon Western Cascade Range and the Klamath Mountains, Geology 9, 127-131.

Magill, J., A. Cox and R. Duncan, 1981, Tillamook Volcanic Series: Further Evidence for Tectonic Rotation of the Oregon Coast Range, JGR 86, 2953-2970.

McBirney, A.R., 1978, Volcanic Evolution of the Cascade Range, Ann. Rev. Earth & Planet. Sci. 6, 437-456.

McBirney, A.R., 1968, Petrochemistry of Cascade Andesite Volcanoes, in Dole, H.M., ed., 1968, Andesite Conference Guidebook, Oregon Dept. Geol. Min. Ind. Bull 62, 101-107.

McBirney, A.R. and C.M. White, 1982, The Cascade Province, in R.S. Thorpe, ed., Andesites, John Wiley & Sons, New York.

McGarr, A., 1982, Analysis of States of Stress Between Provinces of Constant Stress, JGR 87, 9279-9288.

McKee, C.O., P.L. Lowenstein, P. De Saint Ours, B. Talai, I. Itikarai, J.J. Mori, 1984, Seismic and Ground Deformation Crises at Rabaul Caldera: Prelude to an Eruption?, Bull. Volc. 47-2, 397-411.

McKenzie, D.P., 1969, The relationship between fault plane solutions for earthquakes and the directions of the principal stresses, Seis. Soc. Am. Bull. 59, 591-601.

McKenzie, D.P. and W.J. Morgan, 1969, Evolution of Triple Junctions, Nature 224, 125-133.

McKenzie, D.P., 1978, Active Tectonics of the Alpine--Himalayan belt: the Aegean Sea and Surrounding regions, Geophys. J. R. Astr. Soc. 55, 217-254.

MacLeod, N.S., D.R. Sherrod and L.A. Chitwood, 1982, Geologic Map of Newberry Volcano, Deschutes, Klamath and Lake Counties, Oregon, USGS Open File Report 82-847.

MacLeod, N.S., D.R. Sherrod, L.A., Chitwood, E.H., McKee, 1981, Newberry Volcano, Oregon, in Johnston, D.A. and Donnelly-Nolan, eds., USGS Circular 838, 85-91.

MacLeod, N.S. and E.A. Sammel, Newberry Volcano, Oregon: A Cascade Range geothermal prospect, Oregon Geology 44, 11, Nov 82, 123-131.

MacLeod, N.S., G.W. Walker and E.H. McKee, 1975, Geothermal Significance of Eastward Increase in age of upper Cenozoic Rhyolite Domes in Southeast Oregon, in Proc. 2nd U.N. Sympos. on Dev. and use of Geotherm. Res., 1, U.S. Govt Print Ofc, Washington, D.C., 465-474.

Malin, M.C., 1977, Comparison of volcanic features of Elysium (Mars) and Tibesti (Earth), GSA Bull 88, 908-919.

Marsh, B.D., 1982, On the Mechanics of Igneous Diapirism, Stoping, and Zone Melting, AJS 282, 808-855.

Melekestsev, I.V., 1974, Kamchatka, Kuriles and Kommander Islands (in Russian), Nauka: Moscow, 439p.

Menard, H.W., 1978, Fragmentation of the Farallon Plate by pivoting subduction, Jour. Geol. 86, 99-110.

Miller, E.L., P.B. Gans and J. Garing, 1983, The Snake Range Decollement: An Exhumed Mid-Tertiary Ductile-Brittle Transition, Tectonics 2, 239-262.

Miller, T.P. and R.L. Smith, 1977, Spectacular Mobility of Ashflows Around Aniakchak and Fisher Calderas, Alaska, Geology 5, 173-176.

Minato, M., 1977, Japan and Its Nature, Heibonsha Ltd., Pub.: Tokyo, 220p.

Minster, J.B. and T.H. Jordan, 1978, Present-day plate motions, JGR 83, 5331-5354.

Mohr, P., 1983, Perspectives on the Ethiopian Volcanic Province, Bull. Volc. 46-1, 23-43.

Mohr, P., J.G. Mitchell, and R.G.H. Raynolds, 1980, Quaternary Volcanism and Faulting at O'A Caldera, Central Ethiopian Rift, Bull. Volcanol. 43-1, 173-189.

Mohr, P., 1973, Tectonic Maps of the Ethiopian rift System and an Apology, Bull. Volcanol. 36, 507-511.

Mohr, P. and C. Wood, 1976, Volcano Spacings and Lithospheric Attenuation in the Eastern Rift of Africa, EPSL 33, 126-144.

Moore, J.G., 1960, Curvature of Normal Faults in the Basin and Range Province of Western United States, USGS Prof. Pap. 400B, B409-B411.

Morrice, M.G., P.A. Jezek, J.B. Gill, D.J. Whitford and M. Monoarfa, An Introduction to the Sangihe Arc: Volcanism Accompanying Arc-Arc Collision in the Molucca Sea, Indonesia, JVGR 19, 135-165.

Mukaiyama, H., M. Nakaumra, M. Inoue and T. Kimura, 1984, Fractures Related to the Post-Pliocene Volcanism with Pyroclastic Flows in Japan, Bull. Volc. Soc. Japan 29, 45-56.

Mukaiyama, H., M. Nakaumra, M. Inoue and T. Kimura, 1983, Geotectonism and Post-Miocene Volcanism in Northeast Japan, Bull. Volc. Soc. Japan 28, 395-408.

Muller, O.H., and D.D. Pollard, 1977, The Stress State Near Spanish Peaks, Colorado Determined From a Dike Pattern, Pageoph 115, 69-86.

Nakamura, K., 1977, Volcanoes as Possible Indicators of Tectonic Stress Orientation -- Principle and Proposal, JVGR 2, 1-16.

Nakamura, K., K. Shimazaki, and N. Yonekura, 1984, Subduction, Bending and Eduction. Present and Quaternary Tectonics of the Northern Border of the Philippine Sea Plate, Bull. Geol. Soc. France XXVI, 221-243.

Nakamura, K., K.H. Jacob, and J.N. Davies, 1977, Volcanoes as Possible Indicators of Tectonic Stress Orientation -- Aleutians and Alaska, Pageoph 115, 87-112.

Nakamura, K. and S. Uyeda, 1980, Stress Gradient in Arc-Back Arc Regions and Plate Subduction, JGR 85, 6419-6428.

Niccum, M., D. Bice, K. Cline, L. Cluff, and D. Schwartz, 1974, Active faults in Managua, Nicaragua, GSA Abstracts with Prog. 6, 889-890.

Nicks, O.W., ed., 1970, This Island Earth, NASA SP-250, Washington, D.C.

Nielsen, R.L., 1965, Right-Lateral Strike-Slip Faulting in the Walker Lane, West-Central Nevada, GSA Bull. 76, 1301-1308.

Nixon, G.T., 1979, The relationship between Quaternary volcanism in central Mexico and the seismicity and structure of subducted ocean lithosphere, GSA Bull 93, 514-523.

Noble, D.C., 1972, Some Observations on the Cenozoic Volcano-tectonic Evolution of the Great Basin, Western United States, EPSL 17, 142-150.

Ode, H., 1957, Mechanical Analysis of the Dike Pattern of the Spanish Peaks area, Colorado, GSA Bull 68, 567-576.

Oide, K., 1968, Geotectonic Conditions for the Formation of the Krakatau-type Calderas in Japan, Pacific Geology 1, 119-135.

Okaya, D.A. and G.A. Thompson, 1985, Geometry of Cenozoic Extensional Faulting: Dixie Valley, Nevada, Tectonics 4, 107-125.

Oldow, J.S., 1984, Spatial Variability in the Structure of the Roberts Mountains Allochthon, Western Nevada, GSA Bull 95, 174-185.

Pease, R.W., 1969, Normal Faulting and Lateral Shear in Northeastern California, GSA Bull. 80, 715-720.

Peccerillo, A., 1985, Roman Comagmatic Province (central Italy): Evidence for subduction-related magma genesis, Geology 13, 103-106.

Pecora W.T., Proceedings of the First Annual Memorial Symposium, 1975, p 247.

Peterson, N.V. and E.A. Groh, eds., 1966, Lunar Geological Field Conference Guide Book, Oregon Department of Geology and Mineral Industries, 51 p.

Peterson, N.V. and J.R. McIntyre, 1970, The Reconnainssance Geology and Mineral Resources of Eastern Klamath County and Western Lake County, Oregon, Bulletin 66, Oregon Department of Geology and Mineral Resources, Portland.

Pike, R.J. and G.D. Clow, 1981, Revised Classification of Terrestrial Volcanoes and Catalog of Topographic Dimensions, with New Results on Edifice Volume, USGS Open File Report 81-1038, 40 p.885

Pollard D.D., P.T. Delaney, W.A. Duffield, E.T. Endo and A.T. Okamura, 1983, Surface deformation in volcanic rift zones, Tectonophys (in press).

Priest, G.R., N.M. Waller, G.L. Black and S.H. Evans, 1983, Overview of the Geology of the Central Oregon Cascade Range, in Priest, G.R. and B.F. Vogt, eds., Geology and Geothermal Resources of the Central Oregon Cascade Range, Oregon Dept. Geol. Min. Ind. Special Paper 15, 3-28.

Proffett, J.M.Jr, 1977, Cenozoic Geology of the Yerington district, Nevada, and implications for the nature and origin of Basin and Range faulting, GSA Bull 88, 247-266.

Purbo-Hadiwidjojo, M.M., 1971, Geological Map of Bali, Geological Survey of Indonesia, Bandung.

Puxeddu, M., 1984, Structure and Late Cenozoic Evolution of the Upper Lithosphere in Southwest Tuscany (Italy), Tectonphys. 101, 357-382.

Raff, A.D. and Mason, R.G., 1961, Magnetic survey off the west coast of North America, 40 degrees N latitude to 50 degrees N latitude, Geol. Soc. Am. Bull. 72, 1267-1270.

Rehault, J-P, G. Boillot, and A. Mauffret, 1984, The Western Mediterranean Basin Geological Evolution, Marine Geology 55, 447-477.

Reilinger, R. and Adams, J., 1982, Geodetic evidence for active landward tilting of the Oregon and Washington Coastal Ranges, Geophys. Res. Ltrs. 9, 401-403.

Reutter, K.J., K. Gunther and J. Groscurth, 1978, An Approach to the Geodynamics of the Corsica -- Northern Apennines Double Orogene, in Cloos, H., D. Roeder, and K. Schmidt, eds., Alps, Apennines, Hellenides: Interunion Commission on Geodynamics, Science Report no. 38, Schweizerbartsche Verlag, 299-311.

Riddihough, R.P., 1980, Gorda Plate motions from magnetic anomaly analysis, EPSL 51, 163-170.

Riddihough, R.P., 1984, Recent Movements of the Juan de Fuca Plate System, JGR 89, 6980-6994.

Riddihough, R.P. and Hyndman, 1976, Canada's active western margin -- the case for subduction, Geosci. Can. 3, 269-278.

Robin, C., 1982, Mexico, in R.S. Thorpe, ed., Andesites.

Robin, C. and J. Tournon, 1978, Spatial Relations of Andesitic and Alkaline Provinces in Mexico and Central America, Can. J. Earth Sci. 15, 1633-1641.

Robinson, J.H., L.S. Forcella, and M.W. Gannett, 1981, Data from Geothermal Test Wells near Mt. Hood, Oregon, USGS OF 81-1002.

Robyn, T.L. and J.D. Hoover, 1982, Late Cenozoic Deformation and Volcanism in the Blue Mountains of Central Oregon: Microplate Interactions?, Geology 10, 572-576.

Rodgers, D.A., 1980, Analysis of basin development produced by en echelon strike slip faults, in P.F. Ballance and H.G. Reading, eds, International Association of Sedimentologists, 27-41.

Rogan, M., 1982, A Geophysical Study of the Taupo Volcanic Zone, New Zealand, JGR 87, 4073-4088.

Rogers, G.C., 1983, Some Comments on the Seismicity of the Northern Puget Sound -- Southern Vancouver Island Region, in Yount, J.C. and R.S. Crosson, USGS Open File Report 83-19.

Rose, W.I., B.T. Penfield, J.W. Drexler and P.B. Larson, 1980, Geochemistry of the Andesite Flank Lavas of three Composite Cones within the Atitlan Cauldron, Guatemala, Bull. Volc. 43-1, 132-153.

Rowan, L.C. and P.H. Wetlaufer, 1981, Relation Between Regional Lineament Systems and Structural Zones in Nevada, AAPG Bull 65, 1414-1432.

Russell, B.J., M.E. Beck, R.F. Burmester and R.C. Speed, 1982, Cretaceous Magnetizations in Northwestern Nevada and Its Tectonic Implications, Geology 10, 423-428.

Sabins, F.F., 1978, Remote Sensing, W.H. Freeman & Co., San Francisco, 426p.

Saemundsson, K., 1979, Outline of Geology of Iceland, Jokull 29, 7-28.

Sanders, C. O., 1984, Location and Configuration of Magma Bodies beneath Long Valley, California, Determined from Anomalous Earthquake Signals, JGR 89, 8287-8302.

Savage, J.C., 1983, Strain Accumulation in Western United States, Ann. Rev. Earth Planet. Sci. 11, 11-43.

Savage, J.C. and M.M. Clark, 1982, Magmatic Resurgence in Long Valley Caldera, California: Possible Cause of the 1980 Mammoth Lakes Earthquakes, Science 217, 531-532.

Savage, J.C., Lisowski, M., and Prescott, W.H., 1981, Geodetic Strain Measurements in Washington, JGR 86, 4929-4940.

Savostin, L., L. Zonenshain and B. Baranov, 1983, Geology and Plate Tectonics of the Sea of Okhotsk, in T.W.C. Hilde and S. Uyeda, Geodynamics of the Western Pacific-Indonesian Region, Geodynamics Series V. 11, AGU: Washington, D.C., 189-221.

Sbar, M., 1982, Delineation and Interpretation of Seismotectonic Domains in Western North America, JGR 87, 3919-3928.

Scholz, C.H., M. Barazangi, and Sbar, M.L., 1971, Late Cenozoic Evolution of the Great Basin, Western United States, as an Ensialic Interarc Basin, GSA Bull 82, 2979-2990.

Self, S., F. Goff, J.N. Gardner, J.V. Wright and W.M. Kite, 1985, Explosive Rhyolitic Volcanism in the Jemez Mountains: Vent Locations, Caldera Development and Relation to Regional Structure (Abstract), EOS 66, 679.

Seno, T., 1985, "Northern Honshu Microplate" Hypothesis and Tectonics in the Surrounding Region, Jour. Geol. Soc. Japan 31, 106-123.

Shaw, H.R., 1980, The Fracture Mechanisms of Magma Transport from the mantle to the surface, In Hargraves, R.B., ed, Physics of Magmatic Processes, Princeton University Press, Princeton, NJ.

Shawe, D.R., 1965, Strike-slip Control of Basin-Range Structure Indicated by Historical Faults in Western Nevada, GSA Bull 76, 1361-1378.

Sheets, P.D., 1979, Environmental and Cultural Effects of the Ilopango Eruption in Central America, in P.D. Sheets and D.K.Grayson, Volcanic Activity and Human Ecology, Academic Press: New York, 525-564.

Sheffield, C., 1981, Earth Watch, Macmillanh Publishing Co. Inc., New York, 160p.

Short, N.M., P.D. Lowman, S.C. Freden, and W.A. Finch, 1976, Mission to Earth: Landsat Views the World, NASA SP-360, Washington, D.C.

Sigurdsson, H. and R.S.J. Sparks, 1978, Rifting Episode in North Iceland in 1874-1875 and the Eruptions of Askja and Sveinagja, Iceland, Bull. Volc. 41-3, 149-167.

Silver, E.A., 1971, Small Plate tectonics in the Northeastern Pacific, Geol. Soc. Am. 82, 3491-3496.

Silver, E.A., 1978, Geophysical Studies and Tectonic Development of the Continental Margin off the Western U.S., Latitude 34 degrees to 48 degrees, in Smith, R.B. and G.P. Eaton, eds., GSA Memoir 152.

Simkin, T. and R. Fiske, 1983, Krakatau, 1883 -- the Volcanic Eruption and Its Effects, Smithsonian Institution Press, Washington, D.C., 464p.

Simkin, T., L. Siebert, L. McClelland, D. Bridge, C. Newhall, and J.H. Latter, 1981, Volcanoes of the World, Hutchinson Ross Publishing Company, Stroudsburg, Pa., 232p.

Sinton, J.M., D.S. Wilson, D.M. Christie, R.N. Hey, and J.R. Delaney, 1983, Petrologic Consequences of Rift Propagation on Oceanic Spreading Ridges, EPSL 62, 193-207.

Smith, J.G., 1979, Cenozoic volcanism in the Cascade Range, Medford 2 degree sheet, southern Oregon (abs), GSA Abstracts with Programs, 11, 128.

Smith, R.B. and R.L. Christiansen, 1980, Yellowstone Park as a Window on the Earth's Interior, Sci. Am. 242, 104-117.

Smith, R.B. and A.G. Lindh, 1978, Fault-plane solutions of the Western United States: a compilation, in Smith, R.B and G.P, Eaton, eds., GSA Memoir 152.

Smith, R.B., 1978, Seismicity, Crustal Structure and Intraplate tectonics of the Interior of the Western Cordillera, in Smith, R.B. and G.P. Eaton, eds, GSA Memoir 152.

Smith, R.B. and R.L. Bruhn, 1984, Intraplate Extensional Tectonics of the Eastern Basin-Range: Inferences on Structural Style from Seismic Reflection Data, Ragional Tectonics and Thermal-Mechanical Models of Brittle-ductile Deformation, JGR 89, 5733-5762.

Smith, R.B. and M.L. Sbar, 1974, Contemporary Tectonics and Seismicity of the Western United Stated with emphasis on the Intermountain Seismic Belt, GSA Bull 85, 1205-1218.

Smith, R.L. and R.A. Bailey, 1968, Resurgent Cauldrons, GSA Memoir 116, 613-662.

Smith, R.L. and R.G. Luedke, 1984, Potentially Active Volcanic Lineaments and Loci in Western Conterminous United States, in Explosive Volcanism, National Research Council Geophysics Study Committee, National Academy Press, Washington, DC., 47-66.

Smith, R.L., 1979, Ash-flow Magmatism, in Chapin, C.E. and W.E. Elston, eds., Ash-Flow Tuffs, GSA Special Paper 180, 5-28.

Snyder, W.S., W.R. Dickinson and M.L. Silberman, 1976, Tectonic Implications of Space-Time Patterns of Cenozoic Magmatism in the Western United States, EPSL 32, 91-106.

Sparks, R.S.J., 1981, Inside a volcano: the first three-dimensional map, Nature 293, 512.

Sparks, R.S.J., 1975, Stratigraphy and Geology of the Ignimbrites of Vulsini Volcano, Central Italy, Geol. Rundsch. 64, 497-523.

Sparks, R.S.J., L. Wilson and H. Sigurdsson, 1982, The Pyroclastic Deposits of the 1875 Eruption of Askja, Iceland, Phil. Trans. Roy. Soc. London A, 299, 241-273.

Spera, F.J., 1980, Aspects of Magma Transport, in Hargraves, R.B., ed, Physics of Magmatic Processes, Princeton University Press, Princeton, NJ.

Spera, F.J. and J.A. Crisp, 1981, Eruption Volume, Periodicity, and Caldera Area: Relationships and Inferences on Development of Compositional Zonation in Silicic Magma Chambers, JVGR 11, 169-187.

Stewart, J.H. and J.E. Carlson, 1978, Geologic Map of Nevada, 1:500,000, USGS, Washington, D.C.

Stewart, J.H., 1983, Extensional Tectonics in the Death Valley Area, California: Transport of the Panamint Range Structural Block 80 km Northwestward, Geology 11, 153-157.

Stewart, J.H., 1980, Geology of Nevada, Nevada Bur Mines & Geol, Spec. Pub. 4, 136 p.

Stewart, J.H., 1980a, Regional Tilt Patterns of Late Cenozoic Basin-range fault blocks, Western United States, GSA Bull 91, 460-464.

Stewart, J.H., 1978, Basin and Range Structure in North America: a review, in Smith, R.B. and G.P. Eaton, eds., Cenozoic Tectonics and regional geophysics of the Western Cordillera: GSA Memoir 152, 1-31.

Stewart, J.H., W.J. Moore and I. Zeitz, 1977, East-west patterns of Cenozoic Igneous Rocks, Aeromagnetic Anomalies, and Mineral Deposits, Nevada and Utah, GSA Bull 88, 67-77.

Stewart, J.H., G.W. Walker and F.J. Kleinhampl, 1975, Oregon-Nevada Lineament, Geology 3, 265-268.

Stewart, J.H., J.P. Albers and F.G. Poole, 1968, Summary of Regional Evidence for Right-lateral Displacement in the Western Great Basin, GSA Bull 79, 1407-1414.

Stewart, J.H., 1971, Basin and Range Structure: A System of Horsts and Grabens Produced by Deep-seated Extension, GSA Bull 82, 1019-1044.

Stoiber, R.E. and M.J. Carr, 1973, Quaternary Volcanic and Tectonic Segmentation of Central America, Bull Volc 37-3, 304-325.

Strand, R.G., 1963, Weed Sheet, Geologic Map of California, Olaf P. Jenkins Edition, California Division of Mines.

Suggate, R.P., G.R. Stevens and M.T. Te Punga, 1978, The Geology of New Zealand, New Zealand Geological Survey, Govt Printers, Wellington.

Sugi, N., C. Kiyotaka, and S. Uyeda, 1983, Vertical Crustal Movements of Northeast Japan Since Middle Miocene, in T.W.C. Hilde and S. Uyeda, eds., Geodynamics of the Western Pacific- Indonesian Region, Geodynamics Series Volume 11, AGU: Washington, D.C., 317-329.

Suneson, N.H. and I. Luccitta, 1983, Origin of Bimodal Volcanism, Southern Basin and Range Province, GSA Bull 94, 1005-1019.

Suppe, J., C. Powell and R. Berry, 1975, Regional Topography, Seismicity, Quaternary Volcanism, and the Present-day Tectonics of the Western United States, AJS 275-A, 397-436.

Sykes, L., 1978, Intraplate Seismicity, Reactivation of Preexisting Zones of Weakness, Alkaline Magmatism, and other Tectonism posdating Continental Fragmentation, Rev Geophys and Space Phys 16, 621-688.

Tamaki, K. and E. Honza, 1985, Incipient Subduction and Obduction Along the Eastern Margin of the Japan Sea, Tectonophys. 119, 381-406.

Tapponier, P. and P. Molnar, 1976, Slip-line Field Theory and Large-scale Continental Tectonics, Nature 264, 319-324.

Tarney, J., S.D. Weaver, A.D. Saunders, R.J. Pankhurst, and P.F. Barker, 1982, Volcanic Evolution of the Northern Antarctic Peninsula and the Scotia Arc, in R.S. Thorpe, Andesites, John Wiley & Sons: New York, 371-400.

Taylor, E.M., 1980, Volcanic and volcaniclastic rocks on the east flank of the central Cascade Range to the Deschutes River, Oregon, in Oles, K.F., J.G. Johnson, A.R. Niem and W.A. Niem, eds, Geologic field trips in western Oregon and southwestern Washington: Oregon Dept of Geol and Min Ind Bull 101, 1-7.

Taylor, E.M., 1973, Geology of the Dechustes Basin, in Beaulieu, J.D., Geologic Field Trips in Northern Oregon and Southern Washington: Oregon Department of Geology and Mineral Industries, Bull. 77, 29-32.

Tchalenko, J.S., 1970, Similarities Between Shear Zones of Different Magnitudes, GSA Bull. 81, 1625-1640.

Thatcher, W. and J.C. Savage, 1982, Triggering of Large Earthquakes by Magma-Chamber Inflation, Izu Peninsula, Japan, Geology 10, 637-640.

Thorarinsson, S., K. Saemundsson and R.S. Williams, 1973, ERTS-1 Image of Vatnajokull: Analysis of Glaciological, Structural and Volcanic Features, Jokull 23, 7-17.

Thompson, G.A. and D.B.Burke, 1973, Rate and Direction of Spreading in Dixie Valley, Basin and Range Province, Nevada, GSA Bull 84, 627-632.

Thompson, R.N., 1977, Columbia-Snake River-Yellowstone Magmatism in the context of Western USA Cenozoic Geodynamics, Tectonophys. 39, 621-636.

Thompson, R.N. and D.B. Burke, 1974, Regional Geophysics of the Basin and Range province, Ann. Rev. Earth & Planet. Sci. 2, 213-238.

Thornbury, W.D., 1965, Regional Geomorphology of the United States, John Wiley & Sons, Inc.: New York.

Thorpe, R.S., P.W. Francis, M. Hammill, and M.C.W. Baker, 1982, The Andes, in R.S. Thorpe, ed., Andesites, John Wiley and Sons: New York.

Ui, T., 1972, Recent Volcanism in Masaya-Granada Area, Nicaragua, Bull. Volc. 36, 174-190.

Uyeda, S. and H. Kanamori, 1979, Back-arc Opening and the Mode of Subduction, JGR 84, 1049-1061.

Venkatakrishnan, R., J.G. Bond and J.D. Kauffman, 1980, Geological Linears of the Northern Part of the Cascades Range, Oregon, Special Paper 12, Oregon Dept of Geol and Min Ind, Portland, Oregon.

Vincent, P.M., 1970, The evolution of the Tibesti Volcanic Province, eastern Sahara, in T.N. Clifford and I.G. Glass, eds., African Magmatism and Tectonics, Hafner Pub. Co., Darien, Conn., 301-319.

Voight, B., 1967, Interpretations of In Situ Stress Measurements, Proc. Intern. Congr. Rock Mech. 2, 332-348.

Volcano Map of Kamchatka, 1960, Telberg Book Co.: New York.

Volcano News, 1980, Myvatn Volcanism, Volcano News 3, April.

Walker, G.W. and B. Nolf, 1981, High Lava Plains, Brothers Fault Zone to Harney Basin, Oregon, in D.A. Johnston and J. Donnelly-Nolan, eds, Guides to some Volcanic Terranes in Washington, Idaho, Oregon and Northern California, USGS Circular 838, 105-111.

Walker, G.W., 1977, Geologic Map of Oregon East of the 121st Meridian, 1:500,000, USGS Map I-902, Washington, D.C.

Walker, G.W., 1969, Geology of the High Lava Plains province, in Mineral and Water Resources of Oregon, Oregon Dept. Geol. and Min. Ind. Bull. 64, 77-79.

Walker, G.W., 1970, Cenozoic Ash-Flow Tuffs of Oregon, Ore Bin 32, 97-115.

Walker, G.P.L., 1981, New Zealand Case Histories of pyroclastic studies, in Tephra Studies, S. Self and R.S.J. Sparks, D. Reidel, Hingham, Mass., 317-330.

Wallace, R.E., 1984, Patterns and Timing of Late Quaternary Faulting in the Great Basin Province and Relation to Some Regional Tectonic Features, JGR 89, 5763-5769.

Washington Public Power Supply System, 1981, Final Safety Analysis Report, WPPSS Nuclear Project No. 2, Amendment 18.

Waters, A.C., 1962, Basalt Magma Types and Their Tectonic Associations: Pacific Northwest of the United States, in Macdonald, G.A. and H. Kuno, eds., The Crust of the Pacific Basin, AGU Monograph 6, 158-170.

Watts, A.B., M.G. Kogan and J.H. Bodine, 1978, Gravity Field of the Northwest Pacific Ocean Basin and Its Margin: Kuril Island Arc-Trench System, GSA Map MC-27.

Weaver, C.S., W.C. Grant, S.D. Malone and E.T. Endo, 1981, Post-May 18 Seismicity: Volcanic and Tectonic Implications, USGS Prof. Pap. 1250, 109-121.

Weaver, C.S. and S.W. Smith, 1983, Regional Tectonic and Earthquake Hazard Implications of a Crustal Fault Zone in Southwestern Washington, JGR 88, 10371-10383.

Weaver, C.S. and C.A. Michaelson, 1985, Seismicity and Volcanism in the Pacific Northwest: Evidence for the Segmentation of the Juan De Fuca Plate, Geophys. Res. Lttrs. 12, 215-218.

Wells, F.G. and D.L. Peck, 1961, Geologic Map of Oregon west of the 121st meridian: US Geological Survey Misc Inv Map I-325, 1:500,000.

Wells, R.E., D.C. Engebretson, P.D. Snavely, Jr., and R.S. Coe, 1984, Cenozoic Plate Motions and the Volcano-tectonic Evolution of Western Oregon and Washington, Tectonics 3, 275-294.

Wernicke, B., J.E. Spencer, B.C. Burchfiel, P.L. Guth, 1982, Magnitude of Crustal Extension in the Southern Great Basin, Geology 10, 499-502.

Wernicke, B., 1981, Low-angle Normal Faults in the Basin and Range Province: Nappe Tectonics in an Extending Orogen, Nature 291, 645-648.

Wesnousky, S.G., C.H. Scholz, and K. Shimazaki, 1982, Deformation of an Island Arc: Rates of Moment Release and Crustal Shortening in Intraplate Japan Determined From Seismicity and Quaternary Fault Data, JGR 87, 6829-6852.

Westerveld, J., 1954, Quaternary Volcanism on Sumatra, GSA Bull. 63, 561-594.

White, C.M. and A.R. McBirney, 1978, Some Quantitative Aspects of Orogenic Volcanism in the Oregon Cascades, in Smith, R.B. and G.P. Eaton, eds., GSA Memoir 152, 369-388.

Wilcox, R.E., T.P. Harding and D.R. Seely, 1973, Basic Wrench Tectonics, AAPG 57, 74-96.

Williams, H., 1935, Newberry Volcano of Central Oregon, GSA Bull. 46, 253-304.

Williams, H. and A.R. McBirney, 1979, Volcanology: Freeman, Cooper and Co., San Francisco, 391p.

Williams, L.A.J., R. Macdonald, and G.R. Chapman, 1984, Late Quaternary Caldera Volcanoes of the Kenya Rift Valley, JGR 89, 8553-8570.

Williams, S., 1982, Basaltic ignimbrite erupted from Masaya Caldera Complex, Nicaragua [Abs], EOS 63, 1155

Wilson, C.J.N., A.M. Rogan, I.E.M. Smith, D.J. Northey, I.A. Nairn, and B.F. Houghton, 1984, Caldera Volcanoes of the Taupo Volcanic Zone, New Zealand, JGR 89, 8463-8484.

Wilson, D.S., 1984, The Gorda Plate: When is a plate not a plate? EOS 65, 1100.

Wilson, D.S, Hey, R.N., and C. Nishimura, 1984, Propagation as a mechanism of ridge reorientation: a model for the tectonic evolution of the Juan de Fuca Ridge, JGR 89, fall.

Wilson, J.T., 1965, A New Class of Faults and their Bearing on Continental Drift, Nature 207, 343-347.

Wise, D.U., R. Funiciello, M. Parotto, and F. Salvini, 1985, Topographic Lineament Swarms: Clues to Their Origin from Domain Analysis of Italy, GSA Bull. 96, 952-967.

Wise, D.U. and T.A. McCrory, 1982, A New Method of Fracture Analysis: Azimut', versus traverse distance plots, GSA Bull. 93, 889-897.

Wise, D.U., 1963, An Outrageous Hypothesis for the Tectonic Pattern of the North American Cordillera, GSA Bull 74, 357-362.

Wise, W.S., 1968, Geology of Mt. Hood, in Dole, H.M., ed., Andesite Conference Guidebook, Oregon Dept. Geol. Min. Ind. Bull 62, 81-100.

Withjack, M.O. and C. Shreiner, 1982, Fault Patterns Associated with Domes -- An Experimental and Analytical Study, AAPG Bull. 66, 302-316.

Wolfe, J.A., 1981, Philippine geochronology, J. Geol. Soc. Philipp., 35(1), 1-30.

Wolfe, J.A. and S. Self, 1982, Structural Lineaments and Neogene Volcanism in southwestern Luzon, in The Tectonic and Geologic Evolution of Southeast Asian Seas and Islands, Part 2, Geophysical Mono Ser., V 27, AGU.

Woller, N.M. and G.L. Black, 1983, Geology of the Waldo-Swift Creek Area, Lane and Klamath Counties, Oregon, in Priest, G.R. and B.F. Vogt, eds, 1983, Geology and Geothermal Resources of the Central Oregon Cascade Range, Special Paper 15, Oregon Dept of Geol and Min Ind, Portland, Ore.

Woller, N.M. and G.R. Priest, 1983, Geology of the Lookout Point Area, Lane County, Oregon in Priest, G.R. and B.F. Vogt, eds, 1983, Geology and Geothermal Resources of the Central Oregon Cascade Range, Special Paper 15, Oregon Dept of Geol and Min Ind, Portland, Ore.

Wright, L.A., 1976, Late Cenozoic Fault Patterns and Stress Fields in the Great Basin and Westward Displacement of the Sierra Nevada Block, Geology 4, 489-494.

Wright, L.A. and B.W. Troxel, 1973, Shallow Fault Interpretation of Basin & Range Structure, Southwestern Great Basin, in De Jong, K.A. and R. Scholton, eds., Gravity and Tectonics, John Wiley: New York, 397-407.

Wunderman, R.L. and W.I. Rose, 1984, Amatitlan, An Actively Resurging Cauldron 10 km South of Guatemala City, JGR 89, 8525-8539.

Yokoyama, I., 1983, Gravimetric Studies and Drilling Results at the Four Calderas in Japan, in D. Shimozuru and I. Yokoyama, eds., Arc Volcanism: Physics and Tectonics, Terra Scientific Publishing Co.: Tokyo, 29-41.

Yokoyama, I., 1966, Crustal Structures that Produce Eruptions of Welded Tuff and Formation of Calderas, Bull. Volc. 29, 51-60.

Yokoyama, I. and S. Suparto, 1970, Volcanological Survey of Indonesian Volcanoes. Part 5. A Gravity Survey on and around Batur Caldera, Bali., Bull. Earthquake Res. Inst. 48, 317-329.

Yoshikawa, T., S. Kaizuka, and Y. Ota, 1981, The Landforms of Japan, Unversity of Tokyo: Tokyo, 222p.

Yount, J.C. and R.C. Crosson, eds., 1983, Proceedings of Workshop XIV: Earthquake Hazards of the Puget Sound Region, USGS Open File Report 83-19.

Zoback, M.L., R.E. Anderson and G.A. Thompson, 1981, Cainozoic Evolution of the State of stress and Style of Tectonism of the Basin and Range Province of the Western U.S., Phil. Trans. Roy. Soc. London A 300, 407-434.

Zoback, M. and G. Thompson, 1978, Basin and Range Rifting in Northern Nevada: Clues from a Mid-Miocene Rift and Its Subsequent Offsets, Geology 6, 110-116.

Zoback, M.L., R.E. Anderson, and G.A. Thompson, 1981, Cainozoic Evolution of the State of Stress and Style of Tectonism of the Basin and Range Province of the Western U.S., Phil. Trans. Roy. Soc. London A, 300, 407-434.

Zoback, M.L. and Zoback, M., 1980, State of Stress in the Conterminous United States, JGR 85, 6113-6156.

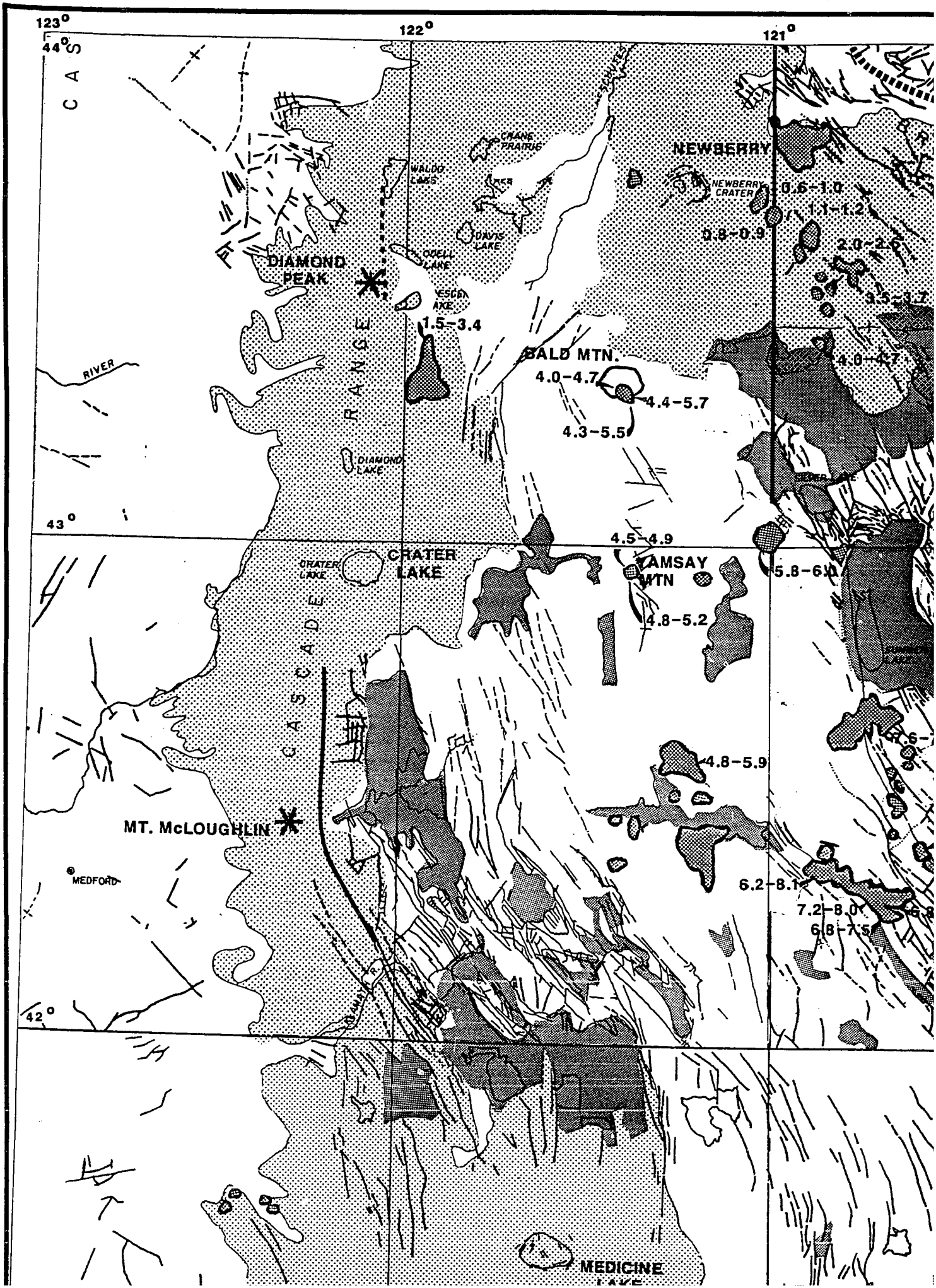
123°
122°
121°
44°
43°
42°
CASCADE RANGE
DIAMOND PEAK
1.5–3.4
CRANE PRAIRIE
WALDO LAKE
DAVIS LAKE
ODELL LAKE
ESCOLA LAKE
DIAMOND LAKE
NEWBERRY
NEWBERRY CRATER
0.6–1.0
1.1–1.2
0.8–0.9
2.0–2.6
3.3–3.7
4.0–4.7
BALD MTN.
4.0–4.7
4.4–5.7
4.3–5.5
4.5–4.9
CRATER LAKE
CRATER LAKE
RAMSAY MTN
5.8–6.0
4.8–5.2
4.8–5.9
6.2–8.1
7.2–8.0
6.8–7.5
MT. McLOUGHLIN
MEDFORD
MEDICINE LAKE
RIVER

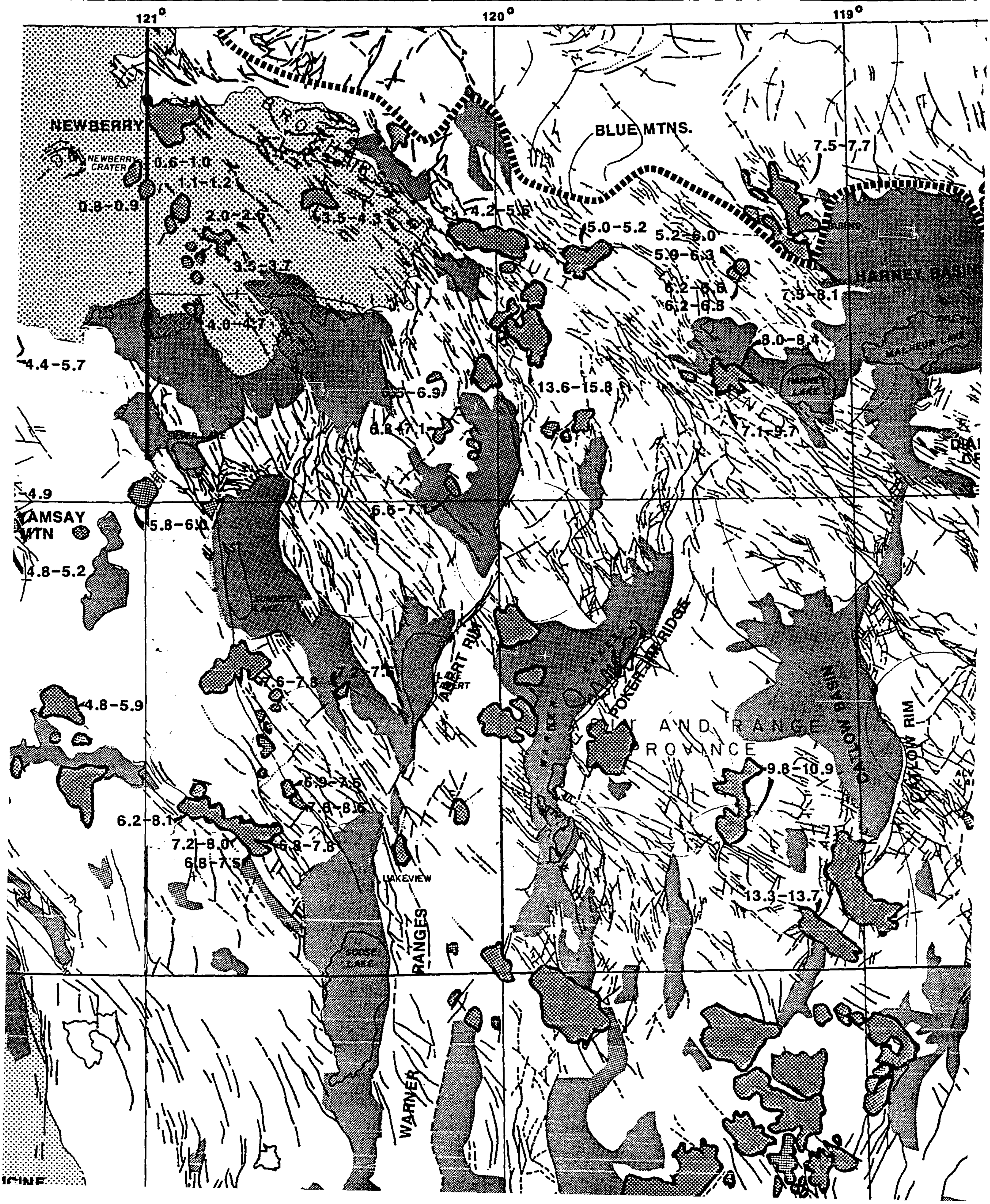
121°
120°
119°
NEWBERRY
NEWBERRY CRATER
BLUE MTNS.
HARNEY BASIN
MALHEUR LAKE
HARNEY LAKE
0.6–1.0
1.1–1.2
0.8–0.9
2.0–2.6
3.5–3.7
4.0–4.7
4.2–5.6
5.0–5.2
5.2–6.0
5.9–6.3
6.2–6.8
7.5–7.7
7.5–8.1
8.0–8.4
4.4–5.7
13.6–15.8
7.1–9.7
4.9
RAMSAY MTN
5.8–6.0
4.8–5.2
6.6–7.1
SUMMER LAKE
ABERT RIM
POKER JIM RIDGE
BASIN AND RANGE PROVINCE
ALVORD BASIN
STEENS MTN.
4.8–5.9
7.6–7.8
7.2–7.5
9.8–10.9
6.9–7.5
7.8–8.6
6.2–8.1
7.2–8.0
6.8–7.5
6.8–7.8
LAKEVIEW
13.3–13.7
WARNER RANGES
GOOSE LAKE

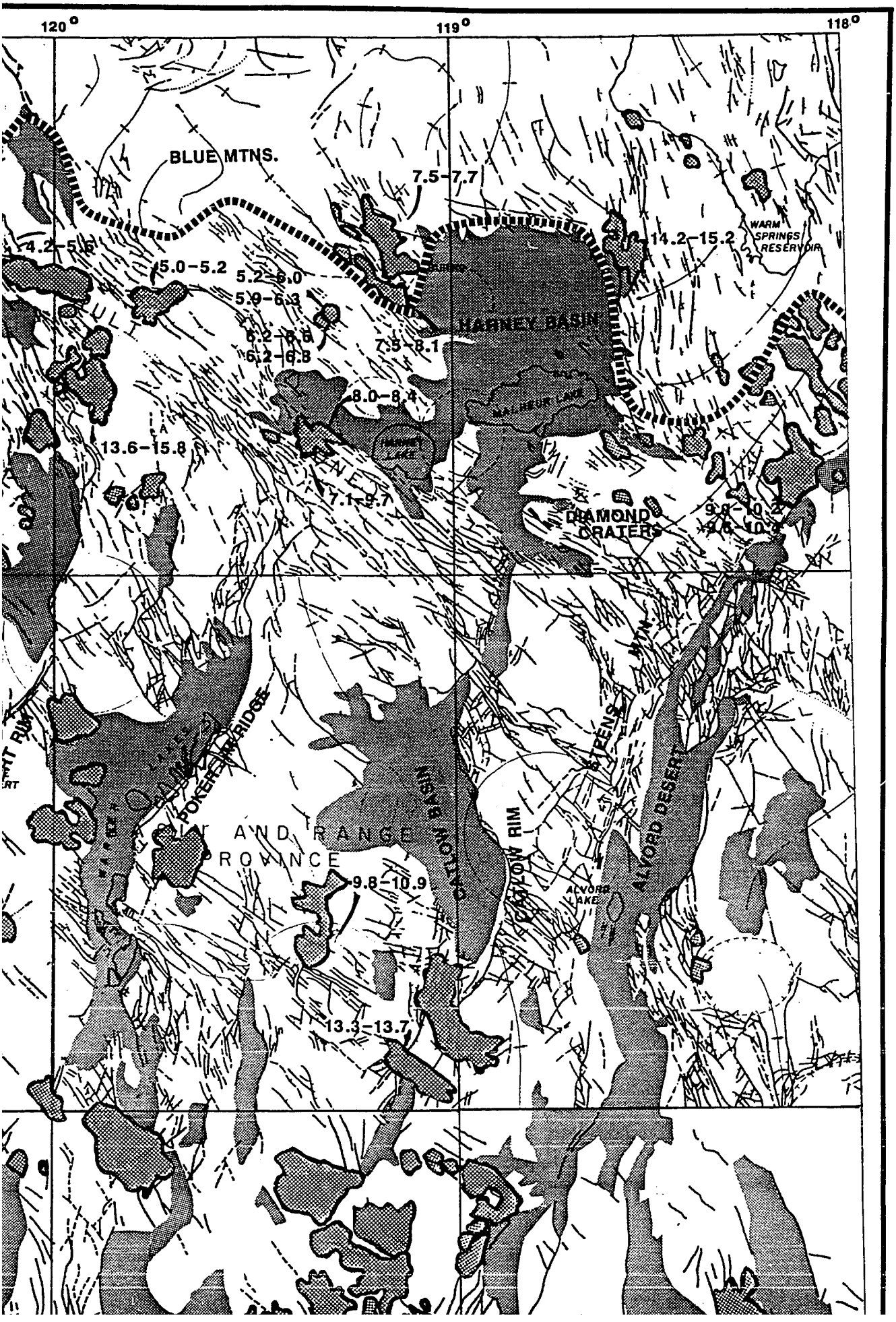
120°
119°
118°
BLUE MTNS.
7.5–7.7
14.2–15.2
WARM SPRINGS RESERVOIR
4.2–5.6
5.0–5.2
5.2–6.0
5.9–6.3
6.2–6.6
6.2–6.8
7.5–8.1
HARNEY BASIN
8.0–8.4
MALHEUR LAKE
13.6–15.8
7.1–9.7
DIAMOND CRATERS
9.8–10.2
9.6–10.7
POKER JIM RIDGE
BASIN AND RANGE PROVINCE
9.8–10.9
CATLOW RIM
ALVORD LAKE
ALVORD DESERT
13.3–13.7

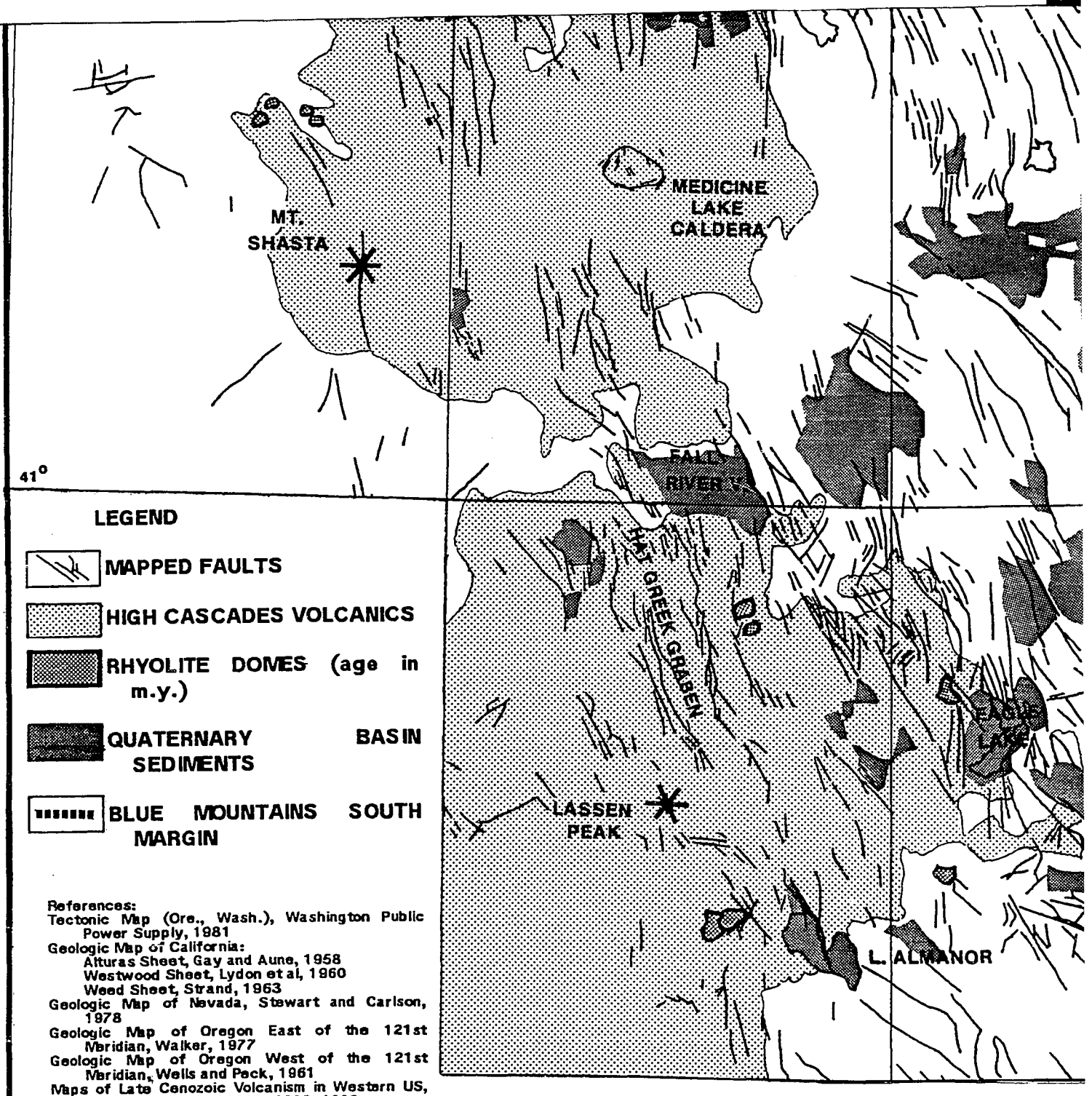

LEGEND

- MAPPED FAULTS
- HIGH CASCADES VOLCANICS
- RHYOLITE DOMES (age in m.y.)
- QUATERNARY BASIN SEDIMENTS
- BLUE MOUNTAINS SOUTH MARGIN

References:
Tectonic Map (Ore., Wash.), Washington Public Power Supply, 1981
Geologic Map of California:
Alturas Sheet, Gay and Aune, 1958
Westwood Sheet, Lydon et al, 1960
Weed Sheet, Strand, 1963
Geologic Map of Nevada, Stewart and Carlson, 1978
Geologic Map of Oregon East of the 121st Meridian, Walker, 1977
Geologic Map of Oregon West of the 121st Meridian, Wells and Peck, 1961
Maps of Late Cenozoic Volcanism in Western US, Luedke and Smith, 1981, 1982, 1983
MacLeod et al, 1975

SCALE 1:1,000,000

0 50 KM

TECTONIC MAP OF THE CASCADES AND BASIN AND RAI OF OREGON, CALIFORNIA AND NEVADA

C. FERRALL

1986

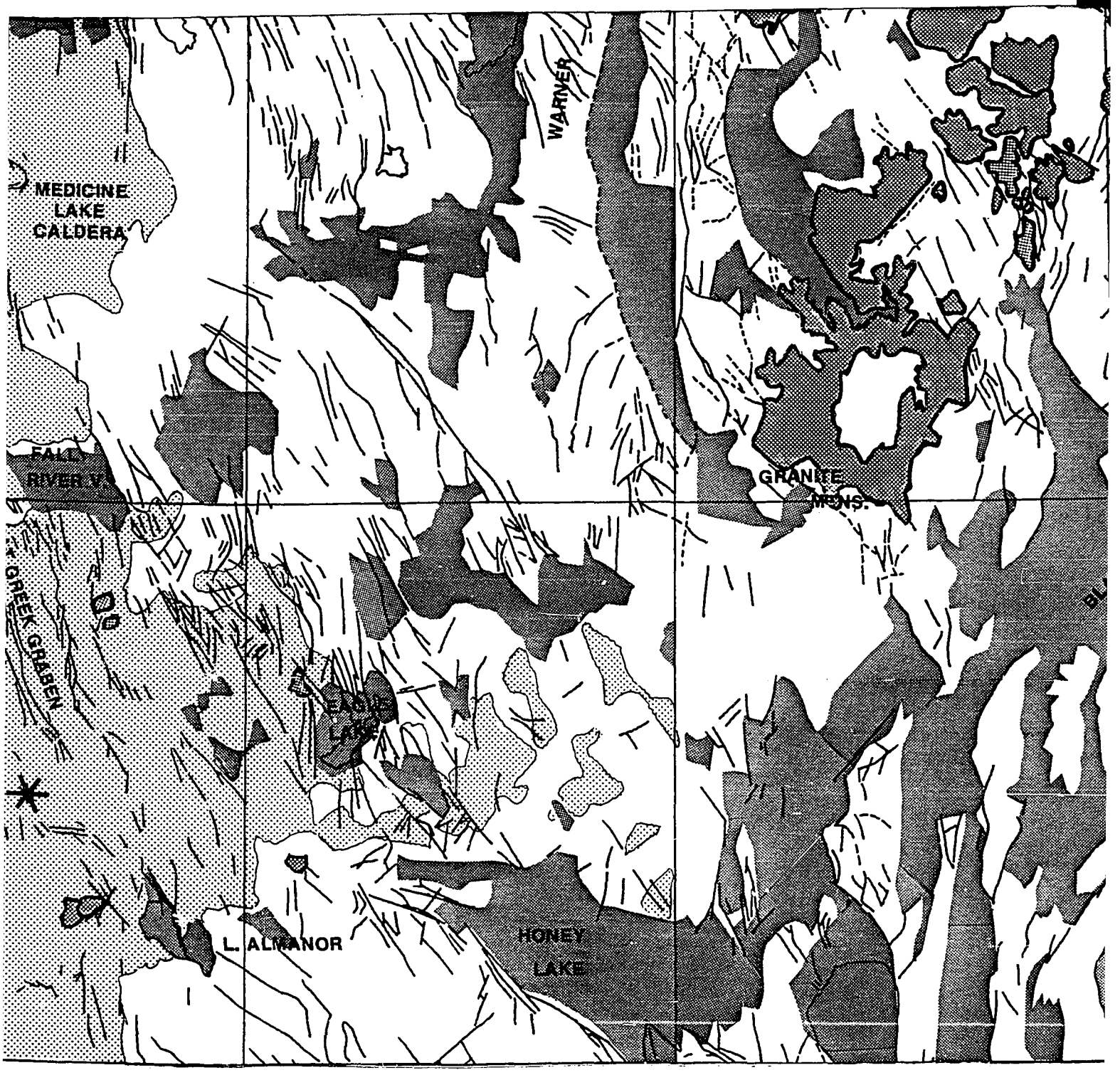

OF THE CASCADES AND BASIN AND RANGE
ON, CALIFORNIA AND NEVADA

ALL

PLATE I